Gene expression and genetic analyses in Parkinson's disease with and without dementia

Alan Edward Mayo Renton

Thesis submitted for the degree of Doctor of Philosophy to University College London

Department of Molecular Neuroscience
Institute of Neurology
Institute of Human Genetics and Health
University College London

2010

Declaration

I declare that the work described in this thesis is solely that of the author, unless stated otherwise in the text. None of the work has been submitted for any other qualification at this or any other university.

Alan Renton

Abstract

Dementia occurs in ~30% of Parkinson's disease (PD) patients, but few studies have examined gene expression in the brains of these individuals. In this thesis, quantitative reverse transcriptase-polymerase chain reaction (qRT-PCR) and microarray were used to investigate gene expression in the dorsolateral prefrontal cortex (DLPFC), comparing idiopathic Parkinson's disease (IPD) patients with and without dementia against each other and controls. Expression of the Extracellular-signal regulated kinase 1/2 (ERK1/2) inhibitor *Dual specificity phosphatase 6* (*DUSP6*) and the tyrosine kinase *Ephrin receptor A2* (*EPHA2*) was significantly decreased and increased, respectively, in IPD versus controls, however these phenotypes were unaffected by dementia status. Expression of the PD gene *α-Synuclein* (*SNCA*) was unaltered in the DLPFC. Further qRT-PCR analyses demonstrated that *DUSP6*, *EPHA2*, and *SNCA* are not differentially-expressed in seven other regions of the IPD brain. Association and imaging analyses indicated that variation at the *DUSP6* single nucleotide polymorphism (SNP) rs1689408 marginally alters IPD risk and profoundly influences grey matter density, possibly through an effect on *DUSP6* splicing. Moreover, variation at the *EPHA2* SNP rs11260822 significantly modified IPD susceptibility. However, variation at these SNPs did not influence the overall expression of *DUSP6* or *EPHA2*, respectively. In addition, a rare haplotype composed of the *SNCA* SNPs rs11931074 and rs3822086 significantly increased IPD risk. Detailed examination of the microarray data suggested that pathways involving inflammation, cell adhesion, the cytoskeleton, synaptic transmission, lipoprotein metabolism, metal binding, and mitochondria are dysregulated in the DLPFC of IPD dementia patients. Furthermore, *in silico* mining of the microarray data suggested that a positive feedback loop involving EPHA2 and ERK1/2 signaling is constitutively-activated in the IPD neurodegeneration DLPFC. Notwithstanding the observed changes, the parkinsonian DLPFC was characterised by an overall lack of gene dysregulation. These findings extend our knowledge of gene expression in IPD dementia and neurodegeneration. Moreover, they suggest that *DUSP6* and *EPHA2* are novel genes involved in IPD pathogenesis.

Acknowledgements

Firstly, I would like to thank my supervisor, Prof. Nicholas Wood, for his support, consumable funding, and critical reading of the manuscript. I would also like to thank Prof. Peter Giese for his supervision. I was funded by the Institute of Human Genetics and Health (stipend) and the Medical Research Council (consumables).

I would like to thank Dr. Rohan da Silva, Dr. Emma Deas, Dr. Simone Sharma, and Dr. Geoffrey Tan for critical reading of the manuscript.

I would especially like to thank the following people for contributing data, performing analyses, and/or carrying out extractions: Dr. Geoffrey Tan, Dr. Mike Hubank and his team at the Gene Microarray Centre, Dr. Sonia Shah, Dr. Simone Sharma, Dr. Coro Paisán-Ruíz, Dr. Andrew Singleton, Dr. Emma Deas, the NHNN Neurogenetics Service team.

I would like to thank the Queen Square Brain Bank for providing brain tissue, and especially the following people for technical assistance, sample selection/information, and/or helpful discussions: Linda Kilford, Prof. David Williams, Dr. Sean O'Sullivan, Dr. Rina Bandopadhyay, Dr. Janice Holton, Prof. Tamas Revesz, Prof. Andrew Lees.

I would like to thank the following people for providing equipment, consumables, and/or sample information: Dr. Jon Beck, Prof. Steve Humphries, Jutta Palmen, Ros Whittall, Dr. Jana Vandrovcova, Dr. Anna Melchers, Dr. Charles Mein, Dr. Stephanie Schorge.

I would to thank the following people for technical and statistical training: Dr. Vaneesha Gibbons, Ese Mudanohwo, Mark Poulter, Dr. Carles Vilariño-Guëll, Dr. Charles Mein, Dr. Geoffrey Tan, Dr. Stephanie Schorge.

I would like to thank the following people in our laboratory and UCL for helpful discussions and moral support: Dr. Simone Sharma, Dr. Carles Vilariño-Guëll, Dr. Geoffrey Tan, Dr. Emma Deas, Dr. Julia Fitzgerald, Dr. Alison Wood-Kaczmar, Dr. Sonia Gandhi, Dr. Patrick Abou-Sleiman, Dr. Lee Stanyer, Emily Fletcher, Dr. Hazel Urwin, Gary Adamson, Dr. Virginie Bros-Facer, Dr. Paul Johns, Dr. Charles Lockwood, Dr. Mark Thomas, Prof. Andrés Ruiz-Linares, and Prof. John Hardy.

I would like to thank the members of the Institute of Human Genetics and Health for their advice and support: Prof. Steve Humphries, Prof. Sue Povey, Prof. Nanneke Redclift, Dr. Simone Sharma, Dr. Jessica Mozersky, Dr. Richard Milne, Alex Calladine.

I would especially like to thank Ayesha Shahid for her unwavering help and support. I then want to thank all my mates for being them and keeping me well fed and watered: Tom, Katie, Marc, Sophie, Michael, Vicki, Nick, Wakana, Jack, Adam, Ben, Anna, Hannah, Karen, the Stephs, the Jesses, Brace, Adam, Avi, Rich, Angela, Grabbit, and the rest of the OKR crew.

And finally, a huge thank you to my family who have supported me throughout: Mum, Haig, Dad, Josh, Zoë, Tom, Grandma, David, Lisa, Roger, Tim, Clare, Granny, Grandfather.

This thesis is dedicated to my grandfather, Kennedy Mayo Harrow, who gave me one of his names and the inspiration to become a scientist.

Contents

List of figures

Chapter 3

Chapter 4

Chapter 5

Appendix

List of tables

Chapter 2

Chapter 3

Chapter 4

Chapter 5

Appendix

List of abbreviations

The list includes common stems which apply to multiple gene symbols as appropriate.

Abbreviation	Meaning
-ve	Negative control
+ve	Positive control
1:3	Splice form 1:3
4:6	Splice form 4:6
ACh	Acetylcholine
AChE	Acetylcholinesterase
ACP1	*Acid phosphatase 1, soluble*
ATF6	*Activating transcription factor 6*
ARC	*Activity-regulated cytoskeleton-associated protein*
AMP	Adenosine monophosphate
cAMP	Cyclic AMP
CREB	*cAMP response element binding protein*
ATP	Adenosine triphosphate
ATPase	Adenosine triphosphatase
ATP13A2	*ATPase type 13A2*
ADCYAP1	*Adenylate cyclase activating polypeptide 1*
AODP	Adult onset dystonia parkinsonism
AMBA	Allen Mouse Brain Atlas
aka	Also known as
AD	Alzheimer's disease
ALAS2	*Aminolevulinate, δ-, synthase 2*
AMPA	α-Amino-3-hydroxy-5-methyl-4-isoxazolepropionic acid
GABA	γ-Aminobutyric acid
APP	Amyloid precursor protein
ALS-PDC	Amyotrophic lateral sclerosis-parkinsonism dementia complex
ANOVA	Analysis of variance
AG	Angular gyrus
ACC	Anterior cingulate cortex
AFC	Anterior frontal cortex
APOA5	*Apolipoprotein A5*
APOE	*Apolipoprotein E*
APE1	Apurinic/apyrimidinic endonuclease 1
AUC	Area under the curve
RARS2	*Arginyl-tRNA synthetase 2, mitochondrial*
APSP	Atypical Progressive supranuclear palsy
bp	Base pairs

BG	BioGRID
BAIAP3	*Brain angiogenesis inhibitor 1-associated protein 3*
BDNF	*Brain-derived neurotrophic factor*
BS	Brain stem
BA	Brodmann area
CACNA2D3	*Calcium channel, voltage-dependent, α2/δ3 subunit*
COMT	*Catechol-O-methyltransferase*
CNS	Central nervous system
CEPH	Centre d'Étude du Polymorphisme Humain
CBF	Cerebral blood flow
CMA	Chaperone-mediated autophagy
CHI3L1	*Chitinase 3-like 1*
ChAT	Choline acetyltransferase
C3orf36	*Chromosome 3 open reading frame 36*
C8orf79	*Chromosome 8 open reading frame 79*
CDR	Clinical dementia rating
COG	A measure of whether patients presented with cognitive impairment or altered personality (within two years of PD diagnosis)
CCDC92	*Coiled-coil domain containing 92*
COL2A1	*Collagen, type II, α 1*
COL27A1	*Collagen, type XXVII, α 1*
CI	Confidence interval
CON	Control
CA1	Cornu ammonis 1
CA2	Cornu ammonis 2
C_t	Cycle threshold
DBS	Deep brain stimulation
DG	Dentate gyrus
DNA	Deoxyribonucleic acid
cDNA	Complementary DNA
gDNA	Genomic DNA
ssDNA	Single-stranded DNA
DDIT3	*DNA-damage-inducible transcript 3*
DNAJC10	*DnaJ homologue, subfamily C, member 10*
DTNBP1	*Dystrobrevin binding protein 1*
DLB	Dementia with Lewy bodies
DEPC	Diethyl pyrocarbonate
DAE	Differential allelic expression
DCS	Direct current stimulation
tDCS	Transcranial DCS
DTT	Dithiothreitol
DA	Dopamine
6-OHDA	6-Hydroxydopamine
DLPFC	Dorsolateral prefrontal cortex
DUSP	*Dual specificity phosphatase*

DUSP6	*Dual specificity phosphatase 6*
DPP	*DUSP6* putative promoter
ETS	*E Twenty-Six oncogene homologue 1*
ELK	*ETS-like kinase*
ELANE	*Elastase, neutrophil expressed*
ETC	Electron transport chain
ER	Endoplasmic reticulum
ERAD	ER-associated degradation
EDEM1	*ER degradation enhanced, mannosidase α-like 1*
ERN1	*ER to nucleus signaling 1*
EC	Entorhinal cortex
EFNA	*Ephrin*
EPHA2	*Ephrin receptor A2*
ECK	Epithelial cell kinase
ESR1	*Estrogen receptor 1*
EDTA	Ethylendiaminetetraacetate
EIF2AK	*Eukaryotic translation initiation factor 2 α kinase*
EIF2S1	*Eukaryotic translation initiation factor 2, subunit 1 α, 35 kDa*
EXOC3L	*Exocyst complex component 3-like*
EM	Expectation-maximisation
ECM	Extracellular matrix
ERK	Extracellular-signal regulated kinase
FDR	False discovery rate
FAD3	Familial Alzheimer's disease 3
FPD	Familial Parkinson's disease
FWE	Family-wise error
FAM83H	*Family with sequence similarity 83, member H*
FTH1	*Ferritin, heavy polypeptide 1*
FTL	*Ferritin, light polypeptide*
FGF	*Fibroblast growth factor*
FU	Fluoresence units
FMR1	*Fragile X mental retardation 1*
FXTAS	Fragile X tremor ataxia syndrome
FC	Frontal cortex
FTDP17	Frontotemporal dementia and parkinsonism linked to chromosome 17
FTLDU	Frontotemporal lobar degeneration with ubiquitin-positive inclusions
FL	Full length
FWHM	Full width at half maximum
FXYD2	*FXYD domain containing ion transport regulator 2*
GPR37	*G-protein-coupled receptor 37*
GRK	*G-protein-coupled receptor kinase*
GO	Gene ontology
GSD	Gerstmann-Straussler disease

GCI	Glial cytoplasmic inclusion
GP	Globus pallidus
GBA	*β-Glucocerebrosidase*
G6PD	*Glucose-6-phosphate dehydrogenase*
GRIA4	*Glutamate receptor, ionotrophic, AMPA 4*
GWAS	Genome wide association study
GTP	Guanosine triphosphate
GTPase	Guanosine triphosphatase
HWE	Hardy-Weinberg equilibrium
HSPA1A	*Heat shock 70 kDa protein 1A*
HSPA5	*Heat shock 70 kDa protein 5*
HNF1A	*Hepatic nuclear factor 1 homeobox A*
HMSN	Hereditary motor and sensory neuropathy
het	Heterozygote
HTRA2	*High temperature requirement A2* (aka *Omi*)
HP	Hippocampus
hom	Homozygote major
H_2O_2	Hydrogen peroxide
HPRT1	*Hypoxanthine phosphoribosyltransferase 1*
HD	Huntington's disease
ID	Identity
IPD	Idiopathic Parkinson's disease (also the combined group of IPDD and IPDND)
IPDD	IPD dementia
IPDND	IPD no dementia
IHC	Immunohistochemistry
IPC	Inferior parietal cortex
IKB	Inhibitor of κ light polypeptide gene enhancer in B-cells
IKBKE	*Inhibitor of κ light polypeptide gene enhancer in B-cells, kinase ε*
IFI27	*Interferon, α-inducible protein 27*
ITGAL	*Integrin, alpha L*
IUBMB	International Union of Biochemistry and Molecular Biology
IREB2	*Iron responsive element binding protein 2*
KRT9	*Keratin 9*
kb	Kilobase pairs
kDa	Kilodaltons
KRAS	*Kirsten rat sarcoma viral oncogene homologue*
KRS	Kufor-Rakeb syndrome
KEGG	Kyoto Encyclopaedia of Genes and Genomes
LCM	Laser capture microdissection
LRRK2	*Leucine-rich repeat kinase 2*
LB	Lewy body
LBD	Lewy body disease

LN	Lewy neurite
LP	Lewy pathology
LIMMA	Linear Modelling for Microarray Analysis
LD	Linkage disequilibrium
LREC	Local Research Ethics Committee
LOESS	Locally weighted scatter plot smoothing
LC	Locus coeruleus
LTP	Long term potentiation
LY6K	*Lymphocyte antigen 6 complex, locus K*
LCK	*Lymphocyte-specific protein tyrosine kinase*
M	A measure of reference gene stability (qRT-PCR)
MRI	Magnetic resonance imaging
fMRI	Functional MRI
MHC	Major histocompatibility complex
MAN1B1	*Mannosidase, α, class 1B, member 1*
MED	Medulla
MARCH7	*Membrane-associated ring finger(C3HC4) 7*
MBTPS1	*Membrane-bound transcription factor peptidase, site 1*
MPTP	1-Methyl-4-phenyl-1,2,3,6-tetrahydropyridine
MPP+	1-Methyl-4-phenylpyridinium
MSP	Methyl-specific PCR
MAPT	*Microtubule-associated protein tau*
MID1	*Midline 1*
MID1IP1	*Midline 1 interacting protein 1*
MLL5-L	Mixed-lineage leukaemia 5-lysine
MAF	Minor allele frequency
MMSE	Mini mental state examination
MAPK	*Mitogen-activated protein kinase*
MKP	Mitogen-activated protein kinase phosphatase
MAO	Monoamine oxidase
MNI	Montreal Neurological Institute
NCBI	National Center for Biotechnology Information
NHNN	National Hospital for Neurology and Neurosurgery
NP	Neuritic plaque
NFT	Neurofibrillary tangle
NLC	Neuronal loss-corrected
NF	Normalisation factor
NTC	Nontemplate control
NA	Not applicable
ND	Not determined
NS	Not significant
NFKB	Nuclear factor κ light polypeptide gene enhancer in B-cells
NURR1	*Nuclear receptor related 1*
NR3C1	*Nuclear receptor subfamily 3, group C, member 1*

NR4A2	*Nuclear receptor subfamily 4, group A, member 2* (aka *NURR1*)
NUP98	*Nucleoporin 98 kDa*
dNTP	Deoxynucleotide triphosphate
NbM	Nucleus basalis of Meynert
OGT	*O-linked N-acetylglucosamine transferase*
OR	Odds ratio
OR2M4	*Olfactory receptor, family 2, subfamily M, member 4*
OMIM	Online Mendelian Inheritance in Man
OFC	Orbitofrontal cortex
ODF2	*Outer dense fibre of sperm tails 2*
PB	Pale body
PARK2	*Parkin*
PD	Parkinson's disease
PDD	PD dementia
PARK7	*Parkinson's disease 7* (aka *DJ1*)
PCNX	*Pecanex homologue*
PINK1	*Phosphatase and tensin homologue-induced putative kinase 1*
PE	Phosphatidylethanolamine
PISD	*Phosphatidylserine decarboxylase*
PLA2	Phospholipase A2
PLA2G	*Phospholipase A2, group*
PCR	Polymerase chain reaction
RT-PCR	Reverse transcriptase-PCR
qRT-PCR	Quantitative RT-PCR
PET	Positron emission tomography
PMD	*Post mortem* delay
PTM	Post translational modification
PCC	Posterior cingulate cortex
POU4F3	*POU class 4 homeobox 3*
PFC	Prefrontal cortex
PSEN1	*Presenilin 1*
PCA	Principal components analysis
PSP	Progressive supranuclear palsy
PTGDS	*Prostaglandin D2 synthase*
PSMB8	*Proteasome (prosome, macropain) subunit, β type, 8*
PPP1R16A	*Protein phosphatase 1, regulatory subunit 16A*
PTP	Protein tyrosine phosphatase
PTPN11	*Protein tyrosine phosphatase, non-receptor type 11*
PTPRR	*Protein tyrosine phosphatase, receptor type, R*
PUM1	*Pumilio homologue 1*
QKI	*Quaking homologue, KH domain RNA binding*
QC	Quality control
QTL	Quantitative trait locus
eQTL	Expression QTL

QSBBND	Queen Square Brain Bank for Neurological Disorders
RN	Raphe nuclei
REM	Rapid eye movement
Ras	Rat sarcoma
RasGAP	Ras GTPase activating protein
RASA1	*Ras p21 protein activator 1*
ROS	Reactive oxygen species
ROC	Receiver operator curve
ROI	Region of interest
RRAS	*Related Ras viral oncogene homologue*
3R	3-Repeat *MAPT*
4R	4-Repeat *MAPT*
RARRES2	*Retinoic acid receptor responder 2*
RICH2	*Rho-type GTPase-activating protein RICH2*
RNA	Ribonucleic acid
cRNA	Complementary RNA
mRNA	Messenger RNA
miRNA	Micro RNA
rRNA	Ribosomal RNA
tRNA	Transfer RNA
RNAi	RNA interference
RNAse	Ribonuclease
RPL13A	*Ribosomal protein L13A*
RPL35A	*Ribosomal protein L35A*
RPS6KA	*Ribosomal protein S6 kinase, 90 kDa, polypeptide*
RSK	Ribosomal S6 kinase
RMA	Robust multi-chip average
RUSC1	*RUN and SH3 domain containing 1*
SEPW1	*Selenoprotein W, 1*
SNP	Single nucleotide polymorphism
htSNP	Haplotype-tagging SNP
mSNP	Marker SNP
rSNP	Regulatory SNP
Src	Sarcoma
SH2	Src homology 2
SH3	Src homology 3
ST	Sense target
STAT4	*Signal transducer and activator of transcription 4*
SPECT	Single photon emission computerised tomography
SDS	Sodium dodecyl sulphate
SD	Standard deviation
SPM	Statistical parametrical mapping
STAU1	*Staufen homologue 1*
STR	Striatum
SN	Substantia nigra
SNpc	SN pars compacta

STN	Subthalamic nucleus
SNCAIP	*Synuclein, α interacting protein* (aka *Synphilin 1*)
SNCA	*α-Synuclein*
SNCB	*β-Synuclein*
TCF/LEF	T-cell factor/lymphoid enhancer binding factor
TBP	*TATA box binding protein*
TC	Temporal cortex
TdT	Terminal deoxynucleotidyl transferase
TEX2	*Testis expressed 2*
TOL	Tower of London
TMS	Transcranial magnetic stimulation
rTMS	Repetitive TMS
TF	Transcription factor
TCF7	*Transcription factor 7*
TCF7L	*Transcription factor 7-like*
TFBS	Transcription factor binding site
TSS	Transcriptional start site
TRPM	*Transient receptor potential cation channel, subfamily M, member*
TMC3	*Transmembrane channel-like 3*
TBE	Tris-borate-EDTA
TFIP11	*Tuftelin interacting protein 11*
TP53	*Tumour protein 53*
UQCRFS1	*Ubiquinol-cytochrome c reductase, Rieske iron-sulphur polypeptide 1*
UCHL1	*Ubiquitin carboxy-terminal hydrolase L1*
UPS	Ubiquitin-proteasome system
UCSC	University of California Santa Cruz
UCL	University College London
UCLH	University College London Hospital
UPR	Unfolded protein response
UTR	Untranslated region
UDG	Uracil DNA glycosylase
dUTP	Deoxyuridine triphosphate
V25	A measure of whether patients presented with cognitive impairment or altered personality (two years or more after PD diagnosis)
RELB	*V-rel reticuloendotheliosis viral oncogene homologue B*
VTA	Ventral tegmental area
VLN	Ventrolateral nucleus
vs	Versus
WT	Wild type
WCST	Wisconsin Card Sorting Task
VBM	Voxel-based morphometry
WM	Working memory

H_2O	Water
mqH_2O	MilliQ H_2O
rfH_2O	RNAse-free H_2O
tH_2O	Tap H_2O
XBP1	*X-box binding protein 1*
YY1	*Yin Yang 1*
ZNF407	*Zinc finger protein 407*

Chapter 1: Introduction

1.1. Parkinson's disease

1.1.1. Clinical and neuropathological characteristics of Lewy body disease

1.1.1.1. Parkinson's disease: introduction and clinical overview

Parkinson's disease (PD) was first identified by James Parkinson, and christened the "shaking palsy" (Parkinson 1817). It is the most common neurodegenerative movement disorder, affecting roughly 1% of people over the age of 60, rising to 4-5% in those 85 or above, and has a higher prevalence in men than in women (Fahn 2003). PD typically has an insidious (it presents during mid to late adulthood) and asymmetrical onset, with a progressive course eventually resulting in death. It is characterised clinically by the presence of four cardinal motor symptoms, collectively known as parkinsonism: bradykinesia (slowed initiation and execution of voluntary movement), resting tremor, muscular rigidity, and postural instability. Bradykinesia and at least one other parkinsonian symptom must be present to ensure clinical diagnosis of PD [reviewed in (Lees *et al.* 2009)].

It is widely accepted that PD motor symptoms are for the most part caused by the death and/or dysfunction of neuromelanin-containing dopaminergic neurons in the pars compacta of the substantia nigra (SN). This leads to a severe reduction of dopamine (DA) levels in the striatum, a vital structure in the basal ganglia whose function is to initiate and coordinate voluntary movement, resulting in parkinsonism (see 1.1.1.2) (Farrer 2006). 5-10% of cases are the result of monogenic mutations that follow a Mendelian inheritance pattern, and as such are termed familial Parkinson's disease (FPD). The vast remainder is known as idiopathic Parkinson's

disease (IPD) (see 1.1.2). Its exact aetiology still escapes elucidation, but most commentators believe it arises from a complex interplay of genetic, epigenetic, and environmental factors (Lesage and Brice 2009).

Confirmation of PD diagnosis requires clinical parkinsonism and the subsequent detection of two essential neuropathological hallmarks *post mortem*. These are loss of the aforementioned substantia nigra pars compacta (SNpc) dopaminergic neurons with concomitant depigmentation, and the presence of proteinaceous cytoplasmic inclusions called Lewy bodies (LBs) and/or dystrophic Lewy neurites (LNs) (collectively known as Lewy pathology [LP]) in the brain stem (see 1.1.1.2) (Lees *et al.* 2009). Several other forms of parkinsonism exist, and these conditions are distinguished from PD by their lack of the diagnostic triad: parkinsonian motor dysfunction, SNpc neuronal loss, and brain stem LP (Farrer 2006). These atypical parkinsonian syndromes are beyond the scope of this chapter, which will concentrate on PD and two very closely related diseases: Parkinson's disease dementia (PDD) and dementia with Lewy bodies (DLB). These conditions are collectively known as Lewy body disease (LBD), and together with multiple system atrophy (MSA), form a group of neurological disorders termed synucleinopathies (Farrer 2006).

In the past, PD was primarily considered as a movement disorder. However this view is increasingly seen as overly simplistic and a plethora of nonmotor symptoms have been described. Moreover, many of these are thought to arise from dysfunction in extranigral structures, highlighting the growing understanding of the role played by nondopaminergic systems in PD (see 1.1.1.2) [reviewed in (Adler 2005; Lim *et al.* 2009)]. Some of these symptoms can present well before the onset of classical motor features, even by decades. Examples include: cognitive impairment (see 1.1.1.3), depression, anxiety, rapid eye movement (REM) behaviour disorder, excessive daytime somnolence (sleepiness), insomnia, pain, hyposmia (olfactory impairment), and autonomic problems e.g. constipation, incontinence, impotence, and orthostatic hypotension (sudden dizziness on standing). Other nonmotor symptoms tend to be associated with more advanced PD. These include: dementia (see 1.1.1.3), psychosis

e.g. visual hallucinations and delusions, dysarthria (speech disorder), and dysphagia (swallowing difficulties) [reviewed in (Adler 2005; Lim *et al.* 2009)].

PD remains incurable, and the primary therapeutic approach is replacement of depleted nigrostriatal DA. Levodopa, the metabolic precursor of DA, alleviates the motor symptoms at first. But after five years of levodopa therapy, ~60% of patients develop a reduced response and/or dyskinesias (involuntary movements) (Fahn 2003). More advanced cases undergo surgery. Stereotactic deep brain stimulation (DBS) is the most popular and successful option. Generally the subthalamic nucleus (STN) is targeted, resulting in reduced bradykinesia severity, however stimulation of the globus pallidus (GP) is also employed to control levodopa-induced dyskinesia (Fahn 2003). Several methodologies are employed to treat the spectrum of nonmotor symptoms, notably acetylcholinesterase inhibitors which can ameliorate the cognitive dysfunction associated with this condition (see 1.1.1.4) (Caballol *et al.* 2007).

1.1.1.2. Parkinson's disease: synaptic pathways and neuropathology

Parkinson's disease is characterised by severe neuronal loss in the ventrolateral tier of the SNpc, which causes marked degeneration of nigrostriatal fibres that project to DA receptors in the putamen (Fearnley and Lees 1991). Under normal circumstances these fibres innervate two synaptic systems, known as the "direct" and "indirect" pathways, both of which result in excitation of cortical motor areas. The direct pathway begins with excitatory signaling of nigrostriatal fibres to DA D1 receptors in the putamen. Inhibitory γ-aminobutyric acid (GABA) pathways then link the putamen to the medial GP, and in turn connect this structure to the thalamic ventrolateral nucleus (VLN). Excitatory glutamergic pathways link the VLN to the cortex (Crossman and Neary 2005). The indirect pathway starts with inhibitory signaling of nigrostriatal fibres to DA D2 receptors in the putamen. GABAergic pathways then signal from the putamen to the lateral GP, and in turn connect this

structure to the subthalamic nucleus (STN). Glutamergic pathways link the STN to the medial GP, which is itself connected to the VLN and cortex, as per the direct pathway. Hence, the akinetic symptoms observed in PD can be accounted for by reduced striatal DA and resultant cortical inhibition via the direct and indirect pathways (Crossman and Neary 2005).

However, cell death and concomitant LP (see below) is not restricted to either the SNpc or dopaminergic neurons. Indeed, extensive noradrenergic and serotonergic neuronal loss can be detected in the locus coeruleus (LC) and raphe nuclei (RN), respectively. Cholinergic neurons in the dorsal motor nuclei of the medulla oblongata, the pons, and the nucleus basalis of Meynert (NbM) are damaged. To a lesser extent, dopaminergic neuronal loss is also observed in the ventral tegmental area (VTA). Moreover, even cells outside the central nervous system (CNS) are affected, such as those in the olfactory bulb and mesenteric system [reviewed in (Lees 2009)]. Neurodegeneration in many of these extranigral regions and the resultant neurotransmitter deficiency at postsynaptic cortical targets is believed to contribute to some of the nonmotor features seen in PD (see 1.1.1.4) (Scatton *et al.* 1983; Perry *et al.* 1985).

Neuronal cell loss in PD is generally accompanied by three types of intracellular inclusion: LBs, LNs, and pale bodies (PBs). LBs, the classical pathological hallmark, exist as two distinct types. Brain stem LBs are easily seen under light microscopy with haematoxylin and eosin staining. They are spherical or elongated cytoplasmic aggregates possessing a dense eosinophilic core and a paler peripheral halo. Cortical LBs tend to be more irregular in shape, often lack a conspicuous halo, and can be difficult to detect with haematoxylin. Both types of LB possess a filamentous ultrastructure and stain positive for α-Synuclein (SNCA). Aggregated SNCA is a major component of LBs and LNs, and its detection is the immunohistochemical marker used to evaluate the severity and extent of LP (see below). Aggregates of this protein are also abundant in PBs, which are large rounded eosinophilic filamentous structures. In the early stages of PD, SNCA can be detected in neurons as punctuate

cytoplasmic staining. It is believed that during pathogenesis, cytoplasmic SNCA aggregation progresses from punctuate staining to PBs to LBs. In addition to SNCA, LBs contain over 70 other molecules whose functions include signal transduction, protein folding, oxidative stress, and protein degradation [reviewed in (Wakabayashi *et al.* 2007)]. The terms incidental Lewy body disease (ILBD) and diffuse Lewy body disease (DLBD) are diagnostic definitions used by neuropathologists to indicate low levels of brain stem LP or widespread cortical LP, respectively.

An influential publication retrospectively studied groups of PD patients and individuals with ILBD at various pathological stages, documenting the spread of accumulated SNCA in the form of LBs and LNs i.e. LP. This has resulted in the development of a system known as Braak staging (Braak *et al.* 2003). The findings indicate that LP begins in the medullary dorsal motor nuclei and the anterior olfactory nucleus (stage 1). As PD progresses, LP ascends rostrally up the brain stem to the pons, affecting the reticular formation, particularly the RN and LC (stage 2), and then to the midbrain and basal forebrain, notably involving the SNpc and the magnocellular nuclei (e.g. the NbM), respectively (stage 3) (Braak *et al.* 2003). Next, LP expands through the basal forebrain, affecting the amygdala and certain thalamic nuclei, and into the temporal mesocortex and the allocortex, involving the perirhinal cortex and hippocampus respectively (stage 4). LP then spreads into the neocortex. Initially, the higher order sensory association areas, insula, anterior cingulate cortex (ACC), and prefrontal cortex (PFC) are affected (stage 5). Subsequently, almost the entire neocortex is involved, including to some extent the first order sensory association areas, primary sensory areas, and premotor and primary motor cortices (stage 6). Note that LNs are generally inferred to precede LBs (Braak *et al.* 2003).

Notwithstanding its apparent success at charting the spread of LP (see below), specific criticisms have been levelled at the Braak system (Kalaitzakis *et al.* 2008c). These have brought an unresolved issue about PD pathophysiology into sharp relief, that being whether LBs themselves are neurotoxic, neuroprotective or simply a marker of excessive protein load with no direct influence on disease progression. The

first issue with the Braak scheme is that the authors introduced a confounding bias, by only selecting individuals demonstrating SNCA positivity in the dorsal motor nuclei, thereby undermining their contention that LP at this site is an obligate trigger for PD (Kalaitzakis *et al.* 2008c). Indeed, two studies have shown that ~7-8% of PD cases do not possess LP at this location, despite exhibiting extensive lesions in the SNpc and neocortex (Kalaitzakis *et al.* 2008b; Attems and Jellinger 2008). The second criticism is that the Braak system fails to correlate the spread of LP with the severity of either neuronal loss or clinical symptoms, and so does not accurately chart PD pathogenesis (Kalaitzakis *et al.* 2008c). In PD, bradykinesia and rigidity correlate with SNpc neuronal loss, but not with SNpc SNCA accumulation (Greffard *et al.* 2006; Greffard *et al.* 2010). Prospective and retrospective studies have shown that ~50-60% of PD brains follow the hierarchical LP pattern proposed by Braak (Halliday *et al.* 2008; Kalaitzakis *et al.* 2008b). Moreover, it was found that amongst 226 SNCA-positive subjects selected regardless of clinical presentation, 83% demonstrated SNCA accumulation broadly compatible with the Braak scheme. However, 55% of individuals with widespread SNCA pathology (stage 5 or 6) lacked parkinsonism or dementia (Parkkinen *et al.* 2008). It has been proposed that transient SNCA oligomers, not LBs, are the toxic species in PD (see 1.1.2.2) (Volles and Lansbury, Jr. 2003). Furthermore, foetal mesencephalic neurons grafted into the striatum of PD patients can develop LBs, suggesting the possibility that the internal milieu of the recipient striatum might facilitate host-to-graft propagation of SNCA pathology (Li *et al.* 2008; Kordower *et al.* 2008), potentially via a prion-like mechanism of permissive templating (Hardy 2005). The recent demonstration that SNCA forms inclusion bodies in neuronal stem cells transplanted into the brains of mice overexpressing human *SNCA* supports this hypothesis (Desplats *et al.* 2009).

Taken together, these findings indicate that Braak staging only applies to a proportion of PD cases, and suggest that SNCA accumulation is probably one of several pathogenic factors that synergise to generate this disorder. Moreover, they also indicate that PD may in fact encompass several disease entities which have been brought together under the same clinical umbrella (see 1.1.1.4) (Lees 2009).

1.1.1.3. Parkinson's disease dementia: clinical overview

Cognitive impairment and dementia are common in PD. Estimates of point prevalence for the latter range from 24 to 31% (Aarsland *et al.* 2005b), and its near inevitability has been demonstrated in two prospective studies, with over 80% of patients developing dementia during the course of their illness (Buter *et al.* 2008; Hely *et al.* 2008). Other reports have shown that the risk of dementia amongst PD patients is approximately four to six times that of age-matched controls (Levy *et al.* 2002b; Aarsland *et al.* 2001a; Hobson and Meara 2004). Several longitudinal studies indicate that older age at baseline, more severe and protracted motor symptoms, akinetic-dominant PD, lower mini mental state examination (MMSE) score at baseline, the presence of hallucinations, and male gender are all risk factors that increase the incidence of dementia in PD (Aarsland *et al.* 2001a; Hughes *et al.* 2000; Levy *et al.* 2000; Aarsland *et al.* 2003a; Hobson and Meara 2004). Moreover, age at baseline and motor impairment act synergistically to increase the risk of this phenotype (Levy *et al.* 2002b). The literature is conflicted with regard to the effect of parkinsonian symptom age of onset, and evidence has been presented both supporting (Hely *et al.* 1995; Mahieux *et al.* 1998; Hobson and Meara 2004) and undermining (Aarsland *et al.* 2001a; Hughes *et al.* 2000; Aarsland *et al.* 2007) the assertion that this factor significantly influences the development of dementia in PD.

Cognitive impairment has been described in nondemented PD patients encompassing a variety of domains, including executive, memory, visuospatial, and language abilities. These deficits are often detected early in the disease course and symptom presentation is heterogeneous [reviewed in (Caballol *et al.* 2007; Goetz *et al.* 2008)]. Executive dysfunction has been demonstrated by impaired performance on tests assessing attentional set shifting (the Wisconsin Card Sorting Task [WCST]), cognitive sequencing (digit ordering tasks), and planning (the Tower of London [TOL] task) (Lees and Smith 1983; Cooper *et al.* 1991; Foltynie *et al.* 2004a). Note that the executive domain is associated with the frontal lobes and relies on several cognitive functions, including attention, working memory (WM), and visual

processing. It controls processes required for goal-directed and adaptive mental behaviour, such as the generation of new concepts, problem solving, organisation, and planning (Dubois and Pillon 1997; Emre 2003). Deficits in numerical, spatial, and verbal WM have been described (Cooper *et al.* 1991; Bradley *et al.* 1989; Owen *et al.* 1992; Cooper and Sagar 1993). Results of word learning and recall trials have demonstrated that early stage PD patients also display impairments in declarative memory with relatively preserved recognition, suggesting that the disability is one of encoding or retrieval but not storage (Taylor *et al.* 1986; Sagar *et al.* 1991; Weintraub *et al.* 2004). Deficits in visuospatial (e.g. facial recognition and visuomotor construction) and language (e.g. verbal fluency) skills have both been reported (Levin *et al.* 1991; Auriacombe *et al.* 1993). Longitudinal studies demonstrate that dysfunction in several of these neuropsychological variables successfully predicts the subsequent development of dementia in PD. Examples include declarative memory impairment, executive dysfunction, deficits in verbal fluency, and visuospatial impairment. These correlations highlight the progression from cognitive dysfunction to full-blown dementia that is a common feature of PD pathogenesis (Hobson and Meara 2004; Levy *et al.* 2002a; Mahieux *et al.* 1998; Williams-Gray *et al.* 2007a).

Parkinson's disease dementia (PDD) has been defined as an insidious progressive dysexecutive-visuospatial syndrome accompanied by declarative memory, language, and behavioural symptoms which together impede daily life (Dubois and Pillon 1997; Goetz *et al.* 2008). These disabilities tend to be qualitatively similar to, but more severe than, those found in nondemented PD patients (Girotti *et al.* 1988). Moreover, symptom presentation is heterogeneous. One study indicates that while a "frontosubcortical" pattern of impairment (i.e. affecting executive abilities) is found in over half of PDD cases, almost a third display the "cortical" pattern (i.e. affecting declarative memory) typically associated with Alzheimer's disease (AD) (Janvin *et al.* 2006). PDD has even been described as cortical dysfunction superimposed on frontosubcortical impairment (Pagonabarraga *et al.* 2008). Executive dysfunction is the core neuropsychological feature of PDD (Emre 2003). Deficits in attention and conceptualisation have been observed when comparing to both controls and AD

patients matched for dementia severity (Litvan *et al.* 1991; Noe *et al.* 2004). Although classically associated with DLB (see 1.1.1.5), fluctuating attention is found in almost one third of PDD cases (Ballard *et al.* 2002). Furthermore, impairments in numerical and verbal WM tasks are seen in this disorder when contrasted against controls and dementia-matched AD patients, respectively (Litvan *et al.* 1991; Bohnen *et al.* 2006; Jefferson *et al.* 2002). Marked visuospatial deficits have been described. Compared to nondemented PD and controls, PDD patients are impaired with regard to visuospatial orientation and reasoning, respectively (Girotti *et al.* 1988; Huber *et al.* 1989). Moreover, one publication demonstrated visuoperceptive deficits in PDD when contrasted against either nondemented PD or controls (Mosimann *et al.* 2004).

Impairments in declarative memory have been identified, yet these tend to be less severe than those found in AD. Verbal free recall trials demonstrate that episodic and semantic memory are both deficient in PDD patients compared to controls, but not to the extent observed in dementia-matched AD patients (Helkala *et al.* 1989; Litvan *et al.* 1991; Noe *et al.* 2004). Subsequent semantic cueing dramatically enhances recall, indicating that storage is intact but retrieval is impaired. Moreover, memory scores significantly correlate with executive abilities in PDD patients, suggesting that frontal dysfunction underlies the defective activation of memory processes (Pillon *et al.* 1993). Language deficits have been reported. Verbal fluency, the most commonly affected ability, is impaired in PDD patients compared to nondemented PD patients, AD patients, and controls (Girotti *et al.* 1988; Huber *et al.* 1989). Behavioural and neuropsychiatric symptoms are frequently found in PDD, and include psychosis e.g. hallucinations (both visual and auditory) and delusions, and mood disturbances e.g. depression, anxiety, and apathy (Aarsland *et al.* 2001b; Aarsland *et al.* 2001c).

Collectively, these results indicate that cognitive impairment and dementia are relatively common in PD, and are characterised by similar neuropsychological symptoms. These symptoms tend to predict progression from one to the other, and are generally more severe in demented compared to nondemented PD patients. Furthermore, PDD is viewed primarily as a dysexecutive-visuospatial syndrome.

1.1.1.4. Parkinson's disease dementia: neurochemistry and neuropathology

Efforts to elucidate the mechanistic principles underlying PDD have employed a variety of approaches drawing on several neuroscientific disciplines. The findings can be broadly subdivided into two areas: neurochemistry and neuropathology. The data generated in each area are not mutually exclusive and there is crossover between them, but unification into an overarching scheme that fully explains PDD aetiopathogenesis remains elusive. This pathophysiological heterogeneity reflects the clinical heterogeneity (see 1.1.1.3). Indeed, attempts to correlate neurochemical and neuropathological states with cognitive symptoms have been relatively successful.

Several lines of evidence suggest that DA deficiency might underlie cognitive impairment in PD. Exposure to 1-methyl-4-phenyl-1,2,3,6-tetrahydropyridine (MPTP) causes selective dopaminergic cell death and parkinsonism in humans, and impaired executive and visuospatial abilities have been described in these individuals (Stern *et al.* 1990). In nondemented PD patients, WM is significantly inhibited and enhanced by levodopa withdrawal and treatment, respectively (Lange *et al.* 1992; Lewis *et al.* 2005). Interestingly, positron emission tomography (PET) analysis of brain perfusion suggests that this levodopa effect could be mediated by altered cerebral blood flow (CBF) in the dorsolateral prefrontal cortex (DLPFC) (Cools *et al.* 2002). This is consistent with PET experiments quantifying 6-[^{18}F]fluoro-levodopa uptake showing that verbal fluency and WM abilities positively correlate with DA synthesis in the PD frontal cortex (FC) (Rinne *et al.* 2000). However, excessive cortical DA can inhibit executive ability in PD, consistent with the "inverted U" relationship between DA signaling and PFC function (see 1.1.2.8) (Cools 2006).

The relevance of DA signaling to PD dementia is less clear. *Post mortem* findings demonstrate that VTA neuronal loss significantly associates with dementia in PD (Zweig *et al.* 1993). This dopaminergic nucleus projects to the PFC via the mesocortical circuit (Van den Heuvel and Pasterkamp 2008). Moreover, neuronal

loss in the medial SNpc significantly correlates with dementia severity in this condition (Rinne *et al.* 1989). The medial SNpc innervates the caudate, which itself receives input from the DLPFC as part of the "dorsolateral prefrontal loop", believed to be important for the manipulation of information in WM [reviewed in (Alexander *et al.* 1986; Owen 2004)]. Single photon emission computerised tomography (SPECT) analysis indicates that dopamine transporter (DAT) activities in the caudate and putamen are both significantly lower in PDD patients compared to nondemented PD or controls (O'Brien *et al.* 2004). However, levodopa use does not predict dementia incidence in this condition (Levy *et al.* 2000), and three months of chronic levodopa treatment does not significantly improve WM ability or MMSE score in PDD patients (Molloy *et al.* 2006). Furthermore, PET data indicate no differences in striatal or cortical DA synthesis between demented and nondemented PD (Hilker *et al.* 2005). These findings suggest that impaired DA signaling resulting from cell death in the ventral mesencephalon fails to account for all aspects of PDD cognitive impairment, but may be involved in the dysexecutive syndrome.

The role of acetylcholine (ACh) in PDD cognitive dysfunction is less controversial. Significantly greater neuronal loss in the NbM and significantly lower frontal, entorhinal, temporal, and parietal choline acetyltransferase (ChAT) activities are observed in demented PD patients when contrasted against their nondemented counterparts *post mortem* (Whitehouse *et al.* 1983; Perry *et al.* 1985). PET studies comparing these two groups have found significantly reduced acetylcholinesterase (AChE) activity in the PDD inferior parietal and temporal cortices, premotor cortex, and posterior cingulate cortex (PCC) (Hilker *et al.* 2005; Shimada *et al.* 2009). These findings are generally consistent with SPECT CBF analyses demonstrating hypoperfusion in the PDD inferior parietal cortex, precuneus, and PCC (Firbank *et al.* 2003; Osaki *et al.* 2009). Moreover, cortical AChE activity significantly correlates with WM ability and MMSE score in combined groups of PD patients with and without dementia (Bohnen *et al.* 2006; Shimada *et al.* 2009), and clinical trials demonstrate that AChE inhibitors modestly but significantly improve cognitive symptoms in PDD, including WM and attention deficits (Emre *et al.* 2004; Ravina *et*

al. 2005). Taken together, these results support the hypothesis that NbM neuronal death resulting in cortical cholinergic denervation could account for executive, memory, visuospatial, and attentional dysfunction in PDD.

Similar research has examined the role of noradrenergic and serotonergic signaling. LC noradrenalin levels and neuronal counts are lower in demented compared to nondemented PD patients *post mortem* (Cash *et al.* 1987; Zweig *et al.* 1993), and cerebrospinal fluid levels of a noradrenalin metabolite significantly correlate with attention in this disorder (Stern *et al.* 1984). Furthermore, when PDD patients are grouped by depression status, significantly greater levels of RN cell death and temporal cortex inhibitory serotonin receptor expression are observed *post mortem* in those that experienced depressive behaviour during the course of their illness (Paulus and Jellinger 1991; Sharp *et al.* 2008). These data suggest that in PDD, loss of LC noradrenergic cells and RN serotonergic neurons might underlie attentional impairment and depression, respectively. Collectively, the neurochemical studies detailed above have resulted in the hypothesis that deficits in each of these neurotransmitters contributes to various aspects of PDD, and that their relative influences partially explains the heterogeneity of cognitive and behavioural symptoms. The contention is that DA is to some extent responsible for executive dysfunction, ACh is involved in executive, memory, attentional, and visuospatial impairment, noradrenalin contributes to attentional dysfunction, and serotonin plays a role in depression [reviewed in (Emre 2003)].

Neuropathological correlates of PDD have been investigated using magnetic resonance imaging (MRI) to quantify gross cortical grey matter atrophy. These studies indicate significantly greater atrophy in the PFC, ACC, superior temporal gyrus, occipital cortex, caudate, thalamus, and hippocampus of demented PD compared to nondemented PD patients (Burton *et al.* 2004; Nagano-Saito *et al.* 2005). At the cellular level, PDD neuropathology is characterised by Lewy pathology, and many *post mortem* clinicopathological studies have examined LB loads in relation to dementia severity (see below). However, coexistent Alzheimer

pathology is frequently detected *post mortem*, albeit at levels below the diagnostic threshold for AD (see below). This pathological class is characterised by β-amyloid-positive neuritic plaques (NPs) and Microtubule-associated protein tau (MAPT)-positive neurofibrillary tangles (NFTs). There has been considerable debate about the nature of the primary pathogenic substrate driving dementia in PD, and disagreement over the relative importance of cortical or subcortical regions.

Several reports have concluded that cortical and/or limbic LBs constitute the primary pathological mechanism underlying PDD. Significantly higher LB counts, but not NFT and NP densities, have been observed in the neocortex and limbic cortex of demented compared to nondemented PD patients (Apaydin *et al.* 2002). Moreover, LB load in several cortical regions significantly correlates with the degree of cognitive impairment, and this is more pronounced after removing cases fulfilling the pathological criteria for AD. Regression analyses in these studies demonstrated that cognitive dysfunction is significantly predicted by LB density in the frontal gyrus, entorhinal cortex (EC), and ACC, but not by the severity of Alzheimer pathology in any region (Mattila *et al.* 2000; Kovari *et al.* 2003). These retrospective data are supported by prospective findings showing that LB counts and Braak stage correlate with MMSE in this condition, whereas AD pathological stage does not (Aarsland *et al.* 2005a; Braak *et al.* 2005). However, some investigators have argued against placing LBs at the forefront of PDD pathogenesis. Indeed, at least two groups have indentified subsets of patients that lack dementia despite extensive neocortical and/or limbic LB infiltration (Colosimo *et al.* 2003; Parkkinen *et al.* 2008).

There is evidence indicating that cortical Alzheimer pathology is the main substrate driving PDD. Overall cortical AD pathological staging has been significantly correlated with MMSE score in prospectively-studied PD (Bancher *et al.* 1993). PD dementia severity significantly correlates with levels of hyperphosphorylated MAPT protein in the prefrontal, entorhinal, and temporal cortices (Vermersch *et al.* 1993). Furthermore, another retrospective report examined the cortices of 200 PD patients and found that of those with Lewy pathology but lacking Alzheimer pathology, only

3% had been demented (Jellinger *et al.* 2002). Recent studies have called this hypothesis into doubt. PET analysis showed that cortical β-amyloid load is unaltered in demented contrasted against nondemented PD (Edison *et al.* 2008). Moreover, no difference in MMSE score is seen when prospectively comparing PDD patients with and without concomitant cortical Alzheimer pathology (Sabbagh *et al.* 2009).

Despite the undoubted conflict over these two interpretations of the primary mechanism underlying PDD pathogenesis, there is evidence to suggest that this dichotomy can be transcended. Several studies demonstrate that in PD with and without dementia, levels of Lewy and Alzheimer pathology significantly and positively intercorrelate in a variety of cortical regions, notably the ACC (Apaydin *et al.* 2002; Mattila *et al.* 2000; Pletnikova *et al.* 2005; Lashley *et al.* 2008). Furthermore, mice transgenic for human *SNCA* and *Amyloid precursor protein* (*APP*) possess more SNCA-reactive neuronal inclusions and learning deficiencies than those transgenic for *SNCA* alone (Masliah *et al.* 2001). These results suggest that β-amyloid and SNCA can synergise to promote dementia progression in PD. This interpretation is consistent with a recent prospective study which found that the LBD course is heterogeneous and divided patients into three clinicopathological phenotypes. All individuals that qualified for an end stage diagnosis of PDD were found to have both cortical/limbic LBs and NPs *post mortem* (Halliday *et al.* 2008).

The third hypothesis proposes that subcortical pathology is the main correlate of PDD. Early studies demonstrated that neuronal loss in the medial SNpc, VTA, NbM, and LC significantly associates with dementia in PD (Rinne *et al.* 1989; Whitehouse *et al.* 1983; Zweig *et al.* 1993). In addition, demented PD patients have significantly more striatal deposition of β-amyloid than their nondemented counterparts, with no difference observed for SNCA or MAPT (Kalaitzakis *et al.* 2008a). However, the focus of this theory has shifted to subcortical and cortical components of the limbic system. In the ACC, amygdala, and claustrum, both SNCA and β-amyloid pathologies significantly associate with dementia and/or cognitive impairment in PD patients (Apaydin *et al.* 2002; Mattila *et al.* 2000; Kalaitzakis *et al.* 2009a;

Kalaitzakis *et al.* 2009b). This relationship also holds true for SNCA and MAPT pathologies in the hippocampus (Apaydin *et al.* 2002; Mattila *et al.* 2000; Kalaitzakis *et al.* 2009a; Churchyard and Lees 1997).

The pathophysiology of PDD is not fully understood. Studies have successfully identified neurochemical, cellular, and anatomical correlates for this disorder, including dysregulated neurotransmission, protein aggregation, and neuronal loss in subcortical, limbic, and cortical regions. Some of these are found to a lesser extent in nondemented PD, highlighting the clinicopathological overlap between these two conditions, and suggesting that PDD can be viewed as one extreme on a spectrum of LBD pathogenesis. There is some conflict in the literature regarding the exact nature and location(s) of the cellular lesion(s) that drive(s) dementia in PD. Nevertheless, the growing appreciation of PDD as a multisystem and heterogeneous illness will probably reconcile these differences. The eventual outcome is likely to be an individualistic approach, whereby the clinical course of each patient is explained in terms of specific combinations of anatomopathological changes.

1.1.1.5. Dementia with Lewy bodies: clinical and neuropathological overview

Lewy body dementias are subdivided into two conditions: PDD and DLB. Clinicians employ the "one year rule" to distinguish between these nosological entities. This states that a diagnosis of DLB is made if dementia is recognised either before or less than one year after the onset of parkinsonism. Otherwise, the patient is classified as having PDD. In clinical and neuropathological terms, PDD and DLB are very similar, yet subtle differences do exist [reviewed in (McKeith *et al.* 2005)]. What follows is a brief overview of DLB, highlighting some of these disparities.

Dementia with Lewy bodies shares numerous clinical features with PDD, including an insidious onset and a generally idiopathic aetiology. However, parkinsonism

seems to be less severe and more symmetrical in DLB compared to PDD (Burn *et al.* 2003). The type of dementia observed in DLB tends to be very comparable with that found in PDD, in that most cases are characterised by a dysexecutive-visuospatial syndrome with fluctuating attention and relatively intact memory capabilities, and that similar levels of cognitive heterogeneity (i.e. deviation from this pattern of frontosubcortical impairment) are observed (Ballard *et al.* 2002; Janvin *et al.* 2006). However when compared to PDD, DLB patients are impaired in executive abilities, such as attention, verbal fluency, and conceptualisation (Downes *et al.* 1998; Aarsland *et al.* 2003b). Moreover, hallucinations and delusions are significantly more frequent in DLB than in PDD (Aarsland *et al.* 2001b).

There is much neuropathological overlap between DLB and PDD, in that both diseases are characterised by Lewy and Alzheimer pathology *post mortem*. In many cortical areas, LB densities are similar in PDD and DLB. However in the temporal cortex, significantly more LBs are found in DLB compared to PDD (Harding and Halliday 2001; Harding *et al.* 2002). Moreover, LB loads in this region significantly correlate with visual hallucinations early in the DLB disease course. Much greater cortical Alzheimer pathology is seen in DLB compared to PDD (Harding *et al.* 2002). The coexistence of Alzheimer and Lewy pathologies significantly associates with memory impairment and cognitive decline in DLB (Kraybill *et al.* 2005). Striatal SNCA pathology is thought to be greater in DLB than in PDD, whereas the reverse is true for SN neuronal loss (Duda *et al.* 2002a; Tsuboi and Dickson 2005).

So many similarities exist between PDD and DLB that it has been proposed they represent different extremes on a spectrum of LBD (Aarsland *et al.* 2004). Indeed, this assertion is supported by a study demonstrating that the duration of parkinsonism prior to dementia in both PDD and DLB correlates with the severity of Lewy and Alzheimer pathology i.e. the one year rule might not distinguish meaningful biological entities (Ballard *et al.* 2006). However, close examination reveals subtle differences, which suggest that the two disorders could be driven by overlapping but distinct biological processes operating within the context of this disease spectrum.

1.1.2. Molecular genetics and pathogenesis of Parkinson's disease with and without dementia

1.1.2.1. Introduction

Familial parkinsonism has been reported in the literature for over a century, yet research into the aetiology of PD historically focused on environmental factors and played down the influence of genetics. This was because of strong epidemiological evidence linking it to neurotoxic compounds and viruses, implying that familial clustering was due to shared environmental exposure (see 1.1.2.10). Underpowered twin studies in the 1980s which indicated similar concordance rates in monozygotic and dizygotic twins further strengthened this conclusion [reviewed in (Nussbaum and Polymeropoulos 1997)].

In the last decade, it has emerged that genetic factors play a critical role in the aetiology of this disorder. Linkage and sequencing analyses have identified numerous pathogenic coding mutations that cause FPD, together accounting for 5-10% of all PD. Such studies have been vital in elucidating the pathways that regulate PD pathophysiology, not only in these monogenic forms but also the majority of cases, which are termed IPD [reviewed in (Lesage and Brice 2009)]. The exact cause(s) of IPD is/are still unknown, but it is believed to arise due to the complex interaction of genetic, epigenetic, and environmental factors. Genetic association studies have been employed to uncover alleles that alter IPD susceptibility, but insufficient statistical power has hampered replication in many instances [reviewed in (Lesage and Brice 2009)]. However, large carefully-designed experiments are beginning to identify genetic variants that unequivocally influence IPD aetiopathogenesis (Maraganore *et al.* 2006; Healy *et al.* 2008; Satake *et al.* 2009; Simon-Sanchez *et al.* 2009).

There is considerable overlap between the various forms of FPD and IPD, both in terms of clinical manifestation and the underlying neuropathology [reviewed in

(Schiesling *et al.* 2008)]. This commonality extends to the genetic level. Polymorphisms residing in and around some of the FPD-causing genes demonstrate association with IPD (Healy *et al.* 2008; Kay *et al.* 2008; Simon-Sanchez *et al.* 2009). Furthermore, microarray studies indicate that the majority of known familial genes are differentially-expressed in the IPD SN (Moran *et al.* 2007; Simunovic *et al.* 2009). It is believed that regulatory variants significantly alter susceptibility to complex disease via their effect on gene expression (see 1.2) [reviewed in (Buckland 2004)]. Estimates suggest that single nucleotide polymorphisms (SNPs) might influence the expression of ~20% of cortical transcripts (Myers *et al.* 2007a), so it is interesting that some of the most compelling IPD-associated variants have regulatory ability or reside in noncoding regions (Chiba-Falek and Nussbaum 2001; Maraganore *et al.* 2006; Satake *et al.* 2009).

Investigation into the molecular pathophysiology of Lewy body dementia is still in its infancy. Due to their prominent role in Lewy body disease pathogenesis, most studies have concentrated on the synucleins. Examples include genetic alterations that result in familial forms of PDD and DLB, and transgenic mice that model their phenotypes *in vivo* (Ross *et al.* 2008a; Ohtake *et al.* 2004; Freichel *et al.* 2007; Fujita *et al.* 2009). However, inherent limitations in these model systems can complicate interpretation and undermine the relevance to cognitive dysfunction in humans. Tentative association with idiopathic Parkinson's disease dementia (IPDD) has been shown for a handful of genetic variants [for example (Williams-Gray *et al.* 2009a; de Lau *et al.* 2005)], but these findings are still controversial [for example (Ezquerra *et al.* 2008; Kurz *et al.* 2009)]. Moreover, expression microarray analysis has identified genetic pathways that demonstrate dysregulation in IPDD (see 4.1), yet these findings await confirmation (Stamper *et al.* 2008). In summary, our understanding of the molecular processes which generate the emergent property we recognise as dementia is still patchy at best.

Given the focus of this thesis, the aim of section 1.1.2 is not to summarise all molecular aspects of PD, but to concentrate on what is known about the molecular

genetics and pathogenesis of PDD and DLB, with particular emphasis on gene expression. As such, those genes relevant to familial and idiopathic Lewy body disease accompanied by a significant degree of dementia and/or cognitive impairment will be discussed first. Genes underlying FPD without cognitive dysfunction will then be considered, followed by the role played by environmental factors.

1.1.2.2. *α-Synuclein* (*PARK1* and *PARK4*)

α-Synuclein (*SNCA*) was the first gene demonstrated to cause familial PD, and it remains an important focus of research into FPD and IPD. Three rare heterozygous missense mutations have been described in *SNCA*: Ala53Thr, Ala30Pro, and Glu46Lys. These all result in a heterogeneous clinical phenotype of variably penetrant autosomal dominant parkinsonism that tends to be early onset (21-40 years), and diagnoses include PD, PDD, and DLB (*PARK1*). A spectrum of cognitive impairment, dementia, and hallucinations is observed in the majority of these individuals, notably the Spanish Glu46Lys kindred who were diagnosed with DLB based on neuropathological criteria (Polymeropoulos *et al.* 1997; Kruger *et al.* 1998; Kruger *et al.* 2001; Zarranz *et al.* 2004). Extensive LP is found in all of the Ala53Thr and Glu46Lys patients, although this exists primarily as LNs and perikaryal inclusions in the former, and LBs and LNs in the latter. Critically, SNCA protein is a major component of LBs and LNs found in IPD, DLB, and the aforementioned familial cases (Spillantini *et al.* 1997; Spillantini *et al.* 1998a; Duda *et al.* 2002b; Yamaguchi *et al.* 2005; Zarranz *et al.* 2004). Taken together, these findings indicate that *SNCA* plays a central role in both familial and idiopathic LBD pathogenesis, and suggest that its mutation tends to precipitate cognitive dysfunction.

Rare multiplications of *SNCA* are also known to cause early onset autosomal dominant parkinsonism with concomitant spectra of cognitive dysfunction and LBD diagnosis (*PARK4*). Several duplication and triplication families have been identified, and one prevailing theme is that patients possessing more copies of *SNCA*

are at increased risk of cognitive impairment, dementia, and hallucinations, and tend to present these symptoms and parkinsonism at an earlier stage (Chartier-Harlin *et al.* 2004; Ibanez *et al.* 2004; Nishioka *et al.* 2006; Singleton *et al.* 2003; Farrer *et al.* 2004). This effect is highlighted by two kindreds where intrafamily variation in the cognitive phenotype clearly correlates with the degree of *SNCA* ploidy (Fuchs *et al.* 2007; Ikeuchi *et al.* 2008). Moreover, FC *SNCA* expression is increased in triplication patients compared to controls (Farrer *et al.* 2004; Miller *et al.* 2004). Interestingly, sparse data suggest that *SNCA* triplication cases exhibit more cortical LBs than their duplication counterparts [reviewed in (Ross *et al.* 2008a)]. These results imply that increased *SNCA* copy number causes parkinsonism and cognitive dysfunction by directly affecting the expression of this gene.

α-Synuclein genetic variation has been shown to significantly alter IPD risk in Caucasians and Asians. Key polymorphisms include the upstream promoter microsatellite Rep1; SNPs residing in the 5' promoter, the large ~93 kb intron, the 3' untranslated region (UTR), the 3' flanking region; and haplotypes constructed thereof (see 5.1) (Maraganore *et al.* 2006; Kay *et al.* 2008; Mueller *et al.* 2005; Mizuta *et al.* 2006; Sutherland *et al.* 2009a; Pals *et al.* 2004; Tan *et al.* 2004; Farrer *et al.* 2001; Simon-Sanchez *et al.* 2009; Satake *et al.* 2009). Interestingly, common variation at Rep1 and five 5' promoter SNPs does not associate with dementia status in Caucasian IPD patients, but the relatively small size of this study may have generated a false negative (De Marco *et al.* 2008). *SNCA* multiplication seems incredibly rare in IPD, as three reports discovered only two examples of duplication in a combined total of 1431 cases (Johnson *et al.* 2004; Nishioka *et al.* 2006; Ahn *et al.* 2008). There is evidence to suggest that common variation at Rep1 and the 3' flanking SNP rs356219 might influence *SNCA* expression in the human brain (see 5.1) (Chiba-Falek and Nussbaum 2001; Fuchs *et al.* 2008). The literature is conflicted concerning *SNCA* expression in IPD. Some studies have observed increases in the SN of IPD patients (Chiba-Falek *et al.* 2006; Grundemann *et al.* 2008), whereas several others have detected reduced expression in this region (see 5.1) (Kingsbury *et al.* 2004; Zhang *et al.* 2005b; Dachsel *et al.* 2007; Moran *et al.* 2007; Simunovic *et al.* 2009).

Contradictory results are also seen in the IPD FC, but one report found that all four spliceforms display increased expression (Kingsbury *et al.* 2004; Zhang *et al.* 2005b; Chiba-Falek *et al.* 2006; Beyer *et al.* 2008). On the other hand, *SNCA* is alternatively-spliced in DLB, with underexpression observed for the full length (FL) isoform (Beyer *et al.* 2008). These data demonstrate that *SNCA* genetic variation influences IPD susceptibility, and suggest that it might affect *SNCA* expression in this disorder. However, variation in this gene appears not to associate with IPDD.

The function of *SNCA* is not fully understood. The full length 140 amino acid protein is expressed throughout the human brain and localises to the cytosol and presynaptic vesicles. In dopaminergic cells it regulates vesicular trafficking, DA release, and synaptic plasticity (Irizarry *et al.* 1996; Abeliovich *et al.* 2000; Murphy *et al.* 2000; Cooper *et al.* 2006). SNCA can aggregate into oligomers (or protofibrils) and fibrils *in vitro*, and this sequence of events is believed to precede LB and LN formation during LBD. The Ala53Thr and Ala30Pro mutations both promote its conversion into pore-like soluble oligomers *in vitro*, whereas only the former promotes its fibrillisation. Moreover, DA stabilises SNCA oligomers and inhibits fibril formation *in vitro* (Conway *et al.* 1998; Conway *et al.* 2000; Conway *et al.* 2001; Lashuel *et al.* 2002). Importantly, SNCA aggregates are detected in the brains of *SNCA* triplication patients (Miller *et al.* 2004). These findings suggest that SNCA oligomers might be the pathogenic species that mediate dopaminergic cell death in LBD, potentially by permeabilising presynaptic vesicles thereby releasing excess DA into the cytosol, resulting in oxidative stress (see below). The recent discovery that SNCA oligomers concentrate at presynaptic terminals in the FC of DLB patients supports this hypothesis and implicates these species in dementia pathophysiology (Kramer and Schulz-Schaeffer 2007; Paleologou *et al.* 2009). SNCA is phosphorylated at Ser129 and this species forms part of LBs and LNs in LBD brains, yet its pathogenic relevance is unclear (Fujiwara *et al.* 2002; Anderson *et al.* 2006). Ser129 phosphorylation correlates with SNCA oligomerisation and enhanced neuronal toxicity in *Drosophila melanogaster* and mice overexpressing human *SNCA* (see below) (Chen and Feany 2005; Chen *et al.* 2009; Ihara *et al.* 2007). In rats however,

SN injection with virus encoding a nonphosphorylateable human *SNCA* mutant either promotes cell death or is as efficient as the wild type (WT) (Gorbatyuk *et al.* 2008; Azeredo da Silveira *et al.* 2009; McFarland *et al.* 2009). Nonetheless, these results are consistent with the notion of SNCA oligomers as the key pathogenic species driving LBD.

The function of *SNCA* has been studied *in vivo* using several model organisms, such as *Caenorhabditis elegans*, *Drosophila*, mice, and marmosets, successfully recapitulating some of the molecular pathophysiology fundamental to LBD. Overexpression of WT or Ala53Thr human *SNCA* in these systems elicits some of the phenotypes which characterise PD, including loss of dopaminergic cells (Ala53Thr only) or terminals, SNCA-positive neuronal inclusions, and motor dysfunction (Lakso *et al.* 2003; Feany and Bender 2000; Masliah *et al.* 2000; Giasson *et al.* 2002; Eslamboli *et al.* 2007). Interestingly, aged mice transgenic for WT, Ala30Pro, or Tyr39Cys human *SNCA* exhibit significant spatial memory impairment (Freichel *et al.* 2007; Nuber *et al.* 2008; Zhou *et al.* 2008).

SNpc ubiquitin-proteasome system (UPS) activity and 20S α subunit levels are significantly reduced in IPD (McNaught *et al.* 2003). Decreased 20S α subunit expression is also seen in the DLB ACC, and its levels significantly correlate with MMSE score in these patients (MacInnes *et al.* 2008). UPS inhibition and reduction of 19S subunits are observed in the midbrain and striatum of aged mice transgenic for doubly mutant (Ala53Thr and Ala30Pro) human *SNCA* (Chen *et al.* 2006). The chaperone-mediated autophagy (CMA) pathway is significantly inhibited in nigral and striatal IPD neurons (Chu *et al.* 2009; Yang *et al.* 2009). Neuronal cell models show that CMA degrades WT SNCA, but not the Ala53Thr or Ala30Pro mutants or DA-modified WT, which actually impair this system for other substrates (Cuervo *et al.* 2004; Martinez-Vicente *et al.* 2008). Importantly, mice transgenic for human WT *SNCA* demonstrate neuronal autophagy dysfunction, but limbic injection with virus encoding the proautophagic gene *Beclin1* ameliorates this phenotype and significantly reduces SNCA immunoreactivity (Spencer *et al.* 2009).

In the IPD SN, mitochondrial complex I activity is reduced, and oxidative damage to lipids and proteins is increased (Schapira *et al.* 1989; Dexter *et al.* 1989; Alam *et al.* 1997). DA stabilises SNCA oligomers *in vitro*, and transfection of dopaminergic cells with *SNCA* induces apoptosis dependent on endogenous DA synthesis (Conway *et al.* 2001; Xu *et al.* 2002). *Snca*-null mice are resistant to dopaminergic cell death after treatment with the oxidative mitochondrial toxin MPTP (see 1.1.2.10) (Dauer *et al.* 2002). Furthermore, aged mice transgenic for human Ala53Thr *SNCA* develop neuronal mitochondrial abnormalities and degeneration (Martin *et al.* 2006). Collectively, these findings demonstrate that impaired protein degradation, oxidative stress, and mitochondrial dysfunction are central facets of LBD pathophysiology, and suggest that they could be involved in the tendency of overexpressed *SNCA* to promote cognitive deficiency in these disorders.

1.1.2.3. *β-Synuclein*

β-Synuclein (*SNCB*) belongs to the same genetic family as *SNCA* (Lavedan 1998). Two rare heterozygous missense *SNCB* mutations, Val70Met and Pro123His, have been described in unrelated DLB patients. Val70Met was found in a seemingly idiopathic case, whereas the Pro123His proband belonged to a DLB kindred (Ohtake *et al.* 2004). Further investigation revealed that the Pro123His clinical phenotype is late onset (> 40 years) dementia and parkinsonism inherited in an autosomal dominant fashion with incomplete penetrance. Its neuropathological phenotype is extensive Lewy and Alzheimer pathology, with high LB levels in the hippocampus and the amygdala. Notably, no SNCB-positive inclusions are observed (see below), but diffuse soluble SNCB immunoreactivity is detected (Ohtake *et al.* 2004).

Two studies have examined variation at a total of four common *SNCB* SNPs for genetic association with IPD, and none were found to influence overall susceptibility in Caucasians. However, variation at the common upstream polymorphism rs1352303 associates with age of onset in females only (Fung *et al.* 2006; Brighina *et*

al. 2007). *SNCB* is significantly underexpressed in the SN and temporal cortex of DLB patients, as well as in the DLPFC [Brodmann area 9 (BA9)] of IPD patients (Rockenstein *et al.* 2001; Zhang *et al.* 2005b). It seems to be unaltered in the IPD SN (Zhang *et al.* 2005b; Moran *et al.* 2006). SNCB is not a component of IPD or DLB LBs (Spillantini *et al.* 1997; Spillantini *et al.* 1998a), however in both diseases, SNCB aggregates are detected within accumulated vesicles localised to degenerating hippocampal axons (Galvin *et al.* 1999).

β-Synuclein is expressed in the cortex, SN, caudate, hippocampus, amygdala, and thalamus, and its encoded protein predominately associates with presynaptic vesicles (Lavedan 1998). SNCB can oligomerise, but these species do not bind and permeabilise synthetic vesicles *in vitro*. SNCB inhibits the oligomerisation and fibrillisation of WT and Ala53Thr *SNCA in vitro*, as well as binding WT *SNCA in vivo* and ameliorating its aggregation in cell models (Park and Lansbury, Jr. 2003; Hashimoto *et al.* 2001). Moreover, overexpression of human *SNCB* in aged mice transgenic for human WT and Ala53Thr *SNCA* significantly improves neuronal SNCA accumulation, loss of dopaminergic terminals (only WT transgenics were assessed), and motor dysfunction (Hashimoto *et al.* 2001; Fan *et al.* 2006). Interestingly, neuronal cells stably transfected with Val70Met or Pro123His *SNCB* develop lysosomal SNCB-positive inclusion bodies, resulting in significantly upregulated lysosomal activity. Treating these cells with autophagy inhibitors significantly reduces inclusion body formation and increases SNCB oligomerisation and apoptosis (Wei *et al.* 2007).

Taken together, these data demonstrate that *SNCB* mutations can cause DLB, and suggest that lysosomal dysfunction might underlie neurodegeneration in these cases. Furthermore, they indicate that *SNCB* might regulate *SNCA* aggregation under normal circumstances, and are consistent with the hypothesis that altered *SNCB* expression affects *SNCA* accumulation in idiopathic LBD. However, the paucity of reported human DLB cases with mutated *SNCB* and the failure to detect SNCB in LBs or LNs casts doubt on these conclusions.

1.1.2.4. *Leucine-rich repeat kinase 2* (*PARK8*)

Mutations in *Leucine-rich repeat kinase 2* (*LRRK2*) were first demonstrated to cause FPD in 2004 (Paisan-Ruiz *et al.* 2004; Zimprich *et al.* 2004). Since then, over 40 mutations have been described, most of which are missense. The few that are definitely pathogenic result in a fairly uniform clinical phenotype of late onset autosomal dominant parkinsonism with variable penetrance (Lesage and Brice 2009). Screening has discovered *LRRK2* mutation(s) in ~5% of IPD cases worldwide, making alteration of this gene the most common single risk factor for IPD (Santpere and Ferrer 2009). One global study of over 10 000 cases demonstrated that the Gly2019Ser mutation significantly increases IPD susceptibility in Caucasians (Healy *et al.* 2008). Cognitive impairment and/or dementia is/are observed in PD patients with mutated *LRRK2*, although at a reduced frequency when compared to PD in general. One report showed that 23% of 162 Gly2019Ser PD cases had evidence of cognitive impairment (Healy *et al.* 2008). These results are consistent with a smaller but more detailed neuropsychological study, which detected frontal lobe dysfunction in 35% of 24 Gly2019Ser PD patients (Goldwurm *et al.* 2006). The neuropathological phenotype of *LRRK2* mutation is quite heterogeneous. SN dopaminergic neuronal loss is seen in all PD cases, but LBs can be either present or absent [reviewed in (Santpere and Ferrer 2009)].

Two recent and well-powered genome wide association studies (GWAS) performed in Caucasians and Asians both identified several *LRRK2* SNPs that might influence IPD risk, although none of these survived the stringent Bonferroni threshold for multiple testing (Simon-Sanchez *et al.* 2009; Satake *et al.* 2009). *LRRK2* is significantly underexpressed in IPD SNpc neurons (Simunovic *et al.* 2009). However, neuronal LRRK2 can aggregate in enlarged granules or vacuoles that stain positive for endosomal markers, and these are more frequent in the SN and EC of IPD and DLB patients compared to controls (Higashi *et al.* 2009). The presence of LRRK2 in IPD and DLB LBs is controversial, potentially resulting from the use of several different antibodies [reviewed in (Santpere and Ferrer 2009)].

Leucine-rich repeat kinase 2 is expressed in neurons and glia, and can be detected in the SNpc, striatum, hippocampus, and cortex (Miklossy *et al.* 2006; Higashi *et al.* 2007; Galter *et al.* 2006). LRRK2 localises primarily to mitochondria, lysosomes, and endosomes (Biskup *et al.* 2006). *LRRK2* pathogenic mutations increase its kinase activity *in vitro*, and inactivation of its kinase domain inhibits the toxicity of mutant *LRRK2* in neuronal cell models (West *et al.* 2005; Smith *et al.* 2006b). Moreover, injecting the SNpc of rats with virus encoding the kinase domain of Gly2019Ser human *LRRK2* promotes MAPT-positive inclusion formation, neurite length reduction, and apoptosis in dopaminergic neurons (MacLeod *et al.* 2006). Interestingly, LRRK2 binds SNCA in the FC of DLB patients but not controls, and Gly2019Ser LRRK2 phosphorylates SNCA at Ser129 *in vitro* more effectively than the wild type (Qing *et al.* 2009b; Qing *et al.* 2009a).

Collectively, these results suggest that *LRRK2* sequence variation can cause and/or increase the risk of both PD and cognitive dysfunction therein, and are consistent with the hypothesis that enhanced LRRK2 kinase activity and its resultant effect on and MAPT and/or SNCA aggregation might be involved in these phenotypes.

1.1.2.5. *β-Glucocerebrosidase*

β-Glucocerebrosidase (*GBA*) encodes a lysosomal enzyme which catalyses the breakdown of glucocerebroside (also known as glucosylceramide) in neurons and macrophages. Homozygous *GBA* mutations cause the lipid storage disorder Gaucher's disease, and a small subgroup of these individuals develop parkinsonism [reviewed in (DePaolo *et al.* 2009)]. *GBA* mutations, notably Asn370Ser, are relatively common in Ashkenazi Jews, and early findings demonstrated that Asn370Ser carrier status significantly increases IPD risk in this population (Aharon-Peretz *et al.* 2004). Larger studies have confirmed that *GBA* mutation significantly increases IPD susceptibility in Ashkenazi Jews, non-Ashkenazi Caucasians, and

Asians, and indicate that Leu444Pro and Asn370Ser are the most frequent alterations in non-Ashkenazi cases (Neumann *et al.* 2009; Sidransky *et al.* 2009).

Cognitive impairment, dementia, and hallucinations are seen in IPD patients with *GBA* mutations (Aharon-Peretz *et al.* 2005; Goker-Alpan *et al.* 2008). One group observed cognitive dysfunction and/or dementia in 52% of 21 IPD cases with mutant *GBA* (Neumann *et al.* 2009). A much larger study reporting data for 1948 individuals found some evidence of cognitive change in 26% of mutated and 19% of nonmutated patients. This difference is significant and implies that cognitive impairment is more common in patients with *GBA* mutations than amongst IPD in general (Sidransky *et al.* 2009). Therefore, it is perhaps unsurprising that *GBA* mutation also significantly increases DLB risk (Goker-Alpan *et al.* 2006; Mata *et al.* 2008). IPD cases with *GBA* mutations display similar patterns of neuropathology as IPD in general, with SNCA-positive LP in subcortical and cortical regions, however there is a trend for higher levels of neocortical involvement (Neumann *et al.* 2009).

These results demonstrate that *GBA* mutations significantly enhance susceptibility to IPD, IPDD, and DLB. Moreover, they suggest that lysosomal dysfunction might play a role in cognitive impairment in these disorders.

1.1.2.6. *Microtubule-associated protein tau*

Microtubule-associated protein tau (*MAPT*) is primarily expressed in neurons where it stabilises microtubules by promoting their polymerisation. Pathological neuronal aggregates of hyperphosphorylated MAPT characterises a group of neurodegenerative disorders known as tauopathies, which includes AD, progressive supranuclear palsy (PSP), and frontotemporal dementia and parkinsonism linked to chromosome 17 (FTDP17) [reviewed in (Iqbal *et al.* 2009)]. Moreover, heterozygous missense (e.g. Pro301Leu) and splice site *MAPT* mutations have been identified in autosomal dominant FTDP17 patients (Hutton *et al.* 1998; Spillantini *et al.* 1998b).

Analysis of *MAPT* polymorphisms uncovered the existence of two major nonrecombining haplotype blocks in Caucasians, called H1 and H2, which originated from an ancestral inversion involving ~900 kb of chromosome 17 (Baker *et al.* 1999; Stefansson *et al.* 2005). Variation within the common H1 clade is significantly associated with idiopathic tauopathies, and further investigation has defined several subhaplotypes that appear to be largely driving these associations, notably H1c (Baker *et al.* 1999; Pastor *et al.* 2004; Pittman *et al.* 2005; Myers *et al.* 2005).

Meta-analysis of older studies shows that amongst Caucasians, *MAPT* H1/H1 homozygotes are significantly more susceptible to IPD, and several publications have replicated this finding (Healy *et al.* 2004b; Zabetian *et al.* 2007; Tobin *et al.* 2008; Vandrovcova *et al.* 2009). Well-powered GWAS analysis demonstrates that variation at three *MAPT* SNPs significantly associates with IPD in Caucasians, and these polymorphisms appear to be tagging the H1 haplotype (Simon-Sanchez *et al.* 2009). Furthermore, *MAPT* haplotype interacts synergistically with the *SNCA* SNP rs356219 to modify IPD risk in this population (Goris *et al.* 2007). There is debate regarding the influence of variation within common H1 subhaplotypes on IPD risk in Caucasians, and at least two reports do not observe association with H1c (Skipper *et al.* 2004; Tobin *et al.* 2008; Vandrovcova *et al.* 2009; Zabetian *et al.* 2007). Amongst Caucasians, *MAPT* H1/H1 homozygous IPD patients have significantly greater rates of cognitive decline, and multivariate analysis demonstrates an age/genotype interaction for this effect (Goris *et al.* 2007). Critically, a recent follow up study of the same longitudinal cohort showed that IPD dementia incidence is significantly higher in *MAPT* H1/H1 homozygotes, and found that the combination of this diplotype, older age, and impaired semantic fluency makes IPD patients 88-fold more likely to develop dementia (Williams-Gray *et al.* 2009a). On the other hand, cross-sectional data indicates that H1 homozygosity is not associated with IPDD (Ezquerra *et al.* 2008).

Microtubule-associated protein tau is expressed as six isoforms which are generated by alternative splicing. These transcripts differ by the presence of either three or four

microtubule-binding domains (3-repeat [3R] and 4-repeat [4R] isoforms) (Iqbal *et al.* 2009) The 4R:3R ratio is significantly increased in the IPD cerebellum, whereas total *MAPT* expression is significantly reduced in PCC neurons of demented compared with nondemented IPD or controls (Tobin *et al.* 2008; Stamper *et al.* 2008). Several groups have investigated the relative expression of *MAPT* H1 and H2 haplotypes in the human brain. In the DLPFC, H1:H2 transcript ratio is significantly increased in IPD patients but not controls, however only when 4R isoforms are specifically quantified (Williams-Gray *et al.* 2009a). This isoform-specific effect has also been shown for H1c:H2a transcript ratio in the frontal and temporal cortices of controls (Myers *et al.* 2007b). The demonstration by another report that H1c status does not influence total *MAPT* H1:H2 transcript ratio in controls is consistent with these results. This study also discovered that age significantly and negatively correlates with H1:H2 transcript ratio (Hayesmoore *et al.* 2009). MAPT can co-localise with SNCA in IPD and DLB LBs (Arima *et al.* 1999; Ishizawa *et al.* 2003). Moreover, MAPT and SNCA promote each other's aggregation *in vitro* and *in vivo* (Giasson *et al.* 2003). Interestingly, suppressing *MAPT* expression ameliorates neuronal loss and spatial memory impairment in mice transgenic for human Pro301Leu *MAPT* (Santacruz *et al.* 2005).

Taken together, these findings indicate that *MAPT* H1 homozygosity most likely enhances IPD susceptibility and progression to dementia, and suggest that these effects might be caused by alternative splicing resulting in increased production of MAPT 4R isoforms with greater ability to induce SNCA aggregation.

1.1.2.7. *Apolipoprotein E*

Apolipoprotein E (*APOE*) is expressed in glia throughout the brain, and it regulates lipid transport, synaptic plasticity, and neuronal repair. Variation at two common nonsynonymous SNPs differentiates three transcript isoforms, known as ε2, ε3, and ε4 [reviewed in (Bu 2009)]. The APOE ε4 allele significantly increases AD risk in Caucasian and Asian populations in a dose-dependent manner (Farrer *et al.* 1997), whereas amongst Caucasians, the ε2 allele is significantly overrepresented in IPD cases (Huang *et al.* 2004; Williams-Gray *et al.* 2009b).

The relationship between *APOE* genotype and IPDD is highly contentious. Meta-analyses indicate that the ε4 allele significantly associates with an increased prevalence of dementia amongst Caucasian IPD patients, however issues over sample sizes, publication bias, and ascertainment bias (diagnostic criteria with regard to PDD, DLB, and AD) have cast doubt on these results (Huang *et al.* 2006; Williams-Gray *et al.* 2009b). Nevertheless, longitudinal and *post mortem* cross-sectional studies corroborate the findings of these meta-analyses, although one observed an even stronger effect for the ε2 allele (de Lau *et al.* 2005; Papapetropoulos *et al.* 2007). On the other hand, several relatively well-powered cross-sectional studies employing good selection criteria indicate no association between the ε4 allele and the prevalence of IPD dementia in Caucasians (Blazquez *et al.* 2006; Jasinska-Myga *et al.* 2007; Ezquerra *et al.* 2008), and this conclusion is supported by longitudinal and *post mortem* cross-sectional data (Camicioli *et al.* 2005; Kurz *et al.* 2009; Williams-Gray *et al.* 2009b).

The *APOE* ε4 allele is significantly more expressed than either ε3 or ε2 in control brains (Bray *et al.* 2004). Moreover, ε4-positive IPD patients possess significantly higher cortical LB counts and levels of Alzheimer pathology (Mattila *et al.* 2000; Mattila *et al.* 1998; Lashley *et al.* 2008). Interestingly, mice transgenic for human Ala53Thr or Ala30Pro *SNCA* exhibit increased levels of endogenous Apoe and β-amyloid in their CNS. Deletion of *Apoe* in these mice reduces levels of SNCA

oligomers and β-amyloid aggregates, concomitant with delayed onset of motor symptoms and improved survival (Gallardo *et al.* 2008).

Collectively, these results indicate that the *APOE* ε4 allele might increase dementia incidence in IPD, although longitudinal studies with thousands of participants will probably be required to confirm or refute this. They also suggest that APOE may regulate SNCA and β-amyloid accumulation in LBD, potentially contributing to cognitive dysfunction in these disorders.

1.1.2.8. *Catechol-O-methyltransferase*

Catechol-O-methyltransferase (*COMT*) is predominately expressed in neurons and catalyses DA breakdown in the PFC but not in the caudate (Matsumoto *et al.* 2003; Yavich *et al.* 2007). Variation at the common nonsynonymous *COMT* SNP Val158Met influences this process. Compared to Val/Val homozygotes, Met/Met homozygotes have significantly lower levels of COMT protein and enzymatic activity in the DLPFC (Chen *et al.* 2004). Association between variation at this polymorphism and schizophrenia has been reported in Caucasian and Asian populations, although meta-analysis casts doubt on this (Egan *et al.* 2001; Ohmori *et al.* 1998; Munafo *et al.* 2005). Met/Met normal controls appear to score significantly better than their Val/Val counterparts on the WCST attentional set shifting task, but this is also a matter of debate (Barnett *et al.* 2007; Barnett *et al.* 2008).

Studies using the TOL task to assess planning ability in nondemented Caucasian IPD patients demonstrate that Met/Met homozygotes perform significantly worse than Val/Val homozygotes. Moreover, functional magnetic resonance imaging (fMRI) shows these Val/Val patients have significantly greater task-related activity increases in the DLPFC, the posterior parietal cortex, and the frontopolar region (Foltynie *et al.* 2004b; Williams-Gray *et al.* 2007b). Investigation of attentional set shifting aptitude in nondemented Caucasian IPD patients reveals similar effects, with significantly

stronger performance and frontoparietal activation in Val/Val homozygotes (Williams-Gray *et al.* 2008). These data can be interpreted in the context of the inverted U model which posits a complex nonlinear relationship between dopaminergic signaling and PFC function. Val/Val homozygotes with higher COMT activity cope better with the inhibitory hyperdopaminergic state characteristic of the PFC in early IPD, resulting in higher prefrontal-dependent task scores (Kaasinen *et al.* 2001; Williams-Gray *et al.* 2008).

Longitudinal examination of the same community-based incident cohort, the largest of its kind, shows that while Val/Val homozygotes score better in early IPD, the reverse is true for later disease. Given that prefrontal DA levels fall in late IPD, this is in keeping with the inverted U model (Williams-Gray *et al.* 2009a). Moreover, Val158Met genotype and prefrontal-dependent TOL ability do not predict dementia incidence in these individuals, whereas *MAPT* haplotype and temporal-dependent semantic fluency aptitude do (see 1.1.2.6). This recent and intriguing finding indicates a dissociation between frontosubcortical and temporal cognitive syndromes in IPD, and contrary to accepted wisdom, suggests a startling conclusion about this disorder: prefrontal executive dysfunction does not develop into dementia (Williams-Gray *et al.* 2009a).

These data demonstrate that *COMT* Val158Met genotype significantly influences executive ability in IPD patients, and that there is a complex nonlinear relationship between this cognitive domain and PFC DA levels in IPD. Furthermore, they suggest that the primary pathogenic substrate driving IPD dementia is more likely to be cortical rather than subcortical.

1.1.2.9. Genes causing familial Parkinson's disease without significant dementia

Juvenile (< 21 years) or early onset highly penetrant autosomal recessive FPD can be caused by missense, nonsense, exonic deletion, and exonic multiplication homozygous and compound heterozygous mutations in *Parkin* (*PARK2*). Cognitive impairment and dementia are almost unheard of in these individuals, although behavioural symptoms (e.g. psychosis and depression) have been described (Kitada *et al.* 1998; Lucking *et al.* 2000; Khan *et al.* 2003; Lohmann *et al.* 2009). All patients with mutant *PARK2* display SN neuronal loss, but the majority lack LBs (Pramstaller *et al.* 2005). Variation at the common *PARK2* promoter SNP -258 T/G significantly alters IPD risk in Caucasians and influences its expression in neuronal cell models but this association is disputed (West *et al.* 2002; Ross *et al.* 2007b). One relatively large study demonstrated that rare heterozygous *PARK2* mutations do not influence IPD susceptibility in Caucasians (Kay *et al.* 2007). *PARK2* is differentially-spliced in the IPD FC, and its protein product can be detected in IPD and DLB LBs (Beyer *et al.* 2008; Schlossmacher *et al.* 2002).

Parkin is an E3 ligase which adds ubiquitin molecules to substrates thereby targeting them for degradation by the UPS. In this regard, FPD-causing mutants are deficient *in vitro* (Shimura *et al.* 2000). *Park2*-null *Drosophila* mutants display muscle mitochondrial pathology, muscle degeneration, and motor defects (Greene *et al.* 2003). However, deleting *Park2* in mice does not cause SN neuronal loss. Instead, the result is a phenotypic spectrum including LC noradrenergic cell death, dysregulated nigrostriatal dopaminergic signaling, and reduction in neuronal electron transport chain (ETC) component expression, concomitant with decreased mitochondrial respiration and increased oxidative damage to lipids and proteins (von Coelln *et al.* 2004; Palacino *et al.* 2004). Interestingly, PARK2 can ubiquitinate glycosylated SNCA *in vitro* and *Park2* ameliorates human Ala30Pro *SNCA*-induced SN dopaminergic neuronal loss *in vivo* (Shimura *et al.* 2001; Lo Bianco *et al.* 2004).

The literature describes one rare missense mutation (Ile93Met) of *Ubiquitin carboxy-terminal hydrolase L1* (*UCHL1*) that is known to cause late onset autosomal dominant FPD with incomplete penetrance (*PARK5*). Only one kindred has been identified and these patients do not display cognitive dysfunction (Leroy *et al.* 1998). This lack of genetic evidence questions whether *UCHL1* should be classified as FPD-causing at all. There is also debate regarding the effect of common *UCHL1* genetic variation on IPD susceptibility. Some studies indicate that Ser18Tyr significantly reduces IPD risk in Caucasians and Asians (Maraganore *et al.* 2004a; Ragland *et al.* 2009), whereas others find no such association (Healy *et al.* 2006; Sutherland *et al.* 2009a). *UCHL1* is significantly underexpressed in the SN and FC of IPD and DLB cases (Zhang *et al.* 2005b; Moran *et al.* 2007; Barrachina *et al.* 2006). UCHL1 colocalises with SNCA in IPD LBs (Yasuda *et al.* 2009).

The protein product of *UCHL1* can free reusable ubiquitin monomers via its ubiquitin hydrolase activity, and the Ile93Met mutation inhibits this process *in vitro* (Leroy *et al.* 1998). Mice transgenic for human Ile93Met *UCHL1* develop neuronal inclusions, SN dopaminergic cell loss, and locomotor dysfunction (Setsuie *et al.* 2007). Overexpression of human *SNCA* enhances dopaminergic cell death in these mice, but not in those transgenic for human WT *UCHL1* (Yasuda *et al.* 2009). Moreover, Ile93Met, but not WT, *UCHL1* inhibits CMA and SNCA degradation in cell models (Kabuta *et al.* 2008).

Moderately frequent homozygous and compound heterozygous missense, nonsense, and frameshift mutations in *Phosphatase and tensin homologue-induced putative kinase 1* (*PINK1*) can cause early onset autosomal recessive FPD with variable penetrance (*PARK6*). Cognitive impairment is extremely infrequent in these cases (Valente *et al.* 2004; Rogaeva *et al.* 2004; Bonifati *et al.* 2005). However, executive dysfunction and/or dementia have been described in a handful of patients with *PINK1* exonic deletion and nonsense mutations. Nevertheless, *PINK1* mutation failed to segregate with this phenotype in one of two sib pairs (Li *et al.* 2005; Ephraty *et al.* 2007; Savettieri *et al.* 2008). Although the Ala340Thr polymorphism is significantly

overrepresented in Asian IPD patients, variation at common *PINK1* SNPs and haplotypes does not influence IPD susceptibility in Caucasians (Wang *et al.* 2006; Healy *et al.* 2004a; Sutherland *et al.* 2009a). Rare heterozygous *PINK1* mutations appear to marginally increase IPD risk in Caucasians but this is debated (Abou-Sleiman *et al.* 2006a; Marongiu *et al.* 2008). Data are conflicted in terms of *PINK1* expression in IPD dopaminergic SN neurons, with both no difference and significant reduction reported (Blackinton *et al.* 2007; Simunovic *et al.* 2009). PINK1 is detected in a subset of IPD LBs (Gandhi *et al.* 2006).

The protein product of *PINK1* is a putative Ser/Thr kinase that localises to the mitochondrial membrane and WT PINK1, but not FPD-causing mutants, protects neuronal cells against mitochondrial dysfunction and apoptosis induced by UPS inhibition (see 1.1.2.10) (Gandhi *et al.* 2006; Valente *et al.* 2004; Abou-Sleiman *et al.* 2006a). Aged *Drosophila Pink1* mutants exhibit dopaminergic cell death, muscle atrophy, and impaired locomotion resulting from mitochondrial dysfunction. These effects are similar to those observed in *Park2*-null flies, and expression of *Park2* can ameliorate the mutant *Pink1* phenotype but not vice-a-versa (Park *et al.* 2006; Clark *et al.* 2006). *Pink1*$^{-/-}$ mice display impaired synaptic plasticity, progressive reduction of spontaneous movement, and progressive neuronal mitochondrial pathology, concomitant with respiratory inhibition and enhanced sensitivity to oxidative stress. However, they do not develop SN dopaminergic cell loss (Kitada *et al.* 2007; Gautier *et al.* 2008; Gispert *et al.* 2009). Interestingly, ribonucleic acid interference (RNAi) directed against *PINK1* in differentiated human midbrain neurons results in lysosomal vesicular aggregation and enhanced cell death over the long term (Wood-Kaczmar *et al.* 2008). Moreover, these cells exhibit mitochondrial Calcium accumulation, which stimulates reactive oxygen species (ROS) production and respiratory impairment (Gandhi *et al.* 2009).

Early onset highly penetrant autosomal recessive FPD can be caused by rare missense and exonic deletion mutations in *Parkinson's disease 7* (*PARK7*) (also known as *DJ1*), but these patients do not develop cognitive dysfunction (Bonifati *et al.* 2003).

Variation at common *PARK7* SNPs and haplotypes does not significantly influence IPD susceptibility in Caucasians, however borderline associations have been observed for two polymorphisms in females only (Maraganore *et al.* 2004b; Sutherland *et al.* 2009a). *PARK7* is significantly underexpressed in the IPD putamen, cortex, and cerebellum. However, results in IPD SN dopaminergic neurons are contradictory, with both significant reduction and no difference reported (Kumaran *et al.* 2009; Simunovic *et al.* 2009; Galter *et al.* 2007). PARK7 is generally not found in IPD and DLB LBs, although it is detected in nigral, striatal, and cortical DLB NFTs (Bandopadhyay *et al.* 2004; Rizzu *et al.* 2004).

The protein encoded by *PARK7* localises to the mitochondrial matrix and intermembrane space and is involved in protecting neurons against oxidative stress (Zhang *et al.* 2005a; Canet-Aviles *et al.* 2004). RNAi knockdown of *Park7* in *Drosophila* causes dopaminergic cell death, elevated neuronal ROS accumulation, and hypersensitivity to hydrogen peroxide (H_2O_2)-induced oxidative stress (Yang *et al.* 2005). *Park7*-null *Drosophila* do not exhibit neuronal loss, but still display enhanced sensitivity to UPS inhibition and agents that promote oxidative stress, such as H_2O_2, paraquat, and rotenone (see 1.1.2.10) (Meulener *et al.* 2005). *Park7*$^{-/-}$ mice develop impaired synaptic plasticity and motor dysfunction, but do not suffer from neuronal loss (Goldberg *et al.* 2005; Chen *et al.* 2005). However, treating these animals with MPTP or paraquat elicits a range of phenotypes including striatal DA deficiency, SNpc dopaminergic cell death, and UPS inhibition (Kim *et al.* 2005; Yang *et al.* 2007).

Rare *Adenosine triphosphatase type 13A2* (*ATP13A2*) homozygous and compound heterozygous frameshift and splice site mutations can cause highly penetrant juvenile onset autosomal recessive Kufor-Rakeb syndrome (KRS) (*PARK9*), and heterozygous missense *ATP13A2* alterations have been detected in early and late onset autosomal recessive FPD cases. KRS is characterised by parkinsonism, dementia, and supranuclear gaze palsy (the inability to look in a particular direction), whereas some of the FPD patients in question experienced visual hallucinations but none were

demented (Ramirez *et al.* 2006; Di Fonzo A. *et al.* 2007; Lin *et al.* 2008). Variation at common *ATP13A2* SNPs and haplotypes does not significantly alter IPD risk in North Africans and Caucasians (Vilarino-Guell *et al.* 2009; Rakovic *et al.* 2009). Analysis of *ATP13A2* expression in IPD SN dopaminergic neurons has yielded conflicting results, with reports of significant increases and decreases (Ramirez *et al.* 2006; Simunovic *et al.* 2009).

The protein product of *ATP13A2* is a lysosomal P-type adenosine triphosphatase (ATPase). ATP13A2 is degraded via the proteasome, and KRS-derived mutants are destroyed more rapidly than the WT in cell models (Ramirez *et al.* 2006). Expressing the relevant WT *ATP13A2* orthologues inhibits human *SNCA*-mediated toxicity in yeast cells, *Caenorhabditis* dopaminergic neurons *in vivo*, and rat primary dopaminergic neurons. KRS-equivalent or ATPase mutants are deficient in this regard. Further experiments in yeast and *Caenorhabditis* indicate that WT ATP13A2 enhances SNCA folding and protects cells from Manganese toxicity (see 1.1.2.10) (Gitler *et al.* 2009).

The genetic evidence for *High temperature requirement A2* (*HTRA2*) (also known as *Omi*) is not as strong. The initial study detected heterozygous Gly399Ser mutations in four late onset apparently idiopathic PD patients but not in 370 normal controls. The authors indicated that this suggests an autosomal dominant mode of inheritance (*PARK13*). They also demonstrated that the heterozygous Ala141Ser mutation is marginally but significantly overrepresented in German IPD cases. The subsequent identification of nine heterozygous substitutions and insertions (one of which is missense) in late onset familial and apparently idiopathic patients but not in 359 controls provided further support for the role of *HTRA2* in autosomal dominant PD. Note that three of the four upstream mutations significantly influence reporter gene expression in neuronal cell models. Cognitive impairment is almost unheard of in these patients (Strauss *et al.* 2005; Bogaerts *et al.* 2008). However, association between IPD and the Gly399Ser and Ala141Ser mutations was not replicated in American Caucasians. Moreover, analyses in combined groups of IPD and late onset

FPD cases indicates that variation at common *HTRA2* SNPs and haplotypes does not significantly influence disease susceptibility in several Caucasian populations (Simon-Sanchez and Singleton 2008; Ross *et al.* 2008b; Bogaerts *et al.* 2008). These conflicting results do not exclude the possibility that rare *HTRA2* mutations can cause FPD in specific populations. In addition, HTRA2 is detected in a significant proportion of IPD and DLB LBs (Strauss *et al.* 2005; Kawamoto *et al.* 2008).

The protein encoded by *HTRA2* is a mitochondrial serine protease. During apoptosis, it is released into the cytosol and regulates caspase activation, partially via its proteolytic function (Suzuki *et al.* 2001; Yang *et al.* 2003). *Htra2*$^{-/-}$ mice or those homozygous for the Ser276Cys *Htra2* mutation (the *motor neuron disease 2* strain) display neuronal mitochondrial pathology, selective death of striatal neurons, enhanced cellular sensitivity to oxidative stress, motor dysfunction, and juvenile mortality (Jones *et al.* 2003; Martins *et al.* 2004). Furthermore, deletion of *Htra2* induces mitochondrial protein accumulation, respiratory dysfunction, increased ROS levels, and a transcriptional stress response that contributes to neuronal cell death (Moisoi *et al.* 2009). The Ser276Cys, Gly399Ser, and Ala141Ser mutations inhibit the protease activity of Htra2 *in vitro*, and the latter two elicit mitochondrial pathology and stress-induced mitochondrial dysfunction in neuronal cell models (Jones *et al.* 2003; Strauss *et al.* 2005). PINK1 promotes HTRA2 phosphorylation in neuronal cells and the IPD caudate, and phosphorylation of HTRA2 appears to enhance its proteolytic activity. Importantly, PINK1 and HTRA2 cooperate to protect primary fibroblasts from apoptosis induced by rotenone and UPS inhibition, and this appears to be dependent on HTRA2 phosphorylation (Plun-Favreau *et al.* 2007).

Taken together, these findings indicate that common variation in genes known to cause FPD without dementia tends not to associate with IPD. Nevertheless, heterozygosity for mutations underlying recessive FPD might increase IPD susceptibility in certain instances. In addition, FPD animal models develop a range of phenotypes including mitochondrial dysfunction, oxidative stress, UPS impairment, lysosomal dysfunction, protein accumulation, deregulated

neurotransmission, and motor dysfunction. However, many of these do not exhibit dopaminergic cell death.

1.1.2.10. Environmental factors and Parkinson's disease

Parkinson's disease with and without dementia are characterised by considerable molecular, neuropathological, and clinical heterogeneity. This suggests that environmental factors play a significant role in the aetiopathogenesis of these conditions. Indeed, various environmental influences can alter PD risk. Studies demonstrate that occupational exposure to herbicides, pesticides, or metals (i.e. Manganese, Copper, and Lead); regular well-water consumption; and being knocked unconscious significantly increase PD susceptibility. To put this in context, these factors each confer slightly less risk than having a positive history of PD in a first degree relative. On the other hand, smoking; coffee and tea consumption; and exposure to general anaesthetic significantly protect against PD (Gorell *et al.* 2004; Dick *et al.* 2007; Hu *et al.* 2007).

The discovery that exposure to MPTP causes parkinsonism and executive dysfunction in humans markedly advanced our understanding of PD and cognitive impairment therein (Langston *et al.* 1983; Stern *et al.* 1990). The active metabolite of MPTP is the 1-methyl-4-phenylpyridinium ion (MPP+). This species is a substrate for the dopamine transporter and inhibits mitochondrial ETC complex I. Therefore, it accumulates specifically in dopaminergic neurons, leading to oxidative stress and death (Javitch *et al.* 1985; Nicklas *et al.* 1985). MPTP-treated mice exhibit Snca-positive neuronal accumulations, SNpc dopaminergic cell death, and locomotor dysfunction (Heikkila *et al.* 1984; Vila *et al.* 2000; Tillerson *et al.* 2002). Similar effects are observed in rats injected with the pesticide rotenone, a highly selective complex I inhibitor (Betarbet *et al.* 2000). Interestingly, macaques exposed to chronic low dose MPTP display attention and planning deficits (Decamp and Schneider 2004).

The ability of environmental agents to recapitulate essential aspects of PD is not solely restricted to those that directly promote oxidative stress. In one seminal study, the authors injected rats with the proteasome inhibitors epoxomicin and PSI. After several weeks, animals developed a parkinsonian-like syndrome and reduced nigrostriatal DA signaling. *Post mortem* analyses demonstrated loss of dopaminergic cells in the SNpc and LC, noradrenergic neurons in the LC, cholinergic cells in the NbM, and neurons in the dorsal motor nucleus. In the majority of the degenerating regions, these changes were accompanied by Snca-positive neuronal inclusions (McNaught *et al.* 2004). These remarkable findings represent what is probably the most comprehensive and accurate animal model of PD neuropathology and motor dysfunction in existence.

Collectively, these results indicate that environmental factors are intimately involved in PD, and potentially, in PD-associated cognitive impairment. Further, they echo the genetic data, by demonstrating that mitochondrial dysfunction, oxidative stress, and UPS inhibition are central components of the molecular pathogenesis driving this condition.

1.1.2.11. Molecular aetiopathogenesis of Parkinson's disease: a modern synthesis

The various manifestations of IPD and FPD exhibit a certain degree of molecular heterogeneity, both within themselves and compared to each other. This is most likely the result of complex gene-gene and gene-environment interactions. Despite this variability, it is striking that similar insults are consistently observed. In essence, the building blocks of disease are more or less the same, but their specific number and combination varies from case to case. This conclusion is based on a large body of work identifying mitochondria, oxidative stress, the UPS, and lysosomal degradation as pathways which regulate the molecular aetiopathogenesis of PD. Moreover, there is strong evidence from various systems that some of the key players

and pathways can interact with each other, converging at the molecular level to drive disease (see also below) [reviewed in (Abou-Sleiman *et al.* 2006b; Lesage and Brice 2009)]. Research in this area has largely concentrated on intergenetic relationships. However, forays are being made into the territory of gene-environment interactions [for example (McCulloch *et al.* 2008)]. This important and necessary direction holds much promise of bringing all the pieces together, enabling us to grasp the complex mechanics of IPD and develop novel forms of effective therapy.

Amongst the various pathway interactions described in the PD brain and model systems, those influencing SNCA accumulation may be particularly relevant to Lewy body dementia pathogenesis. Many of the genes implicated in IPDD or DLB regulate SNCA accumulation *in vivo*, notably *MAPT*, *SNCB*, *LRRK2*, *APOE* (Hashimoto *et al.* 2001; Giasson *et al.* 2003; Gallardo *et al.* 2008; Lin *et al.* 2009b). Moreover, SNCA aggregates are concentrated at presynaptic terminals in DLB, and proteasomal subunit levels significantly correlate with MMSE scores in this disorder (Kramer and Schulz-Schaeffer 2007; MacInnes *et al.* 2008). *Snca*-null mice are resistant to oxidative stress-induced dopaminergic cell death (Dauer *et al.* 2002). Finally, *SNCA* ploidy and cortical SNCA pathology correlate with the severity of cognitive dysfunction in FPD and IPD, respectively (Kovari *et al.* 2003; Aarsland *et al.* 2005a; Braak *et al.* 2005; Ross *et al.* 2008a). Taken together, these findings suggest that pathway interactions influencing SNCA accumulation could be critically-involved in the processes driving cognitive impairment and/or dementia in Lewy body disease.

1.2. Genetic regulation of gene expression

1.2.1. Genetic variation and gene expression

Marked differences exist between the human transcriptome and those of our primate cousins, particularly in the CNS, and natural selection has driven the evolution of gene expression in the human lineage (Enard *et al.* 2002; Gilad *et al.* 2006). Together with the unexpectedly small number of protein-coding genes in the human genome, these observations have generated the hypothesis that heritable differences in the regulation of gene expression account for a large proportion of common human phenotypic variation [reviewed in (Buckland 2004)].

Genetic influences that regulate expression can be subdivided into two classes: *cis*-acting and *trans*-acting. *Cis*-acting factors function in an allele-specific manner. *Cis*-acting variants are situated at the target gene locus itself, residing in regulatory regions, such as promoters or enhancers, exons, or introns. They alter transcription, splicing, translation, RNA stability, or protein stability (Bray and O'Donovan 2006). *Trans*-acting factors act on both gene copies. *Trans*-acting polymorphisms are by definition located far from their target gene (generally on a different chromosome), and tend to influence expression via transcription factors or hormones (Bray and O'Donovan 2006). Since transcription results in a quantitative phenotype, *cis*- and *trans*-acting variants are collectively known as expression quantitative trait loci (eQTLs) (Pastinen and Hudson 2004).

The identification of polymorphisms that influence expression is complicated by our incomplete knowledge of regulatory regions. The positions of all the DNA elements controlling the expression of any specific gene are generally unknown, and may lie in promoters, introns, exons, or at distant locations tens or hundreds of kb from the transcribed sequence (Buckland 2004). However, the human genome possesses extensive linkage disequilibrium (LD), making it possible to screen for these effects indirectly. This involves genotyping marker variants (e.g. marker SNPs [mSNPs])

and using that information to tag unknown or unidentified regulatory polymorphisms (e.g. regulatory SNPs [rSNPs]) (Bray and O'Donovan 2006).

Early small scale estimates suggested that *cis*-acting variants explain a sizeable proportion of interindividual differences in gene expression (Yan *et al.* 2002; Lo *et al.* 2003). Large scale genome wide studies indicate that *cis*-acting variation significantly affects the expression of 25-50% of all human transcripts. They have also identified polymorphisms that act as master regulators or "hotspots"; which influence the expression of many targets in *trans* (Morley *et al.* 2004; Cheung *et al.* 2005; Dixon *et al.* 2007; Goring *et al.* 2007; Ge *et al.* 2009). These data have generally been obtained in cultured lymphoblastoid cells. However, it has been demonstrated that eQTLs operate in the human brain. One genome wide study indicates that SNP variation significantly influences the expression of ~20% of cortical transcripts, with *trans*-acting mechanisms accounting for the bulk of this (Bray *et al.* 2003; Buckland *et al.* 2004; Myers *et al.* 2007a)

Whole genome studies generate the greatest amount of information for identifying regulatory variants. However, the effect of *cis*-acting variation can be detected by quantifying the relative abundance of messenger ribonucleic acid (mRNA) transcripts containing each allele [reviewed in (Bray and O'Donovan 2006)]. This approach relies on the marker polymorphism being located on the transcript, and measures expression exclusively in heterozygotes. Relative quantification is performed in the same sample, with each allele acting as internal control for the other. *Cis*-acting variation is detected as a significant departure from the 1:1 ratio of expressed alleles, which is known as differential allelic expression (DAE) [reviewed in (Bray and O'Donovan 2006)]. This method is sensitive to subtle *cis*-acting factors, as it controls for interindividual differences in *trans*-acting effects caused by sample preparation, mRNA quality, or the environment. It is limited in that strong LD is required between the marker variant and any putative regulatory polymorphisms [reviewed in (Bray and O'Donovan 2006)]. Relative allelic expression has been investigated using a variety of technologies including single base extension, oligo arrays, haplotype

chromatin immunoprecipitation, and reverse transcriptase-coupled 5' nuclease assays (Yan *et al.* 2002; Lo *et al.* 2003; Knight *et al.* 2003; Zhu *et al.* 2004).

1.2.2. *Cis*-acting variation and complex disease

Genetic variation affects the aetiopathogenesis of many complex disorders. It is now widely accepted that many polymorphisms each of small to moderate effect act in concert with environmental factors to generate disease phenotypes [reviewed in (Buckland 2006)]. Many commentators believe that a substantial proportion of these variants are likely to be eQTLs that influence risk via the regulation of gene expression. Moreover, a variety of relatively simple techniques can detect their effects on gene expression as quantitative endophenotypes (see 1.2.1), making them attractive to laboratory researchers [reviewed in (Buckland 2006)].

Cis-acting variation has been demonstrated *post mortem* in the brains of neurological disease cases. Examples include AD, where the ε4 and H1c alleles associate with significant overexpression of *APOE* and 4R *MAPT*, respectively (Bray *et al.* 2004; Myers *et al.* 2007b), and schizophrenia, in which variation at the SNP rs1047631 significantly influences *Dystrobrevin binding protein 1* (*DTNBP1*) expression (Bray *et al.* 2005). Notably, the *APOE* ε4 allele increases AD risk (Farrer *et al.* 1997). *Cis*-acting variation has also been shown in IPD brains. Variation at the polymorphism rs356219 significantly influences *SNCA* expression and IPD susceptibility (Fuchs *et al.* 2008; Mueller *et al.* 2005), and the H1 haplotype significantly increases 4R *MAPT* expression and IPD risk (Williams-Gray *et al.* 2009a; Healy *et al.* 2004b).

1.3. Concluding remarks

Idiopathic Parkinson's disease is a complex, multifactorial disorder: genes and environment are both involved in its genesis. The extent of these factors' individual roles and the specific interactions between them most likely vary from patient to patient. This is exemplified by the considerable clinicopathological and molecular heterogeneity observed in IPD cases, which supports the hypothesis that IPDD and DLB are situated at opposing ends of a Lewy body disease spectrum. Much has been learned about the molecular aetiopathogenesis of PD in general, primarily from the identification of genes that cause familial forms of this condition. However, at this point very little is known about the molecular determinants that drive cognitive impairment and dementia in PD. Monogenic mutation in *SNCA*, *SNCB*, and *LRRK2* can result in familial Lewy body dementia, and alleles in *GBA*, *MAPT*, and *APOE* are believed to alter the susceptibility to cognitive dysfunction in IPD. Nevertheless, if we wish to elucidate the processes underlying these complex phenotypes, significant inroads must still be made. Listed below are three broad questions that highlight current gaps in our knowledge of the molecular aetiopathogenesis of IPDD:

1. Which genes and genetic pathways demonstrate dysregulated expression in the brains of demented compared with nondemented IPD patients?
2. Can eQTLs be identified that influence the expression of these genes?
3. Does variation at these polymorphisms associate with IPD dementia and/or neurodegeneration?

Chapter 2: Materials and Methods

2.1. Chemicals and prepared solutions

Unless stated otherwise, all chemicals were obtained from Sigma, UK, all primers were obtained from Sigma-Genosys, UK, all 1.5 ml microfuge tubes were obtained from Axygen, USA, all falcon tubes were obtained from VWR, UK, and all 96-well plates and adhesive covers were obtained from ABgene, UK.

The following solutions were prepared in milliQ H_2O (mqH_2O):

2x Orange G gel loading dye

Glycerol 50% by volume

Orange G dye to colour

10x Tris-Borate-Ethylendiaminetetraacetate (TBE)

1 M Trizma base

1 M Boric acid (anhydrous)

20 mM Ethylendiaminetetraacetate (EDTA)

pH to 8.3

2.2. Agarose gel electrophoresis

DNA was resolved on agarose gels. Agarose (Roche Diagnostics GmbH, Germany) was dissolved in 1x TBE and ethidium bromide added (to 0.5 μg/ml) before polymerisation. DNA in solution was mixed 1:1 with 2x Orange G dye before loading. Hyperladder II or V DNA ladder (Bioline, UK) was run on each gel. Gels were visualised and photographed using the Gene Genius digital camera system and GeneSnap v4.0.0 (both from SynGene, UK).

2.3. Quantitative reverse transcriptase-polymerase chain reaction

2.3.1. Case and control sample selection

Flash-frozen *post mortem* brain samples from unrelated individuals were obtained from the Queen Square Brain Bank for Neurological Disorders (QSBBND). Ethical approval was gained from both the National Hospital for Neurology and Neurosurgery (NHNN) Local Research Ethics Committee (LREC) (reference: 06/Q0512/11), and the Research and Development Department of University College London Hospital (UCLH) (reference: 06L 306). All QSBBND samples had been previously been acquired with informed consent, and almost exclusively from people of European ancestry. Idiopathic Parkinson's disease (IPD) cases had been diagnosed both clinically and neuropathologically. Controls had been confirmed by neuropathological exam as free of any neurological condition.

Two distinct tissue sets were collected, each from a different group of individuals. The first, called the IPD cognitive series, enabled the comparison the gene expression between three groups: idiopathic Parkinson's disease dementia (IPDD), idiopathic Parkinson's disease no dementia (IPDND), and controls. This series was employed for the IPD cognitive expression analysis (see 2.10.2.2), the *cis*-acting variation analysis (see 2.10.5), and validation of IPD cognitive expression microarray hits (see 2.10.6.2). IPD cases were segregated into IPDD and IPDND according to two measures, both based upon a report of cognitive impairment or change in personality by a family member or General Practitioner. The first measure (termed "COG") was scored as 1 if the patient had presented with such symptoms within two years of IPD diagnosis. The second (termed "V25") was scored as 1 if such symptoms presented at any time after that point. Cases scoring either 1 in V25 or 1 in both COG and V25 were placed into the IPDD group. Cases scoring 0 in both COG and V25 were placed into the IPDND group. Where possible, cases were selected upon whom a mini

mental state examination (MMSE) had been performed, and whose results agreed with the COG and V25 scores (or in cases where the result did not agree, had been performed at least 5 years before death). Two exclusion criteria were employed: cases were to have no family history of Parkinson's disease (PD); cases were to have no pathology indicative of any neurological condition except PD. Tissue from two brain regions obtained from the same individuals was collected for this series: the dorsolateral prefrontal cortex (DLPFC) (Brodmann area 46 [BA46]) and the angular gyrus (AG) in the inferior parietal cortex (IPC) (BA39). AG tissue was unavailable for two individuals (C19/93 and P12/95). Cerebellum tissue was also collected for each individual in order to extract genomic DNA (gDNA) (see 2.6.2) for single nucleotide polymorphism (SNP) genotyping (see 2.6.3) as part of the *cis*-acting variation analysis (see 2.10.5), as well as from two other individuals so as to generate quantitative reverse transcriptase-polymerase chain reaction (qRT-PCR) standard and calibrator complementary DNA (cDNA) (see 2.3.3). Individual clinicopathological data for the cognitive series samples can be seen in table 2.1.

The second tissue set, called the IPD mapping series, facilitated the comparison of gene expression between IPD cases and controls. This was used for the IPD expression mapping analyses (see 2.10.2.2). Note that IPD cases were not segregated according to dementia status. Tissue samples were collected for the mapping series from the following seven brain regions obtained from the same individuals: medulla, putamen, amygdala, entorhinal cortex (EC) (BA28), anterior cingulate cortex (ACC) (BA24), AG (BA39), and frontal cortex (FC) (BA8). Not all regions were available for all individuals. Due to low availability of medulla tissue, several individuals were replaced for this brain region. The mapping series samples were extracted and quantified (see 2.3.2) in collaboration with Simone Sharma from our laboratory. Table 2.2 shows individual clinicopathological data for the mapping series samples.

Table 2.1. IPD cognitive series individual clinicopathological data.

Individual clinicopathological data for the IPD cognitive series samples (below and following pages). Measures of time are in years, except PMD, which is measured in hours. COG and/or V25 scores of 1, backed up by MMSE ≤ 27 (where available), were taken as indicative of dementia. CON = control; F = female; IPD = idiopathic Parkinson's disease; IPDD = idiopathic Parkinson's disease dementia; IPDND = idiopathic Parkinson's disease no dementia; L =left; M = male; MMSE = mini mental state examination; NA = not applicable; ND = not determined; PMD = *post mortem* delay; R = right; SD = standard deviation.

Group (*n*)	Brain Bank code	Sex	Brain hemisphere	Age of onset	Age of death	Disease duration	PMD	Brain pH	COG	V25	MMSE score	Time between MMSE and death
CON (16)	C10/92	M	R	NA	77	NA	27.50	6.49	ND	ND	ND	ND
	C14/93	M	R	NA	74	NA	5.50	6.51	ND	ND	ND	ND
	C16/93	M	L	NA	76	NA	16.00	6.71	ND	ND	ND	ND
	C19/93	M	L	NA	82	NA	33.00	6.79	ND	ND	ND	ND
	C33/93	F	R	NA	84	NA	18.00	6.86	ND	ND	ND	ND
	C10/95	M	L	NA	72	NA	13.00	6.16	ND	ND	ND	ND
	C03/97	M	L	NA	86	NA	53.00	6.65	ND	ND	ND	ND
	C11/97	M	L	NA	63	NA	42.00	6.23	ND	ND	ND	ND
	C03/98	M	L	NA	86	NA	23.30	6.55	ND	ND	ND	ND
	C06/98	M	R	NA	83	NA	117.05	6.81	ND	ND	ND	ND
	C04/99	M	R	NA	91	NA	48.00	6.54	ND	ND	ND	ND
	C08/99	M	L	NA	79	NA	56.40	6.60	ND	ND	ND	ND
	C09/99	M	L	NA	75	NA	64.50	6.18	ND	ND	ND	ND
	C03/00	M	R	NA	85	NA	43.35	6.68	ND	ND	ND	ND
	C04/00	M	L	NA	81	NA	40.00	6.48	ND	ND	ND	ND
	P15/05	M	R	NA	57	NA	78.50	ND	ND	ND	ND	ND
Mean	**NA**	**NA**	**NA**	**NA**	**78.2**	**NA**	**42.4**	**6.55**	**NA**	**NA**	**NA**	**NA**
SD	**NA**	**NA**	**NA**	**NA**	**8.8**	**NA**	**28.2**	**0.22**	**NA**	**NA**	**NA**	**NA**

Group (*n*)	Brain bank code	Sex	Brain hemisphere	Age of onset	Age of death	Disease duration	PMD	Brain pH	COG	V25	MMSE score	Time between MMSE and death
IPDD (15)	P24/94	M	L	53.6	64.1	10.5	23.25	6.18	1	1	13	0.8
	P18/95	M	R	65.9	82.3	16.4	24.00	6.52	0	1	30	7.5
	P25/98	M	R	61.8	68.3	6.5	86.15	6.70	0	1	26	1.7
	P36/98	F	L	74.2	84.8	10.6	18.00	6.64	0	1	22	3.6
	P62/98	M	R	48.0	72.8	24.8	27.00	6.32	0	1	26	4.6
	P30/00	M	R	61.6	77.5	15.9	28.25	6.39	0	1	24	0.2
	P54/00	M	R	58.3	74.9	16.6	51.15	5.77	ND	1	24	7.6
	P59/00	M	L	69.1	74.8	5.7	37.30	5.88	0	1	16	3.7
	P05/01	M	L	42.0	79.0	37.0	38.35	6.20	0	1	17	3.0
	P18/01	M	R	45.9	70.1	24.2	61.20	6.29	0	1	19	0.3
	P01/02	M	L	59.5	70.5	11.0	51.20	6.29	0	1	27	2.0
	P23/02	M	R	55.0	72.0	17.0	25.45	ND	0	1	24	5.0
	P25/03	M	L	71.1	80.1	9.0	62.20	ND	0	1	21	3.0
	P18/05	M	L	44.0	74.0	30.0	38.00	ND	0	1	16	4.0
	P60/05	M	R	54.0	76.0	22.0	ND	ND	0	1	29	17.0
Mean	**NA**	**NA**	**NA**	**57.6**	**74.7**	**17.1**	**40.8**	**6.29**	**NA**	**NA**	**22.3**	**4.3**
SD	**NA**	**NA**	**NA**	**10.0**	**5.5**	**9.0**	**19.3**	**0.29**	**NA**	**NA**	**5.1**	**4.2**

Group (*n*)	Brain bank code	Sex	Brain hemisphere	Age of onset	Age of death	Disease duration	PMD	Brain pH	COG	V25	MMSE score	Time between MMSE and death
IPDND (16)	P16/92	M	L	74.1	80.3	6.2	30.00	6.30	0	0	ND	ND
	P28/94	M	L	55.6	75.7	20.1	17.00	6.44	0	0	ND	ND
	P45/94	M	R	66.9	76.0	9.1	20.50	6.45	0	0	29	1.7
	P12/95	M	L	62.2	82.7	20.5	21.00	ND	0	0	ND	ND
	P17/96	M	L	72.8	81.1	8.3	11.50	6.42	0	0	ND	ND
	P05/97	M	R	44.1	68.2	24.1	39.00	6.42	0	0	ND	ND
	P65/97	F	R	74.1	86.9	12.8	72.00	6.31	0	0	30	7.8
	P50/98	M	R	40.6	66.2	25.6	40.00	6.65	0	0	ND	ND
	P67/98	M	L	54.7	71.3	16.6	115.00	6.35	0	0	ND	ND
	P14/99	M	R	59.4	74.0	14.6	25.30	6.35	0	0	30	6.0
	P40/99	M	L	54.0	73.7	19.7	39.00	6.00	0	0	ND	ND
	P54/99	M	L	79.9	91.8	11.9	60.45	6.22	0	0	ND	ND
	P55/00	M	R	50.4	73.0	22.6	25.20	7.18	0	0	30	15.6
	P75/00	M	R	50.7	66.1	15.4	56.00	6.49	0	0	29	0.1
	P24/01	M	R	58.4	73.2	14.8	20.30	6.22	0	0	ND	ND
	P05/04	M	R	66.5	81.5	15.0	45.20	ND	0	0	ND	ND
Mean	**NA**	**NA**	**NA**	**60.3**	**76.4**	**16.1**	**39.8**	**6.41**	**NA**	**NA**	**29.6**	**6.2**
SD	**NA**	**NA**	**NA**	**11.4**	**7.3**	**5.7**	**26.3**	**0.27**	**NA**	**NA**	**0.5**	**6.1**

Table 2.2. IPD mapping series individual clinicopathological data.

Individual clinicopathological data for the IPD mapping series samples (below and following pages). Measures of time are in years, except PMD, which is measured in hours. CON = control; F = female; IPD = idiopathic Parkinson's disease; L =left; M = male; NA = not applicable; ND = not determined; PMD = *post mortem* delay; R = right; SD = standard deviation.

Group (*n*)	Brain bank code	Sex	Brain hemisphere	Age of onset	Age of death	Disease duration	PMD	Brain pH
CON (20) [All regions except medulla]	C01/96	F	L	NA	77	NA	23.00	5.60
	C05/96	F	L	NA	85	NA	34.00	6.31
	C01/97	F	R	NA	86	NA	46.50	6.17
	C03/97	M	L	NA	86	NA	53.00	6.65
	C04/97	F	R	NA	53	NA	29.50	6.64
	C10/97	F	R	NA	81	NA	13.50	6.39
	C11/97	M	L	NA	63	NA	42.00	6.23
	C03/98	M	L	NA	86	NA	23.30	6.55
	C06/98	M	R	NA	83	NA	117.05	6.81
	C02/99	F	L	NA	84	NA	81.45	6.28
	C04/99	M	R	NA	91	NA	48.00	6.54
	C08/99	M	L	NA	79	NA	56.40	6.60
	C09/99	M	L	NA	75	NA	64.50	6.18
	C03/00	M	R	NA	85	NA	43.35	6.68
	C04/00	M	L	NA	81	NA	40.00	6.48
	C05/00	F	L	NA	88	NA	49.25	6.23
	C06/00	F	L	NA	89	NA	77.30	6.49
	P44/02	F	R	NA	78	NA	23.30	6.07
	P15/05	M	R	NA	57	NA	78.50	ND
	P94/05	M	L	NA	71	NA	38.50	ND
Mean	**NA**	**NA**	**NA**	**NA**	**78.9**	**NA**	**49.1**	**6.38**
SD	**NA**	**NA**	**NA**	**NA**	**10.5**	**NA**	**24.9**	**0.29**

Group (*n*)	Brain bank code	Sex	Brain hemisphere	Age of onset	Age of death	Disease duration	PMD	Brain pH
IPD (20) [All regions except medulla]	P03/01	F	R	36.5	66.5	30.0	125.30	6.20
	P07/01	F	L	53.1	77.1	24.0	80.00	6.53
	P14/01	M	L	64.4	81.0	16.6	103.00	6.15
	P18/01	M	R	45.9	70.1	24.2	61.20	6.29
	P19/01	M	L	67.0	72.2	5.2	40.45	6.10
	P22/01	M	L	82.4	92.1	9.7	31.45	5.81
	P24/01	M	R	58.4	73.2	14.8	20.30	6.22
	P44/01	M	L	56.5	65.2	8.7	8.00	6.37
	P56/01	F	L	77.2	89.0	11.8	11.30	6.38
	P57/01	M	R	57.1	71.2	14.1	81.30	6.76
	P64/01	M	L	73.8	79.9	6.1	27.25	5.88
	P73/01	M	R	50.4	73.3	22.9	71.30	6.17
	P01/02	M	L	59.5	70.5	11.0	51.20	6.29
	P07/02	M	R	73.1	77.7	4.6	46.20	6.73
	P10/02	F	L	55.8	65.1	9.3	46.20	5.88
	P12/02	M	L	65.2	73.8	8.6	11.20	6.32
	P22/02	F	R	73.9	88.2	14.3	47.45	6.62
	P25/02	F	L	49.4	78.7	29.3	75.45	6.46
	P36/02	F	R	59.0	81.5	22.5	24.25	ND
	P52/02	F	L	52.9	81.1	28.2	57.30	ND
Mean	**NA**	**NA**	**NA**	**60.6**	**76.3**	**15.8**	**51.0**	**6.29**
SD	**NA**	**NA**	**NA**	**11.6**	**7.7**	**8.4**	**31.6**	**0.27**

Group (*n*)	Brain bank code	Sex	Brain hemisphere	Age of onset	Age of death	Disease duration	PMD	Brain pH
CON (15) [Medulla only]	C01/96	F	L	NA	77	NA	23.00	5.60
	C01/97	F	R	NA	86	NA	46.50	6.17
	C04/97	F	R	NA	53	NA	29.50	6.64
	C11/97	M	L	NA	63	NA	42.00	6.23
	C06/98	M	R	NA	83	NA	117.05	6.81
	C04/99	M	R	NA	91	NA	48.00	6.54
	C06/99	M	L	NA	82	NA	44.15	ND
	C08/99	M	L	NA	79	NA	56.40	6.60
	C01/00	F	R	NA	83	NA	20.00	6.55
	C03/00	M	R	NA	85	NA	43.35	6.68
	C04/00	M	L	NA	81	NA	40.00	6.48
	C06/00	F	L	NA	89	NA	77.30	6.49
	C07/00	F	L	NA	78	NA	51.30	ND
	P44/02	F	R	NA	78	NA	23.30	6.07
	P94/05	M	L	NA	71	NA	38.50	ND
Mean	**NA**	**NA**	**NA**	**NA**	**78.6**	**NA**	**46.7**	**6.41**
SD	**NA**	**NA**	**NA**	**NA**	**9.9**	**NA**	**24.3**	**0.33**

Group (*n*)	Brain bank code	Sex	Brain hemisphere	Age of onset	Age of death	Disease duration	PMD	Brain pH
IPD (17) [Medulla only]	P38/00	F	R	61.0	71.0	10.0	58.10	6.38
	P07/01	F	L	53.1	77.1	24.0	80.00	6.53
	P14/01	M	L	64.4	81.0	16.6	103.00	6.15
	P18/01	M	R	45.9	70.1	24.2	61.20	6.29
	P19/01	M	L	67.0	72.2	5.2	40.45	6.10
	P22/01	M	L	82.4	92.1	9.7	31.45	5.81
	P24/01	M	R	58.4	73.2	14.8	20.30	6.22
	P44/01	M	L	56.5	65.2	8.7	8.00	6.37
	P56/01	F	L	77.2	89.0	11.8	11.30	6.38
	P57/01	M	R	57.1	71.2	14.1	81.30	6.76
	P64/01	M	L	73.8	79.9	6.1	27.25	5.88
	P73/01	M	R	50.4	73.3	22.9	71.30	6.17
	P01/02	M	L	59.5	70.5	11.0	51.20	6.29
	P07/02	M	R	73.1	77.7	4.6	46.20	6.73
	P10/02	F	L	55.8	65.1	9.3	46.20	5.88
	P22/02	F	R	73.9	88.2	14.3	47.45	6.62
	P25/02	F	L	49.4	78.7	29.3	75.45	6.46
Mean	**NA**	**NA**	**NA**	**62.3**	**76.2**	**13.9**	**50.6**	**6.30**
SD	**NA**	**NA**	**NA**	**10.7**	**7.9**	**7.3**	**26.3**	**0.28**

2.3.2. Ribonucleic acid extraction and quantification

Total ribonucleic acid (RNA) was extracted from human brain samples using TRIzol (Invitrogen, UK), according to the manufacturer's instructions. Before starting the protocol, all surfaces and pipettes were cleaned with Ribonuclease (RNase) AWAY (Invitrogen, UK). All centrifugation steps were performed at 4ºC. Between extractions, homogenisation glass tubes were scrubbed with detergent and thoroughly washed with tap H_2O (tH_2O) to remove any brain material, then rinsed with 70% ethanol followed by mqH_2O.

For each extraction, a frozen piece of brain approximately 1 cm^3 in size was homogenised in a clean glass tube containing 1 ml of ice-cold TRIzol using a dounce homogeniser. The homogenate was transferred to a 2 ml phase-lock tube (Eppendorf, UK). 200 µl chloroform was added and the tube was shaken vigorously by hand before being centrifuged at 12 000 *g* for 15 minutes. The upper aqueous phase (above the phase lock gel barrier) was then transferred to a sterile 2 ml screw cap O-ring tube (Starstedt, UK). RNA was precipitated by adding 500 µl propan-2-ol (molecular biology grade). The tube was mixed by inversion and incubated at room temperature for 10 minutes. The tube was centrifuged at 12 000 *g* for 10 minutes and the supernatant aspirated. The pellet was then washed by adding 1 ml 70% ethanol (molecular biology grade) and inverting. The tube was centrifuged at 7 500 *g* for 5 minutes and the supernatant aspirated. The pellet was air-dried (sealed over with perforated Parafilm to avoid contamination) and resuspended in 100-200 µl H_2O pre-treated with diethyl pyrocarbonate (DEPC) (Ambion, UK). Sample RNAs were stored at –80ºC. RNA concentration and quality was assessed using the NanoDrop ND-1000 (NanoDrop Technologies, USA), enabling the identification of samples contaminated with protein or other organic compounds.

2.3.3. Complementary DNA synthesis

Complementary DNA was generated from total RNA using the SuperScript II Reverse Transcriptase system (Invitrogen, UK), according to the manufacturer's instructions. All pipettes and surfaces were cleaned with RNAse AWAY. Sample cDNA synthesis batches were carried out on a region-by-region basis, each batch comprising all of the IPD and control RNA samples extracted for that region. Standard curve and calibrator cDNA were produced in multiple simultaneous reactions using RNA extracted from one of four different IPD cases (see 2.3.4). Individual RNAs were diluted to 500 ng/µl and plated out onto 96-well plates for ease of manipulation.

First strand cDNA synthesis reactions were performed in a total volume of 40 µl. For each reaction, 2 µg total RNA was mixed with DEPC-treated H_2O, 6 µg random hexamer primers, and deoxynucleotide triphosphates (dNTPs) (to 0.5 mM for each dNTP) and added to a 96-well plate. The plate was sealed and heated to 65ºC for 5 minutes, before being briefly chilled on ice and centrifuged. 10x first strand buffer, dithiothreitol (DTT) (to 10 mM), and 80 U RNaseOUT were added. The reaction was mixed by pipetting and incubated at 25ºC for 2 minutes. 400 U SuperScript II enzyme was added and mixed in by gentle pipetting. The plate was incubated as follows: 25ºC for 10 minutes; 42ºC for 50 minutes; 70ºC for 15 minutes. It was then stored at 4ºC until further processing. Sample cDNA reactions were diluted 10-fold with mqH_2O, and stored in deep-well 96-well plates at –80ºC or 4ºC, avoiding multiple freeze/thaw cycles. For standard curve/calibrator cDNA, multiple reactions were pooled and diluted 2-fold with mqH_2O (to generate the neat standard curve) and then diluted a further 10-fold with mqH_2O (to generate the calibrator), all of which were aliquotted and stored at –20ºC or 4ºC, avoiding multiple freeze/thaw cycles.

2.3.4. Quantitative reverse transcriptase-polymerase chain reaction procedure

Quantitative RT-PCR was carried out in real time using the Power Sybr Green system on an Applied Biosystems 7500 machine running the absolute quantification protocol in 9600 emulation mode (both from Applied Biosystems, UK), according to the manufacturer's instructions. All plates comprised a six-point cDNA standard curve (to enable quantification), a nontemplate control (NTC), a calibrator (to ensure similar C_t [cycle threshold] values between multiple plates quantifying the same gene), and IPD/control cDNA samples. All reactions were performed in triplicate (technical replicates). Multiple plates analysing expression of the same gene in each brain region (termed qRT-PCR runs) were all measured on the same day using the same Power Sybr Green/mqH_2O/primer mix. Reference genes were treated as independent target genes i.e. their expression was quantified using a separate mix in a separate run. Complementary DNA generated from the same individual was used as the standard curve and calibrator samples for each run. Runs quantifying cognitive series cDNA samples used one of three IPD cases as standards/calibrators: P27/00 cerebellum cDNA, P01/02 BA46 cDNA, or P45/94 BA46 cDNA (the latter solely for *Dual specificity phosphatase 6* [*DUSP6*] 1:3 splice form runs). Runs quantifying mapping series cDNA samples used as standards/calibrators IPD case P27/00 cerebellum cDNA for *DUSP6*, and P35/00 cerebellum cDNA for *Ephrin receptor A2* (*EPHA2*) and *α-Synuclein* (*SNCA*). Six-point standard curves were freshly generated for each run, by making serial dilutions of standard cDNA in mqH_2O, producing the following dilutions: neat; 1:5; 1:25; 1:125; 1:250; 1:500.

Amplification was performed in 25 µl reaction volumes. For each reaction, Power Sybr Green Master Mix was mixed with forward and reverse primers (each to 900 nM). The mixture was then made up to 20 µl with mqH_2O and pipetted into a 96-well Optical Reaction polymerase chain reaction (PCR) plate (Applied Biosystems, UK). 5 µl of standard curve cDNA, calibrator cDNA, IPD/control

cDNA sample, or NTC (mqH_2O) was added to the relevant wells. The plate was sealed with an Optical Adhesive Cover (Applied Biosystems, UK). Runs for both target genes and reference genes utilised one of five different sets of conditions (based on the annealing temperatures of the relevant primer pairs). All types of conditions were immediately followed by a dissociation curve stage, in order to confirm that only one amplicon was being generated. This consisted of bringing the plate up to 95ºC for 15 seconds, down to 60ºC for 1 minute, and then up to 99ºC, ramping 1ºC at a time, and remaining at each temperature for 15 seconds. The five sets of cycling conditions are listed as follows (data acquisition steps in bold):

55ºC

50ºC for 2 minutes
95ºC for 10 minutes
95ºC for 15 seconds
55ºC for 30 seconds
72ºC for 45 seconds
} 40 cycles

60ºC

50ºC for 2 minutes
95ºC for 10 minutes
95ºC for 15 seconds
60ºC for 45 seconds
} 40 cycles

64ºC

50ºC for 2 minutes
95ºC for 10 minutes
95ºC for 15 seconds
64ºC for 45 seconds
} 40 cycles

62ºC

50ºC for 2 minutes
95ºC for 10 minutes
95ºC for 15 seconds
62ºC for 45 seconds
} 40 cycles

66ºC

50ºC for 2 minutes
95ºC for 10 minutes
95ºC for 15 seconds
66ºC for 45 seconds
} 40 cycles

Tables 2.3 and 2.4 show the qRT-PCR annealing temperatures and primer sequences used to amplify each target and reference gene. As an added check to ensure that only one amplicon was being produced in each qRT-PCR run, amplified DNA from one well was resolved on 4% agarose gels.

Gene	Class	Annealing temperature (ºC)	Gene	Class	Annealing temperature (ºC)
ALAS2	Target	66	*PTGDS*	Target	60
APOA5 FL	Target	60	*PUM1*	Target	60
APOA5 1:3	Target	62	*SNCA*	Target	62
ARC	Target	60	*STAT4*	Target	60
BDNF	Target	55	*STAU1*	Target	60
CHI3L1	Target	55	*UQCRFS1*	Target	62
DUSP6 FL	Target	60	*ZNF407* FL	Target	60
DUSP6 1:3	Target	62	*ZNF407* 4:6	Target	62
EIF2AK4	Target	55	*G6PD*	Reference	62
EPHA2	Target	64	*HPRT1*	Reference	55
ETS1	Target	64	*NEFH*	Reference	62
PISD	Target	60	*RPL13A*	Reference	55
POU4F3	Target	62	*TBP*	Reference	60

Table 2.3. qRT-PCR annealing temperatures.

The annealing temperatures used for the 26 genes assayed by qRT-PCR. Class columns indicate whether the gene was a target or a reference gene. Annealing temperatures indicate which of the five different sets of conditions apply (see text for details). In cases where qRT-PCR was employed to distinguish specific splice forms, the gene name is followed either by FL, or by the exons flanking the skipped exon (separated by a colon). See list of abbreviations for gene symbol definitions. 1:3 = splice form 1:3; 4:6 = splice form 4:6; FL = full length; qRT-PCR = quantitative reverse transcriptase-polymerase chain reaction.

Table 2.4. qRT-PCR primer sequences.

The qRT-PCR primer sequences and generated amplicon sizes (in bp) (below and following pages). Sense and antisense are in terms of the direction of transcription (except for *POU4F3*). Primers annealing across an exon-exon boundary are indicated by naming the two relevant exons (separated by a dash). Primers were designed based on information available from Ensembl (releases 36, 44, and 48 from December 2005, April 2007, and December 2007 respectively), and BLASTed in Ensembl to ensure the production of a single predicted amplicon. In cases where qRT-PCR was employed to distinguish specific splice forms, the gene name is followed either by FL, or by the exons flanking the skipped exon (separated by a colon). See list of abbreviations for gene symbol definitions. 1:3 = splice form 1:3; 4:6 = splice form 4:6; bp = base pairs; FL = full length; qRT-PCR = quantitative reverse transcriptase-polymerase chain reaction.

Gene (amplicon size in bp)	Primer	Annealing location	Primer sequence (5' to 3')
ALAS2 (117)	Sense	Exon 9-10	TGTGGAGAAGCTGCTGCTGG
	Antisense	Exon 10	TCCCACTCACTCATGAGCTC
APOA5 FL (109)	Sense	Exon 1-2	CTTCTTTCAGCGTTTTCGGC
	Antisense	Exon 2	CCATCTTCTGCTGATGGATC
APOA5 1:3 (57)	Sense	Exon 1	TAATGGCAAGCATGGCTGCC
	Antisense	Exon 1-3	AGGGTCCTGAAAGAAGAGCC
ARC (137)	Sense	Exon 2	CCCGCCTGGAGAAGAATCA
	Antisense	Exon 2-3	TTGAGACCTGTTGTCACTCT
BDNF (130)	Sense	Exon 4	AATATGTAAGGAATGCTTGG
	Antisense	Exon 4	CACTTAACAGATCTGGCC
CHI3L1 (122)	Sense	Exon 6	GAAGGCCGAATTTATAAAGG
	Antisense	Exon 6-7	GGTGTTGGGATATCTTGGC
DUSP6 FL (162)	Sense	Exon 1-2	TACCTGGAAGGTGGCTTCAG
	Antisense	Exon 2	AAGGTCAGACTCGATGTCCG
DUSP6 1:3 (132)	Sense	Exon 1	ACACAGTGGTGCTCTACGAC
	Antisense	Exon 1-3	GGGCTTCATCTTCCAGGTAG
EIF2AK4 (148)	Sense	Exon 26-27	GAGGAATCTGTTACAATAAG
	Antisense	Exon 27-28	CCTCTTGGGACTGTGAC

Gene (amplicon size in bp)	Primer	Annealing location	Primer sequence (5' to 3')
EPHA2 (144)	Sense	Exon 15-16	TTGACCCCCGCGTGTCTATC
	Antisense	Exon 16	TCTCGATGGCAGTGTAGCCG
ETS1 (132)	Sense	Exon 2-3	CTGGGGATCCCAAAAGACCC
	Antisense	Exon 3	GCAGAGGGCTGCTCCATTCA
PISD (157)	Sense	Exon 6	CCGCGTCGTGTGACTCCTTC
	Antisense	Exon 6-7	ATCAGGGAGCCTGGGAAGTG
POU4F3 (109)	Sense	Exon 1-2	CCGCAGCTGCAGGGTAATAT
	Antisense	Exon 1	TGAACGGATGGTTCTTGCCG
PTGDS (86)	Sense	Exon 2-3	CCTTCCTCAGGAAAAACCAG
	Antisense	Exon 3	GGGACTCCGGTAGCTGTAG
PUM1 (158)	Sense	Exon 10	CAGCTGTGGTCCCTCACCAG
	Antisense	Exon 10-11	ACGGAGAACCTGCTGCTGTC
SNCA (134)	Sense	Exon 3-4	TGGCAACAGTGGCTGAGAAG
	Antisense	Exon 4	TTTGACAAAGCCAGTGGCTG
STAT4 (105)	Sense	Exon 20-21	TCTGAAAGTGGGGAAGTGAG
	Antisense	Exon 21	TTGTAGTCTCGCAGGATGTC
STAU1 (157)	Sense	Exon 4-5	TATCCCCCGAGGTACTTTTA
	Antisense	Exon 5	TCTGCAGGATCCTCAACGC

Gene (amplicon size in bp)	Primer	Annealing location	Primer sequence (5' to 3')
UQCRFS1 (233)	Sense	Exon 1	TGTCGCCATGTTGTCGGTAG
	Antisense	Exon 1-2	CAGAAGCAGGGACATTGAGG
ZNF407 FL (89)	Sense	Exon 5	CGAGAAGTCGTTTCTGTGTG
	Antisense	Exon 5-6	TTTCTCCTGTGTGCTGTCTG
ZNF407 4:6 (82)	Sense	Exon 4	AAATGTACCTGGCCCACGTG
	Antisense	Exon 4-6	TTTCTCCTGTGTGCGTCCTG
G6PD (113)	Sense	Exon 3-4	CCACCATCTGGTGGCTGTTC
	Antisense	Exon 4	GAAGGGCTCACTCTGTTTGC
HPRT1 (188)	Sense	Exon 3	TGAACGTCTTGCTCGAGAT
	Antisense	Exon 3-4	GGTCATTACAATAGCTCTTC
NEFH (146)	Sense	Exon 4	GATAACTGAGTACCGGCGTC
	Antisense	Exon 4-5	GCTGAATGGCTTCCTGGTAG
RPL13A (89)	Sense	Exon 6	GATATAATTGACACTGGCAA
	Antisense	Exon 6-7	AGCAAGCTTGCGACCTTGA
TBP (112)	Sense	Exon 4-5	TAATCCCAAGCGGTTTGCTG
	Antisense	Exon 5-6	CTGTTCTTCACTCTTGGCTC

2.4. Splicing reverse transcriptase-polymerase chain reaction

Splicing RT-PCR was used to identify alternative splice forms in cognitive series DLPFC (BA46) cDNA (see 2.3.1). RNA extraction, RNA quantification, and cDNA synthesis were performed as for qRT-PCR (see 2.3.2 and 2.3.3). Amplification was carried out in 25 µl reaction volumes using MolTaq polymerase (Molzym, Germany), according the manufacturer's instructions. For each reaction, 10x Taq buffer was mixed with enhancer solution, dNTPs (to 0.2 mM for each dNTP), forward and reverse primers (each to 600 nM), and 1U Taq polymerase. This mixture was then made up to 23 µl with mqH_2O and pipetted into a 96-well plate. 2 µl of IPD/control BA46 cDNA sample, positive control (P27/00 cerebellum cDNA), or negative control (mqH_2O) was added to the relevant wells. The plate was cycled as follows and then 6 µl of each reaction resolved on 3% agarose gels:

94ºC for 2 minutes
94ºC for 1 minute
62ºC for 1 minute
72ºC for 1 minute
} 30 cycles
72ºC for 7 minutes

Splicing RT-PCR Primers were designed based on information available from Ensembl (release 41 from October 2006), and BLASTed in Ensembl to ensure the production of a single predicted amplicon. Splicing RT-PCR primer sequences were as follows (predicted amplicon size in brackets after gene name; sense and antisense opposite to direction of transcription; annealing location in brackets after primer sequence):

DUSP6 (193 bp):

Sense	5'- TACCTGGAAGATGAAGCCCG -3'	(exon 1-3)
Antisense	5'- GCAGCTGACCCATGAAGTTG -3'	(exon 1)

2.5. Deoxyribonucleic acid sequencing

2.5.1. Case and control samples

Deoxyribonucleic acid sequencing was employed to identify mutations in familial Parkinson's disease (FPD) cases. Blood samples from FPD patients (n = 82) and control individuals (n = 83) were used for this purpose. All samples had been obtained previously with informed consent from individuals almost exclusively of European ancestry. FPD patients had been diagnosed clinically with PD and possessed at least one first-degree relative also diagnosed clinically with PD. Control individuals had been confirmed clinically as free of any neurological condition. No further clinicopathological information was available for these individuals. Where available, blood samples acquired from first-degree relatives were used to ascertain whether novel mutations segregated with FPD. Genomic DNA extraction and quantification had been performed by members of the NHNN Neurogenetics Service team using a similar protocol as that employed for SNP genotyping (see 2.6.2).

2.5.2. Sequencing polymerase chain reaction and cleanup

Sequencing PCR was carried out in 25 µl reaction volumes using MolTaq polymerase (Molzym, Germany), according the manufacturer's instructions. For each reaction, 10x Taq buffer was mixed with enhancer solution, dNTPs (to 0.2 mM for each dNTP), forward and reverse primers (each to 600 nM), and 1U Taq polymerase. This mixture was then made up to 24 µl with mqH_2O and pipetted into a 96-well plate. 50 ng PD/control gDNA sample or 1 µl of negative control (mqH_2O) was added to the relevant wells. The plate was cycled as follows:

61.5ºC

94ºC for 2 minutes

94ºC for 30 seconds
61.5ºC for 45 seconds
72ºC for 45 seconds
} 30 cycles

72ºC for 7 minutes

Table 2.5 show the sequencing PCR primer sequences. In order to demonstrate that PCR had occurred successfully, 5 µl of each reaction was resolved on 3% agarose gels. PCR reaction cleanup was performed using 96-well MultiScreen PCR Cleanup Filter plates (Millipore, UK), according to the manufacturer's instructions. For each reaction, the remaining 20 µl was mixed with 80 µl mqH_2O and added to a PCR Cleanup Filter plate. The mixture was then pulled through the filter using a vacuum manifold. The cleaned PCR product was resuspended in 30 µl mqH_2O by shaking at room temperature for 15 minutes and stored at –20ºC.

Amplicon (size in bp)	Primer	Primer sequence (5' to 3')
Upstream (531)	Sense	**TGTAAAACGACGGCCAGT**GGGAGGGGAGGGTTAAGG
	Antisense	**CAGGAAACAGCTATGACC**GCGAGGCAGCTCCTCAAT
1A (504)	Sense	**TGTAAAACGACGGCCAGT**TCATCAACACAACCTGTTCCA
	Antisense	**CAGGAAACAGCTATGACC**TAATTCCGCCTCGCCTTAC
1B (432)	Sense	**TGTAAAACGACGGCCAGT**GAGAGAGATTCATTGACACTAAGAGC
	Antisense	**CAGGAAACAGCTATGACC**CACGTTGATGGCCGACTC
1C (493)	Sense	**TGTAAAACGACGGCCAGT**GAAATGGCGATCAGCAAGAC
	Antisense	**CAGGAAACAGCTATGACC**TGAGCGGAGCAGAGGTATTT
2 (535)	Sense	**TGTAAAACGACGGCCAGT**AGATGATTGCTTTTCTCGTTCT
	Antisense	**CAGGAAACAGCTATGACC**AAATGTCAGAGCGACGACTATTA
3A (514)	Sense	**TGTAAAACGACGGCCAGT**GGGTGGTTTTCAGTCTGCTG
	Antisense	**CAGGAAACAGCTATGACC**CAGACAGCTGGTGTCATTTTG
3B (533)	Sense	**TGTAAAACGACGGCCAGT**GTCTGGCCCTTCAGCAGTT
	Antisense	**CAGGAAACAGCTATGACC**CACTGTCAAGTGATTCAAGATCAA
3C (500)	Sense	**TGTAAAACGACGGCCAGT**GAGGAGCCAAAGAGAGATTTCA
	Antisense	**CAGGAAACAGCTATGACC**GAGCCCATGATTTGGTGTCT

Table 2.5. *DUSP6* DNA sequencing PCR primer sequences.

Dual specificity phosphatase 6 DNA sequencing PCR primer sequences and generated amplicon sizes (in bp). Amplicon numbers correspond to exon numbers (in the direction of transcription). Generally only exons (including both coding regions, UTRs, and some flanking intronic sequence) were amplified. The last ~330 bp of the 3'UTR was not amplified. Where exons were too large to allow successful dideoxy sequencing in one reaction, multiple overlapping amplicons were generated separately (labelled "1A", "1B", etc.). The "Upstream" amplicon covers ~420 bp immediately upstream of the transcription start site. Sense and antisense are in terms of the direction of transcription. Bold text indicates the portion of primer sequences that are M13 tag (see 2.5.3). Primers were designed using Primer3 (Rozen and Skaletsky 2000) based on information available from Ensembl (release 45 from June 2007), and BLASTed in Ensembl to ensure the production of a single predicted amplicon. bp = base pairs; *DUSP6* = *Dual specificity phosphatase 6*; PCR = polymerase chain reaction; UTR = untranslated region.

2.5.3. Dideoxy sequencing

Dideoxy sequencing was carried out in 10 µl reaction volumes using BigDye Terminator v1.1 (Applied Biosystems, UK), according to the manufacturer's instructions. For each reaction, 1 µl BigDye Terminator v1.1 reagent was mixed with 10x BigDye buffer and either the M13 sense or antisense primer (to 350 nM) (see below). This mixture was then made up to 6.5 µl with mqH_2O and pipetted into a 96-well plate. 3.5 µl of PD/control clean sequencing PCR product was added to the relevant wells. The plate was cycled as follows and stored at –20ºC wrapped in aluminium foil:

96ºC for 10 seconds
50ºC for 5 seconds
60ºC for 4 minutes
} 25 cycles

In order to simplify the dideoxy reaction protocol, all sequencing primers possessed the relevant M13 tag sequence (sense or antisense as appropriate) at their 5'. The M13 sense primer was initially used to perform dideoxy sequencing for all *DUSP6* amplicons. Due to unclear sequencing data, the M13 antisense primer was initially utilised to sequence *DUSP6* amplicon 2. Deviations from the human reference sequence were confirmed by bidirectional resequencing in those specific samples, bringing the total coverage to 2x in the sense direction and 2x in the antisense direction. The M13 primer sequences were as follows:

Sense 5'- TGTAAAACGACGGCCAGT -3'
Antisense 5'- CAGGAAACAGCTATGACC -3'

2.5.4. Dideoxy cleanup and capillary electrophoresis

Dideoxy reaction cleanup was carried out using 96-well Dye Terminator Removal plates (Abgene, UK), according to the manufacturer's instructions. Dye Terminator Removal plates were cleared of storage buffer by centrifugation at 950 *g* at room temperature for 3 minutes. For each reaction, 10 µl dideoxy reaction was mixed with 10 µl mqH_2O and added to a pre-cleared Dye Terminator Removal plate. The mixture was pulled through the plate filter into a 96-well plate by centrifugation at 950 *g* at room temperature for 3 minutes. Cleaned dideoxy reactions were then sequenced by capillary electrophoresis using a 3730XL DNA Analyzer running the BigDye v1.1 protocol (Applied Biosystems, UK). Sequencing data was imported into SeqScape v2.5 (Applied Biosystems, UK) for analysis. Reference sequence was obtained from Ensembl (release 45 from June 2007).

2.6. Single nucleotide polymorphism genotyping

2.6.1. Case and control samples

Four different sample series were used for SNP genotyping: the two IPD association series for the purpose of SNP association analysis (see 2.10.3.2), the imaging series for the purpose of genotypic voxel-based morphometry (VBM) analysis (see 2.10.4), and the IPD cognitive series for the purpose of *cis*-acting variation analysis (see 2.10.5). All samples had been obtained previously with informed consent from individuals almost exclusively of European ancestry.

For all association studies, the IPD case groups were combinations of pathologically-diagnosed QSBBND cerebellum samples and clinically-diagnosed blood samples. These had been extracted previously by members of the NHNN Neurogenetics Service team. For the *DUSP6* and *EPHA2* association studies, the control groups were blood samples obtained from individuals who were confirmed clinically as free of any neurological condition, but who had been diagnosed with familial hypercholesterolaemia. These controls were a kind gift of Prof. Steve Humphries (Rayne Institute, University College London [UCL]), and had been extracted previously by members of Prof. Humphries' laboratory. For the *SNCA* association study, the control group was a combination of cerebellum samples confirmed neuropathologically as free of any neurological condition and blood samples obtained from individuals who were confirmed clinically as free of any neurological condition. These controls were a kind gift of Dr. Jana Vandrovcova (Rita Lila Weston Institute, UCL), and had been extracted previously Dr. Vandrovcova. Table 2.6 shows group clinical data for the IPD association study series samples.

The imaging series comprised normal control blood samples obtained from individuals who had been confirmed clinically as free of any neurological condition. These samples had been collected and extracted previously by Dr. Geoffrey Tan in our laboratory. Group demographic data for the imaging series is shown in table 2.7.

QSBBND cerebellum tissue obtained from the cognitive series was used for the *cis*-acting variation analysis (see 2.3.1). These samples had been extracted previously by members of the NHNN Neurogenetics Service team.

Table 2.6. IPD association study series clinical data.

a. *DUSP6* and *EPHA2* association series group clinical data (below). In the IPD group, 319 were brain samples and 295 were blood samples. Disease duration values for IPD blood samples were measured at a cut-off date in 2003. All of the controls were blood samples. Measures of time are in years. CON = control; IPD = idiopathic Parkinson's disease; NA = not applicable; SD = standard deviation.

Group (*n*)	% males	Statistic	Age of onset	Age of donation	Disease duration
CON (619)	49.6	Mean	NA	47.6	NA
		SD	NA	15.1	NA
IPD (614)	58.3	Mean	60.1	75.1	13.9
		SD	11.1	8.3	8.3

b. *SNCA* association series group clinical data (below). In the IPD group, 319 were brain samples and 386 were blood samples; in the CON group these counts were 94 and 478, respectively. Disease duration values for IPD blood samples were measured at a cut-off date in 2003. Measures of time are in years. CON = control; IPD = idiopathic Parkinson's disease; NA = not applicable; SD = standard deviation.

Group (*n*)	% males	Statistic	Age of onset	Age of donation	Disease duration
CON (572)	50.7	Mean	NA	38.7	NA
		SD	NA	8.2	NA
IPD (705)	58.1	Mean	57.4	72.0	14.1
		SD	12.9	11.5	8.8

Group (*n*)	% males	Statistic	Age of scan
CON (302)	45.4	Mean	31.6
		SD	12.2

Table 2.7. Imaging series demographic data.

Group demographic data for the imaging series. Age of donation is measured in years. CON = control; SD = standard deviation.

2.6.2. Genomic DNA extraction and quantification

Genomic DNA was extracted from human cerebellum samples using the Wizard Genomic DNA Purification Kit (Promega, UK), according to the manufacturer's instructions. All centrifugation steps were performed at room temperature. For each extraction, 960 µl 0.5 M EDTA was added to 4 ml Nuclei Lysis Solution and chilled on ice until cloudy. 4.8 ml of this mixture was added to a frozen piece of brain approximately 1 cm^3 in size in a 15 ml falcon tube. 140 µl proteinase K (at 20 mg/ml) was added and the tube incubated at 55ºC for 16 hours until the brain was completely digested. 24 µl RNAse Solution was added to the nuclear lysate and mixed in by inversion. The tube was incubated at 37ºC for 30 minutes and then allowed to cool to room temperature for 5 minutes. 200 µl Protein Precipitation Solution was added and the tube vortexed vigorously for 20 seconds. The tube was chilled on ice for 5 minutes and centrifuged at 12 000 *g* for 4 minutes. The supernatant was carefully transferred to a new 15 ml falcon containing 4.8 ml propan-2-ol (molecular biology grade). The tube was gently mixed by inversion to precipitate the DNA and then centrifuged at 12 000 *g* for 1 minute. The supernatant was carefully decanted and the pellet was washed by adding 4.8 ml 70% ethanol (molecular biology grade). The tube was centrifuged at 12 000 *g* for 1 minute. The ethanol was carefully aspirated and the pellet air-dried (sealed over with perforated Parafilm avoid contamination). The pellet was resuspended in 800 µl DNA Rehydration Solution and incubated at room temperature for 16 hours. The DNA solution was transferred to a sterile 2 ml screw cap O-ring tube and stored at 4ºC until further processing. DNA concentration and quality were assessed using the NanoDrop ND-1000, enabling the identification of samples contaminated with protein or other organic compounds. Sample gDNAs were diluted to 50 ng/µl and stored in 96-well plates at –20ºC or 4ºC, avoiding multiple freeze/thaw cycles. Blood gDNA extraction and quantification were carried out using a similar protocol.

2.6.3. TaqMan allelic discrimination genotyping

Allelic discrimination genotyping was carried out in 5 µl reaction volumes in 384- or 96-well Optical Reaction PCR plates using the TaqMan system (all from Applied Biosystems, UK), according to the manufacturer's instructions. IPD/control gDNA samples and negative controls (mqH_2O) were plated out and left to evaporate overnight. 2.5 ng gDNA was used for *EPHA2* SNPs; 5 ng gDNA was used for all other SNPs. For each reaction, 2.5 µl TaqMan Genotyping Master Mix was mixed with 0.125 µl of the relevant TaqMan SNP Genotyping Assay and 2.375 µl mqH_2O and pipetted into the plate, which was sealed with an Optical Adhesive Cover (Applied Biosystems, UK). The plate was cycled as follows and stored at –20ºC wrapped in aluminium foil:

95ºC for 10 minutes
92ºC for 15 seconds
60ºC for 60 seconds
} 40 cycles

Alleles were subsequently called using allelic discrimination protocols run on an Applied Biosystems 7900HT machine (384-well plates) or an Applied Biosystems 7500 machine (96-well plates) (both from Applied Biosystems, UK). Table 2.8 shows information about the SNPs interrogated by TaqMan genotyping.

Gene (chromosome)	SNP identity [DNA base ambiguity]	Chromosomal location	HapMap CEPH MAF
DUSP6 (12)	rs11105262 [C/G]	88263586	0.068
	rs770087 [A/C]*	88268904	0.150
	rs2279574 [A/C]*	88269608	0.388
	rs1689408 [C/T]	88278032	0.076
EPHA2 (1)	rs3754334 [G/A]	16324354	0.292
	rs10907223 [G/A]	16332332	0.067
	rs6603855 [T/C]	16333128	0.102
	rs2230597 [G/A]	16337260	0.412
	rs11260822 [T/C]	16358398	0.356
	rs4661717 [T/G]	16368501	0.093
SNCA (4)	rs11931074 [G/T]	90858538	0.100
	rs3822086 [C/T]	90883817	NA

Table 2.8. TaqMan allelic discrimination SNP assays.

SNPs genotyped by TaqMan allelic discrimination. SNP identities, CEPH DNA base ambiguities (positive strand), and CEPH MAFs were obtained from HapMap phase II (release 23a from March 2008). DNA base ambiguity shows the major allele first (single letter codes in accordance with the International Union of Biochemistry and Molecular Biology). Chromosomal locations are according to NCBI assembly build 36. All SNPs were genotyped using predesigned TaqMan assays, except those marked with a *, for which custom assays were designed using File Builder v3.1 (software downloaded from Applied Biosystems, UK). The rs11931074 assay was a kind gift of Dr. Anna Melchers in our laboratory. CEPH = Centre d'Étude du Polymorphisme Humain; *DUSP6 = Dual specificity phosphatase 6*; *EPHA2 = Ephrin receptor A2*; MAF = minor allele frequency; NCBI = National Center for Biotechnology Information; SNP = single nucleotide polymorphism; NA = not applicable; *SNCA = α-Synuclein*.

2.7. Structural magnetic resonance imaging

T1-weighted anatomical brain images were obtained using a Siemens 1.5 Tesla magnetic resonance imaging (MRI) scanner. Images had been acquired previously from the imaging series (see table 2.7) with informed consent. All scans were performed by Dr. Geoffrey Tan.

2.8. Expression microarray

2.8.1. Case and control sample selection

The aim of the expression microarray was to compare genome wide gene expression and alternative splicing between three groups: IPDD, IPDND, and controls. Therefore, *post mortem* QSBBND tissue obtained from cognitive series individuals was used for this purpose (see 2.3.1). However, financial constraints restricted the analysis to only a subset of the original series in only one brain region (the DLPFC [BA46]). Members of the IPD microarray series were selected based on RNA quality. Previously-extracted RNA (see 2.3.2) was assessed by capillary electrophoresis using the RNA 6000 Nano LabChip Kit on an Agilent 2100 Bioanalyzer (both from Agilent, UK). Those samples demonstrating clean 18S and 28S ribosomal RNA (rRNA) peaks and a minimum of low molecular weight degraded RNA were selected. Individual clinicopathological data and RNA quality graphs for the microarray series can be seen in table 2.9 and the Appendix, respectively. All RNA quality assessments and microarray procedures were performed by members of the Gene Microarray Centre (Institute of Child Health, UCL).

2.8.2. Microarray procedure

Genome wide expression and splicing were examined using GeneChip Human Exon 1.0 Sense Target (ST) oligonucleotide microarrays (Affymetrix, UK), according to the manufacturer's instructions. Independent probe sets span each annotated exon, enabling investigation of both differential gene expression and alternative exon splicing. Unless stated otherwise, all kits and equipment were obtained from Affymetrix, UK and tubes were kept on ice at all times. All procedures refer to the processing of one RNA sample.

Poly(A) RNA Controls were generated with the GeneChip Poly(A) RNA Control Kit and added to 2 µg total RNA, producing the Total RNA/Poly(A) RNA Controls Mix. Ribosomal RNA was reduced from the Total RNA/Poly(A) RNA Controls Mix by hybridisation and magnetic isolation using the RiboMinus Concentration Module Kit (Invitrogen, UK). Ribosomal RNA-Reduced Total RNA/Poly(A) RNA Controls Mix was cleaned and concentrated by spin column with the GeneChip In Vitro Translation (IVT) complementary RNA (cRNA) Cleanup Kit, and then eluted in ~9.8 µl RNAse-free H_2O (rfH_2O). RNA quality and rRNA reduction were assessed using the Agilent 2100 Bioanalyzer (see 2.8.1).

T7-$(N)_6$ Primers were generated with the GeneChip Whole Transcript cDNA Synthesis Kit and 500 ng added to 4 µl rRNA-Reduced Total RNA/Poly(A) RNA Controls Mix, producing the Total RNA/Poly(A) RNA Controls/T7-$(N)_6$ Primers Mix. First cycle cDNA synthesis was performed using the GeneChip Whole Transcript cDNA Synthesis Kit. First strand synthesis was carried out by mixing all of the Total RNA/Poly(A) RNA Controls/T7-$(N)_6$ Primers Mix with first strand buffer, DTT (to 10 mM), dNTPs (to 0.5 mM each dNTP), 0.5 µl RNase Inhibitor, 1 µl SuperScript II enzyme, and incubating as follows: 25ºC for 10 minutes; 42ºC for 60 minutes; 70ºC for 10 minutes; 4ºC for not more than 10 minutes. Second strand synthesis was performed by mixing all of the first strand synthesis reaction with $MgCl_2$ (to 3.5 mM), dNTPs (to 0.2 mM for each dNTP), 0.6 µl DNA Polymerase I,

0.2 µl RNase H, rfH_2O, and incubating as follows: 16ºC for 120 minutes; 75ºC for 10 minutes; 4ºC for not more than 10 minutes.

cRNA was synthesised at 37ºC for 16 hours using the GeneChip Whole Transcript cDNA Amplification Kit, cleaned and concentrated by spin column with the GeneChip Sample Cleanup Module, and then eluted in ~13.5 µl rfH_2O. RNA concentration was assessed using the NanoDrop ND-1000. Second cycle cDNA synthesis (first strand only) was carried out using the GeneChip Whole Transcript cDNA Synthesis Kit by mixing 10 µg cRNA with 4.5 µg Random Primers and rfH_2O and incubating as follows: 70ºC for 5 minutes; 25ºC for 5 minutes; 4ºC for at least 2 minutes. First strand buffer, DTT (to 10 mM), deoxyuridine triphosphate (dUTP) and dNTPs (each dNTP and dUTP to 0.625 mM), and 4.75 µl SuperScript II enzyme were mixed with the reaction and incubated as follows: 25ºC for 10 minutes; 42ºC for 90 minutes; 70ºC for 10 minutes; 4ºC for at least 2 minutes. cRNA was hydrolysed at 37ºC for 45 minutes with RNase H enzyme using the GeneChip Whole Transcript cDNA Synthesis Kit. The remaining single-stranded DNA (ssDNA) was cleaned by spin column with the GeneChip Sample Cleanup Module and eluted in ~28 µl cDNA Elution Buffer. DNA concentration was assessed using the NanoDrop ND-1000.

ssDNA fragmentation and biotin-labelling were performed using the GeneChip Whole Transcript Terminal Labeling Kit. 5.5 µg ssDNA was fragmented at 37ºC for 60 minutes with 1000 U Apurinic/Apyrimidinic endonuclease 1 (APE1) and 10 U Uracil DNA glycosylase (UDG). DNA fragmentation was assessed using the Agilent 2100 Bioanalyzer (see 2.8.1). Fragmented ssDNA was biotin-labelled at 37ºC for 60 minutes with 60 U Terminal deoxynucleotidyl transferase (TdT) and DNA Labeling Reagent (to 83 µM). Hybridisation and microarray washing and staining were carried out using the GeneChip Hybridization, Wash and Stain Kit. Fragmented and labelled ssDNA was injected into a microarray and incubated in a hybridisation oven at 60 rpm and 45ºC for 16 hours. Several cycles of washing and streptavidin-staining were performed, before scanning the microarray with a GeneChip Scanner 3000 7G.

Table 2.9. IPD microarray series individual clinicopathological data.

Individual clinicopathological data for the IPD microarray series samples (below and next page). Measures of time are in years, except PMD, which is measured in hours. COG and/or V25 scores of 1, backed up by MMSE ≤ 27 (where available), were taken as indicative of dementia. CON = control; F = female; IPD = idiopathic Parkinson's disease; IPDD = idiopathic Parkinson's disease dementia; IPDND = idiopathic Parkinson's disease no dementia; L =left; M = male; MMSE = mini mental state examination; NA = not applicable; ND = not determined; PMD = *post mortem* delay; R = right; SD = standard deviation.

Group	Brain Bank code	Sex	Brain hemisphere	Age of onset	Age of death	Disease duration	PMD	Brain pH	COG	V25	MMSE score	Time between MMSE and death
CON	C14/93	M	R	NA	74	NA	5.50	6.51	ND	ND	ND	ND
	C16/93	M	L	NA	76	NA	16.00	6.71	ND	ND	ND	ND
	C10/95	M	L	NA	72	NA	13.00	6.16	ND	ND	ND	ND
	C03/98	M	L	NA	86	NA	23.30	6.55	ND	ND	ND	ND
	C04/99	M	R	NA	91	NA	48.00	6.54	ND	ND	ND	ND
	C03/00	M	R	NA	85	NA	43.35	6.68	ND	ND	ND	ND
	C04/00	M	L	NA	81	NA	40.00	6.48	ND	ND	ND	ND
Mean	**NA**	**NA**	**NA**	**NA**	**80.7**	**NA**	**27.0**	**6.52**	**NA**	**NA**	**NA**	**NA**
SD	**NA**	**NA**	**NA**	**NA**	**7.0**	**NA**	**16.7**	**0.18**	**NA**	**NA**	**NA**	**NA**

Group (*n*)	Brain bank code	Sex	Brain hemisphere	Age of onset	Age of death	Disease duration	PMD	Brain pH	COG	V25	MMSE score	Time between MMSE and death
IPDD (7)	P24/94	M	L	53.6	64.1	10.5	23.25	6.18	1	1	13	0.8
	P62/98	M	R	48.0	72.8	24.8	27.00	6.32	0	1	26	4.6
	P30/00	M	R	61.6	77.5	15.9	28.25	6.39	0	1	24	0.2
	P54/00	M	R	58.3	74.9	16.6	51.15	5.77	ND	1	24	7.6
	P59/00	M	L	69.1	74.8	5.7	37.30	5.88	0	1	16	3.7
	P05/01	M	L	42.0	79.0	37.0	38.35	6.20	0	1	17	3.0
	P18/01	M	R	45.9	70.1	24.2	61.20	6.29	0	1	19	0.3
Mean	**NA**	**NA**	**NA**	**54.1**	**73.3**	**19.2**	**38.1**	**6.15**	**NA**	**NA**	**19.9**	**2.9**
SD	**NA**	**NA**	**NA**	**9.6**	**5.0**	**10.4**	**13.8**	**0.23**	**NA**	**NA**	**4.9**	**2.7**
IPDND (7)	P45/94	M	R	66.9	76.0	9.1	20.50	6.45	0	0	29	1.7
	P67/98	M	L	54.7	71.3	16.6	115.00	6.35	0	0	ND	ND
	P14/99	M	R	59.4	74.0	14.6	25.30	6.35	0	0	30	6.0
	P40/99	M	L	54.0	73.7	19.7	39.00	6.00	0	0	ND	ND
	P54/99	M	L	79.9	91.8	11.9	60.45	6.22	0	0	ND	ND
	P55/00	M	R	50.4	73.0	22.6	25.20	7.18	0	0	30	15.6
	P75/00	M	R	50.7	66.1	15.4	56.00	6.49	0	0	29	0.1
Mean	**NA**	**NA**	**NA**	**59.4**	**75.1**	**15.7**	**48.8**	**6.43**	**NA**	**NA**	**29.5**	**5.9**
SD	**NA**	**NA**	**NA**	**10.7**	**8.0**	**4.5**	**33.1**	**0.37**	**NA**	**NA**	**0.6**	**7.0**

2.9. Methyl-specific polymerase chain reaction

2.9.1. Case and control sample selection

The aim of the methyl-specific PCR (MSP) was to compare levels of relative CpG methylation in the *DUSP6* putative promoter (DPP) between IPD patients and control individuals. Therefore, *post mortem* DLPFC (BA46) QSBBND tissue obtained from cognitive series individuals was used for this purpose (see 2.3.1). Six IPD cases (three IPDD and three IPDND) and six control individuals were selected. This choice was based on the qRT-PCR results for *DUSP6* in the DLPFC, whereby the IPD cases had relatively high expression and the control individuals had relatively low expression. Previously-extracted blood gDNA from one hereditary motor and sensory neuropathy (HMSN) patient was used as a positive control. Table 2.10 shows individual clinicopathological data for the IPD MSP series samples.

2.9.2. Genomic deoxyribonucleic acid extraction and quantification

Genomic DNA was extracted from brain tissue using the QIAamp DNA Mini Kit (Qiagen, UK), according to the manufacturer's instructions. All centrifugation steps were performed at room temperature. Buffers AW1 and AW2 were prepared by resuspending the concentrate in 25 ml and 30 ml ethanol (molecular biology grade) respectively. For each extraction, 25 mg frozen brain was homogenised by hand in a 1.5 ml microfuge tube containing 80 µl 1x phosphate-buffered saline (PBS). 100 µl Buffer ATL and 20 µl proteinase K were added and the tube was mixed by vortexing. The tube was incubated at 56ºC for 2 hours (vortexing occasionally to disperse the sample) until the brain was completely digested. The tube was then briefly centrifuged. 200 µl Buffer AL was added and the tube was mixed by vortexing for 15 seconds. The tube was incubated at 70ºC for 10 minutes and briefly centrifuged.

200 µl ethanol (molecular biology grade) was added. The tube was mixed by vortexing for 15 seconds and briefly centrifuged. The contents of the tube (including any precipitate) were carefully applied to a QIAamp Mini spin column (in a 2 ml collection tube), which was then centrifuged at 6000 *g* for 1 minute. The collection tube was discarded and replaced with a fresh collection tube. The column was washed by adding 500 µl Buffer AW1, before being centrifuged at 6000 *g* for 1 minute. The flow-through was discarded. 500 µl Buffer AW2 was added to the column, which was centrifuged at 20 000 *g* for 3 minutes. The collection tube was emptied and returned to the column, which was then cleared of residual wash buffer by centrifugation at 20 000 *g* for 1 minute. The column was placed in a clean 1.5 ml microfuge tube. 100 µl Buffer AE was added to the column, which was incubated at room temperature for 5 minutes. DNA in solution was eluted by centrifugation at 6000 *g* for 1 minute. The addition of Buffer AE and subsequent centrifugation were repeated twice to increase DNA yield. DNA concentration and quality were assayed using the NanoDrop ND-1000, enabling the identification of samples contaminated with protein or other organic compounds. Sample gDNAs were stored at –20ºC or 4ºC, avoiding multiple freeze/thaw cycles.

Group	Brain bank code	Sex	Brain hemisphere	Age of onset	Age of death	Disease duration	PMD	Brain pH	COG	V25	MMSE score	Time between MMSE and death
CON	C14/93	M	R	NA	74	NA	5.50	6.51	ND	ND	ND	ND
	C16/93	M	L	NA	76	NA	16.00	6.71	ND	ND	ND	ND
	C10/95	M	L	NA	72	NA	13.00	6.16	ND	ND	ND	ND
	C04/99	M	R	NA	91	NA	48.00	6.54	ND	ND	ND	ND
	C03/00	M	R	NA	85	NA	43.35	6.68	ND	ND	ND	ND
	C04/00	M	L	NA	81	NA	40.00	6.48	ND	ND	ND	ND
Mean	**NA**	**NA**	**NA**	**NA**	**79.8**	**NA**	**27.6**	**6.51**	**NA**	**NA**	**NA**	**NA**
SD	**NA**	**NA**	**NA**	**NA**	**7.3**	**NA**	**18.2**	**0.20**	**NA**	**NA**	**NA**	**NA**
IPDD	P24/94	M	L	53.6	64.1	10.5	23.25	6.18	1	1	13	0.8
	P30/00	M	R	61.6	77.5	15.9	28.25	6.39	0	1	24	0.2
	P18/01	M	R	45.9	70.1	24.2	61.20	6.29	0	1	19	0.3
IPDND	P45/94	M	R	66.9	76.0	9.1	20.50	6.45	0	0	29	1.7
	P40/99	M	L	54.0	73.7	19.7	39.00	6.00	0	0	ND	ND
	P54/99	M	L	79.9	91.8	11.9	60.45	6.22	0	0	ND	ND
Mean	**NA**	**NA**	**NA**	**60.3**	**75.5**	**15.2**	**38.8**	**6.26**	**NA**	**NA**	**NA**	**NA**
SD	**NA**	**NA**	**NA**	**12.0**	**9.3**	**5.9**	**18.2**	**0.16**	**NA**	**NA**	**NA**	**NA**

Table 2.10. IPD MSP series individual clinicopathological data.

Individual clinicopathological data for the MSP series samples. Measures of time are in years, except PMD, which is measured in hours. COG and/or V25 scores of 1, backed up by MMSE $\leq$ 27 (where available), were taken as indicative of dementia. CON = control; F = female; IPD = idiopathic Parkinson's disease; IPDD = idiopathic Parkinson's disease dementia; IPDND = idiopathic Parkinson's disease no dementia; L =left; M = male; MSP = methyl-specific polymerase chain reaction; MMSE = mini mental state examination; NA = not applicable; ND = not determined; PMD = *post mortem* delay; R = right; SD = standard deviation.

2.9.3. Bisulphite conversion and cleanup

Sample gDNA was bisulphite-converted and cleaned using the EpiTect Bisulphite Kit (Qiagen, UK), according to the manufacturer's instructions. All centrifugation steps were performed at room temperature. Buffers BW and BD were prepared by adding 30 ml and 27 ml ethanol (molecular biology grade) respectively. Bisulphite Mix was prepared by resuspending the concentrate in 800 µl rfH_2O and vortexing vigorously until completely dissolved. For each conversion, 500 ng sample gDNA was pipetted into a 96-well plate and made up to 20 µl with rfH_2O. 85 µl Bisulphite Mix was added, followed by 25 µl DNA Protect Buffer. The plate was sealed and vortexed vigorously, before being briefly centrifuged. The plate was then incubated as follows: 99ºC for 5 minutes; 60ºC for 25 minutes; 99ºC for 5 minutes; 60ºC for 85 minutes; 99ºC for 5 minutes; 60ºC for 175 minutes; 20ºC overnight. The plate was centrifuged briefly and the reaction transferred to a 1.5 ml microfuge tube. 560 µl Buffer BL was added and the mixture was vortexed and briefly centrifuged, before being carefully applied to an EpiTect spin column (with collection tube). The column was centrifuged at 20 000 *g* for 1 minute and the flow-through discarded. Converted DNA was washed by adding 500 µl Buffer BW and centrifuging at 20 000 *g* for 1 minute. The flow-through was discarded. DNA desulphonation was achieved by adding 500 µl Buffer BD and incubating at room temperature for 15 minutes, followed by centrifugation at 20 000 *g* for 1 minute. The flow-through was discarded. DNA was washed a further two times by adding 500 µl Buffer BW, centrifuging at 20 000 *g* for 1 minute, and discarding the flow-through. The column was cleared of residual wash buffer by centrifugation at 20 000 *g* for 5 minutes. The column was placed in a clean 1.5 ml microfuge tube. 20 µl Buffer EB was added to the column and DNA in solution was eluted by centrifugation at 15 000 *g* for 1 minute. DNA yield was increased by adding a further 20 µl Buffer EB to the column and centrifuging it at 20 000 *g* for 1 minute. DNA concentration and quality were assayed using the NanoDrop ND-1000, enabling the identification of samples contaminated with protein or other organic compounds. Clean bisulphite-converted sample gDNA was stored at –20ºC.

2.9.4. Methyl-specific polymerase chain reaction procedure

Reactions was carried out in 15 µl volumes using HotStarTaq Plus polymerase (Qiagen, UK), according the manufacturer's instructions with guidance from a published protocol (Herman *et al.* 1996). Two different E Twenty-Six (ETS) family binding sites in the DPP were interrogated with regard to their CpG methylation status. Bisulphite-converted gDNA from each individual was subjected to two separate amplification reactions at each site, achieved using different combinations of primers. One reaction was specific for methylated alleles, while the other was specific for unmethylated alleles. For each reaction, 10x Taq buffer was mixed with Q solution, dNTPs (to 1.25 mM for each dNTP), forward and reverse primers (each to 1 µM), and 1U HotStarTaq Plus polymerase. This mixture was then made up to 11 µl with mqH_2O and pipetted into a 96-well plate. 4 µl of IPD/control bisulphite-converted BA46 gDNA sample, positive control (bisulphite-converted HMSN blood gDNA), or negative control (mqH_2O) was added to the relevant wells. The plate was cycled as follows:

ETS1-binding site A

95ºC for 5 minutes
94ºC for 30 seconds
48ºC for 30 seconds
72ºC for 45 seconds } 40 cycles
72ºC for 10 minutes

ETS1-binding site B

95ºC for 5 minutes
94ºC for 30 seconds
51ºC for 30 seconds
72ºC for 45 seconds } 35 cycles
72ºC for 10 minutes

Table 2.11 shows the primer sequences for each MSP reaction at each location in the DPP. 13 µl of each reaction was resolved on 3% agarose gels.

ETS binding site (distance relative to *DUSP6* TSS in bp)	Amplicon size (bp)	Primer (M/U allele specificity)	Primer sequence (5' to 3')
A (-192)	95	Sense (M)	CTAAAATACCCTAATTTATATACCCTACTC
		Antisense (M)	AAATAAGTTGTAATAGCGGGTTCGGC
	99	Sense (U)	CTAAAATACCCTAATTTATATACCCTACTC
		Antisense (U)	GTGTAAATAAGTTGTAATAGTGGGTTTGG
B (-136)	194	Sense (M)	GTATTGGGGTTTATTCGGAGC
		Antisense (M)	AAACAACTCCTCAATAAATACAAACAA
	197	Sense (U)	TTTGTATTGGGGTTTATTTGGAGT
		Antisense (U)	AAACAACTCCTCAATAAATACAAACAA

Table 2.11. MSP primer sequences.

MSP primers sequences and generated amplicons sizes (in bp). The numbers in the first column represent the distance between the relevant DPP ETS binding site and the TSS of *DUSP6* (negative values indicate that the sites are upstream in the direction of transcription) (see also figure 4.11). Primers were designed using MethPrimer (Li and Dahiya 2002) based on information available from Ensembl (release 48 from December 2007). For site B, sense and antisense are in terms of the direction of transcription, whereas for site A, the opposite is true (note that *DUSP6* is transcribed from the negative strand). To reduce variability, one primer was common to the methylated allele-specific and unmethylated allele-specific reaction for each ETS binding site: this was the sense primer for site A, and the antisense primer for site B. bp = base pairs; *DUSP6* = *Dual specificity phosphatase 6*; DPP = *DUSP6* putative promoter; ETS = E Twenty-Six; MSP = methyl-specific polymerase chain reaction; M = methylated; TSS = transcriptional start site; U = unmethylated.

2.10. Data analysis

2.10.1. Multiple testing correction methodology

In order to reduce the chance of statistical false positives, correction for multiple testing was employed throughout this thesis. The Bonferroni approach was mostly used, although family-wise error (FWE) and the less severe false discovery rate (FDR) were selected for the genotypic VBM (see 2.10.4) and expression microarray analyses (see 2.10.6.1), respectively [reviewed in (Shaffer 1995)]. In addition, the *in silico* microarray mining results (see 2.10.6.3) were uncorrected due to prior hypothesis (Rothman 1990). The overall Bonferroni strategy was to correct within each experimental type on a chapter-by-chapter basis e.g. correcting across all the qRT-PCR statistical tests in chapter 3 (i.e. cognitive expression analysis, *DUSP6* full length [FL] and 1:3 expression analysis, *DUSP6* expression mapping analysis, *DUSP6 cis*-acting variation analysis) generated a correction factor of 45.

2.10.2. Quantitative reverse transcriptase-polymerase chain reaction

2.10.2.1. Raw data processing and normalisation

Quantitative RT-PCR (see 2.3.4) raw expression data were generated with Applied Biosystems 7500 System Software v1.4 (Applied Biosystems, UK). The standard curve method was employed, which entails the use of said curves to generate raw expression values from C_t values (Giulietti *et al.* 2001). If the standard curve $r^2 < 0.95$, outlying standard curve data points were removed before reanalysis. Dissociation curves were checked to ensure the existence of only one PCR product above the data acquisition temperature, or the relevant data points were excluded from the analysis. Triplicates were examined to ensure that the C_t standard deviation

(SD) < 0.5 (or that the C_t of two replicates differed by < 0.5) for each sample, or the relevant sample was excluded from the analysis. The arithmetic mean of the raw expression values for each triplicate was calculated and used as the raw expression value for that sample.

Potential reference genes were selected based upon statistical modelling performed on experimental gene expression data (Szabo *et al.* 2004). For each brain region, the expression of multiple reference genes was quantified and raw data processed as above. The geometric mean of the raw expression values for these reference genes was calculated on a sample-by-sample basis; this value was termed the normalisation factor (NF) (Vandesompele *et al.* 2002). In certain instances, geNorm v3.5 was used to generate optimal sets of reference genes. It achieves this by calculating the average pairwise variation of a particular reference gene with all other reference genes (the stability measure, *M*). The optimal set contains those reference genes that are most stable across all samples i.e. that have the lowest *M* values (Vandesompele *et al.* 2002). Expression data was normalised on a sample-by-sample basis, by dividing the raw target gene expression value by the NF. As each qRT-PCR run comprised two plates, the mean of this normalised dataset was calculated, and each value divided by the mean in order to distribute the values around 1, producing a set of final relative expression data for each target gene in each brain region. NF group mean and 95% confidence interval (CI) values were calculated and examined to ensure comparability of final relative target gene expression between disease groups.

2.10.2.2. Idiopathic Parkinson's disease cognitive and mapping expression analyses

Final relative expression data were imported into SPSS v12.0.1 (SPSS Inc., USA) for statistical analysis. Data were grouped according to sample type (IPDD, IPDND, IPD, or control) and analysed on a gene-by-gene and region-by-region basis. Clustered boxplots were drawn, and extreme outliers (datapoints further than three

SD from the group mean) were removed from the analysis. Shapiro-Wik and Kolmogorov-Smirnov tests were used to check the data for normality. Given that the data for almost all genes were found not to exhibit normal distribution, two-tailed Mann-Whitney tests were used to analyse qRT-PCR expression data throughout this thesis. Bonferroni-corrected p values ≤ 0.05 were taken as significantly different. Mean expression with 95% CI was plotted in Excel (Microsoft, USA), as appropriate.

Groups were also compared with regard to age of onset, age of death, disease duration, *post mortem* delay (PMD), brain pH, and MMSE, as appropriate. This was performed according to the method outlined above, except that three group comparisons were carried out by two-tailed Kruskal-Wallis test. Bonferroni-corrected p values ≤ 0.05 were taken as significantly different. *Post hoc* statistical power calculations were carried out using an online tool, as appropriate (www.stat.ubc.ca/~rollin/stats/ssize/n2.html). In one instance, clinicopathological data were correlated using the two-tailed Spearman's rho coefficient, and scatter plots were generated. Bonferroni-corrected p values ≤ 0.05 were taken as significantly different.

2.10.3. Idiopathic Parkinson's disease single nucleotide polymorphism association

2.10.3.1. Haplotype tagging

Haplotype tagging SNPs (htSNPs) were generated as follows. Genotypes of common (minor allele frequency [MAF] ≥ 0.05) polymorphic SNPs were downloaded for Centre d'Étude du Polymorphisme Humain (CEPH) trios (Utah residents with ancestry from northern and western Europe) from HapMap phase II (release 23a from March 2008) (Frazer *et al.* 2007). Pairwise tagging was performed using Tagger (de Bakker *et al.* 2005) in Haploview v4.0 (Barrett *et al.* 2005), ensuring that the average

locus haplotype $r^2 \geq 0.8$. Linkage disequilibrium (LD) plots were generated using Haploview.

2.10.3.2. Single nucleotide polymorphism association analysis

Single nucleotide polymorphisms were genotyped by TaqMan allelic discrimination (see 2.6.3). Genotypic data were grouped according to disease status (IPD or control) and imported into Haploview v4.0 for statistical analysis on a gene-by-gene basis. Two-tailed exact tests were employed to identify deviations from the Hardy-Weinberg equilibrium (HWE) (Wigginton *et al.* 2005). Uncorrected p values ≤ 0.05 were taken as significant deviation from HWE. Haplotypes were inferred using an accelerated expectation-maximisation (EM) algorithm similar to the partition-ligation method (Qin *et al.* 2002), as appropriate. Statistical assessments of allelic and haplotypic association were carried out by two-tailed χ^2 test under a multiplicative model. This states that the genotype relative risk of one homozygote is the square of genotype relative risk of the heterozygote, if the other homozygote is taken as reference (Lewis 2002). Bonferroni-corrected p values ≤ 0.05 were taken as significantly different. Odds ratios (ORs) with 95% confidence interval (CI) were estimated based on the null hypothesis (also known as the Peto OR) using an online calculator (Bland and Altman 2000). *Post hoc* statistical power calculations were carried out using the CaTS software, as appropriate (Skol *et al.* 2006).

2.10.4. Genotypic voxel-based morphometry

Single nucleotide polymorphisms were genotyped by TaqMan allelic discrimination (see 2.6.3). Deviation from HWE was assessed in Haploview (see 2.10.3.2). Genotypic VBM analysis (Ashburner and Friston 2000) was carried out using the statistical parametrical mapping 5 (SPM5) software package (Functional Imaging

Laboratory, Institute of Cognitive Neuroscience, UCL) on Matlab 7 (The Mathworks, USA) by Dr. Geoffrey Tan. MRI images were segmented using a unified segmentation procedure (Ashburner and Friston 2005) to obtain grey matter probability maps, spatially normalised into Montreal Neurological Institute (MNI) space with a fast diffeomorphic algorithm (Ashburner 2007), and modulated and smoothed with a 12 mm full width at half maximum (FWHM) isotropic Gaussian kernel. Individuals were grouped by SNP genotype, and the groups subjected to voxel-wise comparisons of grey matter density, based on a generalised linear model. Brain regions of interest (ROIs) were selected based on differential expression in the expression analyses (see 2.10.2.2), expression in the mouse brain according to the Allen Mouse Brain Atlas (Lein *et al.* 2007), or a well-established role in IPD [reviewed in (Lees *et al.* 2009)]. Brain ROIs were used to generate a mask, which was applied to the data, producing the ROI analysis. The global analysis was subsequently generated by examining changes in grey matter density across the entire brain unconstrained by prior hypothesis. Statistical comparisons were performed by two-tailed *t* test, with significance set at corrected $p < 0.05$. The FWE approach was employed in accordance with random field theory to correct for multiple testing across the brain [reviewed in (Shaffer 1995)]. Associated regions were located based on their MNI coordinates using the WFU PickAtlas tool (Lancaster *et al.* 2000; Maldjian *et al.* 2003) in Matlab 7.

2.10.5. *Cis*-acting variation analysis

Single nucleotide polymorphisms were genotyped by TaqMan allelic discrimination (see 2.6.3). Deviation from HWE was assessed in Haploview (see 2.10.3.2). Final relative expression data (see 2.10.2.1) were grouped by genotype and imported into SPSS v12.0.1 for statistical analysis. Extreme outliers were removed as in the cognitive and mapping expression analyses (see 2.10.2.2). If the SNP MAF was so low that the minor allele homozygote group only comprised a few individuals, this group was removed from the analysis. Groups were compared by two-tailed Mann-

Whitney or Kruskal-Wallis test. Bonferroni-corrected p values ≤ 0.05 were taken as significantly different.

2.10.6. Idiopathic Parkinson's disease cognitive expression microarray analysis

2.10.6.1. Data preprocessing, quality control, and analysis

Expression microarray data was analysed in R v2.5.0 using the Bioconductor v2.0 package Linear Modelling for Microarray Analysis (LIMMA) (Gentleman *et al.* 2004). Analysis was performed at both the exon and gene levels. Data preprocessing was conducted using the robust multichip average (RMA) algorithm (Irizarry *et al.* 2003), which consisted of three steps: background correction, summarisation, and normalisation. In background correction, probes were adjusted (array by array) using a global model of probe intensity distribution. This removed cross-hybridising probesets. Summarisation used the median polish algorithm to combine data from several probes and generate exon and gene expression values. In the case of exon level analysis, summarisation combined the multiple probe intensities for each probeset to produce a single expression value for each exon. In the case of gene level analysis, multiple probeset (exon) intensities were combined to produce a single expression value for each transcript cluster (gene). Mapping between probesets and transcript clusters was based on 17817 "core" RefSeq and full length Genbank mRNAs (obtained previously from the National Center for Biotechnology Information). Quantile normalisation was employed to adjust the probeset intensity distributions, thus making microarrays comparable with each other.

Microarray data quality control (QC) analysis was carried out to evaluate the extent to which valid conclusions could be drawn from the data. Receiver operator curves were plotted to assess how well the summarisation method separated exonic (positive) and intronic (negative) controls present on each array. Pairwise microarray

total fluorescence correlations were calculated, in order to identify chips outlying the others and evaluate overall array performance. RNA and technique quality were assessed by plotting intensity distribution histograms. MvA scatter plots were generated to gauge variation between biological replicates (i.e. samples in the same group).

Log_2 exon and gene expression were compared between the various groups (IPDD, IPDND, and controls) by modified *t* test incorporating Bayesian statistics. For the exon level analysis, log_2 probeset intensities were first normalised by log_2 transcript cluster intensities to control for differential expression at the gene level. For both levels, low expressing probesets and transcripts were then filtered out, and intergroup fold change and *p* values were calculated. The FDR approach was used for multiple testing correction, with $p < 0.05$ taken as significantly different (Benjamini and Hochberg 1995). Given the high levels of biological variation, uncorrected $p < 0.01$ was employed as the significance threshold for identifying microarray hits (see 4.3.2). For the gene level analysis, principal components analysis plots were generated. All microarray data analyses up to this point were performed by Dr. Sonia Shah at the Bloomsbury Centre for Bioinformatics (UCL). Groups were also compared with regard to age of onset, age of death, disease duration, PMD, brain pH, and MMSE (as appropriate), according to the procedure outlined for the cognitive and mapping expression analyses (see 2.10.2.2). Bonferroni-corrected *p* values ≤ 0.05 were taken as significantly different.

2.10.6.2. Confirmation and validation

Differential gene expression and alternative exon splicing events detected by the microarray were confirmed using the NetAffx (Liu *et al.* 2003) and X:Map (Yates *et al.* 2008) databases. Dysregulation events involving expression below the signal-noise cut-off point (5 units on the log_2 fluorescence scale) were excluded from further analysis. Gene ontology (GO) terms (release 24th January 2010) associated with

confirmed microarray hits were collected (Ashburner *et al.* 2000). Validation by qRT-PCR was then attempted (see 2.3.4 and 2.10.2).

2.10.6.3. *In silico* data mining

The following bioinformatic resources were consulted to obtain lists of candidate genes: BioGRID, Kyoto Encyclopaedia of Genes and Genomes (KEGG), Online Mendelian Inheritance in Man (OMIM), PROMO (set to a maximum dissimilarity rate of 1%), Ensembl (release 48 from December 2007), and University of California Santa Cruz (UCSC) PhyloP (assembly hg18) (Kanehisa and Goto 2000; Messeguer *et al.* 2002; Siepel *et al.* 2006; Stark *et al.* 2006; Hubbard *et al.* 2007). NetAffx was used to obtain transcript cluster identities for these candidates, and $\log_2$ microarray data were mined *in silico*. Groups were then compared for candidate gene expression according to the procedure outlined for the cognitive and mapping expression analyses (see 2.10.2.2), except that statistical comparisons were carried out by *t* test or Mann-Whitney test (depending on distribution normality), and *p* values were not corrected for multiple testing because of prior hypothesis (Rothman 1990). Uncorrected $p \leq 0.05$ were taken as significantly different. Selected hits arising from the microarray data mining were validated by qRT-PCR (see 2.3.4 and 2.10.2).

2.10.7. Identification of putative functional variants

2.10.7.1. Elucidation of linkage disequilibrium

Haploview was used to elucidate and plot fine scale pairwise r^2 LD relationships in the *SNCA* locus. This was based on SNP genotype data obtained for the *SNCA* IPD association study (see 2.10.3.2) and SNP genotype data obtained previously by Dr. Coro Paisán-Ruíz, from the laboratory of Dr. Andrew Singleton.

2.10.7.2. *In silico* data mining

Single nucleotide polymorphisms putatively driving genetic association were identified as follows. CEPH trio LD data for all the polymorphic SNPs in a defined ROI was downloaded from HapMap phase II (release 23a from March 2008). The UCSC (assembly hg18 from March 2006) PhyloP database was mined for predicted interspecies DNA sequence conservation across 32 placental mammals at these SNP positions. PhyloP computes predicted conservation based on a phylogenetic hidden Markov model. Sites predicted to be conserved are assigned positive scores, whereas sites predicted to be fast-evolving are assigned negative scores. The absolute values represent –log *p* values under a null hypothesis of neutral evolution. The literature was mined for Caucasian and Asian IPD genetic association data pertaining to SNPs residing at positions assigned a positive score by PhyloP (Mueller *et al.* 2005; Mizuta *et al.* 2006; Ross *et al.* 2007a; Westerlund *et al.* 2008; Winkler *et al.* 2007), and SNPs displaying association with IPD were considered as putative functional variants.

Chapter 3: Idiopathic Parkinson's disease cognitive expression analysis and genetic characterisation of *Dual specificity phosphatase 6*

3.1. Introduction

Parkinson's disease (PD) is an incurable neurodegenerative disorder characterised clinically by bradykinesia, rigidity, resting tremor, and postural instability. Its neuropathological hallmarks are dopaminergic cell death in the substantia nigra (SN) and cytoplasmic protein aggregates called Lewy bodies (LBs), of which accumulated α-synuclein is a major component [reviewed in (Lees *et al.* 2009)]. PD is frequently accompanied by dementia, and point prevalence is estimated to be 24-31% (Aarsland *et al.* 2005b). Parkinson's disease dementia (PDD) is defined as a progressive dysexecutive syndrome that impedes daily life. Its neuropsychological features are marked deficits in working memory (WM), attention, verbal fluency, and visuospatial ability. These symptoms are often accompanied by declarative memory impairment and behavioural disturbances [reviewed in (Goetz *et al.* 2008)]. There is much controversy over the neuropathological basis of PDD. For example, dementia in PD has been significantly correlated with cortical LB load, cortical Alzheimer pathology severity, subcortical neuronal loss, and the degree of limbic system pathology (Aarsland *et al.* 2005a; Zweig *et al.* 1993; Bancher *et al.* 1993; Kalaitzakis *et al.* 2009a).

Monogenic mutation accounts for 5-10% of PD. Similarities between these familial Parkinson's disease (FPD) patients and the majority of cases, which are known as idiopathic Parkinson's disease (IPD), suggest that they involve common molecular mechanisms [reviewed in (Schiesling *et al.* 2008)]. Mutations or multiplications in

α-Synuclein (*SNCA*), *β-Synuclein* (*SNCB*), and *Leucine-rich repeat kinase 2* (*LRRK2*) can cause familial forms of PDD and the related condition dementia with Lewy bodies (DLB) (Zarranz *et al.* 2004; Ross *et al.* 2008a; Ohtake *et al.* 2004; Healy *et al.* 2008). Moreover, genetic variation in *β-Glucocerebrosidase* (*GBA*), *Microtubule-associated protein tau* (*MAPT*), and *Apolipoprotein E* (*APOE*) can significantly alter the susceptibility to cognitive impairment and/or dementia in IPD (Sidransky *et al.* 2009; Williams-Gray *et al.* 2009a; de Lau *et al.* 2005). Importantly, several of these mutations and polymorphisms appear to influence gene expression in the human brain (Farrer *et al.* 2004; Williams-Gray *et al.* 2009a; Bray *et al.* 2004).

In the current literature, only two reports specifically compare gene expression in IPD with and without dementia. Genes encoding G-protein-coupled receptor kinases (GRKs) and arrestins are significantly overexpressed in the striatum of demented IPD patients contrasted against their nondemented counterparts (Bychkov *et al.* 2008). This is relevant to IPD as GRK-induced phosphorylation of SNCA at Ser129 may promote its accumulation and neurotoxicity *in vivo* (Chen and Feany 2005; Ihara *et al.* 2007). The only published microarray study comparing IPD with and without dementia demonstrated that numerous genes are differentially-expressed in posterior cingulate cortex (PCC) neurons. The findings indicate that idiopathic Parkinson's disease dementia (IPDD) is associated with dysregulation of molecular pathways encompassing mitochondrial function, inflammation, cell adhesion, ribonucleic acid (RNA) splicing, and axonal transport (see 4.1 for more details) (Stamper *et al.* 2008).

Working memory impairment is a central facet of the IPDD dysexecutive syndrome. Two brain regions involved in WM amongst normal controls have also been implicated in IPD cognitive dysfunction: Brodmann area 46 (BA46) in the dorsolateral prefrontal cortex (DLPFC), and the angular gyrus (AG [BA39]) in the inferior parietal cortex (IPC). The DLPFC plays a role in the monitoring and manipulation of items held in WM (Petrides 2000). Targeting the DLPFC with either repetitive transcranial magnetic stimulation (rTMS) or transcranial direct current stimulation (tDCS) significantly improves WM ability in nondemented IPD patients

(Boggio *et al.* 2005; Boggio *et al.* 2006). Moreover, significantly greater atrophy of BA46 is observed in demented compared to nondemented IPD cases (Nagano-Saito *et al.* 2005). The AG is involved in numerical and verbal WM (Gruber *et al.* 2001; Dronkers *et al.* 2004). Cerebral blood flow (CBF) is significantly reduced in the AG of IPDD patients contrasted against controls (Firbank *et al.* 2003). As yet, no studies have investigated IPDD gene expression in these two brain regions.

In summary, PDD is characterised by executive dysfunction, including deficits in WM. Some of the mutations and polymorphisms implicated in familial and idiopathic PDD appear to influence gene expression in the human brain. Very few studies have investigated gene expression in IPDD, and to date none have examined the DLPFC and AG, two areas known to play a role in WM.

3.2. Aims and methodology

Based on the background literature, it was hypothesised that there might be a relationship between IPD dementia status and target gene expression in the DLPFC and/or AG, and that target gene single nucleotide polymorphism (SNP) variation might influence IPD risk and gene expression. Therefore, the aims and methodology of this chapter were as follows:

1. **Identify genes implicated in IPD dementia and/or neurodegeneration.**
   Sybr Green quantitative reverse transcriptase-polymerase chain reaction (qRT-PCR) (see 2.3.4) was employed to compare the messenger RNA (mRNA) expression of 10 target genes in complementary DNA (cDNA) generated (see 2.3.3) from the IPD cognitive series (idiopathic Parkinson's disease dementia [IPDD]; idiopathic Parkinson's disease no dementia [IPDND]; controls) DLPFC (BA46) and AG (BA39) (see 2.3.1). This was called the IPD cognitive expression analysis (see 2.10.2.2). The three group study design enabled the discrimination of expression signatures associated with specific IPD subtypes i.e. IPD dementia, IPD neurodegeneration, or both (see figure 3.1). Membership in the IPDD or IPDND group was assigned based on reported cognitive impairment and/or change in personality. This was backed up by mini mental state examination (MMSE) scores where available; MMSE $\leq$ 27 was taken as indicative of dementia (see 2.3.1). The DLPFC and AG were selected because of their involvement in WM and IPDD (see 3.1). Target genes were selected based on a connection to working or long term memory (see 3.3.1). In order to control for neuronal cell death and/or gliosis in IPD samples and for technical variation, target gene expression data were normalised with a normalisation factor (NF) calculated as the geometric mean of two reference genes: *Ribosomal protein L13A* (*RPL13A*) and *TATA box binding protein* (*TBP*) (see 2.10.2.1). Only those targets exhibiting significant differential expression underwent further characterisation. For confirmatory purposes, a second batch of DLPFC cDNA (batch 2) was generated from the same RNA samples. For batch 2, target gene expression data

were normalised with a NF calculated from the reference genes *Glucose-6-phosphate dehydrogenase* (*G6PD*), *RPL13A*, and *TBP*. This was termed "total" expression. As an alternative approach to correct for neuronal cell death, "neuronal loss-corrected" (NLC) target gene expression data were normalised with a neuronal marker acting as the reference gene (Fuchs *et al.* 2008). *Neurofilament H* (*NEFH*) was selected for this purpose (Goldstein *et al.* 1983; Schulz *et al.* 2003; Lariviere and Julien 2004; Cahoy *et al.* 2008). Where appropriate, splicing reverse RT-PCR was undertaken (with the products resolved on agarose gels) (see 2.4) and splice form-specific qRT-PCR reactions were performed (see 2.3.4). Statistical comparisons were carried out by Mann-Whitney test, with significance set at corrected $p \leq 0.05$ (see 2.10.2.2). DLPFC and AG expression data were not compared with each other statistically.

2. **Examine target gene mRNA expression in multiple brain regions.** In an effort to provide a more extensive picture of expression, Sybr Green qRT-PCR was employed to compare total and NLC target gene mRNA expression in cDNA generated from seven subcortical and cortical brain regions obtained from the IPD mapping series (IPD; controls) (see 2.3.1). The medulla, putamen, amygdala, entorhinal cortex (EC [BA28]), anterior cingulate cortex (ACC [BA24]), AG (BA39), and frontal cortex (FC [BA8]) were examined. These brain areas were selected based on their susceptibility to Lewy pathology (LP) during the disease process (Braak *et al.* 2003). Figure 3.2 shows the brain regions examined in the cognitive and mapping series. Total expression data were normalised with a NF calculated from the most stable set of the following reference genes: *G6PD*, *Hypoxanthine phosphoribosyltransferase 1* (*HPRT1*), *RPL13A*, and *TBP*. These sets were determined on a region-by-region basis using geNorm (see 2.10.2.1). NLC expression data were normalised with the neuronal marker *NEFH*. Statistical comparisons were carried out by Mann-Whitney test, with significance set at corrected $p \leq 0.05$ (see 2.10.2.2). Brain area expression data were not compared with each other statistically.
3. **Investigate target gene involvement in FPD, IPD, and normal brain structure.** This aim consisted of three parts. In order to identify target gene

mutations that segregate with FPD, patient, control, and first-degree patient relative (where available) genomic DNA (gDNA) was amplified by polymerase chain reaction (PCR) and dideoxy sequencing undertaken (see 2.5). Where appropriate, Ensembl (release 45 from June 2007) and the PROMO online resource were employed for *in silico* transcription factor binding site (TFBS) prediction (see 2.10.6.3). So as to ascertain whether target gene SNP variation influences IPD risk, a case-control genetic association study (see 2.10.3) was performed, by using HapMap phase II Centre d'Étude du Polymorphisme Humain (CEPH) trio genotypic data (release 23a from March 2008) and Tagger (see 2.10.3.1) to generate haplotype-tagging single nucleotide polymorphisms (htSNPs), and TaqMan-genotyping (see 2.6.3) gDNA samples obtained from the IPD association series (IPD; controls) (see 2.6.1). Statistical assessment of allelic association under a multiplicative model was carried out by χ^2 test in Haploview with significance set at corrected $p \leq 0.05$ (see 2.10.3.2). In order to evaluate whether IPD-associated SNPs affect brain structure, genotypic voxel-based morphometry (VBM) analysis was performed. This involved using structural magnetic resonance imaging (MRI) to acquire T1-weighted anatomical brain images (see 2.7) of the imaging series controls (see 2.6.1), TaqMan-genotyping their gDNA, and then employing statistical parametrical mapping (SPM) to carry out voxel-wise comparisons of grey matter density. Statistical comparisons were performed by *t* test, with significance set at corrected $p < 0.05$ (see 2.10.4). The family-wise error (FWE) approach was used for multiple testing correction [reviewed in (Shaffer 1995)].

4. **Investigate the effect of *cis*-acting SNP variation on target gene mRNA expression.** In order to ascertain whether SNP variation influences target gene expression, *cis*-acting variation analysis was carried out, by TaqMan-genotyping gDNA samples obtained from the cognitive series, and regrouping total and NLC DLPFC target gene mRNA expression data (batch 2) by genotype. Statistical comparisons were performed by Mann-Whitney test, with significance set at corrected $p \leq 0.05$ (see 2.10.5).

Expression signature associated with	Significantly different expression in comparison		
	A	B	C
IPD dementia	Yes	No	Yes
IPD neurodegeneration	Yes	Yes	No
Both	Yes	Yes	Yes

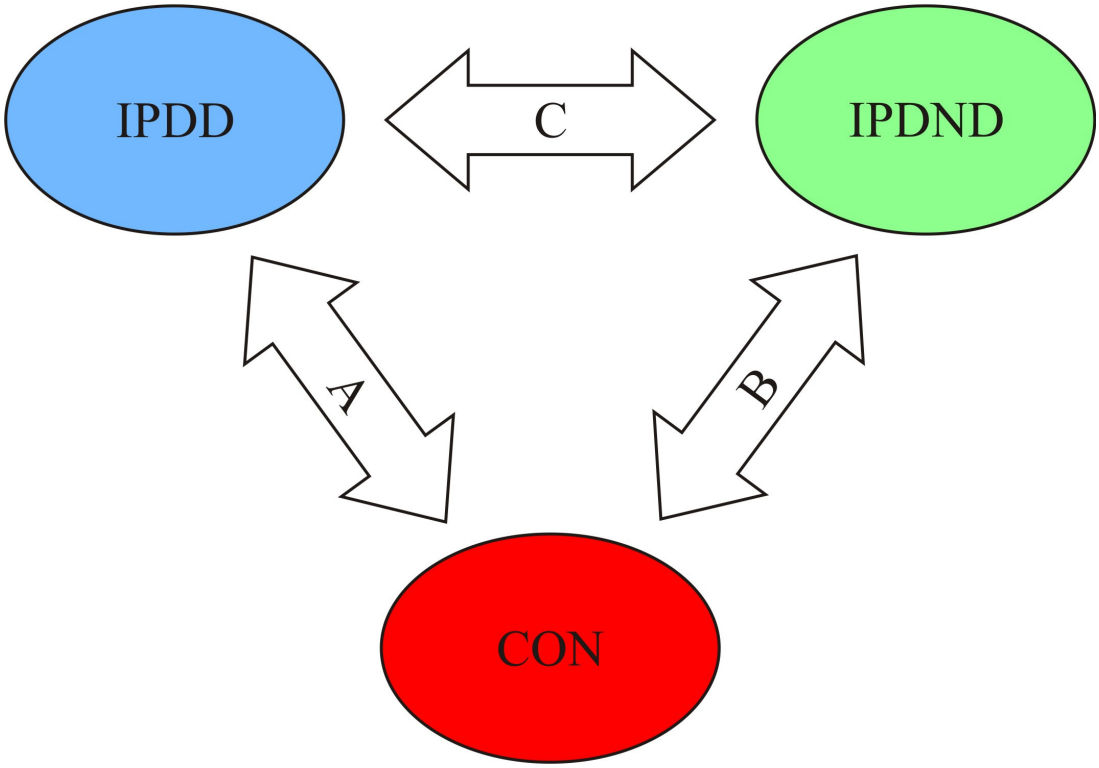

Figure 3.1. IPD cognitive expression analysis design.

Diagrammatic representation of the three group IPD cognitive expression analysis design. Significantly different expression is required in two of the three intergroup comparisons (A, B, and C) to qualify target gene expression signature for association with an IPD subtype. The associated subtype (IPD dementia, IPD neurodegeneration, or both) depends on the specific combination of said comparisons (see table for details). CON = control; IPD = idiopathic Parkinson's disease; IPDD = idiopathic Parkinson's disease dementia; IPDND = idiopathic Parkinson's disease no dementia.

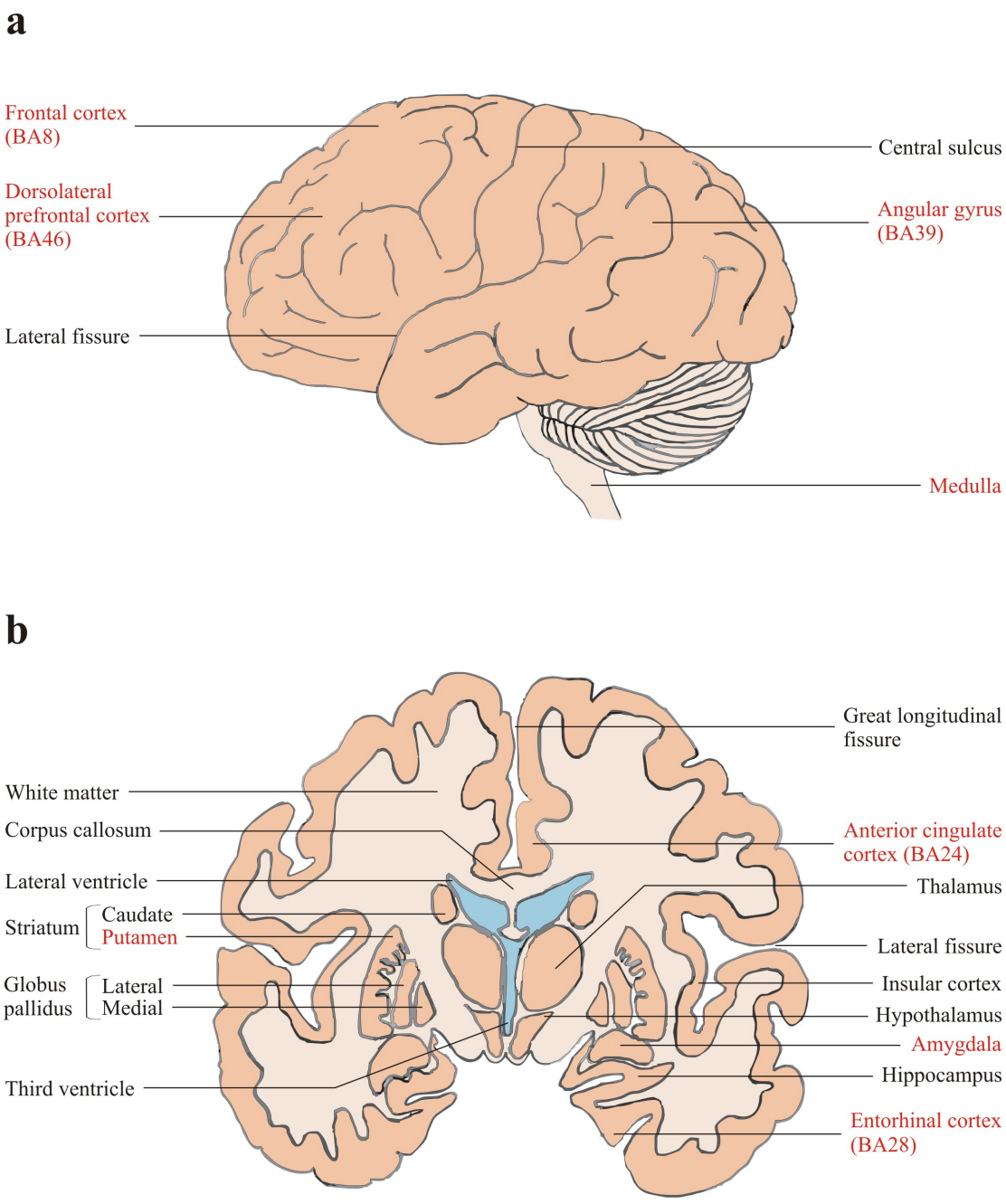

Figure 3.2. Brain regions and structures of interest.

(a) Sagittal aspect of and (b) coronal section through the human brain. Regions and structures of interest are labelled, including those in which gene expression was quantified in the cognitive and mapping series (in red text). Figure adapted from (Crossman and Neary 2005) with permission from the publisher. BA = Brodmann area.

3.3. Results

3.3.1. Idiopathic Parkinson's disease cognitive expression analysis target gene selection

Target selection was founded on the premise that genes involved in working or long term memory function might be differentially-expressed in IPDD individuals. This idea stems from the "generalist brain" hypothesis, which proposes that variation in a specific set of genes affects many cognitive abilities and disabilities (Kovas and Plomin 2006). Target genes were selected using a two step process. The first step consisted of choosing numerous candidate targets from four sources (human orthologues of animal genes were used where appropriate):

1. Genes that display altered expression in the murine hippocampus after contextual fear conditioning, as detected by expression microarray (Levenson *et al.* 2004).
2. Genes that are mutated in *Drosophila* and mice impaired with regard to olfactory conditioning and spatial memory, respectively (Dubnau *et al.* 2003; Costa-Mattioli *et al.* 2005).
3. Genes that exhibit differential expression in the hippocampus of mice doubly transgenic for human Lys670Asn, Met671Leu *Amyloid precursor protein* (*APP*) and Met146Leu *Presenilin 1* (*PSEN1*), as detected by expression microarray and qRT-PCR (Dickey *et al.* 2003). These mice display spatial WM impairment (Morgan *et al.* 2000).
4. Genes that display altered expression in the hippocampus of individuals diagnosed with neurocognitive disorders characterised by WM dysfunction i.e. DLB and schizophrenia, as detected by qRT-PCR (Imamura *et al.* 2005; Chung *et al.* 2003).

In the next step, HapMap phase II CEPH data (release 19 from October 2005) was utilised to assess candidate targets for SNP content and haplotype structure. This was performed to facilitate subsequent genetic analyses. The final list of 10 target genes was generated by selecting candidates of interest that possess several common SNPs (minor allele frequency [MAF] ≥ 0.05) and an adequate r^2 linkage disequilibrium (LD) structure (see table 3.1).

Gene name	Gene symbol	Source	Chromosomal location	Protein function
Activity-regulated cytoskeleton-associated protein	*ARC*	3	8q24.3	Synaptic plasticity
Brain-derived neurotrophic factor	*BDNF*	4	11p13	Synaptic plasticity
Chitinase 3-like 1	*CHI3L1*	4	1q32.1	Inflammation
Dual specificity phosphatase 6	*DUSP6*	1	12q22-q23	Cytoplasmic ERK-directed phosphatase
Eukaryotic translation initiation factor 2 α kinase 4	*EIF2AK4*	2	15q15.1	Synaptic plasticity
Membrane-associated ring finger(C3HC4) 7	*MARCH7*	1	2q24.2	E3 ubiquitin ligase
Phosphatidylserine decarboxylase	*PISD*	1	22q12.2	Mitochondrial PE synthesis
Prostaglandin D2 synthase	*PTGDS*	1	9q34.2-q34.3	Neuromodulation
Pumilio homologue 1	*PUM1*	2	1p35.2	Synaptic plasticity
Staufen homologue 1	*STAU1*	2	20q13.1	Synaptic plasticity

Table 3.1. IPD cognitive expression analysis target genes.

The 10 target genes selected for the IPD cognitive expression analysis. Their sources (see text for details), chromosomal locations, and encoded protein functions are listed. All information was obtained from the NCBI Gene database. ERK = Extracellular-signal regulated kinase; IPD = idiopathic Parkinson's disease; NCBI = National Center for Biotechnology Information; PE = phosphatidylethanolamine.

3.3.2. Mini mental state examination score correlates with cerebellar *post mortem* brain pH

Before quantifying gene expression in the cognitive series samples, it was necessary to ensure that the three groups (IPDD [n = 15]; IPDND [n = 16]; control [n = 16]) were comparable based on the relevant clinicopathological characteristics (see 2.10.2.2). To this end, group data for age of onset, age of death, disease duration, *post mortem* delay (PMD), *post mortem* brain pH, and MMSE were analysed. After correction for multiple testing, the groups were not significantly different with regard to any of the first five metrics, indicating that they are comparable (see table 3.2). However, group MMSE scores for IPDD were significantly lower than those for IPDND (corrected p = 0.048). This indicates that based on carer report and the available MMSE data, these two groups can be considered as IPD patients with and without dementia, respectively. Individual clinicopathological data for each member of the cognitive series is shown in table 2.1.

Hypoperfusion has been demonstrated in several regions of the IPDD brain (Firbank *et al.* 2003; Osaki *et al.* 2009). Given that CBF would be expected to influence pH, it was hypothesised that there might be a relationship between IPD dementia severity and brain pH. Therefore, correlation between MMSE score and cerebellar *post mortem* brain pH was evaluated using the Spearman's rho coefficient (see 2.10.2.2). All of the IPDD and IPDND samples with available data for both metrics (n = 16) were analysed. Significant positive correlation between these two variables was observed (r = 0.557; corrected p = 0.038) (see figure 3.3a). Because of the relatively low number of samples in this analysis, the Queen Square Brain Bank for Neurological Disorders (QSBBND) database was mined for more IPD cases with available pH and MMSE data. The resultant IPD correlation series (n = 37) (see table 3.3) included the 16 cognitive series cases mentioned above. The previous correlation was repeated in the larger series. As with the cognitive series, the

correlation series data demonstrated significant positive correlation between MMSE score and *post mortem* brain pH ($r = 0.412$; corrected $p = 0.022$) (see figure 3.3b).

Group (*n*)	Statistic	Age of onset	Age of death	Disease duration	PMD	Brain pH	MMSE
CON (16)	Mean	NA	78.2	NA	42.4	6.55	ND
	SD	NA	8.8	NA	28.2	0.22	ND
IPDD (15)	Mean	57.6	74.7	17.1	40.8	6.29	22.3
	SD	10.0	5.5	9.0	19.3	0.29	5.1
IPDND (16)	Mean	60.3	76.4	16.1	39.8	6.41	29.6
	SD	11.4	7.3	5.7	26.3	0.27	0.5
p value	Uncorrected	0.514	0.206	0.859	0.873	0.034	0.004
	Corrected	NS	NS	NS	NS	0.408	0.048

Table 3.2. IPD cognitive series clinicopathological data.

Group clinicopathological metrics and statistical results for the IPD cognitive series. After correction for multiple testing, the first five metrics were not significantly different, indicating that the groups are comparable. However, MMSE was significantly lower in the demented patients. Together with carer reports regarding cognitive impairment and/or change in personality (see table 2.1), this result indicates that the IPDD and IPDND groups are correctly labelled as such. Measures of time are in years, except for PMD, which is measured in hours. Groups were compared by Mann-Whitney or Kruskal-Wallis test as appropriate. *p* values were corrected x12. CON = control; IPD = idiopathic Parkinson's disease; IPDD = idiopathic Parkinson's disease dementia; IPDND = idiopathic Parkinson's disease no dementia; MMSE = mini mental state examination; NA = not applicable; ND = not determined; NS = not significant; PMD = *post mortem* delay; SD = standard deviation.

Group (*n*)	Statistic	Age of death	PMD	Brain pH	MMSE
IPD (37)	Mean	76.2	35.4	6.35	25.6
	SD	6.5	20.0	0.29	4.9

Table 3.3. IPD correlation series clinicopathological data.

Group clinicopathological metrics for the IPD correlation series. Age of death is measured in years, and PMD in hours. IPD = idiopathic Parkinson's disease; MMSE = mini mental state examination; PMD = *post mortem* delay; SD = standard deviation.

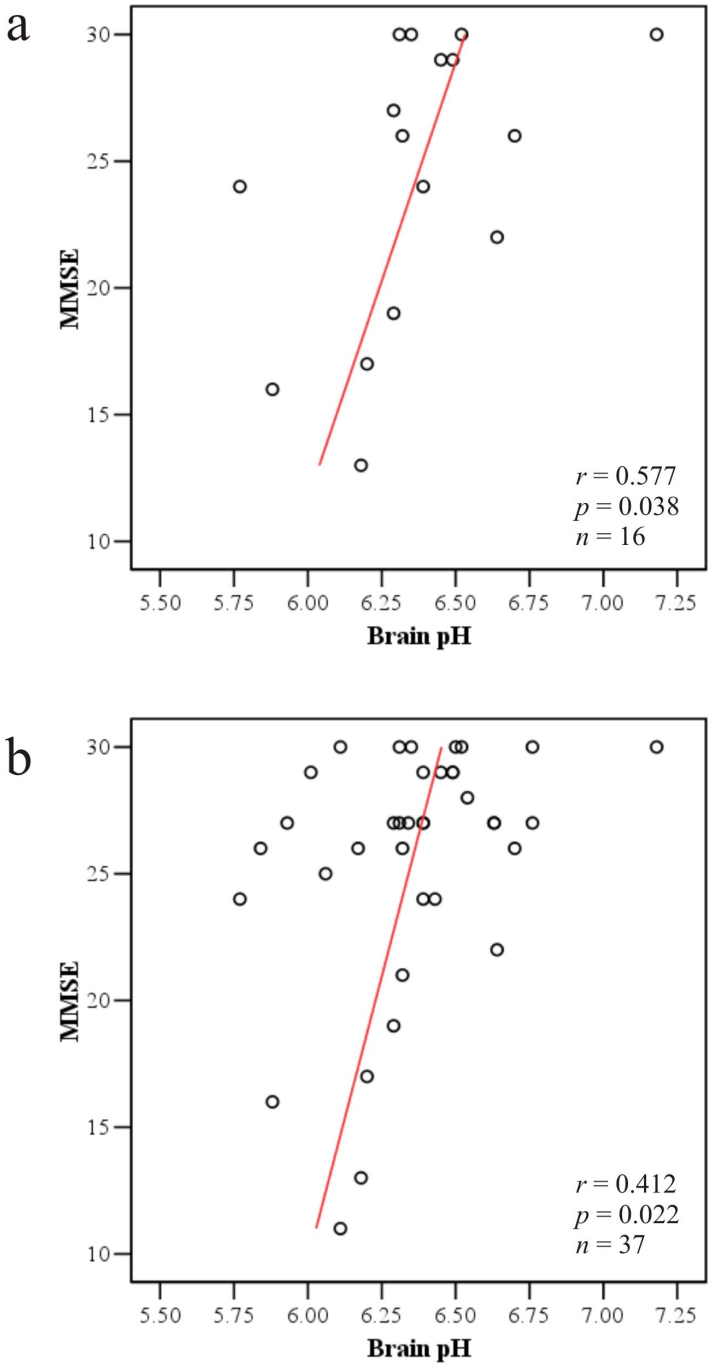

Figure 3.3. MMSE score correlates with cerebellar *post mortem* brain pH.

Scatter plots with linear best fit lines displaying Spearman's rho correlations between cerebellar *post mortem* brain pH and MMSE score in the (a) IPD cognitive and (b) IPD correlation series. Moderate but significant correlations were observed in both series. Spearman's *r* coefficients, corrected *p* values, and *n* values are shown on each plot. *p* values were corrected x2. IPD = idiopathic Parkinson's disease; MMSE = mini mental state examination.

3.3.3. Variation in dorsolateral prefrontal cortex *Dual specificity phosphatase 6* expression is associated with idiopathic Parkinson's disease

Dorsolateral prefrontal cortex and angular gyrus target gene expression were measured in the cognitive series using qRT-PCR. In order to correct for variation in tissue composition and experimental procedure, target expression data were normalised with a NF calculated from the reference genes *RPL13A* and *TBP*. Table 3.4, figure 3.4, and figure 3.5 show the findings of the IPD cognitive expression analysis. Examination of the data indicated high levels of intragroup variation in several instances and an overall lack of intergroup differential expression. Thus only the IPDD and IPDND groups were compared statistically. Clear trends of IPDD vs IPDND overexpression and underexpression were seen for *MARCH7* in the DLPFC and *DUSP6* in the AG, respectively. Both observations were accompanied by altered IPDD expression compared to controls, suggesting that these genes might exhibit IPD dementia expression signatures (see figure 3.1). However, the magnitude of the IPDD vs control differences and relevant levels of intragroup variation indicated that these changes were nonsignificant. After correction for multiple testing, all 10 target genes failed to demonstrate significant IPDD vs IPDND differential expression in either region. Therefore, there is no evidence to support the hypothesis that there is a relationship between IPD dementia status and DLPFC or AG target gene expression.

The data suggested that when contrasted against controls, DLPFC *DUSP6* expression was reduced in both IPDD and IPDND (see figure 3.4). To further investigate this finding, IPDD and IPDND were combined to generate the IPD group. IPD (n = 31) and control (n = 16) *DUSP6* expression in the DLPFC and AG were then compared statistically. Strikingly, IPD *DUSP6* expression was significantly lower than that of controls in the DLPFC (corrected $p = 0.008$), but not in the AG (corrected $p > 1$) (see figure 3.6). This demonstrates that variation in DLPFC *DUSP6* expression is associated with IPD in the cognitive series.

Brain region	Gene	Fold change mean expression/CON		IPDD vs IPDND *p* value	
		IPDD	IPDND	Uncorrected	Corrected
DLPFC (BA46)	*ARC*	0.76	0.63	0.221	NS
	BDNF	0.65	0.76	0.874	NS
	CHI3L1	1.41	0.83	0.262	NS
	DUSP6	0.47	0.60	0.221	NS
	EIF2AK4	0.99	0.92	0.339	NS
	MARCH7	1.31	1.01	0.013	0.585
	PISD	1.03	0.97	0.553	NS
	PTGDS	1.04	0.94	0.548	NS
	PUM1	0.85	0.93	0.527	NS
	STAU1	0.97	0.89	0.664	NS
AG (BA39)	*ARC*	1.03	1.45	0.191	NS
	BDNF	0.89	1.46	0.065	NS
	CHI3L1	1.17	1.20	0.447	NS
	DUSP6	0.63	1.25	0.002	0.090
	EIF2AK4	0.91	0.87	0.188	NS
	MARCH7	0.97	0.89	0.419	NS
	PISD	0.88	1.00	0.239	NS
	PTGDS	1.11	1.57	0.395	NS
	PUM1	1.08	1.12	0.190	NS
	STAU1	0.99	1.14	0.351	NS

Table 3.4. IPD cognitive expression analysis data.

Dorsolateral prefrontal cortex (BA46) and angular gyrus (BA39) fold change mean target gene expression values (relative to controls) and statistical results for the IPD cognitive expression analysis. No significant differences were observed after correction for multiple testing. Expression data were normalised with *RPL13A* and *TBP*. For all targets, IPDD and IPDND groups were compared by Mann-Whitney test. *p* values were corrected x45. Gene symbols are defined in table 3.1. AG = angular gyrus; BA = Brodmann area; CON = control; DLPFC = dorsolateral prefrontal cortex; IPD = idiopathic Parkinson's disease; IPDD = idiopathic Parkinson's disease dementia; IPDND = idiopathic Parkinson's disease no dementia; *RPL13A = Ribosomal protein L13A*; *TBP = TATA box binding protein*.

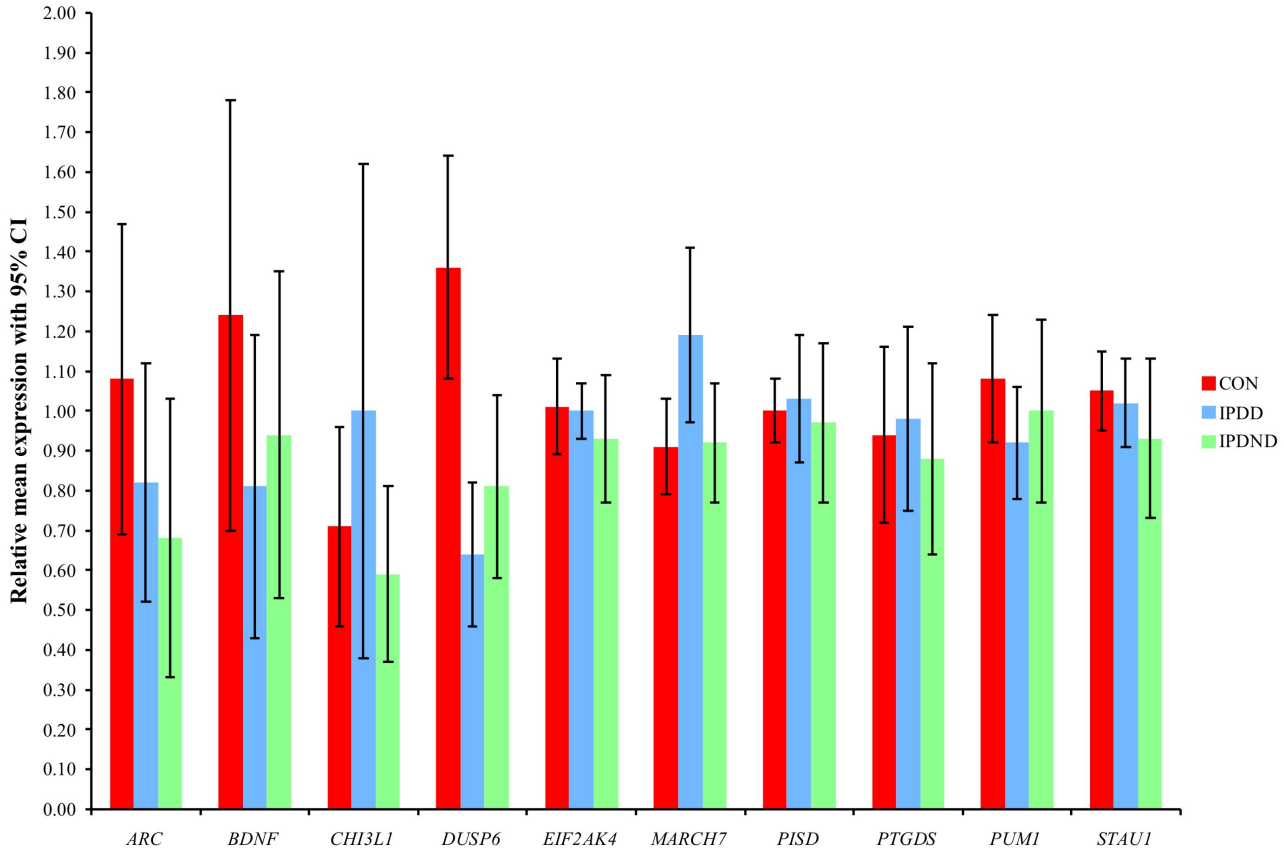

Figure 3.4. IPD cognitive expression analysis data: dorsolateral prefrontal cortex (BA46).

Dorsolateral prefrontal cortex relative mean target gene expression with 95% CI. No significant differences were observed after correction for multiple testing. Expression data were normalised with *RPL13A* and *TBP*. For all targets, IPDD and IPDND groups were compared by Mann-Whitney test. *p* values were corrected x45. Gene symbols are defined in table 3.1. BA = Brodmann area; CI = confidence interval; CON = control; IPD = idiopathic Parkinson's disease; IPDD = idiopathic Parkinson's disease dementia; IPDND = idiopathic Parkinson's disease no dementia; *RPL13A = Ribosomal protein L13A*; *TBP = TATA box binding protein*.

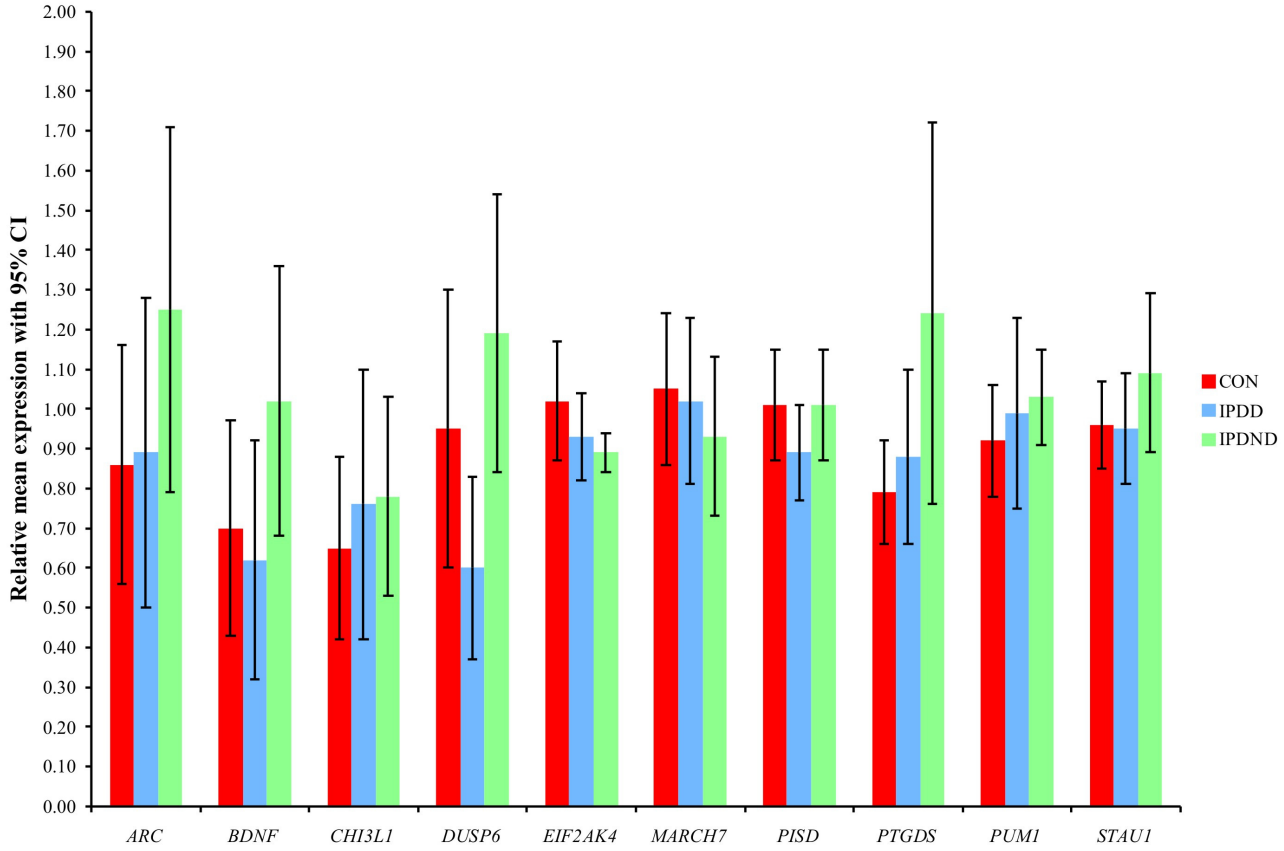

Figure 3.5. IPD cognitive expression analysis data: angular gyrus (BA39).

Angular gyrus relative mean target gene expression with 95% CI. No significant differences were observed after correction for multiple testing. Expression data were normalised with *RPL13A* and *TBP*. For all targets, IPDD and IPDND groups were compared by Mann-Whitney test. *p* values were corrected x45. Gene symbols are defined in table 3.1. BA = Brodmann area; CI = confidence interval; CON = control; IPD = idiopathic Parkinson's disease; IPDD = idiopathic Parkinson's disease dementia; IPDND = idiopathic Parkinson's disease no dementia; *RPL13A = Ribosomal protein L13A*; *TBP = TATA box binding protein*.

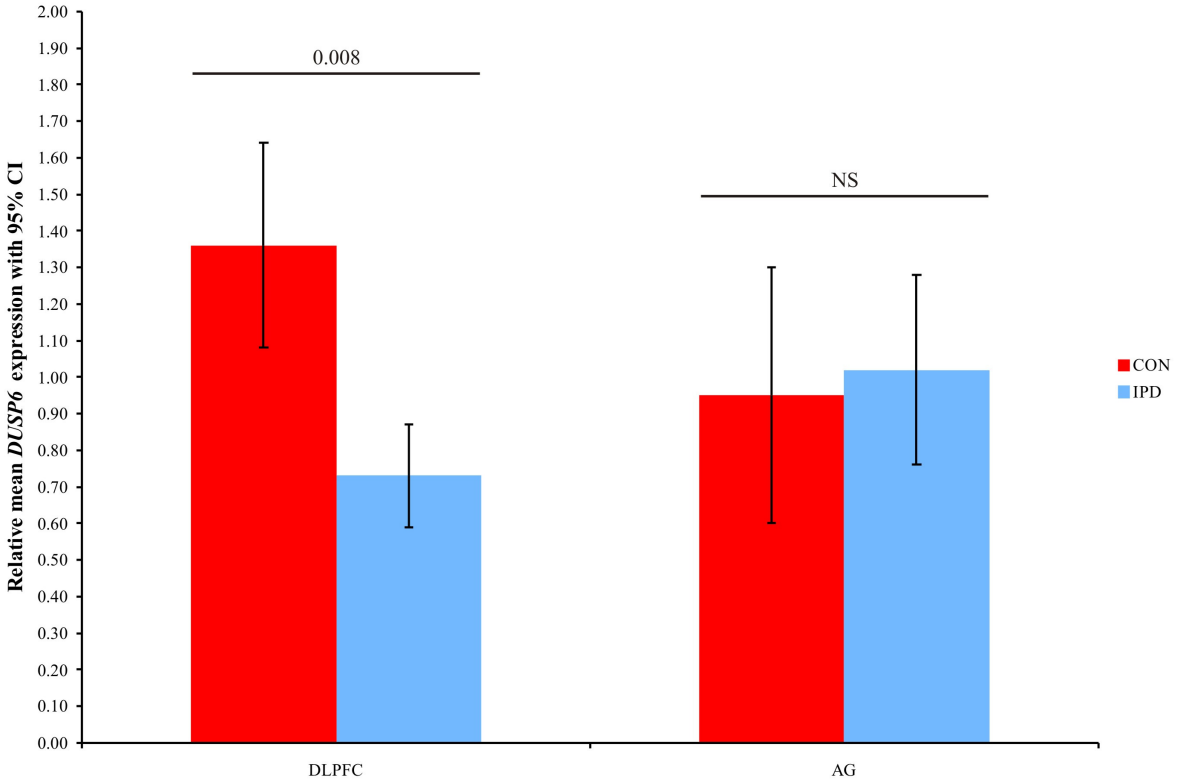

Figure 3.6. Variation in DLPFC *DUSP6* expression is associated with IPD.

Dorsolateral prefrontal cortex (BA46) and angular gyrus (BA39) relative mean *DUSP6* expression values with 95% CI and statistical results. In the DLPFC, *DUSP6* was significantly underexpressed in IPD compared to controls, demonstrating that variation in *DUSP6* expression in this region is associated with IPD. No significant difference was observed in the AG. *DUSP6* expression data were normalised with *RPL13A* and *TBP*. IPD and CON groups were compared by Mann-Whitney test. Uncorrected *p* values were $1.87e^{-4}$ for the DLPFC and 0.847 for the AG. Corrected *p* values are displayed. *p* values were corrected x45. AG = angular gyrus; BA = Brodmann area; CI = confidence interval; CON = control; DLPFC = dorsolateral prefrontal cortex; *DUSP6 = Dual specificity phosphatase 6*; IPD = idiopathic Parkinson's disease; NS = not significant; *RPL13A = Ribosomal protein L13A*; *TBP = TATA box binding protein*.

3.3.4. *Dual specificity phosphatase 6* underexpression in the idiopathic Parkinson's disease dorsolateral prefrontal cortex is not caused by modulated splicing

The human *DUSP6* gene is composed of three exons. According to Ensembl, two splice forms are transcribed from this gene: the full length (FL) transcript, which contains all three exons; and a shorter transcript, comprised of exons 1 and 3 (hereafter known as "*DUSP6* 1:3") (see figure 3.7). This architecture has an important consequence for Sybr Green qRT-PCR, in that it is impossible to design exon-exon boundary-spanning primers able to simultaneously detect both splice forms. Consequently, the underexpression of *DUSP6* observed in the IPD DLPFC could have been an artefact caused by modulated splicing. In order to confirm that *DUSP6* 1:3 is expressed in the DLPFC, splicing RT-PCR was used to amplify cognitive series DLPFC cDNA (batch 1). The results showed that *DUSP6* 1:3 is expressed in the DLPFC of the entire cognitive series (see figure 3.8).

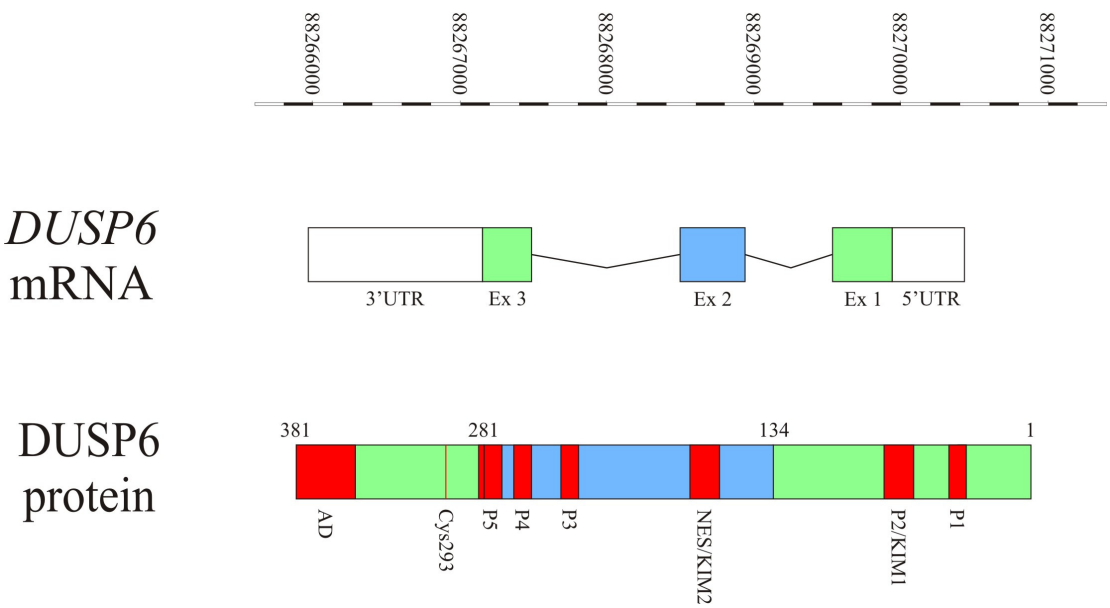

Figure 3.7. *DUSP6* FL mRNA and DUSP6 FL protein architecture.

Human *DUSP6* FL mRNA transcript and DUSP6 FL protein architecture. *DUSP6* is transcribed from the negative strand. Alternative splicing generates two transcripts, the FL and 1:3 splice forms, which contain and lack exon 2, respectively. The FL protein isoform contains five phosphatase domains ("P1" to "P5"), primary and secondary KIMs ("KIM1" and "KIM2", respectively, which regulate ERK1/2 binding), a NES (which regulates nucleocytoplasmic shuttling), and an AD (which regulates enzymatic activation after ERK1/2 binding). Cys293 is the critical phosphatase active site residue. mRNA scale bar indicates locations on chromosome 12 according to NCBI assembly build 36. mRNA information was obtained from Ensembl (release 45 from June 2007). Protein scale bar indicates amino acid locations. Blue and green protein regions are encoded by blue and green exons, respectively, whilst protein domains and critical residues are overlaid in red. Phosphatase domain locations were obtained from the Prints database. Locations of all other protein domains were obtained from (Zhou *et al.* 2001). AD = activation domain; Cys = cysteine; *DUSP6* = *Dual specificity phosphatase 6*; Ex = exon; ERK 1/2 = Extracellular-signal regulated kinase 1/2; FL = full length; KIM = kinase interaction motif; mRNA = messenger ribonucleic acid; NCBI = National Center for Biotechnology Information; NES = nuclear export sequence; UTR = untranslated region.

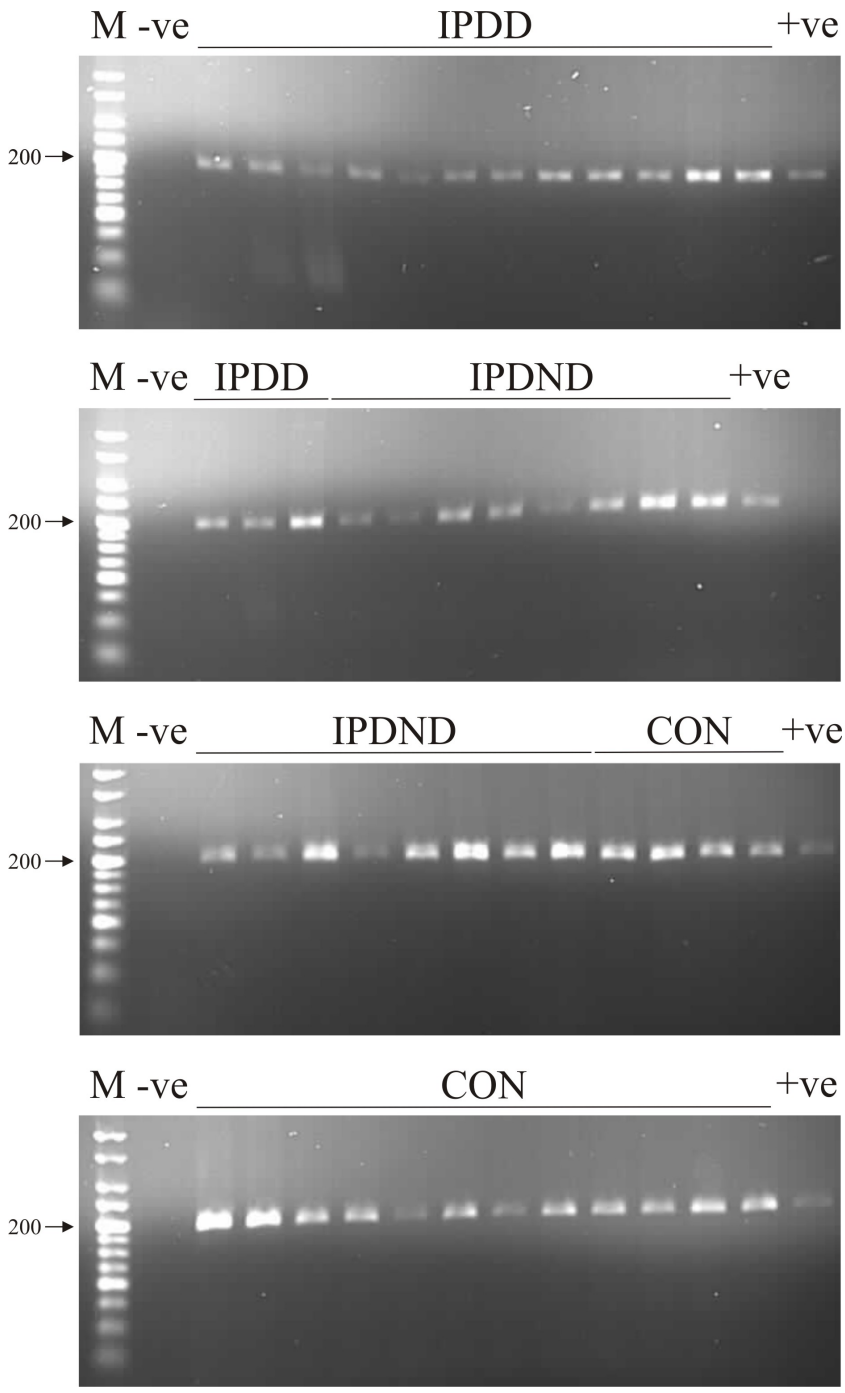

Figure 3.8. *DUSP6* 1:3 is expressed in the DLPFC of the entire IPD cognitive series.

Splicing RT-PCR amplification of *DUSP6* 1:3 from IPD cognitive series DLPFC batch 1 cDNA. This splice form is expressed in the DLPFC of the entire series. RT-PCR products were resolved on agarose gels. Arrows denote the 200 base pair marker on each gel. -ve = negative control (water); +ve = positive control (IPD cerebellum cDNA); 1:3 = splice form 1:3; CON = control; DLPFC = dorsolateral prefrontal cortex; cDNA = complementary DNA; *DUSP6 = Dual specificity phosphatase 6*; IPD = idiopathic Parkinson's disease; IPDD = idiopathic Parkinson's disease dementia; IPDND = idiopathic Parkinson's disease no dementia; M = marker ladder; RT-PCR = reverse transcriptase-polymerase chain reaction.

We wanted to confirm the underexpression of *DUSP6* observed in the IPD DLPFC, evaluate whether this effect is the result of modulated splicing, and attempt an alternative normalisation strategy to correct for neuronal loss in IPD samples. Therefore, qRT-PCR was employed to measure the expression of *DUSP6* FL and 1:3 in cognitive series DLPFC cDNA batches 1 and 2 (IPD [$n = 31$]; controls [$n = 16$]). As before, batch 1 *DUSP6* expression data were normalised with a NF calculated from *RPL13A* and *TBP* (see 3.3.3). For batch 2, two different normalisation approaches were used: the neuronal marker *NEFH*; and a NF calculated from *G6PD*, *RPL13A*, and *TBP*. The resultant normalised datasets were labelled as NLC and total, respectively. NLC data represents an alternative correction strategy and does not equate to neuron-specific expression. Expression in IPD and controls was compared statistically (see table 3.5 and figure 3.9).

In batch 2, total *DUSP6* FL expression was significantly reduced in IPD compared to controls (corrected $p = 0.045$), although to a lesser extent than batch 1, in which mean IPD expression was 0.54-fold of that in controls (corrected $p = 0.008$). Batch-by-batch, total *DUSP6* 1:3 expression patterns tended to recapitulate those of total *DUSP6* FL expression. For example in batch 2, total *DUSP6* 1:3 expression was significantly decreased in IPD compared with controls (corrected $p = 0.045$). However in batch 1, the IPD underexpression of total *DUSP6* 1:3 was less pronounced than that of total *DUSP6* FL, and failed to reach significance after correction for multiple testing (corrected $p = 0.090$). Trends of lower NLC *DUSP6* FL and 1:3 expression were observed in IPD contrasted against controls, but these effects did not survive correction.

Overall, these findings confirm that variation in DLPFC *DUSP6* expression is associated with IPD in the cognitive series. Moreover, there is little evidence to suggest that this phenomenon is a consequence of alternative *DUSP6* splicing. Although changes in transcript ratio might play a minor role, the most parsimonious interpretation of these data is that *DUSP6* underexpression in the cognitive series IPD DLPFC is not caused by modulated splicing.

cDNA synthesis batch	Expression	Splice form	Fold change mean *DUSP6* expression (IPD/CON)	IPD vs CON *p* value	
				Uncorrected	Corrected
1	Total	FL	0.54	$1.87e^{-4}$	0.008
		1:3	0.63	0.002	0.090
2	Total	FL	0.63	0.001	0.045
		1:3	0.60	0.001	0.045
2	NLC	FL	0.64	0.016	0.720
		1:3	0.76	0.037	NS

Table 3.5. IPD cognitive series DLPFC *DUSP6* expression data.

Fold change mean *DUSP6* expression values (relative to controls) and statistical results for cognitive series DLPFC cDNA batches 1 and 2. Batch-by-batch, total *DUSP6* 1:3 expression patterns tended to recapitulate those of total *DUSP6* FL expression, indicating that *DUSP6* underexpression in the cognitive series IPD DLPFC is not caused by modulated splicing. Note that batch 1 total *DUSP6* FL expression data and statistics were already presented in figure 3.6. Batch 1 total expression data were normalised with *RPL13A* and *TBP*, and batch 2 total expression data with *G6PD*, *RPL13A*, and *TBP*. NLC expression data were normalised with *NEFH*. IPD and CON groups were compared by Mann-Whitney test. *p* values were corrected x45. 1:3 = splice form 1:3; CON = control; cDNA = complementary DNA; DLPFC = dorsolateral prefrontal cortex; *DUSP6 = Dual specificity phosphatase 6*; FL = full length; *G6PD = Glucose-6-phosphate dehydrogenase*; IPD = idiopathic Parkinson's disease; *NEFH = Neurofilament H*; NLC = neuronal-loss corrected; NS = not significant; *RPL13A = Ribosomal protein L13A*; *TBP = TATA box binding protein*.

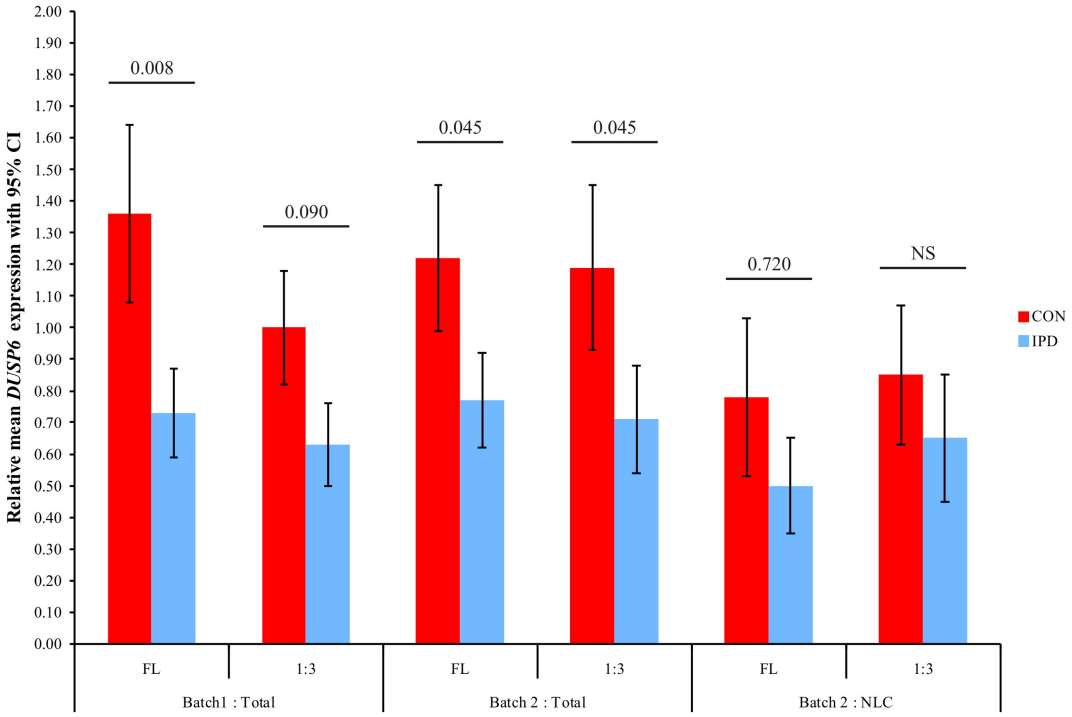

Figure 3.9. *DUSP6* underexpression in the IPD DLPFC is not caused by differential splicing.

Relative mean *DUSP6* expression values with 95% CI and statistical results for cognitive series DLPFC cDNA batches 1 and 2. Batch-by-batch, total *DUSP6* 1:3 expression patterns tended to recapitulate those of total *DUSP6* FL expression, indicating that *DUSP6* underexpression in the cognitive series IPD DLPFC is not caused by modulated splicing. Note that batch 1 total *DUSP6* FL expression data and statistics were already presented in figure 3.6. Batch 1 total expression data were normalised with *RPL13A* and *TBP*, and batch 2 total expression data with *G6PD*, *RPL13A*, and *TBP*. NLC expression data were normalised with *NEFH*. IPD and CON groups were compared by Mann-Whitney test. Corrected *p* values are displayed. *p* values were corrected x45. 1:3 = splice form 1:3; CI = confidence interval; CON = control; cDNA = complementary DNA; DLPFC = dorsolateral prefrontal cortex; *DUSP6 = Dual specificity phosphatase 6*; FL = full length; *G6PD = Glucose-6-phosphate dehydrogenase*; IPD = idiopathic Parkinson's disease; *NEFH = Neurofilament H*; NLC = neuronal-loss corrected; NS = not significant; *RPL13A = Ribosomal protein L13A*; *TBP = TATA box binding protein*.

3.3.5. *Dual specificity phosphatase 6* underexpression in idiopathic Parkinson's disease is restricted to the dorsolateral prefrontal cortex

In order to provide a more extensive picture of *DUSP6* in IPD, qRT-PCR was used to measure expression of the FL isoform in seven subcortical and cortical brain regions obtained from the mapping series. Total expression data were normalised with a NF calculated from the most stable set of the following reference genes: *G6PD*, *HPRT1*, *RPL13A*, and *TBP*. For the medulla, putamen, ACC, AG, and FC, these sets comprised all four reference genes. For the amygdala and EC, these sets consisted of *HPRT1*, *RPL13A*, and *TBP*. All NLC expression data were normalised with *NEFH*. As before, comparability based on clinicopathological characteristics was assessed (see 3.3.2). Group data for age of death, PMD, and *post mortem* brain pH were analysed. Comparisons were not possible for age of onset, disease duration, and MMSE. After correction for multiple testing, the IPD (n = 20) and control (n = 20) groups were not significantly different with regard to any of the metrics, indicating that they are comparable (see table 3.6). This was the case for both the generalised and the medulla-specific mapping series. Individual clinicopathological data for each member of the mapping series is shown in table 2.2. *DUSP6* FL expression in IPD and controls was then compared statistically.

Table 3.7 and figure 3.10 show the results of this analysis. Relatively high levels of intragroup variation were detected in the majority of regions. After correction for multiple testing, no significant changes were observed for total or NLC *DUSP6* FL expression in any of the seven regions obtained from the mapping series. Clear trends of reduction in IPD contrasted against controls were seen for total expression in the ACC, and NLC expression in the AG and FC. However, these effects failed to reach significance after correction. Notably, the lack of differential total *DUSP6* expression observed in the mapping series AG corroborates the cognitive series data for this area (see figure 3.6). Taken together, these findings demonstrate that *DUSP6*

FL is not differentially-expressed in the mapping series. Moreover, they indicate that in all eight brain areas examined thus far, IPD *DUSP6* underexpression is restricted to the DLPFC.

Table 3.6. IPD mapping series clinicopathological data.

a. Putamen, amygdala, entorhinal cortex, anterior cingulate cortex, angular gyrus, frontal cortex (below).

Group (*n*)	Statistic	Age of onset	Age of death	Disease duration	PMD	Brain pH
CON (20)	Mean	NA	78.9	NA	49.1	6.38
	SD	NA	10.5	NA	24.9	0.29
IPD (20)	Mean	60.6	76.3	15.8	51.0	6.29
	SD	11.6	7.7	8.4	31.6	0.27
p value	Uncorrected	NA	0.155	NA	0.935	0.223
	Corrected	NA	NS	NA	NS	NS

b. Medulla only (below).

Group (*n*)	Statistic	Age of onset	Age of death	Disease duration	PMD	Brain pH
CON (15)	Mean	NA	78.6	NA	46.7	6.41
	SD	NA	9.9	NA	24.3	0.33
IPD (17)	Mean	62.3	76.2	13.9	50.6	6.30
	SD	10.7	7.9	7.3	26.3	0.28
p value	Uncorrected	NA	0.186	NA	0.461	0.207
	Corrected	NA	NS	NA	NS	NS

Group clinicopathological metrics and statistical results for the IPD mapping series. After correction for multiple testing, none of the metrics were significantly different, indicating that the groups are comparable. Due to low availability of medulla tissue, several individuals were replaced solely for this region (see table 2.2). Measures of time are in years, except for PMD, which is measured in hours. Groups were compared by Mann-Whitney test. *p* values were corrected x12. CON = control; IPD = idiopathic Parkinson's disease; NS = not significant; PMD = *post mortem* delay; SD = standard deviation.

Brain region	Expression	Fold change mean *DUSP6* FL expression (IPD/CON)	IPD vs CON *p* value	
			Uncorrected	Corrected
Medulla	Total	1.59	0.043	NS
	NLC	0.55	0.576	NS
Putamen	Total	1.00	0.524	NS
	NLC	0.48	0.200	NS
Amygdala	Total	1.12	0.748	NS
	NLC	0.64	0.429	NS
EC (BA28)	Total	1.25	0.957	NS
	NLC	0.59	0.128	NS
ACC (BA24)	Total	0.77	0.013	0.585
	NLC	0.76	0.204	NS
AG (BA39)	Total	1.00	0.267	NS
	NLC	0.39	0.008	0.360
FC (BA8)	Total	0.83	0.116	NS
	NLC	0.46	0.007	0.315

Table 3.7. IPD mapping series *DUSP6* FL expression data.

Fold change mean *DUSP6* FL expression values (relative to controls) and statistical results for the mapping series. No significant differences were observed after correction for multiple testing, indicating that *DUSP6* underexpression in IPD is restricted to the DLPFC. Total expression data were normalised with *G6PD*, *HPRT1*, *RPL13A*, and *TBP*, except for amygdala and EC data, which were normalised with *HPRT1*, *RPL13A*, and *TBP*. NLC expression data were normalised with *NEFH*. IPD and CON groups were compared by Mann-Whitney test. *p* values were corrected x45. AG = angular gyrus (BA39); ACC = anterior cingulate cortex (BA24); BA = Brodmann area; CON = control; DLPFC = dorsolateral prefrontal cortex (BA46); *DUSP6 = Dual specificity phosphatase 6*; EC = entorhinal cortex (BA28); FC = frontal cortex (BA8); FL = full length; *G6PD = Glucose-6-phosphate dehydrogenase*; *HPRT1 = Hypoxanthine phosphoribosyltransferase 1*; IPD = idiopathic Parkinson's disease; *NEFH = Neurofilament H*; NLC = neuronal-loss corrected; NS = not significant; *RPL13A = Ribosomal protein L13A*; *TBP = TATA box binding protein*.

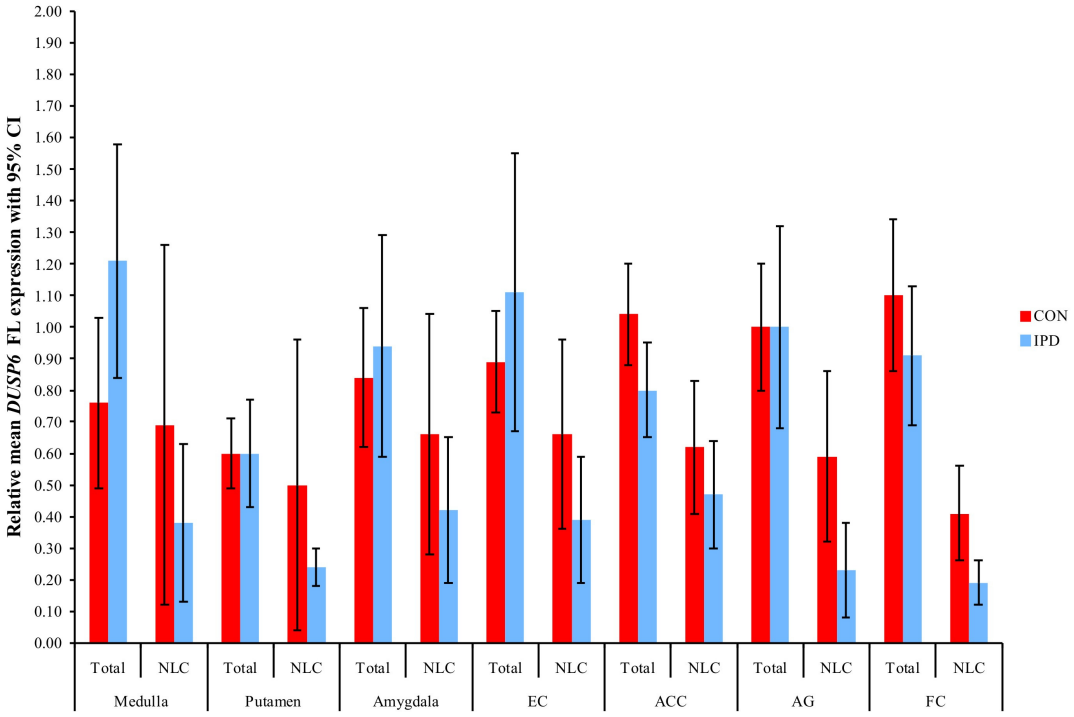

Figure 3.10. *DUSP6* FL is not differentially-expressed in the IPD mapping series.

Relative mean *DUSP6* FL expression values with 95% CI for the mapping series. No significant differences were observed after correction for multiple testing, indicating that *DUSP6* underexpression in IPD is restricted to the DLPFC. Total expression data were normalised with *G6PD*, *HPRT1*, *RPL13A*, and *TBP*, except for amygdala and EC data, which were normalised with *HPRT1*, *RPL13A*, and *TBP*. NLC expression data were normalised with *NEFH*. IPD and CON groups were compared by Mann-Whitney test. *p* values were corrected x45. AG = angular gyrus (BA39); ACC = anterior cingulate cortex (BA24); BA = Brodmann area; CI = confidence interval; CON = control; DLPFC = dorsolateral prefrontal cortex (BA46); *DUSP6 = Dual specificity phosphatase 6*; EC = entorhinal cortex (BA28); FC = frontal cortex (BA8); FL = full length; *G6PD = Glucose-6-phosphate dehydrogenase*; *HPRT1 = Hypoxanthine phosphoribosyltransferase 1*; IPD = idiopathic Parkinson's disease; *NEFH = Neurofilament H*; NLC = neuronal-loss corrected; *RPL13A = Ribosomal protein L13A*; *TBP = TATA box binding protein*.

3.3.6. *Dual specificity phosphatase 6* sequencing identifies one familial Parkinson's disease-restricted mutation and three low frequency polymorphisms

Pathogenic mutations in several different genes are known to cause FPD [reviewed in (Lesage and Brice 2009)]. We wanted to evaluate whether *DUSP6* might exhibit mutations that segregate with FPD. Therefore, gDNA samples obtained from FPD patients (n = 82) were amplified by PCR and dideoxy sequencing was performed. *DUSP6* coverage consisted of ~420 bp of upstream sequence, the 5' untranslated region (UTR), the coding portions of exons 1 to 3, and the majority (the first 830 bp) of the 3'UTR. Deviations from the reference sequence and segregation with FPD were evaluated by sequencing the relevant amplicons in control individuals (n = 83) and in first-degree relatives of known FPD status, respectively.

Four novel heterozygous deviations from the *DUSP6* reference sequence were identified: two transitions and two transversions (see table 3.8). Three of these changes were found in FPD cases and controls, and hence can be classified as low frequency SNPs. These were as follows: -285A/C in the upstream region, +394C/T in the 5'UTR, and +740G/A in exon 1, which is predicted to result in a Thr87Ile substitution. In contrast, the novel +460G>C alteration was detected in only one case and none of the controls, and therefore appears to be a point mutation. Segregation with FPD could not be assessed for this mutation, as no relatives were available. *In silico* TFBS prediction analysis was carried out for +460G>C. Genomic DNA sequence encompassing this position and 60 bp in either direction was downloaded from Ensembl and entered into PROMO. The +460G>C mutation was found to abolish a predicted DNA binding site for the transcription factor (TF) glucocorticoid receptor α, which is encoded by the *nuclear receptor subfamily 3, group C, member 1* (*NR3C1*) gene (see figure 3.11).

These results establish the existence of one FPD-restricted point mutation and three novel low frequency SNPs in the human *DUSP6* locus. They also suggest that *DUSP6* mutation is unlikely to be a significant cause of FPD.

Sequence alteration	Location	Amino acid substitution	FPD allelic frequency	Control allelic frequency	Segregates with FPD?
-285A>C	Upstream	NA	3/144	8/148	ND
+394C>T	5'UTR	NA	3/130	7/138	No*
+460G>C	5'UTR	NA	1/130	0/140	ND
+740G>A	Exon 1	Thr87Ile	3/108	3/84	ND

Table 3.8. *DUSP6* DNA sequencing data.

Dual specificity phosphatase 6 DNA sequencing data obtained in FPD patients, controls, and first-degree patient relatives (where available). All changes were heterozygous. One FPD-restricted 5'UTR mutation and three low frequency SNPs were discovered. Base identities are from the positive strand (note that *DUSP6* is transcribed from the negative strand). Base positions are on the negative strand in relation to the TSS, where the first transcribed base is +1. DNA base and amino acid codes are in accordance with the International Union of Biochemistry and Molecular Biology. * = affected sibling of one heterozygous FPD patient was homozygous wild type; *DUSP6 = Dual specificity phosphatase 6*; FPD = familial Parkinson's disease; NA = not applicable; ND = not determined; SNP = single nucleotide polymorphism; TSS = transcriptional start site; UTR = untranslated region.

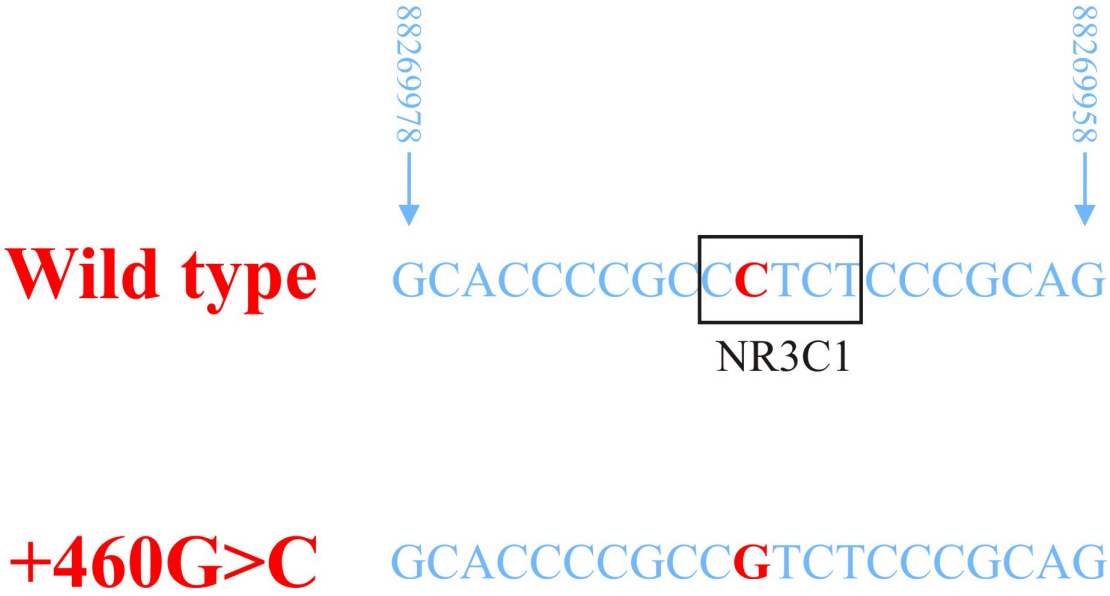

Figure 3.11. The +460G>C *DUSP6* mutation abolishes a predicted NR3C1 DNA binding site.

In silico analysis investigating the effect of *DUSP6* mutation on predicted TF binding. The +460G>C *DUSP6* 5'UTR mutation abolishes a predicted DNA binding site for the TF glucocorticoid receptor α (also known as NR3C1). PROMO maximum binding dissimilarity was 1%. Locations on the negative strand of chromosome 12 are according to NCBI assembly build 36. +460G>C is shown bolded in red. Box indicates predicted NR3C1 binding site. DNA base codes are in accordance with the International Union of Biochemistry and Molecular Biology. *DUSP6 = Dual specificity phosphatase 6*; NCBI = National Center for Biotechnology Information; NR3C1 = nuclear receptor subfamily 3, group C, member 1; TF = transcription factor; UTR = untranslated region.

3.3.7. Variation at rs1689408 is implicated in idiopathic Parkinson's disease risk

Genetic association studies have identified polymorphisms that affect IPD aetiopathogenesis [for example (Simon-Sanchez *et al.* 2009)]. In order to assess SNP variation in the *DUSP6* locus for its potential to influence IPD susceptibility, a case-control association study was undertaken. A region encompassing the *DUSP6* gene (~4.5 kb) and 10 kb upstream and downstream was defined, and HapMap phase II CEPH data were used to evaluate LD relationships between common SNPs and generate htSNPs (see figure 3.12). Four htSNPs were produced, with an average locus haplotype r^2 of 0.994. Taqman was employed to genotype these markers in gDNA extracted from the association series (IPD [n = 614]; controls [n = 619]), and they were tested for allelic association with IPD under a multiplicative model. The novel SNPs identified during *DUSP6* sequencing (see 3.3.6) were not examined due to low MAF. Group clinical data for the association series can be seen in table 3.9.

Table 3.10 shows the findings of the SNP association study. The Hardy-Weinberg equilibrium (HWE) was not violated for any of the htSNPs in either group, indicating that no serious genotyping errors had occurred. Variation at rs1689408 displayed a trend for association with IPD (corrected p = 0.088). The estimated odds ratio (OR) for this effect was 0.747 with a 95% confidence interval (CI) that ranged from 0.582 to 0.958, suggesting that the observation is not a false positive. Comparison of the IPD (0.102) and control (0.133) MAFs suggested that the minor T allele confers reduced susceptibility to IPD. Therefore, these data indicate that variation at rs1689408 is implicated in IPD risk in the association series. According to HapMap, this polymorphism is in perfect LD with three other *DUSP6* locus SNPs in Caucasians: rs1650342, rs704080, and rs808820. This implies uncertainty over which of these four SNPs (or combination thereof) is/are driving the observed trend.

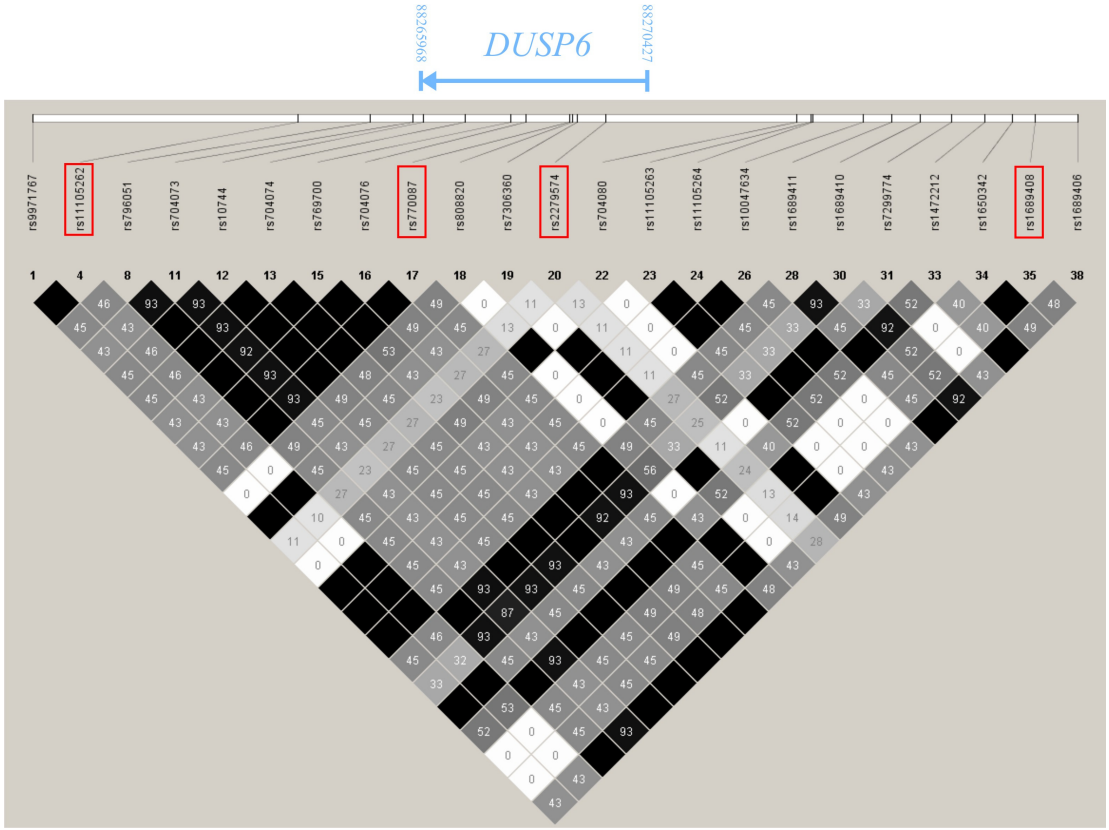

Figure 3.12. *DUSP6* genomic locus SNP LD plot.

Pairwise r^2 LD plot for common SNPs (MAF ≥ 0.05) in the *DUSP6* genomic locus (~24.5 kb). CEPH trio genotypic data were obtained from HapMap phase II (release 23a from March 2008). Tagger was used to generate four htSNPs capturing 95% the SNP variation in this region (average locus haplotype r^2 = 0.994). Pairwise LD values (out of 100) label the relevant squares. Degree of square shading denotes LD magnitude. Empty black squares indicate LD = 1. Red boxes denote htSNPs. Boundaries of *DUSP6* transcribed sequence (~4.5 kb) in relation to the white bar are indicated. Locations on chromosome 12 are according to NCBI assembly build 36. CEPH = Centre d'Étude du Polymorphisme Humain; *DUSP6* = *Dual specificity phosphatase 6*; LD = linkage disequilibrium; MAF = minor allele frequency; NCBI = National Center for Biotechnology Information; SNP = single nucleotide polymorphism; htSNP = haplotype-tagging single nucleotide polymorphism.

Group (*n*)	% males	Statistic	Age of onset	Age of donation	Disease duration
CON (619)	49.6	Mean	NA	47.6	NA
		SD	NA	15.1	NA
IPD (614)	58.3	Mean	60.1	75.1	13.9
		SD	11.1	8.3	8.3

Table 3.9. IPD association series clinical data.

Group clinical metrics for the IPD association series. In the IPD group, 319 were brain samples and 295 were blood samples. Disease duration values for IPD blood samples were measured at a cut-off date in 2003. All of the controls were blood samples. Measures of time are in years. CON = control; IPD = idiopathic Parkinson's disease; NA = not applicable; SD = standard deviation.

SNP identity [DNA base ambiguity]	Location on chromosome 12	HapMap CEPH MAF	*n* alleles		MAF		HWE *p* value		Estimated OR [95% CI]	χ^2 allelic association *p* value	
			CON	IPD	CON	IPD	CON	IPD		Uncorrected	Corrected
rs11105262 [C/G]	88263586	0.068	1214	1220	0.079	0.082	0.141	0.080	1.040 [0.777 – 1.393]	0.793	NS
rs770087 [A/C]	88268904	0.150	1198	1216	0.205	0.184	0.185	0.786	0.874 [0.715 – 1.069]	0.190	0.760
rs2279574 [A/C]	88269608	0.388	1192	1206	0.488	0.454	1.000	0.373	0.884 [0.752 – 1.037]	0.089	0.356
rs1689408 [C/T]	**88278032**	**0.076**	**1198**	**1182**	**0.133**	**0.102**	**0.746**	**0.807**	**0.747 [0.582 – 0.958]**	**0.022**	**0.088**

Table 3.10. *DUSP6* IPD SNP association study data.

Dual specificity phosphatase 6 IPD SNP association study data. Variation at rs1689408 displayed a trend for association with IPD (in bold text), whereby the minor T allele conferred reduced risk of IPD. SNP identities, CEPH DNA base ambiguities (positive strand), and CEPH MAFs were obtained from HapMap phase II (release 23a from March 2008). DNA base ambiguity shows the major allele first (single letter codes in accordance with the International Union of Biochemistry and Molecular Biology). Locations on chromosome 12 are according to NCBI assembly build 36. HWE *p* values were not corrected. χ^2 allelic association *p* values were calculated under a multiplicative model and corrected x4. CEPH = Centre d'Étude du Polymorphisme Humain; CI = confidence interval; CON = control; *DUSP6* = *Dual specificity phosphatase 6*; HWE = Hardy-Weinberg equilibrium; IPD = idiopathic Parkinson's disease; MAF = minor allele frequency; NCBI = National Center for Biotechnology Information; NS = not significant; OR = odds ratio; SNP = single nucleotide polymorphism.

3.3.8. Variation at rs1689408 influences grey matter density in several brain regions

The mechanism underlying the effect of rs1689408 variation on IPD risk is unclear. Structural MRI has been used to examine grey matter density in asymptomatic *Parkin* heterozygous mutation carriers (Binkofski *et al.* 2007). Exploring relationships between this endophenotype and rs1689408 variation might shed further light on its role in IPD and the human brain. Therefore, genotypic VBM analysis was carried out for this SNP. MRI scans were generated for the imaging series (n = 302) (see table 3.11). These normal controls were then genotyped at rs1689408, split into homozygote majors and heterozygotes, and the groups subjected to voxel-wise statistical comparisons of grey matter density. Several regions of interest (ROIs) were selected based on evidence of *DUSP6* differential expression in the IPD expression analyses (see 3.3.3 and 3.3.5), on *Dusp6* expression as demonstrated in the Allen Mouse Brain Atlas (AMBA), or on a well-established role in IPD. The AG and FC were selected as ROIs based on the magnitude of differential NLC *DUSP6* expression, even though these changes did not survive correction. The ROIs were used to generate a mask which was applied to the data, producing the ROI analysis. The global analysis was subsequently generated by examining changes in grey matter density across the entire brain unconstrained by prior hypothesis. This experiment was performed in collaboration with Geoffrey Tan from our laboratory. Dr. Tan carried out the MRI scans, gDNA extractions, and statistical analyses.

Group (n)	% males	Heterozygote frequency	Statistic	Age of scan
CON (302)	45.4	0.179	Mean	31.6
			SD	12.2

Table 3.11. Imaging series demographic data.

Group demographic metrics for the imaging series. Heterozygote frequency refers to rs1689408 genotype. The rs1689408 genotypic data did not violate Hardy-Weinberg equilibrium (uncorrected p = 0.148). Age of donation is measured in years. CON = control; SD = standard deviation.

After FWE correction for multiple testing, the VBM ROI analysis demonstrated significant unilateral associations in several cortical and subcortical regions (see table 3.12 and figure 3.13). The results indicated that compared to C/C homozygotes, C/T heterozygotes possess higher grey matter density in these areas. Starting with the cortex, the right medial EC (corrected $p = 9.52e^{-5}$), right DLPFC (corrected $p = 0.001$), and left FC (corrected $p = 0.001$) were of significantly higher density in heterozygotes. In the subcortical limbic system, the same was true of the left hippocampus (corrected $p = 2.31e^{-5}$) and right amygdala (corrected $p = 2.62e^{-4}$). Within the striatum, the left caudate (corrected $p = 0.008$) was also of significantly higher density in heterozygotes. No significant differences were seen in the AG or the SN.

The VBM global analysis showed that rs1689408 heterozygotes possess significantly higher grey matter density in several regions, most of which were cortical (see table 3.13 and figure 3.14). Significant bilateral effects were observed in the subgenual ACC (corrected $p = 6.60e^{-8}$ and $5.16e^{-4}$ in left and right hemispheres, respectively), lateral orbitofrontal cortex (OFC) (corrected $p = 0.002$ and $3.32e^{-6}$ in left and right hemispheres, respectively), and insular cortex (corrected $p = 1.68e^{-4}$ and $5.21e^{-4}$ in left and right hemispheres, respectively). Significant unilateral differences were seen in the right inferior temporal pole (corrected $p = 2.51e^{-4}$), right superior frontal pole (corrected $p = 2.63e^{-4}$), left superior temporal sulcus (corrected $p = 5.46e^{-4}$), right medial EC (corrected $p = 0.001$), right precuneus (corrected $p = 0.007$), and left FC (corrected $p = 0.008$). Significant effects were also seen in two noncortical areas: the left cerebellar vermis (corrected $p = 1.27e^{-5}$) and left hippocampus (corrected $p = 3.19e^{-4}$).

Taken together, these data demonstrate that normal rs1689408 heterozygotes in the imaging series possess significantly higher levels of grey matter density in a variety of cortical and subcortical regions.

ROI				Statistics (FWE-corrected)			
Source	**Query (BA)**	**Outcome (BA)**	**Hemisphere**	**MNI coordinates**	***Z* score**	***p* value**	**Cluster extent**
IPD *DUSP6* differential expression	AG (39)	None	NA	NA	NA	NA	NA
	DLPFC (46)	DLPFC (46)	Right	42 49 19	4.80	0.001	8
	FC (8)	FC (8)	Left	-10 29 46	5.00	0.001	144
Dusp6 Expression in AMBA	Amygdala	Amygdala	Right	28 -1 -23	5.26	$2.62e^{-4}$	740
	Hippocampal formation	Hippocampus	Left	-23 -17 -19	5.73	$2.31e^{-5}$	952
		Medial EC (28)	Right	24 -17 -24	5.46	$9.52e^{-5}$	740
	Striatum	Caudate	Left	-13 9 14	4.51	0.008	115
Role in IPD	SN	None	NA	NA	NA	NA	NA

Table 3.12. Genotypic rs1689408 VBM data: ROI analysis.

Genotypic rs1689408 VBM ROI analysis data. Individuals heterozygous at rs1689408 exhibited significantly higher grey matter density in the right medial EC, right DLPFC, left FC, left hippocampus, right amygdala, and left caudate. No significant effects were observed in the AG or SN. Source indicates the reasons underlying ROI selection (see text for details). Query denotes the broad ROIs used in the analysis mask, and outcome the specific ROIs that demonstrated association. Cluster extent is the number of voxels making up each associated cluster. Groups were compared by *t* test. *p* values were corrected using the FWE approach. AMBA = Allen Mouse Brain Atlas; AG = angular gyrus (BA39); BA = Brodmann area; DLPFC = dorsolateral prefrontal cortex (BA46); EC = entorhinal cortex (BA28); FWE = family-wise error; FC = frontal cortex (BA8); IPD = idiopathic Parkinson's disease; MNI = Montreal Neurological Institute; NA = not applicable; ROI = region of interest; SN = substantia nigra; VBM = voxel-based morphometry.

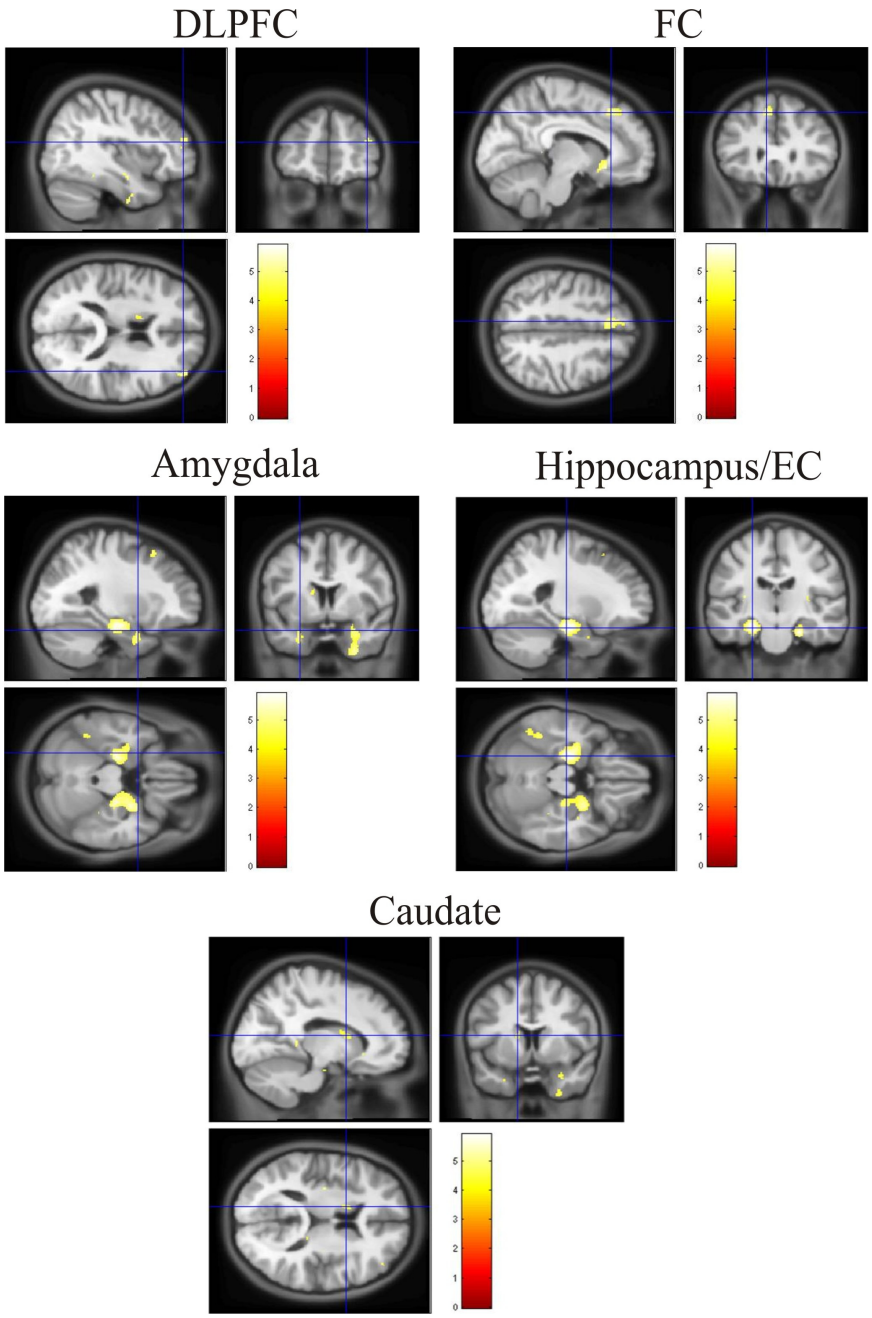

Figure 3.13. Genotypic rs1689408 VBM images: ROI analysis.

Genotypic rs1689408 VBM ROI analysis T1-weighted MRI images. Individuals heterozygous at rs1689408 exhibited significantly higher grey matter density in the right medial EC, right DLPFC, left FC, left hippocampus, right amygdala, and left caudate. No significant effects were observed in the AG or SN. Groups were compared by *t* test. *p* values were corrected using the FWE approach. Blue crosshairs specify the location of the peak associated voxels (and the first titular region in images displaying multiple associations). Heat map scales indicate *T* score gradients within the associated voxel clusters. AG = angular gyrus (BA39); BA = Brodmann area; DLPFC = dorsolateral prefrontal cortex (BA46); EC = entorhinal cortex (BA28); FWE = family-wise error; FC = frontal cortex (BA8); MRI = magnetic resonance imaging; ROI = region of interest; SN = substantia nigra; VBM = voxel-based morphometry.

Global		Statistics (FWE-corrected)			
Region (BA)	**Hemisphere**	**MNI coordinates**	***Z* score**	***p* value**	**Cluster extent**
Subgenual ACC (32)	Left	-10 39 -10	7.12	$6.60e^{-8}$	1699
Subgenual ACC (32)	Right	8 33 -11	5.64	$5.16e^{-4}$	1699
Lateral OFC (11)	Left	-27 39 -14	5.35	0.002	149
Lateral OFC (11)	Right	34 41 -12	6.52	$3.32e^{-6}$	819
Cerebellar vermis	Left	-15 -34 -45	6.29	$1.27e^{-5}$	149
Insular cortex (13)	Left	-37 -9 7	5.84	$1.68e^{-4}$	429
Insular cortex (13)	Right	44 -1 -19	5.63	$5.21e^{-4}$	321
Insular cortex (13)	Right	37 -13 7	4.97	0.013	64
Inferior temporal pole (20)	Right	47 -3 -43	5.77	$2.51e^{-4}$	662
Superior frontal pole (10)	Right	26 58 10	5.76	$2.63e^{-4}$	436
Hippocampus	Left	-23 -17 -19	5.73	$3.19e^{-4}$	439
Superior temporal sulcus (21)	Left	-45 -9 -14	5.62	$5.46e^{-4}$	547
Medial EC (28)	Right	24 -17 -24	5.46	0.001	339
Precuneus	Right	10 -40 6	5.10	0.007	57
FC (8)	Left	-8 29 46	5.08	0.008	68

Table 3.13. Genotypic rs1689408 VBM data: global analysis.

Genotypic rs1689408 VBM global analysis data. Individuals heterozygous at rs1689408 exhibited significantly higher grey matter density in the bilateral subgenual ACC, bilateral lateral OFC, left cerebellar vermis, bilateral insular cortex (BA13), right inferior temporal pole (BA20), right superior frontal pole (BA10), left hippocampus, left superior temporal sulcus (BA21), right medial EC, right precuneus, and left FC. Cluster extent is the number of voxels making up each associated cluster. Groups were compared by *t* test. *p* values were corrected using the FWE approach. ACC = anterior cingulate cortex (BA32); BA = Brodmann area; EC = entorhinal cortex (BA28); FWE = family-wise error; FC = frontal cortex (BA8); MNI = Montreal Neurological Institute; OFC = orbitofrontal cortex (BA11); VBM = voxel-based morphometry.

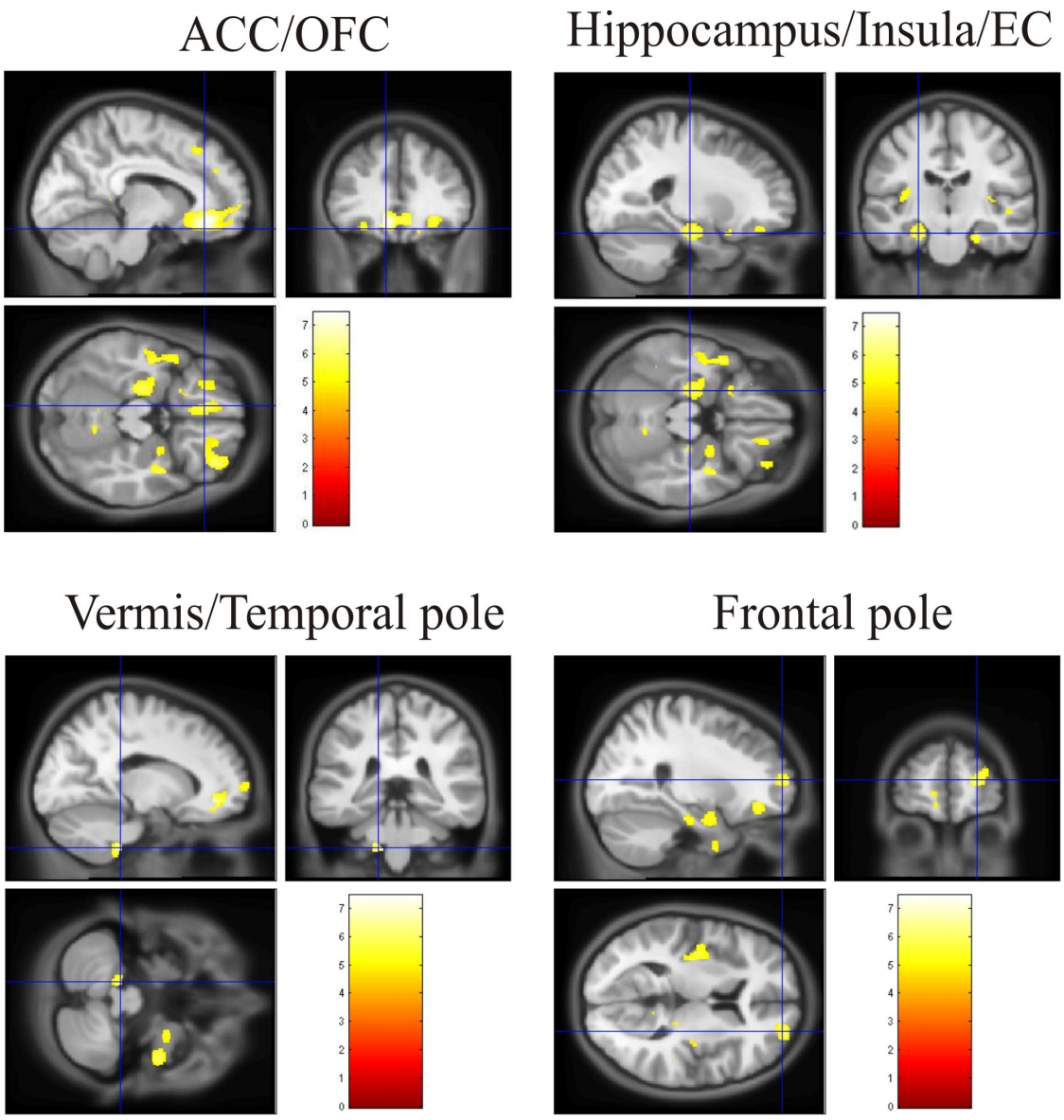

Figure 3.14. Genotypic rs1689408 VBM images: global analysis.

Genotypic rs1689408 VBM global analysis T1-weighted MRI images. Individuals heterozygous at rs1689408 exhibited significantly higher grey matter density in the bilateral subgenual ACC, bilateral lateral OFC, left cerebellar vermis, bilateral insular cortex (BA13), right inferior temporal pole (BA20), right superior frontal pole (BA10), left hippocampus, left superior temporal sulcus (BA21), right medial EC, right precuneus, and left FC. Groups were compared by *t* test. *p* values were corrected using the FWE approach. Blue crosshairs specify the location of the peak associated voxels (and the first titular region in images displaying multiple associations). Heat map scales indicate *T* score gradients within the associated voxel clusters. ACC = anterior cingulate cortex (BA32); BA = Brodmann area; EC = entorhinal cortex (BA28); FWE = family-wise error; FC = frontal cortex (BA8); MRI = magnetic resonance imaging; OFC = orbitofrontal cortex (BA11); VBM = voxel-based morphometry.

3.3.9. Variation at rs1689408 is implicated in *Dual specificity phosphatase 6* splicing in the dorsolateral prefrontal cortex

Variation at rs1689408 could alter brain structure and IPD susceptibility through a variety of mechanisms. This SNP is located ~7.6 kb upstream of the *DUSP6* transcriptional start site (TSS) in an intergenic region of no known regulatory function. One possibility is that rs168408 variation influences *DUSP6* expression. This could occur directly, for example by altering TF binding, or indirectly, by tagging a distant functional polymorphism. According to HapMap, this variant is in perfect LD with rs808820, which resides just 24 bp upstream of the start of *DUSP6* exon 2, and hence might influence *DUSP6* splicing. In order to investigate these possibilities, *cis*-acting variation analysis was performed for rs1689048. The cognitive series individuals were genotyped at this SNP, total and NLC DLPFC *DUSP6* expression data (cDNA batch 2 only) grouped by genotype, and the groups compared statistically (C/C homozygote majors [n = 33]; C/T heterozygotes [n = 13]). Two analyses were carried out on these groups. Initially, *DUSP6* FL expression data were analysed. However to investigate splicing, *DUSP6* FL data were also divided by *DUSP6* 1:3 data on an individual-by-individual basis, and resultant the *DUSP6* FL/1:3 ratios analysed in a similar fashion.

Table 3.14 and figure 3.15 show the results of these analyses. A trend of increased expression in heterozygotes compared to homozygotes was seen for NLC *DUSP6* FL expression. Similar trends were observed for total and NLC *DUSP6* FL/1:3 ratio. For these latter effects, the relative splice form balance was shifted towards *DUSP6* FL in heterozygotes. After correction for multiple testing, no significant effects were observed for variation at rs1689408 on *DUSP6* FL expression or *DUSP6* FL/1:3 ratio. Nevertheless, these data suggest that variation at rs1689408 is implicated in *DUSP6* splicing in the cognitive series DLPFC.

DUSP6 splice form	Expression	Fold change mean expression (het/hom)	het vs hom *p* value	
			Uncorrected	Corrected
FL	Total	1.18	0.453	NS
	NLC	1.98	0.037	NS
FL/1:3 ratio	Total	1.48	0.035	NS
	NLC	1.49	0.035	NS

Table 3.14. DLPFC *DUSP6* rs1689408 *cis*-acting variation analysis data.

Fold change mean *DUSP6* FL expression values and FL/1:3 ratios (rs1689408 hets relative to homs), and statistical results for cognitive series DLPFC cDNA batch 2. No significant differences were observed after correction for multiple testing. However, trends of increased total and NLC *DUSP6* FL/1:3 ratio were observed in hets, suggesting that variation at rs1689048 is implicated in *DUSP6* splicing in the DLPFC. Total expression data were normalised with *G6PD*, *RPL13A*, and *TBP*. NLC expression data were normalised with *NEFH*. FL/1:3 ratios were generated on an individual-by-individual basis; these are taken to be relative guides and do not necessarily represent the absolute ratios of FL to 1:3. Data were grouped by rs1689408 genotype, and hets and homs compared by Mann-Whitney test. *p* values were corrected x45. The rs1689408 genotypic data did not violate Hardy-Weinberg equilibrium (uncorrected $p = 0.747$). 1:3 = splice form 1:3; cDNA = complementary DNA; DLPFC = dorsolateral prefrontal cortex; *DUSP6 = Dual specificity phosphatase 6*; FL = full length; *G6PD = Glucose-6-phosphate dehydrogenase*; het = heterozygote; hom = homozygote major; *NEFH = Neurofilament H*; NLC = neuronal-loss corrected; NS = not significant; *RPL13A = Ribosomal protein L13A*; *TBP = TATA box binding protein*.

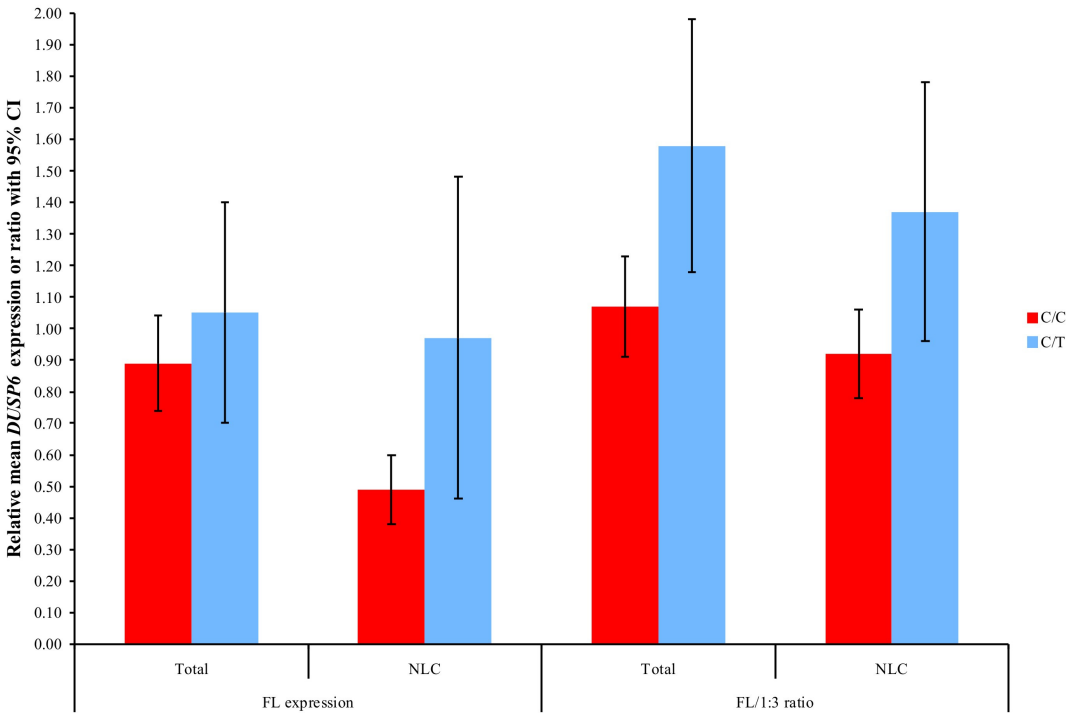

Figure 3.15. rs1689408 is implicated in *DUSP6* splicing in the DLPFC.

Relative mean *DUSP6* expression values and FL/1:3 ratios with 95% CI and statistical results for cognitive series DLPFC cDNA batch 2. No significant differences were observed after correction for multiple testing. However, trends of increased total and NLC *DUSP6* FL/1:3 ratio were observed in hets, suggesting that variation at rs1689048 is implicated in *DUSP6* splicing in the DLPFC. Total expression data were normalised with *G6PD*, *RPL13A*, and *TBP*. NLC expression data were normalised with *NEFH*. FL/1:3 ratios were generated on an individual-by-individual basis; these are taken to be relative guides and do not necessarily represent the absolute ratios of FL to 1:3. Data were grouped by rs1689408 genotype, and hets and homs compared by Mann-Whitney test. *p* values were corrected x45. The rs1689408 genotypic data did not violate Hardy-Weinberg equilibrium (uncorrected $p = 0.747$). 1:3 = splice form 1:3; CI = confidence interval; cDNA = complementary DNA; DLPFC = dorsolateral prefrontal cortex; *DUSP6 = Dual specificity phosphatase 6*; FL = full length; *G6PD = Glucose-6-phosphate dehydrogenase*; het = heterozygote; hom = homozygote major; *NEFH = Neurofilament H*; NLC = neuronal-loss corrected; *RPL13A = Ribosomal protein L13A*; *TBP = TATA box binding protein*.

3.4. Discussion

In this chapter it was demonstrated that MMSE score positively correlates with cerebellar *post mortem* brain pH in IPD patients. We used qRT-PCR to investigate 10 target genes, selected for their involvement in working or long term memory, and found that none were differentially-expressed in the DLPFC or AG of demented compared to nondemented IPD patients. However, variation in DLPFC *DUSP6* expression was shown to significantly associate with IPD. Moreover, it was demonstrated that this association manifests as *DUSP6* underexpression in IPD contrasted against controls, that this underexpression is not caused by modulated splicing, and that variation in *DUSP6* expression is not related to disease status in seven other subcortical and cortical brain regions. *DUSP6* DNA sequencing identified three low frequency SNPs and one 5'UTR point mutation that is restricted to FPD and abolishes a predicted NR3C1 TFBS. SNP allelic association analysis indicated that variation at rs1689408 is implicated in IPD susceptibility by trend of borderline significance. Specifically, the rs1689408 minor allele was found to confer decreased risk of IPD. Furthermore, genotypic VBM experiments demonstrated that normal rs1689048 heterozygotes possess significantly higher grey matter density in several brain regions. These include cortical (the subgenual ACC, lateral OFC, insular cortex, medial EC, DLPFC, and FC) and subcortical (the hippocampus, amygdala, and caudate) areas. Finally, a trend was observed in which rs1689408 heterozygotes exhibit relatively higher DLPFC *DUSP6* FL/1:3 ratios, thus providing a putative mechanism through which variation at this polymorphism might exert its effects on brain structure and IPD risk.

These findings connect *DUSP6* to IPD neurodegenerative processes in general, and not to IPD dementia. Moreover, the experiments detailed in this chapter failed to discover any genes specifically implicated in IPDD. Therefore, our results do not support the hypothesis that there is a relationship between IPD dementia status and gene expression in the DLPFC or AG. The expression of these 10 targets has not previously been investigated in the IPD BA46 or BA39, and so no direct precedent

exists against which we could evaluate the data. However, two microarray studies provide results of some relevance. One of these examined BA9 whole tissue extracts, and observed that IPD *DUSP6* expression was ~0.6-fold of that in controls (Zhang *et al.* 2005b). Given that BA9 and BA46 are DLPFC regions which lie adjacent to one another, this result goes some way to corroborating our own findings regarding *DUSP6* expression in the IPD DLPFC. The other study quantified gene expression in IPDD PCC neurons. This report showed that in IPD compared to controls, *BDNF* was expressed at ~0.6-fold and *PTGDS* at ~2-fold. Interestingly, the results also demonstrated that *DUSP6* was expressed at ~0.5-fold in IPDD vs IPDND and at ~0.4-fold in IPDD vs controls. These data indicate connections between *BDNF*/*PTGDS* and IPD neurodegeneration, and between *DUSP6* and IPD dementia (Stamper *et al.* 2008).

In terms of the relationship between *DUSP6* expression and IPD subtype, the discrepancy between our results and those of Stamper *et al.* might be explained by differences in brain region. Indeed, our data suggest that the association between IPD and variation in *DUSP6* expression is restricted to the DLPFC. SNCA and/or MAPT aggregation in the ACC and EC are the best cortical neuropathological predictors of cognitive dysfunction in IPD (Vermersch *et al.* 1993; Kovari *et al.* 2003; Pletnikova *et al.* 2005). Furthermore, a recent groundbreaking study has demonstrated that IPD dementia incidence is predicted by temporal-dependent semantic fluency skills, but not by prefrontal-dependent planning ability, suggesting that prefrontal executive dysfunction does not develop into dementia in this disorder (Williams-Gray *et al.* 2009a). Imaging studies indicate that semantic fluency tasks mainly activate the perirhinal cortex, parahippocampal cortex, and hippocampus (Pihlajamaki *et al.* 2000). Consequently, despite the classical neuropsychological rationale (WM-prefrontal-parietal) behind their selection, the DLPFC and AG may not have been the ideal regions in which to perform these experiments.

Apart from the choice of brain area, several other confounds could underlie the failure of the cognitive expression analysis to identify genes implicated in IPDD.

Firstly, the criteria for IPDD/IPDND group membership were carer reports of cognitive impairment and/or change in personality, backed up by MMSE scores indicative of dementia. The retrospective nature of the cognitive series meant that the latter was not available for some individuals allocated to the IPDND group, and hence they may have been incorrectly assigned. Moreover, the QSBBND database lacks information about other tests of dementia severity (e.g. the Mattis dementia rating scale), or of executive function (e.g. the Weschler Adult Intelligence Scale digit span, Wisconsin Card Sorting Task, or semantic fluency animal test), the latter of which would be most pertinent to the cognitive deficits that characterise IPDD (Girotti *et al.* 1988; Litvan *et al.* 1991; Bohnen *et al.* 2006; Williams-Gray *et al.* 2009a). Secondly, the two groups may have differed with regard to date of death, PD gene mutation, LB load, or therapeutic drug treatment. However, no clear disparities were observed (see Appendix). Thirdly, the number of individuals in each group may have been too low to robustly demonstrate significant differential expression. Nevertheless, *post hoc* calculations showed that the sample size provided 80% power to detect 1.3-fold ± 0.2-fold (SD) expression differences at a significance of corrected $p \leq 0.05$, suggesting that the numbers were sufficient. Next, the premise used to select targets (i.e. genes with a connection to working or long term memory) may have been flawed in the context of this disease. However, semantic fluency tasks recently found to predict dementia incidence in IPD are known to activate the perirhinal cortex, parahippocampal cortex, and hippocampus (see above) (Pihlajamaki *et al.* 2000; Williams-Gray *et al.* 2009a). The perirhinal cortex and hippocampus are both involved in long term and working memory, which therefore lends to support to our target selection approach (Squire and Zola-Morgan 1991; Cabeza *et al.* 2002; Lee *et al.* 2006a). Finally, the number of target genes could have simply been too few.

The positive correlation between cerebellar *post mortem* brain pH and MMSE score in IPD patients is an interesting result. We were unable to find any published study reporting this finding. One potential explanation might relate to CBF. This is decreased in the IPDD IPC, precuneus, and PCC, suggesting a relationship between

hypoperfusion and cognitive impairment in IPD (Firbank *et al.* 2003; Osaki *et al.* 2009). Reduced CBF would be expected to lower pH in the brain. Therefore our observed correlation between cerebellar pH and MMSE might be indicative of this relationship, adding further evidence in support of the published findings, and suggesting that they could be relevant to the IPD cerebellum. Nevertheless, this conclusion is potentially weakened by several confounding factors. Interindividual differences in agonal state (the state during the time immediately preceding death), notably in cause of death, might have affected *post mortem* pH via the opposing processes of acidosis and alkalosis. Furthermore, MMSE was not consistently measured at the same time before death in these individuals, which could have introduced a bias into the correlation.

The underexpression of *DUSP6* observed in the IPD DLPFC was robust. The best estimate of this effect is that on average, IPD cases express total *DUSP6* FL at ~60% of the level found in controls (see 3.3.4). Expression data for total *DUSP6* 1:3 indicate that this phenomenon is not caused by modulated splicing. Moreover, the majority of *DUSP6* locus SNP variation did not associate with IPD and the detected *cis*-acting influence was relatively weak (see below), which suggests that *DUSP6* underexpression does not have a primary genetic aetiology. Neuronal cell death is a potential confound. Indeed, demented IPD patients exhibit greater atrophy in BA46 than controls or their nondemented counterparts, although no differences are seen when comparing IPDND with controls (Burton *et al.* 2004; Nagano-Saito *et al.* 2005). Furthermore, the detected reductions in NLC *DUSP6* FL and 1:3 expression were merely nonsignificant trends, suggesting that a proportion of the *DUSP6* underexpression in the IPD DLPFC might be caused by neuronal loss. However, this possibility is unlikely to be the case for three main reasons: the total expression data were normalised with multiple reference genes which buffers against variation in tissue composition and experimental procedure (and would be expected to so more effectively than a single neuronal marker gene); NLC expression displayed changes of a similar direction and magnitude as total expression (albeit with more intragroup variation); and total *DUSP6* FL expression values for the IPDD and IPDND groups

were very similar, despite the reported differences in BA46 atrophy. We cannot exclude the possibility that the underexpression of *DUSP6* seen in the IPD DLPFC results in part from altered glial expression. Taken together, these results suggest that two possible explanations remain: changes in *DUSP6* transcriptional activity and/or alterations in *DUSP6* mRNA stability. These could be caused by modulation in many processes, such as TF binding and/or stability, epigenetic modification, or RNA interference. Whatever the reason behind *DUSP6* differential expression, our data suggest that this phenomenon is probably a secondary effect of IPD pathogenesis.

The role played by *DUSP6* in primary disease aetiology was evaluated using DNA sequencing and SNP association analyses. The sequencing data identified one FPD-restricted 5'UTR point mutation, +460G>C, which abolishes a predicted binding site for the TF NR3C1. However, the lack of available relatives precluded our ability to assess whether +460G>C segregates with FPD. Despite the limited number of samples, these findings suggest that *DUSP6* mutation is unlikely to be a significant cause of FPD. In contrast, the results of the SNP association study implied that the rs1689048 minor allele confers reduced susceptibility to IPD. *Post hoc* calculations showed that the sample size provided 80% power to detect an effect of OR ≈ 0.67 with the observed control MAF at a significance of corrected $p \leq 0.05$ (disease prevalence = 0.01). This suggests that the experiment was underpowered to confidently demonstrate significance for the observed trend.

Genotypic VBM analysis demonstrated that normal rs1689048 heterozygotes exhibit significantly higher grey matter density in several cortical and subcortical regions. These findings are not without precedent. Variation at the nonsynonymous Ile62Met polymorphism residing in *Dusp6* exon 1 significantly influences murine brain weight and anterior and hippocampal commissure size (Liu 2008). We observed effects in areas that acquire LP during IPD pathogenesis, such as the caudate, amygdala, hippocampus, medial EC, and subgenual ACC (Braak *et al.* 2003). Interestingly, several of these are known to display significant associations between LP burden and dementia in IPD patients i.e. the medial EC, amygdala, and hippocampus (Kovari *et*

al. 2003; Kalaitzakis *et al.* 2009a). Moreover, results were seen in regions that mediate critical cognitive and/or affective processes, some of which are relevant to IPD dementia. These include the ACC, OFC, and DLPFC which project to the striatum (specifically to the caudate, in the case of the OFC and DLPFC), forming part of the anterior cingulate, lateral orbitofrontal, and dorsolateral prefrontal loops, respectively (Alexander *et al.* 1986). The subgenual ACC is involved in affective processing and is activated by emotional attention tasks and depression (Bush *et al.* 2000). The lateral OFC is believed to regulate both executive ability, specifically the evaluation of novel stimuli that can result in behavioural change e.g. reversal learning, and the extent to which such information is encoded in declarative memory (Kringelbach 2005; Petrides 2007). The DLPFC controls the monitoring and manipulation of items held in WM (Petrides 2000). Other examples include the superior frontal pole, which is thought to be involved in executive functioning, specifically enabling the interposition of two concurrent mental strategies (Koechlin and Hyafil 2007); and the hippocampus and medial EC, which together constitute a well-established interconnected network that mediates the storage of information in declarative memory (Squire and Zola-Morgan 1991). Furthermore, rodent lesion studies suggest that the medial EC may also be implicated in WM and attention (Coutureau and Di Scala 2009). Given our trends potentially connecting AG *DUSP6* expression to IPD dementia, these data hint at the possibility that the role of *DUSP6* might extend to this disease subtype.

The *cis*-acting variation analysis results implied that rs1689408 heterozygotes exhibit increased DLPFC *DUSP6* FL/1:3 ratios. However, variation at this SNP does not seem to influence DLPFC *DUSP6* FL expression *per se*. We arrived at these conclusions because very similar fold change values were detected for total and NLC FL/1:3 ratios, whereas the fold change values for total and NLC FL expression were markedly different from each other. Nevertheless, the FL/1:3 ratio results were nonsignificant trends after correction, indicating that this finding is both preliminary and describing a relatively weak effect. *Post hoc* calculations showed that the sample size provided 80% power to detect 1.5-fold ± 0.34-fold (SD) differences at a

significance of corrected $p \leq 0.05$. This suggests that levels of intragroup variation were too large and/or the sample size too small to confidently demonstrate significance for the observed trends. Critically, our combined data suggest that this effect of SNP variation on *DUSP6* splicing is most likely distinct from the more general *DUSP6* underexpression effect observed in the IPD DLPFC.

In conclusion, it was shown that *DUSP6* expression is significantly decreased in the IPD DLPFC, but unaltered in seven other subcortical and cortical regions of the IPD brain, and that *DUSP6* mutation is unlikely to be a major cause of FPD. Moreover, the results indicated that genetic variation in the *DUSP6* locus marginally alters IPD risk and profoundly affects the structure of several human brain areas, possibly by influencing the splicing of this gene.

Chapter 4: Idiopathic Parkinson's disease cognitive expression microarray analysis and genetic characterisation of *Ephrin receptor A2*

4.1. Introduction

Microarray-based approaches have been used to investigate gene expression in the Parkinson's disease (PD) brain, successfully expanding our understanding of this condition. These findings have strengthened the role of known molecular players and pathways, and provided evidence that corroborates emerging research avenues (see below). Most studies have understandably focused on the substantia nigra (SN), although these techniques have also been employed to scrutinise other brain areas. When one compares publications examining the same region, there is considerable overlap of dysregulated pathways, even if the contents of gene lists vary (see below). Disparities arise from many interacting factors, including differences in array platform, sample quality and preparation (e.g. the use of whole tissues or specific cell types), disease stage(s) and course(s) of the patients under study, and data analysis methodology. The necessary constraint of using *post mortem* tissue usually obtained from late stage disorder suggests that a sizeable proportion of the detected changes are probably secondary effects arising during the disease process. At first glance, this seems disappointing for researchers interested in primary genetic aetiology. However, neuronal cell death in PD is most likely caused by a complex interplay of genetic, epigenetic, and environmental factors operating over many years [reviewed in (Lesage and Brice 2009)]. Consequently, these secondary effects probably drive disease progression at the molecular level and contribute to its clinical manifestation. Therefore, expression microarray techniques represent a powerful approach, with the

potential to elucidate key events in PD pathogenesis and generate novel therapies for this disorder.

One of the first microarray studies investigated gene expression in substantia nigra pars compacta (SNpc) whole tissue extracts. The authors found that in PD, signal transduction, protein degradation, energy/glycolysis, and iron transport pathways were downregulated, whereas those involved in the extracellular matrix (ECM), cytoskeleton/cell adhesion, and inflammation/hypoxia were upregulated (Grunblatt *et al.* 2004). Another early report also assessed SN whole tissues. This demonstrated PD-associated expression increases amongst heat shock genes, and decreases amongst genes mediating mitochondrial function, the ubiquitin-proteasome system (UPS), and protein trafficking. Within the final group, many of the hits regulated neurotransmitter secretion (Hauser *et al.* 2005). Zhang *et al.* analysed the SN, putamen, and dorsolateral prefrontal cortex (DLPFC) (Brodmann area 9 [BA9]) in parallel. They observed several group-based alterations that occurred across all (or two) of the regions tested. In PD, these included upregulation of heat shock, metallothionein, and polypyrimidine tract-binding genes, and downregulation of proteasome and mitochondrial electron transport chain (ETC) components, specifically constituents of complexes I, III, and IV (Zhang *et al.* 2005b). These data support the notion of PD as a multisystem disease involving several areas of the brain, and fit well with the widespread Lewy pathology (LP) detected in patients *post mortem* (Braak *et al.* 2003). This postulate was further bolstered by a study which focused on the SN but also examined the superior frontal gyrus, and observed significant genetic coregulation across these regions. The results identified numerous pathways that displayed PD-based expression changes in the SN, including those involved in metal ion binding, transport, signaling, nucleic acid binding, protein synthesis/breakdown, and cell adhesion (Moran *et al.* 2006).

The microarray experiments discussed so far were all performed using whole tissue extracts. Consequently, reports of dysregulated gene expression might not be "true" hits, but instead could represent artefacts arising from neuronal cell death and/or

gliosis. Moreover, it is difficult to ascertain the relative contribution of specific cell types (e.g. neurons or glia) to observed differences in expression. Cantuti-Castelvetri *et al*. circumvented these problems by employing laser capture microdissection (LCM) to examine expression exclusively in SNpc dopaminergic neurons. They detected PD-associated alterations of several gene groups, such as those mediating metal ion transport, cell-cell signaling, neurotransmitter secretion, and synaptic transmission. Furthermore, this was the first study to investigate gender-specific changes in PD. In females, protein kinase and proteolytic gene groups were dysregulated, whereas in males, the notable groups were those involved in protein-protein interactions and copper binding (Cantuti-Castelvetri *et al.* 2007). Simunovic *et al.* also used LCM to analyse SNpc dopaminergic neurons. In PD, their results demonstrated increased expression of pathways regulating apoptosis, inflammation, and cell survival, and decreased expression of pathways involved in ion transport, synaptic transmission, cytoskeletal maintenance, microtubule function, chaperone function, the UPS, and the mitochondrial ETC. Several PD-linked *PARK* locus genes were also downregulated (Simunovic *et al.* 2009).

Another recent publication assessing the SN took a slightly different approach to control for neuronal loss. The most intact regions (i.e. the most pigmented due to neuromelanin content) were selected for analysis. Moreover, the percentage reduction in neuronal density due to PD was measured, enabling the authors to more accurately evaluate changes in gene expression per neuron. One advantage of this methodology is that it still permits the quantification of nonneuronal (e.g. glial) expression (Bossers *et al.* 2009). The data indicated PD-associated alterations in neurotrophin signaling, axonal guidance, and synaptic transmission pathways, and demonstrated upregulation of gene groups involved in iron binding, cytoskeletal protein binding, and the ECM, as well as downregulation of groups mediating microtubule-based movement, oxidative phosphorylation, and the proteasome (Bossers *et al.* 2009). Consilient themes of dysfunctional pathways emerge from these studies, many of which play well-documented roles in PD and/or animal models thereof. Examples include the UPS, the mitochondrial ETC, oxidative stress, metal

ion binding/transport, synaptic transmission, axonal guidance, cytoskeletal/microtubule function, inflammation, cell adhesion/the ECM, chaperone/heat shock function, signal transduction, and apoptosis [reviewed in (Abou-Sleiman *et al.* 2006b; Sulzer 2007; Lin *et al.* 2009a; Hirsch and Hunot 2009)].

Until recently, microarrays had not been used to investigate gene expression in Parkinson's disease dementia (PDD). However, the study published by Stamper *et al.* changed the landscape of PD cognitive genetics. LCM was employed to isolate layer V and VI pyramidal neurons from the posterior cingulate cortex (PCC) of PD patients with and without dementia (and controls). Affymetrix's Human Genome U133 array was subsequently used to compare expression in these groups (Stamper *et al.* 2008). The results demonstrated that in PD dementia, genes mediating mitochondrial function and inflammation were downregulated and upregulated, respectively. In terms of PD neurodegeneration, differential expression was observed for genes regulating the proteasome, oxidative stress, axonal transport, axonal pathfinding, and synaptic transmission. Interestingly, the authors identified a subset of genes displaying changes of a similar direction in the PD demented vs nondemented and PD nondemented vs control comparisons. These were inferred to represent candidate "initiators" of dementia; cell adhesion, ribonucleic acid (RNA) splicing, and axonal transport were highlighted as key pathways putatively involved in this process (Stamper *et al.* 2008).

In summary, microarrays can reveal primary and secondary changes in gene expression, both of which probably contribute to the molecular pathogenesis of PD. These experiments have demonstrated that numerous genetic pathways exhibit dysregulation in the PD brain, corroborating evidence obtained using alternative genetic and biochemical approaches. The only published expression microarray study of PDD has pinpointed mitochondrial function, inflammation, cell adhesion, RNA splicing, and axonal transport as critical pathways implicated in this disease subtype.

4.2. Aims and methodology

Based on the background literature discussed in this (see 4.1) and the last chapter (see 3.1), it was hypothesised that there might be a relationship between idiopathic Parkinson's disease (IPD) dementia status and gene expression in the DLPFC, and that single nucleotide polymorphism (SNP) variation might influence IPD risk and gene expression. Therefore, the aims and methodology of this chapter were as follows:

1. **Identify genes implicated in IPD dementia and/or neurodegeneration.** Affymetrix GeneChip Exon 1.0 sense target (ST) oligonucleotide microarrays were used to compare genome wide messenger RNA (mRNA) gene expression in complementary DNA (cDNA) generated (see 2.8.2) from IPD microarray series (idiopathic Parkinson's disease with dementia [IPDD]; idiopathic Parkinson's disease no dementia [IPDND]; controls) DLPFC (BA46) (see 2.8.1). This was called the IPD cognitive expression microarray analysis (see 2.10.6). This array platform can detect differential gene expression and alternative exon splicing. Sample RNA quality was assessed using an Agilent 2100 Bioanalyzer (see Appendix) (see 2.8.1). Analysis was performed at the exon and gene levels. Data preprocessing was conducted using the robust multichip average (RMA) algorithm, and microarray quality control (QC) was carried out (see 2.10.6.1). The three group study design was identical to that employed for the IPD cognitive gene expression analysis (and similar to the approach used by Stamper *et al.*). As before, it enabled the discrimination of expression signatures related to specific IPD subtypes i.e. IPD dementia, IPD neurodegeneration, or both (see figure 3.1). Statistical comparisons were performed on $\log_2$ data by modified *t* test, with significance set at uncorrected $p < 0.01$ (see 2.10.6.1). The false discovery rate (FDR) approach was employed for multiple testing correction, but hits were identified by uncorrected significance due to biological variation and experimental constraints (see 4.3.2). Gene ontology (GO) terms (release 24th January 2010) associated with each microarray hit were collected (see 2.10.6.2).

Selected hits were validated using Sybr Green quantitative reverse transcriptase-polymerase chain reaction (qRT-PCR) to measure total and neuronal loss-corrected (NLC) mRNA expression in IPD cognitive series DLPFC cDNA batch 2 (see 3.2). Total expression data were normalised with a normalisation factor (NF) calculated from the reference genes *Glucose-6-phosphate dehydrogenase* (*G6PD*), *Ribosomal protein L13A* (*RPL13A*), and *TATA box binding protein* (*TBP*). NLC expression data were normalised with the neuronal marker *Neurofilament H* (*NEFH*) acting as reference gene (see 3.2). Statistical comparisons were carried out by Mann-Whitney test, with significance set at corrected $p \leq 0.05$ (see 2.10.2.2). So as to reduce the risk of pursuing false positives, only those genes exhibiting significant dysregulation in both the microarray and qRT-PCR analyses underwent further characterisation (henceforth called target genes).

2. **Examine target gene mRNA expression in multiple brain regions.** In order to further investigate target gene expression in IPD, Sybr Green qRT-PCR was employed to measure total and NLC target gene mRNA expression in medulla, putamen, amygdala, entorhinal cortex (EC [BA28]), anterior cingulate cortex (ACC [BA24]), angular gyrus (AG [BA39]), and frontal cortex (FC [BA8]) cDNA obtained from the IPD mapping series (see 3.2). Total expression data were normalised with a NF calculated from the most stable set of the following reference genes: *G6PD*, *RPL13A*, and *TBP*, and *Hypoxanthine phosphoribosyltransferase 1* (*HPRT1*). NLC expression data were normalised with the *NEFH* (see 3.2). Statistical comparisons were carried out by Mann-Whitney test, with significance set at corrected $p \leq 0.05$ (see 2.10.2.2). Brain region expression data were not compared with each other statistically.
3. **Investigate the effect of target gene SNP variation on IPD risk and target gene mRNA expression.** This aim consisted of two parts. In order to ascertain whether target gene SNP variation influences IPD susceptibility, a case-control genetic association study was performed, by using HapMap phase II Centre d'Étude du Polymorphisme Humain (CEPH) trio genotypic data (release 23a from March 2008) and Tagger to generate haplotype-tagging single nucleotide

polymorphisms (htSNPs), and TaqMan-genotyping IPD association series genomic DNA (gDNA) samples (see 3.2). Statistical assessment of allelic association under a multiplicative model was carried out by χ^2 test in Haploview, with significance set at corrected $p \leq 0.05$ (see 2.10.3.2). So as to discover whether target gene SNP variation affects target gene expression, *cis*-acting variation analysis was performed using cognitive series total and NLC DLPFC target gene mRNA expression data (batch 2) (see 3.2). Statistical comparisons were carried out by Mann-Whitney test, with significance set at corrected $p \leq 0.05$ (see 2.10.5).

4. **Evaluate hypotheses relevant to target gene differential expression and IPD pathogenesis.** In order to evaluate hypotheses relevant to target gene differential expression and IPD pathogenesis, *in silico* data mining was performed. The following bioinformatic resources were consulted to obtain lists of candidate genes: BioGRID, Kyoto Encyclopaedia of Genes and Genomes (KEGG), Online Mendelian Inheritance in Man (OMIM), University of California Santa Cruz (UCSC) PhyloP (assembly hg18), Ensembl (release 48 from December 2007), and PROMO. Log_2 microarray data were then mined *in silico*, and groups compared for candidate gene expression. Depending on distribution normality, statistical comparisons were carried out by *t* test or Mann-Whitney test, with significance set at uncorrected $p \leq 0.05$. *p* values were uncorrected due to prior hypothesis (see 2.10.6.3). Selected mining hits were validated using qRT-PCR to measure total and NLC expression in cognitive series DLPFC cDNA batch 2 (see above). Statistical comparisons were performed by Mann-Whitney test, with significance set at corrected $p \leq 0.05$ (see 2.10.2.2).
5. **Investigate the relationship between variation in target gene promoter CpG methylation and IPD.** So as to elucidate mechanisms underlying target gene differential expression, CpG methylation analysis was carried out (see 2.9). Methyl-specific polymerase chain reaction (MSP) (see 2.9.4) was employed to compare target gene relative CpG methylation in bisulphite-converted DLPFC gDNA (see 2.9.3) obtained from the IPD MSP series (IPD; controls) (see 2.9.1). MSP products were then resolved on agarose gels.

4.3. Results

4.3.1. Idiopathic Parkinson's disease cognitive expression microarray analysis: quality control

Microarrays were used to quantify genome wide exon and gene expression in the microarray series DLPFC. The microarray experiment was performed in collaboration with the Gene Microarray Centre (Institute of Child Health, University College London [UCL]) and the Bloomsbury Centre for Bioinformatics (UCL). Members of the former carried out the RNA quality assessments and microarray procedures; Dr. Sonia Shah at the latter performed the microarray preprocessing, QC, and statistical analyses. Before examining the microarray QC data, the microarray series was assessed for comparability based on clinicopathological characteristics. Group data for age of onset, age of death, disease duration, *post mortem* delay (PMD), *post mortem* brain pH, and mini mental state examination (MMSE) were analysed. After correction for multiple testing, the three groups (IPDD [$n = 7$]; IPDND [$n = 7$]; control [$n = 7$]) were not significantly different with regard to any of the first five metrics, indicating that they are comparable (see table 4.1). However, group MMSE scores for IPDD were significantly lower than those for IPDND (corrected $p = 0.048$), indicating that based on carer report and the available MMSE data, these two groups can be considered as IPD patients with and without dementia, respectively. Table 2.9 shows individual clinicopathological data for each member of the microarray series.

The expression microarray QC data can be seen in figures 4.1 and 4.2. Receiver operator curves (ROCs) evaluate how well the summarisation method separates exonic (positive) and intronic (negative) controls present on each array. The area under the curve (AUC) value for each chip fell between 0.8 and 0.9, indicating a low likelihood of false positives (data not shown). Pairwise microarray fluorescence correlations identify chips outlying the others in terms of total fluorescence, thereby

assessing overall array performance. For data normalised at both the exon and gene levels, most of the coefficients were high ($r \geq 0.95$), although the P24/94 and P59/00 chips were slightly less correlated to the others (data not shown). The intensity distribution histogram (IDH) curves for most arrays overlapped relatively well, indicating that microarray technique and RNA quality were of a good standard. However, this was less apparent in the gene level-normalised data.

MvA scatter plots were used to evaluate variation between the biological replicates comprising each group. For the most part, variation between the IPDD samples was relatively high. P18/01 exhibited marked differences from several other members of this group. These were visible in the exon level data, but much more pronounced in the gene level data. Similar patterns were observed for P24/94 and P59/00, although these were less extreme. Variation within the IPDND group was notably lower. One exception was P75/00, which also displayed its differences more extensively in the gene rather than the exon level data. Variation between the control samples fell somewhere between that seen within the two IPD groups. C03/00 was clearly different from the other controls, with C04/99 only slightly less so. Again, these observations were more pronounced in the gene level data when contrasted against the exon level data.

Taken together, these results demonstrate that the expression microarray data is generally high quality but possesses marked levels of biological variation, particularly in terms of the gene level-normalised data. Therefore, the expression array analysis will possess reduced statistical power. This is exemplified by the gene level principal components analysis (PCA) plot, which showed that the majority of samples did not cluster according to group (see figure 4.3).

Group (*n*)	Statistic	Age of onset	Age of death	Disease duration	PMD	Brain pH	MMSE
CON (7)	Mean	NA	80.7	NA	27.0	6.52	ND
	SD	NA	7.0	NA	16.7	0.18	ND
IPDD (7)	Mean	54.1	73.3	19.2	38.1	6.15	19.9
	SD	9.6	5.0	10.4	13.8	0.23	4.9
IPDND (7)	Mean	59.4	75.1	15.7	48.8	6.43	29.5
	SD	10.7	8.0	4.5	33.1	0.37	0.6
p value	Uncorrected	0.338	0.175	0.443	0.318	0.019	0.008
	Corrected	NS	NS	NS	NS	0.114	0.048

Table 4.1. IPD microarray series clinicopathological data.

Group clinicopathological metrics and statistical results for the IPD microarray series. After correction for multiple testing, the first five metrics were not significantly different, indicating that the groups are comparable. However, MMSE was significantly lower in the demented patients. Together with carer reports regarding cognitive impairment or change in personality (see table 2.9), this result indicates that the IPDD and IPDND groups are correctly labelled as such. Measures of time are in years, except for PMD, which is measured in hours. Groups were compared by Mann-Whitney or Kruskal-Wallis test as appropriate. *p* values were corrected x6. CON = control; IPDD = idiopathic Parkinson's disease dementia; IPDND = idiopathic Parkinson's disease no dementia; MMSE = mini mental state examination; NA = not applicable; ND = not determined; NS = not significant; PMD = *post mortem* delay; SD = standard deviation.

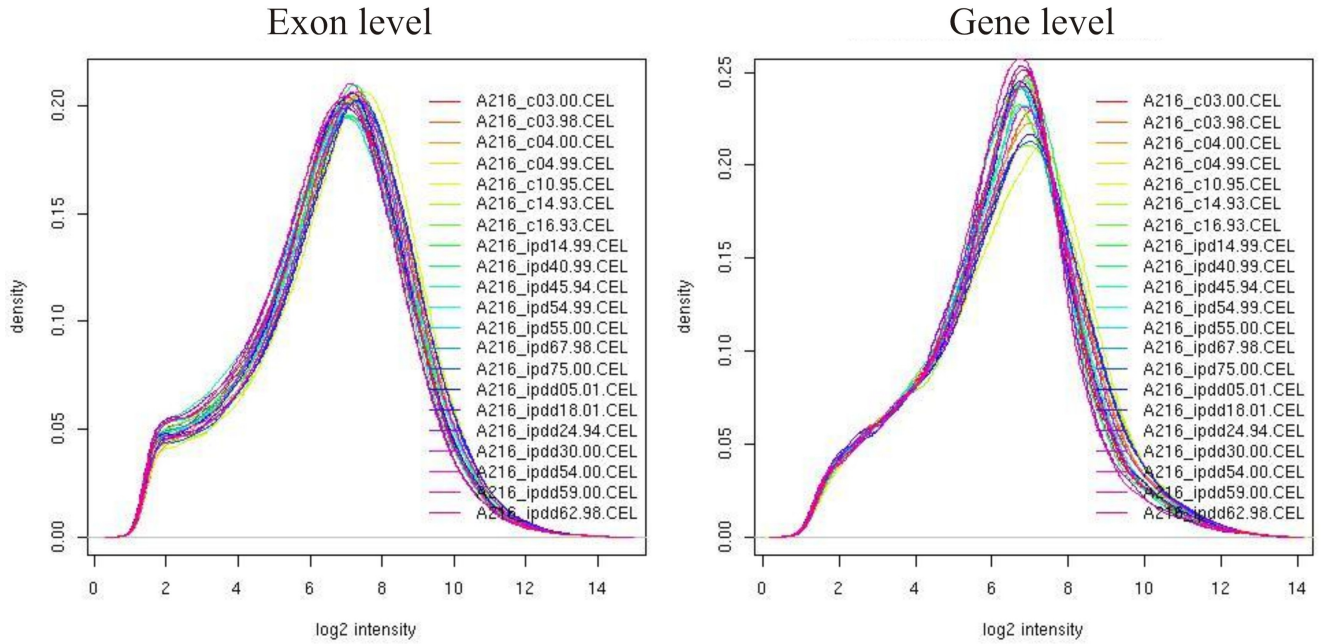

Figure 4.1. Cognitive expression microarray QC: IDH plots.

Cognitive expression microarray IDH plots. For data normalised at both the exon and gene levels, the majority of the distribution curves overlapped well, indicating that microarray technique and RNA quality were of a good standard. However, this was less apparent in gene level data. Density distribution of exon level- and gene level-normalised $\log_2$ fluorescence intensity was plotted for each array. C = control; IPDD = idiopathic Parkinson's disease dementia; IPD = idiopathic Parkinson's disease no dementia; IDH = intensity distribution histogram; QC = quality control; RNA = ribonucleic acid.

Figure 4.2. Cognitive expression microarray QC: MvA scatter plots.

Cognitive expression microarray MvA scatter plots (following pages). Marked biological (intragroup) variation was observed in IPDD, and to a lesser extent, in CON. IPDND was relatively spared. P18/01, P24/94, P59/00, C03/00, C04/99, and P75/00 exhibited notable differences from other members of their respective groups. Gene level-normalised data possessed greater variation than exon level-normalised data. For data normalised at the exon and gene levels, A values (means of $\log_2$ probeset or cluster intensity values) were plotted against M values (ratios of $\log_2$ probeset or cluster intensity values) for all intragroup pairwise sample combinations. LOESS curves (red) indicate deviation from the x axis (blue); this corresponds to intersample variation. CON = control; LOESS = locally weighted scatter plot smoothing; IPDD = idiopathic Parkinson's disease dementia; IPDND = idiopathic Parkinson's disease no dementia; QC = quality control.

Exon level: CON

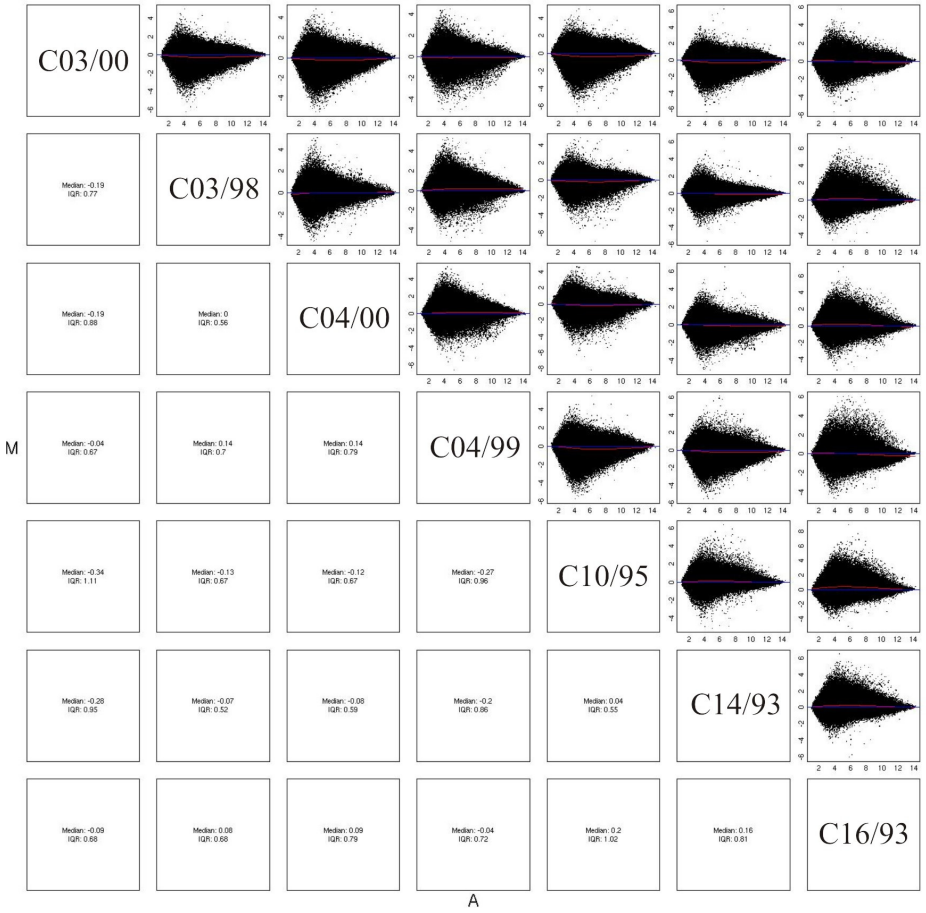

Gene level: CON

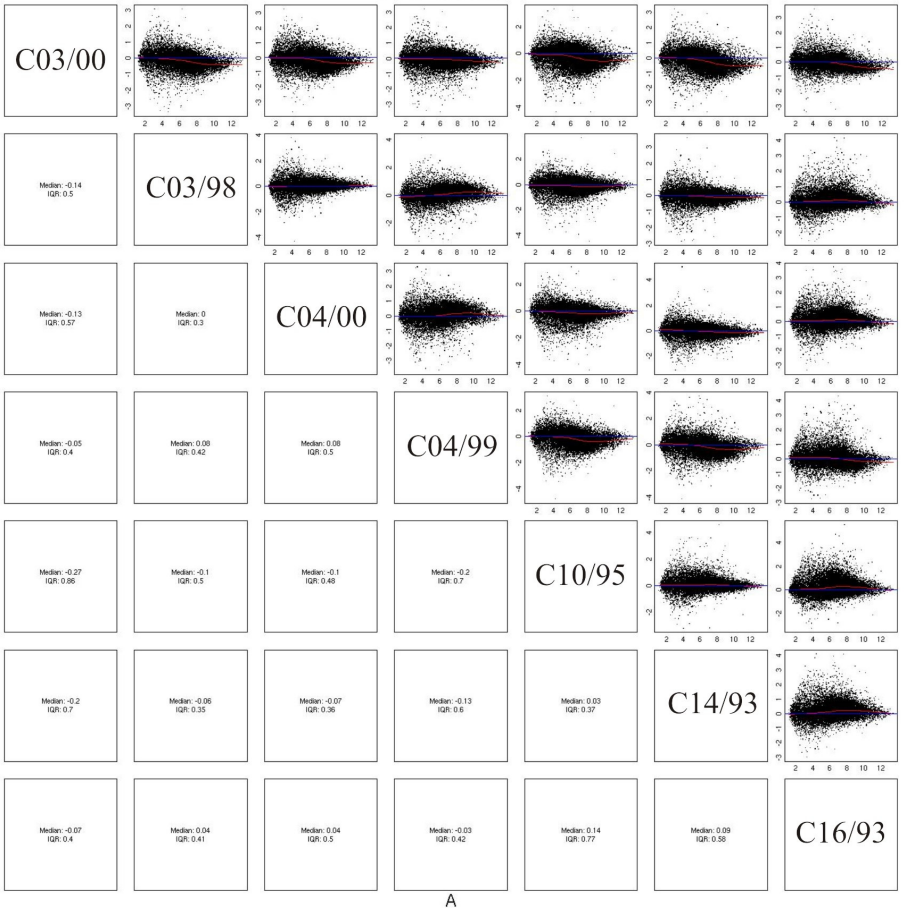

Exon level: IPDD

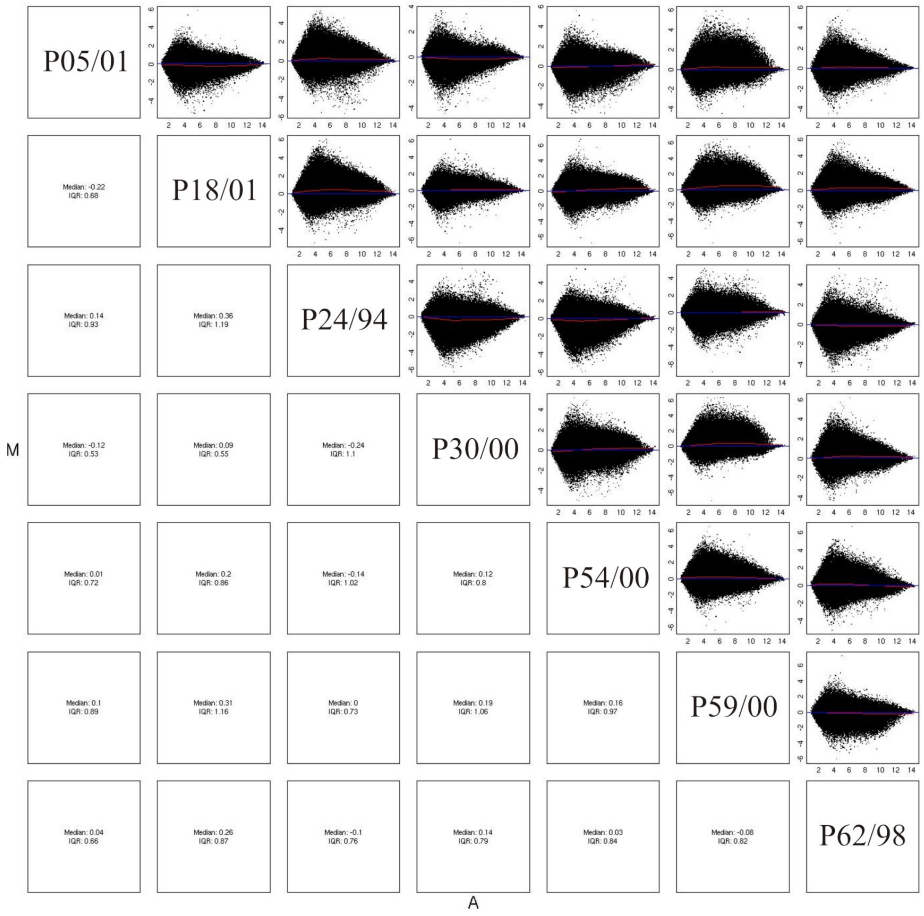

Gene level: IPDD

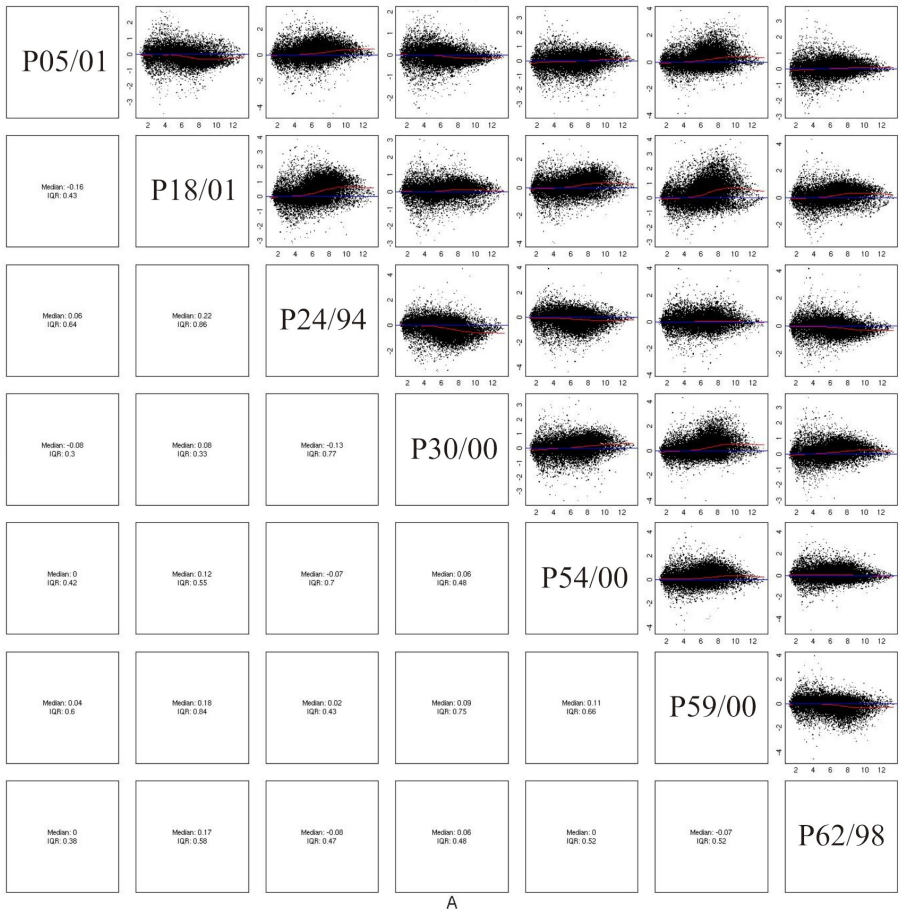

Exon level: IPDND

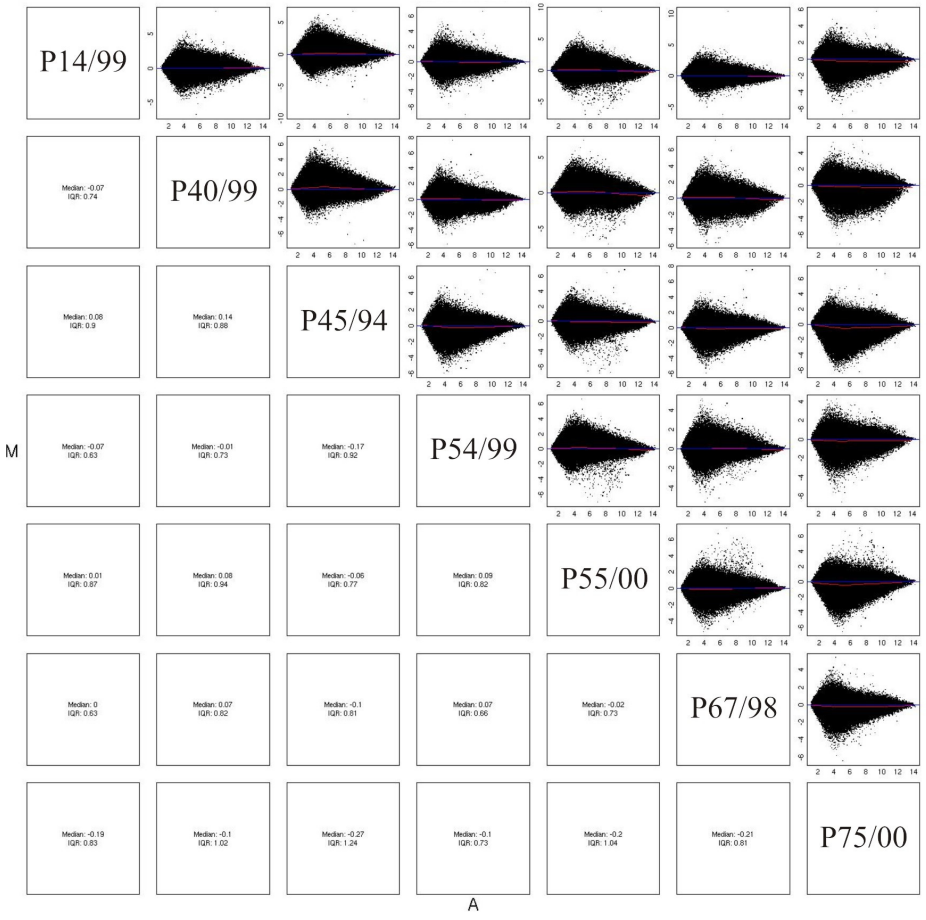

Gene level: IPDND

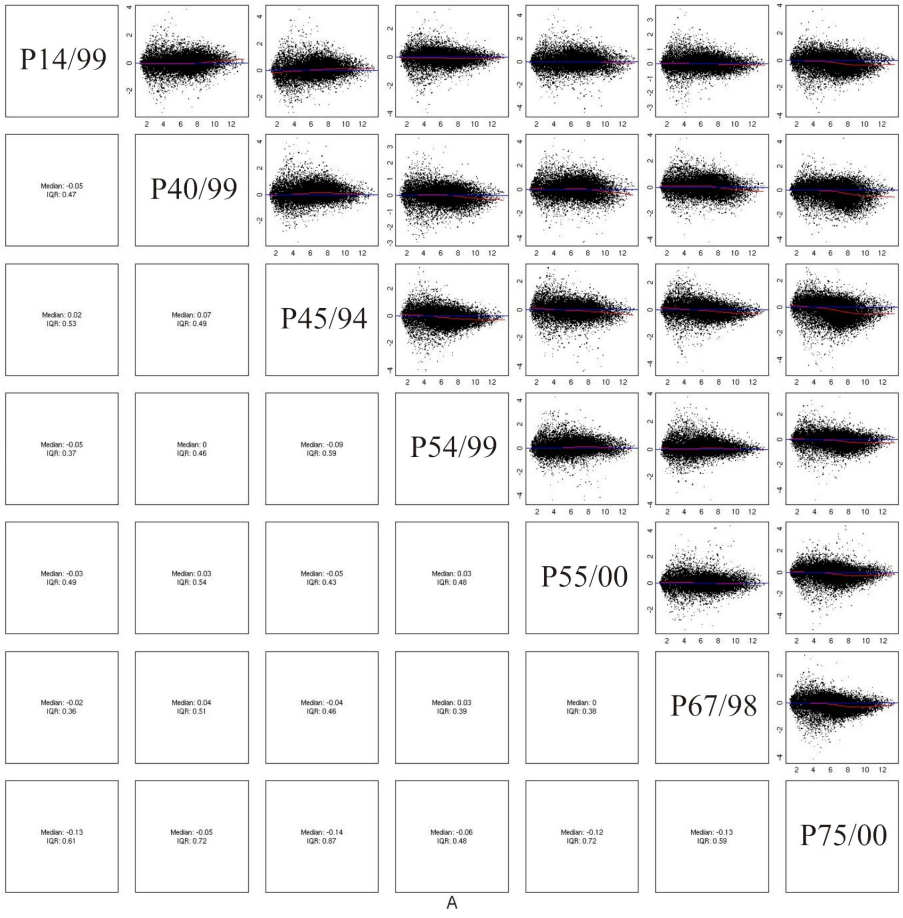

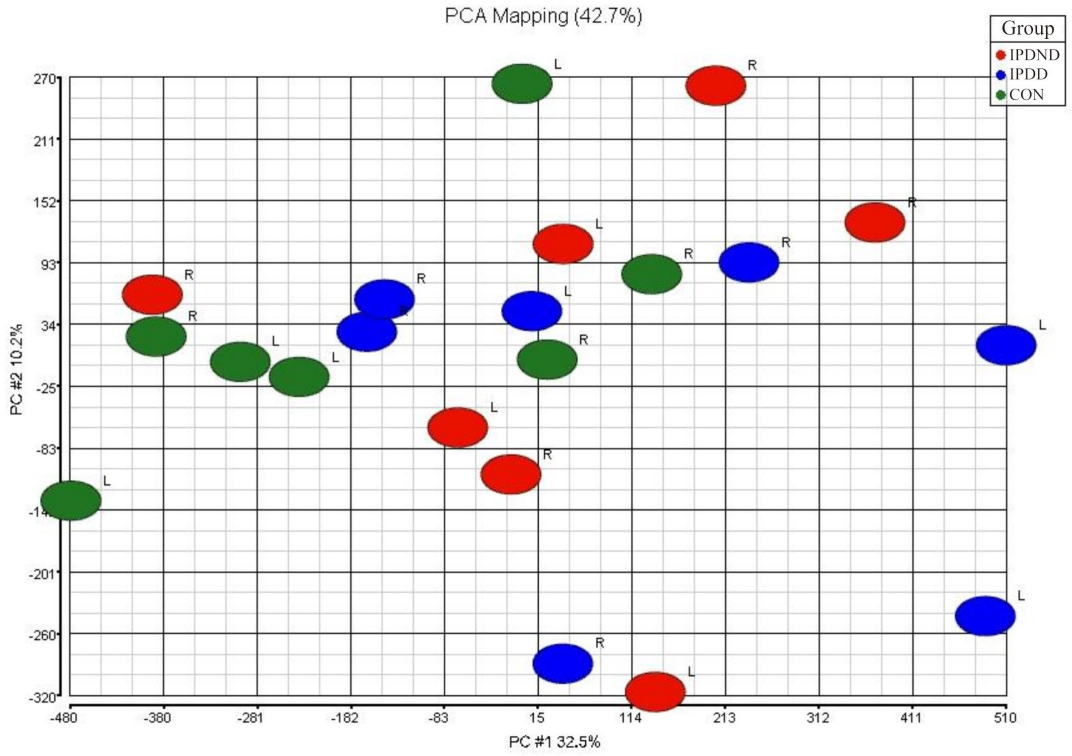

Figure 4.3. Cognitive expression microarray gene level PCA plot.

Cognitive expression microarray PCA plot for gene level-normalised data. PCA mapping identified two principal components that together account for 42.7% of the variation in expression. The majority of samples did not cluster according to group, indicating high levels of intragroup variation. CON = control; IPDD = idiopathic Parkinson's disease dementia; IPDND = idiopathic Parkinson's disease no dementia; L = left hemisphere; PCA = principal components analysis; R = right hemisphere.

4.3.2. Idiopathic Parkinson's disease cognitive expression microarray analysis: results overview

Given the huge number of statistical tests carried out when analysing microarray data, it is necessary to perform correction for multiple testing. Bonferroni correction is generally considered too harsh for this kind of analysis, and other methods are available. The FDR approach was selected for the cognitive expression microarray analysis. Table 4.2 shows the number of differentially-expressed exons and genes for each of the three intergroup comparisons. The results demonstrated that no events pass the FDR threshold $p < 0.05$. The only potential hit was an exon downregulated in IPDD vs controls, but this proved to be expressed below the signal-noise cut-off point (see 2.10.6.2). This lack of hits was perhaps unsurprising, when one considers the relatively high levels of biological variation observed in the IPDD and control groups (see 4.3.1).

Consequently, a more relaxed threshold of uncorrected $p < 0.001$ was applied, so as to gain an overall picture of the extent of dysregulated expression. Using this approach, multiple dysregulation events were observed (see table 4.2). The analysis detected much more alternative splicing than differential expression. For example in the IPDD vs control comparison, 709 exons were alternatively-spliced, whereas only 68 genes were differentially-expressed. Over all three comparisons, 945 alternative splicing and 73 differential expression events were observed. Markedly more dysregulation events were seen in the IPDD vs control comparison than in either the IPDND vs control or IPDD vs IPDND comparisons; similarly low numbers of events were observed in these latter two comparisons. For example, when contrasting IPDD vs controls against IPDND vs controls, 68 and 3 genes were differentially-expressed, respectively. This was the case in both the exon and gene level analyses, and suggests that when both groups are compared to controls, more genetic dysregulation occurs in IPDD than in IPDND.

Exon level analysis			
Corrected $p < 0.05$ threshold	**IPDD vs CON**	**IPDND vs CON**	**IPDD vs IPDND**
Upregulated	0	0	0
No change	175503	175504	175504
Downregulated	1	0	0
Uncorrected $p < 0.001$ threshold	**IPDD vs CON**	**IPDND vs CON**	**IPDD vs IPDND**
Upregulated	403	54	52
No change	174795	175374	175398
Downregulated	306	76	54
Gene level analysis			
Corrected $p < 0.05$ threshold	**IPDD vs CON**	**IPDND vs CON**	**IPDD vs IPDND**
Upregulated	0	0	0
No change	17817	17817	17817
Downregulated	0	0	0
Uncorrected $p < 0.001$ threshold	**IPDD vs CON**	**IPDND vs CON**	**IPDD vs IPDND**
Upregulated	39	1	2
No change	15075	15140	15141
Downregulated	29	2	0

Table 4.2. IPD cognitive expression microarray analysis summary.

Summary of dysregulation events observed in the IPD cognitive expression microarray analysis. Multiple genes demonstrated differential expression or alternative splicing at the uncorrected $p < 0.001$ threshold, but none of these events survived FDR correction. Exon level counts indicate alternative splicing events, and exclude situations where the majority of a gene's exonic complement is dysregulated in the same direction; these are registered as gene level differential expression events. All data are displayed at two significance thresholds: FDR-corrected $p < 0.05$ and uncorrected $p < 0.001$. CON = control; FDR = false discovery rate; IPD = idiopathic Parkinson's disease; IPDD = idiopathic Parkinson's disease dementia; IPDND = idiopathic Parkinson's disease no dementia.

Therefore, multiple genes demonstrated differential expression or alternative splicing in the expression microarray at the uncorrected $p < 0.001$ threshold, but none of these events survived FDR correction. Given the high levels of biological variation (see figure 4.2) and the requirement for genes/exons to be significantly different in two comparisons (see figure 3.1), uncorrected $p < 0.01$ was employed as the significance threshold for identifying microarray hits. We are aware that this decreases statistical confidence in the results. Nonetheless, it is known that when examining microarray data, uncorrected significance is valid as long as certain conditions are met. These conditions are that probes should be expressed above the signal-noise cut-off, group interquartile ranges should be sufficiently distant from each other, and hits should fit into a sensible biological context (M. Hubank, personal communication). Thus, as long as the reduced statistical confidence is kept in mind, these uncorrected findings can be useful for flagging genes of potential importance.

4.3.3. Expression microarray: genes implicated in idiopathic Parkinson's disease neurodegeneration

Genes implicated in IPD neurodegeneration were filtered out of the microarray data, by identifying all of the genes/exons exhibiting dysregulation in both the IPDD vs control and IPDND vs control comparisons (uncorrected $p < 0.01$). Using these criteria, six genes were differentially-expressed and 12 were alternatively-spliced (see table 4.3).

Examining the National Center for Biotechnology Information (NCBI) Gene database, GO term associations, and literature indicates that these hits encompass several functional pathways relevant to IPD. The first of these was synaptic transmission/ion transport. The ion channel subunit-encoding genes *FXYD domain containing ion transport regulator 2* (*FXYD2*) and *Calcium channel, voltage-dependent, α2/δ3 subunit* (*CACNA2D3*) were alternatively-spliced. FXYD2 modulates the activity of the sodium-potassium adenosine triphosphatase (ATPase) which maintains neuronal resting potential (Geering 2006). CACNA2D3 regulates voltage-dependent L-type $Ca_v1.2$ and $Ca_v1.3$ channels which mediate calcium influx during synaptic transmission. Blocking $Ca_v1.3$ protects SNpc dopaminergic neurons from 1-methyl-4-phenyl-1,2,3,6-tetrahydropyridine (MPTP)-induced cell death *in vivo* (Chan *et al.* 2007). Dysregulation of these genes could alter potassium and calcium ion transport, respectively, affecting neuronal viability in IPD (Sulzer 2007). Alternative splicing was also observed for *Exocyst complex component 3-like* (*EXOC3L*), potentially influencing neurotransmitter secretion. *Adenylate cyclase activating polypeptide 1* (*ADCYAP1*) was underexpressed, which may contribute to IPD-associated neuronal loss, as its encoded peptide hormone and neurotransmitter protects SNpc dopaminergic cells and improves parkinsonian symptoms in rats treated with 6-hydroxydopamine (6-OHDA) (Reglodi *et al.* 2004). Given the well-documented hyposmia that occurs early in IPD, it was interesting to see

downregulation of *Olfactory receptor, family 2, subfamily M, member 4* (*OR2M4*) (Katzenschlager and Lees 2004).

The next pathway of note was glycosylation/protein degradation. Genes encoding two enzymes that regulate glycosylation, *Mannosidase, α, class 1B, member 1* (*MAN1B1*) and *O-linked N-acetylglucosamine transferase* (*OGT*), were alternatively-spliced. MAN1B1 is a member of the mannosidase I family, which controls the entry of substrates into the endoplasmic reticulum-associated degradation (ERAD) pathway. This system mediates the retrotranslocation of misfolded proteins from the endoplasmic reticulum (ER) to the cytosol, where they are destroyed by the UPS. ERAD is thought to play a role in protein aggregation during IPD pathogenesis (Yoshida 2007). OGT catalyses the addition of *N*-acetylglucosamine onto Ser/Thr residues in a wide range of substrates, thereby influencing several neuronal processes, including proteasomal degradation, transcription, signaling, and axonal transport. Furthermore, there is evidence to suggest that OGT regulates Microtubule-associated protein tau (MAPT) phosphorylation and stability (Lazarus *et al.* 2009). Dysregulation of these genes could alter glycosylation and/or protein degradation and affect neuronal cell death in IPD.

Inflammation/immune response was the third implicated pathway. Four genes of known or putative immunological function were dysregulated: *Interferon, α-inducible protein 27* (*IFI27*); *Lymphocyte antigen 6 complex, locus K* (*LY6K*); *V-rel reticuloendotheliosis viral oncogene homologue B* (*RELB*); and *Retinoic acid receptor responder 2* (*RARRES2*). RELB is a member of the Nuclear factor κ light polypeptide gene enhancer in B-cells (NFKB) transcription factor (TF) family. This pathway can be induced by multiple stimuli, including inflammation and stress, and influences neuronal cell death outcomes both directly and indirectly, via glial-mediated proinflammatory cytokine release (see below) (Memet 2006). Moreover, NFKB is activated in IPD SNpc dopaminergic cells, and its inhibition protects SNpc dopaminergic neurons and ameliorates locomotor dysfunction in MPTP-treated mice (Hunot *et al.* 1997; Ghosh *et al.* 2007). RARRES2 is a chemotactic protein that

attracts dendritic cells, macrophages, and natural killer cells to sites of inflammation (Moretta *et al.* 2008). In our series, the expression of these four genes may well be glial-derived, and the observed changes could affect inflammatory and/or immune processes and modulate IPD-associated neuronal loss. Indeed, inflammation resulting from reactive gliosis, and possibly even gliodegeneration, are believed to contribute to IPD pathogenesis (Croisier and Graeber 2006).

The final dysregulated pathway was transcription/translation, which encompassed *POU class 4 homeobox 3* (*POU4F3*), *Quaking homologue, KH domain RNA binding* (*QKI*), and *RELB*. *POU4F3* encodes a TF that regulates inner ear hair cell survival and migration in mouse models (Xiang *et al.* 1998). Mutations in this gene cause autosomal dominant deafness in humans (OMIM #602459), apparently through inhibition of DNA binding and transcription (Collin *et al.* 2008). QKI is an RNA-binding protein which controls myelination, oligodendrocyte differentiation, and apoptosis, via its effects on RNA splicing, stabilisation, and translation (Chenard and Richard 2008). Dysregulation of *POU4F3*, *QKI*, and *RELB* (see above) could alter the expression of their target genes and influence neuronal cell death in IPD.

Overall, these results suggest that synaptic transmission/ion transport, glycosylation/protein degradation, inflammation/immune response, and transcription/translation pathways are dysregulated in IPD neurodegeneration.

Table 4.3. Cognitive expression microarray: genes implicated in IPD neurodegeneration.

Genes exhibiting dysregulated expression or splicing implicating them in IPD neurodegeneration (following pages). The results suggest that synaptic transmission/ion transport, glycosylation/protein degradation, inflammation/immune response, and transcription/translation pathways are dysregulated in IPD neurodegeneration. Genes are listed alphabetically, with the differential expression group preceding the alternative splicing group. All *p* values were uncorrected, except those marked with §, which were FDR-corrected. Uncorrected IPDD vs IPDND *p* values were nonsignificant for all listed genes. GO term associations were obtained from the GO database (release 24th January 2010); GO term identity codes are bolded. See list of abbreviations for gene symbol definitions. ATPase = adenosine triphosphatase; CON = control; FDR = false discovery rate; GO = gene ontology; IPD = idiopathic Parkinson's disease; IPDD = idiopathic Parkinson's disease with dementia; IPDND = idiopathic Parkinson's disease no dementia; pwy = pathway; RNA = ribonucleic acid; mRNA = messenger RNA; Src = Sarcoma; SH2 = Src homology 2; SH3 = Src homology 3; sig = signaling.

Gene symbol	Statistic	IPDD vs CON	IPDND vs CON	GO term associations		
				Biological process	**Cellular component**	**Molecular function**
ADCYAP1	Fold change	0.58	0.67	Activation of adenylate cyclase activity **7190**/Cell-cell sig **7267**/Female pregnancy **7565**/G-protein coupled receptor sig pwy **7186**/Negative regulation of cell cycle **45786**/ Transmembrane receptor protein tyrosine kinase sig pwy **7169**	Extracellular region **5576**/Soluble fraction **5625**	Neuropeptide hormone activity **5184**/Receptor sig protein activity **5057**
	p value	$6.40e^{-5}$	$1.61e^{-3}$			
	p value[§]	0.135	0.570			
C3orf36	Fold change	1.41	1.32	None	None	None
	p value	$5.07e^{-4}$	$3.15e^{-3}$			
	p value[§]	0.135	0.570			
LY6K	Fold change	1.34	1.27	None	Anchored to membrane **31225**/Cytoplasm **5737**/Extracellular region **5576**/Plasma membrane **5886**	None
	p value	$4.54e^{-4}$	$2.64e^{-3}$			
	p value[§]	0.135	0.570			
OR2M4	Fold change	0.77	0.82	G-protein coupled receptor sig pwy **7186**/Response to stimulus **50896**/Sensory perception of smell **7608**/Signal transduction **7165**	Integral to membrane **16021**/Plasma membrane **5886**	Olfactory receptor activity **4984**/Receptor activity **4872**
	p value	$3.71e^{-4}$	$3.91e^{-3}$			
	p value[§]	0.135	0.570			
POU4F3	Fold change	1.45	1.38	Auditory receptor cell differentiation **42491**/Axon extension involved in development **48676**/Inner ear morphogenesis **42472**/Neuromuscular process controlling balance **50885**/Neuron apoptosis **51402**/Regulation of transcription from RNA polymerase II promoter **6357**/Retinal ganglion cell axon guidance **31290**/Sensory perception of sound **7605**/Vestibulocochlear nerve development **21562**/Visual perception **7601**	Nucleus **5634**	Sequence-specific DNA binding **43565**/Transcription factor activity **3700**
	p value	$6.26e^{-4}$	$2.47e^{-3}$			
	p value[§]	0.135	0.570			
RPL35A	Fold change	1.63	1.44	Ribosomal large subunit biogenesis **42273**/Ribosomal RNA processing **6364**/Translational elongation **6414**	Cytosol **5829**/Intracellular **5622**/Ribosome **5840**	Protein binding **5515**/Structural constituent of the ribosome **3735**/Transfer RNA binding **49**
	p value	$5.23e^{-4}$	$5.54e^{-3}$			
	p value[§]	0.135	0.570			

Gene symbol	Exon	Statistic	IPDD vs CON	IPDND vs CON	GO term associations		
					Biological process	Cellular component	Molecular function
C8orf79	1	Fold change	1.71	1.48	Metabolic process **8152**	None	Methyltransferase activity **8168**/Transferase activity **16740**
		p value	$3.32e^{-5}$	$9.75e^{-4}$			
		p value[§]	0.217	0.717			
CACNA2D3	Intron 1-2	Fold change	1.96	1.83	Calcium ion transport **6816**/Ion transport **6811**	Integral to membrane **16021**/Membrane **16020**	Calcium ion binding **5509**/Voltage-gated calcium channel activity **5245**/Voltage-gated ion channel activity **5244**
		p value	$2.10e^{-4}$	$6.38e^{-4}$			
		p value[§]	0.234	0.717			
EXOC3L	9	Fold change	1.64	1.60	Exocytosis **6887**/Peptide hormone secretion **30072**	Exocyst **145**/Secretory granule **30141**	None
		p value	$5.10e^{-4}$	$8.29e^{-4}$			
		p value[§]	0.243	0.717			
FXYD2	4	Fold change	1.54	1.51	Ion transport **6811**/Potassium ion transport **6813**/Sodium ion transport **6814**	Integral to membrane **16021**/Membrane **16020**/Sodium:potassium-exchanging ATPase complex **5890**	Ion channel activity **5216**/Potassium ion binding **30955**/Sodium ion binding **31402**/Sodium:potassium-exchanging ATPase activity **5391**/Transporter activity **5215**
		p value	$6.86e^{-5}$	$1.18e^{-4}$			
		p value[§]	0.232	0.717			
IFI27	5	Fold change	0.71	0.76	None	Integral to membrane **16021**/Membrane **16020**	None
		p value	$6.69e^{-5}$	$7.19e^{-4}$			
		p value[§]	0.232	0.717			
MAN1B1	4	Fold change	1.62	1.60	Metabolic process **8152**/Oligosaccharide metabolic process **9311**/Protein amino acid N-linked glycosylation **6487**	Endoplasmic reticulum **5783**/Integral to membrane **16021**/Membrane **16020**/Membrane fraction **5624**	Calcium ion binding **5509**/Hydrolase activity, acting on glycosyl bonds **16798**/Mannosyl-oligosaccharide 1,2-α-mannosidase activity **4571**
		p value	$2.47e^{-4}$	$3.20e^{-4}$			
		p value[§]	0.234	0.717			

Gene symbol	Exon	Statistic	IPDD vs CON	IPDND vs CON	GO term associations		
					Biological process	Cellular component	Molecular function
OGT	11	Fold change	0.56	0.61	Protein amino acid O-linked glycosylation **6493**/Response to nutrient **7584**/Signal transduction **7165**	Cytoplasm **5737**/Cytosol **5829**/Mixed-lineage leukaemia 5-lysine (MLL5-L) complex **70688**/Nucleus **5634**	Acetylglucosaminyltransferase activity **8375**/Protein binding **5515**/Transferase activity, transferring glycosyl groups **16757**
		p value	$1.26e^{-4}$	$6.17e^{-4}$			
		p value[§]	0.234	0.717			
QKI	8 (3'UTR)	Fold change	0.62	0.58	Long-chain fatty acid biosynthetic process **42759**/mRNA processing **6397**/mRNA transport **51028**/Multicellular organismal development **7275**/Muscle cell differentiation **42692**/Myelination **42552**/Regulation of translation **6417**/RNA splicing **8380**/Spermatogenesis **7283**/Transport **6810**/Vasculogenesis **1570**	Cytoplasm **5737**/Nucleus **5634**/Plasma membrane **5886**	Protein binding **5515**/RNA binding **3723**/SH3 domain binding **17124**
		p value	$4.91e^{-4}$	$1.63e^{-4}$			
		p value[§]	0.243	0.717			
RARRES2	4	Fold change	0.65	0.60	Retinoid metabolic process **1523**	Extracellular region **5576**	None
		p value	$7.95e^{-4}$	$1.89e^{-4}$			
		p value[§]	0.245	0.717			
RELB	1 (5'UTR)	Fold change	1.47	1.42	Antigen processing and presentation **19882**/Myeloid dendritic cell differentiation **43011**/Regulation of transcription, DNA-dependent **6355**/T-helper 1 cell differentiation **45063**	Nucleus **5634**	Protein binding **5515**/Transcription corepressor activity **3714**/Transcription factor activity **3700**
		p value	$4.03e^{-4}$	$9.28e^{-4}$			
		p value[§]	0.238	0.717			
RUSC1	3	Fold change	1.51	1.39	None	Cytoplasm **5737**/Nucleus **5634**	SH3/SH2 adaptor activity **5070**
		p value	$7.14e^{-5}$	$7.95e^{-4}$			
		p value[§]	0.232	0.717			
TMC3	11	Fold change	1.62	1.49	None	Integral to membrane **16021**/Membrane **16020**	None
		p value	$6.77e^{-5}$	$5.42e^{-4}$			
		p value[§]	0.232	0.717			

4.3.4. Expression microarray: genes implicated in idiopathic Parkinson's disease dementia

Genes implicated in IPD dementia were filtered out of the microarray data by identifying all of the genes/exons exhibiting dysregulation in both the IPDD vs control and IPDD vs IPDND comparisons (uncorrected $p < 0.01$). Using these criteria, six genes were differentially-expressed and 22 were alternatively-spliced (see table 4.4).

As before, the NCBI Gene database, GO term associations, and literature were examined to identify functional pathways. The first of these was mitochondria/metal binding. Dysregulation was observed for *Arginyl-transfer RNA synthetase 2, mitochondrial* (*RARS2*); *Aminolevulinate, δ-, synthase 2* (*ALAS2*); *Ubiquinol-cytochrome c reductase, Rieske iron-sulphur polypeptide 1* (*UQCRFS1*); *Ferritin, heavy polypeptide 1* (*FTH1*); and *Selenoprotein W, 1* (*SEPW1*). The first three genes encode mitochondrial proteins. The last four are involved in metal binding, specifically iron, in the case of *ALAS2*, *UQCRFS1*, and *FTH1*. *Post mortem* and imaging studies demonstrate increased levels of iron accumulation in the SN of IPD patients compared to controls. Moreover, iron catalyses the Fenton reaction, which converts hydrogen peroxide (H_2O_2) into reactive oxygen species (ROS), thereby enhancing oxidative stress (Rhodes and Ritz 2008). *ALAS2* is expressed in the mitochondrial matrix where it regulates heme biosynthesis (Napier *et al.* 2005). UQCRFS1 is the iron-sulphur-binding subunit of ubiquinol-cytochrome c reductase (also known as complex III), which transfers electrons from ubiquinol to cytochrome c and contributes to the proton gradient as part of the mitochondrial ETC (Trumpower 1990). UQCRFS1 dephosphorylation may play a role in the mitochondrial permeability transition that ultimately results in the cytosolic release of proapoptotic proteins during cellular stress (He and Lemasters 2005). The Ferritin protein, which is composed of subunits encoded by *FTH1* and *Ferritin, light polypeptide* (*FTL*), mediates iron storage in glia, and to a lesser extent, neurons (Rhodes and Ritz 2008).

Excessive ferritin-bound iron can interfere with microglial inflammatory processes (Crichton *et al.* 2002). *FTL* mutation causes a neurodegenerative disease characterised by ferritin-positive intracellular bodies detectable throughout the brain; its symptoms include parkinsonism and cognitive impairment (Vidal *et al.* 2004). Moreover, *Iron responsive element binding protein 2* (*Ireb2*) knockout mice express increased levels of Ferritin and Alas2, and develop a neurodegenerative parkinsonian movement disorder (Lavaute *et al.* 2001; Cooperman *et al.* 2005). *RARS2* encodes a mitochondrial arginyl-transfer RNA (tRNA) synthetase, whose mutation causes autosomal recessive mitochondrial ETC impairment and pontocerebellar atrophy (OMIM #611523) (Edvardson *et al.* 2007). SEPW1 is a selenium-binding oxidoreductase that can protect cells from H_2O_2-mediated toxicity (Chen and Berry 2003). Dysregulation of these five genes could affect mitochondrial function and/or metal binding, thereby altering oxidative stress and neuronal loss in IPDD.

Axonal guidance/cytoskeleton was the next implicated pathway. Dysregulation was observed for *Ephrin receptor A2* (*EPHA2*) (see also figure 4.4a); *Keratin 9* (*KRT9*); *Midline 1 interacting protein 1* (*MID1IP1*); *Outer dense fibre of sperm tails 2* (*ODF2*); *Protein phosphatase 1, regulatory subunit 16A* (*PPP1R16A*); and *Rho-type guanosine triphosphatase-activating protein RICH2* (*RICH2*). EPHA2 is a receptor Tyr kinase that regulates axonal guidance and dopaminergic neurogenesis during development (Brittis *et al.* 2002; Aoki *et al.* 2004). This protein also seems to play a role in inflammatory responses, migration, tumourigenesis, and radiation-induced apoptosis, probably through its Rho family-mediated inhibition of cell adhesion (Ivanov and Romanovsky 2006; Pasquale 2008; Zhang *et al.* 2008). RICH2 promotes Rho family guanosine triphosphatase (GTPase) activity and is involved in actin cytoskeletal dynamics (Richnau and Aspenstrom 2001; Rollason *et al.* 2009). PPP1R16A regulates Protein phosphatase 1 activity towards the cytoskeletal component myosin (Yong *et al.* 2006). MID1IP1 cooperates with the protein product of *Midline 1* (*MID1*) to stabilise microtubules (Berti *et al.* 2004). X-linked Opitz syndrome is characterised by corpus callosum dysplasia and mental retardation (OMIM #300000). This condition is caused by *MID1* mutation, resulting in

stabilisation of Protein phosphatase 2A and hypophosphorylation of microtubule-associated proteins (Trockenbacher *et al.* 2001). ODF2 is necessary for centrosome-mediated microtubule organisation and normal mitotic progression (Soung *et al.* 2006). This protein is also required for primary cilia formation, and may therefore modulate the function of plasma membrane sensory receptors (Ishikawa *et al.* 2005). Dysregulation of these six genes might influence cytoskeletal dynamics and IPDD pathogenesis.

The third highlighted pathway was synaptic transmission/ion transport. *Brain angiogenesis inhibitor 1-associated protein 3* (*BAIAP3*); *Glutamate receptor, ionotrophic, AMPA 4* (*GRIA4*); and *Transient receptor potential cation channel, subfamily M, member 4* (*TRPM4*) were alternatively-spliced. *GRIA4* encodes a subunit of the α-amino-3-hydroxy-5-methyl-4-isoxazolepropionic acid (AMPA) Glu receptor cation channel which regulates postsynaptic membrane depolarisation. AMPA receptors containing GRIA4 may mediate some forms of long term potentiation (LTP) (Sprengel 2006). TRPM4 is a monovalent cation-selective ion channel that regulates postsynaptic membrane depolarisation and cytosolic calcium influx. It is thought that this protein modulates neuronal action potentials and T-cell-mediated cytokine release (Perraud *et al.* 2004; Massullo *et al.* 2006). *BAIAP3* is expressed in the cortex and may be involved in exocytotic neurotransmitter secretion (Palmer *et al.* 2002). Alternative splicing of these genes could alter synaptic transmission and/or ion transport and affect IPDD pathogenesis.

Lipoprotein metabolism was the next pathway of note. *Apolipoprotein A5* (*APOA5*) (see also figure 4.4b) and *Coiled-coil domain containing 92* (*CCDC92*) were alternatively-spliced. APOA5 is involved in triglyceride-rich lipoprotein metabolism; it negatively regulates plasma triglyceride levels (Tai and Ordovas 2008). *APOA5* belongs to the same family as *APOE*, whose expression appears to promote protein aggregation and dementia in IPD patients (Mattila *et al.* 2000; Bray *et al.* 2004; de Lau *et al.* 2005). CCDC92 is an uncharacterised coiled-coil protein. Genetic variation in the *CCDC92* locus influences plasma lipoprotein and triglyceride levels

(Chasman *et al.* 2009). Alternative splicing of *APOA5* and *CCDC92* might affect lipoprotein metabolism and IPDD pathogenesis.

The fifth dysregulated pathway was inflammation/immune response, which encompassed *EPHA2*; *FTH1*; *Inhibitor of κ light polypeptide gene enhancer in B-cells, kinase ε* (*IKBKE*); *Integrin, alpha L* (*ITGAL*); *Proteasome (prosome, macropain) subunit, β type, 8* (*PSMB8*); and *TRPM4*. IKBKE phosphorylates Inhibitor of κ light polypeptide gene enhancer in B-cells (IKB) and promotes its degradation, which relaxes the latter's inhibition of the proinflammatory NFKB transcriptional pathway (see 4.3.3) (Clement *et al.* 2008). ITGAL regulates cell adhesion and is necessary for microglial migration into injured neuronal cultures (Ullrich *et al.* 2001). Furthermore, this protein is expressed on the surface of activated microglia in the IPD putamen (Imamura *et al.* 2003). *PSMB8* encodes a β subunit of the immunoproteasome. This proteolytic complex is found in cells exposed to proinflammatory interferon γ and mature dendritic cells. It exhibits different substrate specificity to the standard proteasome, and is known to regulate the processing of antigens for presentation by major histocompatibility complex (MHC) class I (Van den Eynde and Morel 2001). PSMB8 protein expression is increased in Huntington's disease (HD) cortical and striatal neurons compared to controls (Diaz-Hernandez *et al.* 2003). Dysregulation of these three genes, along with *EPHA2*, *FTH1*, and *TRPM4* (see above), could modulate inflammatory and/or immune processes and influence IPDD-associated neuronal cell death.

Cell adhesion/ECM was the sixth highlighted pathway. Dysregulation was observed for *Collagen, type II, α 1* (*COL2A1*); *Collagen, type XXVII, α 1* (*COL27A1*); *EPHA2*; and *ITGAL*. COL2A1 and COL27A1 homotrimerise to form collagen types II and XXVII, respectively. These ECM fibrillar proteins are found mainly in cartilage (Shoulders and Raines 2009). *COL2A1* expression is dysregulated during inflammatory conditions such as osteoarthritis (Goldring *et al.* 2008). COL27A1 seems to play a role in the transition of cartilage to bone during skeletogenesis (Hjorten *et al.* 2007). Dysregulation of these two genes, as well as *EPHA2* and

ITGAL (see above), might alter cell adhesion and/or the ECM and affect IPDD pathogenesis.

The final notable pathway was transcription/splicing. *IKBKE*, *Tuftelin interacting protein 11* (*TFIP11*), and *Zinc finger protein 407* (*ZNF407*) were alternatively-spliced. TFIP11 appears to mediate intron lariat release during late stage RNA splicing (Yoshimoto *et al.* 2009). *ZNF407* resides in the chromosomal region generally absent in 18q deletion syndrome, one feature of which is mental retardation (OMIM #601808) (Linnankivi *et al.* 2006). ZNF407 contains zinc finger and homeobox domains, making it a putative transcriptional regulator. Alternative splicing of *TFIP11*, *ZNF407*, and *IKBKE* (see above), could influence transcription and/or splicing and modulate IPDD pathogenesis.

Taken together, these results suggest that mitochondrial/metal binding, axonal guidance/cytoskeletal, synaptic transmission/ion transport, lipoprotein metabolism, inflammation/immune response, cell adhesion/ECM, and transcription/splicing pathways are dysregulated in IPD dementia.

Table 4.4. Cognitive expression microarray: genes implicated in IPD dementia.

Genes exhibiting dysregulated expression or splicing implicating them in IPD dementia (following pages). The results suggest that mitochondrial/metal binding, axonal guidance/cytoskeletal, synaptic transmission/ion transport, lipoprotein metabolism, inflammation/immune response, cell adhesion/ECM, and transcription/splicing pathways are dysregulated in IPDD. Genes are listed alphabetically, with the differential expression group preceding the alternative splicing group. All *p* values were uncorrected, except those marked with §, which were FDR-corrected. Uncorrected IPDND vs CON *p* values were nonsignificant for all listed genes. GO term associations were obtained from the GO database (release 24th January 2010); GO term identity codes are bolded. See list of abbreviations for gene symbol definitions. ATP = adenosine triphosphate; AMPA = α-amino-3-hydroxy-5-methyl-4-isoxazolepropionic acid; CON = control; FDR = false discovery rate; GO = gene ontology; GTPase = guanosine triphosphatase; IPD = idiopathic Parkinson's disease; IPDD = idiopathic Parkinson's disease with dementia; IPDND = idiopathic Parkinson's disease no dementia; IKB = Inhibitor of κ light polypeptide gene enhancer in B-cells; MHC = major histocompatibility complex; NFKB = nuclear factor κ light polypeptide gene enhancer in B-cells; pwy = pathway; RNA = ribonucleic acid; mRNA = messenger RNA.

Gene symbol	Statistic	IPDD vs CON	IPDD vs IPDND	GO term associations		
				Biological process	**Cellular component**	**Molecular function**
ALAS2	Fold change	1.26	1.18	Biosynthetic process **9058**/Cellular iron ion homeostasis **6879**/Erythrocyte differentiation **30218**/Heme biosynthetic process **6783**/Haemoglobin biosynthetic process **42541**/Oxygen homeostasis **32364**/Porphyrin metabolic process **6778**/Response to hypoxia **1666**/Tetrapyrrole biosynthetic process **33014**	Mitochondrial inner membrane **5743**/Mitochondrial matrix **5759**/Mitochondrion **5739**	5-Aminolevulinate synthase activity **3870**/Acyltransferase activity **8415**/Coenzyme binding **50662**/Glycine binding **16594**/Protein binding **5515**/Pyridoxal phosphate binding **30170**/Transferase activity, transferring nitrogenous groups **16769**
	p value	$5.53e^{-4}$	$7.46e^{-3}$			
	p value§	0.135	0.989			
EPHA2	Fold change	1.24	1.17	Angiogenesis **1525**/Apoptosis **6915**/Ephrin receptor sig pwy **48013**/Multicellular organismal development **7275**/Neuron differentiation **30182**/Protein amino acid phosphorylation **6468**/Regulation of blood vessel endothelial cell migration **43535**/Signal transduction **7165**	Integral to plasma membrane **5887**/Plasma membrane **5886**	ATP binding **5524**/Ephrin receptor activity **5003**/Nucleotide binding **166**/Protein binding **5515**/Receptor activity **4872**/Transferase activity **16740**
	p value	$2.82e^{-4}$	$4.36e^{-3}$			
	p value§	0.135	0.989			
FAM83H	Fold change	1.28	1.19	Biomineral formation **31214**	None	None
	p value	$3.65e^{-4}$	$6.07e^{-3}$			
	p value§	0.135	0.989			
FTH1	Fold change	0.63	0.71	Immune response **6955**/Intracellular sequestering of iron ion **6880**/Iron ion transport **6826**/Membrane organisation **16044**/Negative regulation of cell proliferation **8285**/Oxidation reduction **55114**/Post Golgi vesicle-mediated transport **6892**	Cytosol **5829**/Intracellular ferritin complex **8043**	Ferric ion binding **8199**/Ferroxidase activity **4322**/Oxidoreductase activity **16491**/Protein binding **5515**
	p value	$3.87e^{-4}$	$6.31e^{-3}$			
	p value§	0.135	0.989			
MID1IP1	Fold change	1.56	1.38	Negative regulation of microtubule depolymerisation **7026**	Cytoplasm **5737**/Microtubule **5874**/Nucleus **5634**	Protein carboxy-terminus binding **8022**
	p value	$2.59e^{-4}$	$4.86e^{-3}$			
	p value§	0.135	0.989			
UQCRFS1	Fold change	1.55	1.27	Electron transport chain **22900**/Response to antibiotic **46677**/Response to drug **42493**/Response to hormone stimulus **9725**/Transport **6810**	Integral to membrane **16021**/Membrane **16020**/ Mitochondrial inner membrane **5743**/Mitochondrial respiratory chain complex III **5750**/Mitochondrion **5739**/Respiratory chain **70469**	Two iron, two sulphur cluster binding **51537**/Iron ion binding **5506**/Metal ion binding **46872**/Oxidoreductase activity, acting on diphenols and related substances as donors **16679**/Protein complex binding **32403**/Ubiquinol-cytochrome-c reductase activity **8121**
	p value	$4.67e^{-6}$	$3.26e^{-3}$			
	p value§	0.071	0.989			

Gene symbol	Exon	Statistic	IPDD vs CON	IPDD vs IPDND	GO term associations		
					Biological process	**Cellular component**	**Molecular function**
APOA5	2	Fold change	0.64	0.72	Acylglycerol homeostasis **55090**/Lipid transport **6869**/Lipoprotein metabolic process **42157**/Positive regulation of fatty acid biosynthetic process **45723**/Positive regulation of lipoprotein lipase activity **51006**/Positive regulation of receptor-mediated endocytosis **48260**/Positive regulation of triglyceride catabolic process **10898**/Positive regulation of very-low-density lipoprotein particle remodelling **10902**/Tissue regeneration **42246**/Triglyceride homeostasis **70328**/Triglyceride-rich lipoprotein particle remodelling **34370**	Chylomicron **42627**/Extracellular region **5576**/Extracellular space **5615**/High-density lipoprotein particle **34364**/Very-low-density lipoprotein particle **34361**	Enzyme binding **19899**/Heparin binding **8201**/Lipoprotein lipase activator activity **60230**/Low-density lipoprotein receptor binding **50750**/Phosphatidyl choline binding **31210**
		p value	$1.53e^{-6}$	$1.04e^{-4}$			
		p value[§]	0.125	0.999			
BAIAP3	26	Fold change	0.73	0.77	G-protein coupled receptor sig pwy **7186**/Neurotransmitter secretion **7269**	None	Protein carboxy-terminus binding **8022**
		p value	$2.56e^{-5}$	$1.70e^{-4}$			
		p value[§]	0.217	0.999			
CCDC92	4	Fold change	0.39	0.38	None	None	None
		p value	$1.89e^{-4}$	$1.39e^{-4}$			
		p value[§]	0.234	0.999			
CDC45L	16	Fold change	1.40	1.40	Cell cycle **7049**/DNA replication **6260**/DNA replication checkpoint **76**/DNA replication initiation **6270**	Centrosome **5813**/Cytoplasm **5737**/Nucleoplasm **5654**/Nucleus **5634**	Protein binding **5515**
		p value	$1.80e^{-4}$	$2.08e^{-4}$			
		p value[§]	0.234	0.999			

Gene symbol	Exon	Statistic	IPDD vs CON	IPDD vs IPDND	GO term associations		
					Biological process	Cellular component	Molecular function
COL2A1	16	Fold change	0.50	0.57	Bone development **60348**/Cartilage condensation **1502**/Cartilage development involved in endochondrial bone morphogenesis **60351**/Chondrocyte differentiation **2062**/Collagen fibril organisation **30199**/Embryonic skeletal joint morphogenesis **60272**/Endochondrial ossification **1958**/Heart morphogenesis **3007**/Inner ear morphogenesis **42472**/Limb morphogenesis **35108**/Negative regulation of apoptosis **43066**/Palate development **60021**/Proteoglycan metabolic process **6029**/Regulation of gene expression **10468**/Sensory perception of sound **7605**/Tissue homeostasis **1894**/Visual perception **7601**	Basement membrane **5604**/Collagen **5581**/Collagen type II **5585**/Cytoplasm **5737**/Extracellular region **5576**/Extracellular space **5615**	Extracellular matrix structural constituent conferring tensile strength **30020**/Identical protein binding **42802**/Platelet-derived growth factor binding **48407**
		p value	$1.17e^{-5}$	$1.42e^{-4}$			
		p value[§]	0.186	0.999			
COL27A1	28	Fold change	0.70	0.75	Cell adhesion **7155**	Collagen **5581**/Extracellular region **5576**	Extracellular matrix structural constituent **5201**
		p value	$1.59e^{-5}$	$1.73e^{-4}$			
		p value[§]	0.186	0.999			
GRIA4	1 (5'UTR)	Fold change	2.31	2.13	Glutamate sig pwy **7215**/Ion transport **6811**/Positive regulation of synaptic transmission, glutamergic **51968**/Regulation of synaptic transmission **50804**	AMPA selective glutamate receptor complex **32281**/Cell junction **30054**/Cell soma **43025**/Dendrite **30425**/Endocytic vesicle membrane **30666**/Integral to membrane **16021**/Plasma membrane **5886**/Postsynaptic density **14069**/Postsynaptic membrane **45211**/Synapse **45202**/Terminal button **43195**	AMPA selective glutamate receptor activity **4971**/Extracellular-glutamate-gated ion channel activity **5234**/Ion channel activity **5216**/Protein binding **5515**/Receptor activity **4872**
		p value	$3.55e^{-4}$	$9.71e^{-4}$			
		p value[§]	0.237	0.999			
IKBKE	23 (3'UTR)	Fold change	1.54	1.55	Immune response **6955**/Positive regulation of IKB kinase/NFKB cascade **43123**/Protein amino acid phosphorylation **6468**	Cytoplasm **5737**	ATP binding **5524**/IKB kinase activity **8384**/NFKB-inducing kinase activity **4704**/Nucleotide binding **166**/Protein binding **5515**/Transferase activity **16740**
		p value	$3.85e^{-5}$	$2.93e^{-5}$			
		p value[§]	0.217	0.999			

Gene symbol	Exon	Statistic	IPDD vs CON	IPDD vs IPDND	GO term associations		
					Biological process	**Cellular component**	**Molecular function**
ITGAL	33 (3'UTR)	Fold change	1.47	1.69	Cellular component movement **6928**/Heterophilic cell adhesion **7157**/Inflammatory response **6954**/Integrin-mediated sig pwy **7229**/Leukocyte adhesion **7159**/Signal transduction **7165**/T-cell activation via T-cell receptor contact with antigen bound to MHC molecule on antigen presenting cell **2291**	Cell surface **9986**/Integral to membrane **16021**/Integrin complex **8305**/Plasma membrane **5886**	Calcium ion binding **5509**/Cell adhesion molecule binding **50839**/Magnesium ion binding **287**/Protein heterodimerisation activity **46982**/Receptor activity **4872**
		p value	$8.64e^{-4}$	$2.78e^{-5}$			
		p value[§]	0.245	0.999			
KRT9	7	Fold change	0.69	0.70	Intermediate filament organisation **45109**/Skin development **43588**/Spermatogenesis **7283**	Cytoplasm **5737**/Cytoskeleton **5856**/Keratin filament **45095**/Perinuclear region of cytoplasm **48471**	Protein binding **5515**/Structural constituent of cytoskeleton **5200**
		p value	$2.66e^{-4}$	$5.51e^{-4}$			
		p value[§]	0.234	0.999			
NUP98	21	Fold change	0.64	0.66	DNA replication **6260**/Interspecies interaction between organisms **44419**/mRNA transport **51028**/Nuclear pore organisation **6999**/Nucleocytoplasmic transport **6913**/Protein import into nucleus, docking **59**/Protein transport **15031**/Transmembrane transport **55085**	Kinetochore **776**/Membrane **16020**/Nuclear membrane **31965**/Nucleoplasm **5654**/Nucleus **5634**/Nup107-160 complex **31080**	Protein binding **5515**/Structural constituent of nuclear pore **17056**/Transporter activity **5215**
		p value	$1.93e^{-4}$	$5.04e^{-4}$			
		p value[§]	0.234	0.999			
ODF2	21	Fold change	1.34	1.32	Cell differentiation **30154**/Multicellular organismal development **7275**/Spermatogenesis **7283**	Centriole **5814**/Cilium **5929**/Cytoplasm **5737**/Cytoskeleton **5856**/Cytosol **5829**/Flagellum **19861**/Microtubule **5874**/Microtubule organising centre **5815**/Spindle pole **922**	Protein binding **5515**/Structural molecule activity **5198**
		p value	$3.38e^{-4}$	$7.01e^{-4}$			
		p value[§]	0.234	0.999			

Gene symbol	Exon	Statistic	IPDD vs CON	IPDD vs IPDND	GO term associations		
					Biological process	Cellular component	Molecular function
PCNX	8	Fold change	0.76	0.75	None	Integral to membrane **16021**/Membrane **16020**	None
		p value	$8.54e^{-4}$	$4.03e^{-4}$			
		p value[§]	0.245	0.999			
PPP1R16A	2 (5'UTR)	Fold change	0.62	0.64	None	Plasma membrane **5886**	Protein binding **5515**
		p value	$1.81e^{-4}$	$3.55e^{-4}$			
		p value[§]	0.234	0.999			
PSMB8	7	Fold change	0.46	0.53	Anaphase-promoting complex-dependent proteasomal ubiquitin-dependent protein catabolic process **31145**/Immune response **6955**/Negative regulation of ubiquitin-protein ligase activity during mitotic cell cycle **51436**/Positive regulation of ubiquitin-protein ligase activity during mitotic cell cycle **51437**/Proteolysis involved in cellular protein catabolic process **51603**	Cytoplasm **5737**/Nucleus **5634**/Proteasome core complex **5839**	Peptidase activity **8233**/Protein binding **5515**/Threonine-type endopeptidase activity **4298**
		p value	$4.01e^{-6}$	$4.45e^{-5}$			
		p value[§]	0.125	0.999			
RARS2	22	Fold change	0.57	0.59	Arginyl-transfer RNA aminoacylation **6420**	Cytoplasm **5737**/Mitochondrial matrix **5759**/Mitochondrion **5739**	Arginine-transfer RNA ligase activity **4814**/ATP binding **5524**/Ligase activity **16874**/Nucleotide binding **166**/Protein binding **5515**
		p value	$4.90e^{-4}$	$9.93e^{-4}$			
		p value[§]	0.243	0.999			

Gene symbol	Exon	Statistic	IPDD vs CON	IPDND vs CON	GO term associations		
					Biological process	**Cellular component**	**Molecular function**
RICH2	6	Fold change	0.67	0.66	Signal transduction **7165**	Cytoplasm **5737**/Intracellular **5622**	GTPase activator activity **5096**/Protein binding **5515**
		p value	$2.59e^{-4}$	$1.89e^{-4}$			
		p value[§]	0.234	0.999			
SEPW1	8 (3'UTR)	Fold change	0.62	0.74	Cell redox homeostasis **45454**	Cytoplasm **5737**	Selenium binding **8430**
		p value	$4.11e^{-6}$	$7.13e^{-4}$			
		p value[§]	0.125	0.999			
TEX2	12 (3'UTR)	Fold change	0.81	0.82	Signal transduction **7165**/Sphingolipid metabolic process **6665**	Integral to membrane **16021**/Membrane **16020**	None
		p value	$5.60e^{-4}$	$7.82e^{-4}$			
		p value[§]	0.245	0.999			
TFIP11	2	Fold change	0.66	0.69	Biomineral formation **31214**/mRNA processing **6397**/RNA splicing **8380**	Cytoplasm **5737**/Intracellular **5622**/Nuclear speck **16607**/Nucleus **5634**/Proteinaceous extracellular matrix **5578**/Spliceosomal complex **5681**	Nucleic acid binding **3676**/Protein binding **5515**
		p value	$2.87e^{-4}$	$9.09e^{-4}$			
		p value[§]	0.234	0.999			
TRPM4	10	Fold change	0.76	0.78	Calcium ion transport **6816**/Immune response **6955**/Ion transport **6811**/Transmembrane transport **55085**	Integral to membrane **16021**/Plasma membrane **5886**	ATP binding **5524**/Calcium channel activity **5262**/Calcium ion binding **5509**/Calmodulin binding **5516**/Ion channel activity **5216**/Nucleotide binding **166**
		p value	$4.71e^{-5}$	$1.19e^{-4}$			
		p value[§]	0.230	0.999			
ZNF407	5	Fold change	1.59	1.42	Regulation of transcription **45449**	Intracellular **5622**/Nucleus **5634**	DNA binding **3677**/Metal ion binding **46872**/Zinc ion binding **8270**
		p value	$3.22e^{-5}$	$6.85e^{-5}$			
		p value[§]	0.217	0.999			

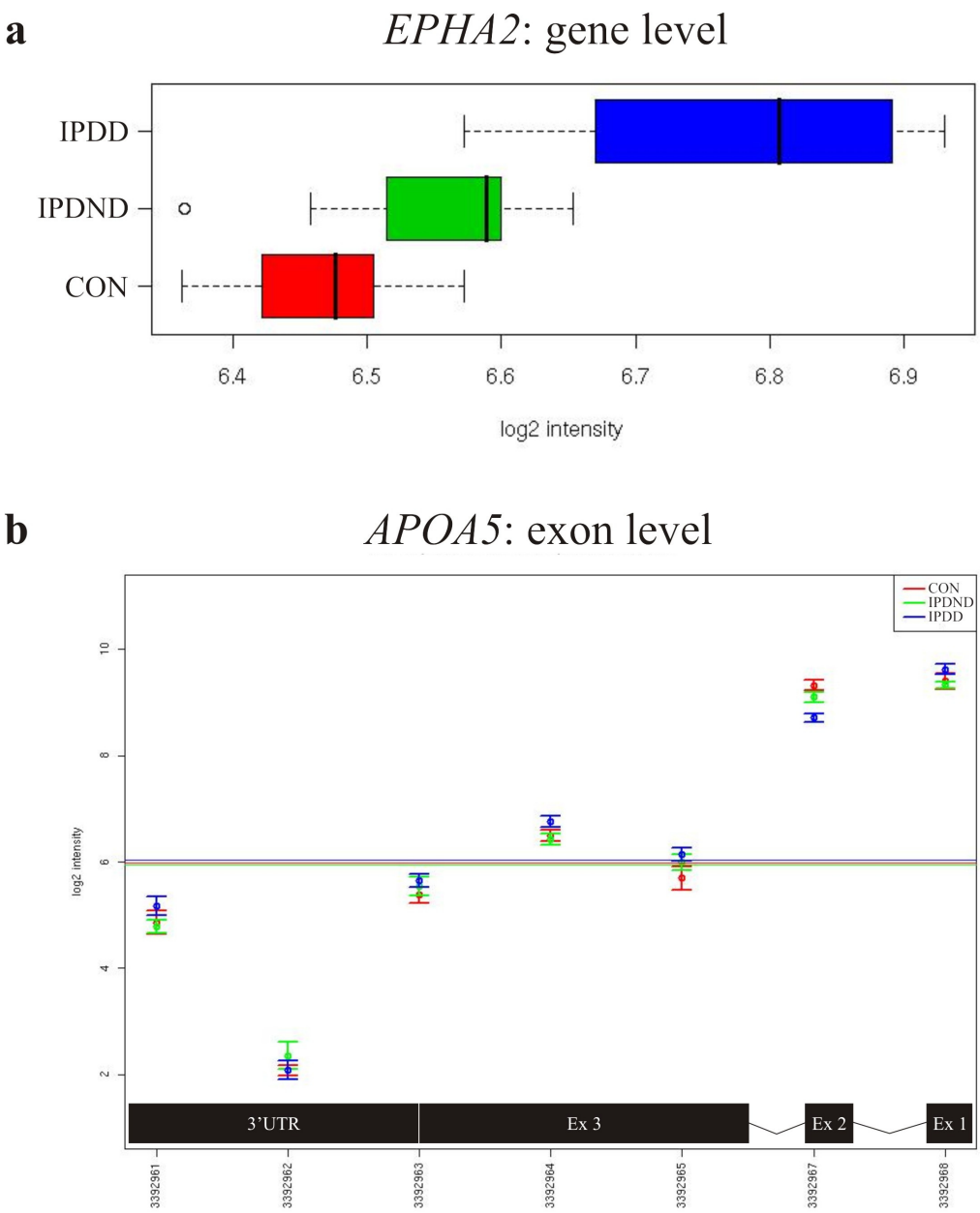

Figure 4.4. Expression microarray plots for *EPHA2* and *APOA5*.

Gene and exon level expression microarray plots for (a) *EPHA2* and (b) *APOA5*, respectively. Differential expression and alternative splicing were observed for *EPHA2* and *APOA5*, respectively, implicating these genes in IPDD. In IPDD vs IPDND or control, *EPHA2* gene expression was increased and *APOA5* exon 2 expression was decreased. (a) *EPHA2* gene level $\log_2$ fluorescence intensity group median and quartile data are shown as a box and whisker plot, with outliers depicted as empty circles. (b) *APOA5* exon level probeset $\log_2$ fluorescence intensity group mean and standard error data are presented as bar chart. *APOA5* gene level group mean fluorescence values are shown as horizontal lines. Probesets are numbered, and their approximate annealing sites in relation to *APOA5* genetic architecture are indicated. *APOA5 = Apoliprotein A5*; CON = control; *EPHA2 = Ephrin receptor A2*; Ex = exon; IPD = idiopathic Parkinson's disease; IPDD = idiopathic Parkinson's disease with dementia; IPDND = idiopathic Parkinson's disease no dementia; UTR = untranslated region.

4.3.5. Variation in dorsolateral prefrontal cortex *Ephrin receptor A2* expression is associated with idiopathic Parkinson's disease

Various microarray hits were selected for validation by qRT-PCR. Our general approach was to concentrate on genes implicated in IPDD. Given the importance of mitochondria and iron metabolism in IPD [reviewed in (Abou-Sleiman *et al.* 2006b; Rhodes and Ritz 2008)], *ALAS2*, *FTH1*, and *UQCRFS1* were chosen. *APOA5* was selected, because this gene belongs to the same family as *APOE*, whose expression appears to promote protein aggregation and dementia in IPD patients (Mattila *et al.* 2000; Bray *et al.* 2004; de Lau *et al.* 2005). As it belongs to several of the pathways implicated in IPDD (see 4.3.4), *EPHA2* was chosen. The TFs *ZNF407* and *POU4F3* were selected, because of their potential for affecting multiple target genes. Due to its neuroprotective ability in IPD models (Reglodi *et al.* 2004), *ADCYAP1* was also chosen. The existence of several *FTH1* pseudogenes made this gene refractory to qRT-PCR primer design. Moreover, the qRT-PCR assay for *ADCYAP1* could not be optimised to ensure the generation of a single amplicon. For the remaining genes, qRT-PCR was employed to measure total and NLC expression in cognitive series DLPFC cDNA batch 2 (IPDD [n = 15]; IPDND [n = 16]; control [n = 16]). Separate qRT-PCR assays were used to interrogate full length (FL) and alternatively-spliced transcripts of the same gene, as appropriate. Clinicopathological group comparisons and expression data normalisation strategies for this series and cDNA batch have been described (see 3.3.2 and 3.3.4). Expression in IPDD and IPDND was compared statistically, and these two groups subsequently combined to generate the IPD group. Expression in IPD (n = 31) and controls (n = 16) was then compared statistically.

Table 4.5 and figure 4.5 show the qRT-PCR microarray validation data. *EPHA2* was confirmed as differentially-expressed. Strikingly, total *EPHA2* expression was significantly higher (2.56-fold) in IPD compared with controls (corrected p = 0.020). A similar trend of higher NLC *EPHA2* expression was observed in IPD contrasted

against controls, but this did not survive correction. However, total and NLC *EPHA2* expression were unaltered in IPDD compared with IPDND. On the other hand, dysregulation was not validated for *ALAS2*, *APOA5*, *POU4F3*, *UQCRFS1*, or *ZNF407*. *APOA5* FL and 1:3 displayed trends of underexpression in IPD compared to controls. But these changes were suggestive of differential expression in IPD neurodegeneration, whereas the array findings indicated alternative splicing in IPD dementia.

These results demonstrate that variation in DLPFC *EPHA2* expression is associated with IPD in the cognitive series. However in contrast to the microarray, this variation is not associated with IPD dementia. Undoubtedly there is discord between the microarray and qRT-PCR expression datasets with regard to this gene. Nevertheless, when one examines the *EPHA2* microarray expression plot (see figure 4.4a), it is clear that the IPDND group lies somewhere in between the other two. Therefore, the most parsimonious and conservative interpretation is that variation in *EPHA2* expression is associated with IPD neurodegeneration, not with IPD dementia.

Gene	Expression	Fold change mean expression/CON			Uncorrected *p* value		Corrected *p* value	
		IPDD	IPDND	IPD	IPDD vs IPDND	IPD vs CON	IPDD vs IPDND	IPD vs CON
ALAS2	Total	1.05	1.13	1.08	0.868	0.509	NS	NS
	NLC	0.69	1.16	0.97	0.526	0.179	NS	NS
APOA5 FL	Total	0.56	0.61	0.58	0.506	0.124	NS	NS
	NLC	0.48	0.87	0.70	0.853	0.078	NS	NS
APOA5 1:3	Total	0.46	0.36	0.48	0.207	0.043	NS	NS
	NLC	0.50	0.74	0.62	0.733	0.042	NS	NS
EPHA2	**Total**	**2.83**	**2.31**	**2.56**	**0.155**	**$3.85e^{-4}$**	**NS**	**0.020**
	NLC	**2.59**	**2.95**	**2.77**	**0.534**	**0.023**	**NS**	**NS**
POU4F3	Total	0.61	0.72	0.67	0.511	0.154	NS	NS
	NLC	0.68	0.85	0.78	0.770	0.078	NS	NS
UQCRFS1	Total	0.86	0.94	0.91	0.304	0.193	NS	NS
	NLC	0.86	0.98	0.92	0.264	0.537	NS	NS
ZNF407 FL	Total	0.88	0.94	0.91	0.678	0.682	NS	NS
	NLC	0.94	1.06	1.00	0.695	0.445	NS	NS
ZNF407 4:6	Total	0.96	0.89	0.88	0.739	0.962	NS	NS
	NLC	0.92	0.92	0.92	0.918	0.552	NS	NS

Table 4.5. Expression microarray qRT-PCR validation data.

Fold change mean gene expression values (relative to controls) and statistical results for expression microarray qRT-PCR validation in cognitive series DLPFC cDNA batch 2. Total *EPHA2* was significantly overexpressed in IPD compared to controls, indicating that variation in DLPFC *EPHA2* expression is associated with IPD (in bold text). However in contrast to the microarray, this variation is not associated with IPD dementia. Validation was not observed for any of the other microarray hits. Total expression data were normalised with *G6PD*, *RPL13A*, and *TBP*, and NLC expression data with *NEFH*. Groups were compared by Mann-Whitney test. *p* values were corrected x52. 1:3 = splice form 1:3; 4:6 = splice form 4:6; *ALAS2 = Aminolevulinate, δ-, synthase 2*; *APOA5 = Apoliprotein A5*; CON = control; cDNA = complementary DNA; DLPFC = dorsolateral prefrontal cortex; *EPHA2 = Ephrin receptor A2*; FL = full length; *G6PD = Glucose-6-phosphate dehydrogenase*; IPD = idiopathic Parkinson's disease; IPDD = idiopathic Parkinson's disease with dementia; IPDND = idiopathic Parkinson's disease no dementia; *NEFH = Neurofilament H*; NLC = neuronal-loss corrected; NS = not significant; *POU4F3 = POU class 4 homeobox 3*; qRT-PCR = quantitative reverse transcriptase-polymerase chain reaction; *RPL13A = Ribosomal protein L13A*; *TBP = TATA box binding protein*; *UQCRFS1 = Ubiquinol-cytochrome c reductase, Rieske iron-sulphur polypeptide 1*; *ZNF407 = Zinc finger protein 407*.

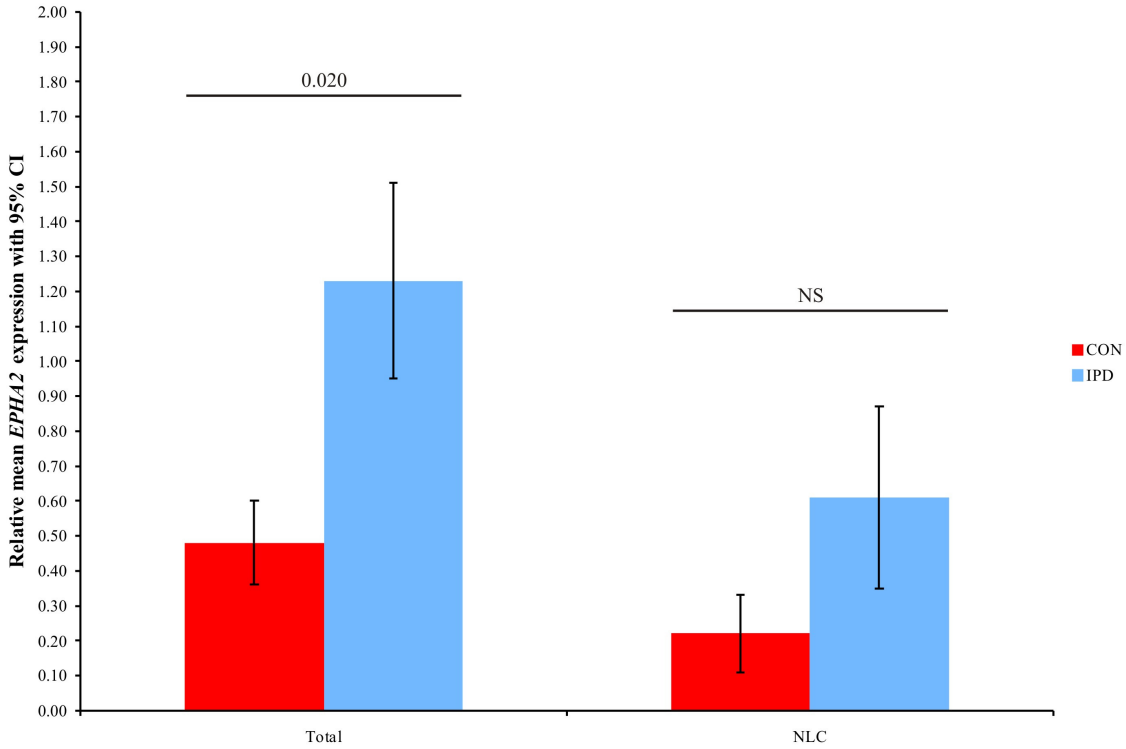

Figure 4.5. Variation in DLPFC *EPHA2* expression is associated with IPD.

Relative mean qRT-PCR *EPHA2* expression values with 95% CI and statistical results for cognitive series DLPFC cDNA batch 2. Total *EPHA2* was significantly overexpressed in IPD compared to controls, indicating that variation in DLPFC *EPHA2* expression is associated with IPD. Total expression data were normalised with *G6PD*, *RPL13A*, and *TBP*, and NLC expression data with *NEFH*. IPD and CON groups were compared by Mann-Whitney test. Corrected *p* values are displayed. *p* values were corrected x52. CI = confidence interval; CON = control; cDNA = complementary DNA; DLPFC = dorsolateral prefrontal cortex; *EPHA2* = *Ephrin receptor A2*; *G6PD* = *Glucose-6-phosphate dehydrogenase*; IPD = idiopathic Parkinson's disease; *NEFH* = *Neurofilament H*; NLC = neuronal-loss corrected; NS = not significant; qRT-PCR = quantitative reverse transcriptase-polymerase chain reaction; *RPL13A* = *Ribosomal protein L13A*; *TBP* = *TATA box binding protein*.

4.3.6. *Ephrin receptor A2* overexpression in idiopathic Parkinson's disease is restricted to the dorsolateral prefrontal cortex

In order to further investigate *EPHA2* in the context of IPD, qRT-PCR was employed to quantify total and NLC expression in seven subcortical and cortical brain regions obtained from the mapping series. Clinicopathological group comparisons and expression data normalisation strategies for this series have been described (see 3.3.5). Expression in IPD (n = 20) and controls (n = 20) was compared statistically.

The results of this analysis can be seen in table 4.6 and figure 4.6. Relatively high levels of intragroup variation were detected in the majority of regions. After correction for multiple testing, no significant changes were observed for total or NLC *EPHA2* expression in any of the seven areas obtained from the mapping series. In IPD compared to controls, trends of increase and decrease were seen for total expression in the medulla and NLC expression in the FC, respectively. However, these effects failed to survive correction. Taken together, these findings demonstrate that *EPHA2* is not differentially-expressed in the mapping series. Furthermore, they indicate that in all eight brain areas examined thus far, IPD *EPHA2* overexpression is restricted to the DLPFC.

Brain region	Expression	Fold change mean *EPHA2* expression (IPD/CON)	IPD vs CON *p* value	
			Uncorrected	Corrected
Medulla	Total	1.88	0.010	0.520
	NLC	0.52	0.600	NS
Putamen	Total	1.32	0.730	NS
	NLC	1.03	0.664	NS
Amygdala	Total	1.33	0.607	NS
	NLC	0.56	0.520	NS
EC (BA28)	Total	1.76	0.595	NS
	NLC	0.89	0.694	NS
ACC (BA24)	Total	0.89	0.801	NS
	NLC	0.63	0.274	NS
AG (BA39)	Total	2.08	0.129	NS
	NLC	2.88	0.704	NS
FC (BA8)	Total	0.93	0.395	NS
	NLC	0.63	0.064	NS

Table 4.6. IPD mapping series *EPHA2* expression data.

Fold change mean qRT-PCR *EPHA2* expression values (relative to controls) and statistical results for the mapping series. No significant differences were observed after correction for multiple testing, indicating that *EPHA2* overexpression in IPD is restricted to the DLPFC. Total expression data were normalised with *G6PD*, *HPRT1*, *RPL13A*, and *TBP*, except for amygdala and EC data, which were normalised with *HPRT1*, *RPL13A*, and *TBP*. NLC expression data were normalised with *NEFH*. IPD and CON groups were compared by Mann-Whitney test. *p* values were corrected x52. AG = angular gyrus (BA39); ACC = anterior cingulate cortex (BA24); BA = Brodmann area; CON = control; DLPFC = dorsolateral prefrontal cortex (BA46); EC = entorhinal cortex (BA28); *EPHA2 = Ephrin receptor A2*; FC = frontal cortex (BA8); *G6PD = Glucose-6-phosphate dehydrogenase*; *HPRT1 = Hypoxanthine phosphoribosyltransferase 1*; IPD = idiopathic Parkinson's disease; *NEFH = Neurofilament H*; NLC = neuronal-loss corrected; NS = not significant; qRT-PCR = quantitative reverse transcriptase-polymerase chain reaction; *RPL13A = Ribosomal protein L13A*; *TBP = TATA box binding protein*.

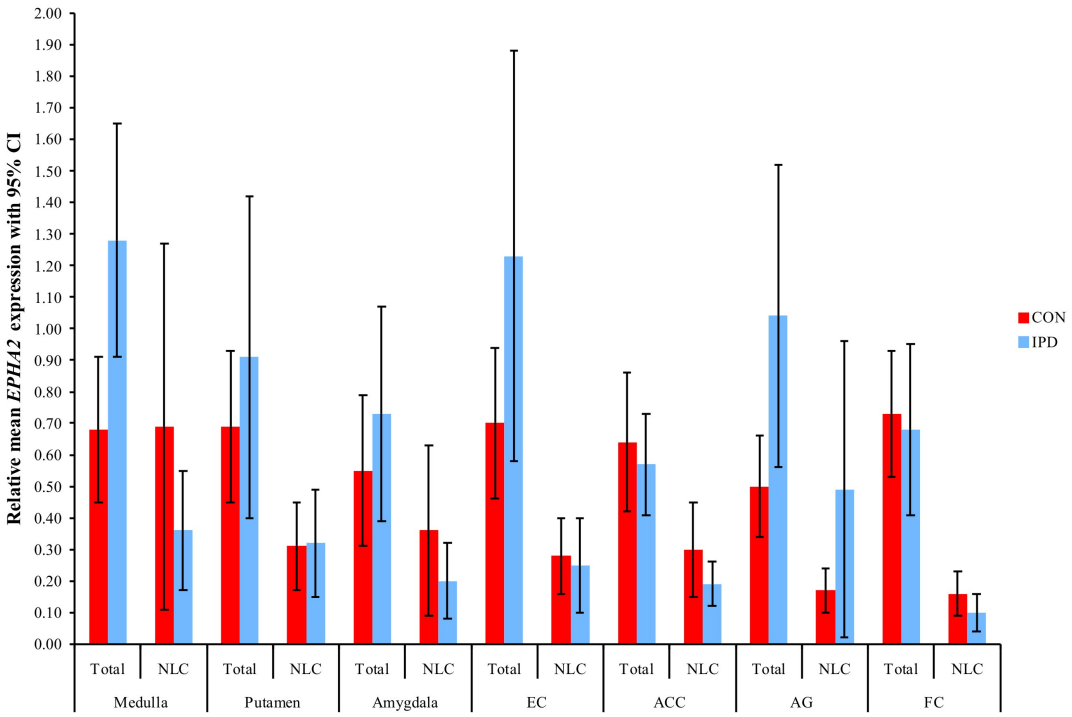

Figure 4.6. *EPHA2* is not differentially-expressed in the mapping series.

Relative mean qRT-PCR *EPHA2* expression values with 95% CI for the mapping series. No significant differences were observed after correction for multiple testing, indicating that *EPHA2* overexpression in IPD is restricted to the DLPFC. Total expression data were normalised with *G6PD*, *HPRT1*, *RPL13A*, and *TBP*, except for amygdala and EC data, which were normalised with *HPRT1*, *RPL13A*, and *TBP*. NLC expression data were normalised with *NEFH*. IPD and CON groups were compared by Mann-Whitney test. *p* values were corrected x52. AG = angular gyrus (BA39); ACC = anterior cingulate cortex (BA24); BA = Brodmann area; CI = confidence interval; CON = control; DLPFC = dorsolateral prefrontal cortex (BA46); EC = entorhinal cortex (BA28); *EPHA2* = *Ephrin receptor A2*; FC = frontal cortex (BA8); *G6PD* = *Glucose-6-phosphate dehydrogenase*; *HPRT1* = *Hypoxanthine phosphoribosyltransferase 1*; IPD = idiopathic Parkinson's disease; *NEFH* = *Neurofilament H*; NLC = neuronal-loss corrected; qRT-PCR = quantitative reverse transcriptase-polymerase chain reaction; *RPL13A* = *Ribosomal protein L13A*; *TBP* = *TATA box binding protein*.

4.3.7. Variation at rs11260822 influences idiopathic Parkinson's disease risk

So as to evaluate SNP variation in the *EPHA2* locus for its effect on IPD risk, a case-control genetic association study was carried out. A region encompassing the *EPHA2* gene (~31.7 kb) and 15 kb upstream was defined. HapMap phase II CEPH data were then used to assess linkage disequilibrium (LD) relationships between common SNPs and generate htSNPs (see figure 4.7). Six htSNPs were produced, with an average locus haplotype r^2 of 0.941. Taqman was employed to genotype these markers in gDNA extracted from the association series (IPD [n = 614]; controls [n = 619]), and they were tested for allelic association with IPD under a multiplicative model. Group clinical data for this series have been presented (see 3.3.7).

Table 4.7 shows the SNP association study data. The Hardy-Weinberg equilibrium (HWE) was not violated for any of the htSNPs in either group, indicating that no serious genotyping errors had occurred. Variation at rs11260822 displayed significant association with IPD (corrected p = 0.018). The estimated odds ratio (OR) for this effect was 1.289 with a 95% confidence interval (CI) that ranged from 1.092 to 1.521. The case (0.423) and control (0.362) minor allele frequencies (MAFs) showed that the minor C allele confers increased susceptibility to IPD.

Therefore, these findings indicate that variation at rs11260822 influences IPD risk in the association series. HapMap data shows that this polymorphism, which is situated ~3.2 kb upstream of the *EPHA2* transcriptional start site (TSS), resides in a block characterised by high levels of LD in Caucasians. Thus it is unclear which of the 13 SNPs in this block (or combination thereof) is/are driving the observed association with IPD. Twelve of these variants (including rs11260822) are intronic or upstream of the *EPHA2* coding sequence, and are not located near to any exons. Hence they would be unlikely to have any effect on *EPHA2* splicing or mRNA stability. According to HapMap, the r^2 LD between the remaining SNP, rs6678616, and

rs11260822 is 0.928 in Caucasians. The rs6678616 polymorphism is a synonymous variant situated in exon 3, and its presence on the *EPHA2* transcript suggests that it might affect the stability of this mRNA.

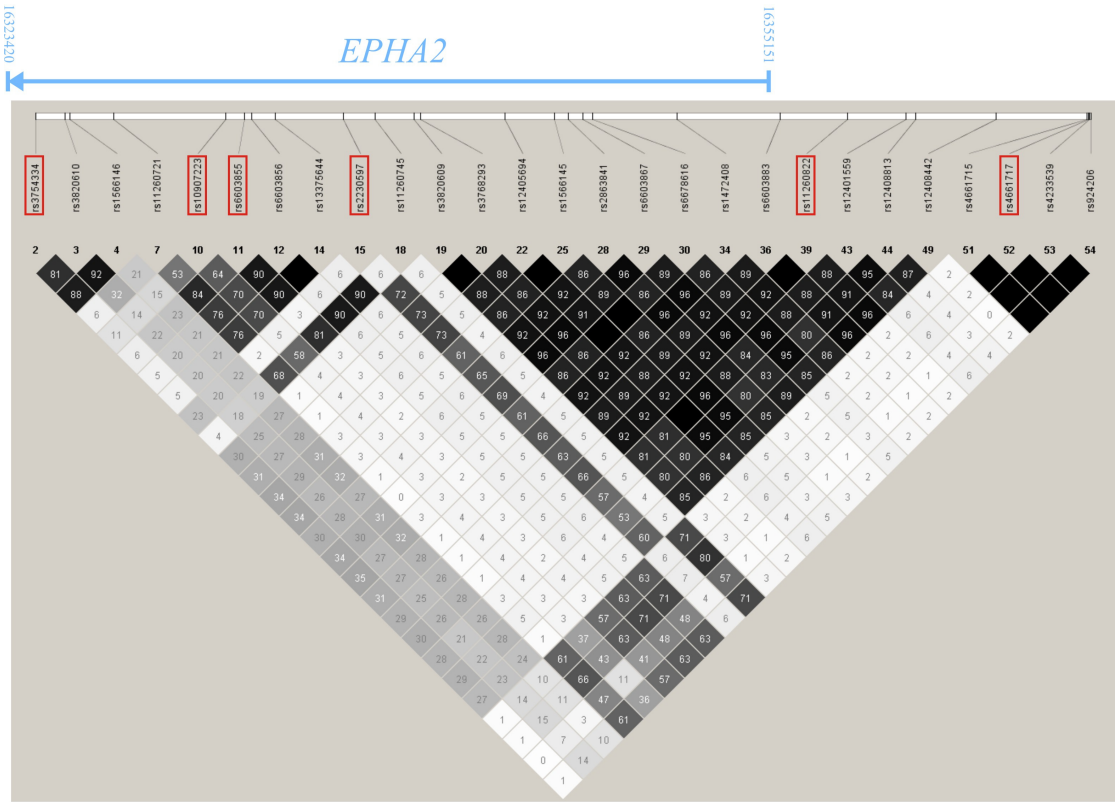

Figure 4.7. *EPHA2* genomic locus SNP LD plot.

Pairwise r^2 LD plot for common SNPs (MAF ≥ 0.05) in the *EPHA2* genomic locus (~46.7 kb). CEPH trio genotypic data were obtained from HapMap phase II (release 23a from March 2008). Tagger was used to generate six htSNPs capturing 95% the SNP variation in this region (average locus haplotype r^2 = 0.941). Pairwise LD values (out of 100) label the relevant squares. Degree of square shading denotes LD magnitude. Empty black squares indicate LD = 1. Red boxes denote htSNPs. Boundaries of *EPHA2* transcribed sequence (~31.7 kb) in relation to the white bar are indicated. Locations on chromosome 1 are according to NCBI assembly build 36. CEPH = Centre d'Étude du Polymorphisme Humain; *EPHA2* = *Ephrin receptor A2*; LD = linkage disequilibrium; MAF = minor allele frequency; NCBI = National Center for Biotechnology Information; SNP = single nucleotide polymorphism; htSNP = haplotype-tagging single nucleotide polymorphism.

SNP identity [DNA base ambiguity]	Location on chromosome 1	HapMap CEPH MAF	*n* alleles		MAF		HWE *p* value		Estimated OR [95% CI]	χ^2 allelic association *p* value	
			CON	IPD	CON	IPD	CON	IPD		Uncorrected	Corrected
rs3754334 [G/A]	16324354	0.292	1206	1150	0.249	0.287	0.472	0.726	1.215 [1.013 – 1.459]	0.036	0.216
rs10907223 [G/A]	16332332	0.067	1206	1192	0.034	0.038	0.990	0.844	1.115 [0.725 – 1.714]	0.621	NS
rs6603855 [T/C]	16333128	0.102	1112	1194	0.049	0.057	1.000	0.833	1.160 [0.806 – 1.668]	0.424	NS
rs2230597 [G/A]	16337260	0.412	1126	1210	0.403	0.428	0.847	0.708	1.108 [0.940 – 1.306]	0.222	NS
rs11260822 [T/C]	**16358398**	**0.356**	**1134**	**1208**	**0.362**	**0.423**	**0.835**	**0.054**	**1.289 [1.092 – 1.521]**	**0.003**	**0.018**
rs4661717 [T/G]	16368501	0.093	1108	1168	0.084	0.086	0.158	0.237	1.022 [0.761 – 1.373]	0.886	NS

Table 4.7. *EPHA2* IPD SNP association study data.

Ephrin receptor A2 IPD SNP association study data. Variation at rs11260822 significantly associated with IPD (in bold text), whereby the minor C allele conferred increased risk of IPD. SNP identities, CEPH DNA base ambiguities (positive strand), and CEPH MAFs were obtained from HapMap phase II (release 23a from March 2008). DNA base ambiguity shows the major allele first (single letter codes in accordance with the International Union of Biochemistry and Molecular Biology). Locations on chromosome 1 are according to NCBI assembly build 36. HWE *p* values were not corrected. χ^2 allelic association *p* values were calculated under a multiplicative model and corrected x6. CEPH = Centre d'Étude du Polymorphisme Humain; CI = confidence interval; CON = control; *EPHA2* = *Ephrin receptor A2*; HWE = Hardy-Weinberg equilibrium; IPD = idiopathic Parkinson's disease; MAF = minor allele frequency; NCBI = National Center for Biotechnology Information; NS = not significant; OR = odds ratio; SNP = single nucleotide polymorphism.

4.3.8. Variation at rs11260822 does not influence *Ephrin receptor A2* expression in the dorsolateral prefrontal cortex

Variation at rs11260822 could alter IPD susceptibility via an effect on *EPHA2* expression. In order to investigate this possibility, *cis*-acting variation analysis was performed for rs11260822. The cognitive series individuals were genotyped at this polymorphism, DLPFC cDNA batch 2 *EPHA2* expression data grouped by genotype, and the groups compared statistically (T/T homozygote majors [n = 12]; T/C heterozygotes [n = 21]; C/C homozygote minors [n = 12]).

Variation at rs11260822 did not significantly associate with either total or NLC DLPFC *EPHA2* expression. An interesting but weak trend was observed of higher NLC expression with increasing C allele ploidy (see figure 4.8). This fits well with the elevated *EPHA2* expression seen in IPD compared to controls (see figure 4.5) and the increased IPD risk conferred by the C allele (see table 4.7). However, the relationship between rs11260822 genotype and NLC *EPHA2* expression was nonsignificant even before correction. Therefore, these results indicate that variation at rs11260822 does not influence *EPHA2* expression in the cognitive series DLPFC.

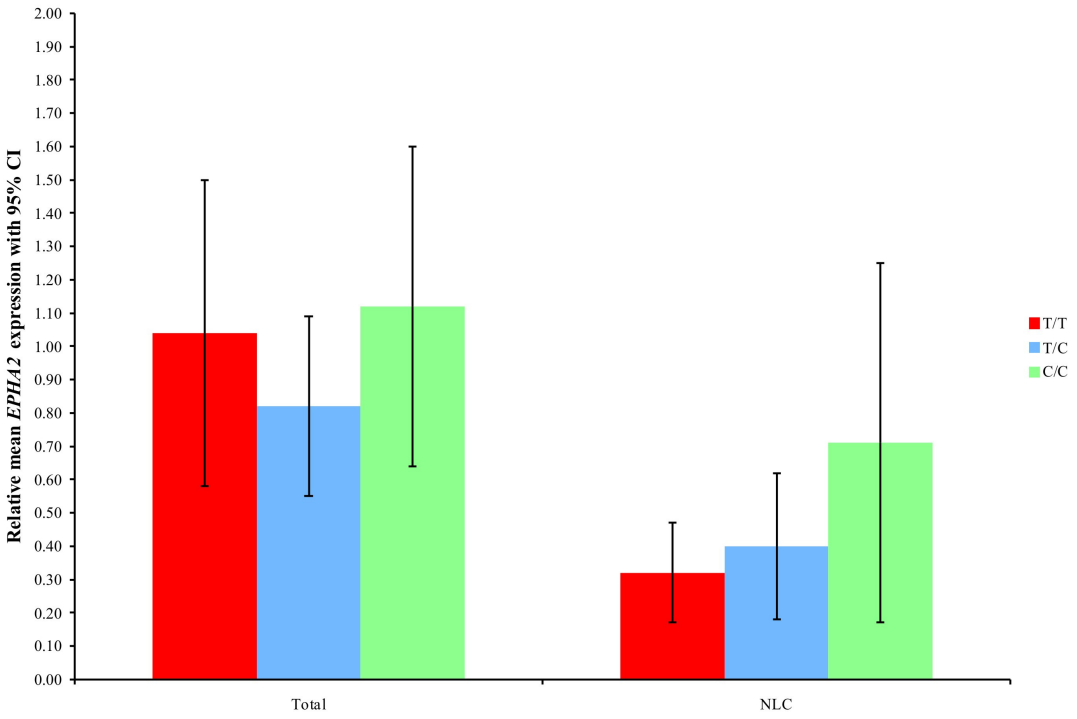

Figure 4.8. Variation at rs11260822 does not influence *EPHA2* expression in the DLPFC.

Relative mean qRT-PCR *EPHA2* expression values with 95% CI for cognitive series DLPFC cDNA batch 2. No significant differences were observed, indicating that variation at rs11260822 does not influence DLPFC *EPHA2* expression. Total expression data were normalised with *G6PD*, *RPL13A*, and *TBP*, and NLC expression data with *NEFH*. Data were grouped by rs11260822 genotype, and groups compared by Kruskal-Wallis test. Uncorrected *p* values were 0.530 for total expression and 0.343 for NLC expression. *p* values were corrected x52. The rs11260822 genotypic data did not violate Hardy-Weinberg equilibrium (uncorrected $p = 0.822$). Single letter codes in accordance with the International Union of Biochemistry and Molecular Biology. CI = confidence interval; cDNA = complementary DNA; DLPFC = dorsolateral prefrontal cortex; *EPHA2 = Ephrin receptor A2*; *G6PD = Glucose-6-phosphate dehydrogenase*; *NEFH = Neurofilament H*; NLC = neuronal-loss corrected; qRT-PCR = quantitative reverse transcriptase-polymerase chain reaction; *RPL13A = Ribosomal protein L13A*; *TBP = TATA box binding protein*.

4.3.9. Expression microarray data mining: *Ephrin receptor A2*-related pathways

The vast amount of data generated by the expression microarray presents interesting opportunities to systematically investigate relationships between IPD pathogenesis and DLPFC gene expression at the pathway level. Previous findings have demonstrated that *EPHA2* is differentially-expressed in this region (see figure 4.5), so we began by examining pathways related to this kinase. It was hypothesised that *EPHA2* overexpression might be accompanied by long term changes in the expression of *EPHA2* pathway genes, potentially resulting in specific patterns of signaling activity. Four groups of candidate genes were selected. The first was EPHA2 interactors; this consisted of the Ephrin A ligand family and other genes whose protein products bind EPHA2, identified using BioGRID. Due to this gene's role in axonal guidance (Brittis *et al.* 2002), the next group comprised axonal guidance pathway genes, chosen using the KEGG database. This resource was also used to select members of the third group: Mitogen-activated protein kinase (MAPK) signaling genes. This group was included because EPHA2 activation has been shown to induce Extracellular-signal regulated kinase 1/2 (ERK1/2) phosphorylation resulting in enhanced ERK1/2 signaling (Pratt and Kinch 2002). The final group consisted of genes known or predicted to regulate *EPHA2* expression. The T-cell factor/lymphoid enhancer binding factor (TCF/LEF) (Katoh and Katoh 2006) and Sarcoma (Src) (Baldwin *et al.* 2006) families were chosen, as well as *Tumour protein 53* (*TP53*) (Yang *et al.* 2006). Microarray data for these 97 candidates were mined *in silico*, and expression in IPD (n = 14) and controls (n = 7) compared statistically.

Table 4.8 shows the results of this analysis. The first point of note is that the majority of evaluated genes were not differentially-expressed. This is perhaps unsurprising, given that most of the candidates belong to the MAPK signaling and axonal guidance groups. These pathways generally operate via sequential cascades of protein-protein

binding and post translational modification (PTM), and not via changes in gene expression. However, differential expression was observed for several candidates.

The EPHA2-directed phosphatase *Acid phosphatase 1, soluble* (*ACP1*) was underexpressed ($p = 0.043$) (Kikawa *et al.* 2002), whereas the EPHA2 ligand *Ephrin A2* (*EFNA2*) was overexpressed ($p = 0.001$). Together with the increase in *EPHA2* expression demonstrated previously, these changes imply enhanced levels of EPHA2 kinase activity. The expression of Rat sarcoma (Ras) inhibitor *Ras p21 protein activator 1* (*RASA1*) and *Related Ras viral oncogene homologue 2* (*RRAS2*) were decreased ($p = 0.020$) and increased ($p = 0.035$), respectively. Notwithstanding the reduction in *Kirsten rat sarcoma viral oncogene homologue* (*KRAS*) expression ($p = 0.012$), these data suggest increased signaling activity of Ras GTPase family members. *Dual specificity phosphatase 4* (*DUSP4*) ($p = 0.024$); *Dual specificity phosphatase 6* (*DUSP6*) ($p = 0.001$); and *Protein tyrosine phosphatase, receptor type, R* (*PTPRR*) ($p = 0.023$) were all underexpressed. Decreased expression of these enzymes, which are known to dephosphorylate and reduce the activity of ERK1/2 (Guan and Butch 1995; Muda *et al.* 1996; Zuniga *et al.* 1999), imply relaxed ERK1/2 inhibition. Notably, IPD *DUSP6* expression was ~50% of that in controls (data not shown). This finding validates the *DUSP6* qRT-PCR results, both in terms of magnitude and direction of effect (see 3.3.4).

Amongst the downstream ERK1/2 effectors, overexpression was observed for *Phospholipase A2, group IID* (*PLA2G2D*) ($p = 0.048$); *Phospholipase A2, group IIE* (*PLA2G2E*) ($p = 0.046$); *Phospholipase A2, group III* (*PLA2G3*) ($p = 0.010$); and *E26-like kinase 1* (*ELK1*) ($p = 0.019$), whereas the expression of *Stathmin 1* (*STMN1*) ($p = 0.037$); *Ribosomal protein S6 kinase, 90 kDa, polypeptide 3* (*RPS6KA3*) ($p = 0.006$); and *Ribosomal protein S6 kinase, 90 kDa, polypeptide 3* (*RPS6KA6*) ($p = 0.022$) were reduced. These data suggest increased activity of Phospholipase A2 (PLA2) and ELK1 pathways, but decreased activity of STMN1 and Ribosomal S6 kinase (RSK)/Cyclic adenosine monophosphate response element binding protein (CREB) pathways. Overexpression was observed for three putative regulators of

EPHA2 transcription: *Transcription factor 7* (*TCF7*) ($p = 0.011$), *Transcription factor 7-like 1* (*TCF7L1*) ($p = 0.007$), and *Lymphocyte-specific protein tyrosine kinase* (*LCK*) ($p = 0.011$). This finding identifies several candidate genes that could be involved in mediating *EPHA2* differential expression in the IPD DLPFC.

Taken together, these mining data indicate that several *EPHA2*-related genes exhibit dysregulation in the microarray series IPD DLPFC (see figure 4.9). Moreover, they validate the qRT-PCR results with regards to IPD *DUSP6* underexpression in this brain region (see 3.3.4).

Table 4.8. Expression microarray data mining: *EPHA2*-related pathways.

Statistical results for the *EPHA2*-related pathways expression microarray *in silico* data mining analysis (following pages). Several *EPHA2*-related genes were differentially-expressed in the microarray series IPD DLPFC (in bold text). IPD and CON $\log_2$ group expression was compared by *t* test, or when the † symbol is shown, by Mann-Whitney test. All *p* values were uncorrected. Positive and negative symbols indicate the direction of differential expression in IPD vs CON. See text for details of pathways and sources. KEGG pathway codes are listed when appropriate. See list of abbreviations for definitions of gene symbols and common gene aliases. BG = BioGRID; CON = control; DLPFC = dorsolateral prefrontal cortex; *EPHA2* = *Ephrin receptor A2*; hsa = *Homo sapiens*; IPD = idiopathic Parkinson's disease; KEGG = Kyoto Encyclopaedia of Genes and Genomes; MAPK = Mitogen-activated protein kinase; ref 1 = (Katoh and Katoh 2006); ref 2 = (Baldwin *et al.* 2006); ref 3 = (Yang *et al.* 2006); Src = Sarcoma; TCF/LEF = T-cell factor/lymphoid enhancer binding factor.

Pathway	Source	Gene (alias)	Uncorrected IPD vs CON *p* value	Change in IPD	Pathway	Source	Gene (alias)	Uncorrected IPD vs CON *p* value	Change in IPD
EPHA2 interactors	BG	***ACP1* (LMWPTP)**	**0.043**	-	Axonal guidance	KEGG hsa 04360	*PAK4*†	0.343	+
	Ligand	*EFNA1*	0.370	+			*PAK6*	0.382	-
		EFNA2	**0.001**	+			*PAK7*	0.133	-
		EFNA3†	0.117	-			*ROCK1*†	0.073	-
		EFNA5	0.143	-			*ROCK2*	0.054	-
	BG	*GRB2*	0.087	-	MAPK signaling	KEGG hsa 04010	*SOS1*	0.072	-
		PIK3R1 (p85α)†	0.156	-			*SOS2*†	0.205	-
		PTK2 (FAK)	0.108	-			*HRAS*	0.946	+
		***PTPN11* (SHP2)**	**0.034**	-			***KRAS***	**0.012**	-
		SHC1	0.143	+			*MRAS*	0.390	+
		SLA†	0.941	-			*NRAS*†	0.052	-
		TNFAIP1†	0.296	-			*RRAS*	0.553	+
Axonal guidance	KEGG hsa 04360	*ABL1*	0.638	+			***RRAS2***	**0.035**	+
		NGEF (Ephexin)	0.417	-			*ARAF*	0.772	+
		***RASA1* (RasGAP)**	**0.020**	-			*BRAF*	0.161	-
		AKT1 (PKB)	0.257	-			*RAF1*	0.269	-
		CDC42†	**0.005**	-			*RAP1A*†	0.296	-
		RAC1	0.058	-			*MAP2K1* (MEK1)	0.084	-
		RAC2	0.239	+			*MAP2K2* (MEK2)	0.649	-
		RAC3	0.439	+			*MAPK1* (ERK2)	0.165	-
		RHOA	0.455	-			*MAPK3* (ERK1)†	0.263	-
		PAK1	0.065	-			***MAPKSP1***	**0.046**	-
		PAK2	0.565	-			*DUSP1*	0.332	-
		PAK3	**0.050**	-			*DUSP2*	0.386	+

Pathway	Source	Gene (alias)	Uncorrected IPD vs CON *p* value	Change in IPD	Pathway	Source	Gene (alias)	Uncorrected IPD vs CON *p* value	Change in IPD
MAPK signaling	KEGG hsa 04010	*DUSP3*†	0.086	-	MAPK signaling	KEGG hsa 04010	***STMN1***†	**0.037**	-
		DUSP4	**0.024**	-			*RPS6KA1* (RSK1)†	0.065	+
		DUSP5	0.668	-			*RPS6KA2* (RSK3)	0.684	-
		***DUSP6* (MKP3)**	**0.001**	-			***RPS6KA3* (RSK2)**	**0.006**	-
		DUSP7†	0.233	-			***RPS6KA6* (RSK4)**	**0.022**	-
		DUSP8	0.438	-			*ATF4* (CREB2)	0.883	+
		DUSP9	0.088	+			*CREB1*	0.363	-
		DUSP10	0.729	-			***ELK1***	**0.019**	+
		DUSP14	0.652	-			*ELK3* (SAP2)†	0.517	+
		DUSP16†	0.823	-			*ELK4* (SAP1)†	0.456	+
		PTPN5	0.148	-			*MYC*†	0.371	+
		PTPN7†	0.100	+			*SRF*†	0.550	+
		PTPRR	**0.023**	-			*FOS*†	0.905	-
		MKNK2	0.055	+			*JUN*	0.953	+
		PLA2G1B	0.541	+	TCF/LEF	Ref 1	*LEF1* (TCF1α)	0.256	-
		PLA2G2A	0.062	+			***TCF7* (TCF1)**	**0.011**	+
		PLA2G2D†	**0.048**	+			***TCF7L1* (TCF3)**†	**0.007**	+
		PLA2G2E	**0.046**	+			*TCF7L2* (TCF4)	0.937	+
		PLA2G2F	0.070	+	Src	Ref 2	*FYN*	0.945	+
		PLA2G3†	**0.010**	+			***LCK***	**0.011**	+
		PLA2G5	0.988	+			*PXN*	0.520	+
		PLA2G6†	0.501	-			*SHC3*	0.092	-
		PLA2G12A	0.377	+			*SHC4*	0.059	-
		PLA2G12B	0.080	+			*SRC*	0.838	-
					p53	Ref 3	*TP53* (p53)†	0.564	+

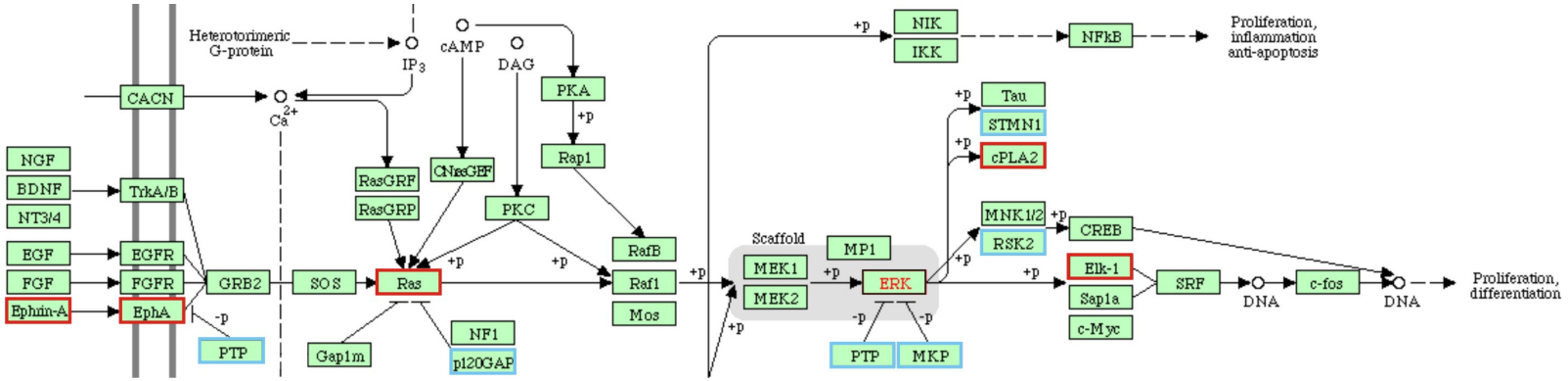

Figure 4.9. Expression microarray data mining: *EPHA2*-related pathways.

Diagrammatic representation of the *EPHA2*-related pathways expression microarray *in silico* data mining analysis results. Several *EPHA2*-related genes were differentially-expressed in the microarray series IPD DLPFC (see table 4.8). Red and blue boxes indicate gene families whose members exhibited increased and decreased expression in IPD vs CON, respectively. Figure adapted from KEGG pathway hsa 04010, (Pratt and Kinch 2002), and (Kikawa *et al.* 2002). -p = dephosphorylation; +p = phosphorylation; CON = control; DLPFC = dorsolateral prefrontal cortex; ELK1 = E26-like kinase 1; *EPHA2* = *Ephrin receptor A2*; ERK1/2 = Extracellular-signal regulated kinase 1/2; hsa = *Homo sapiens*; IPD = idiopathic Parkinson's disease; KEGG = Kyoto Encyclopaedia of Genes and Genomes; MKP = Mitogen-activated protein kinase phosphatase; PLA2 = Phospholipase A2; PTP = Protein tyrosine phosphatase; Ras = Rat sarcoma; p120GAP = Ras guanosine triphosphatase activating protein; RSK = Ribosomal S6 kinase; STMN1 = Stathmin 1.

4.3.10. Expression microarray data mining: the unfolded protein response pathway

The unfolded protein response (UPR) pathway is a collection of cellular stress responses activated by the presence of unfolded and/or misfolded proteins. This process counteracts protein burden by attenuating translation, increasing chaperone gene expression, and promoting ERAD [reviewed in (Rao and Bredesen 2004)]. UPS dysfunction and protein accumulation are thought to induce the UPR pathway in IPD (Lindholm *et al.* 2006). Indeed, UPR gene upregulation has been described in the familial and idiopathic PD brain (Imai *et al.* 2001; Moisoi *et al.* 2009). It was hypothesised that the UPR pathway could be chronically-activated in the IPD DLPFC. Therefore, genes involved in the UPR were selected using OMIM. Microarray data for these 42 candidates were mined *in silico*, and expression in IPD (n = 14) and controls (n = 7) compared statistically.

The results of this analysis are shown in table 4.9. Differential expression was observed for nine genes. Of these, eight were underexpressed and one was overexpressed in IPD contrasted against controls. *Elastase, neutrophil expressed* (*ELANE*) expression was increased (p = 0.004). Impaired UPR activity has been demonstrated in individuals mutated at this gene (Grenda *et al.* 2007). However, the majority of affected genes exhibited reduced expression. These included key members of the UPR, such as *DnaJ homologue, subfamily C, member 10* (*DNAJC10*) (p = 0.008); *ER degradation enhanced, mannosidase α-like 1* (*EDEM1*) (p = 0.033); *Mitogen-activated protein kinase 8* (*MAPK8*) (p = 0.010); and *Membrane-bound transcription factor peptidase, site 1* (*MBTPS1*) (p = 0.035) (Ushioda *et al.* 2008; Urano *et al.* 2000; Ye *et al.* 2000). Essential regulators of this pathway were not differentially-expressed, including *Activating transcription factor 6* (*ATF6*); *DNA-damage-inducible transcript 3* (*DDIT3*); *ER to nucleus signaling 1* (*ERN1*); *G-protein-coupled receptor 37* (*GPR37*); *Heat shock 70 kDa protein 1A* (*HSPA1A*); *Heat shock 70 kDa protein 5* (*HSPA5*); and *X-box binding protein 1* (*XBP1*) (Rao and

Bredesen 2004). Furthermore, the vital UPR initiators *Eukaryotic translation initiation factor 2 α kinase 3* (*EIF2AK3*) ($p = 0.040$) and *Eukaryotic translation initiation factor 2, subunit 1 α, 35 kDa* (*EIF2S1*) ($p = 0.023$) were underexpressed (Harding *et al.* 2000).

Overall, these data suggest that the UPR pathway is not chronically-activated in the microarray series IPD DLPFC. In fact, some of the genes essential for initiating and executing this process were either underexpressed in IPD or unaffected by disease status.

Gene (alias)	Uncorrected IPD vs CON *p* value	Change in IPD	Gene (alias)	Uncorrected IPD vs CON *p* value	Change in IPD
AARS	0.090	-	*HSPA1A* (HSP70-1)	0.332	+
ATF6	0.264	-	*HSPA5* (BIP/GRP78)	0.201	-
BAK1	0.535	+	*KDELR1*	0.500	-
BAX	0.350	-	***MAPK8* (JNK1)**	**0.010**	-
BID	0.680	-	***MBTPS1***	**0.035**	-
BSCL2	0.125	-	*MBTPS2*	0.055	-
CA4	0.291	-	*PHLDA1*†	0.156	+
CYB5R4	**0.006**	-	*PIN1*	0.073	-
DDIT3 (CHOP)	0.897	-	*PLP1*	0.611	-
DERL1	**0.015**	-	*SDF2L1*	0.380	+
DERL2	0.093	-	*SELS* (VIMP)	0.513	-
DERL3†	0.085	+	*SIL1* (BAP)	0.184	-
***DNAJC10* (ERDJ5)**	**0.008**	-	*STUB1*	0.140	-
EDEM1	**0.033**	-	*SYVN1* (HRD1)	0.557	-
EDEM2	0.372	-	*TEGT*†	0.681	-
***EIF2AK3* (PERK)**	**0.040**	-	*TRAF2*	0.158	+
***EIF2S1* (EIF2α)**	**0.023**	-	*UBXD2*	0.134	-
***ELANE* (Elastase 2)**	**0.004**	+	*VAPB*†	0.086	-
ERN1 (IRE1)†	0.262	+	*VCP*	0.094	-
GPR37 (PAELR)	0.953	-	*WFS1*	0.063	+
HERPUD1	0.248	-	*XBP1*	0.342	-

Table 4.9. Expression microarray data mining: the UPR pathway.

Statistical results for the UPR pathway expression microarray *in silico* data mining analysis. Several genes were differentially-expressed (in bold text), but the changes suggest that the UPR pathway is not chronically-activated in the microarray series IPD DLPFC. IPD and CON $\log_2$ group expression was compared by *t* test, or when the † symbol is shown, by Mann-Whitney test. All *p* values were uncorrected. Positive and negative symbols indicate the direction of differential expression in IPD vs CON. See list of abbreviations for definitions of gene symbols and common gene aliases. CON = control; DLPFC = dorsolateral prefrontal cortex; IPD = idiopathic Parkinson's disease; UPR = unfolded protein response.

4.3.11. Expression microarray data mining: Parkinson's disease and parkinsonism-dementia

Several studies have investigated the expression of genes linked to familial Parkinson's disease (FPD) (OMIM #168600) in IPD brain samples. *α-Synuclein* (*SNCA*) is differentially-expressed in both the SN and FC (Kingsbury *et al.* 2004; Beyer *et al.* 2008; Grundemann *et al.* 2008; Simunovic *et al.* 2009). *Parkin* (*PARK2*) is alternatively-spliced in the FC (Beyer *et al.* 2008). *Ubiquitin carboxy-terminal hydrolase L1* (*UCHL1*) is underexpressed in the SN and FC (Moran *et al.* 2007; Zhang *et al.* 2005b). In SN neurons, conflicting results have been observed for *Phosphatase and tensin homologue-induced putative kinase 1* (*PINK1*), *Parkinson's disease 7* (*PARK7*), and *ATPase type 13A2* (*ATP13A2*), whereas *Leucine-rich repeat kinase 2* (*LRRK2*) is underexpressed (Blackinton *et al.* 2007; Galter *et al.* 2006; Ramirez *et al.* 2006; Simunovic *et al.* 2009). The expression of genes with proximal IPD- and IPDD-associated variants has been examined in this disorder. Examples include *β-Glucocerebrosidase* (*GBA*) and *Nuclear receptor subfamily 4, group A, member 2* (*NR4A2*) expression, which are decreased in the SN, and *Synuclein, α interacting protein* (*SNCAIP*), which is overexpressed in the FC (Moran *et al.* 2007; Beyer *et al.* 2008). Various diseases exist in which patients manifest both parkinsonism and dementia, and several of these are thought to result from monogenic mutation. Expression of the relevant genes has generally not been assessed in the IPD brain, however some exceptions do exist. *β-Synuclein* (*SNCB*) mutations are implicated in dementia with Lewy bodies (DLB) (OMIM #127750) (Ohtake *et al.* 2004). In IPD, *SNCB* expression is reduced in BA9 but unaltered in the SN (Zhang *et al.* 2005b). *MAPT* mutations cause frontotemporal dementia and parkinsonism linked to chromosome 17 (FTDP17) (OMIM # 600274); this gene is underexpressed in IPD SNpc dopaminergic neurons (Hutton *et al.* 1998; Simunovic *et al.* 2009). Interestingly, PCC neuronal *MAPT* expression is reduced in IPDD compared to IPDND or controls, implying that it might play a role in IPD dementia (Stamper *et al.* 2008).

It was hypothesised that genes implicated in FPD, IPD, or parkinsonism-dementia might be differentially-expressed in the IPD DLPFC. Consequently, known or predicted *PARK* loci genes and those involved in forms of parkinsonism-dementia were identified using OMIM. Other genes with proximal polymorphisms that demonstrate association with IPD or IPDD were identified using two publications (Sulzer 2007; de Lau *et al.* 2005). Microarray data for these 26 candidates were mined *in silico*, and expression in IPD (n = 14) and controls (n = 7) compared statistically. For those genes involved in parkinsonism-dementia, expression in IPDD (n = 7) and IPDND (n = 7) was also compared statistically.

Table 4.10 shows the results of this analysis. The majority of genes were not differentially-expressed. The four exceptions all displayed reduced expression in IPD contrasted against controls: *Fragile X mental retardation 1* (*FMR1*) (p = 0.022); *GBA* (p = 0.040); *High temperature requirement A2* (*HTRA2*) (p = 0.035); and *Transient receptor potential cation channel, subfamily M, member7* (*TRPM7*) (p = 0.030). *SNCA* exhibited a trend of underexpression in IPD (p = 0.052). None of the parkinsonism-dementia genes displayed differential expression in the IPDD vs IPDND comparison. Taken together, these findings suggest that variation in the DLPFC expression of genes implicated in PD and parkinsonism-dementia is not associated with IPD in the microarray series.

Table 4.10. Expression microarray data mining: PD and parkinsonism-dementia.

Statistical results for the PD and parkinsonism-dementia expression microarray in silico data mining analysis (next page). Only four genes were differentially-expressed (in bold text), suggesting that variation in the DLPFC expression of genes implicated in PD and parkinsonism-dementia is not associated with IPD in the microarray series. Log2 group expression was compared by t test, or when the † symbol is shown, by Mann-Whitney test. All p values were uncorrected. Positive and negative symbols indicate the direction of differential expression in IPDD vs IPDND or IPD vs CON, as appropriate. *LRRK2* expression was not quantified in the microarray. See list of abbreviations for definitions of gene symbols and common gene aliases. AODP = adult onset dystonia parkinsonism (OMIM #612953); ALS-PDC = amyotrophic lateral sclerosis-parkinsonism dementia complex (OMIM #105500); APSP = atypical progressive supranuclear palsy (OMIM #260540); CON = control; DLB = dementia with Lewy bodies (OMIM #127750); DLPFC = dorsolateral prefrontal cortex; FAD3 = familial Alzheimer's disease 3 (OMIM #607822); FPD = familial Parkinson's disease (OMIM #168600); FXTAS = fragile X tremor ataxia syndrome (OMIM #300623); FTDP17 = frontotemporal dementia and parkinsonism linked to chromosome 17 (OMIM #600274); FTLDU = frontotemporal lobar degeneration with ubiquitin-positive inclusions (OMIM #607485); GSD = Gerstmann-Straussler disease (OMIM #137440); IPD = idiopathic Parkinson's disease; IPDD = idiopathic Parkinson's disease with dementia; IPDND = idiopathic Parkinson's disease no dementia; ND = not determined; OMIM = Online Mendelian Inheritance in Man; PD = Parkinson's disease.

Disease(s)	Source	Gene (alias)	Uncorrected *p* value		Change in	
			IPDD vs IPDND	IPD vs CON	IPDD vs IPDND	IPD vs CON
FPD	*PARK1*	*SNCA*†	ND	0.052	ND	-
	PARK2	*PARK2*†	ND	0.063	ND	-
	PARK3	*SPR*	ND	0.400	ND	-
	PARK5	*UCHL1*	ND	0.128	ND	-
	PARK6	*PINK1*	ND	0.261	ND	-
	PARK7	*PARK7* (*DJ1*)	ND	0.105	ND	-
	PARK8	*LRRK2*	ND	ND	ND	ND
	PARK9	*ATP13A2*	ND	0.145	ND	-
	PARK11	*GIGYF2*	ND	0.063	ND	-
	PARK13	***HTRA2* (*Omi*)**	ND	**0.035**	ND	-
	PARK15	*FBXO7*	ND	0.119	ND	-
IPD	Sulzer 2007	*CYP2D6*	ND	0.524	ND	+
	Sulzer 2007	*FGF20*	ND	0.061	ND	-
	Sulzer 2007	***GBA***	ND	**0.040**	ND	-
	Sulzer 2007	*NR4A2* (*NURR1*)†	ND	0.650	ND	+
	Sulzer 2007	*POLG*	ND	0.382	ND	-
	Sulzer 2007	*SNCAIP* (*Synphilin 1*)	ND	0.631	ND	+
IPDD	de Lau *et al.* 2005	*APOE*†	0.565	0.156	+	+
FXTAS	OMIM	***FMR1***	0.661	**0.022**	-	-
FTLDU	OMIM	*GRN* (*Progranulin*)	0.712	0.746	+	-
FTDP17/APSP	OMIM	*MAPT*	0.642	0.138	-	-
AODP	OMIM	*PLA2G6*†	0.198	0.501	-	-
GSD	OMIM	*PRNP*	0.801	0.277	-	-
FAD3	OMIM	*PSEN1*	0.509	0.257	-	-
DLB	OMIM	*SNCB*†	0.749	0.456	-	-
ALS-PDC	OMIM	***TRPM7***	0.339	**0.030**	-	-

4.3.12. Expression microarray data mining: putative regulators of dorsolateral prefrontal cortex *Dual specificity phosphatase 6* expression

The final mining experiment was an attempt to elucidate the mechanism underlying *DUSP6* underexpression in the IPD DLPFC (see 3.3.3 and 4.3.9). This phenomenon is unlikely to be caused by *cis*-acting SNP variation (see 3.3.7). Furthermore, although the low frequency variant rs1689408 is implicated in *DUSP6* splicing (see 3.3.9), there is little evidence to suggest that modulated splicing accounts for the majority of the *DUSP6* underexpression effect (see 3.3.4). It was hypothesised that a TF which regulates *DUSP6* expression could itself be differentially-expressed in the IPD DLPFC. Therefore, the UCSC PhyloP database was consulted to search for putative *DUSP6* regulatory elements, and an upstream region possessing high levels of predicted DNA sequence conservation across 32 placental mammals was identified. This region extends 650 bp upstream from the *DUSP6* TSS (henceforth called the "*DUSP6* putative promoter" [DPP]). It encompasses those elements found to control expression of the murine and human orthologues of this gene (Ekerot *et al.* 2008; Zhang *et al.* 2009). The DPP gDNA sequence was then downloaded from Ensembl, and entered into the PROMO online resource which employs the Transfac database to search for predicted transcription factor binding sites (TFBS). Factors possessing at least one predicted binding site in the DPP were identified. Microarray data for these 16 candidates were mined *in silico*, and expression in IPD (n = 14) and controls (n = 7) compared statistically. Successful candidates were validated using qRT-PCR to measure total and NLC expression in cognitive series DLPFC cDNA batch 2, and expression in IPD (n = 31) and controls (n = 16) compared statistically.

The results of this analysis are shown in table 4.11 and figure 4.10. Differential expression was observed for six genes: *ELK1*, *Estrogen receptor 1* (*ESR1*), *E Twenty-Six oncogene homologue 1* (*ETS1*), *Hepatic nuclear factor 1 homeobox A* (*HNF1A*), *Signal transducer and activator of transcription 4* (*STAT4*), and *Yin Yang 1* (*YY1*). It

was reasoned that factors displaying reduced expression in IPD compared to controls would be most likely to mediate *DUSP6* underexpression. This approach identified *ETS1* and *STAT4* as putative regulators of DLPFC *DUSP6* expression. However, underexpression of *ETS1* and *STAT4* were not validated by qRT-PCR, indicating that these genes are not differentially-expressed in the IPD DLPFC.

Overall, these findings suggest that *DUSP6* underexpression in the IPD DLPFC is not caused by altered expression of a regulatory TF, although the involvement of other putative regulatory elements cannot be excluded.

Gene (alias)	Number of predicted binding sites in the DPP	Uncorrected IPD vs CON *p* value	Change in IPD
CEBPB	20	0.322	+
ELK1	1	0.019	+
ESR1 (ERα)	1	0.011	+
ETS1	**1**	**0.021**	-
FOXP3	2	0.111	+
GTF2I (TFII-I)†	1	0.263	-
HNF1A	2	0.044	+
MAZ (PUR1)	1	0.318	-
NFIC (CTF)†	1	0.156	+
NR3C1 (GR)	14	0.107	-
PAX5	3	0.343	+
PEX5 (PXR1)	1	0.052	-
RXRA	2	0.148	+
STAT4	**1**	**0.042**	-
TBP (TFIID)	2	0.166	-
YY1	2	0.038	+

Table 4.11. Expression microarray data mining: putative DLPFC *DUSP6* expression regulators.

Statistical results for the putative regulators of DLPFC *DUSP6* expression microarray *in silico* data mining analysis. *ETS1* and *STAT4* were underexpressed in the microarray series IPD DLPFC, and hence were designated as putative regulators of DLPFC *DUSP6* expression (in bold text). Transcription factors possessing one or more predicted binding sites in the DPP were identified using PROMO at a maximum binding dissimilarity of 1%. IPD and CON $\log_2$ group expression was compared by *t* test, or when the † symbol is shown, by Mann-Whitney test. All *p* values were uncorrected. Positive and negative symbols indicate the direction of differential expression in IPD vs CON. See list of abbreviations for definitions of gene symbols and common gene aliases. CON = control; DLPFC = dorsolateral prefrontal cortex; *DUSP6 = Dual specificity phosphatase 6*; DPP = *DUSP6* putative promoter; *ETS1 = E Twenty-Six oncogene homologue 1*; IPD = idiopathic Parkinson's disease; *STAT4 = Signal transducer and activator of transcription 4*.

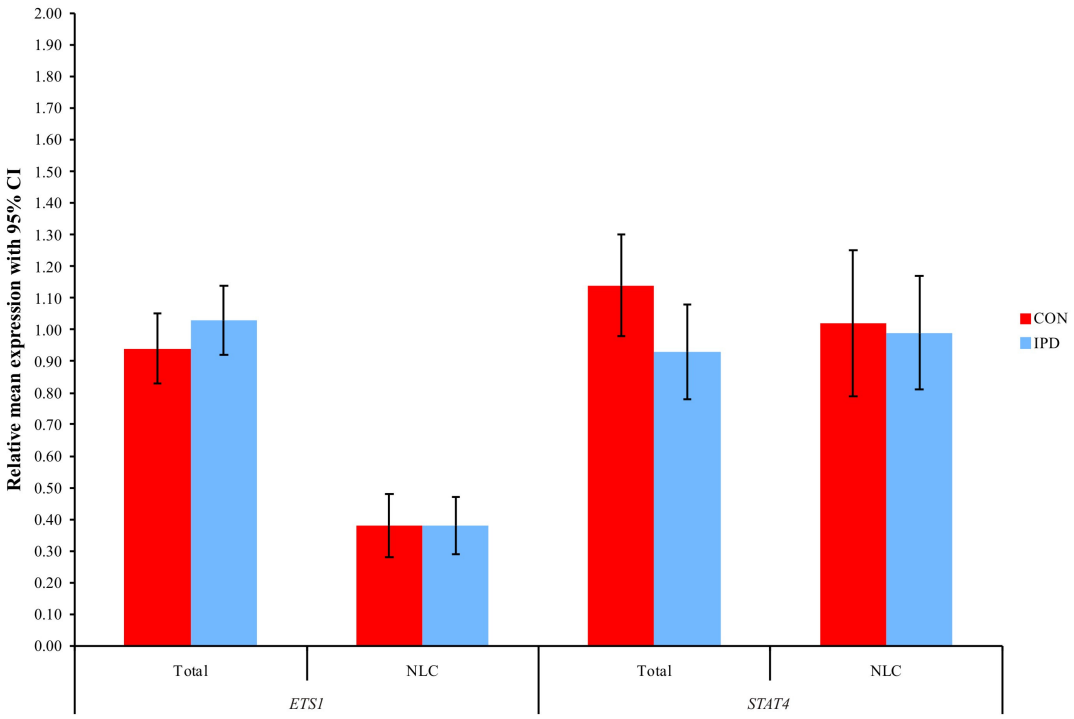

Figure 4.10. *ETS1* and *STAT4* are not differentially-expressed in the IPD DLPFC.

Relative mean qRT-PCR *ETS1* and *STAT4* expression values with 95% CI for cognitive series DLPFC cDNA batch 2. No significant differences were observed, indicating that *ETS1* and *STAT4* are not differentially-expressed in the IPD DLPFC. Total expression data were normalised with *G6PD*, *RPL13A*, and *TBP*, and NLC expression data with *NEFH*. IPD and CON were compared by Mann-Whitney test. Uncorrected *ETS1 p* values were 0.369 for total expression and 0.841 for NLC expression. Uncorrected *STAT4 p* values were 0.178 for total expression and 0.575 for NLC expression. *p* values were corrected x52. CI = confidence interval; CON = control; cDNA = complementary DNA; DLPFC = dorsolateral prefrontal cortex; *ETS1 = E Twenty-Six oncogene homologue 1*; *G6PD = Glucose-6-phosphate dehydrogenase*; IPD = idiopathic Parkinson's disease; *NEFH = Neurofilament H*; NLC = neuronal-loss corrected; qRT-PCR = quantitative reverse transcriptase-polymerase chain reaction; *RPL13A = Ribosomal protein L13A*; *STAT4 = Signal transducer and activator of transcription 4*; *TBP = TATA box binding protein*.

4.3.13. Variation in CpG methylation is implicated in *Dual specificity phosphatase 6* underexpression in the idiopathic Parkinson's disease dorsolateral prefrontal cortex

One possible explanation for *DUSP6* underexpression in the IPD DLPFC is modulated CpG methylation. The murine *Dusp6* promoter contains one conserved Ets family binding site that is necessary for Fgf-induced reporter gene expression (Ekerot *et al.* 2008). Moreover, the orthologous sequence upstream of human *DUSP6* regulates reporter gene expression and mediates ETS binding (Zhang *et al.* 2009). Closer inspection of the Ekerot *et al.* and Zhang *et al.* publications reveal that this ETS target incorporates the predicted STAT4 binding site identified in the DPP by PROMO (see 4.3.12). Due to the laboratory and bioinformatic evidence presented in these papers, this site will be considered as an ETS target, henceforth designated as ETS binding site B. The predicted ETS1 target identified by PROMO (see 4.3.12) will henceforth be called ETS binding site A. Thus, ETS factors are known or predicted to bind two locations in the DPP (see figure 4.11).

It was hypothesised that DPP ETS binding site CpG methylation might be altered in the IPD DLPFC. Therefore, bisulphite-converted DLPFC gDNA extracted from the MSP series (see table 4.12) was amplified using MSP reactions separately interrogating CpG methylation at ETS binding sites A and B, and relative CpG methylation in IPD (n = 6) and controls (n = 6) compared. The bisulphite conversion protocol uses sulphonation to deaminate unmethylated cytosines, followed by desulphonation to convert the deaminated cytosines into uracil. Methylated cytosines are resistant to these modifications and remain as cytosines. Subsequent PCR employs primers specific for converted or unconverted DNA, enabling the specific amplification of unmethylated or methylated alleles, respectively (Herman *et al.* 1996). One caveat should be kept in mind. The constraints of MSP primer design

and the existence of additional CpGs within primer annealing sequences can make it impossible to solely analyse the desired target CpG. ETS binding sites A and B each contain one CpG, however the relevant MSP reactions necessarily interrogated methylation at three and two CpGs, respectively (see figure 4.11). Consequently, the degree of relative methylation at both binding sites was an amalgam of multiple CpGs, only one of which might directly influence transcription.

Figure 4.12 shows the MSP results. Almost all individuals displayed markedly more unmethylated than methylated alleles at ETS binding site A, and relative CpG methylation was similar in IPD and controls. However, the data for ETS binding site B were somewhat different. The controls all exhibited more unmethylated than methylated alleles, except for one individual who displayed approximately equal amounts of the two. On the other hand, relative CpG methylation was marginally higher in the IPD group. Methylated alleles exceeded their unmethylated counterparts in one IPD patient, and these species were roughly equal in two other cases. Nonetheless, the three remaining IPD patients were similar to the controls i.e. unmethylated outnumbered methylated alleles. No clear differences at either binding site were observed when comparing the IPDD and IPDND groups.

These results suggest that variation in CpG methylation at DPP ETS binding site B is implicated in *DUSP6* underexpression in the IPD DLPFC. However, half of the IPD group displayed levels of relative CpG methylation similar to that seen in controls, indicating that this mechanism cannot account for the entire *DUSP6* underexpression effect.

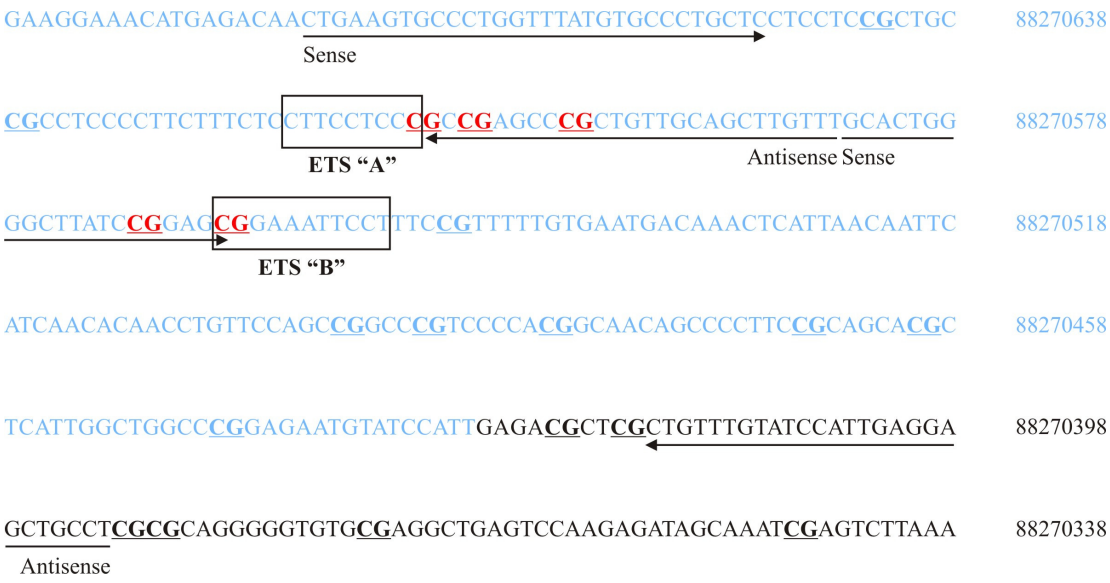

Figure 4.11. *DUSP6* putative promoter ETS family binding sites and CpG locations.

E Twenty-Six family binding sites and CpG locations in the 3' DPP. The DPP is indicated by blue sequence and the *DUSP6* 5'UTR by black. Locations on the negative strand of chromosome 12 are according to NCBI assembly build 36. Boxes indicate ETS binding sites A and B, based on PROMO and (Zhang *et al.* 2009) (see text for details). CpGs are underlined and bolded. CpGs interrogated by MSP reactions are in red. Arrows indicate MSP primer annealing sites. DNA base codes are in accordance with the International Union of Biochemistry and Molecular Biology. *DUSP6* = *Dual specificity phosphatase 6*; DPP = *DUSP6* putative promoter; ETS = E Twenty-Six; MSP = methyl-specific polymerase chain reaction; NCBI = National Center for Biotechnology Information; UTR = untranslated region.

Group (*n*)	Statistic	Age of onset	Age of death	Disease duration	PMD	Brain pH
CON (6)	Mean	NA	79.8	NA	27.6	6.51
	SD	NA	7.3	NA	18.2	0.20
IPD (6)	Mean	60.3	75.5	15.2	38.8	6.26
	SD	12.0	9.3	5.9	18.2	0.16

Table 4.12. IPD MSP series clinicopathological data.

Group clinicopathological metrics for the IPD MSP series. The IPD group consists of three IPDD patients and three IPDND patients. Measures of time are in years, except for PMD, which is measured in hours. Table 2.10 shows individual clinicopathological data for each member of the MSP series. CON = control; IPD = idiopathic Parkinson's disease; IPDD = idiopathic Parkinson's disease with dementia; IPDND = idiopathic Parkinson's disease no dementia; MSP = methyl-specific polymerase chain reaction; NA = not applicable; PMD = *post mortem* delay; SD = standard deviation.

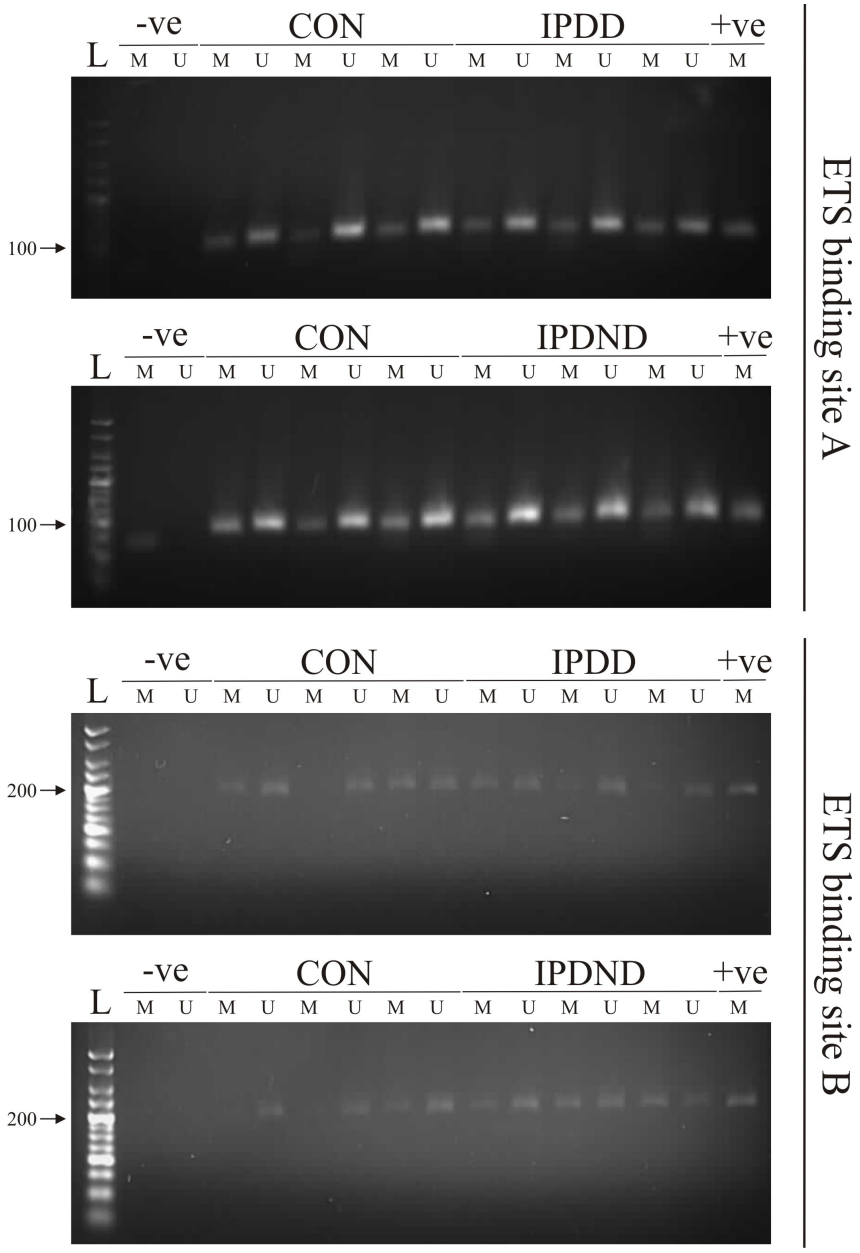

Figure 4.12. Variation in CpG methylation at DPP ETS binding site B is implicated in *DUSP6* underexpression in the IPD DLPFC.

MSP amplification of bisulphite-converted MSP series DLPFC gDNA interrogating CpG methylation at DPP ETS binding sites A and B. Relative CpG methylation at site B was marginally higher in IPD compared to controls, suggesting that variation in CpG methylation at this site is implicated in *DUSP6* underexpression in the IPD DLPFC. MSP products were resolved on agarose gels. Arrows denote the 100 and 200 base pair marker on site A and B gels, respectively. -ve = negative control (water); +ve = positive control (HMSN bisulphite-converted blood gDNA); CON = control; gDNA = genomic DNA; DLPFC = dorsolateral prefrontal cortex; *DUSP6* = *dual specificity phosphatase 6*; DPP = *DUSP6* putative promoter; ETS = E Twenty-Six; HMSN = Hereditary motor and sensory neuropathy; IPD = idiopathic Parkinson's disease; IPDD = idiopathic Parkinson's disease dementia; IPDND = idiopathic Parkinson's disease no dementia; L = marker ladder; MSP = methyl-specific polymerase chain reaction; M = methylated-specific reaction; U = unmethylated-specific reaction.

4.4. Discussion

In this chapter DLPFC expression microarray analysis was carried out to identify genes exhibiting dysregulation in different IPD subtypes. These data suggested that synaptic transmission/ion transport, glycosylation/protein degradation, inflammation/immune response, and transcription/translation pathways are dysregulated in IPD neurodegeneration. Moreover, the array findings suggested that mitochondrial/metal binding, axonal guidance/cytoskeletal, synaptic transmission/ion transport, lipoprotein metabolism, inflammation/immune response, cell adhesion/ECM, and transcription/splicing pathways are dysregulated in IPD dementia. We used qRT-PCR to demonstrate that variation in DLPFC *EPHA2* expression is significantly associated with IPD. This association takes the form of increased expression in IPD compared to controls, but variation in *EPHA2* expression is not related to disease status in seven other cortical and subcortical regions of the IPD brain. SNP allelic association analysis indicated that the rs11260822 minor allele significantly increases IPD risk. However, variation at this SNP does not influence DLPFC *EPHA2* expression. *In silico* mining of the microarray data was performed to evaluate several hypotheses. This approach indicated that several *EPHA2*-related genes exhibit dysregulation in the IPD DLPFC, and validated IPD *DUSP6* underexpression in this region. Furthermore, these analyses suggested that the UPR pathway is not chronically-activated in the IPD DLPFC, and that variation in the DLPFC expression of genes involved in PD and parkinsonism-dementia is not associated with IPD. Array mining also indicated that, of the TFs with predicted binding sites in the conserved DPP, only *ETS1* and *STAT4* exhibit differential expression in the IPD DLPFC consistent with *DUSP6* underexpression; however these observations were not validated by qRT-PCR. Finally, MSP experiments suggested that variation in CpG methylation at DPP ETS binding site B is implicated in, but cannot fully explain, *DUSP6* underexpression in the IPD DLPFC.

The microarray data suggested that genes belonging to a variety of pathways are differentially-expressed in the IPD DLPFC, and that the two IPD subtypes display

some degree of overlap in this regard. Although genome wide gene expression in the IPDD DLPFC has not previously been investigated, our results are mirrored by similar findings reported in array experiments examining several brain regions. Pathways implicated in IPD dementia, such as mitochondria, the cytoskeleton, synaptic transmission, ion transport, cell adhesion, and inflammation, are all known to exhibit dysregulation in IPDD PCC neurons, IPD BA9 whole tissue, and IPD SNpc dopaminergic neurons (Stamper *et al.* 2008; Zhang *et al.* 2005b; Simunovic *et al.* 2009). The same is true for other pathways that our dataset implicated in IPD dementia, including lipid metabolism and metal binding in both IPD BA9 and SN whole tissues (Zhang *et al.* 2005b; Moran *et al.* 2006), and axonal guidance in IPD PCC neurons, IPD SNpc dopaminergic cells, and IPD SN whole tissue (Stamper *et al.* 2008; Simunovic *et al.* 2009; Bossers *et al.* 2009). Pathway-level parallels between our IPD neurodegeneration results and the literature can also be found, such as for protein degradation and glycosylation pathways in both IPD BA9 whole tissue and IPD SNpc dopaminergic neurons (Zhang *et al.* 2005b; Simunovic *et al.* 2009).

Overall, these parallels suggest that similar genetic pathways are dysregulated in the DLPFC and SN, supporting the hypothesis that IPD is a multisystem disorder (Zhang *et al.* 2005b; Moran *et al.* 2006). When viewed collectively with the pathway overlaps we observed between IPD dementia and IPD neurodegeneration, they also suggest that the two disease subtypes are driven by similar pathogenic processes, most likely involving mitochondria, protein degradation, axonal function, synaptic transmission, and inflammation. Moreover, when both groups were compared to controls, IPDD displayed much greater levels of dysregulation than IPDND. Taken together, these findings suggest that IPDD can be seen as an "extension" of the parkinsonian state. This conclusion is supported by the spectrum concept of Lewy body disease (Aarsland *et al.* 2004), and by evidence of positive correlations between cortical Lewy body pathology/gene dysregulation severity and cognitive dysfunction in IPD (Kovari *et al.* 2003; Aarsland *et al.* 2005a; Stamper *et al.* 2008). Interestingly, our IPD dementia data flagged several pleiotropic pathways which mediate neural development during embryogenesis, and neural maintenance and plasticity in

adulthood. Examples include axonal guidance, the cytoskeleton, and synaptic transmission. The involvement of axonal guidance fits well with several SNP association studies demonstrating that this pathway influences IPD susceptibility, and with the detection of misrouted axonal fibres in the IPD brain [reviewed in (Lin *et al.* 2009a)].

Notwithstanding these results, none of the microarray differential expression or alternative splicing events passed the FDR threshold. Furthermore, relatively small numbers of genes were differentially-expressed at the more relaxed uncorrected $p < 0.001$ threshold. Several confounds could have accounted for this situation. Examples, such as choice of brain region, lack of cognitive testing specifically relevant to IPDD, and insufficient numbers of samples (see below), have been discussed (see 3.4). Among these possibilities, the general lack of differential expression observed using microarray and qRT-PCR (see also 3.3.3) suggests that choice of brain region may have been critically important. Indeed, one of the primary conclusions of the microarray experiment could be that, when compared to other brain areas, genetic dysregulation is relatively uncommon in the IPD DLPFC. The issue is one of significance threshold and confidence in the findings. The FDR-corrected data indicated no dysregulation in either IPD subtype, whereas changes were observed in the uncorrected $p < 0.001$ results. However, reduced confidence in these latter findings means that they must be interpreted with caution i.e. as suggestive rather than demonstrative. The conclusion that differential expression is rare in the DLPFC may be particularly relevant to the IPD dementia subtype. Neuropathological and neuropsychological evidence suggests that the ACC (BA24), EC (BA28), perirhinal cortex (BA35), parahippocampal cortex (BA36), or hippocampus could be the most promising regions for identifying genetic dysregulation that associates with IPDD (see 3.4) (Pletnikova *et al.* 2005; Vermersch *et al.* 1993; Kovari *et al.* 2003; Williams-Gray *et al.* 2009a; Pihlajamaki *et al.* 2000).

Although region selection and cognitive testing issues probably contributed to the low number of hits, another important factor was highlighted by the microarray QC.

Relatively high levels of biological variation were detected, particularly in the IPDD and control groups. Moreover, consistently more variation was seen in the gene level compared to the exon level data. This variation may have been a function of the sample number in each group and/or caused by problems with RNA quality. It undoubtedly had a negative effect on statistical power and the total number of significant hits, and might also explain why alternative splicing was detected much more frequently than differential expression. However, this last observation could suggest that alternative splicing is actually of greater biological significance than differential expression in the IPD DLPFC. Furthermore, the high levels of biological variation probably contributed to the general lack of qRT-PCR validation, in that the chance of detecting false positives was increased. Validation was attempted for six genes, and only *EPHA2* was confirmed as differentially-expressed (see below). However, it is likely that inherent differences between the two quantification techniques were also involved. Given the reduced confidence in our array results, the risk of pursuing false positives was minimised by only selecting those hits validated via qRT-PCR for further characterisation.

These findings connect *EPHA2* to IPD neurodegenerative processes in general, and not to IPD dementia. Taken together, the microarray and qRT-PCR validation experiments detailed here failed to confirm any gene as specifically implicated in IPDD. Therefore, our results do not provide strong support for the hypothesis that there is a relationship between IPD dementia status and gene expression in the DLPFC. Notwithstanding the lack of papers investigating gene expression in the IPDD DLPFC, the *EPHA2* data could be evaluated against the Stamper *et al.* microarray study which quantified expression in IPDD PCC neurons. The authors found that *EPHA2* was significantly overexpressed ~2.7-fold in IPDD vs controls, and exhibited a strong trend of ~1.6-fold increased expression in IPDD vs IPDND (Stamper *et al.* 2008). These results are similar to our array findings for *EPHA2*. When viewed together in the context of its axonal guidance function, and despite the fact that our qRT-PCR validation connected this gene to IPD neurodegeneration, these data suggest that *EPHA2* should not be ignored by future attempts to identify

IPD cognitive genes. The mechanism underlying *EPHA2* overexpression in the IPD DLPFC remains unclear. *Cis*-acting SNP variation in the *EPHA2* locus is unlikely to account for this effect. Variation at five of the six *EPHA2* htSNPs, which together capture 95% of the common SNP variation in this region, does not influence IPD susceptibility. Although this relationship was demonstrated for rs11260822, variation at this SNP does not associate with DLPFC *EPHA2* expression. Taken together, these data imply that *EPHA2* overexpression in the IPD DLPFC is not caused by local genetic variation, and probably arises as a secondary effect of IPD pathogenesis. Two major possible causes remain: alterations in *EPHA2* transcriptional activity and/or changes in *EPHA2* mRNA stability (see below). We cannot exclude the possibility that *EPHA2* overexpression results in part from altered glial expression.

In silico mining of the microarray data indicated that several genes belonging to *EPHA2*-related pathways exhibit dysregulation in the IPD DLPFC. Interestingly, these changes could be linked together, enabling us to outline likely patterns of signaling activity in the parkinsonian DLPFC, and to infer putative nodes through which this activity might be transduced. We observed differential expression suggestive of increased EPHA2, Ras, and ERK1/2 signaling. Furthermore, similar changes were seen in certain ERK1/2 effectors, specifically overexpression of *PLA2G* genes and *ELK1*, and underexpression of *RPS6KA* genes and *STMN1*. Overall, these results suggest that signaling patterns in the IPD DLPFC might be characterised by enhanced EPHA2-Ras-ERK1/2 activity, preferentially directed through ELK1 and PLA2 pathways, rather than those involving STMN1 and RSK/CREB. Furthermore, these findings could help elucidate the mechanism driving *EPHA2* overexpression in the IPD DLPFC. Several TFs known or predicted to regulate *EPHA2* expression themselves exhibited differential expression in this region. TCF/LEF family members *TCF7* and *TCF7L1* were overexpressed in IPD. Bioinformatic evidence indicates that the *EPHA2* promoter contains one putative TCF/LEF binding site (Katoh and Katoh 2006), thus increased expression of these factors might be important. However, further inspection of this region with PROMO suggested that the relevant site is bound specifically by *LEF1* and *TCF7L2* but not by the other

family members (data not shown), indicating that TCF/LEF-mediated transcription is unlikely to cause *EPHA2* overexpression in our series. *ELK1* was also found to be overexpressed in IPD. ERK1/2 phosphorylates ELK1, enhancing its DNA-binding and transcriptional activities (Sharrocks 2002). Interestingly, activation of EPHA2 increases ELK1-dependent transcription in a pathway mediated through ERK1/2. In the same cell model, EPHA2 activation upregulates *EPHA2* expression in an ERK1/2-dependent manner (Pratt and Kinch 2002; Pratt and Kinch 2003). These publications indicate the existence of an EPHA2-ERK1/2-ELK1-*EPHA2* positive feedback loop. The differential expression of *ELK1* and of genes suggesting enhanced activity along the EPHA2-Ras-ERK1/2 pathway (see above) implies that this loop could be constitutively activated in the IPD DLPFC, thereby providing a plausible mechanism to explain the overexpression of *EPHA2*.

In silico mining of the microarray also generated several other findings of interest. This approach suggested that the UPR pathway is not chronically-activated in the IPD DLPFC, and that variation in the DLPFC expression of genes implicated in PD and parkinsonism-dementia does not associate with IPD. Both of these results are interesting, in that one would expect the opposite based on the literature. Indeed, UPR components are known to be upregulated in IPD (Moisoi *et al.* 2009), and several genes linked to FPD and parkinsonism-dementia are differentially-expressed in IPD [for example (Moran *et al.* 2007; Simunovic *et al.* 2009)]. However, most of these studies have examined gene expression in midbrain regions e.g. the SN. Therefore, our DLPFC data are entirely plausible. In particular, UPR quiescence in this region might be because the forebrain is one of the last areas to acquire LP, which itself can be thought of as a marker of misfolded protein burden (Braak *et al.* 2003).

The final *in silico* mining, qRT-PCR validation, and MSP experiments were undertaken in order to explain *DUSP6* underexpression in the IPD DLPFC (see 3.3.4). The results indicated that TFs predicted to bind the DPP were not underexpressed in the IPD DLPFC, suggesting that *DUSP6* underexpression is not

caused by differential expression of a regulatory TF. An ETS family binding site located in the DPP is thought to regulate *DUSP6* expression (Ekerot *et al.* 2008; Zhang *et al.* 2009). MSP analysis suggested that increased ETS site CpG methylation in the IPD DLPFC could account for some, but not all, of the *DUSP6* underexpression effect. Despite the inability of this mechanism to fully explain the phenomenon in question, this could be an important finding. Erk1/2 activity induces *Dusp6* expression *in vivo* (Gomez *et al.* 2005; Tsang *et al.* 2004; Eblaghie *et al.* 2003; Smith *et al.* 2006a). As our microarray and qRT-PCR results implied enhanced ERK1/2 activity in the IPD DLPFC, one would also expect increased *DUSP6* expression in this region, especially since ERK1/2 phosphorylates ETS proteins augmenting their transcriptional activity (Foulds *et al.* 2004). Consequently, increased CpG methylation causing reduced ETS binding constitutes an attractive mechanism to explain decreased *DUSP6* expression under the spectre of chronic ERK1/2 activation. Interestingly, *DUSP6* intron 1-2 has recently been shown to induce transcriptional activity which is sensitive to mutation of a resident ETS binding site (Furukawa *et al.* 2008). Therefore, modulated CpG methylation at this intronic location might conceivably explain the remainder of the *DUSP6* underexpression effect.

In conclusion, expression microarray data suggested that mitochondrial/metal binding, axonal guidance/cytoskeletal, synaptic transmission/ion transport, lipoprotein metabolism, inflammation/immune response, cell adhesion/ECM, and transcription/splicing pathways are dysregulated in the IPD dementia DLPFC. It was demonstrated that *EPHA2* expression is significantly increased in the IPD DLPFC, but unaltered in seven other subcortical and cortical regions of the IPD brain. Moreover, genetic variation in the *EPHA2* locus significantly influences IPD susceptibility, but not DLPFC *EPHA2* expression. *In silico* microarray mining suggested that the IPD DLPFC is characterised by enhanced EPHA2-Ras-ERK1/2 signaling, which might explain *EPHA2* overexpression in this region. Finally, epigenetic analysis suggested that increased CpG methylation is implicated in *DUSP6* underexpression in the IPD DLPFC.

Chapter 5: Genetic analyses of *α-Synuclein* in idiopathic Parkinson's disease

5.1. Introduction

Of the genes currently known to cause Parkinson's disease (PD), *α-Synuclein* (*SNCA*) is probably the most investigated. Three autosomal dominant missense mutations as well as multiplications have been described in familial Parkinson's disease (FPD) kindreds (Polymeropoulos *et al.* 1997; Kruger *et al.* 1998; Zarranz *et al.* 2004; Ross *et al.* 2008a), and its protein product is a major constituent of Lewy bodies (LBs) and Lewy neurites (LNs) (Spillantini *et al.* 1997; Spillantini *et al.* 1998a). In pedigrees carrying *SNCA* gene alterations, it is relatively common for parkinsonian symptoms to be accompanied by cognitive impairment, dementia, and hallucinations. This is seen in the missense mutation families, notably the Glu46Lys patients (Polymeropoulos *et al.* 1997; Kruger *et al.* 2001; Zarranz *et al.* 2004). Other examples are derived from studies of *SNCA* multiplication kindreds, in which the number of genomic copies broadly correlates with the age of onset of parkinsonian characteristics and the existence or otherwise of concomitant dementia. Families harbouring *SNCA* duplications tend to either not exhibit dementia or present it much later in the disease course (Chartier-Harlin *et al.* 2004; Ibanez *et al.* 2004; Nishioka *et al.* 2006). Conversely, dementia is a regular feature in pedigrees carrying *SNCA* triplications, and can occur early in the pathogenic process (Singleton *et al.* 2003; Farrer *et al.* 2004). This phenomenon is highlighted by two kindreds where intrafamily variation in the cognitive phenotype clearly correlates with the degree of *SNCA* ploidy (Fuchs *et al.* 2007; Ikeuchi *et al.* 2008). Commentators have suggested that in these multiplication pedigrees, increased *SNCA* ploidy causes parkinsonism and dementia by directly affecting *SNCA* expression, and this hypothesis is supported by analyses of *post mortem* frontal cortex (FC) tissue obtained from these individuals (Singleton *et al.* 2003; Farrer *et al.* 2004; Miller *et al.* 2004).

Publications investigating *SNCA* expression in idiopathic Parkinson's disease (IPD) have arrived at differing and often contradictory conclusions. This is likely to have resulted from heterogeneity in many factors, including sample quality/number, methodological approach, disease stage, and brain region. An early study employing *in situ* hybridisation (ISH) showed that in IPD, *SNCA* expression is reduced in melanised substantia nigra (SN) and FC neurons (Kingsbury *et al.* 2004). Similar results were obtained using expression microarray and quantitative reverse transcriptase-polymerase chain reaction (qRT-PCR) to investigate the SN and putamen (Zhang *et al.* 2005b; Moran *et al.* 2007; Dachsel *et al.* 2007), and more recently in a microarray analysis of isolated substantia nigra pars compacta (SNpc) dopaminergic cells (Simunovic *et al.* 2009). On the other hand, qRT-PCR has also been employed to demonstrate increased *SNCA* expression in the IPD SN, both in whole tissue and isolated dopaminergic neurons (Chiba-Falek *et al.* 2006; Grundemann *et al.* 2008). Moreover, one report used qRT-PCR to specifically examine each of the four main *SNCA* transcript splice forms, which are called 140, 126, 112, and 98, based on the length of their encoded protein. This showed that all four display overexpression in the IPD FC, although greater increases were observed for the 98 and 126 species (Beyer *et al.* 2008). The potential importance of *SNCA* expression in idiopathic Parkinson's disease dementia (IPDD) is highlighted by experiments demonstrating that both neocortical LB load and overall neuropathological disease stage significantly correlate with dementia severity in IPD (Mattila *et al.* 2000; Kovari *et al.* 2003; Aarsland *et al.* 2005a; Braak *et al.* 2005).

Variation at *SNCA* genetic polymorphisms can significantly influence IPD risk. Many groups have investigated the complex dinucleotide promoter microsatellite Rep1, which resides ~10 kb upstream of the translational start. A host of publications have generated conflicting data both in support of and undermining the association of variation at Rep1 with IPD [summarised in (Lesage and Brice 2009)]. Nevertheless, two well-powered multi centre studies have provided strong evidence supporting this relationship in Caucasians. Both demonstrate that amongst the three common Rep1 alleles, IPD susceptibility is significantly increased by the largest allele and reduced

by the smallest. The largest allele also marginally but significantly decreases IPD age of onset (Maraganore *et al.* 2006; Kay *et al.* 2008). Furthermore, significant association has also been shown with haplotypes constructed of Rep1 and 5' promoter single nucleotide polymorphism (SNP) alleles (Farrer *et al.* 2001; Pals *et al.* 2004; Tan *et al.* 2004; Sutherland *et al.* 2009a). *In vitro* neuronal cell culture reporter assays and *in vivo* quantification of SNCA protein in blood both indicate that variation at Rep1 may affect IPD risk by altering the expression of this gene, as the latter phenotype appears to positively correlate with Rep1 allele length (Chiba-Falek and Nussbaum 2001; Fuchs *et al.* 2008).

Association studies examining SNPs residing in the *SNCA* locus have shown that variation at several polymorphisms and haplotypes constructed thereof significantly alters IPD susceptibility in Caucasian and Asian populations. These are concentrated in the 5' promoter, the large ~93 kb intron, the 3' untranslated region (UTR), and the 3' flanking region (Pals *et al.* 2004; Tan *et al.* 2004; Mueller *et al.* 2005; Mizuta *et al.* 2006; Winkler *et al.* 2007; Westerlund *et al.* 2008). Moreover, one of these variants, the 3' flanking SNP rs356219, interacts synergistically with *Microtubule-associated protein tau* (*MAPT*) haplotype to modify IPD risk (Goris *et al.* 2007). Two well-powered genome wide association studies (GWAS) performed in Caucasians and Asians have recently confirmed that *SNCA* is central to IPD aetiopathogenesis. These reports demonstrated highly significant associations with variation at one SNP in the 5' promoter, two in the ~93 kb intron, and one in the 3' flanking region. Two of the associations were common to both populations (Simon-Sanchez *et al.* 2009; Satake *et al.* 2009). Interestingly, variation at Rep1 and five SNPs located in the 5' promoter or haplotypes constructed thereof does not associate with dementia status in Caucasian IPD patients, but the relatively small size of this experiment may have generated a false negative (De Marco *et al.* 2008). Variation at two IPD-associated *SNCA* SNPs has been correlated with *SNCA* messenger RNA (mRNA) levels in *post mortem* brain samples. Significant effects for rs356219 were seen in the SN and cerebellum of a combined set of IPD cases and controls, but a different study failed to replicate the cerebellum result at the protein level (Fuchs *et al.* 2008; Westerlund *et*

al. 2008). Trends were observed for the intronic polymorphism rs7684318 in the IPD and control FC (Mizuta *et al.* 2006). However, whole genome studies correlating SNP genotype with cortical gene expression have not identified any variants demonstrating association with *SNCA* expression, and one of these specifically examined IPD-associated SNPs at this locus (Myers *et al.* 2007a; Simon-Sanchez *et al.* 2009).

In summary, there is evidence to suggest that increasing *SNCA* copy number correlates with a more dementia-prone FPD phenotype, and that this effect could be mediated by changes in *SNCA* expression. Furthermore, variation at polymorphisms situated in the 5' promoter and 3' terminus of *SNCA* significantly associates with IPD and may influence the expression of its mRNA.

5.2. Aims and methodology

Based on the background literature, it was hypothesised that there could be a relationship between IPD dementia status and *SNCA* mRNA expression, and that *SNCA* locus SNP variation might influence IPD risk and *SNCA* mRNA expression. Therefore, the aims of this chapter were as follows:

1. **Examine *SNCA* mRNA expression in IPD dementia and neurodegeneration.** This was accomplished by employing Sybr Green qRT-PCR to compare total and neuronal loss-corrected (NLC) *SNCA* mRNA expression in IPD cognitive series (idiopathic Parkinson's disease with dementia [IPDD]; idiopathic Parkinson's disease no dementia [IPDND]; controls) dorsolateral prefrontal cortex (DLPFC) (Brodmann area 46 [BA46]) complementary DNA (cDNA) batch 2 (see 3.2). The qRT-PCR assay was able to detect the *SNCA* 140 and 112 splice forms. Total expression data were normalised with a normalisation factor (NF) calculated from the reference genes *Glucose-6-phosphate dehydrogenase* (*G6PD*), *Ribosomal protein L13A* (*RPL13A*), and *TATA box binding protein* (*TBP*). NLC expression data were normalised with the neuronal marker *Neurofilament H* (*NEFH*) acting as reference gene (see 3.2). Statistical comparisons were carried out by Mann-Whitney test, with significance set at corrected $p \leq 0.05$ (see 2.10.2.2). DLPFC expression array data obtained from the microarray series were mined *in silico* to corroborate the results (see 4.2). Statistical comparisons were performed by Mann-Whitney test, with significance set at corrected $p \leq 0.05$ (see 2.10.6.3).
2. **Examine *SNCA* mRNA expression in multiple brain regions.** In order to further investigate its role in IPD, Sybr Green qRT-PCR was employed to measure total and NLC *SNCA* mRNA expression in medulla, putamen, amygdala, entorhinal cortex (EC [BA28]), anterior cingulate cortex (ACC [BA24]), angular gyrus (AG [BA39]), and frontal cortex (FC [BA8]) cDNA obtained from the IPD mapping series (see 3.2). The qRT-PCR assay was able to detect the 140 and 112 splice forms. Total expression data were normalised with a NF calculated from the most stable set of the following reference genes: *G6PD*, *RPL13A*, and *TBP*,

and *Hypoxanthine phosphoribosyltransferase 1* (*HPRT1*). NLC expression data were normalised with the neuronal marker *NEFH* (see 3.2). Statistical comparisons were carried out by Mann-Whitney test, with significance set at corrected $p \leq 0.05$ (see 2.10.2.2). Brain region expression data were not compared with each other statistically.

3. **Characterise the influence of *SNCA* SNP variation on IPD risk.** This aim consisted of three parts. Firstly, a case-control study evaluating genetic association with IPD was performed, by TaqMan-genotyping SNPs in genomic DNA (gDNA) samples acquired from the IPD association series (see 3.2). Haplotypes were inferred within Haploview (see 2.10.3.2). Statistical assessments of allelic and haplotypic association under a multiplicative model were carried out by χ^2 test in Haploview, with significance set at corrected $p \leq 0.05$ (see 2.10.3.2). Next, association study genotypic data was used to elucidate fine scale pairwise r^2 SNP linkage disequilibrium (LD), in order to place SNPs in a haplotypic context (see 2.10.7.1). Finally, *in silico* mining was employed to identify putative functional SNPs which might be driving association with disease. HapMap phase II Centre d'Étude du Polymorphisme Humain (CEPH) trio polymorphic SNP LD data was downloaded (release 23a from March 2008). The University of California Santa Cruz (UCSC) PhyloP database (assembly hg18 from March 2006) was mined for predicted DNA conservation across 32 placental mammals, and the literature was then mined for Caucasian and Asian IPD genetic association study data (see 2.10.7.2).

5.3. Results

5.3.1. *α-Synuclein* is not differentially-expressed in the idiopathic Parkinson's disease dorsolateral prefrontal cortex

In order to investigate possible relationships between *SNCA* and IPD dementia status, qRT-PCR was employed to measure total and NLC expression in cognitive series DLPFC cDNA batch 2 (IPDD [*n* = 15]; IPDND [*n* = 16]; control [*n* = 16]). Clinicopathological group comparisons and expression data normalisation strategies for this series and cDNA batch have been described (see 3.3.2 and 3.3.4). So as to corroborate the findings, DLPFC expression array data obtained from the microarray series (IPDD [*n* = 7]; IPDND [*n* = 7]; control [*n* = 7]) were mined *in silico*. Again, clinicopathological comparability of this series has been demonstrated (see 4.3.1). Expression in IPDD and IPDND was compared statistically, and these two groups subsequently combined to generate the IPD group. Expression in IPD (qRT-PCR *n* = 31; microarray *n* = 14) and controls (qRT-PCR *n* = 16; microarray *n* = 7) was then compared statistically.

Table 5.1 and figure 5.1 show the results of this analysis. Notable levels of intragroup variation were detected in the qRT-PCR NLC and microarray data. No significant changes were observed for qRT-PCR total, qRT-PCR NLC, or microarray *SNCA* expression. Indeed, the qRT-PCR results indicated nearly identical expression across the groups. The microarray data displayed a trend of *SNCA* underexpression in IPD contrasted against controls, but this only approached significance even before correction for multiple testing. Taken together, these findings demonstrate that *SNCA* is not differentially-expressed in the IPD DLPFC in these series. Hence, there is no evidence to support the hypothesis that there is a relationship between IPD dementia status and DLPFC *SNCA* expression.

Technique	Expression	Fold change mean *SNCA* expression/CON			Uncorrected *p* value		Corrected *p* value	
		IPDD	IPDND	IPD	IPDD vs IPDND	IPD vs CON	IPDD vs IPDND	IPD vs CON
qRT-PCR	Total	0.93	0.93	0.91	0.756	0.394	NS	NS
	NLC	0.99	0.96	0.97	0.793	0.850	NS	NS
Microarray	Total	0.70	0.78	0.74	0.655	0.052	NS	NS

Table 5.1. IPD DLPFC *SNCA* expression data.

Fold change mean qRT-PCR and microarray DLPFC *SNCA* expression values (normalised to controls) and statistical results for cognitive series cDNA batch 2 and the microarray series, respectively. No significant differences were observed in any comparison, demonstrating that *SNCA* is not differentially-expressed in the IPD DLPFC. For the qRT-PCR, total expression data were normalised with *G6PD*, *RPL13A*, and *TBP*, and NLC expression data with *NEFH*. For the microarray, statistical analyses were performed on $\log_2$ data, but raw fold change data were generated using antilog functions and presented to aid comparison. Groups were compared by Mann-Whitney test. *p* values were corrected x20. CON = control; cDNA = complementary DNA; DLPFC = dorsolateral prefrontal cortex; *G6PD = Glucose-6-phosphate dehydrogenase*; IPD = idiopathic Parkinson's disease; IPDD = idiopathic Parkinson's disease with dementia; IPDND = idiopathic Parkinson's disease no dementia; *NEFH = Neurofilament heavy polypeptide*; NLC = neuronal loss-corrected; NS = not significant; qRT-PCR = quantitative reverse transcriptase-polymerase chain reaction; *RPL13A = Ribosomal protein L13A*; *SNCA = α-Synuclein*; *TBP = TATA box binding protein*.

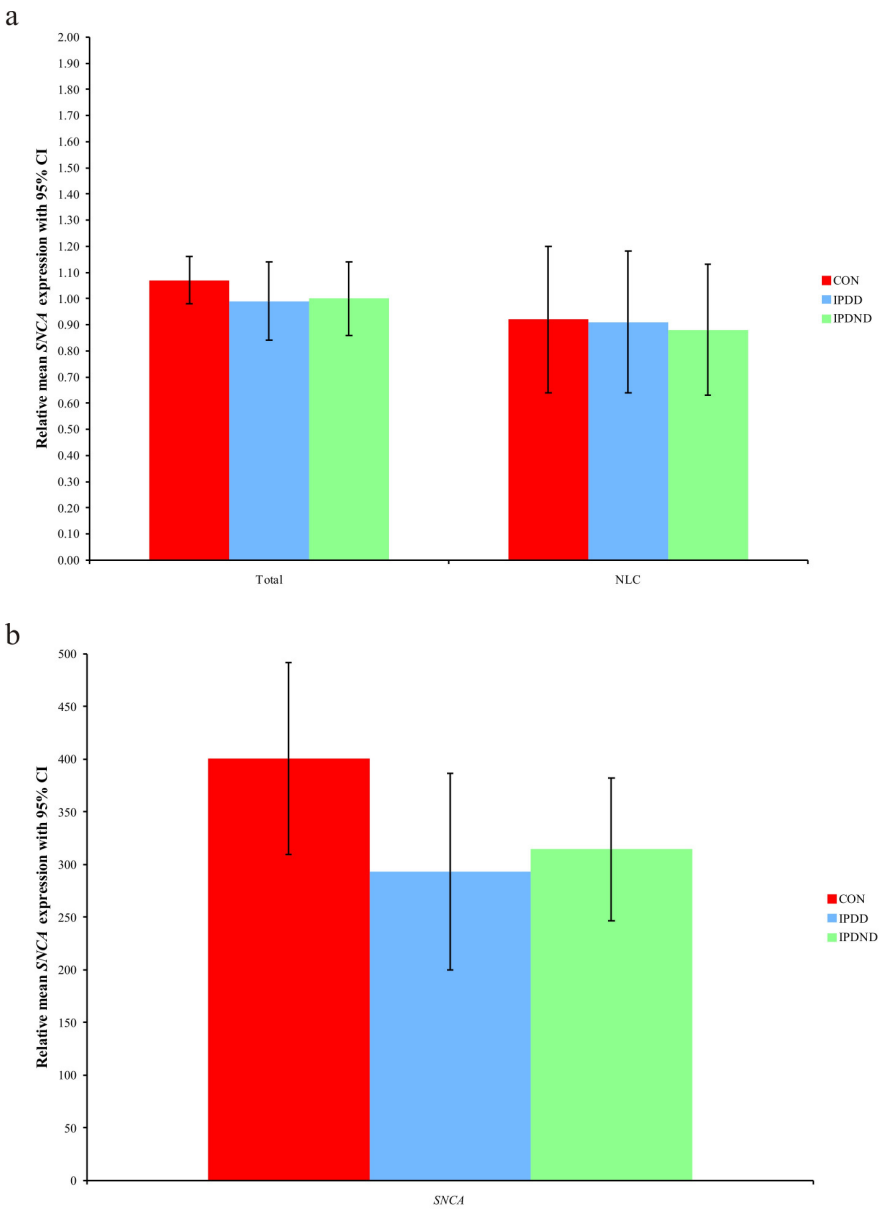

Figure 5.1. *SNCA* is not differentially-expressed in the IPD DLPFC.

Relative mean (a) qRT-PCR and (b) microarray DLPFC *SNCA* expression values with 95% CI for cognitive series cDNA batch 2 and the microarray series, respectively. No significant differences were observed in any comparison, demonstrating that *SNCA* is not differentially-expressed in the IPD DLPFC. For the qRT-PCR, total expression data were normalised with *G6PD*, *RPL13A*, and *TBP*, and NLC expression data with *NEFH*. For the microarray, statistical analyses were performed on $\log_2$ data, but raw mean and CI data were generated using antilog functions and plotted to aid comparison. Groups were compared by Mann-Whitney test. *p* values were corrected x20. CI = confidence interval; CON = control; cDNA = complementary DNA; DLPFC = dorsolateral prefrontal cortex; *G6PD* = *Glucose-6-phosphate dehydrogenase*; IPD = idiopathic Parkinson's disease; IPDD = idiopathic Parkinson's disease with dementia; IPDND = idiopathic Parkinson's disease no dementia; *NEFH* = *Neurofilament heavy polypeptide*; NLC = neuronal loss-corrected; qRT-PCR = quantitative reverse transcriptase-polymerase chain reaction; *RPL13A* = *Ribosomal protein L13A*; *SNCA* = *α-Synuclein*; *TBP* = *TATA box binding protein*.

5.3.2. *α-Synuclein* is not differentially-expressed in seven other subcortical and cortical regions of the idiopathic Parkinson's disease brain

So as to further investigate *SNCA* in the context of IPD, qRT-PCR was used measure total and NLC expression in seven subcortical and cortical brain regions obtained from the mapping series. Clinicopathological group comparisons and expression data normalisation strategies for this series have been described (see 3.3.5). Expression in IPD (n = 20) and controls (n = 20) was compared statistically.

The results of this analysis can be seen in table 5.2 and figure 5.2. Relatively high levels of intragroup variation were detected in the NLC data for several areas, notably the medulla, amygdala, AG, and FC. No significant changes were observed for total or NLC *SNCA* expression in the majority of mapping series regions. The one exception was the FC, in which NLC expression was significantly reduced in IPD contrasted against controls (corrected p = 0.015). However, total expression was unaltered, indicating a general lack of support for *SNCA* differential expression in this area. A trend of decreased NLC expression was also observed in the amygdala, but this was nonsignificant even before correction. Overall, these findings demonstrate that *SNCA* is not differentially-expressed in the mapping series. Therefore, there is little evidence to support the view that variation in *SNCA* expression is associated with IPD in any of these seven regions.

Brain region	Expression	Fold change mean *SNCA* expression (IPD/CON)	IPD vs CON *p* value	
			Uncorrected	Corrected
Medulla	Total	0.95	0.558	NS
	NLC	0.47	0.756	NS
Putamen	Total	0.88	0.411	NS
	NLC	0.75	0.214	NS
Amygdala	Total	1.02	0.346	NS
	NLC	0.58	0.081	NS
EC (BA28)	Total	0.87	0.328	NS
	NLC	0.96	0.523	NS
ACC (BA24)	Total	1.06	0.607	NS
	NLC	0.97	0.757	NS
AG (BA39)	Total	1.02	0.665	NS
	NLC	1.01	0.673	NS
FC (BA8)	Total	0.84	0.116	NS
	NLC	0.45	$7.44e^{-4}$	0.015

Table 5.2. IPD mapping series *SNCA* expression data.

Fold change mean qRT-PCR *SNCA* expression values (relative to controls) and statistical results for the mapping series. No significant differences in both total and NLC *SNCA* expression were observed in any region, demonstrating that *SNCA* is not differentially-expressed in the mapping series. Total expression data were normalised with *G6PD*, *HPRT1*, *RPL13A*, and *TBP*, except for amygdala and EC data, which were normalised with *HPRT1*, *RPL13A*, and *TBP*. NLC expression data were normalised with *NEFH*. IPD and CON groups were compared by Mann-Whitney test. *p* values were corrected x20. AG = angular gyrus (BA39); ACC = anterior cingulate cortex (BA24); BA = Brodmann area; CON = control; DLPFC = dorsolateral prefrontal cortex (BA46); EC = entorhinal cortex (BA28); FC = frontal cortex (BA8); *G6PD = Glucose-6-phosphate dehydrogenase*; *HPRT1 = Hypoxanthine phosphoribosyltransferase 1*; IPD = idiopathic Parkinson's disease; *NEFH = Neurofilament H*; NLC = neuronal-loss corrected; NS = not significant; qRT-PCR = quantitative reverse transcriptase-polymerase chain reaction; *RPL13A = Ribosomal protein L13A*; *SNCA = α-Synuclein*; *TBP = TATA box binding protein*.

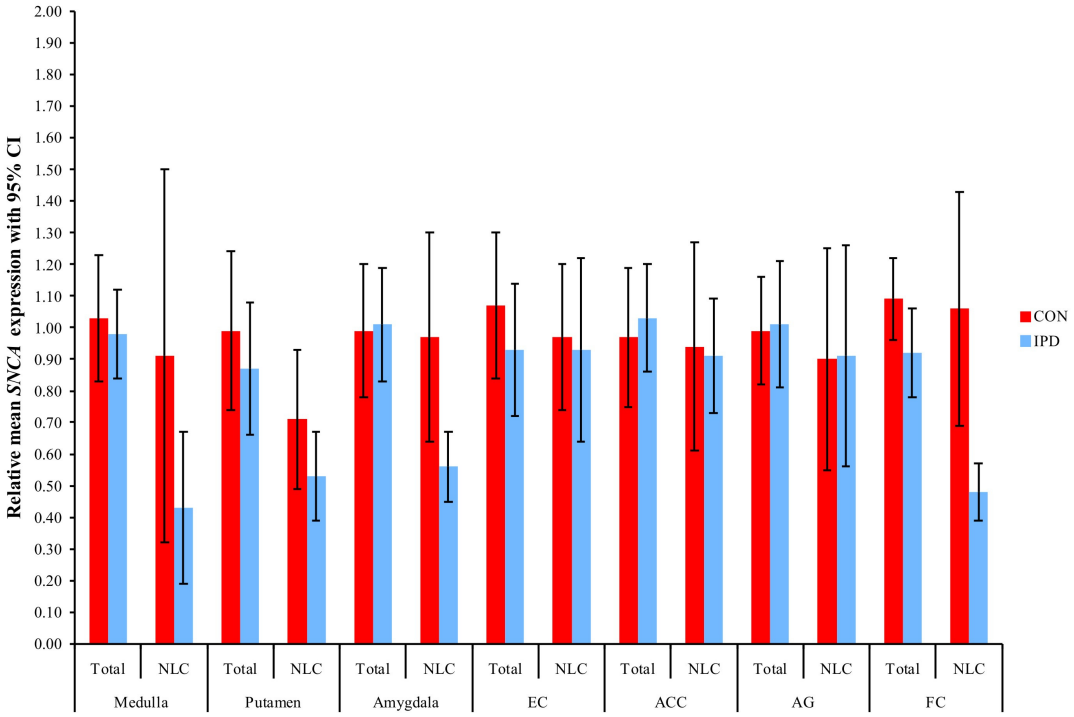

Figure 5.2. *SNCA* is not differentially-expressed in the mapping series.

Relative mean qRT-PCR *SNCA* expression values with 95% CI for the mapping series. No significant differences in both total and NLC *SNCA* expression were observed in any region, demonstrating that *SNCA* is not differentially-expressed in the mapping series. Total expression data were normalised with *G6PD*, *HPRT1*, *RPL13A*, and *TBP*, except for amygdala and EC data, which were normalised with *HPRT1*, *RPL13A*, and *TBP*. NLC expression data were normalised with *NEFH*. IPD and CON groups were compared by Mann-Whitney test. *p* values were corrected x20. AG = angular gyrus (BA39); ACC = anterior cingulate cortex (BA24); BA = Brodmann area; CI = confidence interval; CON = control; DLPFC = dorsolateral prefrontal cortex (BA46); EC = entorhinal cortex (BA28); FC = frontal cortex (BA8); *G6PD = Glucose-6-phosphate dehydrogenase*; *HPRT1 = Hypoxanthine phosphoribosyltransferase 1*; IPD = idiopathic Parkinson's disease; *NEFH = Neurofilament H*; NLC = neuronal-loss corrected; qRT-PCR = quantitative reverse transcriptase-polymerase chain reaction; *RPL13A = Ribosomal protein L13A*; *SNCA = α-Synuclein*; *TBP = TATA box binding protein*.

5.3.3. *α-Synuclein* haplotypic variation influences idiopathic Parkinson's disease risk

Multiple system atrophy (MSA) is an adult onset progressive neurological disorder characterised in most cases by autonomic dysfunction, striatonigral degeneration, and parkinsonism. Its primary neuropathological hallmark is the presence of misfolded protein aggregates within oligodendrocytes. These glial cytoplasmic inclusions (GCIs) are mainly composed of filamentous SNCA. GCIs are associated with demyelination, reactive gliosis, and neuronal loss, all of which occur selectively in the brainstem, SNpc, putamen, and cerebellum. Due to their similarities, MSA and IPD are both classified as synucleinopathies [reviewed in (Wenning *et al.* 2008)].

Based on this clinicopathological overlap, it was hypothesised that genetic variants demonstrating association with both conditions could improve our understanding of IPD. Two recent reports have identified MSA-associated SNPs. The most significant results from each study were rs11931074 and rs3822086, both of which reside in the *SNCA* locus (Scholz *et al.* 2009; Al-Chalabi *et al.* 2009). Notably, variation at these polymorphisms also associates with IPD, however the evidence for rs3822086 is less strong (Simon-Sanchez *et al.* 2009; Mueller *et al.* 2005). Nonetheless, these two markers are amongst the most promising genetic susceptibility factors common to MSA and IPD. Therefore, a case-control genetic association study was performed. Taqman was used to genotype rs3822086 and rs11931074 in gDNA extracted from the association series (IPD [n = 705]; controls [n = 572]) and haplotypes were inferred. SNP alleles and haplotypes were tested for association with IPD under a multiplicative model. Group clinical data for the association series can be seen in table 5.3. This experiment was carried out in collaboration with Coro Paisán-Ruíz from the laboratory of Dr. Andrew Singleton (National Institutes of Health). Dr. Paisán-Ruíz had previously generated the IPD case genotypic data for rs119311074.

Group (*n*)	% males	Statistic	Age of onset	Age of donation	Disease duration
CON (572)	50.7	Mean	NA	38.7	NA
		SD	NA	8.2	NA
IPD (705)	58.1	Mean	57.4	72.0	14.1
		SD	12.9	11.5	8.8

Table 5.3. IPD association series clinical data.

Group clinical metrics for the IPD association series. Due to sample availability, this series differed substantially from chapters 3 and 4 (see table 2.6). In the IPD group, 319 were brain samples and 386 were blood samples; in the CON group these counts were 94 and 478, respectively. Disease duration values for IPD blood samples were measured at a cut-off date in 2003. Measures of time are in years. CON = control; IPD = idiopathic Parkinson's disease; NA = not applicable; SD = standard deviation.

Table 5.4 shows the SNP association study results. The Hardy-Weinberg equilibrium (HWE) was not violated in the case or control groups for either polymorphism, indicating that no serious genotyping errors had occurred. Single marker allelic association with IPD was not demonstrated for variation at rs3822086 or rs11931074. On the other hand, the rare GT haplotype was significantly associated with IPD (corrected $p = 0.030$). The estimated odds ratio (OR) for this effect was 5.935, with a 95% confidence interval (CI) that ranged from 1.714 to 20.555. The case and control frequencies showed that this haplotype confers increased susceptibility to IPD.

Therefore, these findings indicate that the GT haplotype increases IPD risk in the association series. Using Alzheimer's disease (AD) genetic data, it has been demonstrated that haplotypes constructed of markers flanking but not including an associated variant can themselves display association (Fallin *et al.* 2001). Hence, our results suggest that one or more IPD-associated variants is/are being tagged by the GT haplotype and reside(s) in the sequence flanked by these two SNPs i.e. the ~25.2 kb between 90858538 and 90883817 on chromosome 4. *SNCA* is located between 90865728 and 90978489 and is transcribed from the negative strand. Placing this region of interest (ROI) in context of the *SNCA* transcript, rs3822086 lies towards the 3' end of the ~93 kb intron, and rs11931074 is situated downstream. Hence this ROI encompasses Ensembl exons 970014 and 1520237 (including the 3'UTR), the relevant intronic sequences, and ~7.2 kb of downstream sequence (see figure 5.3).

SNP identity [DNA base ambiguity]	Location on chromosome 4	HapMap CEPH MAF	*n* alleles		MAF		HWE *p* value		Estimated OR [95% CI]	χ^2 allelic *p* value	
			CON	IPD	CON	IPD	CON	IPD		Uncorrected	Corrected
rs11931074 [G/T]	90858538	0.100	1136	1126	0.084	0.097	0.446	1.000	1.174 [0.881 – 1.566]	0.274	NS
rs3822086 [C/T]	90883817	NA	1122	1392	0.078	0.088	0.630	0.917	1.138 [0.857 – 1.511]	0.372	NS
SNP haplotype			***n* haplotypes**		**Frequency**				**Estimated OR [95% CI]**	**χ^2 haplotypic *p* value**	
			CON	**IPD**	**CON**	**IPD**				**Uncorrected**	**Corrected**
GC			1142	1402	0.917	0.900			0.821 [0.627 – 1.075]	0.150	0.900
TT			1142	1402	0.080	0.082			1.024 [0.769 – 1.363]	0.877	NS
TC			1142	1402	0.003	0.011			2.966 [1.189 – 7.401]	0.020	0.120
GT			**1142**	**1402**	**0.000**	**0.007**			**5.935 [1.714 – 20.555]**	**0.005**	**0.030**

Table 5.4. *SNCA* IPD SNP association study data.

α-Synuclein IPD SNP association study data. Variation at neither SNP displayed single marker allelic association, however association was observed for the rare GT haplotype (in bold text), whereby it significantly increased IPD risk. SNP identities, CEPH DNA base ambiguities (positive strand), and CEPH MAFs were obtained from HapMap phase II (release 23a from March 2008). DNA base ambiguity shows the major allele first (single letter codes in accordance with the International Union of Biochemistry and Molecular Biology). Locations on chromosome 4 are according to NCBI assembly build 36. Haplotypes were inferred within Haploview using an accelerated EM algorithm. HWE *p* values were not corrected. χ^2 association *p* values were calculated under a multiplicative model and corrected x6. CEPH = Centre d'Étude du Polymorphisme Humain; CI = confidence interval; CON = control; EM = expectation-maximisation; HWE = Hardy-Weinberg equilibrium; IPD = idiopathic Parkinson's disease; MAF = minor allele frequency; NCBI = National Center for Biotechnology Information; NA = not applicable; NS = not significant; OR = odds ratio; SNP = single nucleotide polymorphism; *SNCA* = *α-Synuclein*.

5.3.4. The polymorphisms rs11931074, rs3822086, and rs3857059 reside on the same haplotype block

The polymorphism rs3822086 has not been genotyped as part of the HapMap project. As such, little is known about its LD relationships with SNP haplotype structure in the *SNCA* locus, in particular with rs11931074. Therefore, fine scale pairwise r^2 LD was elucidated from genotypes obtained for the association study (see 5.3.3). This was carried out using rs3822086 and rs11931074 genotypic data for the 572 controls. Subsequently, this was performed using genotypic data for 563 of the IPD cases. In addition to rs3822086 and rs11931074, this second dataset included genotypes at eight *SNCA* locus SNPs. These other variants were located in and around the *SNCA* transcribed region: one ~38 kb upstream; four in the ~93 kb intron; and three downstream, the most distant residing ~94 kb from the 3'UTR (see figure 5.3). This experiment was carried out in collaboration with Coro Paisán-Ruíz from the laboratory of Dr. Andrew Singleton. Dr. Paisán-Ruíz had previously generated the IPD case genotypic data for all SNPs except rs3822086.

Figure 5.3 shows the results. LD between rs11931074 and rs3822086 in controls was very high ($r^2 = 0.96$). In IPD cases, rs3822086 possessed fairly strong LD with rs11931074 ($r^2 = 0.77$) and rs3857059 ($r^2 = 0.78$). However, LD values between rs3822086 and the remaining seven SNPs were markedly lower ($r^2 < 0.55$ in all comparisons). These findings, especially the very strong relationship in controls, indicate that rs11931074 and rs3822086 are probably located on the same haplotype block in Caucasians. In agreement with HapMap CEPH data, the IPD results also suggest that rs3857059 belongs to this block, implying that the ROI suggested to contain one or more IPD-associated variant(s) (see 5.3.3) could be extended to include the genomic space flanked by rs3857059.

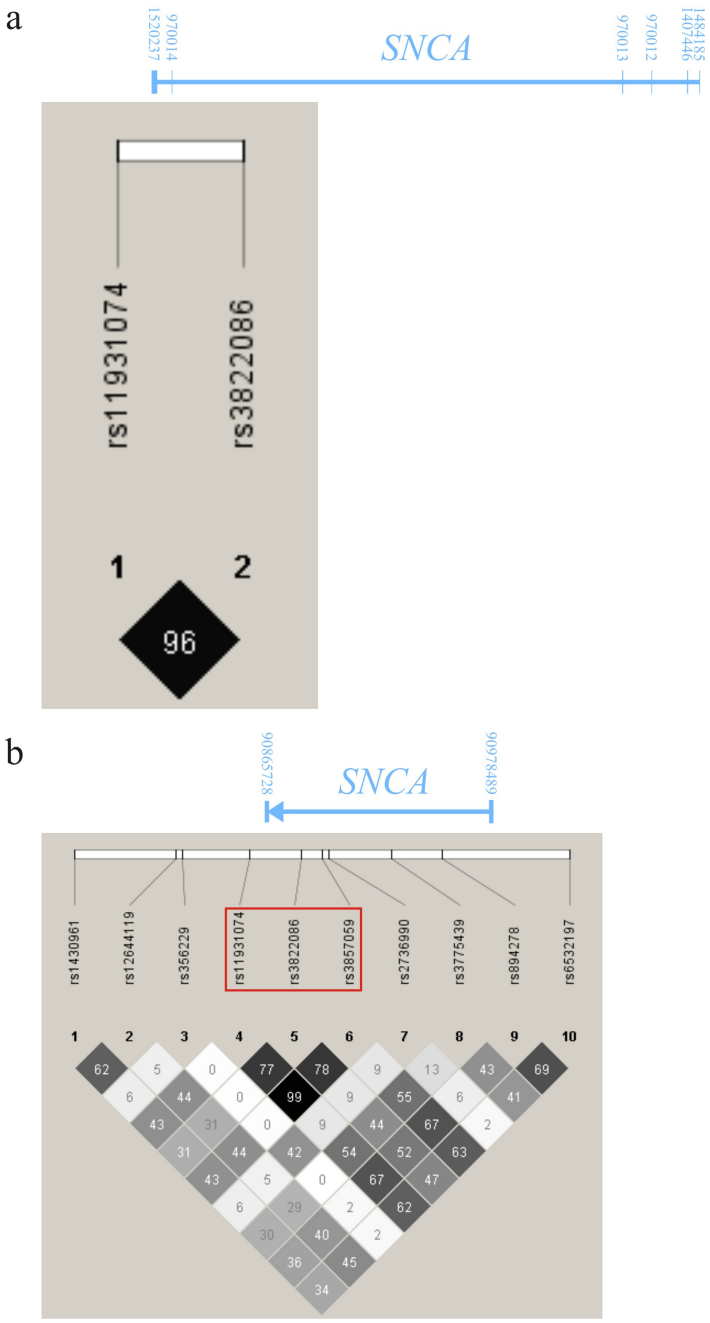

Figure 5.3. SNP LD relationships in the *SNCA* locus.

Fine scale pairwise r^2 LD plots for *SNCA* locus SNPs based on genotyping (a) 572 controls (brain [n = 94]; blood [n = 478]) and (b) 563 IPD cases (brain [n = 318]; blood [n = 245]). LD between rs11931074 and rs3822086 in controls was very high, and in IPD cases, LD between rs3822086 and both rs11931074 and rs3857059 was fairly strong, indicating that these three variants are probably situated on the same haplotype block in Caucasians (boxed in red). Pairwise LD values (out of 100) label the relevant squares. Degree of square shading denotes LD magnitude. (a) Ensembl exon identities and their relative positions along the *SNCA* transcript in relation to the white bar are indicated. (b) Boundaries of *SNCA* transcript (~113.2 kb) on chromosome 1 according to NCBI assembly build 36 in relation to the white bar are indicated. IPD = idiopathic Parkinson's disease LD = linkage disequilibrium; NCBI = National Center for Biotechnology Information; SNP = single nucleotide polymorphism; *SNCA* = *α-Synuclein*.

5.3.5. Identification of putative functional variants in the region flanked by rs11931074 and rs3857059

Linkage disequilibrium architecture in the human genome has an important consequence: it can be difficult to determine exactly which variant(s) within a haplotype block is/are driving genetic association with disease. This can be relatively clear if one of the polymorphisms is obviously functional e.g. a nonsynonymous SNP. However, associated variants often reside in introns or intergenic space. In this instance, how can one sift through a list of polymorphisms and identify the functional variant? Assessment of evolutionary DNA sequence conservation provides a reasonable handle to grasp this problem. Therefore, *in silico* mining was employed to identify putative functional variants which could underlie the haplotypic association with IPD (see 5.3.3). The SNPs rs11931074 and rs3857059 are probably situated on the same haplotype block in Caucasians (see 5.3.4), hence the aforementioned association ROI (see 5.3.3) was redefined as their entire intergenomic space i.e. 90858538 to 90894261 on chromosome 4. LD data for all polymorphic SNPs residing in this ~35.7 kb ROI was downloaded from HapMap, and UCSC PhyloP was mined for predicted mammalian DNA sequence conservation data at these SNP positions. For those variants displaying some degree of predicted conservation, the literature was then mined for IPD genetic association data (Mueller *et al.* 2005; Mizuta *et al.* 2006; Ross *et al.* 2007a; Westerlund *et al.* 2008; Winkler *et al.* 2007).

The results can be seen in table 5.5. Of the 28 SNPs situated in the ROI, only five are located at positions displaying some degree of predicted conservation. The variants rs11931074, rs3822086, and rs3857059 reside at positions predicted by PhyloP to be undergoing rapid evolution. The five aforementioned polymorphisms were: rs7436973, rs356165, rs356204, rs3857057, and rs356168. The SNP rs7436973 is situated ~3 kb downstream of the *SNCA* transcript, rs356165 is located in the 3'UTR, and the remaining three polymorphisms reside in the ~93 kb intron. IPD genetic association study data was available for rs356165, rs356204, and rs356168, but not

for rs7436973 and rs3857057. Variation at rs356165 significantly associated with IPD in four out of five cohorts examined, and an extremely low *p* value was observed in an Asian population (Mueller *et al.* 2005; Mizuta *et al.* 2006; Ross *et al.* 2007a; Westerlund *et al.* 2008; Winkler *et al.* 2007). These findings, together with its 3'UTR location which hypothetically might affect RNA stability, splicing, or microRNA (miRNA) targeting, suggest that rs356165 is an important putative functional variant. The SNP rs356204 exhibited the highest amount of predicted conservation. Furthermore, variation at this polymorphism significantly influenced IPD risk in both of the relevant studies (Mueller *et al.* 2005; Westerlund *et al.* 2008), suggesting that it is also a putative functional variant. On the other hand, variation at rs356168 failed to confidently demonstrate association with IPD (Mueller *et al.* 2005), making it unlikely to be a putative functional variant.

Taken together, these data suggest that rs356165 and rs356204 are both putative functional variants which could be driving the haplotypic association with IPD. However, their status as such is tentative at best, and still requires validation by functional assay.

Table 5.5. Identification of putative functional variants in the *SNCA* ROI.

Predicted DNA sequence conservation and IPD association study literature mining data for SNPs located in the *SNCA* ROI flanked by rs11931074 and rs3857059 (next page). Five SNPs resided at positions exhibiting some degree of predicted conservation (in bold text). Literature mining suggested that two of these variants, rs356165 and rs356204, are putative functional variants. SNP identities and CEPH LD data were obtained from HapMap phase II (release 23a from March 2008), except for rs3822086 LD data (marked with a *), which pertains to the IPD association series controls (see 5.3.4). Locations on chromosome 4 are according to NCBI assembly build 36. PhyloP conservation data were mined from UCSC (assembly hg18 from March 2006). Conservation values are –log *p* values of predicted DNA sequence conservation across 32 placental mammals under a null hypothesis of neutral evolution. Conserved sites are assigned positive scores and fast-evolving sites are assigned negative scores. Literature mining Caucasian and Asian IPD association study allelic *p* values are uncorrected. The significance threshold for each cohort is in parentheses under the first author's name (Mueller *et al.* 2005; Mizuta *et al.* 2006; Ross *et al.* 2007a; Westerlund *et al.* 2008; Winkler *et al.* 2007). For Mueller *et al.*, I and II signify replication cohorts. CEPH = Centre d'Étude du Polymorphisme Humain; chr = chromosome; IPD = idiopathic Parkinson's disease; LD = linkage disequilibrium; NCBI = National Center for Biotechnology Information; NA = not applicable; ND = not determined; ROI = region of interest; SNP = single nucleotide polymorphism; *SNCA* = *α-Synuclein*; UCSC = University of California Santa Cruz.

SNP	Position on chr 4	LD with rs11931074		Predicted conservation	Mizuta (0.0017)	Mueller I (0.00220)	Mueller II (0.00780)	Ross (0.006)	Westerlund (0.050)	Winkler (0.006)
		D'	r^2							
rs11931074	90858538	NA	NA	-0.3	NA	NA	NA	NA	NA	NA
rs356220	90860363	1	0.134	-0.3	NA	NA	NA	NA	NA	NA
rs7655792	90861048	1	1.000	-0.3	NA	NA	NA	NA	NA	NA
rs356221	90861487	1	0.119	-0.3	NA	NA	NA	NA	NA	NA
rs10003708	90862074	1	1.000	-0.3	NA	NA	NA	NA	NA	NA
rs356222	90862146	1	0.054	-0.3	NA	NA	NA	NA	NA	NA
rs168552	90862167	1	0.056	-0.3	NA	NA	NA	NA	NA	NA
rs3857051	90862720	1	0.908	-0.3	NA	NA	NA	NA	NA	NA
rs3857052	90862880	1	1.000	-0.3	NA	NA	NA	NA	NA	NA
rs7436973	**90862944**	**1**	**1.000**	**0.6**	**ND**	**ND**	**ND**	**ND**	**ND**	**ND**
rs17016071	90863304	1	1.000	-0.3	NA	NA	NA	NA	NA	NA
rs8180209	90863477	1	1.000	-0.3	NA	NA	NA	NA	NA	NA
rs8180214	90863531	1	1.000	-0.3	NA	NA	NA	NA	NA	NA
rs7675290	90864026	1	1.000	-0.3	NA	NA	NA	NA	NA	NA
rs356165	**90865909**	**1**	**0.145**	**0.6**	**$2e^{-09}$**	**0.00015**	**0.00555**	**0.023**	**ND**	**0.001**
rs10033209	90872727	1	0.915	-0.3	NA	NA	NA	NA	NA	NA
rs3775423	90876514	1	1.000	-0.3	NA	NA	NA	NA	NA	NA
rs17795208	90878515	1	0.002	-0.3	NA	NA	NA	NA	NA	NA
rs6820267	90879445	1	0.004	-0.3	NA	NA	NA	NA	NA	NA
rs356204	**90882565**	**1**	**0.119**	**1.2**	**ND**	**0.00039**	**ND**	**ND**	**0.048**	**ND**
rs7661330	90882693	1	1.000	-0.3	NA	NA	NA	NA	NA	NA
rs3822086*	90883817	1	0.964	-0.3	NA	NA	NA	NA	NA	NA
rs3775424	90884279	1	0.310	-0.3	NA	NA	NA	NA	NA	NA
rs3857057	**90887042**	**1**	**1.000**	**0.4**	**ND**	**ND**	**ND**	**ND**	**ND**	**ND**
rs356200	90887637	1	0.119	-0.3	NA	NA	NA	NA	NA	NA
rs356168	**90893454**	**1**	**0.119**	**0.8**	**ND**	**0.00031**	**0.17933**	**ND**	**ND**	**ND**
rs3756054	90893474	1	1.000	-0.3	NA	NA	NA	NA	NA	NA
rs3857059	90894261	1	1.000	-0.3	NA	NA	NA	NA	NA	NA

5.4. Discussion

In this chapter we employed qRT-PCR and *in silico* microarray mining to investigate *SNCA* expression, and demonstrated that it is not altered in the IPD DLPFC. Moreover, qRT-PCR experiments showed that variation in *SNCA* expression is not related to disease status in seven other subcortical and cortical regions of the IPD brain. IPD association analysis was carried out for two *SNCA* locus SNPs, rs11931074 and rs3822086. Single marker allelic association was not demonstrated for variation at either polymorphism, however the rare GT haplotype composed of these two SNPs significantly increased IPD risk, suggesting that this haplotype is tagging one or more IPD-associated variant(s). SNP genotype data was used to elucidate fine scale LD relationships in the *SNCA* locus. This demonstrated very high LD between rs3822086 and rs11931074 in controls, and fairly strong LD between rs3822086 and both rs11931074 and rs3857059 in IPD cases, indicating that these three polymorphisms are probably situated on the same haplotype block in Caucasians. Predicted DNA conservation and literature mining were employed to identify SNPs potentially driving the observed haplotypic association with IPD. This approach suggested that rs356165 and rs356204 are putative functional variants which could underlie said association.

No differences in DLPFC *SNCA* expression were seen when comparing IPDD with IPDND, or when contrasting IPD against controls. Therefore, our data do not support the hypothesis that there is a relationship between IPD dementia status and *SNCA* expression. Given the contrasting results in the literature, this is perhaps unsurprising. *SNCA* expression has been shown to be decreased, increased and unaltered in the IPD FC. However, none of the relevant studies specified which parts of the FC were analysed (Kingsbury *et al.* 2004; Chiba-Falek *et al.* 2006; Beyer *et al.* 2008). Two reports have done so, using microarray to demonstrate that in IPD, *SNCA* is underexpressed in BA9 and unaltered in the posterior cingulate cortex (PCC) (Zhang *et al.* 2005b; Stamper *et al.* 2008). Although no studies have quantified *SNCA* expression in BA46, the latter report goes some way to corroborating the

observed data, because this phenotype was found to be unaffected by IPD dementia status. Additional support comes from a study which failed to detect an association between IPD dementia status and variation at the microsatellite Rep1 (De Marco *et al.* 2008), which is thought to influence *SNCA* expression (Chiba-Falek and Nussbaum 2001; Fuchs *et al.* 2008). Taken together, our findings and the literature suggest that changes in *SNCA* expression are not required to maintain the IPD dementia phenotype. Furthermore, *SNCA* was not differentially-expressed in seven other brain regions. IPD *SNCA* expression data have not been published for the majority of these areas. The lack of differential expression in the amygdala reflects similar results in one report (Dachsel *et al.* 2007). However, our data disagree with two studies which showed decreased *SNCA* expression in the IPD putamen (Zhang *et al.* 2005b; Dachsel *et al.* 2007). This disparity is likely due to differences between the relevant sample series, such as genetic background, disease stage, or medication regime. We cannot exclude the possibility that the *SNCA* 126 or 98 splice forms exhibit differential expression in the cognitive or mapping series.

Variation at rs11931074 and rs3822086 both failed to demonstrate single marker association with IPD. This is contrary to the strong rs11931074 association detected by a recent IPD GWAS (Simon-Sanchez *et al.* 2009). Simply comparing allelic frequencies in the two studies shows that differences in statistical power almost certainly explain this disparity. Their MAFs (control = 0.07; case = 0.10) were not dissimilar to ours (control = 0.08; case = 0.10), however the 1713 cases and 3978 controls analysed by Simon-Sanchez *et al.* afforded sufficient power to demonstrate association for this modest genetic effect. This conclusion is borne out by *post hoc* calculations showing that our sample size provided 80% power to detect an effect of OR $\approx$ 1.57 with the observed control MAF at a significance of corrected $p \leq 0.05$ (disease prevalence = 0.01), which implies that this experiment lacked the necessary power. The data for rs3822086 also differ from published work indicating an association with IPD, albeit one that didn't survive correction for multiple testing (Mueller *et al.* 2005). Although our two studies analysed similar numbers, Mueller *et al.* probably observed association because their control MAF (0.06) was lower than

ours (0.08). This discrepancy could have arisen from ancestral differences in the genetic structure of these two control populations. Due to the lack of *SNCA* differential expression (see above), it would have been redundant to undertake *cis*-acting variation analyses for these polymorphisms. This negated our ability to evaluate the hypothesis that *SNCA* locus SNP variation might influence *SNCA* expression.

On the other hand, the results shown here demonstrated that the rare GT haplotype constructed of these two markers does significantly increase IPD risk. Given the lack of single marker association for each polymorphism, this suggests that the haplotype is tagging one or more IPD-associated variant(s) in this population (see below). To begin to explore this possibility, pairwise LD between rs3822086 and other *SNCA* locus SNPs was elucidated. The data indicated that rs3822086, rs11931074, and rs3857059 are probably situated on the same haplotype block in Caucasians. This finding is an important one, because it suggests that the reported associations of variation at rs3822086 and rs11931074 with IPD are not independent (Mueller *et al.* 2005; Simon-Sanchez *et al.* 2009), but in fact arise from the same genetic risk factor i.e. these polymorphisms are tagging each other. This conclusion might also extend to the published associations between variation at these two SNPs and MSA (Al-Chalabi *et al.* 2009; Scholz *et al.* 2009), although confirmation would require clarifying their LD relationship in MSA cases. Our results are broadly corroborated by several studies showing that haplotypes encompassing the ~93 kb intron, the 3' transcribed region, and the 3' downstream region of *SNCA* demonstrate significant association with IPD (Mueller *et al.* 2005; Mizuta *et al.* 2006; Simon-Sanchez *et al.* 2009).

In silico mining suggested that rs356165 and rs356204 are putative functional variants which might be driving the haplotypic association with IPD. Despite their relatively low r^2 LD with rs11931074, this conclusion is supported by the fact that polymorphisms both possess strong *D'* LD with the latter SNP. Due to stronger associations in the literature and the potential for direct influence on *SNCA* transcript

quantity, translational efficiency, or splicing, it is reasonable to infer that the 3'UTR variant rs356165 is the more likely candidate of the two (Mueller *et al.* 2005; Mizuta *et al.* 2006). The miRBase online database was consulted for potential miRNA binding at this site, but unfortunately the relevant sequence is excluded (Griffiths-Jones *et al.* 2008). Nevertheless, it is quite possible that rs356204 is also involved. For example, this polymorphism could be situated in an as yet undefined region which regulates *SNCA* transcription and/or splicing. It is important to mention that these results only suggest putative functionality for rs356165 and rs356204. Functional assays are still required to validate them as true functional candidates. Moreover, the incomplete nature of the HapMap dataset necessarily means that some putative functional SNPs may have been missed by this approach. Furthermore, the true functional variant(s) might belong to a different class of polymorphism e.g. microsatellites. Nonetheless, these data demonstrate the utility of DNA conservation mining for identifying putative functional variants potentially mediating genetic association, particularly if the relevant ROI is intronic and functional prediction is difficult.

In conclusion, it was demonstrated that *SNCA* is not differentially-expressed in eight cortical and subcortical regions of the IPD brain, and that DLPFC *SNCA* expression is not related to IPD dementia status. Furthermore, it was shown that a rare two-marker haplotype in the *SNCA* locus significantly increases IPD risk, and that two SNPs independently reported to influence susceptibility to both IPD and MSA are probably situated on the same haplotype block in Caucasians. Finally, *in silico* mining successfully identified two putative functional variants which might be driving the observed haplotypic association with IPD.

Chapter 6: Discussion

6.1. Introduction and overall experimental rationale

Dementia is a regular feature of Parkinson's disease (PD) (Aarsland *et al.* 2005b; Buter *et al.* 2008; Hely *et al.* 2008). Parkinson's disease dementia (PDD) is a progressive syndrome characterised by neuropsychological deficits affecting working memory (WM), attention, conceptualisation, verbal fluency, visuospatial abilities, and declarative memory (Girotti *et al.* 1988; Litvan *et al.* 1991; Pillon *et al.* 1993; Bohnen *et al.* 2006). Studies have demonstrated that many genes harbour changes which cause and influence susceptibility to familial and idiopathic Parkinson's disease (IPD), respectively [for example (Polymeropoulos *et al.* 1997; Kitada *et al.* 1998; Bonifati *et al.* 2003; Singleton *et al.* 2003; Aharon-Peretz *et al.* 2004; Huang *et al.* 2004; Paisan-Ruiz *et al.* 2004; Valente *et al.* 2004; Healy *et al.* 2008; Simon-Sanchez *et al.* 2009)]. Moreover, a host of reports have shown that numerous genes exhibit differential expression or alternative splicing in the IPD brain [for example (Hauser *et al.* 2005; Zhang *et al.* 2005b; Moran *et al.* 2006; Cantuti-Castelvetri *et al.* 2007; Beyer *et al.* 2008; Tobin *et al.* 2008; Bossers *et al.* 2009; Kumaran *et al.* 2009; Simunovic *et al.* 2009)]. On the other hand, mutation and association analyses have implicated just a handful of genes in familial and idiopathic Parkinson's disease dementia (IPDD) (Ohtake *et al.* 2004; Zarranz *et al.* 2004; de Lau *et al.* 2005; Healy *et al.* 2008; Ross *et al.* 2008a; Sidransky *et al.* 2009; Williams-Gray *et al.* 2009a). Furthermore, studies quantifying gene expression in the IPDD brain have identified numerous dysregulated genes, however the literature contains only two such reports (Bychkov *et al.* 2008; Stamper *et al.* 2008). Despite these findings, the genetic and molecular factors driving IPDD aetiopathogenesis remain largely unexplored.

Therefore, the principal aims of this thesis were to identify and characterise genes implicated in IPD dementia and/or neurodegeneration. Quantifying and comparing

gene expression was the first step in this methodology. IPD is a complex dynamic disorder, underpinned by numerous overlapping and/or interacting processes mediating its initiation and progression, many of which involve dysregulated gene expression [reviewed in (Sulzer 2007; Ferrer 2009)]. In addition, it likely that some of these disease effects are linear and some are circular [reviewed in (Hirsch and Hunot 2009; Ferrer 2009)]. Hence, evaluating intergroup differential expression constituted a versatile approach with the potential to uncover genes involved at any point within these various pathogenic stages. Moreover, the three group design (IPD dementia, IPD no dementia [IPDND], and controls) allowed us to identify genes implicated in either disease subtype i.e. IPD dementia or IPD neurodegeneration. A very similar design was employed in a recent expression microarray study of IPDD (Stamper *et al.* 2008).

Gene expression was measured using hypothesis-driven quantitative reverse transcriptase-polymerase chain reaction (qRT-PCR) and hypothesis-free expression microarray. These complementary techniques enabled validation of observed gene dysregulation events. The qRT-PCR findings were strengthened by the use of a standard curve on every plate, and by measuring each standard curve dilution and sample in triplicate. Neuronal cell death and gliosis in IPD have the potential to generate artefactual expression data. In order to control for neuronal loss and/or gliosis in IPD samples and for technical variation, total qRT-PCR expression data were normalised using a normalisation factor (NF) calculated from multiple reference genes. This strategy is more effective than a single reference gene (Vandesompele *et al.* 2002; Szabo *et al.* 2004).

As an alternative approach to control for neuronal cell death, neuronal loss-corrected (NLC) qRT-PCR expression data were normalised with the neuronal marker *Neurofilament H* (*NEFH*) acting as reference gene [for example (Fuchs *et al.* 2008)]. Neuron-specific expression has been demonstrated for *NEFH* in the human and murine brain (Goldstein *et al.* 1983; Schulz *et al.* 2003; Lariviere and Julien 2004; Cahoy *et al.* 2008). Normalisation with this marker was an alternative but most likely

incomplete attempt to control for neuronal loss in IPD. It is important to note that the concept of NLC expression remains unverified in the *post mortem* qRT-PCR literature, and that compared to normalisation with multiple reference genes, normalisation with one neuronal marker probably generates data less robust to variation in tissue composition and experimental procedure. Critically, the NLC data did not equate to neuron-specific expression. Indeed, the use of whole tissue extracts meant that neither qRT-PCR nor microarray were able to scrutinise cell type-specific expression. Therefore, we were unable determine the relative contributions of neuronal and glial expression to any observed gene dysregulation event.

Subsequently, characterisation of implicated target genes was carried out. The regional specificity of previous effects was gauged by employing qRT-PCR to evaluate differential expression in additional cortical and subcortical brain regions. These were chosen because of their vulnerability to Lewy pathology (LP) in IPD (Braak *et al.* 2003). For these mapping experiments, normalisation of total expression was strengthened by utilising geNorm on a region-by-region basis to select the most stable set from four different reference genes (Vandesompele *et al.* 2002). Single nucleotide polymorphism (SNP) association and *cis*-acting variation analyses were then undertaken. HapMap data was generally employed to select SNPs which captured the vast majority of SNP variation in the relevant loci. These genetic experiments allowed us to determine whether target gene SNP variation plays a primary role in disease aetiology, and whether the relevant mechanisms involve gene dysregulation. Moreover, positive results in these analyses could enrich the initial differential expression findings, by providing further evidence to connect target genes with disease. Because the expression data failed to confirm any gene as specifically implicated in IPD dementia (see 3.3.3, 4.3.5, and 5.3.1), the expression mapping and genetic association experiments did not evaluate correlates of this IPD subtype. *In silico* data mining of the expression microarray and other bioinformatic resources was carried out. For the most part, these approaches utilised the array data to evaluate specific hypotheses concerning gene expression in the IPD brain. In one instance,

predicted DNA conservation and IPD association data were mined to identify putative functional SNPs.

Potential sources of bias in the genetic association analysis were minimised. About half of the IPD cases samples were pathologically-proven. The influences of population stratification and phenotyping errors were reduced by analysing only Caucasian individuals and ensuring accurate diagnoses, respectively. Hardy-Weinberg equilibrium calculation was employed to control against genotyping errors. Statistical confidence was achieved by using the relatively severe Bonferroni approach to correct for multiple testing. The *cis*-acting variation analysis had several weaknesses. In order to obtain sufficient statistical power, it was necessary to analyse cases and controls together. Furthermore, this approach was unable to control for interindividual differences in *trans*-acting effects caused by sample preparation, messenger ribonucleic acid (mRNA) quality, or the environment.

In order to reduce the chance of statistical false positives, correction for multiple testing was employed throughout this thesis. We mostly used the Bonferroni approach, although family-wise error (FWE) and the less severe false discovery rate (FDR) were selected for the genotypic voxel-based morphometry (VBM) and expression microarray analyses, respectively [reviewed in (Shaffer 1995)]. In addition, the *in silico* microarray mining results were uncorrected due to prior hypothesis (Rothman 1990). The overall Bonferroni strategy was to correct within each experimental type on a chapter-by-chapter basis e.g. correcting across all the qRT-PCR statistical tests in chapter 3 (i.e. IPD cognitive expression analysis, *DUSP6* full length [FL] and 1:3 expression analysis, *DUSP6* expression mapping analysis, *DUSP6 cis*-acting variation analysis) generated a correction factor of 45.

6.2. Principal findings

We employed qRT-PCR and *in silico* mining of microarray data to demonstrate that *Dual specificity phosphatase 6* (*DUSP6*) is significantly underexpressed in the IPD dorsolateral prefrontal cortex (DLPFC) (Brodmann area 46 [BA46]). However, variation in DLPFC *DUSP6* expression did not associate with IPD dementia. Combined qRT-PCR, *in silico* microarray mining, and methyl-specific polymerase chain reaction (MSP) analyses indicated that the observed underexpression is not an artefact of modulated splicing, and is unlikely to result from differential expression of a predicted regulatory transcription factor (TF), but may in part be caused by increased CpG methylation at an E Twenty-Six (ETS) family binding site upstream of *DUSP6*. Further qRT-PCR experiments showed that *DUSP6* FL is not differentially-expressed in seven other subcortical and cortical regions of the IPD brain. DNA sequencing of *DUSP6* identified the +460G>C point mutation in the 5'untranslated region (UTR) of one familial Parkinson's disease (FPD) patient, but we were unable to evaluate whether this alteration segregates with disease. Genetic association analysis of 95% of common SNP variation in the *DUSP6* locus indicated that the rs1689408 minor allele marginally lowers IPD susceptibility by trend of borderline significance. Moreover, genotypic VBM demonstrated that normal rs1689408 heterozygotes possess significantly higher grey matter density in several brain regions, including the subgenual anterior cingulate cortex (ACC), lateral orbitofrontal cortex (OFC), medial entorhinal cortex (EC), hippocampus, amygdala, insular cortex, DLPFC, frontal cortex (FC), and caudate. *Cis*-acting variation analysis indicated that variation at rs1689408 does not influence *DUSP6* FL expression *per se*, but did detect a trend whereby DLPFC *DUSP6* FL/1:3 splice form ratios are relatively higher in rs1689408 heterozygotes.

Microarray and qRT-PCR analyses showed that *Ephrin receptor A2* (*EPHA2*) is significantly overexpressed in the IPD DLPFC (BA46). However, association between variation in DLPFC *EPHA2* expression and IPD dementia was not confirmed. *In silico* microarray mining suggested that the observed effect might

result from constitutive activation of an EPHA2-Extraceullular-signal regulated kinase 1/2 (ERK1/2)-ETS-like kinase 1 (ELK1)-*EPHA2* positive feedback loop. Additional qRT-PCR experiments demonstrated that *EPHA2* is not differentially-expressed in seven other subcortical and cortical regions of the IPD brain. Genetic association analysis of 95% of common SNP variation in the *EPHA2* locus indicated that the rs11260822 minor allele significantly increases IPD risk. However, variation at this SNP did not influence DLPFC *EPHA2* expression.

In silico microarray mining and qRT-PCR demonstrated that *α-Synuclein* (*SNCA*) is not differentially-expressed in the IPD DLPFC (BA46). Moreover, variation in DLPFC *SNCA* expression did not associate with IPD dementia. Further qRT-PCR experiments showed that *SNCA* is not differentially-expressed in seven other subcortical and cortical regions of the IPD brain. Single marker *SNCA* locus SNP association analysis indicated that variation at rs11931074 or rs3822086 does not associate with IPD. However, the rare GT haplotype composed of these two SNPs significantly increased IPD susceptibility, suggesting that this haplotype is tagging one or more IPD-associated variant(s). Elucidation of fine scale SNP linkage disequilibrium (LD) in the *SNCA* locus indicated that rs11931074, rs3822086, and rs3857059 are probably situated on the same haplotype block in Caucasians. Predicted DNA conservation and literature mining suggested that rs356165 and rs356204 are putative functional variants which might be driving the observed haplotypic association with IPD.

The cognitive expression qRT-PCR study found that variation in the DLPFC (BA46) and angular gyrus (AG) (BA39) expression of 10 target genes does not associate with IPDD. However, significant positive correlation was observed between cerebellar *post mortem* brain pH and mini mental state examination (MMSE) score in IPD patients. Subsequently, we performed expression microarray to investigate DLPFC (BA46) differential gene expression and alternative exon splicing IPD dementia and neurodegeneration. These analyses suggested that mitochondrial/metal binding, axonal guidance/cytoskeletal, synaptic transmission/ion transport, lipoprotein

metabolism, inflammation/immune response, cell adhesion/extracellular matrix, and transcription/splicing pathways are dysregulated in IPD dementia. They also suggested that synaptic transmission/ion transport, glycosylation/protein degradation, inflammation/immune response, and transcription/translation pathways are dysregulated in IPD neurodegeneration. However, these changes were only significant before correction for multiple testing. FDR-corrected array data indicated an overall lack of gene dysregulation in the IPD DLPFC. Indeed, *in silico* microarray mining suggested that variation in the DLPFC expression of genes involved in PD and parkinsonism-dementia is not associated with IPD neurodegeneration and dementia, respectively, and that the unfolded protein response (UPR) pathway is not chronically-activated in the IPD DLPFC.

6.3. The role of *Dual specificity phosphatase 6* in brain structure and idiopathic Parkinson's disease pathogenesis

Dual specificity phosphatase 6 is expressed throughout the human body, but most extensively in myeloid, bronchial epithelial, and lung cells. Expression of this gene is approximately equivalent across different brain regions, although levels are moderately higher in the amygdala, occipital cortex, and cingulate cortex (Su *et al.* 2004). The DUSP6 protein (also known as Mitogen-activated protein kinase phosphatase 3 [MKP3]) is also broadly expressed in human tissues, but is most abundant in cortical neurons and bronchial epithelial cells (Berglund *et al.* 2008). Early cell culture experiments established that DUSP6 selectively inhibits ERK1/2-mediated transcription by dephosphorylating and anchoring it in the cytoplasm (Muda *et al.* 1996; Brunet *et al.* 1999). Moreover, ERK1/2-DUSP6 binding is required for the catalytic activation of DUSP6, and ERK1/2-mediated phosphorylation of DUSP6

promotes its degradation via the ubiquitin-proteasome system (UPS) (Camps *et al.* 1998; Marchetti *et al.* 2005).

In vivo studies of *Xenopus*, zebrafish, chicken, and mouse embryos have crystallised our understanding of the delicate interplay between these two proteins. They demonstrated that Erk1/2 acts downstream of Fibroblast growth factor (Fgf) to induce *Dusp6* expression, and that Dusp6 protein inhibits Erk1/2 activity, resulting in a negative feedback loop which regulates Erk1/2 signaling. These data indicate that this pathway plays a critical role in limb and nervous tissue development, notably in the anterior forebrain and isthmic organising centre; the latter controls patterning of the neural tube into midbrain and hindbrain (Gomez *et al.* 2005; Tsang *et al.* 2004; Eblaghie *et al.* 2003; Echevarria *et al.* 2005; Smith *et al.* 2006a). Further support for this conclusion has come from observations of *Dusp6*$^{-/-}$ mice, whose phenotype is variably penetrant dominant postnatal lethality, skeletal dwarfism, craniostynostosis (premature fusion of the cranial sutures), and hearing loss. However, the incomplete penetrance suggests some degree of redundancy between Dusp6 and other negative regulators of Fgf signaling (Li *et al.* 2007).

Pancreatic and ovarian cancer tissues exhibit DUSP6 protein underexpression, consistent with the well-established view that increased ERK1/2 signaling enhances cellular proliferation during tumourigenesis (Furukawa *et al.* 2003; Chan *et al.* 2008). Nevertheless, a growing body of evidence suggests that ERK1/2 can promote oxidative neuronal cell death *in vivo*. This may be of particular relevance in neurodegenerative diseases characterised by increased levels of oxidative stress, such as IPD, where this kinase thought to be chronically-activated. One emergent theme is that ERK1/2 subcellular localisation could be vitally important in mediating between the different outcomes of phasic versus chronic ERK1/2 activation [reviewed in (Colucci-D'Amato *et al.* 2003; Chu *et al.* 2004)].

Cytoplasmic aggregates of phosphorylated ERK1/2 are detected *post mortem* in autophagosomes and abnormal mitochondria in IPD and dementia with Lewy bodies

(DLB) substantia nigra (SN) neurons (Zhu *et al.* 2002; Zhu *et al.* 2003). Moreover, neuronal cell models show that oxidative stress resulting from treatment with 1-methyl-4-phenyl-1,2,3,6-tetrahydropyridine and 6-hydroxydopamine induces ERK1/2 activation and cytoplasmic aggregation concomitant with macroautophagy and cell death. These downstream effects are significantly ameliorated by ERK1/2 inhibition, and can be recapitulated in unstressed cells by overexpression of constitutively active ERK2 (Zhu *et al.* 2002; Zhu *et al.* 2007; Dagda *et al.* 2008). DUSP6 phosphatase activity is reversibly inhibited by oxidative stress *in vitro* (Seth and Rudolph 2006). Glu-induced ERK1/2-dependent oxidative toxicity in primary cortical cells is blocked by transient overexpression of either wild type or catalytically inactive *DUSP6*, implying that activated ERK1/2 requires nuclear localisation to elicit cell death in this system (Levinthal and DeFranco 2005). Furthermore, it was recently shown that transient *DUSP6* transfection reduces Glu-induced ERK1/2-dependent apoptosis in astrocytes (Szydlowska *et al.* 2010). Interestingly, *DUSP6* dysregulation has been observed in neurological illness. This gene is significantly underexpressed in the DLPFC and ACC of bipolar disease patients compared to controls (Vawter *et al.* 2006). Overall, these published findings indicate that DUSP6-mediated inhibition of ERK1/2 regulates neural development and might influence stress-induced cell death in the IPD brain.

Underexpression of *DUSP6* was demonstrated in the IPD DLPFC using qRT-PCR and validated by *in silico* mining of the microarray data (see figure 3.6, figure 3.9, and table 4.8). Significant underexpression of total *DUSP6* FL and 1:3 was shown by qRT-PCR in two batches of complementary DNA (cDNA) (see figure 3.9), indicating that this result was not an artefact caused by modulated splicing. Similar but nonsignificant changes were seen when using the alternative qRT-PCR normalisation approach i.e. the NLC data (see figure 3.9). The lack of significance suggests that neuronal cell death may partially account for the observed effect. However, this is unlikely because total *DUSP6* FL expression values for IPDD and IPDND were very similar (see figure 3.4), despite the greater atrophy of BA46 reported in IPDD compared to IPDND (Burton *et al.* 2004; Nagano-Saito *et al.* 2005). Additional qRT-

PCR experiments demonstrated that *DUSP6* FL is not differentially-expressed in seven other subcortical and cortical regions of the IPD brain (see figure 3.10), which suggests that *DUSP6* underexpression is restricted to the DLPFC.

We employed various approaches to elucidate the mechanism driving *DUSP6* underexpression in the IPD DLPFC. Genetic association analysis of 95% of common SNP variation in the *DUSP6* locus suggested that variation at rs1689408 alone might modify IPD risk (see table 3.10) (see below). *Cis*-acting variation analysis indicated that that variation at rs1689408 does not influence *DUSP6* FL expression *per se* (see figure 3.15). Therefore, the observed underexpression phenomenon is unlikely to have a primary genetic aetiology and is probably a secondary effect of IPD pathogenesis. One important caveat is that variation in a different polymorphic class (e.g. microsatellites or copy number variation) might be responsible. *In silico* microarray mining and qRT-PCR indicated that TFs predicted to bind the *DUSP6* putative promoter (DPP) are themselves not underexpressed in the IPD DLPFC (see table 4.11 and figure 4.10). These findings suggest that DLPFC *DUSP6* underexpression does not result from differential expression of a regulatory TF. The DPP was identified as the upstream region exhibiting relatively high levels of predicted DNA sequence conservation across 32 placental mammals, and the Transfac database was queried to identify predicted TF binding sites in this region. Obvious weaknesses were that the DPP identification approach or the incompleteness of Transfac may have excluded critical regulatory sequences or regulatory TFs, respectively. The DPP encompasses the region found to control Fgf-induced murine *Dusp6* expression *in vivo*, and the orthologous human sequence contains an ETS binding site which regulates reporter gene expression in cell models (Ekerot *et al.* 2008; Zhang *et al.* 2009). However, human *DUSP6* intron 1-2 was recently shown to induce transcriptional activity which is sensitive to mutation of a resident ETS binding site (Furukawa *et al.* 2008). MSP analysis showed that relative CpG methylation at the aforementioned DPP ETS site was marginally increased in the IPD DLPFC (see figure 4.12). Because relative CpG methylation in all of the IPD cases was not higher than in all of the controls, this result suggests that increased CpG

methylation at this ETS site might account for some, but not all, of the *DUSP6* underexpression effect. In order to fully investigate the importance of differential CpG methylation at the DPP ETS site, this MSP experiment would need to be repeated using a larger number of samples.

The mechanism which mediates the observed changes in *DUSP6* expression still remains unclear. Nevertheless when viewed together, these findings and the background literature (see above) suggest that *DUSP6* underexpression could synergise with oxidative inhibition of the DUSP6 enzyme, resulting in enhanced stress-induced ERK1/2 activity which might contribute to neuronal cell death in the IPD DLPFC. This conclusion is supported by the recent demonstration that primary cortical neurons treated with the DNA-damaging agent cisplatin exhibit *Dusp6* underexpression and reduced Erk1/2 dephosphorylation (Gozdz *et al.* 2008). Moreover, increased ERK1/2 activity would be expected to induce *DUSP6* expression. Therefore, increased CpG methylation at multiple *DUSP6* regulatory sequences resulting in decreased TF binding represents a plausible mechanism to explain *DUSP6* underexpression under the spectre of chronic ERK1/2 activation. The literature and our experimental evidence suggest that the ETS binding sites in the DPP and intron 1-2 could be the regulatory sequences in question.

Due to the lack of available relatives, we were unable to assess segregation with FPD for the +460G>C point mutation identified during *DUSP6* DNA sequencing (see table 3.8). The overall lack of results suggests that *DUSP6* mutation is unlikely to be a significant cause of FPD. All identified deviations from the reference sequence were confirmed by a total of two sequencing reactions in both 5' and 3' directions. Nevertheless, confidence in the above conclusion would require the sequencing of many more FPD individuals. Genetic association analysis of 95% of common SNP variation in the *DUSP6* locus indicated that the rs1689408 minor allele marginally lowers IPD susceptibility by trend of borderline significance (see table 3.10). However, the findings failed to survive correction, which casts some doubt over the validity and strength of the observed effect, and indicates the need for replication in a

larger population. Although there have been no reports of association between *DUSP6* genetic variation and IPD, variation at the Leu114Val polymorphism (rs2279574) does influence the risk of bipolar disease in female Koreans (Lee *et al.* 2006b).

Genotypic VBM demonstrated that variation at rs1689408 has a profound effect on human brain structure, in that normal heterozygotes possess significantly higher grey matter density in several cortical and subcortical regions (see tables 3.12 and 3.13). These results were strengthened by the use of the relatively severe FWE correction approach, and the fact that several areas demonstrated association in both the region of interest (ROI) and global analyses. According to HapMap, rs1689408 is in perfect LD with rs808820 in Caucasians. This SNP resides just 24 bp upstream of the start of *DUSP6* exon 2, and so might influence *DUSP6* splicing. *Cis*-acting variation analysis detected a trend whereby DLPFC *DUSP6* FL/1:3 splice form ratios are relatively higher in rs1689408 heterozygotes (see figure 3.15). The IPD *post mortem* qRT-PCR literature shows that relative splice form ratios have been calculated in this way [for example (Tobin *et al.* 2008)]. Moreover, the effect was seen in both the total and NLC data. The weakness of these results was that they did not survive correction. This suggests a relatively small effect which requires confirmation with a larger sample size, and importantly, that this effect is most likely distinct from the IPD *DUSP6* underexpression described above.

Collectively, these data for rs1689408 build a fascinating picture. Compared to homozygotes, heterozygotes possess higher grey matter density in several regions, seem to have marginally lower susceptibility to IPD, and appear to exhibit a *DUSP6* splicing profile which is shifted towards the FL splice form. It is tempting to speculate that a common mechanism accounts for the effects on brain structure and IPD risk. Chronically-modulated *DUSP6* splicing is a logical candidate, as alterations to this process are likely to have functional implications. The protein isoform encoded by *DUSP6* 1:3 lacks its nuclear export sequence, and hence would be primarily localised in the nucleus, as well as its secondary kinase interaction motif,

suggesting impaired ERK1/2 binding (see figure 3.7). This isoform also lacks three of the five phosphatase domains present in the FL splice form, and so would be predicted to possess decreased catalytic activity (see figure 3.7) (Karlsson *et al.* 2004; Zhou *et al.* 2001). Thus overall, the isoform encoded by *DUSP6* 1:3 is expected to have relatively reduced abilities to dephosphorylate ERK1/2 and anchor it in the cytoplasm. Therefore, a chronic increase in FL/1:3 ratio might furnish the brain with some degree of protection against oxidative stress-induced cell death. Over time, the cumulative decrease in cell death could result in higher grey matter density and lower susceptibility to IPD. This conclusion is supported by the VBM data showing that rs1689408 heterozygotes possess higher grey matter density in several regions that acquire LP during IPD pathogenesis, such as the caudate, amygdala, hippocampus, medial EC, and subgenual ACC (Braak *et al.* 2003). In addition, this model fits nicely with modern thinking on neuronal cell number and the multiple hit hypothesis of IPD pathogenesis [reviewed in (Weidong *et al.* 2009)].

Dual specificity phosphatase 6 research might be pursued in several future directions. Laser capture microdissection (LCM) could be employed to identify the cell type(s) responsible for *DUSP6* underexpression in the IPD DLPFC [for example (Simunovic *et al.* 2009)]. This approach would have the added advantage of being able to fully control for neuronal loss and/or gliosis. However, even LCM cannot distinguish between primary causes and secondary and effects of pathogenesis. Limited tissue availability and lack of the relevant equipment precluded the use of LCM for the experiments described in this thesis. LCM would also enable the precise investigation of DUSP6 protein expression and ERK1/2 phosphorylation in the IPD brain. We attempted protein extraction from DLPFC brain tissue followed by western blotting for DUSP6 and phosphorylated ERK1/2, but were unable to detect either molecule. Enhanced ERK1/2 activity in this region may have upregulated DUSP6 ubiquitination and degradation (Marchetti *et al.* 2005). Moreover, the relatively large tissue *post mortem* delays (PMDs) were likely to have significantly reduced protein phosphorylation and caused generalised widespread protein degradation (Zhu *et al.* 2002). At present it is not clear if *DUSP6* dysregulation is

specific to IPD, hence it would be interesting to perform these LCM mRNA and protein expression experiments in tissue obtained from other neurodegenerative diseases. Furthermore, the influence of CpG methylation on *DUSP6* mRNA expression could be thoroughly investigated in DLPFC genomic DNA (gDNA) obtained from a large number of individuals by cloning the entire *DUSP6* locus and carrying out bisulphite sequencing [reviewed in (Bernstein *et al.* 2007)].

Genetic association between variation at rs1689408 and IPD could be replicated in a larger population. In order to begin to evaluate the modulated *DUSP6* splicing hypothesis (see above), IPD genetic association and genotypic VBM analyses could be performed for rs808820 variation. If significant associations were demonstrated, the *DUSP6* FL/1:3 *cis*-acting variation analysis could be repeated in much larger numbers of separate cases and controls, with individuals grouped by rs808820 genotype. Unfortunately, the lack of strong LD between these variants and any SNP located on the *DUSP6* transcript would preclude the use of more sensitive relative allelic expression methods e.g. single base extension. In addition, functional validation of this hypothesis could be achieved *in vitro* by cloning rs808820 allelic variants of the *DUSP6* locus into minigene constructs and transfecting them into cultured neuronal cells [for example (Niksic *et al.* 1999)]. Subsequently, more expensive and involved experiments might be performed *in vivo*. Genotypic VBM could be carried out in IPD neurodegeneration and/or dementia cases and compared against the data generated in normal controls. Moreover, human *DUSP6* FL and 1:3 transgenes could be expressed in the forebrain of adult *Dusp6*$^{-/-}$ mice under the control of an inducible tissue-specific promoter [for example (Lin *et al.* 2009b)]. By activating transgene expression at several timepoints and treating with stress-inducing agents (e.g. epoxomicin or rotenone), this system could model the biochemical and neuropathological consequences of interaction between chronically-modulated *DUSP6* splicing and oxidative stress at different stages of development. Furthermore, this approach might even provide evidence clarifying the circumstances under which chronic ERK1/2 activity is neurotoxic or neuroprotective in the IPD prefrontal cortex.

6.4. The role of *Ephrin receptor A2* in idiopathic Parkinson's disease pathogenesis

Ephrin receptor A2 is expressed throughout the human body, but most extensively in dendritic and bronchial epithelial cells. Its expression is approximately equivalent across different brain regions (Su *et al.* 2004). The EPHA2 protein (also known as Epithelial cell kinase [ECK]) is also broadly expressed in human tissues, but is most abundant in cerebellum granular cells and epithelial glandular cells (Berglund *et al.* 2008). Binding of the EPHA2 receptor Tyr kinase by an Ephrin ligand initiates bidirectional signaling cascades known to influence a variety of cellular processes [reviewed in (Pasquale 2008)]. EPHA2 activation inhibits Rho family signaling, thereby destabilising adherens junctions and promoting cell migration (Fang *et al.* 2005; Fang *et al.* 2008). EPHA2 kinase activity increases cell permeability via phosphorylation of tight junction proteins (Tanaka *et al.* 2005). These cell-cell repulsive effects mediate some of its physiological and pathological functions. During vertebrate development, EphA2 guides spinal commissural axons by ensuring that they do not recross the midline (Brittis *et al.* 2002). EPHA2 is thought to induce Rho family-mediated endothelial barrier disruption and leukocyte extravasation and migration during inflammation [reviewed in (Ivanov and Romanovsky 2006)]. EPHA2 protein expression is increased in many cancers. Depending on activation state and cellular context, it can exhibit opposing influences on tumourigenicity via changes in cell adhesion and metastasis [reviewed in (Pasquale 2008)].

Several *EphA2*$^{-/-}$ mouse models have been generated. In an early experiment, mutant mice developed short and kinky tails, indicating that EphA2 regulates tail notochord cell positioning (Naruse-Nakajima *et al.* 2001). Other models confirm its divergent effects on carcinogenesis, and knockouts displaying both increased and decreased tumour progression phenotypes have been reported (Guo *et al.* 2006; Brantley-Sieders *et al.* 2005). The *EphA2*$^{-/-}$ mouse eye lens exhibits heat shock protein overexpression and progressive cataract formation, apparently via mechanisms

involving oxidative stress and protein aggregation (Jun *et al.* 2009). Interestingly, EphA2 activity mediates the Erk1/2-dependent differentiation of telencephalic dopaminergic neuronal precursors in neurosphere cultures, and disruption of neural EphA receptor signaling reduces nigrostriatal dopaminergic developmental innervation *in vivo* (Aoki *et al.* 2004; Sieber *et al.* 2004). Moreover, a meta-analysis of several IPD SN microarray studies was recently reported. After correction for neuronal loss, Ephrin signaling was found to be the most commonly dysregulated pathway (Sutherland *et al.* 2009b). Overall, these literature findings highlight the roles played by EPHA2 in neural development, cell migration, inflammation, and cell viability, as well as suggesting that it may be involved in IPD pathogenesis.

Significant overexpression of *EPHA2* was demonstrated in the IPD DLPFC using microarray and validated by qRT-PCR. However, the former technique suggested implication in IPD dementia (see table 4.4), and the latter, implication in IPD neurodegeneration (see figure 4.5). Nevertheless, the most conservative interpretation of IPD group spacing on the array expression plot (see figure 4.4a) and the qRT-PCR results (see table 4.5) is that variation in EPHA2 expression associates with IPD neurodegeneration. Additional qRT-PCR experiments showed that *EPHA2* is not differentially-expressed in seven other subcortical and cortical regions of the IPD brain (see figure 4.6), which suggests that *EPHA2* overexpression is restricted to the DLPFC. Genetic association analysis of 95% of common SNP variation in the *EPHA2* locus indicated that the rs11260822 minor allele significantly increases IPD risk (see table 4.7). This finding appears relatively sound, but there is still need for replication in a larger population. Variation at rs11260822 was shown not to influence DLPFC *EPHA2* expression (see figure 4.8). Together with the lack of association between IPD and the remaining common SNP variation in the *EPHA2* locus (see table 4.7), this result implies that *EPHA2* overexpression is not caused by local genetic variation, and probably arises as a secondary effect of IPD pathogenesis.

Experiments in cell models indicate the existence of an EPHA2-ERK1/2-ELK1-*EPHA2* positive feedback loop (Pratt and Kinch 2002; Pratt and Kinch 2003). *In*

silico microarray mining suggested that *EPHA2* overexpression in the IPD DLPFC might result from constitutive activation of this loop (see table 4.8 and figure 4.9). Because they are drawn from uncorrected tests, these findings possess reduced statistical confidence. However, it is reasonable to infer that if maintained over time, even small changes in the expression of signaling cascade genes could alter cellular signaling patterns. Given the relatively high number of inflammation gene dysregulation events observed in the array (see 4.3.3 and 4.3.4) and that *EPHA2* is expressed in dendritic cells (Ivanov and Romanovsky 2006), the observed overexpression of *EPHA2* might be ascribed to and/or regulate neuroinflammatory processes in the IPD DLPFC (see 6.7) [reviewed in (Hirsch and Hunot 2009)].

When viewed in the context of a constitutively active EPHA2-ERK1/2-ELK1-*EPHA2* loop, the changes in *DUSP6* and *EPHA2* expression are revealed as single nodes in a larger system, whose functions are as yet unknown. One intriguing possibility could be to ensure chronic ERK1/2 activation in IPD. This kinase constitutes a central player in signal transduction, executing a myriad of functions. Its activation can be neuroprotective or neurotoxic, depending on a multitude of factors, including duration of activity, subcellular localisation, effector choice, cell type, and pathological state. Furthermore, cytoplasmic aggregates of phosphorylated ERK1/2 have been detected in *post mortem* IPD SN neurons (see 6.3) [reviewed in (Colucci-D'Amato *et al.* 2003; Chu *et al.* 2004)]. Given that parkinsonian brain cells are continuously exposed to many factors promoting cell death or survival, chronically active ERK1/2 could enable a rapid response to either influence, providing them with the means and option to initiate protective and/or repair processes or commit apoptosis, as necessary. If ERK1/2 is the central node and its chronic activation the "purpose" of this system, *DUSP6* and *EPHA2* take on more importance, performing signal "gatekeeping" and "replenishment" functions, respectively.

Several lines of *EPHA2* research might be pursued in the future. As before, LCM could be used to quantify cell-type specific *EPHA2* mRNA and protein expression in

the IPD DLPFC and in other neurodegenerative disorders (see 6.3). The association between variation at rs11260822 and IPD could be replicated in a larger population. Given the role played by *EPHA2* in neural development (Brittis *et al.* 2002; Aoki *et al.* 2004; Sieber *et al.* 2004), genotypic VBM analysis might also be warranted for this variant. The constitutive EPHA2 loop hypothesis could be evaluated by investigating protein phosphorylation in IPD DLPFC samples with low PMD, and subsequently explored, by overexpressing *EPHA2* to recapitulate these signaling patterns in oxidatively-stressed neurons and assessing the outcome of treatments which preferentially activate specific pathways downstream of ERK1/2. Finally, the latter experiment could be performed in adult *EphA2*$^{-/-}$ mice induced to overexpress forebrain-specific human *EPHA2*.

6.5. *Dual specificity phosphatase 6* and *Ephrin receptor A2* connect idiopathic Parkinson's disease with tumourigenesis

Dysregulation of the mammalian cell cycle can result in apoptosis and/or tumourigenesis. Although neurons are generally viewed as postmitotic, various stresses and genetic aberrations can cause them to reactivate the cell cycle and commit apoptosis. Critically, evidence suggests that these mechanisms may contribute to neurodegenerative cell death [reviewed in (Staropoli 2008)]. For example, *Parkin* (*PARK2*) promotes the degradation of Cyclin E and protects neurons from excitotoxic and mitochondrial apoptosis (Staropoli *et al.* 2003; Darios *et al.* 2003). Interestingly, *PARK2* locus deletion and underexpression is observed in several forms of cancer (Cesari *et al.* 2003), and PD patients display significantly altered neoplastic susceptibility. Risk is elevated for certain cancer types (e.g. brain, skin, and breast), whereas for others, it is reduced (Olsen *et al.* 2005). Moreover, *in*

silico analysis of expression microarray data has shown that many genes upregulated in the IPD SN are also associated with tumourigenesis (Moran and Graeber 2008).

The results presented in this thesis suggest that *DUSP6* and *EPHA2* may be relevant in this context. The *DUSP6* locus is frequently deleted in neoplasia, and pancreatic and ovarian cancer tissues exhibit DUSP6 protein underexpression (Furukawa *et al.* 1998; Furukawa *et al.* 2003; Chan *et al.* 2008). Our data demonstrate that *DUSP6* underexpressed in IPD (see figure 3.9 and table 4.8). Melanoma cell lines and breast cancer tissues display EPHA2 protein overexpression, and experiments in *EphA2*$^{-/-}$ mice suggest that EphA2 promotes tumour angiogenesis and metastatic progression (Easty *et al.* 1995; Zelinski *et al.* 2001; Brantley-Sieders *et al.* 2005). Our results show that *EPHA2* is overexpressed in IPD (see figures 4.4a and 4.5). Collectively, these findings suggest that *DUSP6* and *EPHA2* could represent new examples of the common ground between IPD and tumourigenesis.

6.6. The role of *α-Synuclein* in idiopathic Parkinson's disease pathogenesis

In silico microarray mining and qRT-PCR demonstrated that *SNCA* is not differentially-expressed in the eight regions of the IPD brain, including the DLPFC (BA46) (see figures 5.1 and 5.2). Furthermore, variation in DLPFC *SNCA* expression did not associate with IPD dementia (see figure 5.1). Significant association with IPD was shown for the rare GT haplotype composed of rs11931074 or rs3822086, but not for single marker analysis (see table 5.4), suggesting that this haplotype is tagging one or more IPD-associated variant(s). There are no published reports of association with this haplotype. However, the low haplotype frequencies observed in both IPD cases and controls casts doubt on this finding, and indicates the need for replication in a larger population. Indeed, highly significant associations between IPD and variation at both rs11931074 and rs3857059 have been demonstrated (Simon-

Sanchez *et al.* 2009; Satake *et al.* 2009), which suggests the haplotypic association may have been a statistical anomaly. Nevertheless, these published associations imply that the ROI selected (see 5.3.5) for identifying putative functional variants (see below) was not equivocal.

Elucidation of fine scale SNP LD in the *SNCA* locus indicated that rs11931074, rs3822086, and rs3857059 are probably situated on the same haplotype block in Caucasians (see figure 5.3). The strength of these data was the relatively high sample numbers, and their weakness, the lack of control genotypes for rs3857059. Predicted DNA conservation and literature mining suggested that rs356165 and rs356204 are putative functional variants which might be driving the observed haplotypic association with IPD (see table 5.5). Although predicted DNA conservation mining appears useful for identifying putative functional variants, the weakness of this approach was the lack of functional validation.

Overall, these results suggest that variation in extranigral *SNCA* expression does not associate with IPD neurodegeneration or dementia. Our DLPFC data for IPD neurodegeneration are consistent with one study of the FC (Chiba-Falek *et al.* 2006), but contradict several others (Kingsbury *et al.* 2004; Zhang *et al.* 2005b; Beyer *et al.* 2008). Nevertheless, our DLPFC results for IPD dementia agree with one report investigating posterior cingulate cortex neurons (Stamper *et al.* 2008). Increased *SNCA* ploidy appears to cause parkinsonism and dementia in FPD multiplication pedigrees by directly affecting *SNCA* expression (Farrer *et al.* 2004; Miller *et al.* 2004; Ross *et al.* 2008a). However, our data and the Stamper *et al.* report suggest that this mechanism is not relevant to the IPDD cortex i.e. that changes in *SNCA* expression are not required to maintain the IPDD phenotype. *SNCA* research might be pursued in several future directions. The haplotypic association with IPD could be replicated in a larger population. Moreover, reporter gene assays could be carried out in neuronal cell models in order to evaluate whether rs356165 and rs356204 are putative functional variants.

6.7. The dorsolateral prefrontal cortex in idiopathic Parkinson's disease dementia and neurodegeneration

The cognitive expression qRT-PCR analysis showed that variation in the DLPFC (BA46) and angular gyrus (AG) (BA39) expression of 10 target genes does not associate with IPDD (see figures 3.4 and 3.5). Brain regions and target genes were selected primarily from a neuropsychological perspective. IPDD is characterised by WM deficits (Litvan *et al.* 1991; Bohnen *et al.* 2006), and the DLPFC and AG are both involved in WM (Petrides 2000; Gruber *et al.* 2001). Furthermore, BA46 exhibits significantly greater atrophy in demented IPD cases compared to their nondemented counterparts or controls (Burton *et al.* 2004; Nagano-Saito *et al.* 2005), and BA39 cerebral blood flow is significantly reduced in IPDD patients contrasted against controls (Firbank *et al.* 2003). Target genes involved in working or long term memory were chosen based on the generalist brain hypothesis, which proposes that variation in a specific set of genes affects many cognitive abilities and disabilities (see 3.3.1) (Kovas and Plomin 2006). The main weakness of this analysis was the cognitive criteria used to allocate patients to IPDD and IPDND groups. The Brain Bank lacks detailed neuropsychological information, and hence this decision was based on carer reports backed up by MMSE scores, where available.

Subsequent to these lacklustre findings, the cognitive expression microarray analysis was performed to investigate DLPFC (BA46) transcriptome dysregulation in IPD dementia and neurodegeneration. The results suggested that several genes are implicated in each disease subtype (see tables 4.3 and 4.4). Moreover, when both were compared to controls, much more dysregulation was seen in IPDD than in IPDND (see table 4.2). However, all of these changes were only significant before correction. The FDR-corrected data indicated an overall lack of gene dysregulation (see table 4.2), which was exemplified by the fact that most of attempts at qRT-PCR

validation failed (see table 4.5). Nevertheless, two recently-published genome wide association studies (GWAS) indicate that only a handful of SNPs display highly significant association with IPD (Simon-Sanchez *et al.* 2009; Satake *et al.* 2009), suggesting that the remainder of its genetic aetiology is probably mediated by many variants each of small effect. Therefore, as long as their reduced statistical confidence is kept in mind, our microarray results are useful in terms of flagging pathways of potential importance (see below). Nevertheless, the low number of hits indicated that it was inappropriate to undertake formal statistical pathway analyses. The strength of microarray Affymetrix GeneChip Exon platform was its ability to detect both differential gene expression and alternative exon splicing. The main weaknesses of this analysis were the group allocation criteria (see above) and the low number of samples.

Expression microarray analysis suggested that several pathways are dysregulated in the IPD dementia DLPFC (see 4.3.4), and some of these are of particular interest. The first is inflammation. There is a growing understanding of the important role that neuroinflammatory processes play in IPD pathogenesis. Numerous reports indicate that neurodegeneration activates glia and peripheral immune cells, which cause oxidative stress and apoptosis thought to contribute to neuronal cell death and disease progression [reviewed in (Hirsch and Hunot 2009)]. Furthermore, array studies have demonstrated dysregulation of inflammatory genes in the IPDD cortex and the IPD SN (Stamper *et al.* 2008; Simunovic *et al.* 2009; Moran and Graeber 2008). In addition, our data suggested that inflammation is also implicated in IPD neurodegeneration (see 4.3.3). The other two interesting pathways are cell adhesion and the cytoskeleton. These are best viewed in relation to the observed inflammation pathway changes. Activated microglia, astrocytes, and T-cells all migrate to sites of brain injury [reviewed in (McGeer and McGeer 2008; Hirsch and Hunot 2009)], and this is mediated by changes in the surface expression of adhesion molecules and reorganisation of the cytoskeleton [reviewed in (Ivanov and Romanovsky 2006)]. As before, the IPDD cortex and IPD SN exhibit dysregulation of cell adhesion and/or cytoskeletal genes (Moran *et al.* 2006; Stamper *et al.* 2008; Bossers *et al.* 2009;

Simunovic *et al.* 2009). Taken together, our data imply that neuroinflammation is an important facet of IPD dementia pathogenesis in the DLPFC, and suggest that the observed dysregulation events might be partially ascribed to glia and/or infiltrating leukocytes.

In silico microarray mining suggested that variation in the DLPFC expression of genes involved in PD and parkinsonism-dementia is not associated with IPD neurodegeneration and dementia, respectively (see table 4.10), and that the UPR pathway is not chronically-activated in the IPD DLPFC (see table 4.9). These uncorrected statistical results necessarily possessed reduced confidence. However, this weakness is problematic for its potential to generate false positives, and so does not detract from these negative findings. The parkinsonism-dementia result implied generalised molecular dissociation between these familial cognitive movement disorders and IPDD. The lack of UPR pathway activation suggested that misfolded protein burden is relatively low in IPD DLPFC, and is in keeping with data showing that the forebrain is one the last areas to acquire LP (Braak *et al.* 2003). Collectively, these results add to growing picture suggesting that gene dysregulation is relatively rare in the IPD DLPFC.

When viewed in context of the literature, several conclusions can be drawn from the microarray findings and subsequent *in silico* analyses. Common pathways are dysregulated in IPD dementia and IPD neurodegeneration, as well as in different regions of the disease brain, however, overall genetic dysregulation is much more extensive in demented compared to nondemented IPD patients (see also 4.4) (Zhang *et al.* 2005b; Moran *et al.* 2006; Stamper *et al.* 2008; Simunovic *et al.* 2009). These observations support the hypothesis that IPD is a multisystem disease at the transcriptomic level (Zhang *et al.* 2005b; Moran *et al.* 2006), and imply that the same is true for IPDD. Moreover, they suggest that IPDD can be viewed as an extension of the parkinsonian state. This conclusion is bolstered by correlations between neuropathological/expression changes and cognitive dysfunction in IPD (Kovari *et al.* 2003; Aarsland *et al.* 2005a; Stamper *et al.* 2008). However, there was an overall

lack of differential expression in the qRT-PCR and microarray cognitive expression analyses, the PD and parkinsonism-dementia *in silico* analysis, the UPR pathway *in silico* analysis, and qRT-PCR *SNCA* analysis (see 6.6). These results imply that the DLPFC is not critically-involved in late stage IPD dementia or neurodegeneration. Therefore, this brain region is not well suited for identifying genes implicated in IPDD. Nevertheless, some genetic dysregulation was detected. These limited changes suggest that, although it is subject to relatively low pathological burden (Braak *et al.* 2003), the DLPFC does experience neuroinflammation by late stage IPD. Moreover, these effects may be marginally more pronounced in IPD dementia.

In the future, several approaches might be employed to identify genes implicated in IPDD cognitive dysfunction. It could be pertinent to repeat the cognitive expression microarray using a similar multiple group design. However, certain critical changes would be needed. Firstly, the study population should be a larger prospective cohort with excellent clinical, neuropathological, and neuropsychological information. This would enable several distinct analyses to be carried out, each based on allocating IPD patients to different groups according to specific neuropsychological [e.g. semantic fluency, WM ability, attention, conceptualisation, or Mattis dementia rating scale score (Girotti *et al.* 1988; Litvan *et al.* 1991; Bohnen *et al.* 2006; Williams-Gray *et al.* 2009a)] and/or neuropathological [e.g. cortical LP; cortical Alzheimer pathology; SNCA, Microtubule-associated protein tau (MAPT), and/or β-amyloid pathology in the ACC; SNCA and/or MAPT pathology in the EC; or SNCA and/or MAPT pathology in the hippocampus (Vermersch *et al.* 1993; Jellinger *et al.* 2002; Kovari *et al.* 2003; Aarsland *et al.* 2005a; Pletnikova *et al.* 2005; Kalaitzakis *et al.* 2009a)] criteria.

Secondly, several different brain regions could be selected, and LCM used to enable specific interrogation of neuronal and/or glial expression. Recent neuropathological and neuropsychological evidence suggests that the ACC, EC, perirhinal cortex, parahippocampal cortex, or hippocampus would be the most promising choices (see 3.4 for details) (Pletnikova *et al.* 2005; Vermersch *et al.* 1993; Kovari *et al.* 2003;

Williams-Gray *et al.* 2009a; Pihlajamaki *et al.* 2000). This approach could identify genes implicated in IPDD cognitive dysfunction and evaluate correlations in gene expression across different regions of the IPDD brain. In order to implicate genes in IPDD aetiology, validated array hits could be subjected to SNP tagging and genetic association analysis using a large series of IPDD gDNA samples [for example (Elstner *et al.* 2009)]. An alternative approach might be to undertake a GWAS in the same series. Furthermore, the relatively novel RNA sequencing technique could enable genome wide investigation of the relationship between genetic variation and expression and/or splicing in IPDD.

6.8. Idiopathic Parkinson's disease dementia molecular aetiopathogenesis research horizons

Elucidating the molecular aetiopathogenesis of IPDD will require research based on a variety of concepts drawn from several neuroscientific disciplines. The debate over the specific neuropathological and/or neurochemical determinant(s) of IPDD still rages on, in terms of both brain region(s) and molecular substrate(s). Holistic models based on multiple interacting factors will probably best explain the various facets of IPD cognitive dysfunction and concomitant behavioural disturbances [reviewed in (Kalaitzakis and Pearce 2009)]. Nevertheless, prospective and retrospective clinicopathological studies suggest that SNCA accumulation is potentially of most importance (Kovari *et al.* 2003; Aarsland *et al.* 2005a; Braak *et al.* 2005; Kalaitzakis *et al.* 2009a). This is supported by significant associations between IPDD and variation in genes whose encoded proteins promote SNCA accumulation in animal models (de Lau *et al.* 2005; Gallardo *et al.* 2008; Giasson *et al.* 2003; Williams-Gray *et al.* 2009a). Given the recent association based on the largest incident cohort to date, *MAPT* may be confirmed as most pertinent in this regard (Williams-Gray *et al.* 2009a). Moreover, gene expression analyses suggest that apoptotic, inflammation, cell adhesion, cytoskeletal, axonal transport, mitochondrial, and splicing pathways

could turn out to be critical parts of the puzzle [see 6.4, 6.5, 6.7 and (Stamper *et al.* 2008)]. Several of these pathways intersect at the point of glia, and future IPDD aetiopathogenesis research will probably focus increasingly on this often overlooked cellular lineage [reviewed in (McGeer and McGeer 2008; Hirsch and Hunot 2009)].

The technical approaches employed to investigate IPDD molecular aetiopathogenesis are likely to be just as varied. Given that human clinicopathological studies will remain at the forefront, high quality patient phenotyping and material cataloguing will be essential. Genome wide studies will best determine the genetic variants and expression phenotypes which associate with IPDD. Integrated approaches examining variation in SNPs, copy number, microsatellites, gene expression, noncoding RNA expression, and protein expression will be most beneficial, especially if these genetic and/or expression data are correlated with clinicopathological and neuropsychological information (for example see 6.7). These experiments will probably employ LCM to examine cell-type specific expression. Furthermore, gene-environment and gene-gene studies are likely to become more common [for example (McCulloch *et al.* 2008)], as researchers seek to build conceptual syntheses of the real word interactions that mediate IPDD. These might take the form of longitudinal imaging studies [for example (Pavese *et al.* 2009; Osaki *et al.* 2009)], such as genotype-phenotype correlations in presymptomatic individuals carrying IPDD susceptibility alleles, and genotype-treatment interactions in IPDD disease cases. Meanwhile, promising genetic and environmental factors will be explored in animal models. Only through concerted effort using various methodologies will we make headway in elucidating the molecular aetiopathogenesis of this debilitating disorder.

References

Aarsland, D., Andersen, K., Larsen, J.P., Lolk, A., & Kragh-Sorensen, P. (2003a). Prevalence and characteristics of dementia in Parkinson disease: an 8-year prospective study. *Arch. Neurol.* **60**, 387-392.

Aarsland, D., Andersen, K., Larsen, J.P., Lolk, A., Nielsen, H., & Kragh-Sorensen, P. (2001a). Risk of dementia in Parkinson's disease: a community-based, prospective study. *Neurology* **56**, 730-736.

Aarsland, D., Ballard, C., Larsen, J.P., & McKeith, I. (2001b). A comparative study of psychiatric symptoms in dementia with Lewy bodies and Parkinson's disease with and without dementia. *Int. J. Geriatr. Psychiatry* **16**, 528-536.

Aarsland, D., Ballard, C.G., & Halliday, G. (2004). Are Parkinson's disease with dementia and dementia with Lewy bodies the same entity? *J. Geriatr. Psychiatry Neurol.* **17**, 137-145.

Aarsland, D., Cummings, J.L., & Larsen, J.P. (2001c). Neuropsychiatric differences between Parkinson's disease with dementia and Alzheimer's disease. *Int. J. Geriatr. Psychiatry* **16**, 184-191.

Aarsland, D., Kvaloy, J.T., Andersen, K., Larsen, J.P., Tang, M.X., Lolk, A., Kragh-Sorensen, P., & Marder, K. (2007). The effect of age of onset of PD on risk of dementia. *J. Neurol.* **254**, 38-45.

Aarsland, D., Litvan, I., Salmon, D., Galasko, D., Wentzel-Larsen, T., & Larsen, J.P. (2003b). Performance on the dementia rating scale in Parkinson's disease with dementia and dementia with Lewy bodies: comparison with progressive supranuclear palsy and Alzheimer's disease. *J. Neurol. Neurosurg. Psychiatry* **74**, 1215-1220.

Aarsland, D., Perry, R., Brown, A., Larsen, J.P., & Ballard, C. (2005a). Neuropathology of dementia in Parkinson's disease: a prospective, community-based study. *Ann. Neurol.* **58**, 773-776.

Aarsland, D., Zaccai, J., & Brayne, C. (2005b). A systematic review of prevalence studies of dementia in Parkinson's disease. *Mov Disord.* **20**, 1255-1263.

Abeliovich, A., Schmitz, Y., Farinas, I., Choi-Lundberg, D., Ho, W.H., Castillo, P.E., Shinsky, N., Verdugo, J.M., Armanini, M., Ryan, A., Hynes, M., Phillips, H., Sulzer, D., & Rosenthal, A. (2000). Mice lacking alpha-synuclein display functional deficits in the nigrostriatal dopamine system. *Neuron* **25**, 239-252.

Abou-Sleiman, P.M., Muqit, M.M., McDonald, N.Q., Yang, Y.X., Gandhi, S., Healy, D.G., Harvey, K., Harvey, R.J., Deas, E., Bhatia, K., Quinn, N., Lees, A., Latchman, D.S., & Wood, N.W. (2006a). A heterozygous effect for PINK1 mutations in Parkinson's disease? *Ann. Neurol.* **60**, 414-419.

Abou-Sleiman, P.M., Muqit, M.M., & Wood, N.W. (2006b). Expanding insights of mitochondrial dysfunction in Parkinson's disease. *Nat. Rev. Neurosci.* **7**, 207-219.

Adler, C.H. (2005). Nonmotor complications in Parkinson's disease. *Mov Disord.* **20 Suppl 11**, S23-S29.

Aharon-Peretz, J., Badarny, S., Rosenbaum, H., & Gershoni-Baruch, R. (2005). Mutations in the glucocerebrosidase gene and Parkinson disease: phenotype-genotype correlation. *Neurology* **65**, 1460-1461.

Aharon-Peretz, J., Rosenbaum, H., & Gershoni-Baruch, R. (2004). Mutations in the glucocerebrosidase gene and Parkinson's disease in Ashkenazi Jews. *N. Engl. J. Med.* **351**, 1972-1977.

Ahn, T.B., Kim, S.Y., Kim, J.Y., Park, S.S., Lee, D.S., Min, H.J., Kim, Y.K., Kim, S.E., Kim, J.M., Kim, H.J., Cho, J., & Jeon, B.S. (2008). alpha-Synuclein gene duplication is present in sporadic Parkinson disease. *Neurology* **70**, 43-49.

Al-Chalabi, A., Durr, A., Wood, N.W., Parkinson, M.H., Camuzat, A., Hulot, J.S., Morrison, K.E., Renton, A., Sussmuth, S.D., Landwehrmeyer, B.G., Ludolph, A., Agid, Y., Brice, A., Leigh, P.N., & Bensimon, G. (2009). Genetic variants of the alpha-synuclein gene SNCA are associated with multiple system atrophy. *PLoS. ONE.* **4**, e7114.

Alam, Z.I., Daniel, S.E., Lees, A.J., Marsden, D.C., Jenner, P., & Halliwell, B. (1997). A generalised increase in protein carbonyls in the brain in Parkinson's but not incidental Lewy body disease. *J. Neurochem.* **69**, 1326-1329.

Alexander, G.E., DeLong, M.R., & Strick, P.L. (1986). Parallel organization of functionally segregated circuits linking basal ganglia and cortex. *Annu. Rev. Neurosci.* **9**, 357-381.

Anderson, J.P., Walker, D.E., Goldstein, J.M., de, L.R., Banducci, K., Caccavello, R.J., Barbour, R., Huang, J., Kling, K., Lee, M., Diep, L., Keim, P.S., Shen, X., Chataway, T., Schlossmacher, M.G., Seubert, P., Schenk, D., Sinha, S., Gai, W.P., & Chilcote, T.J. (2006). Phosphorylation of Ser-129 is the dominant pathological modification of alpha-synuclein in familial and sporadic Lewy body disease. *J. Biol. Chem.* **281**, 29739-29752.

Aoki, M., Yamashita, T., & Tohyama, M. (2004). EphA receptors direct the differentiation of mammalian neural precursor cells through a mitogen-activated protein kinase-dependent pathway. *J. Biol. Chem.* **279**, 32643-32650.

Apaydin, H., Ahlskog, J.E., Parisi, J.E., Boeve, B.F., & Dickson, D.W. (2002). Parkinson disease neuropathology: later-developing dementia and loss of the levodopa response. *Arch. Neurol.* **59**, 102-112.

Arima, K., Hirai, S., Sunohara, N., Aoto, K., Izumiyama, Y., Ueda, K., Ikeda, K., & Kawai, M. (1999). Cellular co-localization of phosphorylated tau- and NACP/alpha-synuclein-epitopes in lewy bodies in sporadic Parkinson's disease and in dementia with Lewy bodies. *Brain Res.* **843**, 53-61.

Ashburner, J. (2007). A fast diffeomorphic image registration algorithm. *Neuroimage.* **38**, 95-113.

Ashburner, J. & Friston, K.J. (2005). Unified segmentation. *Neuroimage.* **26**, 839-851.

Ashburner, J. & Friston, K.J. (2000). Voxel-based morphometry--the methods. *Neuroimage.* **11**, 805-821.

Ashburner, M., Ball, C.A., Blake, J.A., Botstein, D., Butler, H., Cherry, J.M., Davis, A.P., Dolinski, K., Dwight, S.S., Eppig, J.T., Harris, M.A., Hill, D.P., Issel-Tarver, L., Kasarskis, A., Lewis, S., Matese, J.C., Richardson, J.E., Ringwald, M., Rubin, G.M., & Sherlock, G. (2000). Gene ontology: tool for the unification of biology. The Gene Ontology Consortium. *Nat. Genet.* **25**, 25-29.

Attems, J. & Jellinger, K.A. (2008). The dorsal motor nucleus of the vagus is not an obligatory trigger site of Parkinson's disease. *Neuropathol. Appl. Neurobiol.* **34**, 466-467.

Auriacombe, S., Grossman, M., Carvell, S., Gollomp, S., Stern, M.B., & Hurtig H.I. (1993). Verbal Fluency Deficits in Parkinson's Disease. *Neuropsychology* **7**, 182-192.

Azeredo da Silveira, S., Schneider, B.L., Cifuentes-Diaz, C., Sage, D., bbas-Terki, T., Iwatsubo, T., Unser, M., & Aebischer, P. (2009). Phosphorylation does not prompt, nor prevent, the formation of alpha-synuclein toxic species in a rat model of Parkinson's disease. *Hum. Mol. Genet.* **18**, 872-887.

Baker, M., Litvan, I., Houlden, H., Adamson, J., Dickson, D., Perez-Tur, J., Hardy, J., Lynch, T., Bigio, E., & Hutton, M. (1999). Association of an extended haplotype in the tau gene with progressive supranuclear palsy. *Hum. Mol. Genet.* **8**, 711-715.

Baldwin, C., Chen, Z.W., Bedirian, A., Yokota, N., Nasr, S.H., Rabb, H., & Lemay, S. (2006). Upregulation of EphA2 during in vivo and in vitro renal ischemia-reperfusion injury: role of Src kinases. *Am. J. Physiol Renal Physiol* **291**, F960-F971.

Ballard, C., Ziabreva, I., Perry, R., Larsen, J.P., O'Brien, J., McKeith, I., Perry, E., & Aarsland, D. (2006). Differences in neuropathologic characteristics across the Lewy body dementia spectrum. *Neurology* **67**, 1931-1934.

Ballard, C.G., Aarsland, D., McKeith, I., O'Brien, J., Gray, A., Cormack, F., Burn, D., Cassidy, T., Starfeldt, R., Larsen, J.P., Brown, R., & Tovee, M. (2002). Fluctuations in attention: PD dementia vs DLB with parkinsonism. *Neurology* **59**, 1714-1720.

Bancher, C., Braak, H., Fischer, P., & Jellinger, K.A. (1993). Neuropathological staging of Alzheimer lesions and intellectual status in Alzheimer's and Parkinson's disease patients. *Neurosci. Lett.* **162**, 179-182.

Bandopadhyay, R., Kingsbury, A.E., Cookson, M.R., Reid, A.R., Evans, I.M., Hope, A.D., Pittman, A.M., Lashley, T., Canet-Aviles, R., Miller, D.W., McLendon, C., Strand, C., Leonard, A.J., Abou-Sleiman, P.M., Healy, D.G., Ariga, H., Wood, N.W., de, S.R., Revesz, T., Hardy, J.A., & Lees, A.J. (2004). The expression of DJ-1 (PARK7) in normal human CNS and idiopathic Parkinson's disease. *Brain* **127**, 420-430.

Barnett, J.H., Jones, P.B., Robbins, T.W., & Muller, U. (2007). Effects of the catechol-O-methyltransferase Val158Met polymorphism on executive function: a meta-analysis of the Wisconsin Card Sort Test in schizophrenia and healthy controls. *Mol. Psychiatry* **12**, 502-509.

Barnett, J.H., Scoriels, L., & Munafo, M.R. (2008). Meta-analysis of the cognitive effects of the catechol-O-methyltransferase gene Val158/108Met polymorphism. *Biol. Psychiatry* **64**, 137-144.

Barrachina, M., Castano, E., Dalfo, E., Maes, T., Buesa, C., & Ferrer, I. (2006). Reduced ubiquitin C-terminal hydrolase-1 expression levels in dementia with Lewy bodies. *Neurobiol. Dis.* **22**, 265-273.

Barrett, J.C., Fry, B., Maller, J., & Daly, M.J. (2005). Haploview: analysis and visualization of LD and haplotype maps. *Bioinformatics.* **21**, 263-265.

Benjamini, Y. & Hochberg, Y. (1995). Controlling the False Discovery Rate: A Practical and Powerful Approach to Multiple Testing. *J. Roy Stat Soc, Ser B (Methodological)* **57**, 289-300.

Berglund, L., Bjorling, E., Oksvold, P., Fagerberg, L., Asplund, A., Szigyarto, C.A., Persson, A., Ottosson, J., Wernerus, H., Nilsson, P., Lundberg, E., Sivertsson, A., Navani, S., Wester, K., Kampf, C., Hober, S., Ponten, F., & Uhlen, M. (2008). A genecentric Human Protein Atlas for expression profiles based on antibodies. *Mol. Cell Proteomics.* **7**, 2019-2027.

Bernstein, B.E., Meissner, A., & Lander, E.S. (2007). The mammalian epigenome. *Cell* **128**, 669-681.

Berti, C., Fontanella, B., Ferrentino, R., & Meroni, G. (2004). Mig12, a novel Opitz syndrome gene product partner, is expressed in the embryonic ventral midline and co-operates with Mid1 to bundle and stabilize microtubules. *BMC. Cell Biol.* **5**, 9.

Betarbet, R., Sherer, T.B., MacKenzie, G., Garcia-Osuna, M., Panov, A.V., & Greenamyre, J.T. (2000). Chronic systemic pesticide exposure reproduces features of Parkinson's disease. *Nat. Neurosci.* **3**, 1301-1306.

Beyer, K., Domingo-Sabat, M., Humbert, J., Carrato, C., Ferrer, I., & Ariza, A. (2008). Differential expression of alpha-synuclein, parkin, and synphilin-1 isoforms in Lewy body disease. *Neurogenetics.* **9**, 163-172.

Binkofski, F., Reetz, K., Gaser, C., Hilker, R., Hagenah, J., Hedrich, K., van, E.T., Thiel, A., Buchel, C., Pramstaller, P.P., Siebner, H.R., & Klein, C. (2007). Morphometric fingerprint of asymptomatic Parkin and PINK1 mutation carriers in the basal ganglia. *Neurology* **69**, 842-850.

Biskup, S., Moore, D.J., Celsi, F., Higashi, S., West, A.B., Andrabi, S.A., Kurkinen, K., Yu, S.W., Savitt, J.M., Waldvogel, H.J., Faull, R.L., Emson, P.C., Torp, R., Ottersen, O.P., Dawson, T.M., & Dawson, V.L. (2006). Localization of LRRK2 to membranous and vesicular structures in mammalian brain. *Ann. Neurol.* **60**, 557-569.

Blackinton, J.G., Anvret, A., Beilina, A., Olson, L., Cookson, M.R., & Galter, D. (2007). Expression of PINK1 mRNA in human and rodent brain and in Parkinson's disease. *Brain Res.* **1184**, 10-16.

Bland, J.M. & Altman, D.G. (2000). Statistics notes. The odds ratio. *BMJ* **320**, 1468.

Blazquez, L., Otaegui, D., Saenz, A., Paisan-Ruiz, C., Emparanza, J.I., Ruiz-Martinez, J., Moreno, F., Marti-Masso, J.F., & Lopez de, M.A. (2006). Apolipoprotein E epsilon4 allele in familial and sporadic Parkinson's disease. *Neurosci. Lett.* **406**, 235-239.

Bogaerts, V., Nuytemans, K., Reumers, J., Pals, P., Engelborghs, S., Pickut, B., Corsmit, E., Peeters, K., Schymkowitz, J., De Deyn, P.P., Cras, P., Rousseau, F., Theuns, J., & Van, B.C. (2008). Genetic variability in the mitochondrial serine protease HTRA2 contributes to risk for Parkinson disease. *Hum. Mutat.* **29**, 832-840.

Boggio, P.S., Ferrucci, R., Rigonatti, S.P., Covre, P., Nitsche, M., Pascual-Leone, A., & Fregni, F. (2006). Effects of transcranial direct current stimulation on working memory in patients with Parkinson's disease. *J. Neurol. Sci.* **249**, 31-38.

Boggio, P.S., Fregni, F., Bermpohl, F., Mansur, C.G., Rosa, M., Rumi, D.O., Barbosa, E.R., Odebrecht, R.M., Pascual-Leone, A., Rigonatti, S.P., Marcolin, M.A., & raujo Silva, M.T. (2005). Effect of repetitive TMS and fluoxetine on cognitive function in patients with Parkinson's disease and concurrent depression. *Mov Disord.* **20**, 1178-1184.

Bohnen, N.I., Kaufer, D.I., Hendrickson, R., Ivanco, L.S., Lopresti, B.J., Constantine, G.M., Mathis, C., Davis, J.G., Moore, R.Y., & Dekosky, S.T. (2006). Cognitive correlates of cortical cholinergic denervation in Parkinson's disease and parkinsonian dementia. *J. Neurol.* **253**, 242-247.

Bonifati, V., Rizzu, P., van Baren, M.J., Schaap, O., Breedveld, G.J., Krieger, E., Dekker, M.C., Squitieri, F., Ibanez, P., Joosse, M., van Dongen, J.W., Vanacore, N., van Swieten, J.C., Brice, A., Meco, G., van Duijn, C.M., Oostra, B.A., & Heutink, P. (2003). Mutations in the DJ-1 gene associated with autosomal recessive early-onset parkinsonism. *Science* **299**, 256-259.

Bonifati, V., Rohe, C.F., Breedveld, G.J., Fabrizio, E., De, M.M., Tassorelli, C., Tavella, A., Marconi, R., Nicholl, D.J., Chien, H.F., Fincati, E., Abbruzzese, G., Marini, P., De, G.A., Horstink, M.W., Maat-Kievit, J.A., Sampaio, C., Antonini, A., Stocchi, F., Montagna, P., Toni, V., Guidi, M., Dalla, L.A., Tinazzi, M., De, P.F., Fabbrini, G., Goldwurm, S., de, K.A., Barbosa, E., Lopiano, L., Martignoni, E., Lamberti, P., Vanacore, N., Meco, G., & Oostra, B.A. (2005). Early-onset parkinsonism associated with PINK1 mutations: frequency, genotypes, and phenotypes. *Neurology* **65**, 87-95.

Bossers, K., Meerhoff, G., Balesar, R., van Dongen, J.W., Kruse, C.G., Swaab, D.F., & Verhaagen, J. (2009). Analysis of gene expression in Parkinson's disease: possible involvement of neurotrophic support and axon guidance in dopaminergic cell death. *Brain Pathol.* **19**, 91-107.

Braak, H., Del, T.K., Rub, U., de Vos, R.A., Jansen Steur, E.N., & Braak, E. (2003). Staging of brain pathology related to sporadic Parkinson's disease. *Neurobiol. Aging* **24**, 197-211.

Braak, H., Rub, U., Jansen Steur, E.N., Del, T.K., & de Vos, R.A. (2005). Cognitive status correlates with neuropathologic stage in Parkinson disease. *Neurology* **64**, 1404-1410.

Bradley, V.A., Welch, J.L., & Dick, D.J. (1989). Visuospatial working memory in Parkinson's disease. *J. Neurol. Neurosurg. Psychiatry* **52**, 1228-1235.

Brantley-Sieders, D.M., Fang, W.B., Hicks, D.J., Zhuang, G., Shyr, Y., & Chen, J. (2005). Impaired tumor microenvironment in EphA2-deficient mice inhibits tumor angiogenesis and metastatic progression. *FASEB J.* **19**, 1884-1886.

Bray, N.J., Buckland, P.R., Owen, M.J., & O'Donovan, M.C. (2003). Cis-acting variation in the expression of a high proportion of genes in human brain. *Hum. Genet.* **113**, 149-153.

Bray, N.J., Jehu, L., Moskvina, V., Buxbaum, J.D., Dracheva, S., Haroutunian, V., Williams, J., Buckland, P.R., Owen, M.J., & O'Donovan, M.C. (2004). Allelic expression of APOE in human brain: effects of epsilon status and promoter haplotypes. *Hum. Mol. Genet.* **13**, 2885-2892.

Bray, N.J. & O'Donovan, M.C. (2006). Investigating cis-acting regulatory variation using assays of relative allelic expression. *Psychiatr. Genet.* **16**, 173-177.

Bray, N.J., Preece, A., Williams, N.M., Moskvina, V., Buckland, P.R., Owen, M.J., & O'Donovan, M.C. (2005). Haplotypes at the dystrobrevin binding protein 1 (DTNBP1) gene locus mediate risk for schizophrenia through reduced DTNBP1 expression. *Hum. Mol. Genet.* **14**, 1947-1954.

Brighina, L., Okubadejo, N.U., Schneider, N.K., Lesnick, T.G., de, A.M., Cunningham, J.M., Farrer, M.J., Lincoln, S.J., Rocca, W.A., & Maraganore, D.M. (2007). Beta-synuclein gene variants and Parkinson's disease: a preliminary case-control study. *Neurosci. Lett.* **420**, 229-234.

Brittis, P.A., Lu, Q., & Flanagan, J.G. (2002). Axonal protein synthesis provides a mechanism for localized regulation at an intermediate target. *Cell* **110**, 223-235.

Brunet, A., Roux, D., Lenormand, P., Dowd, S., Keyse, S., & Pouyssegur, J. (1999). Nuclear translocation of p42/p44 mitogen-activated protein kinase is required for growth factor-induced gene expression and cell cycle entry. *EMBO J.* **18**, 664-674.

Bu, G. (2009). Apolipoprotein E and its receptors in Alzheimer's disease: pathways, pathogenesis and therapy. *Nat. Rev. Neurosci.* **10**, 333-344.

Buckland, P.R. (2006). The importance and identification of regulatory polymorphisms and their mechanisms of action. *Biochim. Biophys. Acta* **1762**, 17-28.

Buckland, P.R. (2004). Allele-specific gene expression differences in humans. *Hum. Mol. Genet.* **13 Spec No 2**, R255-R260.

Buckland, P.R., Hoogendoorn, B., Guy, C.A., Coleman, S.L., Smith, S.K., Buxbaum, J.D., Haroutunian, V., & O'Donovan, M.C. (2004). A high proportion of polymorphisms in the promoters of brain expressed genes influences transcriptional activity. *Biochim. Biophys. Acta* **1690**, 238-249.

Burn, D.J., Rowan, E.N., Minett, T., Sanders, J., Myint, P., Richardson, J., Thomas, A., Newby, J., Reid, J., O'Brien, J.T., & McKeith, I.G. (2003). Extrapyramidal features in Parkinson's disease with and without dementia and dementia with Lewy bodies: A cross-sectional comparative study. *Mov Disord.* **18**, 884-889.

Burton, E.J., McKeith, I.G., Burn, D.J., Williams, E.D., & O'Brien, J.T. (2004). Cerebral atrophy in Parkinson's disease with and without dementia: a comparison with Alzheimer's disease, dementia with Lewy bodies and controls. *Brain* **127**, 791-800.

Bush, G., Luu, P., & Posner, M.I. (2000). Cognitive and emotional influences in anterior cingulate cortex. *Trends Cogn Sci.* **4**, 215-222.

Buter, T.C., van den, H.A., Matthews, F.E., Larsen, J.P., Brayne, C., & Aarsland, D. (2008). Dementia and survival in Parkinson disease: a 12-year population study. *Neurology* **70**, 1017-1022.

Bychkov, E.R., Gurevich, V.V., Joyce, J.N., Benovic, J.L., & Gurevich, E.V. (2008). Arrestins and two receptor kinases are upregulated in Parkinson's disease with dementia. *Neurobiol. Aging* **29**, 379-396.

Caballol, N., Marti, M.J., & Tolosa, E. (2007). Cognitive dysfunction and dementia in Parkinson disease. *Mov Disord.* **22 Suppl 17**, S358-S366.

Cabeza, R., Dolcos, F., Graham, R., & Nyberg, L. (2002). Similarities and differences in the neural correlates of episodic memory retrieval and working memory. *Neuroimage.* **16**, 317-330.

Cahoy, J.D., Emery, B., Kaushal, A., Foo, L.C., Zamanian, J.L., Christopherson, K.S., Xing, Y., Lubischer, J.L., Krieg, P.A., Krupenko, S.A., Thompson, W.J., & Barres, B.A. (2008). A transcriptome database for astrocytes, neurons, and

oligodendrocytes: a new resource for understanding brain development and function. *J. Neurosci.* **28**, 264-278.

Camicioli, R., Rajput, A., Rajput, M., Reece, C., Payami, H., Hao, C., & Rajput, A. (2005). Apolipoprotein E epsilon4 and catechol-O-methyltransferase alleles in autopsy-proven Parkinson's disease: relationship to dementia and hallucinations. *Mov Disord.* **20**, 989-994.

Camps, M., Nichols, A., Gillieron, C., Antonsson, B., Muda, M., Chabert, C., Boschert, U., & Arkinstall, S. (1998). Catalytic activation of the phosphatase MKP-3 by ERK2 mitogen-activated protein kinase. *Science* **280**, 1262-1265.

Canet-Aviles, R.M., Wilson, M.A., Miller, D.W., Ahmad, R., McLendon, C., Bandyopadhyay, S., Baptista, M.J., Ringe, D., Petsko, G.A., & Cookson, M.R. (2004). The Parkinson's disease protein DJ-1 is neuroprotective due to cysteine-sulfinic acid-driven mitochondrial localization. *Proc. Natl. Acad. Sci. U. S. A* **101**, 9103-9108.

Cantuti-Castelvetri, I., Keller-McGandy, C., Bouzou, B., Asteris, G., Clark, T.W., Frosch, M.P., & Standaert, D.G. (2007). Effects of gender on nigral gene expression and parkinson disease. *Neurobiol. Dis.* **26**, 606-614.

Cash, R., Dennis, T., L'Heureux, R., Raisman, R., Javoy-Agid, F., & Scatton, B. (1987). Parkinson's disease and dementia: norepinephrine and dopamine in locus ceruleus. *Neurology* **37**, 42-46.

Cesari, R., Martin, E.S., Calin, G.A., Pentimalli, F., Bichi, R., McAdams, H., Trapasso, F., Drusco, A., Shimizu, M., Masciullo, V., D'Andrilli, G., Scambia, G., Picchio, M.C., Alder, H., Godwin, A.K., & Croce, C.M. (2003). Parkin, a gene implicated in autosomal recessive juvenile parkinsonism, is a candidate tumor suppressor gene on chromosome 6q25-q27. *Proc. Natl. Acad. Sci. U. S. A* **100**, 5956-5961.

Chan, C.S., Guzman, J.N., Ilijic, E., Mercer, J.N., Rick, C., Tkatch, T., Meredith, G.E., & Surmeier, D.J. (2007). 'Rejuvenation' protects neurons in mouse models of Parkinson's disease. *Nature* **447**, 1081-1086.

Chan, D.W., Liu, V.W., Tsao, G.S., Yao, K.M., Furukawa, T., Chan, K.K., & Ngan, H.Y. (2008). Loss of MKP3 mediated by oxidative stress enhances tumorigenicity and chemoresistance of ovarian cancer cells. *Carcinogenesis* **29**, 1742-1750.

Chartier-Harlin, M.C., Kachergus, J., Roumier, C., Mouroux, V., Douay, X., Lincoln, S., Levecque, C., Larvor, L., Andrieux, J., Hulihan, M., Waucquier, N., Defebvre, L.,

Amouyel, P., Farrer, M., & Destee, A. (2004). Alpha-synuclein locus duplication as a cause of familial Parkinson's disease. *Lancet* **364**, 1167-1169.

Chasman, D.I., Pare, G., Mora, S., Hopewell, J.C., Peloso, G., Clarke, R., Cupples, L.A., Hamsten, A., Kathiresan, S., Malarstig, A., Ordovas, J.M., Ripatti, S., Parker, A.N., Miletich, J.P., & Ridker, P.M. (2009). Forty-three loci associated with plasma lipoprotein size, concentration, and cholesterol content in genome-wide analysis. *PLoS. Genet.* **5**, e1000730.

Chen, J. & Berry, M.J. (2003). Selenium and selenoproteins in the brain and brain diseases. *J. Neurochem.* **86**, 1-12.

Chen, J., Lipska, B.K., Halim, N., Ma, Q.D., Matsumoto, M., Melhem, S., Kolachana, B.S., Hyde, T.M., Herman, M.M., Apud, J., Egan, M.F., Kleinman, J.E., & Weinberger, D.R. (2004). Functional analysis of genetic variation in catechol-O-methyltransferase (COMT): effects on mRNA, protein, and enzyme activity in postmortem human brain. *Am. J. Hum. Genet.* **75**, 807-821.

Chen, L., Cagniard, B., Mathews, T., Jones, S., Koh, H.C., Ding, Y., Carvey, P.M., Ling, Z., Kang, U.J., & Zhuang, X. (2005). Age-dependent motor deficits and dopaminergic dysfunction in DJ-1 null mice. *J. Biol. Chem.* **280**, 21418-21426.

Chen, L. & Feany, M.B. (2005). Alpha-synuclein phosphorylation controls neurotoxicity and inclusion formation in a Drosophila model of Parkinson disease. *Nat. Neurosci.* **8**, 657-663.

Chen, L., Periquet, M., Wang, X., Negro, A., McLean, P.J., Hyman, B.T., & Feany, M.B. (2009). Tyrosine and serine phosphorylation of alpha-synuclein have opposing effects on neurotoxicity and soluble oligomer formation. *J. Clin. Invest* **119**, 3257-3265.

Chen, L., Thiruchelvam, M.J., Madura, K., & Richfield, E.K. (2006). Proteasome dysfunction in aged human alpha-synuclein transgenic mice. *Neurobiol. Dis.* **23**, 120-126.

Chenard, C.A. & Richard, S. (2008). New implications for the QUAKING RNA binding protein in human disease. *J. Neurosci. Res.* **86**, 233-242.

Cheung, V.G., Spielman, R.S., Ewens, K.G., Weber, T.M., Morley, M., & Burdick, J.T. (2005). Mapping determinants of human gene expression by regional and genome-wide association. *Nature* **437**, 1365-1369.

Chiba-Falek, O., Lopez, G.J., & Nussbaum, R.L. (2006). Levels of alpha-synuclein mRNA in sporadic Parkinson disease patients. *Mov Disord.* **21**, 1703-1708.

Chiba-Falek, O. & Nussbaum, R.L. (2001). Effect of allelic variation at the NACP-Rep1 repeat upstream of the alpha-synuclein gene (SNCA) on transcription in a cell culture luciferase reporter system. *Hum. Mol. Genet.* **10**, 3101-3109.

Chu, C.T., Levinthal, D.J., Kulich, S.M., Chalovich, E.M., & DeFranco, D.B. (2004). Oxidative neuronal injury. The dark side of ERK1/2. *Eur. J. Biochem.* **271**, 2060-2066.

Chu, Y., Dodiya, H., Aebischer, P., Olanow, C.W., & Kordower, J.H. (2009). Alterations in lysosomal and proteasomal markers in Parkinson's disease: relationship to alpha-synuclein inclusions. *Neurobiol. Dis.* **35**, 385-398.

Chung, C., Tallerico, T., & Seeman, P. (2003). Schizophrenia hippocampus has elevated expression of chondrex glycoprotein gene. *Synapse* **50**, 29-34.

Churchyard, A. & Lees, A.J. (1997). The relationship between dementia and direct involvement of the hippocampus and amygdala in Parkinson's disease. *Neurology* **49**, 1570-1576.

Clark, I.E., Dodson, M.W., Jiang, C., Cao, J.H., Huh, J.R., Seol, J.H., Yoo, S.J., Hay, B.A., & Guo, M. (2006). Drosophila pink1 is required for mitochondrial function and interacts genetically with parkin. *Nature* **441**, 1162-1166.

Clement, J.F., Meloche, S., & Servant, M.J. (2008). The IKK-related kinases: from innate immunity to oncogenesis. *Cell Res.* **18**, 889-899.

Collin, R.W., Chellappa, R., Pauw, R.J., Vriend, G., Oostrik, J., van, D.W., Huygen, P.L., Admiraal, R., Hoefsloot, L.H., Cremers, F.P., Xiang, M., Cremers, C.W., & Kremer, H. (2008). Missense mutations in POU4F3 cause autosomal dominant hearing impairment DFNA15 and affect subcellular localization and DNA binding. *Hum. Mutat.* **29**, 545-554.

Colosimo, C., Hughes, A.J., Kilford, L., & Lees, A.J. (2003). Lewy body cortical involvement may not always predict dementia in Parkinson's disease. *J. Neurol. Neurosurg. Psychiatry* **74**, 852-856.

Colucci-D'Amato, L., Perrone-Capano, C., & di, P.U. (2003). Chronic activation of ERK and neurodegenerative diseases. *Bioessays* **25**, 1085-1095.

Conway, K.A., Harper, J.D., & Lansbury, P.T. (1998). Accelerated in vitro fibril formation by a mutant alpha-synuclein linked to early-onset Parkinson disease. *Nat. Med.* **4**, 1318-1320.

Conway, K.A., Lee, S.J., Rochet, J.C., Ding, T.T., Williamson, R.E., & Lansbury, P.T., Jr. (2000). Acceleration of oligomerization, not fibrillization, is a shared property of both alpha-synuclein mutations linked to early-onset Parkinson's disease: implications for pathogenesis and therapy. *Proc. Natl. Acad. Sci. U. S. A* **97**, 571-576.

Conway, K.A., Rochet, J.C., Bieganski, R.M., & Lansbury, P.T., Jr. (2001). Kinetic stabilization of the alpha-synuclein protofibril by a dopamine-alpha-synuclein adduct. *Science* **294**, 1346-1349.

Cools, R. (2006). Dopaminergic modulation of cognitive function-implications for L-DOPA treatment in Parkinson's disease. *Neurosci. Biobehav. Rev.* **30**, 1-23.

Cools, R., Stefanova, E., Barker, R.A., Robbins, T.W., & Owen, A.M. (2002). Dopaminergic modulation of high-level cognition in Parkinson's disease: the role of the prefrontal cortex revealed by PET. *Brain* **125**, 584-594.

Cooper, A.A., Gitler, A.D., Cashikar, A., Haynes, C.M., Hill, K.J., Bhullar, B., Liu, K., Xu, K., Strathearn, K.E., Liu, F., Cao, S., Caldwell, K.A., Caldwell, G.A., Marsischky, G., Kolodner, R.D., Labaer, J., Rochet, J.C., Bonini, N.M., & Lindquist, S. (2006). Alpha-synuclein blocks ER-Golgi traffic and Rab1 rescues neuron loss in Parkinson's models. *Science* **313**, 324-328.

Cooper, J.A. & Sagar, H.J. (1993). Encoding deficits in untreated Parkinson's disease. *Cortex* **29**, 251-265.

Cooper, J.A., Sagar, H.J., Jordan, N., Harvey, N.S., & Sullivan, E.V. (1991). Cognitive impairment in early, untreated Parkinson's disease and its relationship to motor disability. *Brain* **114 (Pt 5)**, 2095-2122.

Cooperman, S.S., Meyron-Holtz, E.G., Olivierre-Wilson, H., Ghosh, M.C., McConnell, J.P., & Rouault, T.A. (2005). Microcytic anemia, erythropoietic protoporphyria, and neurodegeneration in mice with targeted deletion of iron-regulatory protein 2. *Blood* **106**, 1084-1091.

Costa-Mattioli, M., Gobert, D., Harding, H., Herdy, B., Azzi, M., Bruno, M., Bidinosti, M., Ben, M.C., Marcinkiewicz, E., Yoshida, M., Imataka, H., Cuello, A.C., Seidah, N., Sossin, W., Lacaille, J.C., Ron, D., Nader, K., & Sonenberg, N. (2005). Translational control of hippocampal synaptic plasticity and memory by the eIF2alpha kinase GCN2. *Nature* **436**, 1166-1173.

Coutureau, E. & Di Scala, G. (2009). Entorhinal cortex and cognition. *Prog. Neuropsychopharmacol. Biol. Psychiatry* **33**, 753-761.

Crichton, R.R., Wilmet, S., Legssyer, R., & Ward, R.J. (2002). Molecular and cellular mechanisms of iron homeostasis and toxicity in mammalian cells. *J. Inorg. Biochem.* **91**, 9-18.

Croisier, E. & Graeber, M.B. (2006). Glial degeneration and reactive gliosis in alpha-synucleinopathies: the emerging concept of primary gliodegeneration. *Acta Neuropathol.* **112**, 517-530.

Crossman,A.R. & Neary,D. (2005). *Neuroanatomy.* Elsevier Churchill Livingstone, London.

Cuervo, A.M., Stefanis, L., Fredenburg, R., Lansbury, P.T., & Sulzer, D. (2004). Impaired degradation of mutant alpha-synuclein by chaperone-mediated autophagy. *Science* **305**, 1292-1295.

Dachsel, J.C., Lincoln, S.J., Gonzalez, J., Ross, O.A., Dickson, D.W., & Farrer, M.J. (2007). The ups and downs of alpha-synuclein mRNA expression. *Mov Disord.* **22**, 293-295.

Dagda, R.K., Zhu, J., Kulich, S.M., & Chu, C.T. (2008). Mitochondrially localized ERK2 regulates mitophagy and autophagic cell stress: implications for Parkinson's disease. *Autophagy.* **4**, 770-782.

Darios, F., Corti, O., Lucking, C.B., Hampe, C., Muriel, M.P., Abbas, N., Gu, W.J., Hirsch, E.C., Rooney, T., Ruberg, M., & Brice, A. (2003). Parkin prevents mitochondrial swelling and cytochrome c release in mitochondria-dependent cell death. *Hum. Mol. Genet.* **12**, 517-526.

Dauer, W., Kholodilov, N., Vila, M., Trillat, A.C., Goodchild, R., Larsen, K.E., Staal, R., Tieu, K., Schmitz, Y., Yuan, C.A., Rocha, M., Jackson-Lewis, V., Hersch, S., Sulzer, D., Przedborski, S., Burke, R., & Hen, R. (2002). Resistance of alpha - synuclein null mice to the parkinsonian neurotoxin MPTP. *Proc. Natl. Acad. Sci. U. S. A* **99**, 14524-14529.

de Bakker, P.I., Yelensky, R., Pe'er, I., Gabriel, S.B., Daly, M.J., & Altshuler, D. (2005). Efficiency and power in genetic association studies. *Nat. Genet.* **37**, 1217-1223.

de Lau, L.M., Schipper, C.M., Hofman, A., Koudstaal, P.J., & Breteler, M.M. (2005). Prognosis of Parkinson disease: risk of dementia and mortality: the Rotterdam Study. *Arch. Neurol.* **62**, 1265-1269.

De Marco, E.V., Tarantino, P., Rocca, F.E., Provenzano, G., Civitelli, D., De, L., V, Annesi, F., Carrideo, S., Ciro, C., I, Romeo, N., Nicoletti, G., Marconi, R., Novellino, F., Morelli, M., Quattrone, A., & Annesi, G. (2008). Alpha-synuclein promoter haplotypes and dementia in Parkinson's disease. *Am. J. Med. Genet. B Neuropsychiatr. Genet.* **147**, 403-407.

Decamp, E. & Schneider, J.S. (2004). Attention and executive function deficits in chronic low-dose MPTP-treated non-human primates. *Eur. J. Neurosci.* **20**, 1371-1378.

DePaolo, J., Goker-Alpan, O., Samaddar, T., Lopez, G., & Sidransky, E. (2009). The association between mutations in the lysosomal protein glucocerebrosidase and parkinsonism. *Mov Disord.* **24**, 1571-1578.

Desplats, P., Lee, H.J., Bae, E.J., Patrick, C., Rockenstein, E., Crews, L., Spencer, B., Masliah, E., & Lee, S.J. (2009). Inclusion formation and neuronal cell death through neuron-to-neuron transmission of alpha-synuclein. *Proc. Natl. Acad. Sci. U. S. A* **106**, 13010-13015.

Dexter, D.T., Carter, C.J., Wells, F.R., Javoy-Agid, F., Agid, Y., Lees, A., Jenner, P., & Marsden, C.D. (1989). Basal lipid peroxidation in substantia nigra is increased in Parkinson's disease. *J. Neurochem.* **52**, 381-389.

Di Fonzo A., Chien, H.F., Socal, M., Giraudo, S., Tassorelli, C., Iliceto, G., Fabbrini, G., Marconi, R., Fincati, E., Abbruzzese, G., Marini, P., Squitieri, F., Horstink, M.W., Montagna, P., Libera, A.D., Stocchi, F., Goldwurm, S., Ferreira, J.J., Meco, G., Martignoni, E., Lopiano, L., Jardim, L.B., Oostra, B.A., Barbosa, E.R., & Bonifati, V. (2007). ATP13A2 missense mutations in juvenile parkinsonism and young onset Parkinson disease. *Neurology* **68**, 1557-1562.

Diaz-Hernandez, M., Hernandez, F., Martin-Aparicio, E., Gomez-Ramos, P., Moran, M.A., Castano, J.G., Ferrer, I., Avila, J., & Lucas, J.J. (2003). Neuronal induction of the immunoproteasome in Huntington's disease. *J. Neurosci.* **23**, 11653-11661.

Dick, F.D., De, P.G., Ahmadi, A., Scott, N.W., Prescott, G.J., Bennett, J., Semple, S., Dick, S., Counsell, C., Mozzoni, P., Haites, N., Wettinger, S.B., Mutti, A., Otelea, M., Seaton, A., Soderkvist, P., & Felice, A. (2007). Environmental risk factors for Parkinson's disease and parkinsonism: the Geoparkinson study. *Occup. Environ. Med.* **64**, 666-672.

Dickey, C.A., Loring, J.F., Montgomery, J., Gordon, M.N., Eastman, P.S., & Morgan, D. (2003). Selectively reduced expression of synaptic plasticity-related genes in amyloid precursor protein + presenilin-1 transgenic mice. *J. Neurosci.* **23**, 5219-5226.

Dixon, A.L., Liang, L., Moffatt, M.F., Chen, W., Heath, S., Wong, K.C., Taylor, J., Burnett, E., Gut, I., Farrall, M., Lathrop, G.M., Abecasis, G.R., & Cookson, W.O. (2007). A genome-wide association study of global gene expression. *Nat. Genet.* **39**, 1202-1207.

Downes, J.J., Priestley, N.M., Doran, M., Ferran, J., Ghadiali, E., & Cooper, P. (1998). Intellectual, mnemonic, and frontal functions in dementia with Lewy bodies: A comparison with early and advanced Parkinson's disease. *Behav. Neurol.* **11**, 173-183.

Dronkers, N.F., Wilkins, D.P., Van, V.R., Jr., Redfern, B.B., & Jaeger, J.J. (2004). Lesion analysis of the brain areas involved in language comprehension. *Cognition* **92**, 145-177.

Dubnau, J., Chiang, A.S., Grady, L., Barditch, J., Gossweiler, S., McNeil, J., Smith, P., Buldoc, F., Scott, R., Certa, U., Broger, C., & Tully, T. (2003). The staufen/pumilio pathway is involved in Drosophila long-term memory. *Curr. Biol.* **13**, 286-296.

Dubois, B. & Pillon, B. (1997). Cognitive deficits in Parkinson's disease. *J. Neurol.* **244**, 2-8.

Duda, J.E., Giasson, B.I., Mabon, M.E., Lee, V.M., & Trojanowski, J.Q. (2002a). Novel antibodies to synuclein show abundant striatal pathology in Lewy body diseases. *Ann. Neurol.* **52**, 205-210.

Duda, J.E., Giasson, B.I., Mabon, M.E., Miller, D.C., Golbe, L.I., Lee, V.M., & Trojanowski, J.Q. (2002b). Concurrence of alpha-synuclein and tau brain pathology in the Contursi kindred. *Acta Neuropathol.* **104**, 7-11.

Easty, D.J., Guthrie, B.A., Maung, K., Farr, C.J., Lindberg, R.A., Toso, R.J., Herlyn, M., & Bennett, D.C. (1995). Protein B61 as a new growth factor: expression of B61 and up-regulation of its receptor epithelial cell kinase during melanoma progression. *Cancer Res.* **55**, 2528-2532.

Eblaghie, M.C., Lunn, J.S., Dickinson, R.J., Munsterberg, A.E., Sanz-Ezquerro, J.J., Farrell, E.R., Mathers, J., Keyse, S.M., Storey, K., & Tickle, C. (2003). Negative feedback regulation of FGF signaling levels by Pyst1/MKP3 in chick embryos. *Curr. Biol.* **13**, 1009-1018.

Echevarria, D., Martinez, S., Marques, S., Lucas-Teixeira, V., & Belo, J.A. (2005). Mkp3 is a negative feedback modulator of Fgf8 signaling in the mammalian isthmic organizer. *Dev. Biol.* **277**, 114-128.

Edison, P., Rowe, C.C., Rinne, J.O., Ng, S., Ahmed, I., Kemppainen, N., Villemagne, V.L., O'Keefe, G., Nagren, K., Chaudhury, K.R., Masters, C.L., & Brooks, D.J. (2008). Amyloid load in Parkinson's disease dementia and Lewy body dementia measured with [11C]PIB positron emission tomography. *J. Neurol. Neurosurg. Psychiatry* **79**, 1331-1338.

Edvardson, S., Shaag, A., Kolesnikova, O., Gomori, J.M., Tarassov, I., Einbinder, T., Saada, A., & Elpeleg, O. (2007). Deleterious mutation in the mitochondrial arginyl-transfer RNA synthetase gene is associated with pontocerebellar hypoplasia. *Am. J. Hum. Genet.* **81**, 857-862.

Egan, M.F., Goldberg, T.E., Kolachana, B.S., Callicott, J.H., Mazzanti, C.M., Straub, R.E., Goldman, D., & Weinberger, D.R. (2001). Effect of COMT Val108/158 Met genotype on frontal lobe function and risk for schizophrenia. *Proc. Natl. Acad. Sci. U. S. A* **98**, 6917-6922.

Ekerot, M., Stavridis, M.P., Delavaine, L., Mitchell, M.P., Staples, C., Owens, D.M., Keenan, I.D., Dickinson, R.J., Storey, K.G., & Keyse, S.M. (2008). Negative-feedback regulation of FGF signalling by DUSP6/MKP-3 is driven by ERK1/2 and mediated by Ets factor binding to a conserved site within the DUSP6/MKP-3 gene promoter. *Biochem. J.* **412**, 287-298.

Elstner, M., Morris, C.M., Heim, K., Lichtner, P., Bender, A., Mehta, D., Schulte, C., Sharma, M., Hudson, G., Goldwurm, S., Giovanetti, A., Zeviani, M., Burn, D.J., McKeith, I.G., Perry, R.H., Jaros, E., Kruger, R., Wichmann, H.E., Schreiber, S., Campbell, H., Wilson, J.F., Wright, A.F., Dunlop, M., Pistis, G., Toniolo, D., Chinnery, P.F., Gasser, T., Klopstock, T., Meitinger, T., Prokisch, H., & Turnbull, D.M. (2009). Single-cell expression profiling of dopaminergic neurons combined with association analysis identifies pyridoxal kinase as Parkinson's disease gene. *Ann. Neurol.* **66**, 792-798.

Emre, M. (2003). What causes mental dysfunction in Parkinson's disease? *Mov Disord.* **18 Suppl 6**, S63-S71.

Emre, M., Aarsland, D., Albanese, A., Byrne, E.J., Deuschl, G., De Deyn, P.P., Durif, F., Kulisevsky, J., van, L.T., Lees, A., Poewe, W., Robillard, A., Rosa, M.M., Wolters, E., Quarg, P., Tekin, S., & Lane, R. (2004). Rivastigmine for dementia associated with Parkinson's disease. *N. Engl. J. Med.* **351**, 2509-2518.

Enard, W., Khaitovich, P., Klose, J., Zollner, S., Heissig, F., Giavalisco, P., Nieselt-Struwe, K., Muchmore, E., Varki, A., Ravid, R., Doxiadis, G.M., Bontrop, R.E., & Paabo, S. (2002). Intra- and interspecific variation in primate gene expression patterns. *Science* **296**, 340-343.

Ephraty, L., Porat, O., Israeli, D., Cohen, O.S., Tunkel, O., Yael, S., Hatano, Y., Hattori, N., & Hassin-Baer, S. (2007). Neuropsychiatric and cognitive features in autosomal-recessive early parkinsonism due to PINK1 mutations. *Mov Disord.* **22**, 566-569.

Eslamboli, A., Romero-Ramos, M., Burger, C., Bjorklund, T., Muzyczka, N., Mandel, R.J., Baker, H., Ridley, R.M., & Kirik, D. (2007). Long-term consequences of human alpha-synuclein overexpression in the primate ventral midbrain. *Brain* **130**, 799-815.

Ezquerra, M., Campdelacreu, J., Gaig, C., Compta, Y., Munoz, E., Marti, M.J., Valldeoriola, F., & Tolosa, E. (2008). Lack of association of APOE and tau polymorphisms with dementia in Parkinson's disease. *Neurosci. Lett.* **448**, 20-23.

Fahn, S. (2003). Description of Parkinson's disease as a clinical syndrome. *Ann. N. Y. Acad. Sci.* **991**, 1-14.

Fallin, D., Cohen, A., Essioux, L., Chumakov, I., Blumenfeld, M., Cohen, D., & Schork, N.J. (2001). Genetic analysis of case/control data using estimated haplotype frequencies: application to APOE locus variation and Alzheimer's disease. *Genome Res.* **11**, 143-151.

Fan, Y., Limprasert, P., Murray, I.V., Smith, A.C., Lee, V.M., Trojanowski, J.Q., Sopher, B.L., & La Spada, A.R. (2006). Beta-synuclein modulates alpha-synuclein neurotoxicity by reducing alpha-synuclein protein expression. *Hum. Mol. Genet.* **15**, 3002-3011.

Fang, W.B., Brantley-Sieders, D.M., Parker, M.A., Reith, A.D., & Chen, J. (2005). A kinase-dependent role for EphA2 receptor in promoting tumor growth and metastasis. *Oncogene* **24**, 7859-7868.

Fang, W.B., Ireton, R.C., Zhuang, G., Takahashi, T., Reynolds, A., & Chen, J. (2008). Overexpression of EPHA2 receptor destabilizes adherens junctions via a RhoA-dependent mechanism. *J. Cell Sci.* **121**, 358-368.

Farrer, L.A., Cupples, L.A., Haines, J.L., Hyman, B., Kukull, W.A., Mayeux, R., Myers, R.H., Pericak-Vance, M.A., Risch, N., & van Duijn, C.M. (1997). Effects of age, sex, and ethnicity on the association between apolipoprotein E genotype and

Alzheimer disease. A meta-analysis. APOE and Alzheimer Disease Meta Analysis Consortium. *JAMA* **278**, 1349-1356.

Farrer, M., Kachergus, J., Forno, L., Lincoln, S., Wang, D.S., Hulihan, M., Maraganore, D., Gwinn-Hardy, K., Wszolek, Z., Dickson, D., & Langston, J.W. (2004). Comparison of kindreds with parkinsonism and alpha-synuclein genomic multiplications. *Ann. Neurol.* **55**, 174-179.

Farrer, M., Maraganore, D.M., Lockhart, P., Singleton, A., Lesnick, T.G., de, A.M., West, A., de, S.R., Hardy, J., & Hernandez, D. (2001). alpha-Synuclein gene haplotypes are associated with Parkinson's disease. *Hum. Mol. Genet.* **10**, 1847-1851.

Farrer, M.J. (2006). Genetics of Parkinson disease: paradigm shifts and future prospects. *Nat. Rev. Genet.* **7**, 306-318.

Feany, M.B. & Bender, W.W. (2000). A Drosophila model of Parkinson's disease. *Nature* **404**, 394-398.

Fearnley, J.M. & Lees, A.J. (1991). Ageing and Parkinson's disease: substantia nigra regional selectivity. *Brain* **114 (Pt 5)**, 2283-2301.

Ferrer, I. (2009). Early involvement of the cerebral cortex in Parkinson's disease: convergence of multiple metabolic defects. *Prog. Neurobiol.* **88**, 89-103.

Firbank, M.J., Colloby, S.J., Burn, D.J., McKeith, I.G., & O'Brien, J.T. (2003). Regional cerebral blood flow in Parkinson's disease with and without dementia. *Neuroimage.* **20**, 1309-1319.

Foltynie, T., Brayne, C.E., Robbins, T.W., & Barker, R.A. (2004a). The cognitive ability of an incident cohort of Parkinson's patients in the UK. The CamPaIGN study. *Brain* **127**, 550-560.

Foltynie, T., Goldberg, T.E., Lewis, S.G., Blackwell, A.D., Kolachana, B.S., Weinberger, D.R., Robbins, T.W., & Barker, R.A. (2004b). Planning ability in Parkinson's disease is influenced by the COMT val158met polymorphism. *Mov Disord.* **19**, 885-891.

Foulds, C.E., Nelson, M.L., Blaszczak, A.G., & Graves, B.J. (2004). Ras/mitogen-activated protein kinase signaling activates Ets-1 and Ets-2 by CBP/p300 recruitment. *Mol. Cell Biol.* **24**, 10954-10964.

Frazer, K.A., Ballinger, D.G., Cox, D.R., Hinds, D.A., Stuve, L.L., Gibbs, R.A., Belmont, J.W., Boudreau, A., Hardenbol, P., Leal, S.M., Pasternak, S., Wheeler,

D.A., Willis, T.D., Yu, F., Yang, H., Zeng, C., Gao, Y., Hu, H., Hu, W., Li, C., Lin, W., Liu, S., Pan, H., Tang, X., Wang, J., Wang, W., Yu, J., Zhang, B., Zhang, Q., Zhao, H., Zhao, H., Zhou, J., Gabriel, S.B., Barry, R., Blumenstiel, B., Camargo, A., Defelice, M., Faggart, M., Goyette, M., Gupta, S., Moore, J., Nguyen, H., Onofrio, R.C., Parkin, M., Roy, J., Stahl, E., Winchester, E., Ziaugra, L., Altshuler, D., Shen, Y., Yao, Z., Huang, W., Chu, X., He, Y., Jin, L., Liu, Y., Shen, Y., Sun, W., Wang, H., Wang, Y., Wang, Y., Xiong, X., Xu, L., Waye, M.M., Tsui, S.K., Xue, H., Wong, J.T., Galver, L.M., Fan, J.B., Gunderson, K., Murray, S.S., Oliphant, A.R., Chee, M.S., Montpetit, A., Chagnon, F., Ferretti, V., Leboeuf, M., Olivier, J.F., Phillips, M.S., Roumy, S., Sallee, C., Verner, A., Hudson, T.J., Kwok, P.Y., Cai, D., Koboldt, D.C., Miller, R.D., Pawlikowska, L., Taillon-Miller, P., Xiao, M., Tsui, L.C., Mak, W., Song, Y.Q., Tam, P.K., Nakamura, Y., Kawaguchi, T., Kitamoto, T., Morizono, T., Nagashima, A., Ohnishi, Y., Sekine, A., Tanaka, T., Tsunoda, T., Deloukas, P., Bird, C.P., Delgado, M., Dermitzakis, E.T., Gwilliam, R., Hunt, S., Morrison, J., Powell, D., Stranger, B.E., Whittaker, P., Bentley, D.R., Daly, M.J., de Bakker, P.I., Barrett, J., Chretien, Y.R., Maller, J., McCarroll, S., Patterson, N., Pe'er, I., Price, A., Purcell, S., Richter, D.J., Sabeti, P., Saxena, R., Schaffner, S.F., Sham, P.C., Varilly, P., Altshuler, D., Stein, L.D., Krishnan, L., Smith, A.V., Tello-Ruiz, M.K., Thorisson, G.A., Chakravarti, A., Chen, P.E., Cutler, D.J., Kashuk, C.S., Lin, S., Abecasis, G.R., Guan, W., Li, Y., Munro, H.M., Qin, Z.S., Thomas, D.J., McVean, G., Auton, A., Bottolo, L., Cardin, N., Eyheramendy, S., Freeman, C., Marchini, J., Myers, S., Spencer, C., Stephens, M., Donnelly, P., Cardon, L.R., Clarke, G., Evans, D.M., Morris, A.P., Weir, B.S., Tsunoda, T., Mullikin, J.C., Sherry, S.T., Feolo, M., Skol, A., Zhang, H., Zeng, C., Zhao, H., Matsuda, I., Fukushima, Y., Macer, D.R., Suda, E., Rotimi, C.N., Adebamowo, C.A., Ajayi, I., Aniagwu, T., Marshall, P.A., Nkwodimmah, C., Royal, C.D., Leppert, M.F., Dixon, M., Peiffer, A., Qiu, R., Kent, A., Kato, K., Niikawa, N., Adewole, I.F., Knoppers, B.M., Foster, M.W., Clayton, E.W., Watkin, J., Gibbs, R.A., Belmont, J.W., Muzny, D., Nazareth, L., Sodergren, E., Weinstock, G.M., Wheeler, D.A., Yakub, I., Gabriel, S.B., Onofrio, R.C., Richter, D.J., Ziaugra, L., Birren, B.W., Daly, M.J., Altshuler, D., Wilson, R.K., Fulton, L.L., Rogers, J., Burton, J., Carter, N.P., Clee, C.M., Griffiths, M., Jones, M.C., McLay, K., Plumb, R.W., Ross, M.T., Sims, S.K., Willey, D.L., Chen, Z., Han, H., Kang, L., Godbout, M., Wallenburg, J.C., L'Archeveque, P., Bellemare, G., Saeki, K., Wang, H., An, D., Fu, H., Li, Q., Wang, Z., Wang, R., Holden, A.L., Brooks, L.D., McEwen, J.E., Guyer, M.S., Wang, V.O., Peterson, J.L., Shi, M., Spiegel, J., Sung, L.M., Zacharia, L.F., Collins, F.S., Kennedy, K., Jamieson, R., & Stewart, J. (2007). A second generation human haplotype map of over 3.1 million SNPs. *Nature.* **449**, 851-861.

Freichel, C., Neumann, M., Ballard, T., Muller, V., Woolley, M., Ozmen, L., Borroni, E., Kretzschmar, H.A., Haass, C., Spooren, W., & Kahle, P.J. (2007). Age-dependent cognitive decline and amygdala pathology in alpha-synuclein transgenic mice. *Neurobiol. Aging* **28**, 1421-1435.

Fuchs, J., Nilsson, C., Kachergus, J., Munz, M., Larsson, E.M., Schule, B., Langston, J.W., Middleton, F.A., Ross, O.A., Hulihan, M., Gasser, T., & Farrer, M.J. (2007).

Phenotypic variation in a large Swedish pedigree due to SNCA duplication and triplication. *Neurology* **68**, 916-922.

Fuchs, J., Tichopad, A., Golub, Y., Munz, M., Schweitzer, K.J., Wolf, B., Berg, D., Mueller, J.C., & Gasser, T. (2008). Genetic variability in the SNCA gene influences alpha-synuclein levels in the blood and brain. *FASEB J.* **22**, 1327-1334.

Fujita, M., Sekigawa, A., Sekiyama, K., Sugama, S., & Hashimoto, M. (2009). Neurotoxic conversion of beta-synuclein: a novel approach to generate a transgenic mouse model of synucleinopathies? *J. Neurol.* **256 Suppl 3**, 286-292.

Fujiwara, H., Hasegawa, M., Dohmae, N., Kawashima, A., Masliah, E., Goldberg, M.S., Shen, J., Takio, K., & Iwatsubo, T. (2002). alpha-Synuclein is phosphorylated in synucleinopathy lesions. *Nat. Cell Biol.* **4**, 160-164.

Fung, H.C., Scholz, S., Matarin, M., Simon-Sanchez, J., Hernandez, D., Britton, A., Gibbs, J.R., Langefeld, C., Stiegert, M.L., Schymick, J., Okun, M.S., Mandel, R.J., Fernandez, H.H., Foote, K.D., Rodriguez, R.L., Peckham, E., De Vrieze, F.W., Gwinn-Hardy, K., Hardy, J.A., & Singleton, A. (2006). Genome-wide genotyping in Parkinson's disease and neurologically normal controls: first stage analysis and public release of data. *Lancet Neurol.* **5**, 911-916.

Furukawa, T., Sunamura, M., Motoi, F., Matsuno, S., & Horii, A. (2003). Potential tumor suppressive pathway involving DUSP6/MKP-3 in pancreatic cancer. *Am. J. Pathol.* **162**, 1807-1815.

Furukawa, T., Tanji, E., Xu, S., & Horii, A. (2008). Feedback regulation of DUSP6 transcription responding to MAPK1 via ETS2 in human cells. *Biochem. Biophys. Res. Commun.* **377**, 317-320.

Furukawa, T., Yatsuoka, T., Youssef, E.M., Abe, T., Yokoyama, T., Fukushige, S., Soeda, E., Hoshi, M., Hayashi, Y., Sunamura, M., Kobari, M., & Horii, A. (1998). Genomic analysis of DUSP6, a dual specificity MAP kinase phosphatase, in pancreatic cancer. *Cytogenet. Cell Genet.* **82**, 156-159.

Gallardo, G., Schluter, O.M., & Sudhof, T.C. (2008). A molecular pathway of neurodegeneration linking alpha-synuclein to ApoE and Abeta peptides. *Nat. Neurosci.* **11**, 301-308.

Galter, D., Westerlund, M., Belin, A.C., & Olson, L. (2007). DJ-1 and UCH-L1 gene activity patterns in the brains of controls, Parkinson and schizophrenia patients and in rodents. *Physiol Behav.* **92**, 46-53.

Galter, D., Westerlund, M., Carmine, A., Lindqvist, E., Sydow, O., & Olson, L. (2006). LRRK2 expression linked to dopamine-innervated areas. *Ann. Neurol.* **59**, 714-719.

Galvin, J.E., Uryu, K., Lee, V.M., & Trojanowski, J.Q. (1999). Axon pathology in Parkinson's disease and Lewy body dementia hippocampus contains alpha-, beta-, and gamma-synuclein. *Proc. Natl. Acad. Sci. U. S. A* **96**, 13450-13455.

Gandhi, S., Muqit, M.M., Stanyer, L., Healy, D.G., Abou-Sleiman, P.M., Hargreaves, I., Heales, S., Ganguly, M., Parsons, L., Lees, A.J., Latchman, D.S., Holton, J.L., Wood, N.W., & Revesz, T. (2006). PINK1 protein in normal human brain and Parkinson's disease. *Brain* **129**, 1720-1731.

Gandhi, S., Wood-Kaczmar, A., Yao, Z., Plun-Favreau, H., Deas, E., Klupsch, K., Downward, J., Latchman, D.S., Tabrizi, S.J., Wood, N.W., Duchen, M.R., & Abramov, A.Y. (2009). PINK1-associated Parkinson's disease is caused by neuronal vulnerability to calcium-induced cell death. *Mol. Cell* **33**, 627-638.

Gautier, C.A., Kitada, T., & Shen, J. (2008). Loss of PINK1 causes mitochondrial functional defects and increased sensitivity to oxidative stress. *Proc. Natl. Acad. Sci. U. S. A* **105**, 11364-11369.

Ge, B., Pokholok, D.K., Kwan, T., Grundberg, E., Morcos, L., Verlaan, D.J., Le, J., Koka, V., Lam, K.C., Gagne, V., Dias, J., Hoberman, R., Montpetit, A., Joly, M.M., Harvey, E.J., Sinnett, D., Beaulieu, P., Hamon, R., Graziani, A., Dewar, K., Harmsen, E., Majewski, J., Goring, H.H., Naumova, A.K., Blanchette, M., Gunderson, K.L., & Pastinen, T. (2009). Global patterns of cis variation in human cells revealed by high-density allelic expression analysis. *Nat. Genet.* **41**, 1216-1222.

Geering, K. (2006). FXYD proteins: new regulators of Na-K-ATPase. *Am. J. Physiol Renal Physiol* **290**, F241-F250.

Gentleman, R.C., Carey, V.J., Bates, D.M., Bolstad, B., Dettling, M., Dudoit, S., Ellis, B., Gautier, L., Ge, Y., Gentry, J., Hornik, K., Hothorn, T., Huber, W., Iacus, S., Irizarry, R., Leisch, F., Li, C., Maechler, M., Rossini, A.J., Sawitzki, G., Smith, C., Smyth, G., Tierney, L., Yang, J.Y., & Zhang, J. (2004). Bioconductor: open software development for computational biology and bioinformatics. *Genome Biol.* **5**, R80.

Ghosh, A., Roy, A., Liu, X., Kordower, J.H., Mufson, E.J., Hartley, D.M., Ghosh, S., Mosley, R.L., Gendelman, H.E., & Pahan, K. (2007). Selective inhibition of NF-kappaB activation prevents dopaminergic neuronal loss in a mouse model of Parkinson's disease. *Proc. Natl. Acad. Sci. U. S. A* **104**, 18754-18759.

Giasson, B.I., Duda, J.E., Quinn, S.M., Zhang, B., Trojanowski, J.Q., & Lee, V.M. (2002). Neuronal alpha-synucleinopathy with severe movement disorder in mice expressing A53T human alpha-synuclein. *Neuron* **34**, 521-533.

Giasson, B.I., Forman, M.S., Higuchi, M., Golbe, L.I., Graves, C.L., Kotzbauer, P.T., Trojanowski, J.Q., & Lee, V.M. (2003). Initiation and synergistic fibrillization of tau and alpha-synuclein. *Science* **300**, 636-640.

Gilad, Y., Oshlack, A., Smyth, G.K., Speed, T.P., & White, K.P. (2006). Expression profiling in primates reveals a rapid evolution of human transcription factors. *Nature* **440**, 242-245.

Girotti, F., Soliveri, P., Carella, F., Piccolo, I., Caffarra, P., Musicco, M., & Caraceni, T. (1988). Dementia and cognitive impairment in Parkinson's disease. *J. Neurol. Neurosurg. Psychiatry* **51**, 1498-1502.

Gispert, S., Ricciardi, F., Kurz, A., Azizov, M., Hoepken, H.H., Becker, D., Voos, W., Leuner, K., Muller, W.E., Kudin, A.P., Kunz, W.S., Zimmermann, A., Roeper, J., Wenzel, D., Jendrach, M., Garcia-Arencibia, M., Fernandez-Ruiz, J., Huber, L., Rohrer, H., Barrera, M., Reichert, A.S., Rub, U., Chen, A., Nussbaum, R.L., & Auburger, G. (2009). Parkinson phenotype in aged PINK1-deficient mice is accompanied by progressive mitochondrial dysfunction in absence of neurodegeneration. *PLoS. ONE.* **4**, e5777.

Gitler, A.D., Chesi, A., Geddie, M.L., Strathearn, K.E., Hamamichi, S., Hill, K.J., Caldwell, K.A., Caldwell, G.A., Cooper, A.A., Rochet, J.C., & Lindquist, S. (2009). Alpha-synuclein is part of a diverse and highly conserved interaction network that includes PARK9 and manganese toxicity. *Nat. Genet.* **41**, 308-315.

Giulietti, A., Overbergh, L., Valckx, D., Decallonne, B., Bouillon, R., & Mathieu, C. (2001). An overview of real-time quantitative PCR: applications to quantify cytokine gene expression. *Methods* **25**, 386-401.

Goetz, C.G., Emre, M., & Dubois, B. (2008). Parkinson's disease dementia: definitions, guidelines, and research perspectives in diagnosis. *Ann. Neurol.* **64 Suppl 2**, S81-S92.

Goker-Alpan, O., Giasson, B.I., Eblan, M.J., Nguyen, J., Hurtig, H.I., Lee, V.M., Trojanowski, J.Q., & Sidransky, E. (2006). Glucocerebrosidase mutations are an important risk factor for Lewy body disorders. *Neurology* **67**, 908-910.

Goker-Alpan, O., Lopez, G., Vithayathil, J., Davis, J., Hallett, M., & Sidransky, E. (2008). The spectrum of parkinsonian manifestations associated with glucocerebrosidase mutations. *Arch. Neurol.* **65**, 1353-1357.

Goldberg, M.S., Pisani, A., Haburcak, M., Vortherms, T.A., Kitada, T., Costa, C., Tong, Y., Martella, G., Tscherter, A., Martins, A., Bernardi, G., Roth, B.L., Pothos, E.N., Calabresi, P., & Shen, J. (2005). Nigrostriatal dopaminergic deficits and hypokinesia caused by inactivation of the familial Parkinsonism-linked gene DJ-1. *Neuron* **45**, 489-496.

Goldring, M.B., Otero, M., Tsuchimochi, K., Ijiri, K., & Li, Y. (2008). Defining the roles of inflammatory and anabolic cytokines in cartilage metabolism. *Ann. Rheum. Dis.* **67 Suppl 3**, iii75-iii82.

Goldstein, M.E., Sternberger, L.A., & Sternberger, N.H. (1983). Microheterogeneity ("neurotypy") of neurofilament proteins. *Proc. Natl. Acad. Sci. U. S. A* **80**, 3101-3105.

Goldwurm, S., Zini, M., Di, F.A., De, G.D., Siri, C., Simons, E.J., van, D.M., Tesei, S., Antonini, A., Canesi, M., Zecchinelli, A., Mariani, C., Meucci, N., Sacilotto, G., Cilia, R., Isaias, I.U., Bonetti, A., Sironi, F., Ricca, S., Oostra, B.A., Bonifati, V., & Pezzoli, G. (2006). LRRK2 G2019S mutation and Parkinson's disease: a clinical, neuropsychological and neuropsychiatric study in a large Italian sample. *Parkinsonism. Relat Disord.* **12**, 410-419.

Gomez, A.R., Lopez-Varea, A., Molnar, C., de, l.C.-M., Ruiz-Gomez, M., Gomez-Skarmeta, J.L., & de Celis, J.F. (2005). Conserved cross-interactions in Drosophila and Xenopus between Ras/MAPK signaling and the dual-specificity phosphatase MKP3. *Dev. Dyn.* **232**, 695-708.

Gorbatyuk, O.S., Li, S., Sullivan, L.F., Chen, W., Kondrikova, G., Manfredsson, F.P., Mandel, R.J., & Muzyczka, N. (2008). The phosphorylation state of Ser-129 in human alpha-synuclein determines neurodegeneration in a rat model of Parkinson disease. *Proc. Natl. Acad. Sci. U. S. A* **105**, 763-768.

Gorell, J.M., Peterson, E.L., Rybicki, B.A., & Johnson, C.C. (2004). Multiple risk factors for Parkinson's disease. *J. Neurol. Sci.* **217**, 169-174.

Goring, H.H., Curran, J.E., Johnson, M.P., Dyer, T.D., Charlesworth, J., Cole, S.A., Jowett, J.B., Abraham, L.J., Rainwater, D.L., Comuzzie, A.G., Mahaney, M.C., Almasy, L., MacCluer, J.W., Kissebah, A.H., Collier, G.R., Moses, E.K., & Blangero, J. (2007). Discovery of expression QTLs using large-scale transcriptional profiling in human lymphocytes. *Nat. Genet.* **39**, 1208-1216.

Goris, A., Williams-Gray, C.H., Clark, G.R., Foltynie, T., Lewis, S.J., Brown, J., Ban, M., Spillantini, M.G., Compston, A., Burn, D.J., Chinnery, P.F., Barker, R.A., & Sawcer, S.J. (2007). Tau and alpha-synuclein in susceptibility to, and dementia in, Parkinson's disease. *Ann. Neurol.* **62**, 145-153.

Gozdz, A., Vashishta, A., Kalita, K., Szatmari, E., Zheng, J.J., Tamiya, S., Delamere, N.A., & Hetman, M. (2008). Cisplatin-mediated activation of extracellular signal-regulated kinases 1/2 (ERK1/2) by inhibition of ERK1/2 phosphatases. *J. Neurochem.* **106**, 2056-2067.

Greene, J.C., Whitworth, A.J., Kuo, I., Andrews, L.A., Feany, M.B., & Pallanck, L.J. (2003). Mitochondrial pathology and apoptotic muscle degeneration in Drosophila parkin mutants. *Proc. Natl. Acad. Sci. U. S. A* **100**, 4078-4083.

Greffard, S., Verny, M., Bonnet, A.M., Beinis, J.Y., Gallinari, C., Meaume, S., Piette, F., Hauw, J.J., & Duyckaerts, C. (2006). Motor score of the Unified Parkinson Disease Rating Scale as a good predictor of Lewy body-associated neuronal loss in the substantia nigra. *Arch. Neurol.* **63**, 584-588.

Greffard, S., Verny, M., Bonnet, A.M., Seilhean, D., Hauw, J.J., & Duyckaerts, C. (2010). A stable proportion of Lewy body bearing neurons in the substantia nigra suggests a model in which the Lewy body causes neuronal death. *Neurobiol. Aging* **31**, 99-103.

Grenda, D.S., Murakami, M., Ghatak, J., Xia, J., Boxer, L.A., Dale, D., Dinauer, M.C., & Link, D.C. (2007). Mutations of the ELA2 gene found in patients with severe congenital neutropenia induce the unfolded protein response and cellular apoptosis. *Blood* **110**, 4179-4187.

Griffiths-Jones, S., Saini, H.K., van, D.S., & Enright, A.J. (2008). miRBase: tools for microRNA genomics. *Nucleic Acids Res.* **36**, D154-D158.

Gruber, O., Indefrey, P., Steinmetz, H., & Kleinschmidt, A. (2001). Dissociating neural correlates of cognitive components in mental calculation. *Cereb. Cortex* **11**, 350-359.

Grunblatt, E., Mandel, S., Jacob-Hirsch, J., Zeligson, S., Amariglo, N., Rechavi, G., Li, J., Ravid, R., Roggendorf, W., Riederer, P., & Youdim, M.B. (2004). Gene expression profiling of parkinsonian substantia nigra pars compacta; alterations in ubiquitin-proteasome, heat shock protein, iron and oxidative stress regulated proteins, cell adhesion/cellular matrix and vesicle trafficking genes. *J. Neural Transm.* **111**, 1543-1573.

Grundemann, J., Schlaudraff, F., Haeckel, O., & Liss, B. (2008). Elevated alpha-synuclein mRNA levels in individual UV-laser-microdissected dopaminergic substantia nigra neurons in idiopathic Parkinson's disease. *Nucleic Acids Res.* **36**, e38.

Guan, K.L. & Butch, E. (1995). Isolation and characterization of a novel dual specific phosphatase, HVH2, which selectively dephosphorylates the mitogen-activated protein kinase. *J. Biol. Chem.* **270**, 7197-7203.

Guo, H., Miao, H., Gerber, L., Singh, J., Denning, M.F., Gilliam, A.C., & Wang, B. (2006). Disruption of EphA2 receptor tyrosine kinase leads to increased susceptibility to carcinogenesis in mouse skin. *Cancer Res.* **66**, 7050-7058.

Halliday, G., Hely, M., Reid, W., & Morris, J. (2008). The progression of pathology in longitudinally followed patients with Parkinson's disease. *Acta Neuropathol.* **115**, 409-415.

Harding, A.J., Broe, G.A., & Halliday, G.M. (2002). Visual hallucinations in Lewy body disease relate to Lewy bodies in the temporal lobe. *Brain* **125**, 391-403.

Harding, A.J. & Halliday, G.M. (2001). Cortical Lewy body pathology in the diagnosis of dementia. *Acta Neuropathol.* **102**, 355-363.

Harding, H.P., Zhang, Y., Bertolotti, A., Zeng, H., & Ron, D. (2000). Perk is essential for translational regulation and cell survival during the unfolded protein response. *Mol. Cell* **5**, 897-904.

Hardy, J. (2005). Expression of normal sequence pathogenic proteins for neurodegenerative disease contributes to disease risk: 'permissive templating' as a general mechanism underlying neurodegeneration. *Biochem. Soc. Trans.* **33**, 578-581.

Hashimoto, M., Rockenstein, E., Mante, M., Mallory, M., & Masliah, E. (2001). beta-Synuclein inhibits alpha-synuclein aggregation: a possible role as an anti-parkinsonian factor. *Neuron* **32**, 213-223.

Hauser, M.A., Li, Y.J., Xu, H., Noureddine, M.A., Shao, Y.S., Gullans, S.R., Scherzer, C.R., Jensen, R.V., McLaurin, A.C., Gibson, J.R., Scott, B.L., Jewett, R.M., Stenger, J.E., Schmechel, D.E., Hulette, C.M., & Vance, J.M. (2005). Expression profiling of substantia nigra in Parkinson disease, progressive supranuclear palsy, and frontotemporal dementia with parkinsonism. *Arch. Neurol.* **62**, 917-921.

Hayesmoore, J.B., Bray, N.J., Cross, W.C., Owen, M.J., O'Donovan, M.C., & Morris, H.R. (2009). The effect of age and the H1c MAPT haplotype on MAPT expression in human brain. *Neurobiol. Aging* **30**, 1652-1656.

He, L. & Lemasters, J.J. (2005). Dephosphorylation of the Rieske iron-sulfur protein after induction of the mitochondrial permeability transition. *Biochem. Biophys. Res. Commun.* **334**, 829-837.

Healy, D.G., Abou-Sleiman, P.M., Ahmadi, K.R., Muqit, M.M., Bhatia, K.P., Quinn, N.P., Lees, A.J., Latchmann, D.S., Goldstein, D.B., & Wood, N.W. (2004a). The gene responsible for PARK6 Parkinson's disease, PINK1, does not influence common forms of parkinsonism. *Ann. Neurol.* **56**, 329-335.

Healy, D.G., Abou-Sleiman, P.M., Casas, J.P., Ahmadi, K.R., Lynch, T., Gandhi, S., Muqit, M.M., Foltynie, T., Barker, R., Bhatia, K.P., Quinn, N.P., Lees, A.J., Gibson, J.M., Holton, J.L., Revesz, T., Goldstein, D.B., & Wood, N.W. (2006). UCHL-1 is not a Parkinson's disease susceptibility gene. *Ann. Neurol.* **59**, 627-633.

Healy, D.G., Abou-Sleiman, P.M., Lees, A.J., Casas, J.P., Quinn, N., Bhatia, K., Hingorani, A.D., & Wood, N.W. (2004b). Tau gene and Parkinson's disease: a case-control study and meta-analysis. *J. Neurol. Neurosurg. Psychiatry* **75**, 962-965.

Healy, D.G., Falchi, M., O'Sullivan, S.S., Bonifati, V., Durr, A., Bressman, S., Brice, A., Aasly, J., Zabetian, C.P., Goldwurm, S., Ferreira, J.J., Tolosa, E., Kay, D.M., Klein, C., Williams, D.R., Marras, C., Lang, A.E., Wszolek, Z.K., Berciano, J., Schapira, A.H., Lynch, T., Bhatia, K.P., Gasser, T., Lees, A.J., & Wood, N.W. (2008). Phenotype, genotype, and worldwide genetic penetrance of LRRK2-associated Parkinson's disease: a case-control study. *Lancet Neurol.* **7**, 583-590.

Heikkila, R.E., Hess, A., & Duvoisin, R.C. (1984). Dopaminergic neurotoxicity of 1-methyl-4-phenyl-1,2,5,6-tetrahydropyridine in mice. *Science* **224**, 1451-1453.

Helkala, E.L., Laulumaa, V., Soininen, H., & Riekkinen, P.J. (1989). Different error pattern of episodic and semantic memory in Alzheimer's disease and Parkinson's disease with dementia. *Neuropsychologia* **27**, 1241-1248.

Hely, M.A., Morris, J.G., Reid, W.G., O'Sullivan, D.J., Williamson, P.M., Broe, G.A., & Adena, M.A. (1995). Age at onset: the major determinant of outcome in Parkinson's disease. *Acta Neurol. Scand.* **92**, 455-463.

Hely, M.A., Reid, W.G., Adena, M.A., Halliday, G.M., & Morris, J.G. (2008). The Sydney multicenter study of Parkinson's disease: the inevitability of dementia at 20 years. *Mov Disord.* **23**, 837-844.

Herman, J.G., Graff, J.R., Myohanen, S., Nelkin, B.D., & Baylin, S.B. (1996). Methylation-specific PCR: a novel PCR assay for methylation status of CpG islands. *Proc. Natl. Acad. Sci. U. S. A* **93**, 9821-9826.

Higashi, S., Biskup, S., West, A.B., Trinkaus, D., Dawson, V.L., Faull, R.L., Waldvogel, H.J., Arai, H., Dawson, T.M., Moore, D.J., & Emson, P.C. (2007). Localization of Parkinson's disease-associated LRRK2 in normal and pathological human brain. *Brain Res.* **1155**, 208-219.

Higashi, S., Moore, D.J., Yamamoto, R., Minegishi, M., Sato, K., Togo, T., Katsuse, O., Uchikado, H., Furukawa, Y., Hino, H., Kosaka, K., Emson, P.C., Wada, K., Dawson, V.L., Dawson, T.M., Arai, H., & Iseki, E. (2009). Abnormal localization of leucine-rich repeat kinase 2 to the endosomal-lysosomal compartment in lewy body disease. *J. Neuropathol. Exp. Neurol.* **68**, 994-1005.

Hilker, R., Thomas, A.V., Klein, J.C., Weisenbach, S., Kalbe, E., Burghaus, L., Jacobs, A.H., Herholz, K., & Heiss, W.D. (2005). Dementia in Parkinson disease: functional imaging of cholinergic and dopaminergic pathways. *Neurology* **65**, 1716-1722.

Hirsch, E.C. & Hunot, S. (2009). Neuroinflammation in Parkinson's disease: a target for neuroprotection? *Lancet Neurol.* **8**, 382-397.

Hjorten, R., Hansen, U., Underwood, R.A., Telfer, H.E., Fernandes, R.J., Krakow, D., Sebald, E., Wachsmann-Hogiu, S., Bruckner, P., Jacquet, R., Landis, W.J., Byers, P.H., & Pace, J.M. (2007). Type XXVII collagen at the transition of cartilage to bone during skeletogenesis. *Bone* **41**, 535-542.

Hobson, P. & Meara, J. (2004). Risk and incidence of dementia in a cohort of older subjects with Parkinson's disease in the United Kingdom. *Mov Disord.* **19**, 1043-1049.

Hu, G., Bidel, S., Jousilahti, P., Antikainen, R., & Tuomilehto, J. (2007). Coffee and tea consumption and the risk of Parkinson's disease. *Mov Disord.* **22**, 2242-2248.

Huang, X., Chen, P., Kaufer, D.I., Troster, A.I., & Poole, C. (2006). Apolipoprotein E and dementia in Parkinson disease: a meta-analysis. *Arch. Neurol.* **63**, 189-193.

Huang, X., Chen, P.C., & Poole, C. (2004). APOE-[epsilon]2 allele associated with higher prevalence of sporadic Parkinson disease. *Neurology* **62**, 2198-2202.

Hubbard, T.J., Aken, B.L., Beal, K., Ballester, B., Caccamo, M., Chen, Y., Clarke, L., Coates, G., Cunningham, F., Cutts, T., Down, T., Dyer, S.C., Fitzgerald, S., Fernandez-Banet, J., Graf, S., Haider, S., Hammond, M., Herrero, J., Holland, R., Howe, K., Howe, K., Johnson, N., Kahari, A., Keefe, D., Kokocinski, F., Kulesha, E., Lawson, D., Longden, I., Melsopp, C., Megy, K., Meidl, P., Ouverdin, B., Parker, A., Prlic, A., Rice, S., Rios, D., Schuster, M., Sealy, I., Severin, J., Slater, G., Smedley, D., Spudich, G., Trevanion, S., Vilella, A., Vogel, J., White, S., Wood, M., Cox, T., Curwen, V., Durbin, R., Fernandez-Suarez, X.M., Flicek, P., Kasprzyk, A., Proctor, G., Searle, S., Smith, J., Ureta-Vidal, A., & Birney, E. (2007). Ensembl 2007. *Nucleic Acids Res.* **35**, D610-D617.

Huber, S.J., Shuttleworth, E.C., & Freidenberg, D.L. (1989). Neuropsychological differences between the dementias of Alzheimer's and Parkinson's diseases. *Arch. Neurol.* **46**, 1287-1291.

Hughes, T.A., Ross, H.F., Musa, S., Bhattacherjee, S., Nathan, R.N., Mindham, R.H., & Spokes, E.G. (2000). A 10-year study of the incidence of and factors predicting dementia in Parkinson's disease. *Neurology* **54**, 1596-1602.

Hunot, S., Brugg, B., Ricard, D., Michel, P.P., Muriel, M.P., Ruberg, M., Faucheux, B.A., Agid, Y., & Hirsch, E.C. (1997). Nuclear translocation of NF-kappaB is increased in dopaminergic neurons of patients with parkinson disease. *Proc. Natl. Acad. Sci. U. S. A* **94**, 7531-7536.

Hutton, M., Lendon, C.L., Rizzu, P., Baker, M., Froelich, S., Houlden, H., Pickering-Brown, S., Chakraverty, S., Isaacs, A., Grover, A., Hackett, J., Adamson, J., Lincoln, S., Dickson, D., Davies, P., Petersen, R.C., Stevens, M., de, G.E., Wauters, E., van, B.J., Hillebrand, M., Joosse, M., Kwon, J.M., Nowotny, P., Che, L.K., Norton, J., Morris, J.C., Reed, L.A., Trojanowski, J., Basun, H., Lannfelt, L., Neystat, M., Fahn, S., Dark, F., Tannenberg, T., Dodd, P.R., Hayward, N., Kwok, J.B., Schofield, P.R., Andreadis, A., Snowden, J., Craufurd, D., Neary, D., Owen, F., Oostra, B.A., Hardy, J., Goate, A., van, S.J., Mann, D., Lynch, T., & Heutink, P. (1998). Association of missense and 5'-splice-site mutations in tau with the inherited dementia FTDP-17. *Nature* **393**, 702-705.

Ibanez, P., Bonnet, A.M., Debarges, B., Lohmann, E., Tison, F., Pollak, P., Agid, Y., Durr, A., & Brice, A. (2004). Causal relation between alpha-synuclein gene duplication and familial Parkinson's disease. *Lancet* **364**, 1169-1171.

Ihara, M., Yamasaki, N., Hagiwara, A., Tanigaki, A., Kitano, A., Hikawa, R., Tomimoto, H., Noda, M., Takanashi, M., Mori, H., Hattori, N., Miyakawa, T., & Kinoshita, M. (2007). Sept4, a component of presynaptic scaffold and Lewy bodies, is required for the suppression of alpha-synuclein neurotoxicity. *Neuron* **53**, 519-533.

Ikeuchi, T., Kakita, A., Shiga, A., Kasuga, K., Kaneko, H., Tan, C.F., Idezuka, J., Wakabayashi, K., Onodera, O., Iwatsubo, T., Nishizawa, M., Takahashi, H., & Ishikawa, A. (2008). Patients homozygous and heterozygous for SNCA duplication in a family with parkinsonism and dementia. *Arch. Neurol.* **65**, 514-519.

Imai, Y., Soda, M., Inoue, H., Hattori, N., Mizuno, Y., & Takahashi, R. (2001). An unfolded putative transmembrane polypeptide, which can lead to endoplasmic reticulum stress, is a substrate of Parkin. *Cell* **105**, 891-902.

Imamura, K., Hishikawa, N., Ono, K., Suzuki, H., Sawada, M., Nagatsu, T., Yoshida, M., & Hashizume, Y. (2005). Cytokine production of activated microglia and

decrease in neurotrophic factors of neurons in the hippocampus of Lewy body disease brains. *Acta Neuropathol. (Berl)* **109**, 141-150.

Imamura, K., Hishikawa, N., Sawada, M., Nagatsu, T., Yoshida, M., & Hashizume, Y. (2003). Distribution of major histocompatibility complex class II-positive microglia and cytokine profile of Parkinson's disease brains. *Acta Neuropathol.* **106**, 518-526.

Iqbal, K., Liu, F., Gong, C.X., Alonso, A.C., & Grundke-Iqbal, I. (2009). Mechanisms of tau-induced neurodegeneration. *Acta Neuropathol.* **118**, 53-69.

Irizarry, M.C., Kim, T.W., McNamara, M., Tanzi, R.E., George, J.M., Clayton, D.F., & Hyman, B.T. (1996). Characterization of the precursor protein of the non-A beta component of senile plaques (NACP) in the human central nervous system. *J. Neuropathol. Exp. Neurol.* **55**, 889-895.

Irizarry, R.A., Hobbs, B., Collin, F., Beazer-Barclay, Y.D., Antonellis, K.J., Scherf, U., & Speed, T.P. (2003). Exploration, normalization, and summaries of high density oligonucleotide array probe level data. *Biostatistics.* **4**, 249-264.

Ishikawa, H., Kubo, A., Tsukita, S., & Tsukita, S. (2005). Odf2-deficient mother centrioles lack distal/subdistal appendages and the ability to generate primary cilia. *Nat. Cell Biol.* **7**, 517-524.

Ishizawa, T., Mattila, P., Davies, P., Wang, D., & Dickson, D.W. (2003). Colocalization of tau and alpha-synuclein epitopes in Lewy bodies. *J. Neuropathol. Exp. Neurol.* **62**, 389-397.

Ivanov, A.I. & Romanovsky, A.A. (2006). Putative dual role of ephrin-Eph receptor interactions in inflammation. *IUBMB. Life* **58**, 389-394.

Janvin, C.C., Larsen, J.P., Salmon, D.P., Galasko, D., Hugdahl, K., & Aarsland, D. (2006). Cognitive profiles of individual patients with Parkinson's disease and dementia: comparison with dementia with lewy bodies and Alzheimer's disease. *Mov Disord.* **21**, 337-342.

Jasinska-Myga, B., Opala, G., Goetz, C.G., Tustanowski, J., Ochudlo, S., Gorzkowska, A., & Tyrpa, J. (2007). Apolipoprotein E gene polymorphism, total plasma cholesterol level, and Parkinson disease dementia. *Arch. Neurol.* **64**, 261-265.

Javitch, J.A., D'Amato, R.J., Strittmatter, S.M., & Snyder, S.H. (1985). Parkinsonism-inducing neurotoxin, N-methyl-4-phenyl-1,2,3,6 -tetrahydropyridine: uptake of the

metabolite N-methyl-4-phenylpyridine by dopamine neurons explains selective toxicity. *Proc. Natl. Acad. Sci. U. S. A* **82**, 2173-2177.

Jefferson, A.L., Cosentino, S.A., Ball, S.K., Bogdanoff, B., Leopold, N., Kaplan, E., & Libon, D.J. (2002). Errors produced on the mini-mental state examination and neuropsychological test performance in Alzheimer's disease, ischemic vascular dementia, and Parkinson's disease. *J. Neuropsychiatry Clin. Neurosci.* **14**, 311-320.

Jellinger, K.A., Seppi, K., Wenning, G.K., & Poewe, W. (2002). Impact of coexistent Alzheimer pathology on the natural history of Parkinson's disease. *J. Neural Transm.* **109**, 329-339.

Johnson, J., Hague, S.M., Hanson, M., Gibson, A., Wilson, K.E., Evans, E.W., Singleton, A.A., Inerney-Leo, A., Nussbaum, R.L., Hernandez, D.G., Gallardo, M., McKeith, I.G., Burn, D.J., Ryu, M., Hellstrom, O., Ravina, B., Eerola, J., Perry, R.H., Jaros, E., Tienari, P., Weiser, R., Gwinn-Hardy, K., Morris, C.M., Hardy, J., & Singleton, A.B. (2004). SNCA multiplication is not a common cause of Parkinson disease or dementia with Lewy bodies. *Neurology* **63**, 554-556.

Jones, J.M., Datta, P., Srinivasula, S.M., Ji, W., Gupta, S., Zhang, Z., Davies, E., Hajnoczky, G., Saunders, T.L., Van Keuren, M.L., Fernandes-Alnemri, T., Meisler, M.H., & Alnemri, E.S. (2003). Loss of Omi mitochondrial protease activity causes the neuromuscular disorder of mnd2 mutant mice. *Nature* **425**, 721-727.

Jun, G., Guo, H., Klein, B.E., Klein, R., Wang, J.J., Mitchell, P., Miao, H., Lee, K.E., Joshi, T., Buck, M., Chugha, P., Bardenstein, D., Klein, A.P., Bailey-Wilson, J.E., Gong, X., Spector, T.D., Andrew, T., Hammond, C.J., Elston, R.C., Iyengar, S.K., & Wang, B. (2009). EPHA2 is associated with age-related cortical cataract in mice and humans. *PLoS. Genet.* **5**, e1000584.

Kaasinen, V., Nurmi, E., Bruck, A., Eskola, O., Bergman, J., Solin, O., & Rinne, J.O. (2001). Increased frontal [(18)F]fluorodopa uptake in early Parkinson's disease: sex differences in the prefrontal cortex. *Brain* **124**, 1125-1130.

Kabuta, T., Furuta, A., Aoki, S., Furuta, K., & Wada, K. (2008). Aberrant interaction between Parkinson disease-associated mutant UCH-L1 and the lysosomal receptor for chaperone-mediated autophagy. *J. Biol. Chem.* **283**, 23731-23738.

Kalaitzakis, M.E., Christian, L.M., Moran, L.B., Graeber, M.B., Pearce, R.K., & Gentleman, S.M. (2009a). Dementia and visual hallucinations associated with limbic pathology in Parkinson's disease. *Parkinsonism. Relat Disord.* **15**, 196-204.

Kalaitzakis, M.E., Graeber, M.B., Gentleman, S.M., & Pearce, R.K. (2008a). Striatal beta-amyloid deposition in Parkinson disease with dementia. *J. Neuropathol. Exp. Neurol.* **67**, 155-161.

Kalaitzakis, M.E., Graeber, M.B., Gentleman, S.M., & Pearce, R.K. (2008c). Controversies over the staging of alpha-synuclein pathology in Parkinson's disease. *Acta Neuropathol.* **116**, 125-128.

Kalaitzakis, M.E., Graeber, M.B., Gentleman, S.M., & Pearce, R.K. (2008b). The dorsal motor nucleus of the vagus is not an obligatory trigger site of Parkinson's disease: a critical analysis of alpha-synuclein staging. *Neuropathol. Appl. Neurobiol.* **34**, 284-295.

Kalaitzakis, M.E. & Pearce, R.K. (2009). The morbid anatomy of dementia in Parkinson's disease. *Acta Neuropathol.* **118**, 587-598.

Kalaitzakis, M.E., Pearce, R.K., & Gentleman, S.M. (2009b). Clinical correlates of pathology in the claustrum in Parkinson's disease and dementia with Lewy bodies. *Neurosci. Lett.* **461**, 12-15.

Kanehisa, M. & Goto, S. (2000). KEGG: kyoto encyclopedia of genes and genomes. *Nucleic Acids Res.* **28**, 27-30.

Karlsson, M., Mathers, J., Dickinson, R.J., Mandl, M., & Keyse, S.M. (2004). Both nuclear-cytoplasmic shuttling of the dual specificity phosphatase MKP-3 and its ability to anchor MAP kinase in the cytoplasm are mediated by a conserved nuclear export signal. *J. Biol. Chem.* **279**, 41882-41891.

Katoh, M. & Katoh, M. (2006). Comparative integromics on Eph family. *Int. J. Oncol.* **28**, 1243-1247.

Katzenschlager, R. & Lees, A.J. (2004). Olfaction and Parkinson's syndromes: its role in differential diagnosis. *Curr. Opin. Neurol.* **17**, 417-423.

Kawamoto, Y., Kobayashi, Y., Suzuki, Y., Inoue, H., Tomimoto, H., Akiguchi, I., Budka, H., Martins, L.M., Downward, J., & Takahashi, R. (2008). Accumulation of HtrA2/Omi in neuronal and glial inclusions in brains with alpha-synucleinopathies. *J. Neuropathol. Exp. Neurol.* **67**, 984-993.

Kay, D.M., Factor, S.A., Samii, A., Higgins, D.S., Griffith, A., Roberts, J.W., Leis, B.C., Nutt, J.G., Montimurro, J.S., Keefe, R.G., Atkins, A.J., Yearout, D., Zabetian, C.P., & Payami, H. (2008). Genetic association between alpha-synuclein and

idiopathic Parkinson's disease. *Am. J. Med. Genet. B Neuropsychiatr. Genet.* **147B**, 1222-1230.

Kay, D.M., Moran, D., Moses, L., Poorkaj, P., Zabetian, C.P., Nutt, J., Factor, S.A., Yu, C.E., Montimurro, J.S., Keefe, R.G., Schellenberg, G.D., & Payami, H. (2007). Heterozygous parkin point mutations are as common in control subjects as in Parkinson's patients. *Ann. Neurol.* **61**, 47-54.

Khan, N.L., Graham, E., Critchley, P., Schrag, A.E., Wood, N.W., Lees, A.J., Bhatia, K.P., & Quinn, N. (2003). Parkin disease: a phenotypic study of a large case series. *Brain* **126**, 1279-1292.

Kikawa, K.D., Vidale, D.R., Van Etten, R.L., & Kinch, M.S. (2002). Regulation of the EphA2 kinase by the low molecular weight tyrosine phosphatase induces transformation. *J. Biol. Chem.* **277**, 39274-39279.

Kim, R.H., Smith, P.D., Aleyasin, H., Hayley, S., Mount, M.P., Pownall, S., Wakeham, A., You-Ten, A.J., Kalia, S.K., Horne, P., Westaway, D., Lozano, A.M., Anisman, H., Park, D.S., & Mak, T.W. (2005). Hypersensitivity of DJ-1-deficient mice to 1-methyl-4-phenyl-1,2,3,6-tetrahydropyrindine (MPTP) and oxidative stress. *Proc. Natl. Acad. Sci. U. S. A* **102**, 5215-5220.

Kingsbury, A.E., Daniel, S.E., Sangha, H., Eisen, S., Lees, A.J., & Foster, O.J. (2004). Alteration in alpha-synuclein mRNA expression in Parkinson's disease. *Mov Disord.* **19**, 162-170.

Kitada, T., Asakawa, S., Hattori, N., Matsumine, H., Yamamura, Y., Minoshima, S., Yokochi, M., Mizuno, Y., & Shimizu, N. (1998). Mutations in the parkin gene cause autosomal recessive juvenile parkinsonism. *Nature* **392**, 605-608.

Kitada, T., Pisani, A., Porter, D.R., Yamaguchi, H., Tscherter, A., Martella, G., Bonsi, P., Zhang, C., Pothos, E.N., & Shen, J. (2007). Impaired dopamine release and synaptic plasticity in the striatum of PINK1-deficient mice. *Proc. Natl. Acad. Sci. U. S. A* **104**, 11441-11446.

Knight, J.C., Keating, B.J., Rockett, K.A., & Kwiatkowski, D.P. (2003). In vivo characterization of regulatory polymorphisms by allele-specific quantification of RNA polymerase loading. *Nat. Genet.* **33**, 469-475.

Koechlin, E. & Hyafil, A. (2007). Anterior prefrontal function and the limits of human decision-making. *Science* **318**, 594-598.

Kordower, J.H., Chu, Y., Hauser, R.A., Freeman, T.B., & Olanow, C.W. (2008). Lewy body-like pathology in long-term embryonic nigral transplants in Parkinson's disease. *Nat. Med.* **14**, 504-506.

Kovari, E., Gold, G., Herrmann, F.R., Canuto, A., Hof, P.R., Bouras, C., & Giannakopoulos, P. (2003). Lewy body densities in the entorhinal and anterior cingulate cortex predict cognitive deficits in Parkinson's disease. *Acta Neuropathol.* **106**, 83-88.

Kovas, Y. & Plomin, R. (2006). Generalist genes: implications for the cognitive sciences. *Trends Cogn Sci.* **10**, 198-203.

Kramer, M.L. & Schulz-Schaeffer, W.J. (2007). Presynaptic alpha-synuclein aggregates, not Lewy bodies, cause neurodegeneration in dementia with Lewy bodies. *J. Neurosci.* **27**, 1405-1410.

Kraybill, M.L., Larson, E.B., Tsuang, D.W., Teri, L., McCormick, W.C., Bowen, J.D., Kukull, W.A., Leverenz, J.B., & Cherrier, M.M. (2005). Cognitive differences in dementia patients with autopsy-verified AD, Lewy body pathology, or both. *Neurology* **64**, 2069-2073.

Kringelbach, M.L. (2005). The human orbitofrontal cortex: linking reward to hedonic experience. *Nat. Rev. Neurosci.* **6**, 691-702.

Kruger, R., Kuhn, W., Leenders, K.L., Sprengelmeyer, R., Muller, T., Woitalla, D., Portman, A.T., Maguire, R.P., Veenma, L., Schroder, U., Schols, L., Epplen, J.T., Riess, O., & Przuntek, H. (2001). Familial parkinsonism with synuclein pathology: clinical and PET studies of A30P mutation carriers. *Neurology* **56**, 1355-1362.

Kruger, R., Kuhn, W., Muller, T., Woitalla, D., Graeber, M., Kosel, S., Przuntek, H., Epplen, J.T., Schols, L., & Riess, O. (1998). Ala30Pro mutation in the gene encoding alpha-synuclein in Parkinson's disease. *Nat. Genet.* **18**, 106-108.

Kumaran, R., Vandrovcova, J., Luk, C., Sharma, S., Renton, A., Wood, N.W., Hardy, J.A., Lees, A.J., & Bandopadhyay, R. (2009). Differential DJ-1 gene expression in Parkinson's disease. *Neurobiol. Dis.* **36**, 393-400.

Kurz, M.W., Dekomien, G., Nilsen, O.B., Larsen, J.P., Aarsland, D., & Alves, G. (2009). APOE alleles in Parkinson disease and their relationship to cognitive decline: a population-based, longitudinal study. *J. Geriatr. Psychiatry Neurol.* **22**, 166-170.

Lakso, M., Vartiainen, S., Moilanen, A.M., Sirvio, J., Thomas, J.H., Nass, R., Blakely, R.D., & Wong, G. (2003). Dopaminergic neuronal loss and motor deficits in

Caenorhabditis elegans overexpressing human alpha-synuclein. *J. Neurochem.* **86**, 165-172.

Lancaster, J.L., Woldorff, M.G., Parsons, L.M., Liotti, M., Freitas, C.S., Rainey, L., Kochunov, P.V., Nickerson, D., Mikiten, S.A., & Fox, P.T. (2000). Automated Talairach atlas labels for functional brain mapping. *Hum. Brain Mapp.* **10**, 120-131.

Lange, K.W., Robbins, T.W., Marsden, C.D., James, M., Owen, A.M., & Paul, G.M. (1992). L-dopa withdrawal in Parkinson's disease selectively impairs cognitive performance in tests sensitive to frontal lobe dysfunction. *Psychopharmacology (Berl)* **107**, 394-404.

Langston, J.W., Ballard, P., Tetrud, J.W., & Irwin, I. (1983). Chronic Parkinsonism in humans due to a product of meperidine-analog synthesis. *Science* **219**, 979-980.

Lariviere, R.C. & Julien, J.P. (2004). Functions of intermediate filaments in neuronal development and disease. *J. Neurobiol.* **58**, 131-148.

Lashley, T., Holton, J.L., Gray, E., Kirkham, K., O'Sullivan, S.S., Hilbig, A., Wood, N.W., Lees, A.J., & Revesz, T. (2008). Cortical alpha-synuclein load is associated with amyloid-beta plaque burden in a subset of Parkinson's disease patients. *Acta Neuropathol.* **115**, 417-425.

Lashuel, H.A., Hartley, D., Petre, B.M., Walz, T., & Lansbury, P.T., Jr. (2002). Neurodegenerative disease: amyloid pores from pathogenic mutations. *Nature* **418**, 291.

Lavaute, T., Smith, S., Cooperman, S., Iwai, K., Land, W., Meyron-Holtz, E., Drake, S.K., Miller, G., bu-Asab, M., Tsokos, M., Switzer, R., III, Grinberg, A., Love, P., Tresser, N., & Rouault, T.A. (2001). Targeted deletion of the gene encoding iron regulatory protein-2 causes misregulation of iron metabolism and neurodegenerative disease in mice. *Nat. Genet.* **27**, 209-214.

Lavedan, C. (1998). The synuclein family. *Genome Res.* **8**, 871-880.

Lazarus, B.D., Love, D.C., & Hanover, J.A. (2009). O-GlcNAc cycling: implications for neurodegenerative disorders. *Int. J. Biochem. Cell Biol.* **41**, 2134-2146.

Lee, A.C., Bandelow, S., Schwarzbauer, C., Henson, R.N., & Graham, K.S. (2006a). Perirhinal cortex activity during visual object discrimination: an event-related fMRI study. *Neuroimage.* **33**, 362-373.

Lee, K.Y., Ahn, Y.M., Joo, E.J., Chang, J.S., & Kim, Y.S. (2006b). The association of DUSP6 gene with schizophrenia and bipolar disorder: its possible role in the development of bipolar disorder. *Mol. Psychiatry* **11**, 425-426.

Lees, A.J. (2009). The Parkinson chimera. *Neurology* **72**, S2-11.

Lees, A.J., Hardy, J., & Revesz, T. (2009). Parkinson's disease. *Lancet* **373**, 2055-2066.

Lees, A.J. & Smith, E. (1983). Cognitive deficits in the early stages of Parkinson's disease. *Brain* **106 (Pt 2)**, 257-270.

Lein, E.S., Hawrylycz, M.J., Ao, N., Ayres, M., Bensinger, A., Bernard, A., Boe, A.F., Boguski, M.S., Brockway, K.S., Byrnes, E.J., Chen, L., Chen, L., Chen, T.M., Chin, M.C., Chong, J., Crook, B.E., Czaplinska, A., Dang, C.N., Datta, S., Dee, N.R., Desaki, A.L., Desta, T., Diep, E., Dolbeare, T.A., Donelan, M.J., Dong, H.W., Dougherty, J.G., Duncan, B.J., Ebbert, A.J., Eichele, G., Estin, L.K., Faber, C., Facer, B.A., Fields, R., Fischer, S.R., Fliss, T.P., Frensley, C., Gates, S.N., Glattfelder, K.J., Halverson, K.R., Hart, M.R., Hohmann, J.G., Howell, M.P., Jeung, D.P., Johnson, R.A., Karr, P.T., Kawal, R., Kidney, J.M., Knapik, R.H., Kuan, C.L., Lake, J.H., Laramee, A.R., Larsen, K.D., Lau, C., Lemon, T.A., Liang, A.J., Liu, Y., Luong, L.T., Michaels, J., Morgan, J.J., Morgan, R.J., Mortrud, M.T., Mosqueda, N.F., Ng, L.L., Ng, R., Orta, G.J., Overly, C.C., Pak, T.H., Parry, S.E., Pathak, S.D., Pearson, O.C., Puchalski, R.B., Riley, Z.L., Rockett, H.R., Rowland, S.A., Royall, J.J., Ruiz, M.J., Sarno, N.R., Schaffnit, K., Shapovalova, N.V., Sivisay, T., Slaughterbeck, C.R., Smith, S.C., Smith, K.A., Smith, B.I., Sodt, A.J., Stewart, N.N., Stumpf, K.R., Sunkin, S.M., Sutram, M., Tam, A., Teemer, C.D., Thaller, C., Thompson, C.L., Varnam, L.R., Visel, A., Whitlock, R.M., Wohnoutka, P.E., Wolkey, C.K., Wong, V.Y., Wood, M., Yaylaoglu, M.B., Young, R.C., Youngstrom, B.L., Yuan, X.F., Zhang, B., Zwingman, T.A., & Jones, A.R. (2007). Genome-wide atlas of gene expression in the adult mouse brain. *Nature* **445**, 168-176.

Leroy, E., Boyer, R., Auburger, G., Leube, B., Ulm, G., Mezey, E., Harta, G., Brownstein, M.J., Jonnalagada, S., Chernova, T., Dehejia, A., Lavedan, C., Gasser, T., Steinbach, P.J., Wilkinson, K.D., & Polymeropoulos, M.H. (1998). The ubiquitin pathway in Parkinson's disease. *Nature* **395**, 451-452.

Lesage, S. & Brice, A. (2009). Parkinson's disease: from monogenic forms to genetic susceptibility factors. *Hum. Mol. Genet.* **18**, R48-R59.

Levenson, J.M., Choi, S., Lee, S.Y., Cao, Y.A., Ahn, H.J., Worley, K.C., Pizzi, M., Liou, H.C., & Sweatt, J.D. (2004). A bioinformatics analysis of memory consolidation reveals involvement of the transcription factor c-rel. *J. Neurosci.* **24**, 3933-3943.

Levin, B.E., Llabre, M.M., Reisman, S., Weiner, W.J., Sanchez-Ramos, J., Singer, C., & Brown, M.C. (1991). Visuospatial impairment in Parkinson's disease. *Neurology* **41**, 365-369.

Levinthal, D.J. & DeFranco, D.B. (2005). Reversible oxidation of ERK-directed protein phosphatases drives oxidative toxicity in neurons. *J. Biol. Chem.* **280**, 5875-5883.

Levy, G., Jacobs, D.M., Tang, M.X., Cote, L.J., Louis, E.D., Alfaro, B., Mejia, H., Stern, Y., & Marder, K. (2002a). Memory and executive function impairment predict dementia in Parkinson's disease. *Mov Disord.* **17**, 1221-1226.

Levy, G., Schupf, N., Tang, M.X., Cote, L.J., Louis, E.D., Mejia, H., Stern, Y., & Marder, K. (2002b). Combined effect of age and severity on the risk of dementia in Parkinson's disease. *Ann. Neurol.* **51**, 722-729.

Levy, G., Tang, M.X., Cote, L.J., Louis, E.D., Alfaro, B., Mejia, H., Stern, Y., & Marder, K. (2000). Motor impairment in PD: relationship to incident dementia and age. *Neurology* **55**, 539-544.

Lewis, C.M. (2002). Genetic association studies: design, analysis and interpretation. *Brief. Bioinform.* **3**, 146-153.

Lewis, S.J., Slabosz, A., Robbins, T.W., Barker, R.A., & Owen, A.M. (2005). Dopaminergic basis for deficits in working memory but not attentional set-shifting in Parkinson's disease. *Neuropsychologia* **43**, 823-832.

Li, C., Scott, D.A., Hatch, E., Tian, X., & Mansour, S.L. (2007). Dusp6 (Mkp3) is a negative feedback regulator of FGF-stimulated ERK signaling during mouse development. *Development* **134**, 167-176.

Li, J.Y., Englund, E., Holton, J.L., Soulet, D., Hagell, P., Lees, A.J., Lashley, T., Quinn, N.P., Rehncrona, S., Bjorklund, A., Widner, H., Revesz, T., Lindvall, O., & Brundin, P. (2008). Lewy bodies in grafted neurons in subjects with Parkinson's disease suggest host-to-graft disease propagation. *Nat. Med.* **14**, 501-503.

Li, L.C. & Dahiya, R. (2002). MethPrimer: designing primers for methylation PCRs. *Bioinformatics.* **18**, 1427-1431.

Li, Y., Tomiyama, H., Sato, K., Hatano, Y., Yoshino, H., Atsumi, M., Kitaguchi, M., Sasaki, S., Kawaguchi, S., Miyajima, H., Toda, T., Mizuno, Y., & Hattori, N. (2005). Clinicogenetic study of PINK1 mutations in autosomal recessive early-onset parkinsonism. *Neurology* **64**, 1955-1957.

Lim, S.Y., Fox, S.H., & Lang, A.E. (2009). Overview of the extranigral aspects of Parkinson disease. *Arch. Neurol.* **66**, 167-172.

Lin, C.H., Tan, E.K., Chen, M.L., Tan, L.C., Lim, H.Q., Chen, G.S., & Wu, R.M. (2008). Novel ATP13A2 variant associated with Parkinson disease in Taiwan and Singapore. *Neurology* **71**, 1727-1732.

Lin, L., Lesnick, T.G., Maraganore, D.M., & Isacson, O. (2009a). Axon guidance and synaptic maintenance: preclinical markers for neurodegenerative disease and therapeutics. *Trends Neurosci.* **32**, 142-149.

Lin, X., Parisiadou, L., Gu, X.L., Wang, L., Shim, H., Sun, L., Xie, C., Long, C.X., Yang, W.J., Ding, J., Chen, Z.Z., Gallant, P.E., Tao-Cheng, J.H., Rudow, G., Troncoso, J.C., Liu, Z., Li, Z., & Cai, H. (2009b). Leucine-rich repeat kinase 2 regulates the progression of neuropathology induced by Parkinson's-disease-related mutant alpha-synuclein. *Neuron* **64**, 807-827.

Lindholm, D., Wootz, H., & Korhonen, L. (2006). ER stress and neurodegenerative diseases. *Cell Death. Differ.* **13**, 385-392.

Linnankivi, T., Tienari, P., Somer, M., Kahkonen, M., Lonnqvist, T., Valanne, L., & Pihko, H. (2006). 18q deletions: clinical, molecular, and brain MRI findings of 14 individuals. *Am. J. Med. Genet. A* **140**, 331-339.

Litvan, I., Mohr, E., Williams, J., Gomez, C., & Chase, T.N. (1991). Differential memory and executive functions in demented patients with Parkinson's and Alzheimer's disease. *J. Neurol. Neurosurg. Psychiatry* **54**, 25-29.

Liu, B. (2008). Association of the dusp6 (mkp3) gene with mouse brain weight and forebrain structure. *J. Child Neurol.* **23**, 624-627.

Liu, G., Loraine, A.E., Shigeta, R., Cline, M., Cheng, J., Valmeekam, V., Sun, S., Kulp, D., & Siani-Rose, M.A. (2003). NetAffx: Affymetrix probesets and annotations. *Nucleic Acids Res.* **31**, 82-86.

Lo Bianco, C., Schneider, B.L., Bauer, M., Sajadi, A., Brice, A., Iwatsubo, T., & Aebischer, P. (2004). Lentiviral vector delivery of parkin prevents dopaminergic degeneration in an alpha-synuclein rat model of Parkinson's disease. *Proc. Natl. Acad. Sci. U. S. A* **101**, 17510-17515.

Lo, H.S., Wang, Z., Hu, Y., Yang, H.H., Gere, S., Buetow, K.H., & Lee, M.P. (2003). Allelic variation in gene expression is common in the human genome. *Genome Res.* **13**, 1855-1862.

Lohmann, E., Thobois, S., Lesage, S., Broussolle, E., du Montcel, S.T., Ribeiro, M.J., Remy, P., Pelissolo, A., Dubois, B., Mallet, L., Pollak, P., Agid, Y., & Brice, A. (2009). A multidisciplinary study of patients with early-onset PD with and without parkin mutations. *Neurology* **72**, 110-116.

Lucking, C.B., Durr, A., Bonifati, V., Vaughan, J., De, M.G., Gasser, T., Harhangi, B.S., Meco, G., Denefle, P., Wood, N.W., Agid, Y., & Brice, A. (2000). Association between early-onset Parkinson's disease and mutations in the parkin gene. *N. Engl. J. Med.* **342**, 1560-1567.

MacInnes, N., Iravani, M.M., Perry, E., Piggott, M., Perry, R., Jenner, P., & Ballard, C. (2008). Proteasomal abnormalities in cortical Lewy body disease and the impact of proteasomal inhibition within cortical and cholinergic systems. *J. Neural Transm.* **115**, 869-878.

MacLeod, D., Dowman, J., Hammond, R., Leete, T., Inoue, K., & Abeliovich, A. (2006). The familial Parkinsonism gene LRRK2 regulates neurite process morphology. *Neuron* **52**, 587-593.

Mahieux, F., Fenelon, G., Flahault, A., Manifacier, M.J., Michelet, D., & Boller, F. (1998). Neuropsychological prediction of dementia in Parkinson's disease. *J. Neurol. Neurosurg. Psychiatry* **64**, 178-183.

Maldjian, J.A., Laurienti, P.J., Kraft, R.A., & Burdette, J.H. (2003). An automated method for neuroanatomic and cytoarchitectonic atlas-based interrogation of fMRI data sets. *Neuroimage.* **19**, 1233-1239.

Maraganore, D.M., de, A.M., Elbaz, A., Farrer, M.J., Ioannidis, J.P., Kruger, R., Rocca, W.A., Schneider, N.K., Lesnick, T.G., Lincoln, S.J., Hulihan, M.M., Aasly, J.O., Ashizawa, T., Chartier-Harlin, M.C., Checkoway, H., Ferrarese, C., Hadjigeorgiou, G., Hattori, N., Kawakami, H., Lambert, J.C., Lynch, T., Mellick, G.D., Papapetropoulos, S., Parsian, A., Quattrone, A., Riess, O., Tan, E.K., & Van, B.C. (2006). Collaborative analysis of alpha-synuclein gene promoter variability and Parkinson disease. *JAMA* **296**, 661-670.

Maraganore, D.M., Lesnick, T.G., Elbaz, A., Chartier-Harlin, M.C., Gasser, T., Kruger, R., Hattori, N., Mellick, G.D., Quattrone, A., Satoh, J., Toda, T., Wang, J., Ioannidis, J.P., de, A.M., & Rocca, W.A. (2004a). UCHL1 is a Parkinson's disease susceptibility gene. *Ann. Neurol.* **55**, 512-521.

Maraganore, D.M., Wilkes, K., Lesnick, T.G., Strain, K.J., de, A.M., Rocca, W.A., Bower, J.H., Ahlskog, J.E., Lincoln, S., & Farrer, M.J. (2004b). A limited role for DJ1 in Parkinson disease susceptibility. *Neurology* **63**, 550-553.

Marchetti, S., Gimond, C., Chambard, J.C., Touboul, T., Roux, D., Pouyssegur, J., & Pages, G. (2005). Extracellular signal-regulated kinases phosphorylate mitogen-activated protein kinase phosphatase 3/DUSP6 at serines 159 and 197, two sites critical for its proteasomal degradation. *Mol. Cell Biol.* **25**, 854-864.

Marongiu, R., Ferraris, A., Ialongo, T., Michiorri, S., Soleti, F., Ferrari, F., Elia, A.E., Ghezzi, D., Albanese, A., Altavista, M.C., Antonini, A., Barone, P., Brusa, L., Cortelli, P., Martinelli, P., Pellecchia, M.T., Pezzoli, G., Scaglione, C., Stanzione, P., Tinazzi, M., Zecchinelli, A., Zeviani, M., Cassetta, E., Garavaglia, B., Dallapiccola, B., Bentivoglio, A.R., & Valente, E.M. (2008). PINK1 heterozygous rare variants: prevalence, significance and phenotypic spectrum. *Hum. Mutat.* **29**, 565.

Martin, L.J., Pan, Y., Price, A.C., Sterling, W., Copeland, N.G., Jenkins, N.A., Price, D.L., & Lee, M.K. (2006). Parkinson's disease alpha-synuclein transgenic mice develop neuronal mitochondrial degeneration and cell death. *J. Neurosci.* **26**, 41-50.

Martinez-Vicente, M., Talloczy, Z., Kaushik, S., Massey, A.C., Mazzulli, J., Mosharov, E.V., Hodara, R., Fredenburg, R., Wu, D.C., Follenzi, A., Dauer, W., Przedborski, S., Ischiropoulos, H., Lansbury, P.T., Sulzer, D., & Cuervo, A.M. (2008). Dopamine-modified alpha-synuclein blocks chaperone-mediated autophagy. *J. Clin. Invest* **118**, 777-788.

Martins, L.M., Morrison, A., Klupsch, K., Fedele, V., Moisoi, N., Teismann, P., Abuin, A., Grau, E., Geppert, M., Livi, G.P., Creasy, C.L., Martin, A., Hargreaves, I., Heales, S.J., Okada, H., Brandner, S., Schulz, J.B., Mak, T., & Downward, J. (2004). Neuroprotective role of the Reaper-related serine protease HtrA2/Omi revealed by targeted deletion in mice. *Mol. Cell Biol.* **24**, 9848-9862.

Masliah, E., Rockenstein, E., Veinbergs, I., Mallory, M., Hashimoto, M., Takeda, A., Sagara, Y., Sisk, A., & Mucke, L. (2000). Dopaminergic loss and inclusion body formation in alpha-synuclein mice: implications for neurodegenerative disorders. *Science* **287**, 1265-1269.

Masliah, E., Rockenstein, E., Veinbergs, I., Sagara, Y., Mallory, M., Hashimoto, M., & Mucke, L. (2001). beta-amyloid peptides enhance alpha-synuclein accumulation and neuronal deficits in a transgenic mouse model linking Alzheimer's disease and Parkinson's disease. *Proc. Natl. Acad. Sci. U. S. A* **98**, 12245-12250.

Massullo, P., Sumoza-Toledo, A., Bhagat, H., & Partida-Sanchez, S. (2006). TRPM channels, calcium and redox sensors during innate immune responses. *Semin. Cell Dev. Biol.* **17**, 654-666.

Mata, I.F., Samii, A., Schneer, S.H., Roberts, J.W., Griffith, A., Leis, B.C., Schellenberg, G.D., Sidransky, E., Bird, T.D., Leverenz, J.B., Tsuang, D., &

Zabetian, C.P. (2008). Glucocerebrosidase gene mutations: a risk factor for Lewy body disorders. *Arch. Neurol.* **65**, 379-382.

Matsumoto, M., Weickert, C.S., Akil, M., Lipska, B.K., Hyde, T.M., Herman, M.M., Kleinman, J.E., & Weinberger, D.R. (2003). Catechol O-methyltransferase mRNA expression in human and rat brain: evidence for a role in cortical neuronal function. *Neuroscience* **116**, 127-137.

Mattila, P.M., Koskela, T., Roytta, M., Lehtimaki, T., Pirttila, T.A., Ilveskoski, E., Karhunen, P., & Rinne, J.O. (1998). Apolipoprotein E epsilon4 allele frequency is increased in Parkinson's disease only with co-existing Alzheimer pathology. *Acta Neuropathol.* **96**, 417-420.

Mattila, P.M., Rinne, J.O., Helenius, H., Dickson, D.W., & Roytta, M. (2000). Alpha-synuclein-immunoreactive cortical Lewy bodies are associated with cognitive impairment in Parkinson's disease. *Acta Neuropathol.* **100**, 285-290.

McCulloch, C.C., Kay, D.M., Factor, S.A., Samii, A., Nutt, J.G., Higgins, D.S., Griffith, A., Roberts, J.W., Leis, B.C., Montimurro, J.S., Zabetian, C.P., & Payami, H. (2008). Exploring gene-environment interactions in Parkinson's disease. *Hum. Genet.* **123**, 257-265.

McFarland, N.R., Fan, Z., Xu, K., Schwarzschild, M.A., Feany, M.B., Hyman, B.T., & McLean, P.J. (2009). Alpha-synuclein S129 phosphorylation mutants do not alter nigrostriatal toxicity in a rat model of Parkinson disease. *J. Neuropathol. Exp. Neurol.* **68**, 515-524.

McGeer, P.L. & McGeer, E.G. (2008). Glial reactions in Parkinson's disease. *Mov Disord.* **23**, 474-483.

McKeith, I.G., Dickson, D.W., Lowe, J., Emre, M., O'Brien, J.T., Feldman, H., Cummings, J., Duda, J.E., Lippa, C., Perry, E.K., Aarsland, D., Arai, H., Ballard, C.G., Boeve, B., Burn, D.J., Costa, D., del, S.T., Dubois, B., Galasko, D., Gauthier, S., Goetz, C.G., Gomez-Tortosa, E., Halliday, G., Hansen, L.A., Hardy, J., Iwatsubo, T., Kalaria, R.N., Kaufer, D., Kenny, R.A., Korczyn, A., Kosaka, K., Lee, V.M., Lees, A., Litvan, I., Londos, E., Lopez, O.L., Minoshima, S., Mizuno, Y., Molina, J.A., Mukaetova-Ladinska, E.B., Pasquier, F., Perry, R.H., Schulz, J.B., Trojanowski, J.Q., & Yamada, M. (2005). Diagnosis and management of dementia with Lewy bodies: third report of the DLB Consortium. *Neurology* **65**, 1863-1872.

McNaught, K.S., Belizaire, R., Isacson, O., Jenner, P., & Olanow, C.W. (2003). Altered proteasomal function in sporadic Parkinson's disease. *Exp. Neurol.* **179**, 38-46.

McNaught, K.S., Perl, D.P., Brownell, A.L., & Olanow, C.W. (2004). Systemic exposure to proteasome inhibitors causes a progressive model of Parkinson's disease. *Ann. Neurol.* **56**, 149-162.

Memet, S. (2006). NF-kappaB functions in the nervous system: from development to disease. *Biochem. Pharmacol.* **72**, 1180-1195.

Messeguer, X., Escudero, R., Farre, D., Nunez, O., Martinez, J., & Alba, M.M. (2002). PROMO: detection of known transcription regulatory elements using species-tailored searches. *Bioinformatics.* **18**, 333-334.

Meulener, M., Whitworth, A.J., rmstrong-Gold, C.E., Rizzu, P., Heutink, P., Wes, P.D., Pallanck, L.J., & Bonini, N.M. (2005). Drosophila DJ-1 mutants are selectively sensitive to environmental toxins associated with Parkinson's disease. *Curr. Biol.* **15**, 1572-1577.

Miklossy, J., Arai, T., Guo, J.P., Klegeris, A., Yu, S., McGeer, E.G., & McGeer, P.L. (2006). LRRK2 expression in normal and pathologic human brain and in human cell lines. *J. Neuropathol. Exp. Neurol.* **65**, 953-963.

Miller, D.W., Hague, S.M., Clarimon, J., Baptista, M., Gwinn-Hardy, K., Cookson, M.R., & Singleton, A.B. (2004). Alpha-synuclein in blood and brain from familial Parkinson disease with SNCA locus triplication. *Neurology* **62**, 1835-1838.

Mizuta, I., Satake, W., Nakabayashi, Y., Ito, C., Suzuki, S., Momose, Y., Nagai, Y., Oka, A., Inoko, H., Fukae, J., Saito, Y., Sawabe, M., Murayama, S., Yamamoto, M., Hattori, N., Murata, M., & Toda, T. (2006). Multiple candidate gene analysis identifies alpha-synuclein as a susceptibility gene for sporadic Parkinson's disease. *Hum. Mol. Genet.* **15**, 1151-1158.

Moisoi, N., Klupsch, K., Fedele, V., East, P., Sharma, S., Renton, A., Plun-Favreau, H., Edwards, R.E., Teismann, P., Esposti, M.D., Morrison, A.D., Wood, N.W., Downward, J., & Martins, L.M. (2009). Mitochondrial dysfunction triggered by loss of HtrA2 results in the activation of a brain-specific transcriptional stress response. *Cell Death. Differ.* **16**, 449-464.

Molloy, S.A., Rowan, E.N., O'Brien, J.T., McKeith, I.G., Wesnes, K., & Burn, D.J. (2006). Effect of levodopa on cognitive function in Parkinson's disease with and without dementia and dementia with Lewy bodies. *J. Neurol. Neurosurg. Psychiatry* **77**, 1323-1328.

Moran, L.B., Croisier, E., Duke, D.C., Kalaitzakis, M.E., Roncaroli, F., Deprez, M., Dexter, D.T., Pearce, R.K., & Graeber, M.B. (2007). Analysis of alpha-synuclein,

dopamine and parkin pathways in neuropathologically confirmed parkinsonian nigra. *Acta Neuropathol.* **113**, 253-263.

Moran, L.B., Duke, D.C., Deprez, M., Dexter, D.T., Pearce, R.K., & Graeber, M.B. (2006). Whole genome expression profiling of the medial and lateral substantia nigra in Parkinson's disease. *Neurogenetics.* **7**, 1-11.

Moran, L.B. & Graeber, M.B. (2008). Towards a pathway definition of Parkinson's disease: a complex disorder with links to cancer, diabetes and inflammation. *Neurogenetics.* **9**, 1-13.

Moretta, A., Marcenaro, E., Parolini, S., Ferlazzo, G., & Moretta, L. (2008). NK cells at the interface between innate and adaptive immunity. *Cell Death. Differ.* **15**, 226-233.

Morgan, D., Diamond, D.M., Gottschall, P.E., Ugen, K.E., Dickey, C., Hardy, J., Duff, K., Jantzen, P., DiCarlo, G., Wilcock, D., Connor, K., Hatcher, J., Hope, C., Gordon, M., & Arendash, G.W. (2000). A beta peptide vaccination prevents memory loss in an animal model of Alzheimer's disease. *Nature* **408**, 982-985.

Morley, M., Molony, C.M., Weber, T.M., Devlin, J.L., Ewens, K.G., Spielman, R.S., & Cheung, V.G. (2004). Genetic analysis of genome-wide variation in human gene expression. *Nature* **430**, 743-747.

Mosimann, U.P., Mather, G., Wesnes, K.A., O'Brien, J.T., Burn, D.J., & McKeith, I.G. (2004). Visual perception in Parkinson disease dementia and dementia with Lewy bodies. *Neurology* **63**, 2091-2096.

Muda, M., Theodosiou, A., Rodrigues, N., Boschert, U., Camps, M., Gillieron, C., Davies, K., Ashworth, A., & Arkinstall, S. (1996). The dual specificity phosphatases M3/6 and MKP-3 are highly selective for inactivation of distinct mitogen-activated protein kinases. *J. Biol. Chem.* **271**, 27205-27208.

Mueller, J.C., Fuchs, J., Hofer, A., Zimprich, A., Lichtner, P., Illig, T., Berg, D., Wullner, U., Meitinger, T., & Gasser, T. (2005). Multiple regions of alpha-synuclein are associated with Parkinson's disease. *Ann. Neurol.* **57**, 535-541.

Munafo, M.R., Bowes, L., Clark, T.G., & Flint, J. (2005). Lack of association of the COMT (Val158/108 Met) gene and schizophrenia: a meta-analysis of case-control studies. *Mol. Psychiatry* **10**, 765-770.

Murphy, D.D., Rueter, S.M., Trojanowski, J.Q., & Lee, V.M. (2000). Synucleins are developmentally expressed, and alpha-synuclein regulates the size of the presynaptic vesicular pool in primary hippocampal neurons. *J. Neurosci.* **20**, 3214-3220.

Myers, A.J., Gibbs, J.R., Webster, J.A., Rohrer, K., Zhao, A., Marlowe, L., Kaleem, M., Leung, D., Bryden, L., Nath, P., Zismann, V.L., Joshipura, K., Huentelman, M.J., Hu-Lince, D., Coon, K.D., Craig, D.W., Pearson, J.V., Holmans, P., Heward, C.B., Reiman, E.M., Stephan, D., & Hardy, J. (2007a). A survey of genetic human cortical gene expression. *Nat. Genet.* **39**, 1494-1499.

Myers, A.J., Kaleem, M., Marlowe, L., Pittman, A.M., Lees, A.J., Fung, H.C., Duckworth, J., Leung, D., Gibson, A., Morris, C.M., de, S.R., & Hardy, J. (2005). The H1c haplotype at the MAPT locus is associated with Alzheimer's disease. *Hum. Mol. Genet.* **14**, 2399-2404.

Myers, A.J., Pittman, A.M., Zhao, A.S., Rohrer, K., Kaleem, M., Marlowe, L., Lees, A., Leung, D., McKeith, I.G., Perry, R.H., Morris, C.M., Trojanowski, J.Q., Clark, C., Karlawish, J., Arnold, S., Forman, M.S., Van, D., V, de, S.R., & Hardy, J. (2007b). The MAPT H1c risk haplotype is associated with increased expression of tau and especially of 4 repeat containing transcripts. *Neurobiol. Dis.* **25**, 561-570.

Nagano-Saito, A., Washimi, Y., Arahata, Y., Kachi, T., Lerch, J.P., Evans, A.C., Dagher, A., & Ito, K. (2005). Cerebral atrophy and its relation to cognitive impairment in Parkinson disease. *Neurology* **64**, 224-229.

Napier, I., Ponka, P., & Richardson, D.R. (2005). Iron trafficking in the mitochondrion: novel pathways revealed by disease. *Blood* **105**, 1867-1874.

Naruse-Nakajima, C., Asano, M., & Iwakura, Y. (2001). Involvement of EphA2 in the formation of the tail notochord via interaction with ephrinA1. *Mech. Dev.* **102**, 95-105.

Neumann, J., Bras, J., Deas, E., O'Sullivan, S.S., Parkkinen, L., Lachmann, R.H., Li, A., Holton, J., Guerreiro, R., Paudel, R., Segarane, B., Singleton, A., Lees, A., Hardy, J., Houlden, H., Revesz, T., & Wood, N.W. (2009). Glucocerebrosidase mutations in clinical and pathologically proven Parkinson's disease. *Brain* **132**, 1783-1794.

Nicklas, W.J., Vyas, I., & Heikkila, R.E. (1985). Inhibition of NADH-linked oxidation in brain mitochondria by 1-methyl-4-phenyl-pyridine, a metabolite of the neurotoxin, 1-methyl-4-phenyl-1,2,5,6-tetrahydropyridine. *Life Sci.* **36**, 2503-2508.

Niksic, M., Romano, M., Buratti, E., Pagani, F., & Baralle, F.E. (1999). Functional analysis of cis-acting elements regulating the alternative splicing of human CFTR exon 9. *Hum. Mol. Genet.* **8**, 2339-2349.

Nishioka, K., Hayashi, S., Farrer, M.J., Singleton, A.B., Yoshino, H., Imai, H., Kitami, T., Sato, K., Kuroda, R., Tomiyama, H., Mizoguchi, K., Murata, M., Toda, T., Imoto, I., Inazawa, J., Mizuno, Y., & Hattori, N. (2006). Clinical heterogeneity of alpha-synuclein gene duplication in Parkinson's disease. *Ann. Neurol.* **59**, 298-309.

Noe, E., Marder, K., Bell, K.L., Jacobs, D.M., Manly, J.J., & Stern, Y. (2004). Comparison of dementia with Lewy bodies to Alzheimer's disease and Parkinson's disease with dementia. *Mov Disord.* **19**, 60-67.

Nuber, S., Petrasch-Parwez, E., Winner, B., Winkler, J., von, H.S., Schmidt, T., Boy, J., Kuhn, M., Nguyen, H.P., Teismann, P., Schulz, J.B., Neumann, M., Pichler, B.J., Reischl, G., Holzmann, C., Schmitt, I., Bornemann, A., Kuhn, W., Zimmermann, F., Servadio, A., & Riess, O. (2008). Neurodegeneration and motor dysfunction in a conditional model of Parkinson's disease. *J. Neurosci.* **28**, 2471-2484.

Nussbaum, R.L. & Polymeropoulos, M.H. (1997). Genetics of Parkinson's disease. *Hum. Mol. Genet.* **6**, 1687-1691.

O'Brien, J.T., Colloby, S., Fenwick, J., Williams, E.D., Firbank, M., Burn, D., Aarsland, D., & McKeith, I.G. (2004). Dopamine transporter loss visualized with FP-CIT SPECT in the differential diagnosis of dementia with Lewy bodies. *Arch. Neurol.* **61**, 919-925.

Ohmori, O., Shinkai, T., Kojima, H., Terao, T., Suzuki, T., Mita, T., & Abe, K. (1998). Association study of a functional catechol-O-methyltransferase gene polymorphism in Japanese schizophrenics. *Neurosci. Lett.* **243**, 109-112.

Ohtake, H., Limprasert, P., Fan, Y., Onodera, O., Kakita, A., Takahashi, H., Bonner, L.T., Tsuang, D.W., Murray, I.V., Lee, V.M., Trojanowski, J.Q., Ishikawa, A., Idezuka, J., Murata, M., Toda, T., Bird, T.D., Leverenz, J.B., Tsuji, S., & La Spada, A.R. (2004). Beta-synuclein gene alterations in dementia with Lewy bodies. *Neurology* **63**, 805-811.

Olsen, J.H., Friis, S., Frederiksen, K., McLaughlin, J.K., Mellemkjaer, L., & Moller, H. (2005). Atypical cancer pattern in patients with Parkinson's disease. *Br. J. Cancer* **92**, 201-205.

Osaki, Y., Morita, Y., Fukumoto, M., Akagi, N., Yoshida, S., & Doi, Y. (2009). Cross-sectional and longitudinal studies of three-dimensional stereotactic surface projection SPECT analysis in Parkinson's disease. *Mov Disord.* **24**, 1475-1480.

Owen, A.M. (2004). Cognitive dysfunction in Parkinson's disease: the role of frontostriatal circuitry. *Neuroscientist.* **10**, 525-537.

Owen, A.M., James, M., Leigh, P.N., Summers, B.A., Marsden, C.D., Quinn, N.P., Lange, K.W., & Robbins, T.W. (1992). Fronto-striatal cognitive deficits at different stages of Parkinson's disease. *Brain* **115 (Pt 6)**, 1727-1751.

Pagonabarraga, J., Kulisevsky, J., Llebaria, G., Garcia-Sanchez, C., Pascual-Sedano, B., & Gironell, A. (2008). Parkinson's disease-cognitive rating scale: a new cognitive scale specific for Parkinson's disease. *Mov Disord.* **23**, 998-1005.

Paisan-Ruiz, C., Jain, S., Evans, E.W., Gilks, W.P., Simon, J., van der, B.M., Lopez de, M.A., Aparicio, S., Gil, A.M., Khan, N., Johnson, J., Martinez, J.R., Nicholl, D., Carrera, I.M., Pena, A.S., de, S.R., Lees, A., Marti-Masso, J.F., Perez-Tur, J., Wood, N.W., & Singleton, A.B. (2004). Cloning of the gene containing mutations that cause PARK8-linked Parkinson's disease. *Neuron* **44**, 595-600.

Palacino, J.J., Sagi, D., Goldberg, M.S., Krauss, S., Motz, C., Wacker, M., Klose, J., & Shen, J. (2004). Mitochondrial dysfunction and oxidative damage in parkin-deficient mice. *J. Biol. Chem.* **279**, 18614-18622.

Paleologou, K.E., Kragh, C.L., Mann, D.M., Salem, S.A., Al-Shami, R., Allsop, D., Hassan, A.H., Jensen, P.H., & El-Agnaf, O.M. (2009). Detection of elevated levels of soluble alpha-synuclein oligomers in post-mortem brain extracts from patients with dementia with Lewy bodies. *Brain* **132**, 1093-1101.

Palmer, R.E., Lee, S.B., Wong, J.C., Reynolds, P.A., Zhang, H., Truong, V., Oliner, J.D., Gerald, W.L., & Haber, D.A. (2002). Induction of BAIAP3 by the EWS-WT1 chimeric fusion implicates regulated exocytosis in tumorigenesis. *Cancer Cell* **2**, 497-505.

Pals, P., Lincoln, S., Manning, J., Heckman, M., Skipper, L., Hulihan, M., Van den, B.M., de, P.T., Cras, P., Crook, J., Van, B.C., & Farrer, M.J. (2004). alpha-Synuclein promoter confers susceptibility to Parkinson's disease. *Ann. Neurol.* **56**, 591-595.

Papapetropoulos, S., Farrer, M.J., Stone, J.T., Milkovic, N.M., Ross, O.A., Calvo, L., McQuorquodale, D., & Mash, D.C. (2007). Phenotypic associations of tau and ApoE in Parkinson's disease. *Neurosci. Lett.* **414**, 141-144.

Park, J., Lee, S.B., Lee, S., Kim, Y., Song, S., Kim, S., Bae, E., Kim, J., Shong, M., Kim, J.M., & Chung, J. (2006). Mitochondrial dysfunction in Drosophila PINK1 mutants is complemented by parkin. *Nature* **441**, 1157-1161.

Park, J.Y. & Lansbury, P.T., Jr. (2003). Beta-synuclein inhibits formation of alpha-synuclein protofibrils: a possible therapeutic strategy against Parkinson's disease. *Biochemistry* **42**, 3696-3700.

Parkinson,J. (1817). *An Essay on the Shaking Palsy.* Sherwood, Neely and Jones, London.

Parkkinen, L., Pirttila, T., & Alafuzoff, I. (2008). Applicability of current staging/categorization of alpha-synuclein pathology and their clinical relevance. *Acta Neuropathol.* **115**, 399-407.

Pasquale, E.B. (2008). Eph-ephrin bidirectional signaling in physiology and disease. *Cell* **133**, 38-52.

Pastinen, T. & Hudson, T.J. (2004). Cis-acting regulatory variation in the human genome. *Science* **306**, 647-650.

Pastor, P., Ezquerra, M., Perez, J.C., Chakraverty, S., Norton, J., Racette, B.A., McKeel, D., Perlmutter, J.S., Tolosa, E., & Goate, A.M. (2004). Novel haplotypes in 17q21 are associated with progressive supranuclear palsy. *Ann. Neurol.* **56**, 249-258.

Paulus, W. & Jellinger, K. (1991). The neuropathologic basis of different clinical subgroups of Parkinson's disease. *J. Neuropathol. Exp. Neurol.* **50**, 743-755.

Pavese, N., Khan, N.L., Scherfler, C., Cohen, L., Brooks, D.J., Wood, N.W., Bhatia, K.P., Quinn, N.P., Lees, A.J., & Piccini, P. (2009). Nigrostriatal dysfunction in homozygous and heterozygous parkin gene carriers: an 18F-dopa PET progression study. *Mov Disord.* **24**, 2260-2266.

Perraud, A.L., Knowles, H.M., & Schmitz, C. (2004). Novel aspects of signaling and ion-homeostasis regulation in immunocytes. The TRPM ion channels and their potential role in modulating the immune response. *Mol. Immunol.* **41**, 657-673.

Perry, E.K., Curtis, M., Dick, D.J., Candy, J.M., Atack, J.R., Bloxham, C.A., Blessed, G., Fairbairn, A., Tomlinson, B.E., & Perry, R.H. (1985). Cholinergic correlates of cognitive impairment in Parkinson's disease: comparisons with Alzheimer's disease. *J. Neurol. Neurosurg. Psychiatry* **48**, 413-421.

Petrides, M. (2000). The role of the mid-dorsolateral prefrontal cortex in working memory. *Exp. Brain Res.* **133**, 44-54.

Petrides, M. (2007). The orbitofrontal cortex: novelty, deviation from expectation, and memory. *Ann. N. Y. Acad. Sci.* **1121**, 33-53.

Pihlajamaki, M., Tanila, H., Hanninen, T., Kononen, M., Laakso, M., Partanen, K., Soininen, H., & Aronen, H.J. (2000). Verbal fluency activates the left medial

temporal lobe: a functional magnetic resonance imaging study. *Ann. Neurol.* **47**, 470-476.

Pillon, B., Deweer, B., Agid, Y., & Dubois, B. (1993). Explicit memory in Alzheimer's, Huntington's, and Parkinson's diseases. *Arch. Neurol.* **50**, 374-379.

Pittman, A.M., Myers, A.J., Abou-Sleiman, P., Fung, H.C., Kaleem, M., Marlowe, L., Duckworth, J., Leung, D., Williams, D., Kilford, L., Thomas, N., Morris, C.M., Dickson, D., Wood, N.W., Hardy, J., Lees, A.J., & de, S.R. (2005). Linkage disequilibrium fine mapping and haplotype association analysis of the tau gene in progressive supranuclear palsy and corticobasal degeneration. *J. Med. Genet.* **42**, 837-846.

Pletnikova, O., West, N., Lee, M.K., Rudow, G.L., Skolasky, R.L., Dawson, T.M., Marsh, L., & Troncoso, J.C. (2005). Abeta deposition is associated with enhanced cortical alpha-synuclein lesions in Lewy body diseases. *Neurobiol. Aging* **26**, 1183-1192.

Plun-Favreau, H., Klupsch, K., Moisoi, N., Gandhi, S., Kjaer, S., Frith, D., Harvey, K., Deas, E., Harvey, R.J., McDonald, N., Wood, N.W., Martins, L.M., & Downward, J. (2007). The mitochondrial protease HtrA2 is regulated by Parkinson's disease-associated kinase PINK1. *Nat. Cell Biol.* **9**, 1243-1252.

Polymeropoulos, M.H., Lavedan, C., Leroy, E., Ide, S.E., Dehejia, A., Dutra, A., Pike, B., Root, H., Rubenstein, J., Boyer, R., Stenroos, E.S., Chandrasekharappa, S., Athanassiadou, A., Papapetropoulos, T., Johnson, W.G., Lazzarini, A.M., Duvoisin, R.C., Di, I.G., Golbe, L.I., & Nussbaum, R.L. (1997). Mutation in the alpha-synuclein gene identified in families with Parkinson's disease. *Science* **276**, 2045-2047.

Pramstaller, P.P., Schlossmacher, M.G., Jacques, T.S., Scaravilli, F., Eskelson, C., Pepivani, I., Hedrich, K., Adel, S., Gonzales-McNeal, M., Hilker, R., Kramer, P.L., & Klein, C. (2005). Lewy body Parkinson's disease in a large pedigree with 77 Parkin mutation carriers. *Ann. Neurol.* **58**, 411-422.

Pratt, R.L. & Kinch, M.S. (2002). Activation of the EphA2 tyrosine kinase stimulates the MAP/ERK kinase signaling cascade. *Oncogene* **21**, 7690-7699.

Pratt, R.L. & Kinch, M.S. (2003). Ligand binding up-regulates EphA2 messenger RNA through the mitogen-activated protein/extracellular signal-regulated kinase pathway. *Mol. Cancer Res.* **1**, 1070-1076.

Qin, Z.S., Niu, T., & Liu, J.S. (2002). Partition-ligation-expectation-maximization algorithm for haplotype inference with single-nucleotide polymorphisms. *Am. J. Hum. Genet.* **71**, 1242-1247.

Qing, H., Wong, W., McGeer, E.G., & McGeer, P.L. (2009a). Lrrk2 phosphorylates alpha synuclein at serine 129: Parkinson disease implications. *Biochem. Biophys. Res. Commun.* **387**, 149-152.

Qing, H., Zhang, Y., Deng, Y., McGeer, E.G., & McGeer, P.L. (2009b). Lrrk2 interaction with alpha-synuclein in diffuse Lewy body disease. *Biochem. Biophys. Res. Commun.* **390**, 1229-1234.

Ragland, M., Hutter, C., Zabetian, C., & Edwards, K. (2009). Association between the ubiquitin carboxyl-terminal esterase L1 gene (UCHL1) S18Y variant and Parkinson's Disease: a HuGE review and meta-analysis. *Am. J. Epidemiol.* **170**, 1344-1357.

Rakovic, A., Stiller, B., Djarmati, A., Flaquer, A., Freudenberg, J., Toliat, M.R., Linnebank, M., Kostic, V., Lohmann, K., Paus, S., Nurnberg, P., Kubisch, C., Klein, C., Wullner, U., & Ramirez, A. (2009). Genetic association study of the P-type ATPase ATP13A2 in late-onset Parkinson's disease. *Mov Disord.* **24**, 429-433.

Ramirez, A., Heimbach, A., Grundemann, J., Stiller, B., Hampshire, D., Cid, L.P., Goebel, I., Mubaidin, A.F., Wriekat, A.L., Roeper, J., Al-Din, A., Hillmer, A.M., Karsak, M., Liss, B., Woods, C.G., Behrens, M.I., & Kubisch, C. (2006). Hereditary parkinsonism with dementia is caused by mutations in ATP13A2, encoding a lysosomal type 5 P-type ATPase. *Nat. Genet.* **38**, 1184-1191.

Rao, R.V. & Bredesen, D.E. (2004). Misfolded proteins, endoplasmic reticulum stress and neurodegeneration. *Curr. Opin. Cell Biol.* **16**, 653-662.

Ravina, B., Putt, M., Siderowf, A., Farrar, J.T., Gillespie, M., Crawley, A., Fernandez, H.H., Trieschmann, M.M., Reichwein, S., & Simuni, T. (2005). Donepezil for dementia in Parkinson's disease: a randomised, double blind, placebo controlled, crossover study. *J. Neurol. Neurosurg. Psychiatry* **76**, 934-939.

Reglodi, D., Tamas, A., Lubics, A., Szalontay, L., & Lengvari, I. (2004). Morphological and functional effects of PACAP in 6-hydroxydopamine-induced lesion of the substantia nigra in rats. *Regul. Pept.* **123**, 85-94.

Rhodes, S.L. & Ritz, B. (2008). Genetics of iron regulation and the possible role of iron in Parkinson's disease. *Neurobiol. Dis.* **32**, 183-195.

Richnau, N. & Aspenstrom, P. (2001). Rich, a rho GTPase-activating protein domain-containing protein involved in signaling by Cdc42 and Rac1. *J. Biol. Chem.* **276**, 35060-35070.

Rinne, J.O., Portin, R., Ruottinen, H., Nurmi, E., Bergman, J., Haaparanta, M., & Solin, O. (2000). Cognitive impairment and the brain dopaminergic system in Parkinson disease: [18F]fluorodopa positron emission tomographic study. *Arch. Neurol.* **57**, 470-475.

Rinne, J.O., Rummukainen, J., Paljarvi, L., & Rinne, U.K. (1989). Dementia in Parkinson's disease is related to neuronal loss in the medial substantia nigra. *Ann. Neurol.* **26**, 47-50.

Rizzu, P., Hinkle, D.A., Zhukareva, V., Bonifati, V., Severijnen, L.A., Martinez, D., Ravid, R., Kamphorst, W., Eberwine, J.H., Lee, V.M., Trojanowski, J.Q., & Heutink, P. (2004). DJ-1 colocalizes with tau inclusions: a link between parkinsonism and dementia. *Ann. Neurol.* **55**, 113-118.

Rockenstein, E., Hansen, L.A., Mallory, M., Trojanowski, J.Q., Galasko, D., & Masliah, E. (2001). Altered expression of the synuclein family mRNA in Lewy body and Alzheimer's disease. *Brain Res.* **914**, 48-56.

Rogaeva, E., Johnson, J., Lang, A.E., Gulick, C., Gwinn-Hardy, K., Kawarai, T., Sato, C., Morgan, A., Werner, J., Nussbaum, R., Petit, A., Okun, M.S., McInerney, A., Mandel, R., Groen, J.L., Fernandez, H.H., Postuma, R., Foote, K.D., Salehi-Rad, S., Liang, Y., Reimsnider, S., Tandon, A., Hardy, J., St George-Hyslop, P., & Singleton, A.B. (2004). Analysis of the PINK1 gene in a large cohort of cases with Parkinson disease. *Arch. Neurol.* **61**, 1898-1904.

Rollason, R., Korolchuk, V., Hamilton, C., Jepson, M., & Banting, G. (2009). A CD317/tetherin-RICH2 complex plays a critical role in the organization of the subapical actin cytoskeleton in polarized epithelial cells. *J. Cell Biol.* **184**, 721-736.

Ross, O.A., Braithwaite, A.T., Skipper, L.M., Kachergus, J., Hulihan, M.M., Middleton, F.A., Nishioka, K., Fuchs, J., Gasser, T., Maraganore, D.M., Adler, C.H., Larvor, L., Chartier-Harlin, M.C., Nilsson, C., Langston, J.W., Gwinn, K., Hattori, N., & Farrer, M.J. (2008a). Genomic investigation of alpha-synuclein multiplication and parkinsonism. *Ann. Neurol.* **63**, 743-750.

Ross, O.A., Gosal, D., Stone, J.T., Lincoln, S.J., Heckman, M.G., Irvine, G.B., Johnston, J.A., Gibson, J.M., Farrer, M.J., & Lynch, T. (2007a). Familial genes in sporadic disease: common variants of alpha-synuclein gene associate with Parkinson's disease. *Mech. Ageing Dev.* **128**, 378-382.

Ross, O.A., Haugarvoll, K., Stone, J.T., Heckman, M.G., White, L.R., Aasly, J.O., Mark, G.J., Lynch, T., Wszolek, Z.K., Uitti, R.J., & Farrer, M.J. (2007b). Lack of evidence for association of Parkin promoter polymorphism (PRKN-258) with increased risk of Parkinson's disease. *Parkinsonism. Relat Disord.* **13**, 386-388.

Ross, O.A., Soto, A.I., Vilarino-Guell, C., Heckman, M.G., Diehl, N.N., Hulihan, M.M., Aasly, J.O., Sando, S., Gibson, J.M., Lynch, T., Krygowska-Wajs, A., Opala, G., Barcikowska, M., Czyzewski, K., Uitti, R.J., Wszolek, Z.K., & Farrer, M.J. (2008b). Genetic variation of Omi/HtrA2 and Parkinson's disease. *Parkinsonism. Relat Disord.* **14**, 539-543.

Rothman, K.J. (1990). No adjustments are needed for multiple comparisons. *Epidemiology* **1**, 43-46.

Rozen, S. & Skaletsky, H. (2000). Primer3 on the WWW for general users and for biologist programmers. *Methods Mol. Biol.* **132**, 365-386.

Sabbagh, M.N., Adler, C.H., Lahti, T.J., Connor, D.J., Vedders, L., Peterson, L.K., Caviness, J.N., Shill, H.A., Sue, L.I., Ziabreva, I., Perry, E., Ballard, C.G., Aarsland, D., Walker, D.G., & Beach, T.G. (2009). Parkinson disease with dementia: comparing patients with and without Alzheimer pathology. *Alzheimer Dis. Assoc. Disord.* **23**, 295-297.

Sagar, H.J., Sullivan, E.V., Cooper, J.A., & Jordan, N. (1991). Normal release from proactive interference in untreated patients with Parkinson's disease. *Neuropsychologia* **29**, 1033-1044.

Santacruz, K., Lewis, J., Spires, T., Paulson, J., Kotilinek, L., Ingelsson, M., Guimaraes, A., DeTure, M., Ramsden, M., McGowan, E., Forster, C., Yue, M., Orne, J., Janus, C., Mariash, A., Kuskowski, M., Hyman, B., Hutton, M., & Ashe, K.H. (2005). Tau suppression in a neurodegenerative mouse model improves memory function. *Science* **309**, 476-481.

Santpere, G. & Ferrer, I. (2009). LRRK2 and neurodegeneration. *Acta Neuropathol.* **117**, 227-246.

Satake, W., Nakabayashi, Y., Mizuta, I., Hirota, Y., Ito, C., Kubo, M., Kawaguchi, T., Tsunoda, T., Watanabe, M., Takeda, A., Tomiyama, H., Nakashima, K., Hasegawa, K., Obata, F., Yoshikawa, T., Kawakami, H., Sakoda, S., Yamamoto, M., Hattori, N., Murata, M., Nakamura, Y., & Toda, T. (2009). Genome-wide association study identifies common variants at four loci as genetic risk factors for Parkinson's disease. *Nat. Genet.* **41**, 1303-1307.

Savettieri, G., Annesi, G., Civitelli, D., Ciro, C., I, Salemi, G., Ragonese, P., Annesi, F., Tarantino, P., Terruso, V., D'Amelio, M., & Quattrone, A. (2008). Identification of the novel D297fsX318 PINK1 mutation and phenotype variation in a family with early-onset Parkinson's disease. *Parkinsonism. Relat Disord.* **14**, 509-512.

Scatton, B., Javoy-Agid, F., Rouquier, L., Dubois, B., & Agid, Y. (1983). Reduction of cortical dopamine, noradrenaline, serotonin and their metabolites in Parkinson's disease. *Brain Res.* **275**, 321-328.

Schapira, A.H., Cooper, J.M., Dexter, D., Jenner, P., Clark, J.B., & Marsden, C.D. (1989). Mitochondrial complex I deficiency in Parkinson's disease. *Lancet* **333**, 1269.

Schiesling, C., Kieper, N., Seidel, K., & Kruger, R. (2008). Review: Familial Parkinson's disease--genetics, clinical phenotype and neuropathology in relation to the common sporadic form of the disease. *Neuropathol. Appl. Neurobiol.* **34**, 255-271.

Schlossmacher, M.G., Frosch, M.P., Gai, W.P., Medina, M., Sharma, N., Forno, L., Ochiishi, T., Shimura, H., Sharon, R., Hattori, N., Langston, J.W., Mizuno, Y., Hyman, B.T., Selkoe, D.J., & Kosik, K.S. (2002). Parkin localizes to the Lewy bodies of Parkinson disease and dementia with Lewy bodies. *Am. J. Pathol.* **160**, 1655-1667.

Scholz, S.W., Houlden, H., Schulte, C., Sharma, M., Li, A., Berg, D., Melchers, A., Paudel, R., Gibbs, J.R., Simon-Sanchez, J., Paisan-Ruiz, C., Bras, J., Ding, J., Chen, H., Traynor, B.J., Arepalli, S., Zonozi, R.R., Revesz, T., Holton, J., Wood, N., Lees, A., Oertel, W., Wullner, U., Goldwurm, S., Pellecchia, M.T., Illig, T., Riess, O., Fernandez, H.H., Rodriguez, R.L., Okun, M.S., Poewe, W., Wenning, G.K., Hardy, J.A., Singleton, A.B., & Gasser, T. (2009). SNCA variants are associated with increased risk for multiple system atrophy. *Ann. Neurol.* **65**, 610-614.

Schulz, T.C., Palmarini, G.M., Noggle, S.A., Weiler, D.A., Mitalipova, M.M., & Condie, B.G. (2003). Directed neuronal differentiation of human embryonic stem cells. *BMC. Neurosci.* **4**, 27.

Seth, D. & Rudolph, J. (2006). Redox regulation of MAP kinase phosphatase 3. *Biochemistry* **45**, 8476-8487.

Setsuie, R., Wang, Y.L., Mochizuki, H., Osaka, H., Hayakawa, H., Ichihara, N., Li, H., Furuta, A., Sano, Y., Sun, Y.J., Kwon, J., Kabuta, T., Yoshimi, K., Aoki, S., Mizuno, Y., Noda, M., & Wada, K. (2007). Dopaminergic neuronal loss in transgenic mice expressing the Parkinson's disease-associated UCH-L1 I93M mutant. *Neurochem. Int.* **50**, 119-129.

Shaffer, J.P. (1995). Multiple Hypothesis Testing. *Annu. Rev. Psychol.* **46**, 561-584.

Sharp, S.I., Ballard, C.G., Ziabreva, I., Piggott, M.A., Perry, R.H., Perry, E.K., Aarsland, D., Ehrt, U., Larsen, J.P., & Francis, P.T. (2008). Cortical serotonin 1A receptor levels are associated with depression in patients with dementia with Lewy bodies and Parkinson's disease dementia. *Dement. Geriatr. Cogn Disord.* **26**, 330-338.

Sharrocks, A.D. (2002). Complexities in ETS-domain transcription factor function and regulation: lessons from the TCF (ternary complex factor) subfamily. The Colworth Medal Lecture. *Biochem. Soc. Trans.* **30**, 1-9.

Shimada, H., Hirano, S., Shinotoh, H., Aotsuka, A., Sato, K., Tanaka, N., Ota, T., Asahina, M., Fukushi, K., Kuwabara, S., Hattori, T., Suhara, T., & Irie, T. (2009). Mapping of brain acetylcholinesterase alterations in Lewy body disease by PET. *Neurology* **73**, 273-278.

Shimura, H., Hattori, N., Kubo, S., Mizuno, Y., Asakawa, S., Minoshima, S., Shimizu, N., Iwai, K., Chiba, T., Tanaka, K., & Suzuki, T. (2000). Familial Parkinson disease gene product, parkin, is a ubiquitin-protein ligase. *Nat. Genet.* **25**, 302-305.

Shimura, H., Schlossmacher, M.G., Hattori, N., Frosch, M.P., Trockenbacher, A., Schneider, R., Mizuno, Y., Kosik, K.S., & Selkoe, D.J. (2001). Ubiquitination of a new form of alpha-synuclein by parkin from human brain: implications for Parkinson's disease. *Science* **293**, 263-269.

Shoulders, M.D. & Raines, R.T. (2009). Collagen structure and stability. *Annu. Rev. Biochem.* **78**, 929-958.

Sidransky, E., Nalls, M.A., Aasly, J.O., haron-Peretz, J., Annesi, G., Barbosa, E.R., Bar-Shira, A., Berg, D., Bras, J., Brice, A., Chen, C.M., Clark, L.N., Condroyer, C., De Marco, E.V., Durr, A., Eblan, M.J., Fahn, S., Farrer, M.J., Fung, H.C., Gan-Or, Z., Gasser, T., Gershoni-Baruch, R., Giladi, N., Griffith, A., Gurevich, T., Januario, C., Kropp, P., Lang, A.E., Lee-Chen, G.J., Lesage, S., Marder, K., Mata, I.F., Mirelman, A., Mitsui, J., Mizuta, I., Nicoletti, G., Oliveira, C., Ottman, R., Orr-Urtreger, A., Pereira, L.V., Quattrone, A., Rogaeva, E., Rolfs, A., Rosenbaum, H., Rozenberg, R., Samii, A., Samaddar, T., Schulte, C., Sharma, M., Singleton, A., Spitz, M., Tan, E.K., Tayebi, N., Toda, T., Troiano, A.R., Tsuji, S., Wittstock, M., Wolfsberg, T.G., Wu, Y.R., Zabetian, C.P., Zhao, Y., & Ziegler, S.G. (2009). Multicenter analysis of glucocerebrosidase mutations in Parkinson's disease. *N. Engl. J. Med.* **361**, 1651-1661.

Sieber, B.A., Kuzmin, A., Canals, J.M., Danielsson, A., Paratcha, G., Arenas, E., Alberch, J., Ogren, S.O., & Ibanez, C.F. (2004). Disruption of EphA/ephrin-a signaling in the nigrostriatal system reduces dopaminergic innervation and dissociates behavioral responses to amphetamine and cocaine. *Mol. Cell Neurosci.* **26**, 418-428.

Siepel, A., Pollard, K.S., & Haussler, D. (2006). New Methods for Detecting Lineage-Specific Selection. *Proceedings of the 10th International Conference on Research in Computational Molecular Biology*.

Simon-Sanchez, J., Schulte, C., Bras, J.M., Sharma, M., Gibbs, J.R., Berg, D., Paisan-Ruiz, C., Lichtner, P., Scholz, S.W., Hernandez, D.G., Kruger, R., Federoff, M., Klein, C., Goate, A., Perlmutter, J., Bonin, M., Nalls, M.A., Illig, T., Gieger, C., Houlden, H., Steffens, M., Okun, M.S., Racette, B.A., Cookson, M.R., Foote, K.D., Fernandez, H.H., Traynor, B.J., Schreiber, S., Arepalli, S., Zonozi, R., Gwinn, K., van der, B.M., Lopez, G., Chanock, S.J., Schatzkin, A., Park, Y., Hollenbeck, A., Gao, J., Huang, X., Wood, N.W., Lorenz, D., Deuschl, G., Chen, H., Riess, O., Hardy, J.A., Singleton, A.B., & Gasser, T. (2009). Genome-wide association study reveals genetic risk underlying Parkinson's disease. *Nat. Genet.* **41**, 1308-1312.

Simon-Sanchez, J. & Singleton, A.B. (2008). Sequencing analysis of OMI/HTRA2 shows previously reported pathogenic mutations in neurologically normal controls. *Hum. Mol. Genet.* **17**, 1988-1993.

Simunovic, F., Yi, M., Wang, Y., Macey, L., Brown, L.T., Krichevsky, A.M., Andersen, S.L., Stephens, R.M., Benes, F.M., & Sonntag, K.C. (2009). Gene expression profiling of substantia nigra dopamine neurons: further insights into Parkinson's disease pathology. *Brain* **132**, 1795-1809.

Singleton, A.B., Farrer, M., Johnson, J., Singleton, A., Hague, S., Kachergus, J., Hulihan, M., Peuralinna, T., Dutra, A., Nussbaum, R., Lincoln, S., Crawley, A., Hanson, M., Maraganore, D., Adler, C., Cookson, M.R., Muenter, M., Baptista, M., Miller, D., Blancato, J., Hardy, J., & Gwinn-Hardy, K. (2003). alpha-Synuclein locus triplication causes Parkinson's disease. *Science* **302**, 841.

Skipper, L., Wilkes, K., Toft, M., Baker, M., Lincoln, S., Hulihan, M., Ross, O.A., Hutton, M., Aasly, J., & Farrer, M. (2004). Linkage disequilibrium and association of MAPT H1 in Parkinson disease. *Am. J. Hum. Genet.* **75**, 669-677.

Skol, A.D., Scott, L.J., Abecasis, G.R., & Boehnke, M. (2006). Joint analysis is more efficient than replication-based analysis for two-stage genome-wide association studies. *Nat. Genet.* **38**, 209-213.

Smith, T.G., Karlsson, M., Lunn, J.S., Eblaghie, M.C., Keenan, I.D., Farrell, E.R., Tickle, C., Storey, K.G., & Keyse, S.M. (2006a). Negative feedback predominates over cross-regulation to control ERK MAPK activity in response to FGF signalling in embryos. *FEBS Lett.* **580**, 4242-4245.

Smith, W.W., Pei, Z., Jiang, H., Dawson, V.L., Dawson, T.M., & Ross, C.A. (2006b). Kinase activity of mutant LRRK2 mediates neuronal toxicity. *Nat. Neurosci.* **9**, 1231-1233.

Soung, N.K., Kang, Y.H., Kim, K., Kamijo, K., Yoon, H., Seong, Y.S., Kuo, Y.L., Miki, T., Kim, S.R., Kuriyama, R., Giam, C.Z., Ahn, C.H., & Lee, K.S. (2006). Requirement of hCenexin for proper mitotic functions of polo-like kinase 1 at the centrosomes. *Mol. Cell Biol.* **26**, 8316-8335.

Spencer, B., Potkar, R., Trejo, M., Rockenstein, E., Patrick, C., Gindi, R., Adame, A., Wyss-Coray, T., & Masliah, E. (2009). Beclin 1 gene transfer activates autophagy and ameliorates the neurodegenerative pathology in alpha-synuclein models of Parkinson's and Lewy body diseases. *J. Neurosci.* **29**, 13578-13588.

Spillantini, M.G., Crowther, R.A., Jakes, R., Hasegawa, M., & Goedert, M. (1998a). alpha-Synuclein in filamentous inclusions of Lewy bodies from Parkinson's disease and dementia with lewy bodies. *Proc. Natl. Acad. Sci. U. S. A* **95**, 6469-6473.

Spillantini, M.G., Murrell, J.R., Goedert, M., Farlow, M.R., Klug, A., & Ghetti, B. (1998b). Mutation in the tau gene in familial multiple system tauopathy with presenile dementia. *Proc. Natl. Acad. Sci. U. S. A* **95**, 7737-7741.

Spillantini, M.G., Schmidt, M.L., Lee, V.M., Trojanowski, J.Q., Jakes, R., & Goedert, M. (1997). Alpha-synuclein in Lewy bodies. *Nature* **388**, 839-840.

Sprengel, R. (2006). Role of AMPA receptors in synaptic plasticity. *Cell Tissue Res.* **326**, 447-455.

Squire, L.R. & Zola-Morgan, S. (1991). The medial temporal lobe memory system. *Science* **253**, 1380-1386.

Stamper, C., Siegel, A., Liang, W.S., Pearson, J.V., Stephan, D.A., Shill, H., Connor, D., Caviness, J.N., Sabbagh, M., Beach, T.G., Adler, C.H., & Dunckley, T. (2008). Neuronal gene expression correlates of Parkinson's disease with dementia. *Mov Disord.* **23**, 1588-1595.

Stark, C., Breitkreutz, B.J., Reguly, T., Boucher, L., Breitkreutz, A., & Tyers, M. (2006). BioGRID: a general repository for interaction datasets. *Nucleic Acids Res.* **34**, D535-D539.

Staropoli, J.F. (2008). Tumorigenesis and neurodegeneration: two sides of the same coin? *Bioessays* **30**, 719-727.

Staropoli, J.F., McDermott, C., Martinat, C., Schulman, B., Demireva, E., & Abeliovich, A. (2003). Parkin is a component of an SCF-like ubiquitin ligase complex and protects postmitotic neurons from kainate excitotoxicity. *Neuron* **37**, 735-749.

Stefansson, H., Helgason, A., Thorleifsson, G., Steinthorsdottir, V., Masson, G., Barnard, J., Baker, A., Jonasdottir, A., Ingason, A., Gudnadottir, V.G., Desnica, N., Hicks, A., Gylfason, A., Gudbjartsson, D.F., Jonsdottir, G.M., Sainz, J., Agnarsson, K., Birgisdottir, B., Ghosh, S., Olafsdottir, A., Cazier, J.B., Kristjansson, K., Frigge, M.L., Thorgeirsson, T.E., Gulcher, J.R., Kong, A., & Stefansson, K. (2005). A common inversion under selection in Europeans. *Nat. Genet.* **37**, 129-137.

Stern, Y., Mayeux, R., & Cote, L. (1984). Reaction time and vigilance in Parkinson's disease. Possible role of altered norepinephrine metabolism. *Arch. Neurol.* **41**, 1086-1089.

Stern, Y., Tetrud, J.W., Martin, W.R., Kutner, S.J., & Langston, J.W. (1990). Cognitive change following MPTP exposure. *Neurology* **40**, 261-264.

Strauss, K.M., Martins, L.M., Plun-Favreau, H., Marx, F.P., Kautzmann, S., Berg, D., Gasser, T., Wszolek, Z., Muller, T., Bornemann, A., Wolburg, H., Downward, J., Riess, O., Schulz, J.B., & Kruger, R. (2005). Loss of function mutations in the gene encoding Omi/HtrA2 in Parkinson's disease. *Hum. Mol. Genet.* **14**, 2099-2111.

Su, A.I., Wiltshire, T., Batalov, S., Lapp, H., Ching, K.A., Block, D., Zhang, J., Soden, R., Hayakawa, M., Kreiman, G., Cooke, M.P., Walker, J.R., & Hogenesch, J.B. (2004). A gene atlas of the mouse and human protein-encoding transcriptomes. *Proc. Natl. Acad. Sci. U. S. A* **101**, 6062-6067.

Sulzer, D. (2007). Multiple hit hypotheses for dopamine neuron loss in Parkinson's disease. *Trends Neurosci.* **30**, 244-250.

Sutherland, G.T., Halliday, G.M., Silburn, P.A., Mastaglia, F.L., Rowe, D.B., Boyle, R.S., O'Sullivan, J.D., Ly, T., Wilton, S.D., & Mellick, G.D. (2009a). Do polymorphisms in the familial Parkinsonism genes contribute to risk for sporadic Parkinson's disease? *Mov Disord.* **24**, 833-838.

Sutherland, G.T., Matigian, N.A., Chalk, A.M., Anderson, M.J., Silburn, P.A., kay-Sim, A., Wells, C.A., & Mellick, G.D. (2009b). A cross-study transcriptional analysis of Parkinson's disease. *PLoS. ONE.* **4**, e4955.

Suzuki, Y., Imai, Y., Nakayama, H., Takahashi, K., Takio, K., & Takahashi, R. (2001). A serine protease, HtrA2, is released from the mitochondria and interacts with XIAP, inducing cell death. *Mol. Cell* **8**, 613-621.

Szabo, A., Perou, C.M., Karaca, M., Perreard, L., Quackenbush, J.F., & Bernard, P.S. (2004). Statistical modeling for selecting housekeeper genes. *Genome Biol.* **5**, R59.

Szydlowska, K., Gozdz, A., Dabrowski, M., Zawadzka, M., & Kaminska, B. (2010). Prolonged activation of ERK triggers glutamate-induced apoptosis of astrocytes: neuroprotective effect of FK506. *J. Neurochem.* **113**, 904-918.

Tai, E.S. & Ordovas, J.M. (2008). Clinical significance of apolipoprotein A5. *Curr. Opin. Lipidol.* **19**, 349-354.

Tan, E.K., Chai, A., Teo, Y.Y., Zhao, Y., Tan, C., Shen, H., Chandran, V.R., Teoh, M.L., Yih, Y., Pavanni, R., Wong, M.C., Puvan, K., Lo, Y.L., & Yap, E. (2004). Alpha-synuclein haplotypes implicated in risk of Parkinson's disease. *Neurology* **62**, 128-131.

Tanaka, M., Kamata, R., & Sakai, R. (2005). EphA2 phosphorylates the cytoplasmic tail of Claudin-4 and mediates paracellular permeability. *J. Biol. Chem.* **280**, 42375-42382.

Taylor, A.E., Saint-Cyr, J.A., & Lang, A.E. (1986). Frontal lobe dysfunction in Parkinson's disease. The cortical focus of neostriatal outflow. *Brain* **109 (Pt 5)**, 845-883.

Tillerson, J.L., Caudle, W.M., Reveron, M.E., & Miller, G.W. (2002). Detection of behavioral impairments correlated to neurochemical deficits in mice treated with moderate doses of 1-methyl-4-phenyl-1,2,3,6-tetrahydropyridine. *Exp. Neurol.* **178**, 80-90.

Tobin, J.E., Latourelle, J.C., Lew, M.F., Klein, C., Suchowersky, O., Shill, H.A., Golbe, L.I., Mark, M.H., Growdon, J.H., Wooten, G.F., Racette, B.A., Perlmutter, J.S., Watts, R., Guttman, M., Baker, K.B., Goldwurm, S., Pezzoli, G., Singer, C., Saint-Hilaire, M.H., Hendricks, A.E., Williamson, S., Nagle, M.W., Wilk, J.B., Massood, T., Laramie, J.M., DeStefano, A.L., Litvan, I., Nicholson, G., Corbett, A., Isaacson, S., Burn, D.J., Chinnery, P.F., Pramstaller, P.P., Sherman, S., Al-hinti, J., Drasby, E., Nance, M., Moller, A.T., Ostergaard, K., Roxburgh, R., Snow, B., Slevin, J.T., Cambi, F., Gusella, J.F., & Myers, R.H. (2008). Haplotypes and gene expression implicate the MAPT region for Parkinson disease: the GenePD Study. *Neurology* **71**, 28-34.

Trockenbacher, A., Suckow, V., Foerster, J., Winter, J., Krauss, S., Ropers, H.H., Schneider, R., & Schweiger, S. (2001). MID1, mutated in Opitz syndrome, encodes an ubiquitin ligase that targets phosphatase 2A for degradation. *Nat. Genet.* **29**, 287-294.

Trumpower, B.L. (1990). The protonmotive Q cycle. Energy transduction by coupling of proton translocation to electron transfer by the cytochrome bc1 complex. *J. Biol. Chem.* **265**, 11409-11412.

Tsang, M., Maegawa, S., Kiang, A., Habas, R., Weinberg, E., & Dawid, I.B. (2004). A role for MKP3 in axial patterning of the zebrafish embryo. *Development* **131**, 2769-2779.

Tsuboi, Y. & Dickson, D.W. (2005). Dementia with Lewy bodies and Parkinson's disease with dementia: are they different? *Parkinsonism. Relat Disord.* **11 Suppl 1**, S47-S51.

Ullrich, O., Diestel, A., Eyupoglu, I.Y., & Nitsch, R. (2001). Regulation of microglial expression of integrins by poly(ADP-ribose) polymerase-1. *Nat. Cell Biol.* **3**, 1035-1042.

Urano, F., Wang, X., Bertolotti, A., Zhang, Y., Chung, P., Harding, H.P., & Ron, D. (2000). Coupling of stress in the ER to activation of JNK protein kinases by transmembrane protein kinase IRE1. *Science* **287**, 664-666.

Ushioda, R., Hoseki, J., Araki, K., Jansen, G., Thomas, D.Y., & Nagata, K. (2008). ERdj5 is required as a disulfide reductase for degradation of misfolded proteins in the ER. *Science* **321**, 569-572.

Valente, E.M., Abou-Sleiman, P.M., Caputo, V., Muqit, M.M., Harvey, K., Gispert, S., Ali, Z., Del, T.D., Bentivoglio, A.R., Healy, D.G., Albanese, A., Nussbaum, R., Gonzalez-Maldonado, R., Deller, T., Salvi, S., Cortelli, P., Gilks, W.P., Latchman, D.S., Harvey, R.J., Dallapiccola, B., Auburger, G., & Wood, N.W. (2004). Hereditary early-onset Parkinson's disease caused by mutations in PINK1. *Science* **304**, 1158-1160.

Van den Eynde, B.J. & Morel, S. (2001). Differential processing of class-I-restricted epitopes by the standard proteasome and the immunoproteasome. *Curr. Opin. Immunol.* **13**, 147-153.

Van den Heuvel, D.M. & Pasterkamp, R.J. (2008). Getting connected in the dopamine system. *Prog. Neurobiol.* **85**, 75-93.

Vandesompele, J., De, P.K., Pattyn, F., Poppe, B., Van, R.N., De, P.A., & Speleman, F. (2002). Accurate normalization of real-time quantitative RT-PCR data by geometric averaging of multiple internal control genes. *Genome Biol.* **3**, R34.

Vandrovcova, J., Pittman, A.M., Malzer, E., Abou-Sleiman, P.M., Lees, A.J., Wood, N.W., & de, S.R. (2009). Association of MAPT haplotype-tagging SNPs with sporadic Parkinson's disease. *Neurobiol. Aging* **30**, 1477-1482.

Vawter, M.P., Tomita, H., Meng, F., Bolstad, B., Li, J., Evans, S., Choudary, P., Atz, M., Shao, L., Neal, C., Walsh, D.M., Burmeister, M., Speed, T., Myers, R., Jones, E.G., Watson, S.J., Akil, H., & Bunney, W.E. (2006). Mitochondrial-related gene expression changes are sensitive to agonal-pH state: implications for brain disorders. *Mol. Psychiatry* **11**, 615, 663-615, 679.

Vermersch, P., Delacourte, A., Javoy-Agid, F., Hauw, J.J., & Agid, Y. (1993). Dementia in Parkinson's disease: biochemical evidence for cortical involvement using the immunodetection of abnormal Tau proteins. *Ann. Neurol.* **33**, 445-450.

Vidal, R., Ghetti, B., Takao, M., Brefel-Courbon, C., Uro-Coste, E., Glazier, B.S., Siani, V., Benson, M.D., Calvas, P., Miravalle, L., Rascol, O., & Delisle, M.B. (2004). Intracellular ferritin accumulation in neural and extraneural tissue characterizes a neurodegenerative disease associated with a mutation in the ferritin light polypeptide gene. *J. Neuropathol. Exp. Neurol.* **63**, 363-380.

Vila, M., Vukosavic, S., Jackson-Lewis, V., Neystat, M., Jakowec, M., & Przedborski, S. (2000). Alpha-synuclein up-regulation in substantia nigra dopaminergic neurons following administration of the parkinsonian toxin MPTP. *J. Neurochem.* **74**, 721-729.

Vilarino-Guell, C., Soto, A.I., Lincoln, S.J., Ben, Y.S., Kefi, M., Heckman, M.G., Hulihan, M.M., Chai, H., Diehl, N.N., Amouri, R., Rajput, A., Mash, D.C., Dickson, D.W., Middleton, L.T., Gibson, R.A., Hentati, F., & Farrer, M.J. (2009). ATP13A2 variability in Parkinson disease. *Hum. Mutat.* **30**, 406-410.

Volles, M.J. & Lansbury, P.T., Jr. (2003). Zeroing in on the pathogenic form of alpha-synuclein and its mechanism of neurotoxicity in Parkinson's disease. *Biochemistry* **42**, 7871-7878.

von Coelln, R., Thomas, B., Savitt, J.M., Lim, K.L., Sasaki, M., Hess, E.J., Dawson, V.L., & Dawson, T.M. (2004). Loss of locus coeruleus neurons and reduced startle in parkin null mice. *Proc. Natl. Acad. Sci. U. S. A* **101**, 10744-10749.

Wakabayashi, K., Tanji, K., Mori, F., & Takahashi, H. (2007). The Lewy body in Parkinson's disease: molecules implicated in the formation and degradation of alpha-synuclein aggregates. *Neuropathology.* **27**, 494-506.

Wang, F., Feng, X., Ma, J., Zou, H., & Chan, P. (2006). A common A340T variant in PINK1 gene associated with late-onset Parkinson's disease in Chinese. *Neurosci. Lett.* **410**, 121-125.

Wei, J., Fujita, M., Nakai, M., Waragai, M., Watabe, K., Akatsu, H., Rockenstein, E., Masliah, E., & Hashimoto, M. (2007). Enhanced lysosomal pathology caused by beta-synuclein mutants linked to dementia with Lewy bodies. *J. Biol. Chem.* **282**, 28904-28914.

Weidong, L., Shen, C., & Jankovic, J. (2009). Etiopathogenesis of Parkinson disease: a new beginning? *Neuroscientist.* **15**, 28-35.

Weintraub, D., Moberg, P.J., Culbertson, W.C., Duda, J.E., & Stern, M.B. (2004). Evidence for impaired encoding and retrieval memory profiles in Parkinson disease. *Cogn Behav. Neurol.* **17**, 195-200.

Wenning, G.K., Stefanova, N., Jellinger, K.A., Poewe, W., & Schlossmacher, M.G. (2008). Multiple system atrophy: a primary oligodendrogliopathy. *Ann. Neurol.* **64**, 239-246.

West, A.B., Maraganore, D., Crook, J., Lesnick, T., Lockhart, P.J., Wilkes, K.M., Kapatos, G., Hardy, J.A., & Farrer, M.J. (2002). Functional association of the parkin gene promoter with idiopathic Parkinson's disease. *Hum. Mol. Genet.* **11**, 2787-2792.

West, A.B., Moore, D.J., Biskup, S., Bugayenko, A., Smith, W.W., Ross, C.A., Dawson, V.L., & Dawson, T.M. (2005). Parkinson's disease-associated mutations in leucine-rich repeat kinase 2 augment kinase activity. *Proc. Natl. Acad. Sci. U. S. A* **102**, 16842-16847.

Westerlund, M., Belin, A.C., Anvret, A., Hakansson, A., Nissbrandt, H., Lind, C., Sydow, O., Olson, L., & Galter, D. (2008). Cerebellar alpha-synuclein levels are decreased in Parkinson's disease and do not correlate with SNCA polymorphisms associated with disease in a Swedish material. *FASEB J.* **22**, 3509-3514.

Whitehouse, P.J., Hedreen, J.C., White, C.L., III, & Price, D.L. (1983). Basal forebrain neurons in the dementia of Parkinson disease. *Ann. Neurol.* **13**, 243-248.

Wigginton, J.E., Cutler, D.J., & Abecasis, G.R. (2005). A note on exact tests of Hardy-Weinberg equilibrium. *Am. J. Hum. Genet.* **76**, 887-893.

Williams-Gray, C.H., Evans, J.R., Goris, A., Foltynie, T., Ban, M., Robbins, T.W., Brayne, C., Kolachana, B.S., Weinberger, D.R., Sawcer, S.J., & Barker, R.A.

(2009a). The distinct cognitive syndromes of Parkinson's disease: 5 year follow-up of the CamPaIGN cohort. *Brain* **132**, 2958-2969.

Williams-Gray, C.H., Foltynie, T., Brayne, C.E., Robbins, T.W., & Barker, R.A. (2007a). Evolution of cognitive dysfunction in an incident Parkinson's disease cohort. *Brain* **130**, 1787-1798.

Williams-Gray, C.H., Goris, A., Saiki, M., Foltynie, T., Compston, D.A., Sawcer, S.J., & Barker, R.A. (2009b). Apolipoprotein E genotype as a risk factor for susceptibility to and dementia in Parkinson's disease. *J. Neurol.* **256**, 493-498.

Williams-Gray, C.H., Hampshire, A., Barker, R.A., & Owen, A.M. (2008). Attentional control in Parkinson's disease is dependent on COMT val 158 met genotype. *Brain* **131**, 397-408.

Williams-Gray, C.H., Hampshire, A., Robbins, T.W., Owen, A.M., & Barker, R.A. (2007b). Catechol O-methyltransferase Val158Met genotype influences frontoparietal activity during planning in patients with Parkinson's disease. *J. Neurosci.* **27**, 4832-4838.

Winkler, S., Hagenah, J., Lincoln, S., Heckman, M., Haugarvoll, K., Lohmann-Hedrich, K., Kostic, V., Farrer, M., & Klein, C. (2007). alpha-Synuclein and Parkinson disease susceptibility. *Neurology* **69**, 1745-1750.

Wood-Kaczmar, A., Gandhi, S., Yao, Z., Abramov, A.Y., Miljan, E.A., Keen, G., Stanyer, L., Hargreaves, I., Klupsch, K., Deas, E., Downward, J., Mansfield, L., Jat, P., Taylor, J., Heales, S., Duchen, M.R., Latchman, D., Tabrizi, S.J., & Wood, N.W. (2008). PINK1 is necessary for long term survival and mitochondrial function in human dopaminergic neurons. *PLoS. ONE.* **3**, e2455.

Xiang, M., Gao, W.Q., Hasson, T., & Shin, J.J. (1998). Requirement for Brn-3c in maturation and survival, but not in fate determination of inner ear hair cells. *Development* **125**, 3935-3946.

Xu, J., Kao, S.Y., Lee, F.J., Song, W., Jin, L.W., & Yankner, B.A. (2002). Dopamine-dependent neurotoxicity of alpha-synuclein: a mechanism for selective neurodegeneration in Parkinson disease. *Nat. Med.* **8**, 600-606.

Yamaguchi, K., Cochran, E.J., Murrell, J.R., Polymeropoulos, M.H., Shannon, K.M., Crowther, R.A., Goedert, M., & Ghetti, B. (2005). Abundant neuritic inclusions and microvacuolar changes in a case of diffuse Lewy body disease with the A53T mutation in the alpha-synuclein gene. *Acta Neuropathol.* **110**, 298-305.

Yan, H., Yuan, W., Velculescu, V.E., Vogelstein, B., & Kinzler, K.W. (2002). Allelic variation in human gene expression. *Science* **297**, 1143.

Yang, G., Zhang, G., Pittelkow, M.R., Ramoni, M., & Tsao, H. (2006). Expression profiling of UVB response in melanocytes identifies a set of p53-target genes. *J. Invest Dermatol.* **126**, 2490-2506.

Yang, Q., She, H., Gearing, M., Colla, E., Lee, M., Shacka, J.J., & Mao, Z. (2009). Regulation of neuronal survival factor MEF2D by chaperone-mediated autophagy. *Science* **323**, 124-127.

Yang, Q.H., Church-Hajduk, R., Ren, J., Newton, M.L., & Du, C. (2003). Omi/HtrA2 catalytic cleavage of inhibitor of apoptosis (IAP) irreversibly inactivates IAPs and facilitates caspase activity in apoptosis. *Genes Dev.* **17**, 1487-1496.

Yang, W., Chen, L., Ding, Y., Zhuang, X., & Kang, U.J. (2007). Paraquat induces dopaminergic dysfunction and proteasome impairment in DJ-1-deficient mice. *Hum. Mol. Genet.* **16**, 2900-2910.

Yang, Y., Gehrke, S., Haque, M.E., Imai, Y., Kosek, J., Yang, L., Beal, M.F., Nishimura, I., Wakamatsu, K., Ito, S., Takahashi, R., & Lu, B. (2005). Inactivation of Drosophila DJ-1 leads to impairments of oxidative stress response and phosphatidylinositol 3-kinase/Akt signaling. *Proc. Natl. Acad. Sci. U. S. A* **102**, 13670-13675.

Yasuda, T., Nihira, T., Ren, Y.R., Cao, X.Q., Wada, K., Setsuie, R., Kabuta, T., Wada, K., Hattori, N., Mizuno, Y., & Mochizuki, H. (2009). Effects of UCH-L1 on alpha-synuclein over-expression mouse model of Parkinson's disease. *J. Neurochem.* **108**, 932-944.

Yates, T., Okoniewski, M.J., & Miller, C.J. (2008). X:Map: annotation and visualization of genome structure for Affymetrix exon array analysis. *Nucleic Acids Res.* **36**, D780-D786.

Yavich, L., Forsberg, M.M., Karayiorgou, M., Gogos, J.A., & Mannisto, P.T. (2007). Site-specific role of catechol-O-methyltransferase in dopamine overflow within prefrontal cortex and dorsal striatum. *J. Neurosci.* **27**, 10196-10209.

Ye, J., Rawson, R.B., Komuro, R., Chen, X., Dave, U.P., Prywes, R., Brown, M.S., & Goldstein, J.L. (2000). ER stress induces cleavage of membrane-bound ATF6 by the same proteases that process SREBPs. *Mol. Cell* **6**, 1355-1364.

Yong, J., Tan, I., Lim, L., & Leung, T. (2006). Phosphorylation of myosin phosphatase targeting subunit 3 (MYPT3) and regulation of protein phosphatase 1 by protein kinase A. *J. Biol. Chem.* **281**, 31202-31211.

Yoshida, H. (2007). ER stress and diseases. *FEBS J.* **274**, 630-658.

Yoshimoto, R., Kataoka, N., Okawa, K., & Ohno, M. (2009). Isolation and characterization of post-splicing lariat-intron complexes. *Nucleic Acids Res.* **37**, 891-902.

Zabetian, C.P., Hutter, C.M., Factor, S.A., Nutt, J.G., Higgins, D.S., Griffith, A., Roberts, J.W., Leis, B.C., Kay, D.M., Yearout, D., Montimurro, J.S., Edwards, K.L., Samii, A., & Payami, H. (2007). Association analysis of MAPT H1 haplotype and subhaplotypes in Parkinson's disease. *Ann. Neurol.* **62**, 137-144.

Zarranz, J.J., Alegre, J., Gomez-Esteban, J.C., Lezcano, E., Ros, R., Ampuero, I., Vidal, L., Hoenicka, J., Rodriguez, O., Atares, B., Llorens, V., Gomez, T.E., del, S.T., Munoz, D.G., & de Yebenes, J.G. (2004). The new mutation, E46K, of alpha-synuclein causes Parkinson and Lewy body dementia. *Ann. Neurol.* **55**, 164-173.

Zelinski, D.P., Zantek, N.D., Stewart, J.C., Irizarry, A.R., & Kinch, M.S. (2001). EphA2 overexpression causes tumorigenesis of mammary epithelial cells. *Cancer Res.* **61**, 2301-2306.

Zhang, G., Njauw, C.N., Park, J.M., Naruse, C., Asano, M., & Tsao, H. (2008). EphA2 is an essential mediator of UV radiation-induced apoptosis. *Cancer Res.* **68**, 1691-1696.

Zhang, J., Nomura, J., Maruyama, M., Nishimoto, M., Muramatsu, M., & Okuda, A. (2009). Identification of an ES cell pluripotent state-specific DUSP6 enhancer. *Biochem. Biophys. Res. Commun.* **378**, 319-323.

Zhang, L., Shimoji, M., Thomas, B., Moore, D.J., Yu, S.W., Marupudi, N.I., Torp, R., Torgner, I.A., Ottersen, O.P., Dawson, T.M., & Dawson, V.L. (2005a). Mitochondrial localization of the Parkinson's disease related protein DJ-1: implications for pathogenesis. *Hum. Mol. Genet.* **14**, 2063-2073.

Zhang, Y., James, M., Middleton, F.A., & Davis, R.L. (2005b). Transcriptional analysis of multiple brain regions in Parkinson's disease supports the involvement of specific protein processing, energy metabolism, and signaling pathways, and suggests novel disease mechanisms. *Am. J. Med. Genet. B Neuropsychiatr. Genet.* **137B**, 5-16.

Zhou, B., Wu, L., Shen, K., Zhang, J., Lawrence, D.S., & Zhang, Z.Y. (2001). Multiple regions of MAP kinase phosphatase 3 are involved in its recognition and activation by ERK2. *J. Biol. Chem.* **276**, 6506-6515.

Zhou, W., Milder, J.B., & Freed, C.R. (2008). Transgenic mice overexpressing tyrosine-to-cysteine mutant human alpha-synuclein: a progressive neurodegenerative model of diffuse Lewy body disease. *J. Biol. Chem.* **283**, 9863-9870.

Zhu, G., Lipsky, R.H., Xu, K., Ali, S., Hyde, T., Kleinman, J., Akhtar, L.A., Mash, D.C., & Goldman, D. (2004). Differential expression of human COMT alleles in brain and lymphoblasts detected by RT-coupled 5' nuclease assay. *Psychopharmacology (Berl)* **177**, 178-184.

Zhu, J.H., Guo, F., Shelburne, J., Watkins, S., & Chu, C.T. (2003). Localization of phosphorylated ERK/MAP kinases to mitochondria and autophagosomes in Lewy body diseases. *Brain Pathol.* **13**, 473-481.

Zhu, J.H., Horbinski, C., Guo, F., Watkins, S., Uchiyama, Y., & Chu, C.T. (2007). Regulation of autophagy by extracellular signal-regulated protein kinases during 1-methyl-4-phenylpyridinium-induced cell death. *Am. J. Pathol.* **170**, 75-86.

Zhu, J.H., Kulich, S.M., Oury, T.D., & Chu, C.T. (2002). Cytoplasmic aggregates of phosphorylated extracellular signal-regulated protein kinases in Lewy body diseases. *Am. J. Pathol.* **161**, 2087-2098.

Zimprich, A., Biskup, S., Leitner, P., Lichtner, P., Farrer, M., Lincoln, S., Kachergus, J., Hulihan, M., Uitti, R.J., Calne, D.B., Stoessl, A.J., Pfeiffer, R.F., Patenge, N., Carbajal, I.C., Vieregge, P., Asmus, F., Muller-Myhsok, B., Dickson, D.W., Meitinger, T., Strom, T.M., Wszolek, Z.K., & Gasser, T. (2004). Mutations in LRRK2 cause autosomal-dominant parkinsonism with pleomorphic pathology. *Neuron* **44**, 601-607.

Zuniga, A., Torres, J., Ubeda, J., & Pulido, R. (1999). Interaction of mitogen-activated protein kinases with the kinase interaction motif of the tyrosine phosphatase PTP-SL provides substrate specificity and retains ERK2 in the cytoplasm. *J. Biol. Chem.* **274**, 21900-21907.

Zweig, R.M., Cardillo, J.E., Cohen, M., Giere, S., & Hedreen, J.C. (1993). The locus ceruleus and dementia in Parkinson's disease. *Neurology* **43**, 986-991.

Appendix

Group (*n*)	Brain bank code	Year of death	*GBA* status	*PARK2* status	*PINK1* status
IPDD (15)	P24/94	1994	WT	WT	WT
	P18/95	1995	WT	WT	WT
	P25/98	1998	Arg502Cys	WT	WT
	P36/98	1998	WT	WT	WT
	P62/98	1998	WT	WT	WT
	P30/00	2000	ND	ND	ND
	P54/00	2000	WT	WT	WT
	P59/00	2000	WT	WT	WT
	P05/01	2001	WT	WT	WT
	P18/01	2001	WT	WT	WT
	P01/02	2002	WT	WT	WT
	P23/02	2002	ND	ND	ND
	P25/03	2003	WT	ND	ND
	P18/05	2005	WT	WT	WT
	P60/05	2005	WT	ND	ND
IPDND (16)	P16/92	1992	WT	WT	WT
	P28/94	1994	WT	WT	WT
	P45/94	1994	WT	WT	WT
	P12/95	1995	WT	WT	WT
	P17/96	1996	WT	WT	WT
	P05/97	1997	WT	WT	WT
	P65/97	1997	WT	WT	WT
	P50/98	1998	WT	WT	WT
	P67/98	1998	WT	WT	WT
	P14/99	1999	WT	WT	WT
	P40/99	1999	ND	ND	ND
	P54/99	1999	Asn409Ser	WT	WT
	P55/00	2000	WT	WT	WT
	P75/00	2000	WT	WT	WT
	P24/01	2001	WT	WT	WT
	P05/04	2004	ND	ND	ND

Supplementary Table 1. IPD cognitive series: PD gene mutation data.

Individual PD gene mutation data for the IPD cognitive series case samples. Mutation investigations consisted of dideoxy DNA sequencing of all transcribed exons, and were previously performed by Drs. Patrick Abou-Sleiman and Emma Deas. *GBA = β-Glucocerebrosidase*; IPD = idiopathic Parkinson's disease; IPDD = idiopathic Parkinson's disease with dementia; IPDND = idiopathic Parkinson's disease no dementia; ND = not determined; *PARK2 = Parkin*; PD = Parkinson's disease; *PINK1 = Phosphatase and tensin homologue-induced putative kinase 1*; WT = wild type.

Supplementary Table 2. IPD cognitive series: neuropathological data.

Individual neuropathological data for the IPD cognitive series case samples (below and following page). Regional LB load was scored semiquantitatively according to the following scale: 0 = none; 1 = low; 2 = medium; 3 = high. Cell loss indicates the region(s) in which neuronal cell death was observed. Neuropathological investigations were previously performed by Dr. Janice Holton. ACC = anterior cingulate cortex; AFC = anterior frontal cortex; BS = brain stem; EC = entorhinal cortex; HP = hippocampus; IPD = idiopathic Parkinson's disease; IPDD = idiopathic Parkinson's disease with dementia; IPDND = idiopathic Parkinson's disease no dementia; IHC = immunohistochemistry; LB = Lewy body; LC = locus coeruleus; MED = medulla; ND = not determined; NbM = nucleus basalis of Meynert; PC = parietal cortex; STR = striatum; SN = substantia nigra; TC = temporal cortex.

Group (*n*)	Brain bank code	Year of death	LB IHC target	Regional LB load			Regional cell loss
				Brain stem	Limbic system	Cortex	
IPDD (15)	P24/94	1994	Ubiquitin	BS 1; LC 1; SN 1	ND	ACC 1	LC; SN
	P18/95	1995	Ubiquitin	BS 1; LC 2; STR 0; SN 1	ND	ACC 1; NbM 1	LC; SN
	P25/98	1998	α-Synuclein	LC 2; SN 2; STR 0	ND	ACC 1	LC; SN
	P36/98	1998	α-Synuclein	BS 1	ND	Cortex 1	LC; SN
	P62/98	1998	α-Synuclein	LC 1; SN 1; STR 0	Amygdala 3; HP 1	ACC 2; AFC 3; TC 3	LC; SN
	P30/00	2000	α-Synuclein	LC 1; SN 1	ND	Cortex 1	LC; SN
	P54/00	2000	α-Synuclein	SN 1	ND	Cortex 1; NbM 1	LC; SN
	P59/00	2000	α-Synuclein	LC 1; SN 1	ND	None	LC; SN
	P05/01	2001	α-Synuclein	BS 3	ND	ACC 2	LC; SN
	P18/01	2001	α-Synuclein	ND	ND	ND	ND
	P01/02	2002	α-Synuclein	SN 1	EC 2	ACC 2; AFC 1; PC 0; TC 1	HP; LC; SN
	P23/02	2002	α-Synuclein	SN 1	EC 2; HP 1	ACC 2; AFC 1; PC 2; TC 2	SN
	P25/03	2003	α-Synuclein	LC 3; SN 3	EC 2; HP 1	ACC 2; AFC 1; PC 0; TC 2	LC; SN
	P18/05	2005	α-Synuclein	LC 1; SN 1; STR 0	EC 2	ACC 2; AFC 1; PC 0; TC 1	ND
	P60/05	2005	α-Synuclein	LC 1; MED 1; SN 1; STR 0	EC 2; HP 1	ACC 1; AFC 2; PC 1; TC 1	SN

Group (*n*)	Brain bank code	Year of death	LB IHC target	Regional LB loads			Regional cell losses
				Brain stem	Limbic system	Cortex	
IPDND (16)	P16/92	1992	Ubiquitin	LC 1; SN 1; STR 0	ND	ACC 1	LC; SN
	P28/94	1994	Ubiquitin	LC 1; MED 0; SN 0; STR 0	ND	ACC 1	LC; SN
	P45/94	1994	Ubiquitin	BS 1; LC 1; SN 1; STR 0	ND	ACC 1; NbM 1	LC; SN
	P12/95	1995	Ubiquitin	BS 1; SN 1; STR 0	ND	ACC 1	LC; SN
	P17/96	1996	Ubiquitin	BS 1; LC 1; SN 1; STR 0	Amygdala 1; EC 1	ACC 1; TC 1	LC; SN
	P05/97	1997	Ubiquitin	LC 1; MED 0; SN 1	Amygdala 1; HP 1	ACC 1; NbM 1	LC; SN
	P65/97	1997	Ubiquitin	LC 1; SN 1; STR 0	EC 1	Cortex 0	LC; SN
	P50/98	1998	α-Synuclein	LC 1; SN 1	EC 1; HP 1	ACC 1; NbM 1	LC; SN
	P67/98	1998	α-Synuclein	BS 1; LC 1; SN 1; STR 0	EC 0	ACC 1; NbM 3	LC; SN
	P14/99	1999	α-Synuclein	LC 1; SN 1	EC 1; HP 1	ACC 2; TC 1	LC; SN
	P40/99	1999	α-Synuclein	BS 3	ND	Cortex 1	LC; SN
	P54/99	1999	α-Synuclein	ND	EC 2	ACC 2	LC; SN
	P55/00	2000	α-Synuclein	LC 1; SN 1	None	AFC 2; TC 1	LC; SN
	P75/00	2000	α-Synuclein	BS 3; LC 3; SN 3	None	Cortex 1; NbM 3	LC; SN
	P24/01	2001	α-Synuclein	LC 1; SN 1	EC 2	ACC 2; AFC 1; PC 1; TC 1	LC; SN
	P05/04	2004	α-Synuclein	LC 2; SN 2	EC 2; HP 1	ACC 2; AFC 2; PC 0; TC 2	LC; SN

Group (*n*)	Brain bank code	Year of death	Drug regime
IPDD (15)	P24/94	1994	1984 to death: levodopa
	P18/95	1995	1988 to death: carbidopa, DA agonist, levodopa
	P25/98	1998	1989 to death: carbidopa, levodopa
	P36/98	1998	1989 to death: levodopa, MAO inhibitor
	P62/98	1998	1991 to death: carbidopa, levodopa, MAO inhibitor
	P30/00	2000	1990 to death: levodopa; 1993 to death: MAO inhibitor
	P54/00	2000	Carbidopa, levodopa
	P59/00	2000	1995 to death: DA agonist, levodopa
	P05/01	2001	ND
	P18/01	2001	ACh antagonist, levodopa
	P01/02	2002	Carbidopa, levodopa
	P23/02	2002	DA agonist, levodopa, MAO inhibitor
	P25/03	2003	ND
	P18/05	2005	1974 to 1975: ACh antagonist; 1975 to death: levodopa
	P60/05	2005	1982 to death: levodopa
IPDND (16)	P16/92	1992	1991 to death: carbidopa, levodopa
	P28/94	1994	1976 to death: ACh antagonist; 1976 to 1988: carbidopa, levodopa; 1990 to death: MAO inhibitor
	P45/94	1994	1988 to 1992: carbidopa, levodopa; 1992 to death: MAO inhibitor
	P12/95	1995	1979 to 1993: carbidopa, levodopa; 1993 to death: MAO inhibitor
	P17/96	1996	1990 to 1992: carbidopa, levodopa; 1992 to death: MAO inhibitor
	P05/97	1997	1977 to death: ACh antagonist, carbidopa, levodopa
	P65/97	1997	1984 to death: levodopa, MAO inhibitor
	P50/98	1998	1980 to death: ACh antagonist, carbidopa, levodopa; 1996 to death: DA agonist, MAO inhibitor
	P67/98	1998	ND
	P14/99	1999	1985 to death: levodopa, MAO inhibitor
	P40/99	1999	1979 to death: ACh antagonist, carbidopa, levodopa, MAO inhibitor
	P54/99	1999	1989 to death: levodopa, MAO inhibitor
	P55/00	2000	1975 to death: ACh antagonist, carbidopa, DA agonist, levodopa
	P75/00	2000	1987 to death: levodopa; 1994 to death: ACh antagonist, carbidopa, DA agonist
	P24/01	2001	ND
	P05/04	2004	Levodopa

Supplementary Table 3. IPD cognitive series: therapeutic drug regime data.

Individual therapeutic drug regime data for the IPD cognitive series case samples. Duration of treatment with each drug is displayed where known. ACh = acetylcholine; DA = dopamine; IPD = idiopathic Parkinson's disease; IPDD = idiopathic Parkinson's disease with dementia; IPDND = idiopathic Parkinson's disease no dementia; MAO = monoamine oxidase; ND = not determined.

Supplementary Figure 1. Microarray: Agilent RNA quality graphs.

Agilent RNA quality graphs for the IPD microarray series (below and following pages). For each RNA sample, the original capillary electrophoresis gel photograph and the resultant graph plot are shown. The gel and graph for P62/98 were unavailable. RNA quality graphs were generated using the RNA 6000 Nano LabChip Kit on an Agilent 2100 Bioanalyzer. [FU] = fluorescence units; IPD = idiopathic Parkinson's disease; RNA = ribonucleic acid; [s] = Svedberg.

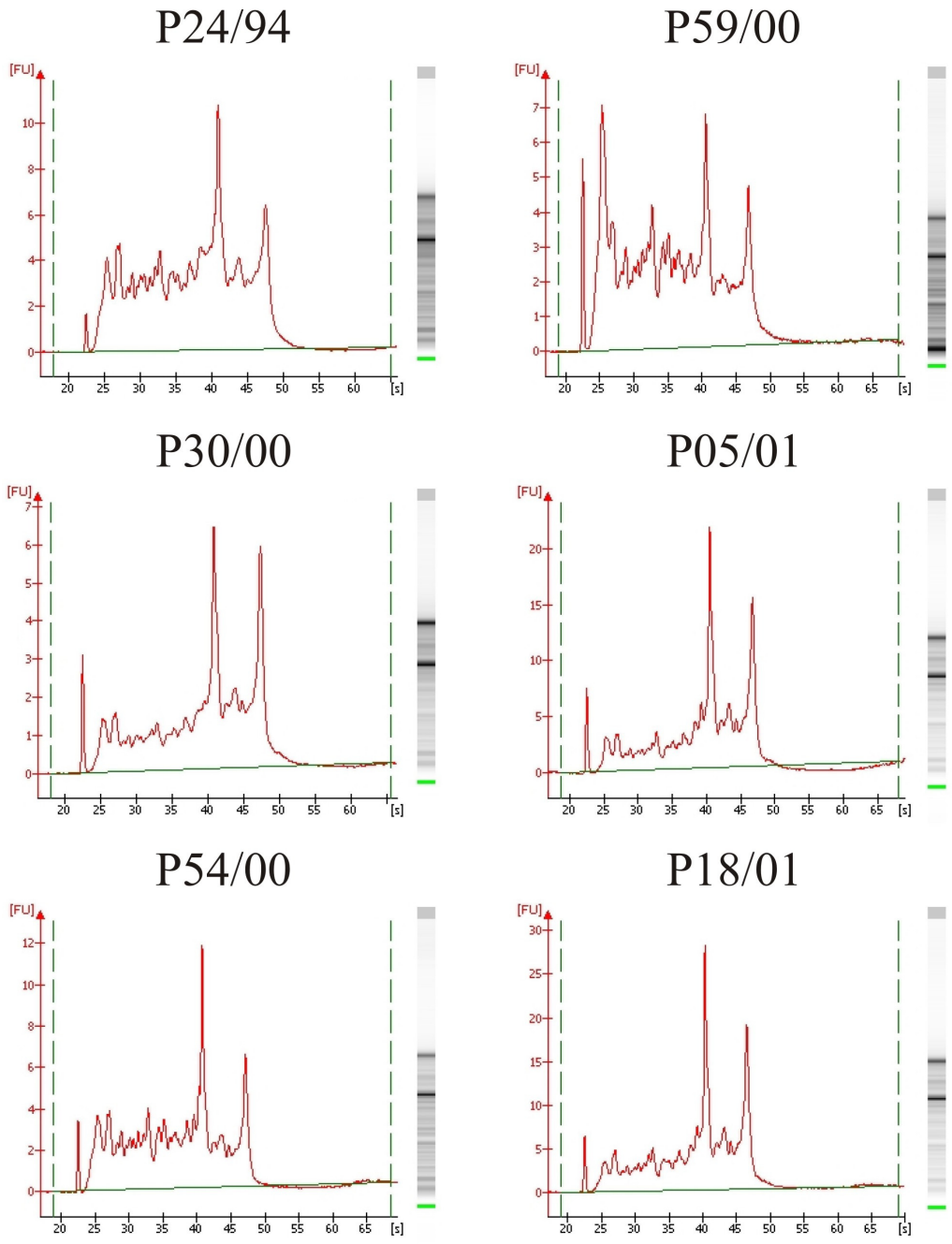

P45/94

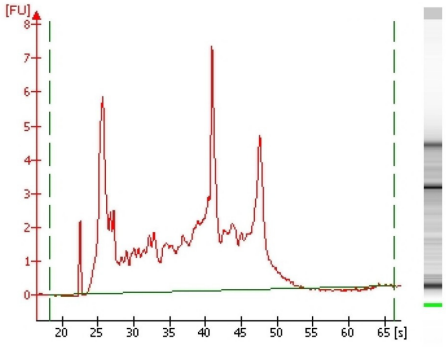

P54/99

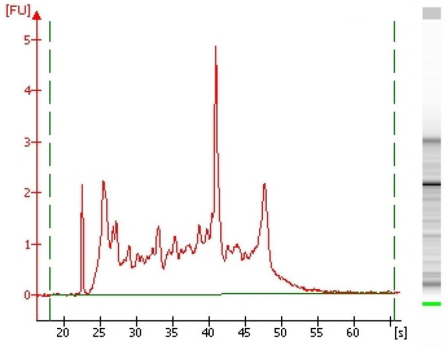

P67/98

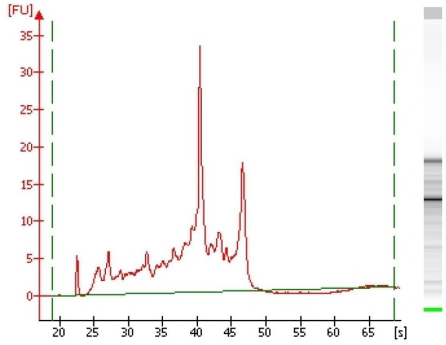

P55/00

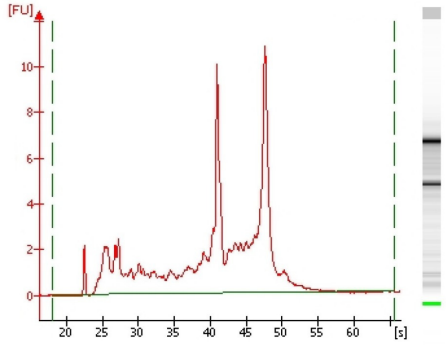

P14/99

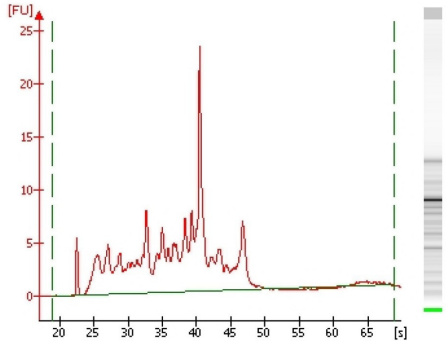

P75/00

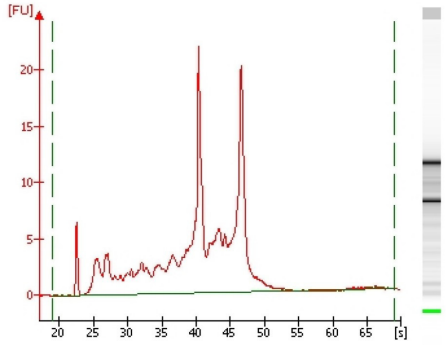

P40/99

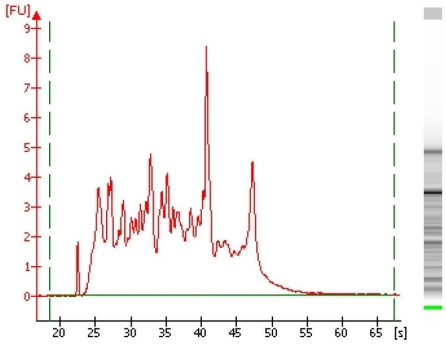

C14/93

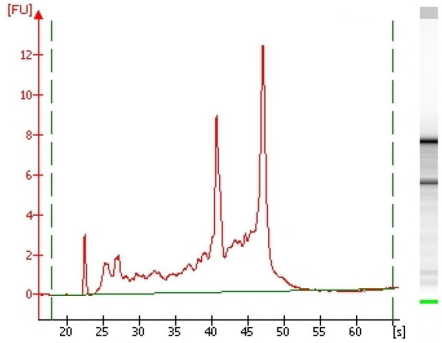

C04/99

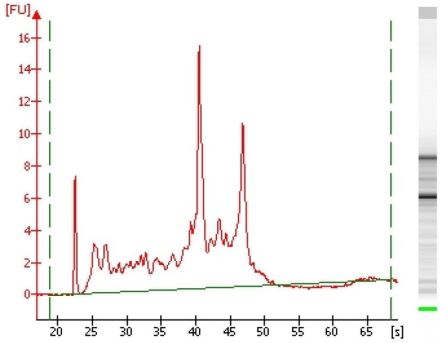

C16/93

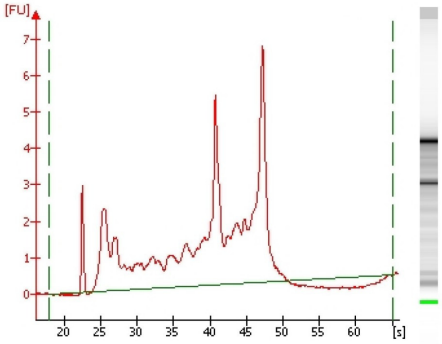

C03/00

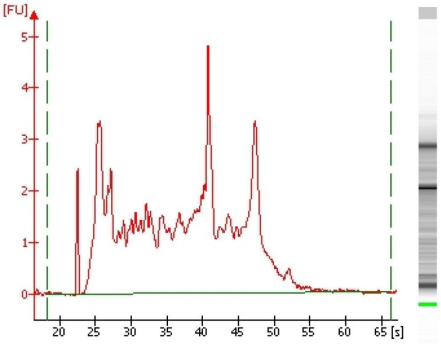

C10/95

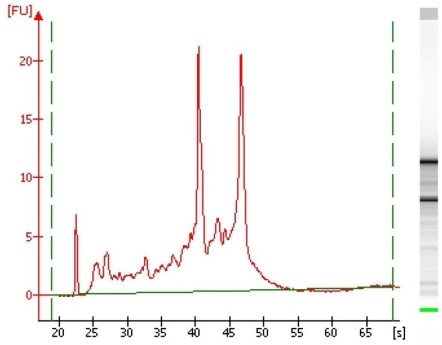

C04/00

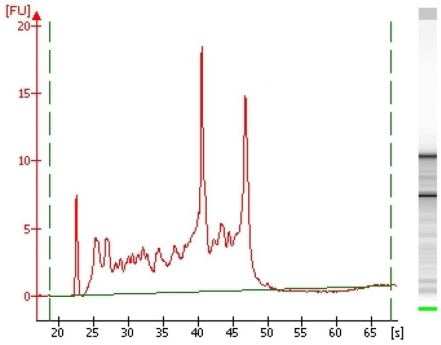

C03/98

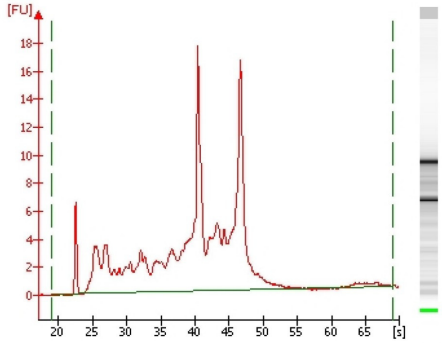

Gene symbol	Affymetrix transcript cluster ID	Ensembl gene ID	Affymetrix probeset ID	Ensembl exon ID
ADCYAP1	3775906	141433	NA	NA
C3orf36	2696109	221972	NA	NA
LY6K	3119213	160886	NA	NA
OR2M4	2390355	171180	NA	NA
POU4F3	2834025	091010	NA	NA
RPL35A	2660013	182899	NA	NA
C8orf79	3086774	170941	3086780	1541420
*CACNA2D3**	2624639	157445	2624642	1594725
EXOC3L	3695450	179044	3695483	1795450
FXYD2	3393446	137731	3393451	1130350
IFI27	3549575	165949	3549592	1484740
MAN1B1	3195174	177239	3195189	1815512
OGT	3981120	147162	3981134	1958312
QKI	2935475	112531	2935592	1894355
RARRES2	3079005	106538	3079009	0729823
RELB	3835966	104856	3835967	1048624
RUSC1	2360887	160753	2360899	1885620
TMC3	3635578	188869	3635603	1391451

Supplementary Table 4. Microarray: clusters and probesets for genes implicated in IPD neurodegeneration.

Affymetrix and Ensembl IDs for genes implicated in IPD neurodegeneration. Affymetrix transcript cluster IDs and Ensembl gene IDs are listed for genes and exons dysregulated in the microarray. For dysregulated exons, Affymetrix probeset IDs and Ensembl exon IDs are also listed. Genes are listed alphabetically, with the differential expression group preceding the alternative splicing group (see table 4.3). See list of abbreviations for gene symbol definitions. * = probeset binds an intronic location 10 bp upstream of this exon (in the direction of transcription); bp = base pairs; ID = identity; IPD = idiopathic Parkinson's disease; NA = not applicable.

Gene symbol	Affymetrix transcript cluster ID	Ensembl gene ID	Affymetrix probeset ID	Ensembl exon ID
ALAS2	4009849	158578	NA	NA
EPHA2	2397948	142627	NA	NA
FAM83H	3157722	180921	NA	NA
FTH1	4037708	167996	NA	NA
MID1IP1	3974098	165175	NA	NA
UQCRFS1	3857691	169021	NA	NA
APOA5	3392957	110243	3392967	0747556
BAIAP3	3643752	007516	3643788	0665665
CCDC92	3476330	119242	3476339	0805119
CDC45L	3936913	093009	3936942	0650790
COL2A1	3452865	139219	3452919	1729865
COL27A1	3185976	196739	3186068	0983778
GRIA4	3347118	152578	3347122	1514240
IKBKE	2376799	143466	2376840	1959016
ITGAL	3656223	005844	3656278	1399855
KRT9	3757138	171403	3757142	1118285
NUP98	3359910	110713	3359948	0988546
ODF2	3190463	136811	3190507	1667665
PCNX	3542689	100731	3542722	1136831
PPP1R16A	3120613	160972	3120631	1473528
PSMB8	2950199	204264	2950201	1842282
RARS2	2963707	146282	2963740	1937897
RICH2	3710870	006740	3710897	1676651
SEPW1	3837504	178980	3837520	1264160
TEX2	3766716	136478	3766723	0947953
TFIP11	3955875	100109	3955903	1851651
TRPM4	3838317	130529	3838334	0896129
ZNF407	3793888	215421	3793949	1104021

Supplementary Table 5. Microarray: clusters and probesets for genes implicated in IPD dementia.

Affymetrix and Ensembl IDs for genes implicated in IPD dementia. Affymetrix transcript cluster IDs and Ensembl gene IDs are listed for genes and exons dysregulated in the microarray. For dysregulated exons, Affymetrix probeset IDs and Ensembl exon IDs are also listed. Genes are listed alphabetically, with the differential expression group preceding the alternative splicing group (see table 4.4). See list of abbreviations for gene symbol definitions. ID = identity; IPD = idiopathic Parkinson's disease; NA = not applicable.

Supplementary Table 6. Microarray: GO term association hits.

GO term association hits for genes implicated in IPD neurodegeneration and IPD dementia by the microarray (below and following pages). Overall occurrences of each term in each disease subtype are shown (see also tables 4.3 and 4.4). Occurrence values are displayed both raw and corrected by the total number of human associations for each term (calculated as raw value divided by total human value). Terms and total human values grouped by ontology type are listed alphabetically and were obtained from the GO database (release 4th September 2010); GO term identity codes are bolded. ATP = adenosine triphosphate; ATPase = adenosine triphosphatase; AMPA = α-amino-3-hydroxy-5-methyl-4-isoxazolepropionic acid; GO = gene ontology; GTPase = guanosine triphosphatase; IPD = idiopathic Parkinson's disease; IKB = inhibitor of κ light polypeptide gene enhancer in B-cells; MHC = major histocompatibility complex; NFKB = nuclear factor κ light polypeptide gene enhancer in B-cells; RNA = ribonucleic acid; Src = Sarcoma; SH2 = Src homology 2; SH3 = Src homology 3.

GO term: Biological process	Total human GO term associations	IPD neurodegeneration GO term associations		IPD dementia GO term associations	
		Raw	Corrected	Raw	Corrected
Activation of adenylate cyclase activity **7190**	57	1	0.018	0	0.000
Acylglycerol homeostasis **55090**	2	0	0.000	1	0.500
Anaphase-promoting complex-dependent proteasomal ubiquitin-dependent protein catabolic process **31145**	64	0	0.000	1	0.016
Angiogenesis **1525**	237	0	0.000	1	0.004
Antigen processing and presentation **19882**	143	1	0.007	0	0.000
Apoptosis **6915**	1134	0	0.000	1	0.001
Arginyl-transfer RNA aminoacylation **6420**	3	0	0.000	1	0.333
Auditory receptor cell differentiation **42491**	17	1	0.059	0	0.000
Axon extension involved in development **48676**	5	1	0.200	0	0.000
Biomineral formation **31214**	67	0	0.000	2	0.030
Biosynthetic process **9058**	4476	0	0.000	1	0.000
Bone development **60348**	38	0	0.000	1	0.026
Calcium ion transport **6816**	196	1	0.005	1	0.005
Cartilage condensation **1502**	16	0	0.000	1	0.063
Cartilage development involved in endochondrial bone morphogenesis **60351**	10	0	0.000	1	0.100
Cell-cell signaling **7267**	722	1	0.001	0	0.000
Cell adhesion **7155**	831	0	0.000	1	0.001
Cell cycle **7049**	1008	0	0.000	1	0.001
Cell differentiation **30154**	1836	0	0.000	1	0.001

GO term: Biological process	Total human GO term associations	IPD neurodegeneration GO term associations		IPD dementia GO term associations	
		Raw	Corrected	Raw	Corrected
Cell redox homeostasis **45454**	66	0	0.000	1	0.015
Cellular component movement **6928**	657	0	0.000	1	0.002
Cellular iron ion homeostasis **6879**	31	0	0.000	1	0.032
Chondrocyte differentiation **2062**	36	0	0.000	1	0.028
Collagen fibril organisation **30199**	27	0	0.000	1	0.037
DNA replication **6260**	248	0	0.000	2	0.008
DNA replication checkpoint **76**	7	0	0.000	1	0.143
DNA replication initiation **6270**	27	0	0.000	1	0.037
Electron transport chain **22900**	117	0	0.000	1	0.009
Embryonic skeletal joint morphogenesis **60272**	5	0	0.000	1	0.200
Endochondrial ossification **1958**	12	0	0.000	1	0.083
Ephrin receptor signaling pathway **48013**	7	0	0.000	1	0.143
Erythrocyte differentiation **30218**	61	0	0.000	1	0.016
Exocytosis **6887**	143	1	0.007	0	0.000
Female pregnancy **7565**	119	1	0.008	0	0.000
G-protein coupled receptor signaling pathway **7186**	546	2	0.004	1	0.002
Glutamate signaling pathway **7215**	24	0	0.000	1	0.042
Haemoglobin biosynthetic process **42541**	5	0	0.000	1	0.200
Heart morphogenesis **3007**	96	0	0.000	1	0.010
Heme biosynthetic process **6783**	21	0	0.000	1	0.048
Heterophilic cell adhesion **7157**	20	0	0.000	1	0.050
Immune response **6955**	926	0	0.000	4	0.004
Inflammatory response **6954**	380	0	0.000	1	0.003

GO term: Biological process	Total human GO term associations	IPD neurodegeneration GO term associations		IPD dementia GO term associations	
		Raw	Corrected	Raw	Corrected
Inner ear morphogenesis **42472**	52	1	0.019	1	0.019
Integrin-mediated signaling pathway **7229**	57	0	0.000	1	0.018
Intermediate filament organisation **45109**	10	0	0.000	1	0.100
Interspecies interaction between organisms **44419**	410	0	0.000	1	0.002
Intracellular sequestering of iron ion **6880**	2	0	0.000	1	0.500
Ion transport **6811**	832	2	0.002	2	0.002
Iron ion transport **6826**	33	0	0.000	1	0.030
Leukocyte adhesion **7159**	28	0	0.000	1	0.036
Limb morphogenesis **35108**	102	0	0.000	1	0.010
Lipid transport **6869**	162	0	0.000	1	0.006
Lipoprotein metabolic process **42157**	86	0	0.000	1	0.012
Long-chain fatty acid biosynthetic process **42759**	2	1	0.500	0	0.000
Membrane organisation **16044**	444	0	0.500	1	0.002
Messenger RNA processing **6397**	318	1	0.003	1	0.003
Messenger RNA transport **51028**	100	1	0.010	1	0.010
Metabolic process **8152**	8520	2	0.000	0	0.000
Multicellular organismal development **7275**	3073	1	0.000	2	0.001
Muscle cell differentiation **42692**	143	1	0.007	0	0.000
Myelination **42552**	48	1	0.021	0	0.000
Myeloid dendritic cell differentiation **43011**	9	1	0.111	0	0.000
Negative regulation of apoptosis **43066**	405	0	0.000	1	0.002
Negative regulation of cell cycle **45786**	189	1	0.005	0	0.000
Negative regulation of cell proliferation **8285**	384	0	0.000	1	0.003

GO term: Biological process	Total human GO term associations	IPD neurodegeneration GO term associations		IPD dementia GO term associations	
		Raw	Corrected	Raw	Corrected
Negative regulation of microtubule depolymerisation **7026**	17	0	0.000	1	0.059
Negative regulation of ubiquitin-protein ligase activity during mitotic cell cycle **51436**	62	0	0.000	1	0.016
Neuromuscular process controlling balance **50885**	31	1	0.032	0	0.000
Neuron apoptosis **51402**	98	1	0.010	0	0.000
Neuron differentiation **30182**	547	0	0.000	1	0.002
Neurotransmitter secretion **7269**	52	0	0.000	1	0.019
Nuclear pore organisation **6999**	5	0	0.000	1	0.200
Nucleocytoplasmic transport **6913**	222	0	0.000	1	0.005
Oligosaccharide metabolic process **9311**	32	1	0.031	0	0.000
Oxidation reduction **55114**	651	0	0.000	1	0.002
Oxygen homeostasis **32364**	6	0	0.000	1	0.167
Palate development **60021**	44	0	0.000	1	0.023
Peptide hormone secretion **30072**	88	1	0.011	0	0.000
Porphyrin metabolic process **6778**	38	0	0.000	1	0.026
Positive regulation of fatty acid biosynthetic process **45723**	11	0	0.000	1	0.091
Positive regulation of IKB kinase/NFKB cascade **43123**	118	0	0.000	1	0.008
Positive regulation of lipoprotein lipase activity **51006**	8	0	0.000	1	0.125
Positive regulation of receptor-mediated endocytosis **48260**	14	0	0.000	1	0.071
Positive regulation of synaptic transmission, glutamergic **51968**	7	0	0.000	1	0.143
Positive regulation of triglyceride catabolic process **10898**	6	0	0.000	1	0.167
Positive regulation of ubiquitin-protein ligase activity during mitotic cell cycle **51437**	64	0	0.000	1	0.016
Positive regulation of very-low-density lipoprotein particle remodelling **10902**	2	0	0.000	1	0.500
Post Golgi vesicle-mediated transport **6892**	59	0	0.000	1	0.017

GO term: Biological process	Total human GO term associations	IPD neurodegeneration GO term associations		IPD dementia GO term associations	
		Raw	Corrected	Raw	Corrected
Potassium ion transport **6813**	138	1	0.007	0	0.000
Protein amino acid N-linked glycosylation **6487**	35	1	0.029	0	0.000
Protein amino acid O-linked glycosylation **6493**	27	1	0.037	0	0.000
Protein amino acid phosphorylation **6468**	802	0	0.000	2	0.002
Protein import into nucleus, docking **59**	2	0	0.000	1	0.500
Protein transport **15031**	891	0	0.000	1	0.001
Proteoglycan metabolic process **6029**	46	0	0.000	1	0.022
Proteolysis involved in cellular protein catabolic process **51603**	346	0	0.000	1	0.003
Regulation of blood vessel endothelial cell migration **43535**	22	0	0.000	1	0.045
Regulation of gene expression **10468**	2976	0	0.000	1	0.000
Regulation of synaptic transmission **50804**	126	0	0.000	0	0.000
Regulation of transcription **45449**	2664	0	0.000	1	0.000
Regulation of transcription, DNA-dependent **6355**	1827	1	0.001	0	0.000
Regulation of transcription from RNA polymerase II promoter **6357**	760	1	0.001	0	0.000
Regulation of translation **6417**	151	1	0.007	0	0.000
Response to antibiotic **46677**	29	0	0.000	1	0.034
Response to drug **42493**	264	0	0.000	1	0.004
Response to hormone stimulus **9725**	460	0	0.000	1	0.002
Response to hypoxia **1666**	150	0	0.000	1	0.007
Response to nutrient **7584**	172	1	0.006	0	0.000
Response to stimulus **50896**	3971	1	0.000	0	0.000
Retinal ganglion cell axon guidance **31290**	15	1	0.067	0	0.000
Retinoid metabolic process **1523**	30	1	0.033	0	0.000
RNA splicing **8380**	301	1	0.003	1	0.003

GO term: Biological process	Total human GO term associations	IPD neurodegeneration GO term associations		IPD dementia GO term associations	
		Raw	Corrected	Raw	Corrected
Ribosomal large subunit biogenesis **42273**	11	1	0.091	0	0.000
Ribosomal RNA processing **6364**	97	1	0.010	0	0.000
Sensory perception of smell **7608**	435	1	0.002	0	0.000
Sensory perception of sound **7605**	96	1	0.010	1	0.010
Signal transduction **7165**	2240	2	0.001	4	0.002
Skin development **43588**	34	0	0.000	1	0.029
Sodium ion transport **6814**	133	1	0.008	0	0.000
Spermatogenesis **7283**	327	1	0.003	2	0.006
Sphingolipid metabolic process **6665**	80	0	0.000	1	0.013
T-cell activation via T-cell receptor contact with antigen bound to MHC molecule on antigen presenting cell **2291**	2	0	0.000	1	0.500
T-helper 1 cell differentiation **45063**	7	1	0.143	0	0.000
Tetrapyrrole biosynthetic process **33014**	26	0	0.000	1	0.038
Tissue homeostasis **1894**	79	0	0.000	1	0.013
Tissue regeneration **42246**	31	0	0.000	1	0.032
Translational elongation **6414**	104	1	0.010	0	0.000
Transmembrane receptor protein tyrosine kinase signaling pathway **7169**	292	1	0.003	0	0.000
Transmembrane transport **55085**	765	0	0.000	2	0.003
Transport **6810**	2913	1	0.000	1	0.000
Triglyceride homeostasis **70328**	14	0	0.000	1	0.071
Triglyceride-rich lipoprotein particle remodelling **34370**	11	0	0.000	1	0.091
Vasculogenesis **1570**	43	1	0.023	0	0.000
Vestibulocochlear nerve development **21562**	2	1	0.500	0	0.000
Visual perception **7601**	219	1	0.005	1	0.005

GO term: Cellular component	Total human GO term associations	IPD neurodegeneration GO term associations		IPD dementia GO term associations	
		Raw	Corrected	Raw	Corrected
AMPA selective glutamate receptor complex **32281**	2	0	0.000	1	0.500
Anchored to membrane **31225**	133	1	0.008	0	0.000
Basement membrane **5604**	73	0	0.000	1	0.014
Cell junction **30054**	539	0	0.000	1	0.002
Cell soma **43025**	183	0	0.000	1	0.005
Cell surface **9986**	348	0	0.000	1	0.003
Centriole **5814**	38	0	0.000	1	0.026
Centrosome **5813**	166	0	0.000	1	0.006
Chylomicron **42627**	12	0	0.000	1	0.083
Cilium **5929**	144	0	0.000	1	0.007
Collagen **5581**	35	0	0.000	2	0.057
Collagen type II **5585**	1	0	0.000	1	1.000
Cytoplasm **5737**	7751	4	0.001	11	0.001
Cytoskeleton **5856**	1422	0	0.000	2	0.001
Cytosol **5829**	1324	2	0.002	2	0.002
Dendrite **30425**	187	0	0.000	1	0.005
Endocytic vesicle membrane **30666**	38	0	0.000	1	0.026
Endoplasmic reticulum **5783**	1042	1	0.001	0	0.000
Exocyst **145**	9	1	0.111	0	0.000
Extracellular region **5576**	2169	3	0.001	3	0.001

GO term: Cellular component	Total human GO term associations	IPD neurodegeneration GO term associations		IPD dementia GO term associations	
		Raw	Corrected	Raw	Corrected
Extracellular space **5615**	755	0	0.000	2	0.003
Flagellum **19861**	36	0	0.000	1	0.028
High-density lipoprotein particle **34364**	24	0	0.000	1	0.042
Integral to membrane **16021**	5422	6	0.001	6	0.001
Integral to plasma membrane **5887**	1198	0	0.000	1	0.001
Integrin complex **8305**	28	0	0.000	1	0.036
Intracellular **5622**	11459	1	0.000	3	0.000
Intracellular ferritin complex **8043**	2	0	0.000	1	0.500
Keratin filament **45095**	94	0	0.000	1	0.011
Kinetochore **776**	92	0	0.000	1	0.011
Membrane **16020**	7463	5	0.001	4	0.001
Membrane fraction **5624**	801	1	0.001	0	0.000
Microtubule **5874**	285	0	0.000	2	0.007
Microtubule organising centre **5815**	277	0	0.000	1	0.004
Mitochondrial inner membrane **5743**	307	0	0.000	2	0.007
Mitochondrial matrix **5759**	223	0	0.000	2	0.009
Mitochondrial respiratory chain complex III **5750**	7	0	0.000	1	0.143
Mitochondrion **5739**	1278	0	0.000	3	0.002
Mixed-lineage leukaemia 5-lysine (MLL5-L) complex **70688**	8	1	0.125	0	0.000
Nuclear membrane **31965**	127	0	0.000	1	0.008

GO term: Cellular component	Total human GO term associations	IPD neurodegeneration GO term associations		IPD dementia GO term associations	
		Raw	Corrected	Raw	Corrected
Nuclear speck **16607**	116	0	0.000	1	0.009
Nucleoplasm **5654**	940	0	0.000	2	0.002
Nucleus **5634**	5237	5	0.001	6	0.001
Nup107-160 complex **31080**	10	0	0.000	1	0.100
Perinuclear region of cytoplasm **48471**	331	0	0.000	1	0.003
Plasma membrane **5886**	3882	3	0.001	5	0.001
Postsynaptic density **14069**	80	0	0.000	1	0.013
Postsynaptic membrane **45211**	155	0	0.000	1	0.006
Proteasome core complex **5839**	20	0	0.000	1	0.050
Proteinaceous extracellular matrix **5578**	314	0	0.000	1	0.003
Respiratory chain **70469**	78	0	0.000	1	0.013
Ribosome **5840**	201	1	0.005	0	0.000
Secretory granule **30141**	187	1	0.005	0	0.000
Sodium:potassium-exchanging ATPase complex **5890**	8	1	0.125	0	0.000
Soluble fraction **5625**	320	1	0.003	0	0.000
Spindle pole **922**	63	0	0.000	1	0.016
Spliceosomal complex **5681**	136	0	0.000	1	0.007
Synapse **45202**	371	0	0.000	1	0.003
Terminal button **43195**	26	0	0.000	1	0.038
Very-low-density lipoprotein particle **34361**	20	0	0.000	1	0.050

GO term: Molecular function	Total human GO term associations	IPD neurodegeneration GO term associations		IPD dementia GO term associations	
		Raw	Corrected	Raw	Corrected
Acetylglucosaminyltransferase activity **8375**	40	1	0.025	0	0.000
Acyltransferase activity **8415**	199	0	0.000	1	0.005
ATP binding **5524**	1490	0	0.000	4	0.003
5-Aminolevulinate synthase activity **3870**	2	0	0.000	1	0.500
AMPA selective glutamate receptor activity **4971**	3	0	0.000	1	0.333
Arginine-transfer RNA ligase activity **4814**	3	0	0.000	1	0.333
Calcium channel activity **5262**	80	0	0.000	1	0.013
Calcium ion binding **5509**	630	2	0.003	2	0.003
Calmodulin binding **5516**	141	0	0.000	1	0.007
Cell adhesion molecule binding **50839**	36	0	0.000	1	0.028
Coenzyme binding **50662**	177	0	0.000	1	0.006
DNA binding **3677**	2054	0	0.000	1	0.000
Enzyme binding **19899**	641	0	0.000	1	0.002
Ephrin receptor activity **5003**	17	0	0.000	1	0.059
Extracellular-glutamate-gated ion channel activity **5234**	19	0	0.000	1	0.053
Extracellular matrix structural constituent **5201**	81	0	0.000	1	0.012
Extracellular matrix structural constituent conferring tensile strength **30020**	6	0	0.000	1	0.167
Ferric ion binding **8199**	11	0	0.000	1	0.091
Ferroxidase activity **4322**	4	0	0.000	1	0.250
Glycine binding **16594**	11	0	0.000	1	0.091
GTPase activator activity **5096**	233	0	0.000	1	0.004
Heparin binding **8201**	114	0	0.000	1	0.009
Hydrolase activity, acting on glycosyl bonds **16798**	116	1	0.009	0	0.000
Identical protein binding **42802**	692	0	0.000	1	0.001
IKB kinase activity **8384**	3	0	0.000	1	0.333

GO term: Molecular function	Total human GO term associations	IPD neurodegeneration GO term associations		IPD dementia GO term associations	
		Raw	Corrected	Raw	Corrected
Ion channel activity **5216**	385	1	0.003	2	0.005
Iron ion binding **5506**	209	0	0.000	1	0.005
Ligase activity **16874**	434	0	0.000	1	0.002
Lipoprotein lipase activator activity **60230**	3	0	0.000	1	0.333
Low-density lipoprotein receptor binding **50750**	12	0	0.000	1	0.083
Magnesium ion binding **287**	164	0	0.000	1	0.006
Mannosyl-oligosaccharide 1,2-α-mannosidase activity **4571**	8	1	0.125	0	0.000
Metal ion binding **46872**	3829	0	0.000	2	0.001
Methyltransferase activity **8168**	175	1	0.006	0	0.000
Neuropeptide hormone activity **5184**	22	1	0.045	0	0.000
NFKB-inducing kinase activity **4704**	6	0	0.000	1	0.167
Nucleic acid binding **3676**	3043	0	0.000	1	0.000
Nucleotide binding **166**	2280	0	0.000	4	0.002
Olfactory receptor activity **4984**	422	1	0.002	0	0.000
Oxidoreductase activity **16491**	694	0	0.000	1	0.001
Oxidoreductase activity, acting on diphenols and related substances as donors **16679**	10	0	0.000	1	0.100
Peptidase activity **8233**	584	0	0.000	1	0.002
Phosphatidyl choline binding **31210**	7	0	0.000	1	0.143
Platelet-derived growth factor binding **48407**	11	0	0.000	1	0.091
Potassium ion binding **30955**	6	1	0.167	0	0.000
Protein binding **5515**	8192	4	0.000	14	0.002
Protein carboxy-terminus binding **8022**	146	0	0.000	2	0.014
Protein complex binding **32403**	247	0	0.000	1	0.004
Protein heterodimerisation activity **46982**	220	0	0.000	1	0.005
Pyridoxal phosphate binding **30170**	54	0	0.000	1	0.019

GO term: Molecular function	Total human GO term associations	IPD neurodegeneration GO term associations		IPD dementia GO term associations	
		Raw	Corrected	Raw	Corrected
Receptor activity **4872**	1712	1	0.001	3	0.002
Receptor signaling protein activity **5057**	162	1	0.006	0	0.000
RNA binding **3723**	754	1	0.001	0	0.000
SH3 domain binding **17124**	100	1	0.010	0	0.000
SH3/SH2 adaptor activity **5070**	50	1	0.020	0	0.000
Selenium binding **8430**	14	0	0.000	1	0.071
Sequence-specific DNA binding **43565**	639	1	0.002	0	0.000
Sodium ion binding **31402**	5	1	0.200	0	0.000
Sodium:potassium-exchanging ATPase activity **5391**	10	1	0.100	0	0.000
Structural constituent of cytoskeleton **5200**	73	0	0.000	1	0.014
Structural constituent of nuclear pore **17056**	5	0	0.000	1	0.200
Structural constituent of the ribosome **3735**	161	1	0.006	0	0.000
Structural molecule activity **5198**	641	0	0.000	1	0.002
Threonine-type endopeptidase activity **4298**	21	0	0.000	1	0.048
Transcription corepressor activity **3714**	147	1	0.007	0	0.000
Transcription factor activity **3700**	969	2	0.002	0	0.000
Transfer RNA binding **49**	24	1	0.042	0	0.000
Transferase activity **16740**	1698	1	0.001	2	0.001
Transferase activity, transferring glycosyl groups **16757**	257	1	0.004	0	0.000
Transferase activity, transferring nitrogenous groups **16769**	30	0	0.000	1	0.033
Transporter activity **5215**	1181	1	0.001	1	0.001
Two iron, two sulphur cluster binding **51537**	19	0	0.000	1	0.053
Ubiquinol-cytochrome-c reductase activity **8121**	9	0	0.000	1	0.111
Voltage-gated calcium channel activity **5245**	27	1	0.037	0	0.000
Voltage-gated ion channel activity **5244**	191	1	0.005	0	0.000
Zinc ion binding **8270**	2041	0	0.000	1	0.000